Digital Surgery

Sam Atallah
Editor

Springer

Digital Surgery

Sam Atallah
Editor

Digital Surgery

Springer

Editor
Sam Atallah
Orlando, FL
USA

ISBN 978-3-030-49099-7   ISBN 978-3-030-49100-0 (eBook)
https://doi.org/10.1007/978-3-030-49100-0

This Springer imprint is published by the registered company Springer Nature Switzerland AG
The registered company address is: Gewerbestrasse 11, 6330 Cham, Switzerland

To my youngest child, Addyson.
What wonders await you in your lifetime?

Preface

The future. Sometimes, we can close our eyes and almost see it. In the years leading up to 2020, *digital surgery* had reached a fever pitch. Abraham Lincoln once said, *"the best way to predict the future is to create it."* In this context, the coming age of surgery will be formed in the present by our own design. This book is written by many of those who, today, are laying the foundation for tomorrow's operating environment. This textbook provides a trove of insightful perspectives on where we are at this instant in time … and the trek ahead toward the realization of digital surgery.

What *is* digital surgery? Perhaps its definition should be left bound not by diction but rather by imagination. To some degree, digital surgery is kaleidoscopic—its facets and shapes, shifting. In its commonest context, it entails the application of artificial intelligence toward computer vision and automation in robotic-assisted surgery. More generally, however, the objective is to *digitally define* the patient, the surgical field, and the surgical problem or task at hand—*to operate based on information, rather than based on anatomic planes alone.*

But digital surgery has shapeshifted into other, equally intriguing facets—many of which are exemplified by chapter headings throughout this book. Digital surgery is fundamental to 3D-printed organs, mind-controlled limbs, image-guided navigation, and tele-mentoring. It is the key that unlocks the metaphorical doorway to surgical access, thereby creating a global framework for surgical training, education, planning, and much more. This 4.0-version of surgery will also provide methods of measurement and perception outside of the human umwelt—including the ability to visualize fields beyond the visible light spectrum, via near infrared fluorescent organic dyes which are rapidly being bioengineered to target specific tumors, as well as native anatomic structures of interest.

Digital surgery ushers in the era of patient centricity. Rather than focusing solely on the anatome, surgeons will operate with an enriched understanding of an individual's *specific* attributes: including the human phenome, physiome, microbiome, genome, and epigenome. In parallel, digital surgery will harness the power and fluidity of the cloud. The cloud is poised to emerge as a significant resource for surgeons over the next decade—especially through shared machine learning, both regionally and globally. It is important to understand that digital surgery is *not* the last step in evolution, but only the next. A touchstone towards computer-centric surgery and the new age of surgical automation, robotic-machine learning, augmented environments, and the like.

In 2005, when I was a fourth-year surgical resident in training, I was reminded of where we stand with regard to innovation in surgery on a grand scale. I had the opportunity to meet famed surgeon Michael DeBakey that year. At our encounter, I asked him with genuine curiosity, *"do you think the era of innovation and discovery in surgery is over and done?"* I went on to ramble off several seismic milestones—the first heart transplant in a human, the development of general anesthetics, the creation of the lung-heart bypass machine, electrocautery, and so on. He shook his head at me and, with a wide grin and a sparkle of certainty in his eyes, said, *"Not at all!"* … he added with a chuckle, "*This is just the beginning!"*

DeBakey was right. Indeed, we are at one of the most exciting times in the history of surgery, and we are only getting started. Off we go... a great odyssey lies ahead!

> *We are at the very beginning of time for the human race. It is not unreasonable that we grapple with problems. But there are tens of thousands of years in the future. Our responsibility is to do what we can, learn what we can, improve the solutions, and pass them on.* — Richard P. Feynman

Orlando, FL, USA Sam Atallah, MD

Contents

Contributors

Nureddin Ashammakhi, PhD, FRCSEd, MBBCh Center for Minimally Invasive Therapeutics (C-MIT), California NanoSystems Institute (CNSI), Department of Radiological Sciences, David Geffen School of Medicine, Department of Biomedical Engineering, Henry Samueli School of Engineering, University of California, Los Angeles, Los Angeles, CA, USA

Joanna Ashby, BSc Program in Global Surgery and Social Change, Harvard Medical School, Boston, MA, USA

Asa B. Atallah, BS, MS Apple Inc., Los Gatos, CA, USA

Sam Atallah, MD University of Central Florida, College of Medicine, Orlando, FL, USA

Kulvinder S. Bajwa, MD Department of Surgery, UT Health McGovern Medical School, Houston, TX, USA

Thomas George Barnes, MBChB (Hons), MRCS, DPhil Department of Colorectal Surgery, Oxford University Hospitals NHS Foundation Trust, Nuffield Department of Surgery, University of Oxford, Oxford, UK

Yanick Beaulieu, MDCM Cardiology and Critical Care, Hôpital Sacré-Coeur de Montréal and Montreal Heart Institute, Montreal, QC, Canada

Fernando Bello, BSc(Hons), PhD Centre for Engagement and Simulation Science, Imperial College London, London, UK

Manuel Birlo, Dipl. -Inform Computer Science/WEISS, University College London, London, UK

Michael F. Byrne, MA, MD(Cantab), MRCP, FRCPC Department of Gastroenterology, Vancouver General Hospital, University of British Columbia, Vancouver, BC, Canada

Daljeet Chahal, MD, MASc Department of Gastroenterology, University of British Columbia, Vancouver, BC, Canada

Manish Chand, MBBS, FRCS, FASCRS, MBA, PhD Surgery and Interventional Sciences, University College London, London, UK

Justin W. Collins, MBChB, MD, FRCS (Urol) Department of Urology, University College London Hospitals NHS, London, UK

Toby Collins, MSc Research & Development, Research Institute Against Digestive Cancers (IRCAD), Strasbourg, France

Esther Consten, MD, PhD Department of Surgery, University Medical Center Groningen, Meander Medical Centre, Groningen, The Netherlands

Mohammad Ali Darabi, PhD Center for Minimally Invasive Therapeutics (C-MIT), California NanoSystems Institute (CNSI), University of California, Los Angeles, Los Angeles, CA, USA

Prokar Dasgupta, MSc, MD, DLS, FRCS(Urol), FEBU MRC Centre for Transplantation, King's College London, London, UK

Hossein Dehghani, PhD Activ Surgical, Boston, MA, USA

Roger Daglius Dias, MD, MBA, PhD Human Factors & Cognitive Engineering Lab, STRATUS Center for Medical Simulation, Department of Emergency Medicine, Brigham and Women's Hospital, Harvard Medical School, Boston, MA, USA

Mischa Dohler, PhD, MSC, PhD DHC Department of Engineering, King's College London, London, UK

P. J. " Eddie" Edwards, BA(Hons), MSc, PhD Computer Science/WEISS, University College London, London, UK

Joseph J. Eid, MD Department of Surgery, University of Nebraska Medical Center, Omaha, NE, USA

Ahmet Erdem, BS Department of Chemistry, Department of Biomedical Engineering, Kocaeli University, Kocaeli, Turkey

Melissa M. Felinski, DO Department of Surgery, UT Health McGovern Medical School, Houston, TX, USA

Danyal M. Fer, MD Applied Research, Verb Surgical, Inc., Santa Clara, CA, USA

Department of Surgery, University of California San Francisco East Bay, Oakland, CA, USA

Laboratory for Automation Science and Engineering, University of California Berkeley, Berkeley, CA, USA

Marco Ferrara, MD Department of Colon and Rectal Surgery, Colon and Rectal Clinic of Orlando, Orlando, FL, USA

Rebecca A. Fisher, BSc (Hons), MBChB MRC Centre for Transplantation, King's College London, London, UK

Jordan Fletcher, MbChB(Hons), BSc, PGC, MRCS Department of Colorectal Surgery, St. Marks Hospital, London, UK

Molly L. Flexman, PhD Philips Research, Cambridge, MA, USA

Bernhard Fuerst, PhD Applied Research, Verb Surgical, Inc., Santa Clara, CA, USA

Ahmed E. Ghazi, MDFEBU Department of Urology, University of Rochester, Rochester, NY, USA

Simulation Innovation Laboratory, University of Rochester, Department of Urology, Rochester, NY, USA

Atul Gupta, MD Philips, Cambridge, MA, USA

Murat Guvendiren, PhD Otto H. York Department of Chemical and Materials Engineering, Department of Biomedical Engineering, New Jersey Institute of Technology, Newark, NJ, USA

Nadine Hachach-Haram, BEM MBBS, MRCS, FRCS(Plast) Plastic Surgery and Clinical Innovation, Guy's & St. Thomas' NHS Foundation Trust, London, UK

David Herrmann, BS, MBA Marketing and Business Development, Verb Surgical, Inc., Santa Clara, CA, USA

David Hindin, MD, MS Stanford Byers Center for Biodesign, Stanford, CA, USA

Alexandre Hostettler, PhD Research & Development, Research Institute Against Digestive Cancers (IRCAD), Strasbourg, France

Andrew J. Hung, MD Catherine & Joseph Aresty Department of Urology, University of Southern California Institute of Urology, Center for Robotic Simulation & Education, Keck School of Medicine, University of Southern California, Los Angeles, CA, USA

Thomas Hurkxkens, MSc Digital Learning Hub, Imperial College London, London, UK

Shalmali Joshi, PhD, MS Vector Institute for Artificial Intelligence, Toronto, ON, Canada

Deborah Keller, MS, MD Department of Surgery, Columbia University Medical Center, New York, NY, USA

William Kethman, MD, BSE Department of Surgery, Case Western Reserve University, University Hospitals – Cleveland Medical Center, Cleveland, OH, USA

Pablo Garcia Kilroy, MSME Research and Digital Technologies, Verb Surgical, Inc., Santa Clara, CA, USA

Peter C. W. Kim, MD, PhD Department of Surgery, Brown University; Active Surgical, Boston, MA, USA

Suewan Kim, MBBS, BSc(Hons) MRC Centre for Transplantation, King's College London, London, UK

Çetin Kaya Koç, PhD College of Engineering, Istinye University, Istanbul, Turkey

Christos Kontovounisios, MD, PhD, FACS, FRCS Department of Surgery and Cancer, Imperial College London – Chelsea and Westminster and the Royal Marsden Campus, London, UK

Przemyslaw Korzeniowski, MSc, PhD Department of Surgery and Cancer, Imperial College London, London, UK

Runzhuo Ma, MD Catherine & Joseph Aresty Department of Urology, University of Southern California Institute of Urology, Center for Robotic Simulation & Education, Keck School of Medicine, University of Southern California, Los Angeles, CA, USA

Jacques Marescaux, MD Research Institute Against Digestive Cancers (IRCAD), Strasbourg, France

Institute of Image-Guided Surgery (IHU Strasbourg), Strasbourg, France

Ozanan Meireles, MD Surgical and Innovation Laboratory, Department of Surgery, Massachusetts General Hospital, Boston, MA, USA

Armando Errando Franchini Melani, MD, MSc Department of Surgery, IRCAD Latin America/Americas Medical Service, Rio de Janeiro, Brazil

Danilo Miskovic, PhD, FRCS Department of Colorectal Surgery, St. Marks Hospital, London, UK

Tamer Mohamed, PhD, MASc, BASc Aspect Biosystems, Vancouver, BC, Canada

Arsen Muhumuza, BSc Medicine and Surgery, University Teaching Hospital of Kigali, Kigali, Rwanda

Didier Mutter, MD, PhD, FACS University of Medicine of Strasbourg, Strasbourg, France

Research Institute Against Digestive Cancers (IRCAD), Strasbourg, France

Department of Digestive and Endocrine Surgery, Institute of Image-Guided Surgery, University Hospital of Strasbourg, Strasbourg, France

Isaac Ndayishimiye, BSc Medicine and Surgery, University of Rwanda, Kigali, Rwanda

Jean Nehme, MSc, MBBS Digital Surgery, London, UK

Sylvine Niyoyita, BSc Medicine and Surgery, University of Rwanda, Kigali, Rwanda

Dmitry Oleynikov, MD Department of Surgery, University of Nebraska Medical Center, Omaha, NE, USA

Virtual Incision Corp, Omaha, NE, USA

Asutay Ozmen, MSci Department of Electrical and Computer Engineering, University of California Santa Barbara, Santa Barbara, CA, USA

M. Mahir Ozmen, MD, MS, FACS, FRCS, FEBS, FASMBS Department of Surgery, Istinye University Medical School, Istanbul, Turkey

Eduardo Parra-Davila, MD, FACS, FASCRS Colorectal and General Surgery, Good Samaritan Medical Center, West Palm Beach, FL, USA

Patrick Pessaux, MD, PhD Hepato-Biliary and Pancreatic Surgical Unit, Department of Digestive and Endocrine Surgery, Institute of Image-Guided Surgery, University Hospital of Strasbourg, Strasbourg, France

University of Medicine of Strasbourg, Strasbourg, France

Research Institute Against Digestive Cancers (IRCAD), Strasbourg, France

Ippokratis Pountos, MB, BSc, MSc, MD Academic Department of Trauma and Orthopaedics, University of Leeds, Leeds, UK

Chapel Allerton Hospital, Leeds Teaching Hospitals, Leeds, UK

Pratik, M.S. Gurung, MD, PhD, FRCS, FEBU Department of Urology, University of Rochester, Rochester, NY, USA

Anna Przedlacka, FRCS Department of Surgery and Cancer, Imperial College London – Chelsea and Westminster Hospital, London, UK

Luis Gustavo Capochin Romagnolo, MD Surgical Oncologic of Colon and Rectal, Barretos Cancer Hospital/IRCAD Latin America, Barretos, Sao Paulo, Brazil

Frank Rudzicz, BSc, MEng, PhD International Centre for Surgical Safety, Toronto, ON, Canada

Li Ka Shing Knowledge Institute, St. Michael's Hospital, Toronto, ON, Canada

Department of Computer Science, University of Toronto, Toronto, ON, Canada

Surgical Safety Technologies Inc., Toronto, ON, Canada

Vector Institute for Artificial Intelligence, Toronto, ON, Canada

Daniel Ruijters, PhD Philips Image Guided Therapy, Best, The Netherlands

Stephanie Schipmann, MD Department of Neurosurgery, University Hospital Münster, Münster, Germany

Rithvik Seela Department of Economics, Stanford University, Palo Alto, CA, USA

Barbara Seeliger, MD, PhD Institute of Image-Guided Surgery, IHU Strasbourg; Research Institute Against Digestive Cancer, IRCAD, Strasbourg, Alsace, France

Shinil K. Shah, DO Department of Surgery, UT Health McGovern Medical School, Houston, TX, USA

Neal Shahidi, MD, FRCPC Department of Gastroenterology, University of British Columbia, Vancouver, BC, Canada

Luc Soler, PhD Visible Patient, Strasbourg, Grand Est, France

University of Medicine of Strasbourg, Strasbourg, France

Mark K. Soliman, MD Department of Colon and Rectal Surgery, Colon and Rectal Clinic of Orlando, Orlando, FL, USA

Danail Stoyanov, BEng, PhD Computer Science/WEISS, University College London, London, UK

Walter Stummer, MD, PhD Department of Neurosurgery, University Hospital Münster, Münster, Germany

Paris Tekkis, BMedSci, BM BS, MD, HonD, FRCS Department of Surgery and Cancer, Imperial College London – Chelsea and Westminster and the Royal Marsden Campus, London, UK

Nazzar Tellisi, MSc, Mmed Sci, FRCS, FRCS Academic Department of Trauma and Orthopaedics, University of Leeds, Leeds, UK

Chapel Allerton Hospital, Leeds Teaching Hospitals, Leeds, UK

Diana Velazquez-Pimentel, BSc Barts and the London School of Medicine and Dentistry, London, UK

Thomas M. Ward, MD Department of Surgery, Massachusetts General Hospital, Boston, MA, USA

Richard F. ff. Weir, PhD Biomechatronics Development Laboratory, Department of Bioengineering, College of Engineering, Design, and Computing, University of Colorado - Denver/Anschutz Medical Campus, Aurora, CO, USA

Arthur Randolph Wijsmuller, MD, PhD Department of Surgery, University Medical Center Groningen, Groningen, The Netherlands

Erik B. Wilson, MD Department of Surgery, UT Health McGovern Medical School, Houston, TX, USA

Todd D. Wilson, MD Department of Surgery, UT Health McGovern Medical School, Houston, TX, USA

Steven J. Yule, PhD STRATUS Center for Medical Simulation, Department of Surgery, Center for Surgery and Public Health, Department of Surgery, Brigham and Women's Hospital, Harvard Medical School, Boston, MA, USA

Marco A. Zenati, MD Department of Surgery, U.S. Department of Veterans Affairs, Brigham and Women's Hospital, Harvard Medical School, Boston, MA, USA

The Cognitive Revolution

1

Thomas M. Ward and Ozanan Meireles

Introduction

In the last decade, we have been witnessing the great potential of a Cognitive Revolution in Medicine that promises to completely transform surgery. Before exploring its history and potential, we must establish some basic definitions. First, cognition is "the action or faculty of knowing" [1]. Cognition is fundamental, but formal study only started in the 1950s [2]. Recent progress in one of its major subfields, artificial intelligence (AI), has created the promise of revolution.

A revolution is a "dramatic or wide-reaching change in conditions" [1]. Examples include the Industrial Revolution, which jump-started modern society with its transition of manual labor into machine-assisted processes. Surgery has also undergone many revolutions. In the nineteenth century, the development of general anesthesia and asepsis allowed for surgeons to humanely, and safely, foray into invasive surgical procedures. The twentieth-century innovations of surgical staplers, endoscopy, and laparoscopy have created modern surgery as we know it [3].

T. M. Ward (✉)
Department of Surgery, Massachusetts General Hospital, Boston, MA, USA
e-mail: tmward@mgh.harvard.edu

O. Meireles
Surgical and Innovation Laboratory, Department of Surgery, Massachusetts General Hospital, Boston, MA, USA

Despite this progress, surgery is still fraught with dangers: almost 30% of surgical patients will suffer a complication [4]. Surgery needs to improve, and AI offers a potential solution: the Cognitive Revolution.

Artificial Intelligence

AI is "the study of computations that make it possible to perceive, reason, and act" [5]. The breadth and extent of these computational abilities lead to different types of AI. Movies and popular science portray AI as computers and automatons with cognition equivalent to humans'. This all-encompassing AI is termed *generalized* AI [6]. Taken to the extreme, some people even believe that AI will obtain superhuman intelligence and end humanity's reign, with an event known as the *singularity* [7]. Despite Hollywood's hyperboles, a more realistic and obtainable intelligence is a *narrow* one, where computer algorithms focus on specific tasks and excel. Narrow AI is pervasive throughout today's society, from movie recommendation systems to autonomous vehicles.

Narrow AI aligns closely to Warren McCulloch and Walter Pitts' original conception of AI in 1943. Based upon a knowledge of basic neurophysiology, propositional logic, and Turing's theory of computation, they proposed that any function could be computed with a network of neurons that were either on or off [8]. Minsky and Edmonds made this "neural network computer" a

S. Atallah (ed.), *Digital Surgery*, https://doi.org/10.1007/978-3-030-49100-0_1

reality in 1950 with their SNARC, a computer that simulated 40 neurons [9]. These neural networks led to initial great success in the 1950s, with an early prototype capable of winning games of Checkers [10]. Unfortunately, the early gains and lofty promises failed to deliver in the ensuing decades. Public and private sector opinion soured on AI, as epitomized by the Lighthill Report in 1973 which led to almost total cessation of governmental funding for AI in the United Kingdom [11]. The ensuing "AI Winter" brought with it a near total collapse of the AI industry in the 1980s and early 1990s [12]. As the 1990s progressed though, AI began to succeed, particularly with narrow tasks. Four decades after Samuel's machine learning success with Checkers, IBM created "Deep Blue," a chess computer capable of beating the World Chess Champion Garry Kasparov [13]. This landmark achievement was one of many to follow in the years ahead.

Artificial Intelligence Revolution

AI in the twentieth century had been a plodding field, filled with many promises but few results. AI's fortunes, though, have changed in the past two decades. AI, particularly *narrow* AI, is undergoing a resurgence and revolution – but why now? Its success results from the alignment of four major factors: (1) big data, (2) adequate compute power, (3) deep learning algorithms, and (4) increased investment.

The first key to the AI revolution is big data. Data inputs form the foundation for AI and its subfield – machine learning (ML). Without data, the algorithms cannot learn. Early successes in ML came with application to problems that have a small, finite data space. For example, Tic-Tac-Toe only has nine squares to fill with two possible markers (X or O), with only a thousand legal possible different positions. Checkers has over 10^{20} possibilities, and the game Go has 10^{170} possibilities [14, 15]. Mapping these possibilities is relatively easy for a computer but imagine the amount of data needed for an algorithm to not just play a board game, but classify objects, understand human speech, or even operate a motor vehicle.

Prior to 2003, humanity had generated 5 exabytes ($5 * 10^{18}$) of data. As of 2012, that much data was generated every 2 days [16]. Medicine has seen a similar explosion in data availability, with 1 minute of high-definition surgical video containing 25 times the amount of information in one CT scan image [17]. This glut of data has given AI and ML algorithms the information they need to learn and perform at human levels.

The second key to the AI revolution is adequate compute power. AI and ML algorithms, particularly those of the "deep learning" variety, are extraordinarily resource intensive. Much of AI's failure to launch in the mid-to-late twentieth century stemmed from lack of compute power. As Moore famously postulated in 1975, computer circuits have doubled in circuit complexity every 2 years, which roughly translates to a doubling in compute power [18]. Even this doubling of compute power failed to reach adequate levels for some of the newer ML algorithms found with "deep learning" which require millions of complex linear algebra calculations. The relatively recent employment of graphical processing units (GPUs) made these algorithms' utilization feasible. GPUs are special computer chips initially developed for computer graphical tasks, such as video games. For ML tasks, they perform calculations orders of magnitude faster than traditional computer chips [19]. Companies, such as Google, have expanded upon this idea with their creation of ML-specific chips like tensor processing units which run with improved energy costs and speed [20]. This additional computer "horsepower" has allowed for actual implementations of all the algorithms that AI's inventors could heretofore only imagine.

The third key to the AI revolution is deep learning algorithms. AI's inception started with the theory that computer networks could mirror a human's own neural networks to create intelligence. Relatively simple tasks with totally knowable data (such as a Checkers game) were quickly implemented [10]. However, complex tasks that many would define as a marker of true intelligence, such as image and speech recognition, escaped AI designers. Krizhevsky et al. created the breakthrough with their application of deep convolutional neural networks. They realized that the natural resources for AI, big data, and compute power finally were bountiful. To tackle complex tasks like image recognition, however, required development of a neural architecture – like the human brain, complex enough to use a limited set of training data to extrapolate recognition to all permutations. Their use of deep convolutional neural networks halved the error rate for image recognition compared to all other competitors [21]. These deep learning algorithms have become the primary approach to create intelligence and cognition at levels that meet or exceed a human's capabilities, from image recognition (with computer vision [CV]) to language (natural language processing [NLP]) [22].

The fourth key to the AI revolution is the increased investment that has accompanied the previous foundation. No longer is AI trapped in the unfundable "AI Winter" where private and public sector funding disappeared [12]. The US government invested $1.1 billion towards AI in 2015 alone [23]. The private sector has seen a similar increase, with a doubling in AI private equity investment from 2016 to 2017. In fact, 12% of worldwide private equity investment went to the AI industry in 2018 alone [24]. Healthcare, in particular, is seeing an order-of-magnitude increase in funding, from $600 million in 2014 to a projected $6.6 billion by 2021 [25]. Big data, adequate compute power, deep learning algorithms, and increased investment have generated the rich AI landscape of today.

AI in Healthcare

The AI revolution has led to an explosion of healthcare-related applications. The foundations of AI in healthcare rest upon the deep learning algorithm's ability, through CV and NLP, to emulate humans' cognitive capabilities. In the surgical arena, it mainly has served to augment, rather than supplant, the human element. Successful AI utilization is found in all phases of the surgery, from preoperative diagnosis and risk assessment to intraoperative assistance and postoperative complication prediction.

The preoperative phase has seen the largest application of AI technology. AI algorithms can go head-to-head with physicians – particularly in the image-predominant fields of radiology and pathology for preoperative diagnosis. Some examples of applications include diagnosis of intracranial hemorrhage from CT images, breast cancer from mammography, and lung cancer from tissue slides [26]. One exceptional example comes from work in dermatology. Esteva et al. developed a diagnostic system based on convolutional neural networks capable of classifying dermatologic lesions as malignant or benign with superior sensitivity and specificity when compared to board-certified dermatologists [27]. AI has also helped with preoperative patient risk stratification. One example includes the POTTER score, an algorithm based on the ML technology of optimal classification trees that outperformed traditional multivariable logistic regression model surgical risk calculators, such as the ACS-NSQIP calculator [28].

The postoperative phase has also begun to see the introduction of AI technology. The majority of efforts have focused on complication prediction, as previous works have identified the concept of "failure to rescue," where overall complication rates between high- and low-performing hospitals are identical, but the lower-performing hospital have twice the mortality rates. These efforts hope to, through integration of myriad variables, detect complications early and therefore prevent a snowball effect that ultimately leads to higher mortality rates – which, in the case of pancreatic cancer, is over an order of magnitude higher [29, 30]. For example, one model considers over 175,000 data points per patient to predict mortality and morbidity [31]. Similar efforts aimed to predict postoperative surgical site infections from pre- and postoperative laboratory values [32].

Despite the development of AI technology for the pre- and postoperative phases, there has been relatively fewer applications to the intraoperative phase. A few computer vision groups focus on *temporal segmentation* of laparoscopic intraoperative videos with analysis of cholecystectomies, sleeve gastrectomies, and colectomies

[33–35]. One other group has worked to link intraoperative performance metrics from robotic surgery to predict postoperative events. For example, investigators could predict, based on intraoperative metrics alone, if a patient's length of stay postoperatively would exceed 2 days [36]. The past 7 years have generated significant progress for AI in healthcare, but there continues to remain numerous unexplored avenues for further applications.

Future Applications for AI in Surgery

The previously described AI innovations in healthcare are technologically revolutionary. The seemingly impossible tasks of image, speech, and language classification are now obtainable, at least at a rudimentary level. However, with respect to patient care, the advancements hardly seem to warrant the label of a "Cognitive Revolution." Fortunately, with the ever-increasing amount of generated data, more powerful computers, improved algorithms, and influx of funds, AI in healthcare is primed for a revolution.

This revolution will progress in incremental steps. Decision-support systems will become more pervasive at every stage of a patient's care. Consider a patient referred with a diagnosis of colon cancer. In the next few years, the patient's initial visit will seem relatively similar to the one from today, but it will incorporate ML algorithms throughout to augment their care. For example, an algorithm will classify their tumor at a granularity far superior to our currently crude TNM staging system to create an individualized treatment plan. Additionally, their metrics, including history, vitals, lab values, and imaging, will combine to form a comprehensive risk assessment. Initially, the risk assessment will help determine surgical readiness. However, in the coming years, it will evolve so that it is capable of providing recommendations for appropriate "pre-habilitation" to optimize the patient for surgery.

Intraoperative decision support will also start to slowly pervade the operating room. It will likely start with simple guidance, for example, to optimize laparoscopic port placement or help correlate preoperative imaging (such as tumor and major vasculature locations) with intraoperative displays. Work with *temporal-phase segmentation* will continue to build and begin to provide true operative guidance. Early implementations may offer a simple traffic light system, with a "green light" when dissection is going well, a "yellow light" when the surgeon is off course from a typical operation, and a "red light" when they are about to injure a vital structure. It will also offer a "phone-a-friend" functionality to connect to consultants for assistance. With continued development, this technology will ultimately develop into an intraoperative "GPS," guiding a surgeon through an operation step-by-step.

Postoperative decision support will include *early warning systems* to flag surgeons that a patient may have a certain complication. In the near future, integration of postoperative patient metrics with intraoperative video findings may lead to enhanced prediction that will predict not only that a complication may occur, but exactly the complication that will occur. Since these technologies will incorporate data from across hospitals and even countries, *their fund of knowledge will far exceed that of any surgeon and create a unified "collective surgical consciousness" that will provide the optimal care*.

Outside of decision-support systems, *automation* with underlying AI technology will also start to be incorporated into the operating room. It will start with automation of small tasks. For example, after recommending laparoscopic port placements, the machine may be able to dock a robotic-assisted surgery platform independently. Other small tasks may include fascial closure or anastomoses. Already, the Smart Tissue Autonomous Robot (STAR) can perform linear suturing and even autonomous sutured bowel anastomoses. In fact, its anastomoses can resist double the leak pressure compared to a human-sutured bowel anastomosis [37, 38]. In the coming years, the surgeon will perform the majority of the dissection, prepare the bowel, and then just press a "bowel anastomosis" button for a picture-perfect anastomosis constructed with optimal tension and precise bite-size throughout. In the more distant future, these incremental autonomous steps will combine until perhaps fully autonomous surgery is realized.

Challenges

AI promises a Cognitive Revolution, but with this revolution will come numerous hurdles and challenges. Without careful treatment, AI's progress may again derail, as it did in the 1980s, for a second coming of the AI Winter.

Ethics

AI and ML technologies present multiple ethical dilemmas. First is the issue of the "moral machine." The original "moral machine" problem asked a variety of questions to people across the world about autonomous driving scenarios, such as whether an autonomous vehicle should hit pedestrians to save the vehicle's passengers or swerve to avoid the pedestrian, thereby striking a barrier and killing the car's occupants. Answers depended on the scenario. For example, participants were more likely to favor saving the vehicle's occupants if they were younger than the pedestrian, or if the pedestrian was illegally crossing the street. *Interestingly, answers varied greatly across different world regions* [39]. Similar scenarios could arise as AI becomes pervasive in medicine. For example, will decision-support algorithms recommend against surgery for certain patients based upon their potential future societal contributions – or favor more aggressive treatment to wealthier patients? *AI model designers will need to provide algorithmic customization based on the locale's cultural norms and regularly work with communities to provide ethically acceptable decisions.*

A second ethical dilemma arises in the bias inherent to many AI algorithms. A recent analysis found one commercial prediction algorithm significantly under-triaged black patients compared to white patients due to use of healthcare costs as a surrogate for a patient's medical complexity. Since black patients had less access to more expensive treatment, their less-expensive care triaged them to an incorrect healthier risk strata [40]. *Training datasets need meticulous curation for fair representation of all patients; otherwise, algorithms unfairly trained may augment already present disparities* [41].

A third ethical dilemma comes from the training process for these models. ML model training is incredibly energy intensive, requiring powerful computers with hours to days of training time over multiple iterations before adequate model performance achievement. Since 2012, the amount of compute power used to train models has increased by 300,000-fold [42]. Training one model generates almost 80,000 pounds of carbon dioxide, which surpasses double the amount an average American produces annually [43]. *Development of these models must be done in an ordered and thoughtful fashion to minimize environmental repercussions.*

Privacy

AI and ML require big data, but big data raises numerous privacy issues. "De-identified" data should be anonymous; however, true "de-identification" is difficult, if not impossible. One researcher could link over 40% of newspaper stories regarding hospital admissions to "anonymized" public databases for hospital stays in the state of Washington [44]. In fact, based off gender, postal zip code, and date of birth (common information in "de-identified" datasets), 87% of United States' citizens are uniquely identified

[45]. Beyond issues with anonymity, many ML algorithms can make inferences about a patient to fill in missing data. As an example, some can infer smoking status (even if it is unknown) to help predict lung cancer risk. Future algorithms may be able to infer more sensitive information, such as HIV status, that the patient may not want known [46]. Other issues include ownership of data and patients' rights to withdraw their data and consent. Laws such as the European General Data Protection Regulation (GDPR) aim to protect the data rights of subjects. Concerted effort must be made to protect patients' privacy. One such solution may lie in split learning, where neural networks train across multiple data sources at different locations to prevent information leak from a central source [47].

Policy

To safely go forth and tackle the above issues, governmental and societal organizations must create sound policy. AI and ML algorithms continually "learn" and update, so regulatory agency approval and guarantee of safety may no longer apply after future training iterations. From a US perspective, the Food and Drug Administration (FDA) made a push in the early 2000s to classify software (smart phone application, stand-alone software, cloud-based solution) as a *medical device.* Congress then passed the 21st Century Cures Act as a response after software lobbying to remove many instances of software from the medical device list. Unfortunately, the Cures Act left a significant loophole for clinical decision support software, allowing it to be unregulated as long as it *intends* to explain to physicians its reasoning, even if this explanation is unsuccessful [48]. On the wings of this relative deregulation, the FDA has been approving increasing numbers of AI-related technologies and devices, from smart watches that can detect atrial fibrillation to algorithms that diagnose diabetic retinopathy [26]. Thus far, however, only "locked" algorithms (ones that will always return the same answer for a certain input) have been approved. The FDA recognized two main issues: first, the loophole and, second, the need for a framework that addressed evolving algorithms. As a response, they are working on a new regulatory framework [49]. As we march towards our AI future, concerted efforts, at the corporate, governmental, and societal level, must occur to ensure we proceed safely while still maximally benefiting from the new technology.

Annotations

The majority of the aforementioned algorithms represent *supervised learning,* where machines effectively learn from human-labeled examples. To teach a model surgical intraoperative phases, a surgeon will watch a video and label each phase, and then the algorithm will be given both the labels and the video and learn what constitutes each phase. *Learning requires immense amounts of data and a commensurate amount of labelling time.* Other areas solved this labelling problem through outsourcing, such as the "reCAPTCHA" tests seen online to ascertain whether a user is a human or computer. Ahn et al. used the reCAPTCHA tests to have regular Internet users transcribe over 440 million words from ancient texts with 99% accuracy [50]. Unfortunately for healthcare, the data is too complex for labelling by untrained annotators, so our annotation capabilities are severely limited by the relatively few expert annotators.

To solve the labor requirement, recent efforts have looked at streamlining the process. One group looked at pretraining models with unlabeled data to hopefully reduce the amount of required labelled data for accurate model training [51]. Others used a clever trick: they trained the model on a small number of videos and then used the model to auto-annotate further videos, achieving similar accuracy to models trained with four times the amount of data [52]. Future efforts will hopefully continue this "auto-annotation" process. The ML model's strength and ability to truly revolutionize surgery will require it to obtain superhuman knowledge and capabilities. Training with thousands to ultimately millions of videos from across the world will give it the collective experience of countless surgeons. A rare example seen in rural Canada could then prevent a complication the next day on the opposite side of the globe. *The sum of surgical experience will create a collective surgical consciousness greater than its individual parts.*

Surgical Training

The Cognitive Revolution that AI promises will require a different workforce in the future. Fewer physicians will be needed, particularly in fields that decision-support systems are well-suited to replacing (such as radiology and pathology). Automation will remove the need for physicians to do more quotidian tasks. Instead, the physician of the future will need more training in probability and statistical learning to accurately interpret algorithms that will assist their care. They will also need increased exposure to ethics to help morally apply these recommendations and computer science to understand the machinations providing them with daily assistance.

AI also promises to revolutionize surgical credentialing. The current process of regular written examinations fails to test actual surgical skills. With intraoperative ML models, surgeons in the future will be able to submit videos for recertification. If the video falls within a level of acceptable practice, they will then successfully recertify (of course, provided they also demonstrate aptitude in the management and care of the surgical patient). Similarly, when new procedures and technologies are introduced into surgical practice, the certification process will start first with intraoperative GPS guidance to train the surgeon, followed by automated video assessment to certify practice-ready performance.

Conclusion

We are at the start of the Cognitive Revolution driven by advancements in AI. The combination of big data, improved compute power, deep learning algorithms, and increased investment has led to an explosion in AI innovation and applications. Despite less than 10 years of innovation, AI models are matching, and often exceeding, human performance across all phases of patient care. This explosion brings with it numerous challenges, ranging from ethical dilemmas to privacy issues, which will require thoughtful and measured policies. The power of a collective surgical consciousness promises an exciting future and, more importantly, a safer future for patients.

References

1. Stevenson A, editor. Oxford dictionary of English. 3rd ed. New York: Oxford University Press; 2010.
2. Paul Thagard. Cognitive science. The Stanford Encyclopedia of Philosophy https://plato.stanford.edu/archives/spr2019/entries/cognitive-science/. Accessed 17 Dec 2019.
3. Tilney NL. Invasion of the body: revolutions in surgery. Cambridge: Harvard University Press; 2011.
4. Healey MA, Shackford SR, Osler TM, Rogers FB, Burns E. Complications in surgical patients. Arch Surg. 2002;137(5):611–8. https://doi.org/10.1001/archsurg.137.5.611.
5. Winston PH. Artificial intelligence. 3rd ed. Reading: Addison-Wesley Pub. Co; 1992.
6. Goertzel B, Pennachin C, editors. Artificial general intelligence. Berlin/New York: Springer; 2007.
7. Vinge V. The coming technological singularity: how to survive in the post-human era. 1993. http://hdl.handle.net/2060/19940022856.
8. McCulloch W, Pitts W. A logical calculus of the ideas immanent in nervous activity. Bull Math Biophys. 1943;5(4):115–33.
9. Russell SJ, Norvig P, Davis E. Artificial intelligence: a modern approach. 3rd ed. Upper Saddle River: Prentice Hall; 2010.
10. Samuel AL. Some studies in machine learning using the game of checkers. IBM J Res Dev. 1959;3(3):210–29.
11. Mccarthy J. Artificial intelligence: a paper symposium: professor sir James Lighthill, FRS. Artificial intelligence: a general survey. In: science research council, 1973. Artif Intell. 1974;5(3):317–22.
12. Crevier D. AI: the tumultuous history of the search for artificial intelligence. New York: Basic Books; 1993.
13. Simon HA, Munakata T. AI lessons. (Artificial intelligence; IBM's Deep Blue chess computer). Communicat ACM. 1997;40(8):23.
14. Schaeffer J, Burch N, Björnsson Y, et al. Checkers is solved. Science. 2007;317(5844):1518–22. https://www.jstor.org/stable/20037797. Accessed 29 Dec 2019.
15. Tromp J, Farnebäck G. Combinatorics of Go. In: van den Herik HJ, Ciancarini P, HHLM D, editors.

Computers and games. Lecture notes in computer science. Berlin, Heidelberg: Springer; 2007. p. 84–99. https://doi.org/10.1007/978-3-540-75538-8_8.
16. Sagiroglu S, Sinanc D. Big data: a review. In: 2013 International Conference on Collaboration Technologies and Systems (CTS); 2013. p. 42–7. https://doi.org/10.1109/CTS.2013.6567202.
17. Natarajan P, Frenzel JC, Smaltz DH. Demystifying big data and machine learning for healthcare. Boca Raton: CRC Press, Taylor & Francis Group; 2017.
18. Moore GE. Progress in Digital Integrated Electronics. In: International Electron Devices Meeting. Vol 21. Washington, DC; 1975:35–40.
19. Mittal S, Vaishay S. A survey of techniques for optimizing deep learning on GPUs. J Syst Archit. 2019;99.
20. Jouppi N, Young C, Patil N, Patterson D. Motivation for and evaluation of the first tensor processing unit. IEEE Micro. 2018;38(3):10–9. https://doi.org/10.1109/MM.2018.032271057.
21. Krizhevsky A, Sutskever I, Hinton GE. ImageNet Classification with Deep Convolutional Neural Networks. In: Pereira F, Burges CJC, Bottou L, Weinberger KQ, eds. Advances in Neural Information Processing Systems 25. Curran Associates, Inc.; 2012:1097–1105.
22. LeCun Y, Bengio Y, Hinton G. Deep learning. Nature. 2015;521(7553):436–44. https://doi.org/10.1038/nature14539.
23. Preparing for the Future of Artificial Intelligence. Executive Office of the President; 2016.
24. OECD. Private equity investment in artificial intelligence. 2018. www.oecd.org/going-digital/ai/private-equity-investment-in-artificial-intelligence.pdf.
25. Collier M, Fu R, Yin L, Christiansen P. Artificial intelligence: healthcare's new nervous system. Viewable at https://www.accenture.com/_acnmedia/pdf-49/accenture-health-artificial-intelligence.pdf.
26. Topol EJ. High-performance medicine: the convergence of human and artificial intelligence. Nat Med. 2019;25(1):44. https://doi.org/10.1038/s41591-018-0300-7.
27. Esteva A, Kuprel B, Novoa RA, et al. Dermatologist-level classification of skin cancer with deep neural networks. Nature, London. 2017;542(7639):115–8G. http://dx.doi.org.ezp-prod1.hul.harvard.edu/10.1038/nature21056
28. Bertsimas D, Dunn J, Velmahos GC, Kaafarani HMA. Surgical risk is not linear: derivation and validation of a novel, user-friendly, and machine-learning-based Predictive OpTimal Trees in Emergency Surgery Risk (POTTER) calculator. Ann Surg. 2018;268(4):574–83. https://doi.org/10.1097/SLA.0000000000002956.
29. Silber JH, Williams SV, Krakauer H, Schwartz JS. Hospital and patient characteristics associated with death after surgery. A study of adverse occurrence and failure to rescue. Med Care. 1992;30(7):615–29.
30. Ghaferi AA, Birkmeyer JD, Dimick JB. Complications, failure to rescue, and mortality with major inpatient surgery in medicare patients. Ann Surg. 2009;250(6):1029–34. https://doi.org/10.1097/SLA.0b013e3181bef697.
31. Rajkomar A, Oren E, Chen K, et al. Scalable and accurate deep learning with electronic health records. NPJ Digit Med. 2018;1(1):18. https://doi.org/10.1038/s41746-018-0029-1.
32. Soguero-Ruiz C, Fei WME, Jenssen R, et al. Data-driven temporal prediction of surgical site infection. AMIA Ann Symp Proc 2015;2015:1164–1173. https://www.ncbi.nlm.nih.gov/pmc/articles/PMC4765613/. Accessed 18 Feb 2019.
33. Twinanda AP, Shehata S, Mutter D, Marescaux J, de Mathelin M, Padoy N. EndoNet: a deep architecture for recognition tasks on laparoscopic videos. IEEE Trans Med Imaging. 2017;36(1):86–97. https://doi.org/10.1109/TMI.2016.2593957.
34. Hashimoto DA, Rosman G, Witkowski ER, et al. Computer vision analysis of intraoperative video: automated recognition of operative steps in laparoscopic sleeve gastrectomy. Ann Surg. 2019;270(3):414–21. https://doi.org/10.1097/SLA.0000000000003460.
35. Kitaguchi D, Takeshita N, Matsuzaki H, et al. Real-time automatic surgical phase recognition in laparoscopic sigmoidectomy using the convolutional neural network-based deep learning approach. Surg Endosc. 2019; https://doi.org/10.1007/s00464-019-07281-0.
36. Hung AJ, Chen J, Gill IS. Automated performance metrics and machine learning algorithms to measure surgeon performance and anticipate clinical outcomes in robotic surgery. JAMA Surg. 2018;153(8):770. https://doi.org/10.1001/jamasurg.2018.1512.
37. Leonard S, Wu KL, Kim Y, Krieger A, Kim PCW. Smart Tissue Anastomosis Robot (STAR): a vision-guided robotics system for laparoscopic suturing. IEEE Trans Biomed Eng. 2014;61(4):1305–17. https://doi.org/10.1109/TBME.2014.2302385.
38. Shademan A, Decker RS, Opfermann JD, Leonard S, Krieger A, Kim PCW. Supervised autonomous robotic soft tissue surgery. Science Translational Medicine. 2016;8(337):337ra64. https://doi.org/10.1126/scitranslmed.aad9398.
39. Awad E, Dsouza S, Kim R, et al. The moral machine experiment. Nature. 2018;563(7729):59–64. https://doi.org/10.1038/s41586-018-0637-6.
40. Obermeyer Z, Powers B, Vogeli C, Mullainathan S. Dissecting racial bias in an algorithm used to manage the health of populations. Science. 2019;366(6464):447–53. https://doi.org/10.1126/science.aax2342.
41. O'neil C. Weapons of math destruction: how big data increases inequality and threatens democracy. Broadway Books; 2016.
42. AI and Compute. OpenAI. 2018. https://openai.com/blog/ai-and-compute/. Accessed 30 Dec 2019.
43. Strubell E, Ganesh A, McCallum A. Energy and policy considerations for deep learning in NLP. arXiv:190602243 [cs]. 2019. http://arxiv.org/abs/1906.02243. Accessed 4 Sept 2019.

44. Sweeney L. Only you, your doctor, and many others may know. Technol Sci. 2015. /a/2015092903/. Accessed 12 Sept 2019.
45. Sweeney L. Simple demographics often identify people uniquely. Health (San Francisco). 2000;671:1–34.
46. Wiens J, Saria S, Sendak M, et al. Do no harm: a roadmap for responsible machine learning for health care. Nat Med. 2019;25(9):1337–40. https://doi.org/10.1038/s41591-019-0548-6.
47. Gupta O, Raskar R. Distributed learning of deep neural network over multiple agents. arXiv:181006060 [cs, stat]. 2018. http://arxiv.org/abs/1810.06060. Accessed 17 Sept 2019.
48. Evans B, Ossorio P. The challenge of regulating clinical decision support software after 21st century cures. Am J Law Med. 2018;44(2–3):237–51. https://doi.org/10.1177/0098858818789418.
49. Food US, Administration D, others. Proposed Regulatory Framework for Modifications to Artificial Intelligence. Machine learning (AI/ML)-based Software as a Medical Device (SaMD) discussion paper and request for feedback. Available at: https://www.fda.gov/media/122535/download. Accessed 12 June 2019.
50. von Ahn L, Maurer B, Mcmillen C, Abraham D, Blum M. reCAPTCHA: human-based character recognition via web security measures. Science. 2008;321(5895):1465–8. https://doi.org/10.1126/science.1160379.
51. Funke I, Jenke A, Mees ST, Weitz J, Speidel S, Bodenstedt S. Temporal coherence-based self-supervised learning for laparoscopic workflow analysis. In: Stoyanov D, Taylor Z, Sarikaya D, et al., eds. OR 2.0 context-aware operating theaters, computer assisted robotic endoscopy, clinical image-based procedures, and skin image analysis. Lecture notes in computer science. Springer International Publishing; 2018. p. 85–93.
52. Yu T, Mutter D, Marescaux J, Padoy N. Learning from a tiny dataset of manual annotations: a teacher/student approach for surgical phase recognition. arXiv:181200033 [cs, stat]. 2018. http://arxiv.org/abs/1812.00033. Accessed 11 Sept 2019.

The Vision of Digital Surgery

2

Bernhard Fuerst, Danyal M. Fer, David Herrmann, and Pablo Garcia Kilroy

The Need for a New Paradigm in Surgery

There are 310 million surgical procedures performed worldwide every year, with approximately 50 million complications (16%) and 1.4 million deaths (0.4%) [1, 2]. Some of these complications can be avoided because there is a high degree of variability in outcomes depending on the institution where the surgical procedure is performed and the level of experience the operating surgeon has [3, 4]. A fraction of these complications are attributed to poor information, lack of coordination, variation of physicians' patterns, and lack of accountability. The science of surgery is one of the most complex and therefore one of the least transparent and least understood. Digital surgery aims to bring a new level of scientific rigor and transparency to the field of surgery by providing tools that augment the surgeon and staff with better perception and judgment. With technological advances, we may harness the collective knowledge gathered over millions of procedures worldwide to provide the best choices for every patient. In this chapter, we will briefly outline the areas of opportunity in the operating room and the building blocks required to bring digital surgery into common practice. Some of the key areas of focus are as follows:

- Disrupting training
- Bringing transparency to the operating room
- Uncovering the breadth of factors that influence patient outcomes
- Managing technology complexity in patient care

Disrupting Surgical Training

The conventional, Halstedian paradigm of educating and training staff and surgeons has not significantly evolved over the decades. Surgical knowledge is transmitted through one-on-one training to communicate the knowledge and tools surgical teams utilize to carry out their tasks. These teaching methods are inefficient and

B. Fuerst (✉)
Applied Research, Verb Surgical, Inc., Santa Clara, CA, USA
e-mail: benfuerst@verbsurgical.com

D. M. Fer
Applied Research, Verb Surgical, Inc., Santa Clara, CA, USA

Department of Surgery, University of California San Francisco East Bay, Oakland, CA, USA

Laboratory for Automation Science and Engineering, University of California Berkeley, Berkeley, CA, USA

D. Herrmann
Marketing and Business Development, Verb Surgical, Inc., Santa Clara, CA, USA

P. G. Kilroy
Research and Digital Technologies, Verb Surgical, Inc., Santa Clara, CA, USA

S. Atallah (ed.), *Digital Surgery*, https://doi.org/10.1007/978-3-030-49100-0_2

limited, especially in the context of an increasingly complex disease science and patient treatments. In the United States, the average surgeon graduates from residency with thousands of hours of surgical training, by performing or assisting in a minimum of 850 operations [5]. A registered nurse, on average, trains approximately 4 years prior to beginning their careers. However, clinicians are tasked with taking care of patients with a unique set of medical issues. Even with extensive medical training, this remains an ongoing challenge and requires a sustained practice dynamic [6]. We still rely on paper documents, one-on-one case mentorship, scientific publications, and conferences to exchange the latest techniques and discuss future improvements. Robotic surgery has reduced the necessity of certain psychomotor skills for specific tasks (compared to laparoscopic techniques), and it has flattened the learning curve for the execution of minimally invasive surgical tasks. However, robotics has not expanded the decision-making capacity of surgeons, and training continues to follow the conventional paradigm of apprenticeship. Figure 2.1 illustrates a model for the adoption and progression from open to laparoscopic, to digital surgery, where robotics are simply a bridge from laparoscopy to digital. Through digital surgery, the surgical community has the opportunity to completely disrupt this conventional method of education and training; by building an ecosystem of knowledge with curated information to seamlessly foster the interactions, continued learning, and the desire to evolve surgical techniques.

Bringing Transparency to the Operating Room

Preoperatively and postoperatively, decisions are driven by objective data points guided by patient's overall clinical picture, through radiographic images, histologic pathology, and/or hematologic tests. In contrast, intraoperative data is limited to anesthesia reports, blood loss estimations, fluid balance metrics, and generic operative reports. The majority of the critical information from an operation is unstructured and not captured in a way that can be analyzed. As a consequence, there is no established way to quantify events critical to a patient's care in a way that can be compared across institutions. Data is limited due to the subjective nature of documentation and lack of standardization of the actions taken by the surgeon. The variety of interventions has become increasingly complex and surgeons are mostly constrained to their own experience. There is no objective and systematic feedback system.

Performance improvement relies on self-reflection and self-motivation. Discussions pertaining to the best possible techniques for surgeons to implement are only brought to light at departmental morbidity and mortality conferences, in written publications, or at medical and surgical congresses. Only minimal data from the

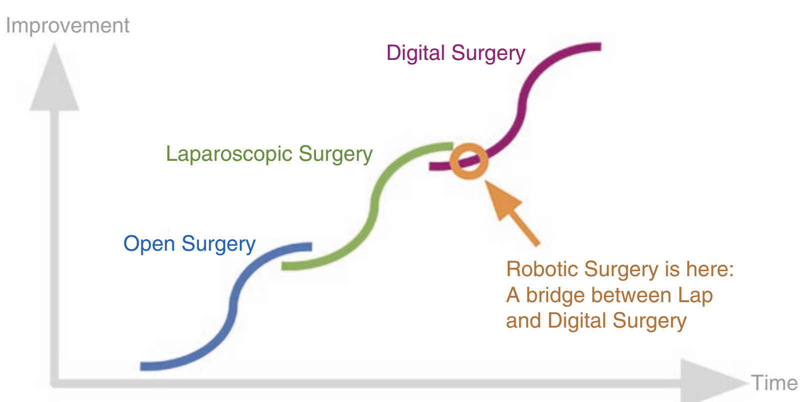

Fig. 2.1 The S-curve of surgery shows the progress from open and laparoscopic techniques to digital surgery

operating room is provided in such discourse, and propagation of information to all surgeons experiencing the same difficulties therefore remains extremely limited.

There is an opportunity to bring a new level of granularity and transparency to the data collected during procedures and to make it accessible to the surgical community in real time. Analytics tools can filter key information relevant to the success of the procedure, so that the practicing surgical community can learn from such educational opportunities and make better decisions in future procedures.

While this data is critical, it is also extremely sensitive which creates significant (yet appropriate) barriers to access. Due to the sensitivity of the data involved (patient demographics and personal data, data pertaining to the planning and execution of surgical procedures, etc.), as well as the sources from which the data is obtained (electronic medical records, surgical video, and other digital imaging), it is expected that a single surgical procedure could generate hundreds of gigabytes of data triggering multiple legal, regulatory, and technical requirements to protect the confidentiality, integrity, and authenticity of the data. One design approach is to de-identify personal information as much as possible before transfer of data from the on-site medical device to an off-site cloud storage system. By reducing the level of identifiability of information, there is a reduced risk to the compromise of patient privacy and inadvertent patient harm.

To bring transparency to the OR and optimize critical decisions, the surgical community will need to drive the creation of data sets which can be mined to uncover disruptive insights and thereby improve the global delivery of surgical care.

Uncovering Breadth of Factors That Influence Patient Outcomes

Successful outcomes are dependent on a complex combination of factors, including the type of surgical procedure, surgeon proficiency, and patient and disease factors [7–10]. An optimum treatment plan should take all these factors into account and ultimately recommend the steps required for the specific patient being treated. Currently, these factors are often analyzed in isolation and they are focused on minimizing mortality and morbidity risks, but not on maximizing the chances of success for the intervention. In bariatric surgery, patients are assessed for risk of stroke and myocardial infarction [11, 12], but predicting the chance of success of any given surgery remains elusive [13]. There is a need for analytical models which take into account a broad number of factors and determine the best course of action based on a cost/benefit calculation [14, 15].

Part of the reason these models are not pursued is because they would involve very complex, lengthy, and costly clinical studies to analyze the correlation between highly heterogeneous variables and outcomes. The only practical way of determining these correlations and causations is to regularly collect relevant data points on a very large number of patients to produce statistically significant results. Ubiquitous sensing technologies, scalable data collection infrastructure, and powerful machine learning analytics tools will enable conducting these studies routinely, as part of continuous quality improvement programs in healthcare systems. As a result, our understanding of how to treat disease in a way that is optimized and personalized for a specific patient will grow exponentially.

Addressing Complexity in the Operation Room

Technology has improved industry and academics alike. By 2020, we have witnessed the introduction of increasingly complex systems into the operating room. Introduction of these new technologies has led to increased operative times (by impacting workflow), increased staff learning curves, crowding of the operating room, and encroaching on surgeon workspace [16–22]. Even the integration of electronic medical records has resulted in an increase of documentation demands which is a source of ongoing frustration for surgeons and operating room staff. New technologies often “stand alone” and function in an independent ecosystem. This makes the decisions on which technologies to employ to be burdensome for various stakeholders in any given surgical service, as it is difficult to integrate such tools so as to render the best possible operation in every instance. The steep learning curves, large physical footprints, and the often high price tags make incorporating potentially lifesaving technologies difficult for healthcare systems. There is a need to manage the complexity without burdening the clinical staff. A more intelligent device connectivity inside and outside the operating room will enable utilization of the information generated in a more efficient and effective way. It will also increase the level of satisfaction of the clinical and surgical teams by allowing them to focus on the care of the patient—as opposed to maintaining and caring for demanding technology applications.

The Objective of Digital Surgery

The ultimate goal for the new digital surgical technologies is to improve the efficiency of treatment rendered by surgeons, thereby improving clinical outcomes for patients. By delivering care more efficiently, surgical care will become more accessible to a larger number of patients worldwide. By harnessing data, optimizing best practices, and mentoring surgeons on how to deliver quality care consistently, digital surgery will reduce the variability of outcomes and identify the key factors to improve them.

Digital surgery is the third wave of surgical innovation, with open and laparoscopic surgery preceding it. It will help the surgeon to better understand the best way to manage surgical problems, to interpret a complex surgical environment, and to effectively manage the surgical team. Digital surgery will help staff to better understand the needs of the surgeon and the operative team, so as to provide more effective and efficient care to patients. It will aid in educating all participants on how to best fulfill their role and provide effective feedback for continuous improvement. It will help administrators to have a more comprehensive insight into what happens in the operating room so they can best manage resources. Digital surgery will leverage connected intelligence to deliver enhanced experiences and outcomes for patients, surgeons, and the healthcare system (Fig. 2.2). With access to this information, it can be most effectively utilized to enhance communication between all parties, reducing the overall stress of the team and even burnout. Most importantly, it will directly help patients. Their care will be provided with better quality and at a lower cost.

To realize the vision for digital surgery, the following steps are required:

- Establish an infrastructure to collect all appropriate patient and procedure-related data in

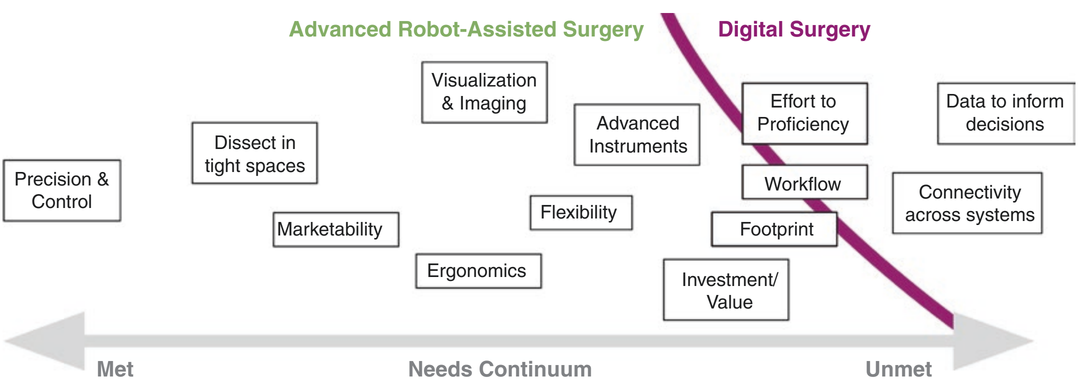

Fig. 2.2 Some unmet needs across the continuum of needs will be met through the introduction of digital surgery

order to inform the clinician and staff at the right time.
- Build and provide access to a global ecosystem of surgical knowledge.
- Build tools to autonomously filter and curate relevant data in the ecosystem of knowledge to present to the clinician and surgeons.
- Grant seamless access to information and knowledge, which can be expected to result in reproducible and consistent outcomes throughout the surgical community.
- Systematically generate objective data to improve efficiency, effectiveness, and outcomes.

This new paradigm of digital surgery requires the shift from components and devices to a unified platform and ecosystem to analyze procedures and train surgeons and clinical teams. It will require a cultural change in the way new surgeons are trained, clinicians continue to educate themselves, complications and difficulties are discussed, and how clinical data can be shared.

The Five Pillars of Digital Surgery

As illustrated in the previous section, five critical pillars have been identified (Fig. 2.3) to enable an intelligent and connected surgical system that can provide safer and efficacious surgery. Each of these is core to the foundation of digital surgery and will be detailed herein.

Surgical Robotics

Surgical robotics systems have already shown the capability to improve dexterity and increase the penetration of minimally invasive techniques for complex operations. Future systems will support the surgeons by executing assist tasks, such as acquisition of medical images which are reproducible, performing specific subtask autonomously, or establishing virtual boundaries [23–26].

Advanced Instrumentation

Instrumentation is a key enabling component in many procedures, and the standardization of instrumentation allows for an easier transfer of knowledge between surgeons (Fig. 2.4). New instruments will not only include advanced energy, suturing, or stapling functions, but also a variety of sensors to analyze and optimize tissue interactions.

Enhanced Visualization

The success of any surgery is dependent on the clear visualization of critical structures and target anatomy. Surgeons and assistants need to locate or avoid critical structures. Better visualization will require the combination of conventional imaging, novel imaging techniques, and machine

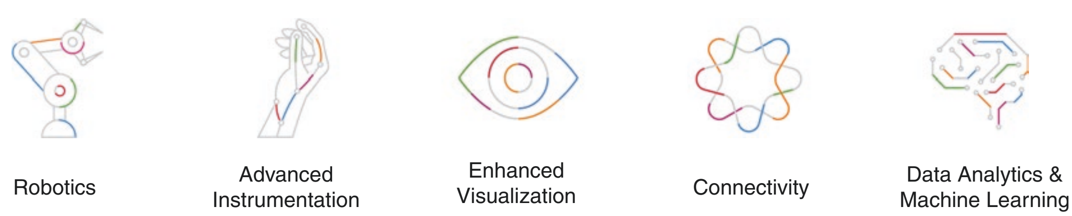

Fig. 2.3 The five pillars of digital surgery: (1) robotics, (2) advanced instrumentation, (3) enhanced visualization, (4) connectivity, and (5) data analytics and machine learning. Digital surgery can be viewed as an amalgam of advanced technologies that span all surgical approaches, leveraging robotics, enhanced visualization, advanced instrumentation, connectivity, and artificial intelligence to deliver exceptional outcomes for patients, surgeons, and the broader healthcare system. Such a platform is intended to connect the benefits and technology of these five pillars

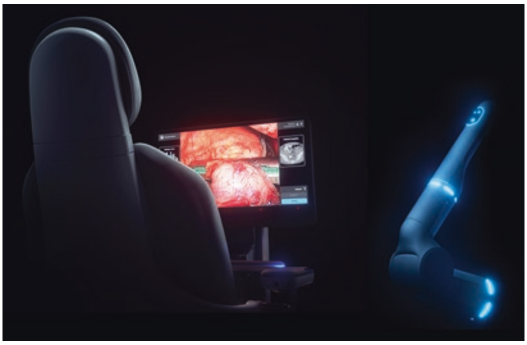

Fig. 2.4 The surgeon's command center is fully connected and enables direct access to medical imaging, analytics, and teleoperation with advanced instrumentation

learning algorithms to enhance what the surgeon perceives from the operative field. In addition, a modern digital surgery platform needs to be capable of connecting and incorporating other imaging sources and to allow for the seamless and transparent fusion of imaging [27–29]. Novel imaging techniques, such as intraoperative SPECT imaging [30], can guide the surgeon towards deeply seated structures and other anatomic targets which require a complex approach, while machine learning algorithms can extract information from imaging and other datasets [31, 32].

Connectivity

It is vital for all systems and devices in the operating room and hospital to be able to communicate with a central gateway, logging all events and data points. Once all local signals are synchronized and collected, information can, in real time, be extracted and studied [33]. In terms of this paradigm shift, a single device standing somewhere inside the operating room is perhaps not the best model. Instead, there should exist a gateway which enables the true connectivity of the digital platform. Digital surgery is not comprised of a single technology or tool and goes beyond a simple collection of data streams available in the operating room. Connectivity will enable the construction of a virtual platform of anonymized data to enable an entire ecosystem.

Data Analytics

Analytics will turn data into actionable insights by extracting information, curating knowledge, and providing it to all surgeons, staff members, and patients. For digital surgery, this is the most complex and difficult building block to create. The variability of processes, patients and anatomy, and surgical techniques presents a challenge at a scale never before experienced and should not be addressed by a singular entity. Given that the conventional dataset currently obtained from operative records have been limited, formatting the data for the age of digital surgery provides significant opportunity as well as challenge, as the breadth of data which may be captured can be vast. Importantly, this information will not be confined to the operating room; data structures will be required to easily incorporate preoperative and postoperative data to seamlessly integrate the data from a patient's care experience. Through this integration, validation of the utility of the digitization of the patient's experience may be achieved through objective demonstration of improved cost and outcomes. This data can then be leveraged to iterate on continuous improvement in patient care.

The Virtuous Cycle (Fig. 2.5)

Digital surgery provides the substrate to inform the continuum of sustained deliberate practice in surgery. Prior to a given operation, the surgeon will have access to the datasets which identify anatomic areas of caution, areas for improvement, and areas of focus (such as the target organ or tumor of interest). Critical anatomy and steps may be identified and the practitioner can quickly access globally recognized best practices, as well as data unique to a given institution. This allows for rapid preparation of all parties involved in patient care.

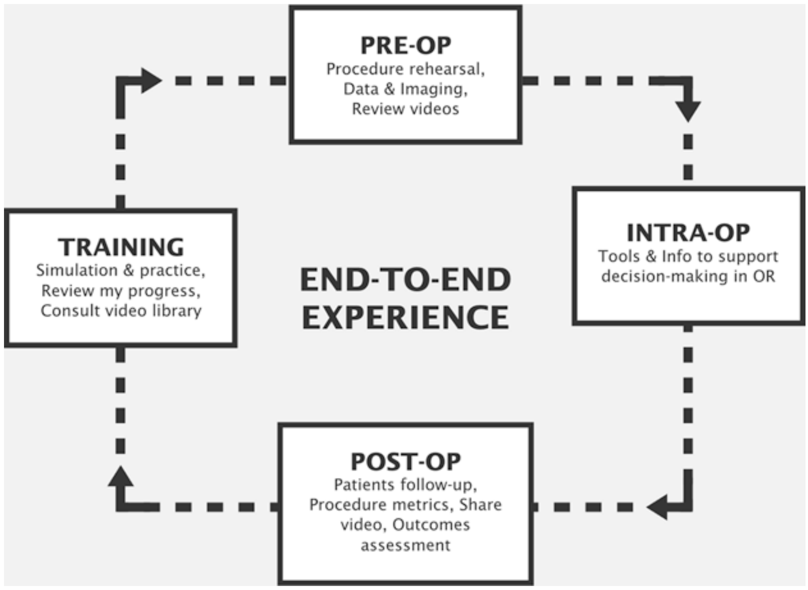

Fig. 2.5 The virtuous cycle of digital surgery

Once in the operating room, data can be used to provide guidance to practitioners and teams in real time to understand what tools are needed, what critical anatomy is exposed, which step of the procedure is being performed, and how much progress is being made towards the completion of a given surgical task. The goal is to enable a real-time mentor into the OR which can provide guidance on the optimum path to follow and the pitfalls to avoid.

Postoperative critical areas of improvement may be identified and clinically relevant information can be uploaded into the EHR so as to provide guidance in postoperative care. A complete postoperative report can be used to further evaluate and optimize the decisions taken in the operating room.

This data then further informs trainees, providing constructive feedback and specific guidance. Moreover, these data can direct training and simulation allowing for surgeons to practice complex clinical situations and surgical scenarios without exposing the patients to risk. Such a digital platform would also allow surgeons to learn from other's operative errors, so that patient harm can be limited globally and so that surgeon education can be enhanced. This continuum of persistent improvement will both drive innovation based on clinical outcomes and also help in standardization of surgical practice.

Transforming Data into Insights Through Artificial Intelligence

Advances in computational power, near limitless data storage capacity, and robotics have now enabled a surgical revolution that seeks to apply the successes of big data and the reproducibility of modern engineering to the relative subjectivity of surgery. This process entails the cataloguing of surgical events, seemingly obvious to a human user. The immediate goal is to have a computer recognize and describe scenes immediately apparent to the average surgeon. By aggregating thousands of procedures, we will eventually be able to reveal trends and events that clinicians are not capable of recognizing on their own.

This mass cataloguing of data requires a series of novel tools in order to filter the information collected and effectively maximize the signal-to-noise ratio. The commonly utilized subfields of artificial intelligence which may be leveraged in surgery involve machine learning, neural networks, natural language processing, and computer vision. These technologies allow for the development of complex statistical models to automatically recognize and categorize specific events and features of a surgical procedure [34] based on a variety of sensors, such as video, audio, imaging, encoders, vital signs, etc.

To autonomously recognize events and features in the operating room environment, an objective language to describe surgery is required. Computers must be able to describe what task is being done, the target anatomy, the tools being used, how the task is being performed, and why it is performed. Early work on classifying the tasks within an operation began in earnest with the classification of the basic building blocks of surgery; these were identified within an operation with impressive accuracy [35–37]. There has also been significant work on recognition and tracking tools and anatomy [37, 38]. These solutions to automatically segment an operation are the basis for providing automated and specific feedback to the surgeon.

Based on the machine language to describe surgery, computers can generate metrics to improve surgical education, performance, and efficiency. It is therefore critical that members of the community generate the definitions of machine learning targets in collaboration [39] and reach consensus on the ontology of how we describe surgery [36]. Early work has begun in this area of surgical description and digital surgery will apply these principles utilizing machine learning to automatically categorize surgical insights of individual and groups of surgeons [39, 40] (Fig. 2.6).

The analysis of surgical video in particular has the potential to both bring transparency to the operating room [41, 42] and to accelerate learning of surgeons [43, 44]. Through video analysis, critical difference between surgeons performing operations has demonstrated significant technique variances, which, when analyzed and implemented, can lead to better outcomes [45, 46]. These tools can potentially provide targeted and specific feedback to training surgeons in the context of a busy clinical setting when time is scarce.

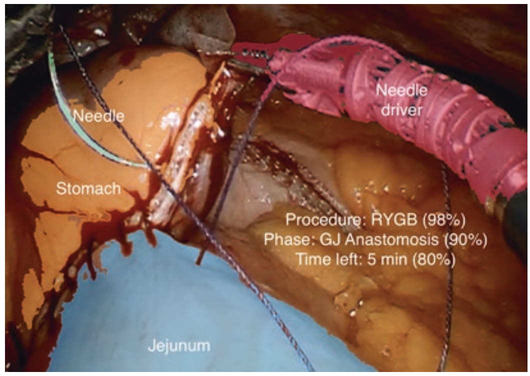

Fig. 2.6 Machine learning provides a powerful tool to automatically recognize and curate the critical components of a given operation. Agreement on the language in which these components are described is critical

Artificial intelligence is already an essential tool for assisting practitioners in the pathological and radiologic fields [47]. In the operating room, the majority of solutions remains under research and development, or are heavily reliant on in-depth manual analysis of large data sets. Part of the reason for this is that there are significant investments required for operating room infrastructures to accommodate, store, and analyze data in a secure setting. This limits the development of new algorithms and their deployment at scale. Therefore, it is important to support innovation by giving researchers and clinicians access to basic tools to accelerate algorithm development and provide a means to scale some of the technologies which promise benefit.

The Future Life as a Digital Surgeon

In the not too distant future, a day in the life of a digital surgeon begins like most days. She/he uses a computer or mobile device to access a secure clinical portal where a list of the scheduled operative cases can be viewed. Details on the required and recommended instruments are instantaneously available and are shared with the operating room staff to avoid delays. Through the portal, the surgeon can directly access an ecosystem of knowledge. Utilizing extensive machine learning algorithms [48, 49], detailed feedback on the performance during past cases is provided. Furthermore, curated information is presented to highlight the procedure steps and techniques which are most critical and which are known to impact outcome. This information can be shared with surgical assistants, residents, or other OR team members. Finally, for the most complex cases, surgeons can elicit help through their local, regional, or global community to improve their technique and efficiency. The digital surgeon is able to directly dialogue with experienced colleagues for telementoring and for technical advice. One can envision that under this framework, a surgeon could invite a remote mentor to virtually participate in the procedure. Digital mentorship provides a critical portion of next-generation platforms; through a combination of automated and manual tools, surgical knowledge from an expert of how to perform a specific technique will provide directed feedback to allow surgeons to quickly adapt the techniques that are both the most efficient and that provide the greatest probability for the best patient outcomes. Furthermore, all OR team members will have had the opportunity for immersive training utilizing augmented and virtual reality under such a framework [50–52]. The training is personalized and aims to support each individual role. Prior to entering the operating room, new members are trained through a surgeon, a team, a procedure, and/or an OR-specific experience. This information and guidance are transferred into the OR, where visual and auditory feedback assists all stakeholders throughout the pre-, intra-, and postoperative phases of any given procedure [53]. Specialized mobile or augmented reality devices will enable direct visualization of tasks, provide discrete and role-specific alerts, and augment the users' view if necessary [54, 55]. This will ensure the efficient utilization of the operating room and will limit frustration and psychological strain within teams by eliminating communication barriers.

Artificial intelligence-powered case setup will eliminate idle time, allowing for the robotic platform and surgeon console to be ready and supportive of the team's tasks. This streamlines the operative process and further eliminates frustration, when a digital surgical platform is utilized.

With an efficient operative workflow, the critical tasks of surgery transpire seamlessly, without distraction. Digital surgery will not just provide the dexterity of a robotic systems, but it will also provide decision-making support for surgeons, translating into optimal care for patients. This support commences when the surgeon accessed the ecosystem of knowledge prior to the surgery and extends into the operating room during the procedure. The surgeon and operative staff actions will be recognized by the system to ensure all team members are aware of the steps of the procedure. In a proposed design, the system unobtrusively notifies the surgeon (and all team members) of next steps during the operation; the system can also be designed to more actively alert surgeons prior to the commencement of the most critical steps, which correlate with the highest impact on outcomes. This information should also be available to the OR staff, allowing for an uninterrupted execution of the procedure, smooth exchange of instrumentation, and clear guidance on other assisting tasks. Extending outside the operating room, the digital surgery platform can communicate the progress of the procedure, allowing for materials or services to be ordered, ultimately meeting patient care demands in an efficient manner. This comprehensive situational awareness will allow for better coordination of preoperative and recovery rooms as well.

Within the confines of the operating theater, the surgeon can focus exclusively on the procedure at hand, using advanced instruments to delicately handle tissue and perform precise dissections. In digital surgery, advanced controls will expand the dexterity of the human hand and will leverage the entire range of motion of the robotic system and robotic instruments. Furthermore, a surgeon will have the option to allow the computer-centric system to cooperatively control instruments, ensuring that critical structures are avoided and a virtual boundary is enforced [56–58], or even allow the system to perform subtasks on its own [59–63]. These technologies in combination with the growing knowledge generated through the deconstruction of surgical tasks will allow the surgeon to not just rely on themselves, but they will have access to a global ecosystem of knowledge and the collective wealth of surgeon experience it will entail. Such a global ecosystem may provide automated suggestions based upon the techniques of a "digital mentor," or may even be more specific with intraoperative, live telementoring.

During critical operative steps, the platform of digital surgery will provide surgeons with imaging technologies which can be accessed in real time and can thereby provide invaluable information relevant to critical structure identification. These include advanced multi- and hyperspectral optical imaging, enhanced ultrasound imaging with tissue characterization, and preoperative imaging modalities. This information can be further overlaid and integrated into the surgical view [64, 65]. In addition, this information can also be presented to the team at bedside to provide an additional level of safety and guidance to achieve the end goal of optimal patient care.

Postoperative metrics will be generated to allow the surgeon to advance along her/his proficiency-gain curve. This information can be shared with peers and experts for more specific feedback and for learning from the global surgical community. The creation of these metrics through the global community will provide a common language for information to be shared between surgeons which will lead to standardization of surgical procedures as the most efficient and highest-quality techniques are elicited through leveraging the surgical community's collective knowledge. These analytics will allow for curated content to be directed to the surgeon so they may understand the highest-yield segments in their own technique for improvement.

In sum, the digital surgeon's day promises a dramatic reduction in frustration that can currently be associated with the disconnected operating theater. Targeting information to key stakeholders will ultimately improve the efficiency of the operating room and empower the surgeon to focus on the delivery of optimum patient care in the operative and perioperative setting.

The Path Forward

As a surgical community, we are striving to make digital surgery a reality. A key hurdle towards the integrated future of digital surgery is the creation of a core, centralized data repository. Another important challenge involves resolving the "disconnected nature" of the operating room. The status quo of the latter and a lack on a unified standard results in the friction of adoption and leaves nonlinked components (such as standalone robotic platforms) isolated from the global ecosystem fundamental to the vision of digital surgery. It also limits the opportunity for iterative improvement and the design and ability of the artificial intelligence behind it. Many of the tools that can contribute to digital surgery are isolated to research institutions and small entities. To meaningfully implement these technologies and to democratize surgery, a venue for these tools to be integrated into the operating room must be developed.

The path forward requires the establishment of a virtual platform which is able to integrate the multitude of surgical systems and robotic tools commonly used today. It is inefficient and unrealistic to expect each component to exist separately, disconnected from the other data streams in the operating room and hospital settings. The goal is to not only integrate these data streams, but also to be discerning and clear-sighted as to how data is presented to practitioners and administrators. High-yield data with a great opportunity to improve outcomes should not be overlooked, and information overload needs to be avoided.

Establishing a critical infrastructure to allow for seamless integration of robotics, AI, advanced instrumentation, advanced training modalities, and educational programs will allow for rapid innovation and lowering of barriers of entry. In this manner and under the framework of digital surgery outlined herein, the global delivery of advanced surgical care will continue to improve.

References

1. Meara JG, Leather AJ, Hagander L, Alkire BC, Alonso N, Ameh EA, et al. Global surgery 2030: evidence and solutions for achieving health, welfare, and economic development. Lancet. 2015;386(9993):569–624.
2. International Surgical Outcomes Study group. Global patient outcomes after elective surgery: prospective cohort study in 27 low-, middle-and high-income countries. BJA Br J Anaesth. 2016;117(5):601–9.
3. Ely S, Rothenberg KA, Gologorsky RC, Dominguez DA, Chang C, Velotta JB. Differences in NSQIP esophagectomy outcomes by surgeon specialty. J Am Coll Surg. 2019;229(4):S276.
4. Ho V, Heslin MJ. Effect of hospital volume and experience on inhospital mortality for pancreaticoduodenectomy. Ann Surg. 2003;237(4):509.
5. ©2019 Accreditation Council for Graduate Medical Education (ACGME). Defined category minimum numbers for general surgery residents and credit role review committee for surgery. 2019 (Accessed: 2019-10-10). Available at https://www.acgme.org/Portals/0/DefinedCategoryMinimumNumbersforGeneralSurgeryResidentsandCreditRole.pdf.
6. Collins JW, Levy J, Stefanidis D, Gallagher A, Coleman M, Cecil T, et al. Utilising the Delphi process to develop a proficiency-based progression train-the-trainer course for robotic surgery training. Eur Urol. 2019;75(5):775–85.
7. Ficarra V, Novara G, Rosen RC, Artibani W, Carroll PR, Costello A, et al. Systematic review and meta-analysis of studies reporting urinary continence recovery after robot-assisted radical prostatectomy. Eur Urol. 2012;62(3):405–17.
8. Davenport DL, Henderson WG, Khuri SF, Mentzer RM Jr. Preoperative risk factors and surgical complexity are more predictive of costs than postoperative complications: a case study using the National Surgical Quality Improvement Program (NSQIP) database. Ann Surg. 2005;242(4):463.
9. Sereysky J, Parsikia A, Stone M, Castaldi M, McNelis J. Predictive factors for the development of surgical site infection in adults undergoing initial open inguinal hernia repair. Hernia. 2019; https://doi.org/10.1007/s10029-019-02050-3.
10. Matikainen M, Aro E, Vironen J, Kossi J, Hulmi T, Silvasti S, et al. Factors predicting chronic pain after open inguinal hernia repair: a regression analysis of randomized trial comparing three different meshes with three fixation methods (FinnMesh Study). Hernia. 2018;22(5):813–8.
11. Quilliot D, Sirveaux MA, Nomine-Criqui C, Fouquet T, Reibel N, Brunaud L. Evaluation of risk factors for complications after bariatric surgery. J Visc Surg. 2018;155(3):201–10.
12. Mechanick JI, Youdim A, Jones DB, Garvey WT, Hurley DL, McMahon MM, et al. Clinical practice guidelines for the perioperative nutritional, metabolic, and nonsurgical support of the bariatric surgery patient—2013 update: cosponsored by American Association of Clinical Endocrinologists, the Obesity Society, and American Society for Metabolic & Bariatric Surgery. Obesity. 2013;21(S1):S1–S27.
13. King WC, Hinerman AS, Belle SH, Wahed AS, Courcoulas AP. Comparison of the performance of common measures of weight regain after bariatric surgery for association with clinical outcomes. JAMA. 2018;320(15):1560–9.
14. Lindmark M, Strigard K, Lowenmark T, Dahlstrand U, Gunnarsson U. Risk factors for surgical complications in ventral hernia repair. World J Surg. 2018;42(11):3528–36.
15. Kim E, Kang JS, Han Y, Kim H, Kwon W, Kim JR, et al. Influence of preoperative nutritional status on clinical outcomes after pancreatoduodenectomy. HPB. 2018;20(11):1051–61.
16. Van Dam P, Hauspy J, Verkinderen L, Trinh XB, Van Dam PJ, Van Looy L, et al. Are costs of robot-assisted surgery warranted for gynecological procedures? Obstet Gynecol Int. 2011;2011:973830.
17. Lotan Y. Is robotic surgery cost-effective: no. Curr Opin Urol. 2012;22(1):66–9.
18. Anderberg M, Kockum CC, Arnbjornsson E. Paediatric robotic surgery in clinical practice: a cost analysis. Eur J Pediatr Surg. 2009;19(05):311–5.
19. Baek SJ, Kim SH, Cho JS, Shin JW, Kim J. Robotic versus conventional laparoscopic surgery for rectal cancer: a cost analysis from a single institute in Korea. World J Surg. 2012;36(11):2722–9.
20. Bertani E, Chiappa A, Biffi R, Bianchi PP, Radice D, Branchi V, et al. Assessing appropriateness for elective colorectal cancer surgery: clinical, oncological, and quality-of-life short-term outcomes employing different treatment approaches. Int J Color Dis. 2011;26(10):1317.
21. Bodner J, Kafka-Ritsch R, Lucciarini P, Fish JH III, Schmid T. A critical comparison of robotic versus conventional laparoscopic splenectomies. World J Surg. 2005;29(8):982–5.
22. Breitenstein S, Nocito A, Puhan M, Held U, Weber M, Clavien PA. Robotic-assisted versus laparoscopic cholecystectomy: outcome and cost analyses of a case-matched control study. Ann Surg. 2008;247(6):987–93.
23. Navab N, Hennersperger C, Frisch B, Fuerst B. Personalized, relevance- based multimodal robotic imaging and augmented reality for computer assisted interventions. Med Image Anal. 2016;33:64–71.
24. Fuerst B. Multi-modal registration and robotic imaging for computer assisted surgery. Munich, Germany: Technische Universitat Munchen; 2016.

25. Hennersperger C, Fuerst B, Virga S, Zettinig O, Frisch B, Neff T, et al. Towards MRI-based autonomous robotic US acquisitions: a first feasibility study. IEEE Trans Med Imaging. 2016;36(2):538–48.
26. Kojcev R, Khakzar A, Fuerst B, Zettinig O, Fahkry C, DeJong R, et al. On the reproducibility of expert-operated and robotic ultrasound acquisitions. Int J Comput Assist Radiol Surg. 2017;12(6):1003–11.
27. Fuerst B, Wein W, Muller M, Navab N. Automatic ultrasound–MRI registration for neurosurgery using the 2D and 3D LC2 metric. Med Image Anal. 2014;18(8):1312–9.
28. Fuerst B, Fotouhi J, Lee SC, Fischer M, Kojcev R, Navab N, et al. Can intraoperative ultrasound assist transoral robotic surgery? In: Hopkins imaging conference. Baltimore, MD, USA: Hopkins Imaging Initiative; 2015.
29. Zettinig O, Fuerst B, Kojcev R, Esposito M, Salehi M, Wein W, et al. Toward real-time 3D ultrasound registration-based visual servoing for interventional navigation. In: 2016 IEEE International Conference on Robotics and Automation (ICRA). Montreal, Canada: IEEE; 2016. p. 945–50.
30. Fuerst B, Sprung J, Pinto F, Frisch B, Wendler T, Simon H, et al. First robotic SPECT for minimally invasive sentinel lymph node mapping. IEEE Trans Med Imaging. 2016;35(3):830–8.
31. Barker J, Hoogi A, Depeursinge A, Rubin DL. Automated classification of brain tumor type in whole-slide digital pathology images using local representative tiles. Med Image Anal. 2016;30:60–71.
32. Milletari F, Navab N, Ahmadi SA. V-net: Fully convolutional neural networks for volumetric medical image segmentation. In: 2016 Fourth international conference on 3D Vision (3DV). Los Alamitos, CA, USA: IEEE; 2016. p. 565–71.
33. Ahmadi SA, Sielhorst T, Stauder R, Horn M, Feussner H, Navab N. Recovery of surgical workflow without explicit models. In: International conference on medical image computing and computer-assisted intervention. Copenhagen, Denmark: Springer; 2006. p. 420–28.
34. Hashimoto DA, Rosman G, Rus D, Meireles OR. Artificial intelligence in surgery: promises and perils. Ann Surg. 2018;268(1):70–6.
35. Yu F, Croso GS, Kim TS, Song Z, Parker F, Hager GD, et al. Assessment of automated identification of phases in videos of cataract surgery using machine learning and deep learning techniques. JAMA Netw Open. 2019;2(4):e191860.
36. Hashimoto DA, Rosman G, Witkowski ER, Stafford C, Navarette-Welton AJ, Rattner DW, et al. Computer vision analysis of intraoperative video: automated recognition of operative steps in laparoscopic sleeve gastrectomy. Ann Surg. 2019;270(3):414–21.
37. Twinanda AP, Shehata S, Mutter D, Marescaux J, De Mathelin M, Padoy N. Endonet: a deep architecture for recognition tasks on laparoscopic videos. IEEE Trans Med Imaging. 2016;36(1):86–97.
38. Meeuwsen F, van Luyn F, Blikkendaal MD, Jansen F, van den Dobbelsteen J. Surgical phase modelling in minimal invasive surgery. Surg Endosc. 2019;33(5):1426–32.
39. Katic D, Julliard C, Wekerle AL, Kenngott H, Muller-Stich BP, Dillmann R, et al. LapOntoSPM: an ontology for laparoscopic surgeries and its application to surgical phase recognition. Int J Comput Assist Radiol Surg. 2015;10(9):1427–34.
40. Hashimoto DA, Axelsson CG, Jones CB, Phitayakorn R, Petrusa E, McKinley SK, et al. Surgical procedural map scoring for decision-making in laparoscopic cholecystectomy. Am J Surg. 2019;217(2):356–61.
41. Dimick JB, Scott JW. A video is worth a thousand operative notes. JAMA Surg. 2019;154(5): 389–90.
42. Langerman A, Grantcharov TP. Are we ready for our close-up? Why and how we must embrace video in the OR. Ann Surg. 2017;266(6):934–6.
43. Soucisse ML, Boulva K, Sideris L, Drolet P, Morin M, Dube P. Video coaching as an efficient teaching method for surgical residents—a randomized controlled trial. J Surg Educ. 2017;74(2):365–71.
44. Rindos NB, Wroble-Biglan M, Ecker A, Lee TT, Donnellan NM. Impact of video coaching on gynecologic resident laparoscopic suturing: a randomized controlled trial. J Minim Invasive Gynecol. 2017;24(3):426–31.
45. Hung AJ, Chen J, Ghodoussipour S, Oh PJ, Liu Z, Nguyen J, et al. A deep- learning model using automated performance metrics and clinical features to predict urinary continence recovery after robot-assisted radical prostatectomy. BJU Int. 2019;124(3):487–95.
46. Scally CP, Varban OA, Carlin AM, Birkmeyer JD, Dimick JB. Video ratings of surgical skill and late outcomes of bariatric surgery. JAMA Surg. 2016;151(6):e160428.
47. Fotouhi J, Unberath M, Taylor G, Farashahi AG, Bier B, Taylor RH, et al. Exploiting partial structural symmetry for patient-specific image augmentation in trauma interventions. In: International conference on medical image computing and computer-assisted intervention. Granada, Spain: Springer; 2018. p. 107–15.
48. Barker J. Machine learning in M4: what makes a good unstructured model? Int J Forecast. 2020;36(1):150–5.
49. Padoy N. Machine and deep learning for workflow recognition during surgery. Minim Invasive Ther Allied Technol. 2019;28(2):82–90.
50. Forster T, Taylor G, Mehrfard A, Fotouhi J, Fer D, Nagle D, et al. Submitted: on the effectiveness of virtual reality-based training for robotic setup. Robot Automat Lett (RA-L). 2020.
51. Bork F, Barmaki R, Eck U, Fallavolita P, Fuerst B, Navab N. Exploring non-reversing magic mirrors for screen-based augmented reality systems. In: 2017 IEEE Virtual Reality (VR). Los Angeles, CA, USA: IEEE; 2017. p. 373–74.
52. Mehrfard A, Fotouhi J, Taylor G, Forster T, Navab N, Fuerst B. Submitted: A comparative analysis of

virtual reality head-mounted display systems. IEEE Virtual Reality. 2020.
53. Bork F, Fuerst B, Schneider AK, Pinto F, Graumann C, Navab N. Auditory and visio-temporal distance coding for 3-dimensional perception in medical augmented reality. In: Mixed and augmented reality (ISMAR), 2015 IEEE international symposium on. Fukuoka, Japan: IEEE; 2015. p. 7–12.
54. Qian L, Winkler A, Fuerst B, Kazanzides P, Navab N. Modeling physical structure as additional constraints for stereoscopic optical see-through head-mounted display calibration. In: 15th IEEE International Symposium on Mixed and Augmented Reality (ISMAR). Beijing, China: IEEE; 2016.
55. Sielhorst T, Feuerstein M, Navab N. Advanced medical displays: a literature review of augmented reality. J Disp Technol. 2008;4(4):451–67.
56. Zhang H, Gonenc B, Iordachita I. Admittance control for robot assisted retinal vein micro-cannulation under human-robot collaborative mode. In: 2017 17th international conference on control, automation and systems (ICCAS). Jeju, Korea: IEEE; 2017. p. 862–6.
57. Torabi M, Hauser K, Alterovitz R, Duindam V, Goldberg K. Guiding medical needles using single-point tissue manipulation. In: 2009 IEEE international conference on robotics and automation. Kobe, Japan: IEEE; 2009. p. 2705–10.
58. Kojcev R. Google summer of code project – ROS interface for impedance/force control by Risto Kojcev; 2016. Accessed: 2019-10-10. Available at: https://rosindustrial.org/news/2016/9/16/google-summer-of-code-project-.
59. Kojcev R, Fuerst B, Zettinig O, Fotouhi J, Lee SC, Frisch B, et al. Dual- robot ultrasound-guided needle placement: closing the planning-imaging- action loop. Int J Comput Assist Radiol Surg. 2016;11(6):1173–81.
60. Garcia P, Rosen J, Kapoor C, Noakes M, Elbert G, Treat M, et al. Trauma pod: a semi-automated telerobotic surgical system. Int J Med Robot Comput Assist Surg. 2009;5(2):136–46.
61. Seita D, Krishnan S, Fox R, McKinley S, Canny J, Goldberg K. Fast and reliable autonomous surgical debridement with cable-driven robots using a two-phase calibration procedure. In: 2018 IEEE International Conference on Robotics and Automation (ICRA). Brisbane, Australia: IEEE; 2018. p. 6651–8.
62. Sundaresan P, Thananjeyan B, Chiu J, Fer D, Goldberg K. Automated extraction of surgical needles from tissue phantoms. In: 2019 IEEE 15th International Conference on Automation Science and Engineering (CASE). Vancouver, Canada: IEEE; 2019. p. 170–7.
63. Thananjeyan B, Tanwani A, Ji J, Fer D, Patel V, Krishnan S, et al. Optimizing robot-assisted surgery suture plans to avoid joint limits and singularities. In: 2019 International Symposium on Medical Robotics (ISMR). Atlanta, GA, USA: IEEE; 2019. p. 1–7.
64. Fischer M, Fuerst B, Lee SC, Fotouhi J, Habert S, Weidert S, et al. Preclinical usability study of multiple augmented reality concepts for K-wire placement. Int J Comput Assist Radiol Surg. 2016;11(6):1007–14.
65. Fotouhi J, Fuerst B, Lee SC, Keicher M, Fischer M, Weidert S, et al. Interventional 3D augmented reality for orthopedic and trauma surgery. In: 16th annual meeting of the International Society for Computer Assisted Orthopedic Surgery (CAOS). Osaka, Japan: International Society for Computer Assisted Orthopaedic Surgery; 2016.

3

Artificial Intelligence for Next-Generation Medical Robotics

M. Mahir Ozmen, Asutay Ozmen, and Çetin Kaya Koç

Introduction

Since the first use of the word "robot" by a Czechoslovakian author Karel Čapek in a drama as *Rossum's Universal Robots in 1920*, it spread quickly all over the world and became a common term for artificial beings. Robots have been used in surgery since 1978; however, to justify the cost of robotic surgery, a quest for proven advantage over existing surgical techniques remains ongoing. Artificial intelligence (AI) is understood to be near-human intelligence exhibited by a machine for pattern recognition and decision-making. Future systems posing a certain degree of intelligence together with the increased possibility of connectivity will provide the answer for the questions being raised by traditional surgeons. Building these new intelligent robots will be one of the future tasks for humanity.

M. M. Ozmen (✉)
Department of Surgery, Istinye University Medical School, Istanbul, Turkey
e-mail: mahir.ozmen@istinye.edu.tr

A. Ozmen
Department of Electrical and Computer Engineering, University of California Santa Barbara, Santa Barbara, CA, USA

Ç. K. Koç
College of Engineering, Istinye University, Istanbul, Turkey

Artificial Intelligence

Nowadays, vast amounts of data are being generated in every field of medicine, making data analysis an immense task for humans. However, the level of analysis by humans alone of this big data has clearly been surpassed by artificial intelligence (AI) in an age where healthcare is dependent on human precision more than ever. An AI machine displays qualities of human intelligence by using algorithms to perform pattern recognition and decision-making. AI is broadly classified as *general* AI and *narrow* AI where the former describes machines that exhibit and imitate human thought, emotion, and reason (i.e., machines that can pass the Turing test remain elusive for now), whereas the latter is used for technologies that can perform as well or better than humans for specific tasks (like analyzing vast medical data in diverse fields).

AI, by eliminating human error, is expected to significantly reduce the number of misdiagnosis cases, excessive waste of resources, errors in treatment, and workflow inefficiencies and also *increase (not subtract from) the interaction times* between patients and clinicians. It is, therefore, important for surgeons to know about AI and to understand its effect on modern healthcare as they will be increasingly interacting with AI systems within the healthcare environment.

AI currently serves many purposes as a powerful tool in various areas – such as renewable energy systems, economics, weather predictions, manu-

S. Atallah (ed.), *Digital Surgery*, https://doi.org/10.1007/978-3-030-49100-0_3

facturing, and medicine – helping researchers worldwide. Its roots are found in robotics, philosophy, psychology, linguistics, and statistics [1, 2]. The popularity of AI soared with the major advances in computer science, mainly processing power and speed, which enabled the efficient implementation of long developed algorithms within the area. AI can be divided into four main subfields. They are (a) machine learning, (b) natural language processing, (c) artificial neural networks, and (d) computer vision. Although it seems complicated, we will try to explain each field separately and connect them – especially for robotic surgery applications [1–3]. These four subfields are the very foundation of digital surgery.

Machine Learning

Machine learning (ML) is a subfield of AI which can be described as the practice of solving a problem by enabling the machines to learn and make predictions by using a dataset and algorithmically building a statistical model. ML is useful for identifying subtle patterns which are impossible to be seen by humans in large datasets. There are four types of learning algorithms which are termed as follows: *supervised*, *semi-supervised*, *unsupervised*, and *reinforcement* [4].

In *supervised learning*, human-labeled training data are fed into an ML algorithm to teach the computer a function such as recognizing an organ (stomach, duodenum, colon, liver, etc.) in an image. This kind of learning is useful in predicting known results or outcomes, as it focuses on classification.

In *unsupervised learning*, the training dataset consists of unlabeled examples and this unlabeled data is fed into the learning algorithm. Unlike supervised learning, unsupervised learning does not involve a predefined outcome; hence, it is exploratory and used to find naturally occurring undefined patterns or clusters within datasets. The significance of such groups learned through unsupervised learning is evaluated by its performance in subsequent supervised learning tasks (i.e., are these new patterns useful in some way?).

In *semi-supervised learning*, the training dataset contains a small amount of labeled data and a large amount of unlabeled data. It can be viewed as a mix between supervised and unsupervised learning. Training data is clustered similar to unsupervised learning and the labeled training data is used to classify these clusters in a supervised learning fashion. It has been found that unlabeled data can produce significant improvement in learning accuracy when used in conjunction with a small amount of labeled data. Semi-supervised learning is similar to supervised learning in its goals.

Reinforcement learning consists of learning algorithms where the machine attempts to accomplish a specified task (playing games, driving, robotics, resource management, or logistics) with the help of a specifically designed reward function. Through its own mistakes and successes, the reinforcement learning algorithm assigns a negative or a positive reward to the agent which learns a policy to perform a task. A policy defines the learning agent's way of behaving at a given time, and it maps the state that the agent is in, to the action the agent should execute in that state. Reinforcement learning is suitable for particular problems in which the decision-making is sequential, and the goal is long term.

Natural Language Processing

Natural language processing (NLP) is the subfield of artificial intelligence where the ability to understand human language is built into a machine [5]. For this purpose, NLP recognizes words and understands semantics and syntax. NLP has been used to identify words and phrases in operative reports and progress notes for surgical patients that predicted anastomotic leak after colorectal surgery. Although the majority of these predictions coincided with simple clinical knowledge (operation type and difficulty), the algorithm was also, quite interestingly, able to adjust predictive weights of phrases that describe patient temperament such as "irritated" or "tired" relative to the post-op day to predict a leak with a sensitivity of 100% and a specificity of 72% [6].

Artificial Neural Networks and Deep Learning

Artificial neural networks (ANNs) are of outstanding importance in many AI applications. ANNs are based on layers of connected nodes (artificial neurons) which model the basic functions of a biological neuron. In this regard, each connection is a pathway to transmit signals to other nodes (neurons) similar to synapses in the brain. *In deep learning, a special structure of neural networks is used that are called deep neural networks (DNNs) with multiple layers between the input and output layers as opposed to simple 1 or 2-layer ANNs, and this complexity in structure enables them to learn more complex and subtle patterns (*Fig. 3.1*). Deep learning's autodidactic quality is what sets it apart from the other subtypes of AI. The neural network is not predesigned, but instead, the number of layers is determined by the data itself with this quality.* A DNN consists of digitized inputs (i.e., speech or image data) which go through multiple layers of connected nodes that detect features progressively and provide an output (i.e., label) in the end. For example, a DNN achieved an unprecedentedly low error rate for automated image classification by analyzing 1.2 million carefully annotated images from over 15 million in the ImageNet database [3, 5, 7].

Computer Vision

Computer vision, also known as machine vision, is an area of science that focuses on how computers gain high-level understanding of images and videos. Image acquisition and interpretation in axial imaging with applications such as image-guided surgery, virtual colonoscopy, and computer-aided diagnosis are all important utilizations of computer vision from a healthcare per-

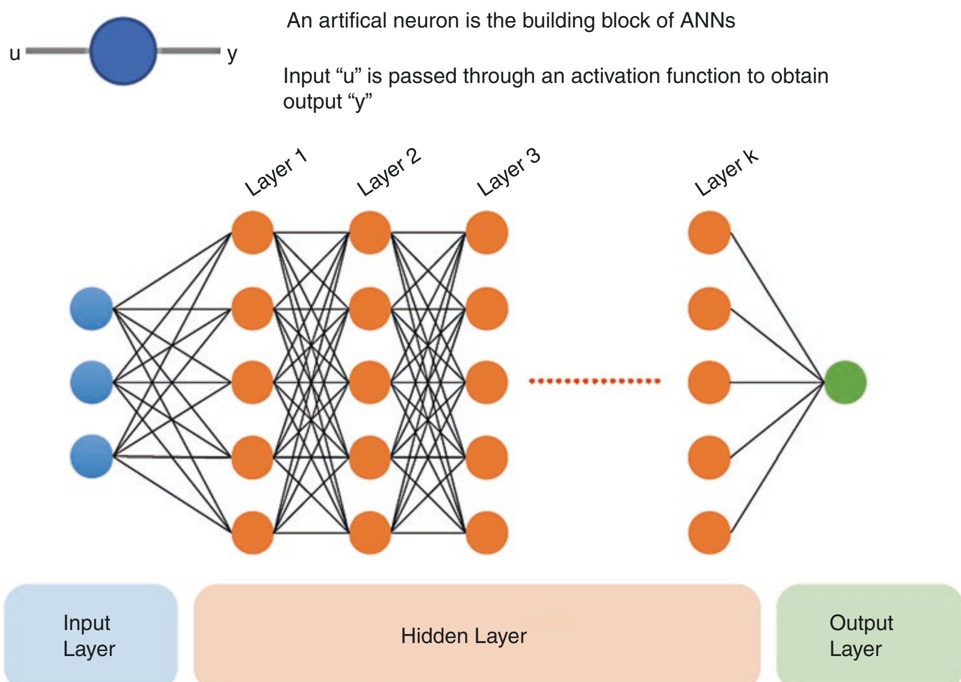

Fig. 3.1 (**a**) Model of a single neuron in machine learning. (**b**) An example of a deep neural network with multiple layers

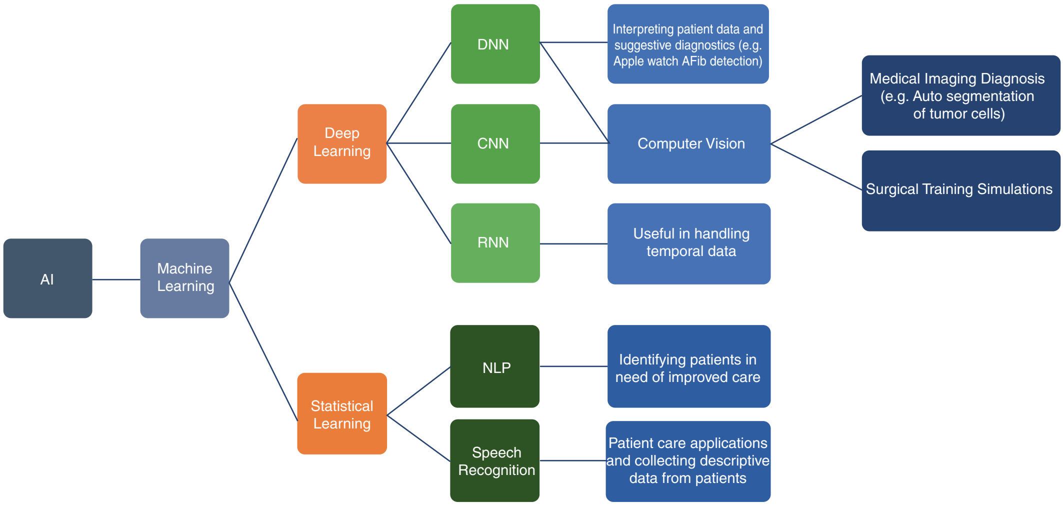

Fig. 3.2 AI, machine learning, and their use in medicine

spective. Current work in computer vision concentrates on understanding higher-level concepts. In surgery, real-time analysis of a laparoscopic video has yielded 92.8% accuracy in automated identification of the steps of a sleeve gastrectomy and noted missing or unexpected steps [3]. In addition, recent research efforts exist in the field in hopes of "digitizing surgery." This consists of observation of the surgical team and equipment in the operating room and performance of the surgeon with the help of computer vision (real-time, high-resolution, AI-processed imaging of the relevant anatomy of the patient) and integration of a patient's comprehensive preoperative data which includes full medical history, labs, and scans [5].

AI is a powerful tool in medicine and different methods are used from diagnostics to patient care. Figure 3.2 provides a summary of different methods and their respective application areas.

History of Robotic Surgery

The word "robot" was first defined by the Robots Institute of America in 1979 as "*a reprogrammable, multifunctional manipulator designed to move materials, parts, tools, or specialized devices through various programmed motions for the performance of a variety of tasks*" [8]. The first robot used in a real surgery was PUMA (*programmable universal machine for assembly*) developed by Scheinman in 1978 [9]. It was used by Kwoh in 1985 for neurosurgical biopsies and then by urologists in 1988 [10]. It was changed to surgeon-assistant robot for prostatectomy (SARP). This robot could only be used on some *fixed* anatomic targets and was not suitable for operations like gastrointestinal surgery where the surgical targets are dynamic and fluid.

At the Stanford Research Institute, Richard Satava, a military surgeon, developed an operating system for instrument tele-manipulation after the introduction of laparoscopic cholecystectomy. In 1988, Satava and his group started working on a robotic system for laparoscopic surgery. In 1993, AESOP (*automated endoscopic system for optimal positioning*) was developed by Yulin Wang and his company, Computer Motion, Inc., in Goleta, CA, USA. This was the first FDA-approved surgical robot [11]. In 1998, ZEUS, the new robot capable of reproducing the movements of the arms of the surgeon, was developed by DARPA (*Defense Advanced Research Projects Agency*). It was later used in 2001 by Prof. Marescaux to perform transcontinental telesurgery, a landmark achievement [12]. Computer Motion, Inc. was eventually acquired by Intuitive Surgical, Inc., which retired the development of the ZEUS robot, supplanting it with a new system. Intuitive Surgical then developed da Vinci as a master–slave robot, which received CE mark in 1999 and the full FDA approval in 2001. The da Vinci Surgical System is currently the most widely used, which has the models of *S, Si, Xi,* and, more recently, *SP*. This master–slave system overcame the limitations of laparoscopic surgery, its technical improvements including magnified 3D optics, precisely controlled wristed instruments with tremor filtration, and seven degrees of freedom. With the preservation of natural eye–hand–instrument alignment, it made the robotic platform highly suitable for a wide range of surgical procedures. The da Vinci *Xi,* the robotic effectors, have a much slimmer design than previous renditions as well as a longer "arm span," which greatly minimizes instrument clashing and collision. Adjunctive tools and accessories include stapling devices with 6 degrees of freedom (dof) or 6-dof flexible instruments, single site, firefly system, Tilpro system, and double console. Recent advancements on robotic technology also resulted in the development of the VeSPA single-port system. However, the VeSPA system has suboptimal ergonomics with clashing of instruments and provides only 4-dof instruments. The *SP* system designed for single-port access has a single arm that delivers three multi-jointed instruments and a fully wristed 3D HD camera for visualization and control in narrow surgical spaces [10]. Robotics surgery devices such as these are used in many areas in medicine and new applications are emerging with each technological development (Fig. 3.3).

Emerging Robotic Surgical Systems

The Italian healthcare company Sofar, Milan, Italy (which was later acquired by TransEnterix, *Morrisville, NC, USA*) developed an alternative robotic system, the Telelap ALF-X (currently known as *Senhance*). The design featured a remote surgeon workstation and three cable-actuated robotic arms featuring instruments and a telescope mounted on three separate carts. The device utilizes an open console design with 3D polarized glasses and a monitor with an integrated eye-tracking system which controls camera movements (e.g., the image is zoomed in,

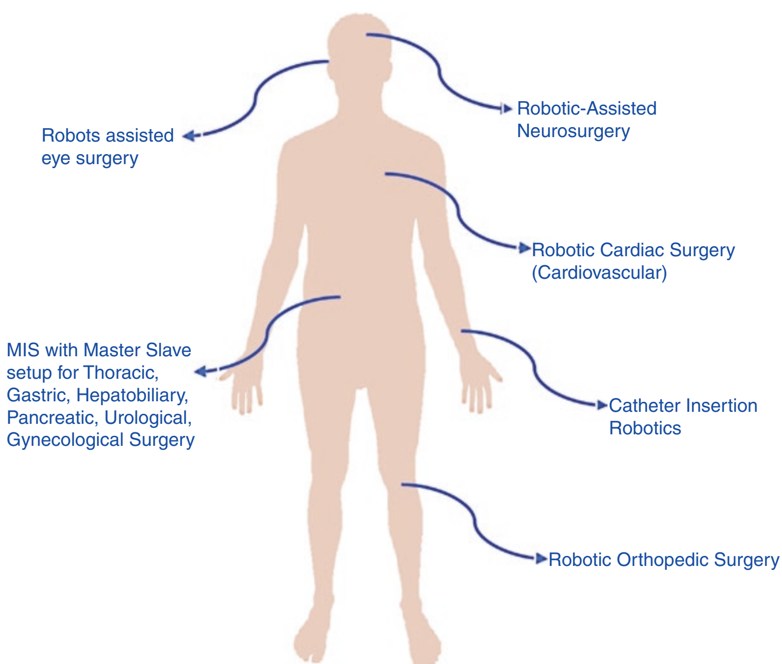

Fig. 3.3 Applications of robotic surgery

when the surgeon's head approaches the screen). Two handles similar to laparoscopic effectors manipulate instruments with 4 dof and 6 dof attached to the robotic arms. Tuebingen Scientific (*Tuebingen, Germany*) developed instruments based on Radius technology. Haptic feedback together with eye tracking is a unique feature of Senhance, when compared to standard da Vinci robots. Haptic feedback is realized by counter-movements of the laparoscopic handle at the console according to force and direction applied at the tip of the instrument [13, 14].

Upcoming Robotic Systems

Robotic surgical systems are evolving to include specific features and improvements of the bedside cart and effector arms (*lightweight, smaller size, mounted on operating table or on separate carts, single arm with a variety of instruments inside*), instruments (*tactile feedback, micro-motors*), console (*open, closed, semi-open*) or without a console, and 3D HD video technology (*polarized glasses, oculars, mirror technology*).

Several modifications of master–slave systems have been developed and the implementation of the console is one design aspect which separates these systems (discussed below). Intuitive Surgical and Avateramedical have chosen to design their robotic systems with a *closed console,* with in-line 3D video technology. An advantage of this is that polarized glasses are not needed, but an important disadvantage is that closed consoles are generally associated with loss of brightness at the periphery of the field of view. An *open console* system may provide better communication with the team at bedside and the flexibility to integrate future technologies such as ultra-HD (4K) video or full HD 3D screens.

Avatera

Avateramedical (*Jena, Germany*), in collaboration with Force Dimension (*Nyon, Switzerland*) and with Tuebingen Scientific (*Tuebingen, Germany*), has been developing Avatera which, as previously mentioned, was designed with a closed console configuration with an integrated seat using microscope-like technology with two adjustable oculars for in-line 3D image with full-HD resolution. Four robotic arms are mounted on a single cart and 6 degrees of freedom (dof) instruments with a diameter of 5mm are used. The system has no force feedback and only been used in preclinical experimentation [15].

Medicaroid

In 2016, Medicaroid (*Kobe, Japan*) started a corporation in Silicon Valley to prime the US market for medical robots made in Japan with the R&D and manufacturing expertise of Sysmex and Kawasaki Heavy Industries. The device features three robotic arms attached to the operating table; a semi-closed console with ocular-like in-line technology, which still requires polarized glasses; and a telescope with 3D HD technology. However, the system has no force feedback. Clinical launch is expected in 2020 [16].

Medtronic

In 2013, Covidien (Dublin, Ireland, later in 2015 Medtronic) acquired the license for versatile system by MiroSurge (German Aerospace Centre, Oberpfaffenhofen, Germany) and included further developments including instruments in their two research and development centers in the USA and announced the robot in 2019. The system comprises three to four modular robotic arms, an open console with an autofocusing monitor, 3D HD telescope and 3D glasses, fingertip-controlled handles, clutch mechanism, and foot switches to activate bipolar energy. The robotic arms are composed of seven joints with serial kinematics, comparable to human arms, and the instruments are driven by micro-motors optionally providing tactile feedback via potentiometers [17].

Raven

The Raven Project (Universities of Santa Cruz, Berkeley, Davis) has an open-source system that would allow two surgeons to operate on a single patient simultaneously. The prototype system included two portable surgical robotic arms, each offering 7 dof, and a portable surgical console. Raven III offers four robotic arms and (optionally) two cameras. Raven III is one of the most advanced surgical robotic research platforms, focused on battlefield and underwater remote surgery [18].

Revo-I

In collaboration with Yonsei University and multiple Korean academic and industry groups, Meerecompany (Hwasong, Korea) designed the Revo-I platform which features an open console, two handles, and foot controller for clutch mode and cautery. The four-arm system mounted on a single cart uses a 3D HD stereoscope and 6-dof instruments with a diameter of 8mm. In 2016, the first results of animal studies were published in collaboration with Samsung and approval for human trials in South Korea has been received [19].

SPORT™

After the unsuccessful introduction of the Amadeus RSS, Titan Medical focused on the SPORT™ Surgical System as a platform for robotic laparoendoscopic single-site surgery (LESS). SPORT™ has an open console with 3D HD vision controlling, a 3D flexible telescope with fiber-optic-based illumination, and two flexible instruments on a single robotic boom. Its main application is expected to be LESS cholecystectomy. Recently, robotic single-port partial nephrectomy was performed in animal models requiring additional trocars for retraction. The FDA approval for the system is currently pending [20].

Da Vinci *SP*

The da Vinci *Xi* system also allows the use of the robotic single-port *SP* 1098 platform including a 3D HD flexible telescope and three flexible instruments. This system has a master console and slave patient cart with a single arm. Once introduced into the abdominal cavity (or, alternatively, through a natural orifice), the flexible instruments, with a snake-style wrist, can separate to achieve triangulation [10, 14].

Verb Surgical

Verb Surgical was formed in 2015 as an independent start-up company, backed by Google and Johnson & Johnson to harness the unique capabilities of both companies [21]. It is detailed elsewhere in this textbook.

EndoMaster

Developed in Singapore originally for endoscopic resection of gastrointestinal polyps and tumors, EndoMaster has been used for natural orifice transluminal endoscopic surgery (NOTES) as well as transoral robotic surgery. This system has been designed with robotic arms (a grasper and a probe for monopolar diathermy) that are incorporated into the end of a flexible endoscope. It consists of a master telesurgical workstation and a slave manipulator (endoscope with robotic arms). Thus far, EndoMaster has only been used for preclinical trials on cadavers and animal models [22].

Computer Technology Drives Progress in Robotics

Innovation in robotic surgery will continue to parallel advancements in technology; especially with the considerable progress in computer science and AI. Novel distinct features, such as haptic gloves, cellular image guidance, or even autonomy might be the next step in the evolution of next-generation devices. Shademan et al. have described in vivo supervised autonomous soft tissue surgery in an open surgical setting, enabled by a plenoptic 3D and near-infrared fluorescent imaging system that supports an autonomous suturing algorithm. A computer program generates a plan to complete complex surgical tasks on deformable soft tissue, such as suturing an intestinal anastomosis based on expert human surgical practices [23]. Despite dynamic scene changes and tissue movement during surgery, they were able to show that the outcome of supervised autonomous procedures was superior to surgery performed by expert surgeons and robot-assisted techniques. The Smart Tissue Autonomous Robot (STAR) results show the potential for autonomous robots to improve efficacy, consistency, functional outcome, and accessibility of surgical techniques. By 2020, robotic surgery, once a simple master–slave device, is poised to merge fundamental concepts in AI as it evolves into digital surgery [24].

Autonomous Robotic Surgery

What Is Autonomy?

Physical, mental, technical variables dictate the performance of the surgeon and these factors affect the outcome. Surgical robots have the advantage of tremor cancellation, scalable motion, insusceptibility to fatigue, and greater range of axial movement which should, in turn, positively impact the quality of surgical care rendered.

Autonomy is defined as "an ability to perform intended tasks based on current state and sensing without human intervention." Although da Vinci is a master–slave robot and completely dependent on human control, to some extent, it has a variable degree of autonomy, since there is "built-in" tremor resistance and scalable motion. If equipped with cognitive capabilities, surgical robots could accomplish more supervised tasks and thus provide a greater level of assistance to the surgeon. Partially autonomous robots such as TSolution-One (Think Surgical, Fremont, CA), Mazor X (Mazor Robotics, Caesarea, Israel), and CyberKnife (Accuracy, Sunnyvale, CA) are currently in clinical use.

A robot is not a *single* device; rather it is a system with three components, *sensors, end effectors, and control architecture*, that process data and perform actions. During the procedure, there is continuous interaction between the robot, the surgeon, and the patient. A learning system is augmented with a process that allows a surgeon to watch the robot and provide feedback based on the behavior of the robot.

Combining AI (*machine learning, natural language processing, artificial neural networks, and computer vision*) with surgical robots may reduce technical and human errors, operative time, and rates of complications and improve the outcome as an ultimate end point. The robots can be taught specific procedures. There are certain methods proposed to "teach" the robots either by directly programming it (*explicit learning*) or by having the robot observe a surgeon or video directly (*implicit learning*); in this case, the robot may even be trained in simulation or virtual reality.

Prior knowledge (*collected data*) is of key importance in machine learning, and in surgery, prior knowledge is typically obtained from an experienced surgeon. *The skills, in this case, are collected from robotic surgery videos and from the data provided by the robot's sensory apparatus during similar procedures that were performed by a skilled surgeon.* A surgical activity dataset by Johns Hopkins University and Intuitive Surgical Inc. consisting of motion and video data is available for researchers interested in this problem [24, 25]. However, having access to all this data and video content is not enough for a robot to perform surgery autonomously. The learning model would also need a large database of explicit knowledge on how to accomplish a specific task in surgery. This sort of database would (and should) depend on the inputs from the surgical community, based on the international surgical consensus for each type of operation. In any case, it is highly unlikely that either implicit or explicit learning alone would be sufficient for automation in robotic surgery. However, a merger of both techniques with constant reinforcement and adjustment by human surgical experts could achieve acceptable levels of autonomy in surgical robotics.

Machine Learning in Autonomous Robotic Surgery

Future surgical robots will have the ability to virtually see, think, and act without active human intervention. Certain surgical tasks (suturing, cauterizing a leak in gastric bypass, clamping a certain area, etc.) could be autonomously performed with varying levels of human supervision. Of course, this would only be considered when an automated robotic system has repeatedly demonstrated its ability to achieve an acceptable level of performance in executing the necessary surgical tasks.

Three parameters define the task of an autonomous surgical robot: complexity of the surgical task, environmental difficulty (properties of the surgical site), and human independence. Versatile autonomous surgical devices will require extensive R&D and integration of control algorithms, robotics, computer vision, and smart sensor technology – in addition to extensive trial periods with surgeon-led vetting. Careful study is needed due to the highly deformable nature of soft tissue environments, the presence of hollow organs that are susceptible to rupture, and the delicacy of tissues.

There are certain autonomous systems that have been able to execute confined surgical tasks based on an exemplary dataset (provided by human input). For suture knot-tying tasks on a laparoscopic telesurgical workstation [26], faster and smoother trajectory executions were achieved (compared to a human) via *trajectory smoothing* of surgeon-provided motion examples. The parameters of a controller function were iteratively updated based on the error of a target trajectory (which is derived from the provided examples) to achieve faster trajectories [27]. The EndoPAR system (Technical University of Munich, Germany), a ceiling-mounted experimental surgical platform, was able to execute knot-tying tasks autonomously using recurrent neural networks (RNNs) using a database of 25 expert trajectories [25]. RNNs are a class of artificial neural networks that allows previous outputs to be used as inputs (feedback connections) while having hidden states. In other words, such a machine remembers from the past, and its decisions are influenced by what it has learnt in the past – so the same input could produce a different output depending on previous inputs in the series (sequential memory). This means that RNNs can (in principle) approximate any dynamic system and can be used to implement sequence to sequence mappings that require memory such as the set of trajectories involved in suture knot-tying [28]. The da Vinci Research Kit (DVRK) is used as a platform to apply learning by observation techniques with the aim of automating multilateral subtasks, such as debridement and pattern cutting. This approach involved segmenting motion examples by a human demonstrator into *structural gestures* such as grasping, retraction, penetration, and cutting, which is then used to define a finite state machine (FSM). An FSM is a mathematical model for any system that has a limited number of conditional states it can exist in for any point in time. In a study by Murali et al., 96% repeatability for 50 trials were achieved for the debridement task of 3D Viscoelastic Tissue phantoms and a repeatability of 70% for 20 trials of pattern cutting of 2D Orthotropic Tissue phantoms [29].

A novel endovascular surgery (ES) robot (currently experimental only) was recently used to test a convolutional neural network (CNN)-based framework to navigate the ES robot based on surgeons' skills. The CNN-based method shows capability of adapting to different situations while achieving a similar success rate in average operating time compared to known standards. Compared to manual operation, robotic operation was observed to demonstrate similar operating trajectory and maintained a similar level of operating force [30]. Finally, STAR (mentioned previously) was used for performing supervised autonomous robot-assisted surgery in various soft tissue surgical tasks such as ex vivo linear suturing of a longitudinal cut along a length of suspended intestine, ex vivo end-to-end anastomosis, and in vivo end-to-end anastomosis of porcine small intestine [31].

Although systems that can perform autonomous surgical tasks exist, considerable work will be required to bring fully autonomous surgical robots into fruition. The existing systems are only used in experimental setups on inanimate or animal models. However, the advances and improvements enabled by the power of machine learning cannot be neglected. The automation operations, with the aid of ML, will decrease the time of surgery, enhance the performance, and reduce miscommunication. As mentioned above, ML approaches have the potential to learn a model of surgical skills of experienced surgeons, provided by data points collected in the operating room. Such data could also be used for quantitatively evaluating surgical skills of trainees and to improve existing trainers by accurately modeling the interaction amongst surgeons, patients, and robots [32]. It is apparent that the future of surgery and surgeons will be shaped by these improvements.

Limitations of Artificial Intelligence

Although AI and ML have the potential to revolutionize the way surgery is taught and practiced, it is not a panacea that can solve all problems in surgery. In some cases, traditional analytical methods outperformed AI/ML. Thus, the addition of ML does not always improve results [33].

ML and other AI analyses are highly data driven and the outputs are naturally limited by the types and accuracy of available data. Hence, the patterns AI can recognize, or the predictions it can make, *are susceptible to the systematic biases in clinical data collection.* Furthermore, despite advances in causal inference, AI cannot yet determine causal relationships in data at a level necessary for clinical implementation nor can it provide an automated clinical interpretation of its analyses as of yet. Instead of a <u>single</u> surgeon's error resulting in <u>single</u> patient's harm, in the era of digital surgery and AI, the potential exists for a machine algorithm to result in iatrogenic harm affecting <u>multiple</u> surgical patients. The possibility of such an inadvertent outcome must be carefully considered before AI/ML systems are deployed in operation theaters. Specifically, systematic debugging, audit, extensive simulation, and validation, along with prospective scrutiny, are required when an AI algorithm is introduced into clinical and surgical practice.

As Professor Stephen Hawking has warned, the creation of powerful AI will be *"either the best, or the worst thing, ever to happen to humanity"*. Hawking had praised the creation of an academic institute dedicated to researching the future of intelligence as "crucial to the future of our civilization and our species" [34].

What Surgeons Should Do?

What does the future hold for surgeons as machine learning and deep learning technologies advance? Data will become increasingly voluminous, and to properly interpret such vast datasets, AI and ML will be integral. Where engineers can provide automated, computational solutions to data analytics problems that would otherwise be too costly or time-consuming for manual methods, surgeons have the clinical insight that can guide data scientists and engineers to answer the *right* questions with the *right* data.

Technology-based advancements have the potential to empower every surgeon with the ability to improve the quality of global surgical care. Given that research has indicated that high-quality surgical techniques and skill sets correlate positively with patient outcomes, AI could help *pool this surgical experience* – similar to efforts in genomics and biobanks – to *standardize* decision-making, thus creating a global consensus in operating theaters worldwide. Surgeons can prove to be essential to data scientists by imparting their understanding of the relevance and importance of the relationship between seemingly simple topics, such as anatomy and physiology, to more complex phenomena, such as a disease pathophysiology, operative course, or postoperative complications. AI needs to be held accountable for its predictions and recommendations in medicine; hence, it is up to the surgeons and engineers to push for transparent and interpretable algorithms to ensure that more professionals have an in-depth understanding of its implications. Next-generation surgical robots will be integral in augmenting a surgeon's skills effectively to achieve accuracy and high precision during complex procedures [35]. The next level of surgery that will be achieved by surgical robotics will likely evolve to include AI and ML [36].

At the beginning of the twentieth century, robotics, machine learning, artificial intelligence, surgical robots, and telesurgery were the stuff of science fiction. Yet today, they are all proven reality. We believe everything will change much faster in the twenty-first century as compared to the twentieth century. Although robots will become an indispensable part of routine life, in the field of medicine, surgical robots with artificial intelligence will evolve to have at least some autonomy and ML-/AI-based decision analysis in the near future. Fully autonomous surgical robots probably remain far from reach. However, in the coming decade, the use of machine learning, deep learning, big data analysis, and computer vision, will translate into (appropriately equipped) surgical robots capable of learning every step of an operation – a harbinger for the age of digital surgery.

References

1. Kalogirou SA. Artificial neural networks in renewable energy systems applications: a review. Renew Sust Energ Rev. 2001;5(4):373–401.
2. Buchanan BGA. (Very) Brief history of artificial intelligence. AI Magazine. 2005;26(4):53. https://doi.org/10.1609/aimag.v26i4.1848.
3. Hashimato DA, Rosman G, Rus D, Meireles OR. Artificial intelligence in surgery: promises and perils. Ann Surg. 2018;268:70–6. https://doi.org/10.1097/SLA.0000000000002693.
4. Burkov A. The hundred-page machine learning book, Andriy Burkov; 2019.
5. Topol EJ. High-performance medicine: the convergence of human and artificial intelligence. Nat Med. 2019;25:44–56. https://doi.org/10.1038/s41591-018-0300-7.
6. Soguero-Ruiz C, Hindberg K, Rojo-Alvarez JL, et al. Support vector feature selection for early detection of anastomosis leakage from bag-of-words in electronic health records. IEEE J Biomed Health Inform. 2016;20(5):1404–15. https://doi.org/10.1109/JBHI.2014.2361688.
7. Jones LD, Golan D, Hanna SA, Ramachandran M. Artificial intelligence, machine learning and the evolution of healthcare: a bright future or cause for concern? Bone Joint Res. 2018;7(3):223–5. https://doi.org/10.1302/2046-3758.73.Bjr-2017-0147.R1.
8. Hockstein NG, Gourtin CG, Faust RA. History of robots: from science fiction to surgical robotics. J Robot Surg. 2007;1:113–8.
9. Kwoh YS, Hou J, Jonckheere EA, et al. A robot with improved absolute positioning accuracy for CT guided stereotactic brain surgery. IEEE Trans Biomed Eng. 1988;35(2):153–60.
10. Ghezzi LT, Corleta CO. 30 years of robotic surgery. World J Surg. 2016;40:2550–7. https://doi.org/10.1007/s00268-016-3543-9.
11. Satava RM. Robotic surgery: from past to future: a personal journey. Surg Clin North Am. 2003;83:1491–500.
12. Marescaux J, Leroy J, Gagner M, et al. Transatlantic robot-assisted telesurgery. Nature. 2001;413(6854):379–80.
13. Gidaro S, Buscarini M, Ruzi E, et al. Telelap Alf-X: a novel telesurgical system for the 21st century. Surg Technol Int. 2012;22:20–5.
14. Rassweiler JJ, Autorino R, Klein J, et al. Future of robotic surgery in urology. BJU Int. 2017;120(6):822–41. https://doi.org/10.1111/bju.13851.
15. www.transenterix.com/news-item/transenterix-aquires-alf-x-surgical-robotsystem/.
16. http://www.sysmex.co.jp/en/corporate/news/2016/160113.html.
17. http://newsroom.medtronic.com/phoenix.zhtml?c=251324&p=irolnewsArticle&ID=2010595.
18. Hannaford B, Rosen J, Friedman DW, et al. Raven-II: an open platform for surgical robotics research. IEEE Trans Biomed Eng. 2013;60:954–9.
19. http://www.meerecompany.com/en/product/surgical_01.asp.
20. http://www.titanmedicalinc.com/titan-medical-inc-completes-amadeuscomposertm-pre-production-console-and-video-tower.
21. http://www.bidnessetc.com/38230-google-inc-joins-hands-with-johnsonjohnson-for-developing-robot-surgical/.
22. Tay G, Tan HK, Nguyen TK, Phee SJ, Iyer NG. Use of the EndoMaster robot-assisted surgical system in transoral robotic surgery: a cadaveric study. Int J Med Robotics Comput Assist Surg. 2018, 2018:e1930. https://doi.org/10.1002/rcs.1930.
23. Cha J, Shademan A, Le HN, Decker R, et al. Multispectral tissue characterization for intestinal anastomosis optimization. J Biomed Opt. 2015;20:106001.
24. Panesar S, Cagle Y, Chander D, Morey J, Fernandez-Miranda J, Kliot M. Artificial intelligence and the future of surgical robotics. Ann Surg. 2019;270(2):223–6.
25. Gao Y, Vedula SS, Reiley CE, Ahmidi N, Varadarajan B, Lin HC, Tao L, Zappella LL, Bejar B, Yuh DD, Chen CCG, Vidal R, Khudanpur S, Hager GD. "The JHU-ISI Gesture and Skill Assessment Working Set (JIGSAWS): A Surgical Activity Dataset for Human Motion Modeling", In Modeling and Monitoring of Computer Assisted Interventions (M2CAI) – MICCAI Workshop, Boston, MA 2014. p. 1–10.
26. Cavu MC, Tendick F, Cohn M, Sastry SS. A laparoscopic telesurgical workstation. IEEE Trans Robot Autom. 1999;15(4):728–39.
27. Berg JVD, Miller S, Duckworth D, Hu H, Wan A, Fu XY, Goldberg K, Abbeel P. "Superhuman performance of surgical tasks by robots using iterative learning from human-guided demonstrations," 2010 IEEE International Conference on Robotics and Automation, Anchorage, AK, 2010, pp. 2074–81. https://doi.org/10.1109/ROBOT.2010.5509621.
28. Mayer H, Gomez F, Wierstra D, Nagy I, Knoll A, Schmidhuber J. "A System for Robotic Heart Surgery that Learns to Tie Knots Using Recurrent Neural Networks," 2006 IEEE/RSJ International Conference on Intelligent Robots and Systems, Beijing, 2006, pp. 543–8. https://doi.org/10.1109/IROS.2006.282190.
29. Murali A, Sen S, Kehoe B, Garg A, Mcfarland S, Patil S, Boyd WD, Lim S, Abbeel P, Goldberg K. "Learning by observation for surgical subtasks: Multilateral cutting of 3D viscoelastic and 2D Orthotropic Tissue Phantoms," 2015 IEEE International Conference on Robotics and Automation (ICRA), Seattle, WA, 2015, pp. 1202–9. https://doi.org/10.1109/ICRA.2015.7139344.

30. Zhao Y, Guo S, Wang Y, et al. A CNN-based prototype method of unstructured surgical state perception and navigation for an endovascular surgery robot. Med Biol Eng Comput. 2019;57(9):1875–87. https://doi.org/10.1007/s11517-019-02002-0.
31. Shademan A, Decker RS, Opfermann JD, et al. Supervised autonomous robotic soft tissue surgery. Sci Transl Med. 2016;8:337–42.
32. Kassahun Y, Yu B, Tibebu AT, et al. Surgical robotics beyond enhanced dexterity instrumentation: a survey of machine learning techniques and their role in intelligent and autonomous surgical actions. Int J Comput Assist Radiol Surg. 2016;11:553–68. https://doi.org/10.1007/s11548-015-1305-z.
33. Hutson M. Artificial intelligence faces reproducibility crisis. Science. 2018;359(6377):725–6. https://doi.org/10.1126/science.359.6377.725.
34. Hern A, Hawking S. AI will be 'either best or worst thing' for humanity. https://www.theguardian.com/science/2016/oct/19/stephen-hawking-ai-best-orworst-thing-for-humanity-cambridge. Date last accessed 20 Dec 2018.
35. Kawashima K, Kanno T, Tadano K. Robots in laparoscopic surgery: current and future status. BMC Biomed Eng. 2019;1:12. https://doi.org/10.1186/s42490-019-0012-1.
36. Feußner H, Park A. Surgery 4.0: the natural culmination of the industrial revolution? Innov Surg Sci. 2017;2(3):105–8.

4 Cloud Computing for Robotics and Surgery

Asa B. Atallah and Sam Atallah

Introduction

In 1961, Stanford University computer scientist and core founder of artificial intelligence (AI) John McCarthy (1927–2011) predicted the age of cloud computing when he stated the following:

> Computing may someday be organized as a computer utility, just as the telephone system is a public utility … the computer utility could become the basis of a new and important industry [1]. In 2007, McCarthy's prediction would come to fruition as it precisely described the very basis of cloud computing today.

In this chapter, the reader is introduced to the history of the cloud, the general basis of its architecture for both storage and computing, as well as potential applications for robotics and surgery. The ability to integrate cloud computing into operating theaters, and the ability to apply this toward the development of AI-equipped next-generation surgical robots is also examined. The possibility of utilizing such a framework in this mode toward the field of surgery is here proposed. Machine learning via the cloud versus single device machine learning is also addressed.

A. B. Atallah (✉)
Apple Inc., Los Gatos, CA, USA
e-mail: atallah@utexas.edu

S. Atallah
College of Medicine, University of Central Florida, Orlando, FL, USA

History and Basics of the Cloud

In the field of computing, networks involve complex connections, both wired and unwired. This can often be overwhelming to illustrate, and so computer scientists, in order to simplify matters, reduce these complex networks by representing them with the icon of a cumulus cloud. Joseph Licklider (1915–1990) is among those credited for the origins of cloud computing in the early 1960s, through his key role with the Advanced Research Projects Agency Network (APRANET). The actual term "cloud computing" was first used in 1996 by Compaq executive George Favaloro [2], but it would take a decade of incubation before the emergence of modern cloud computing. At a Search Engines Strategies Conference in 2006, Eric Schmidt reintroduced the concept of cloud computing [3, 4]. This was the year that Amazon Web Services (AWS) launched a cloud-based storage service. This defined a key aspect of the cloud – namely, utilization of the cloud for virtually infinite digital file storage. The following year (2007) cloud *computing* became a new kind of service. Today, the primary global cloud computing service providers are AWS, Google Cloud Platform (GCP), and Microsoft Azure.

Cloud data storage is near infinite, highly secure, and extremely reliable. It is estimated that for every 10,000 files stored, it would take 10 million years to lose just one of them. Cloud storage is maintained at actual physical locations

S. Atallah (ed.), *Digital Surgery*, https://doi.org/10.1007/978-3-030-49100-0_4

(termed datacenters), where information is maintained on hard drives and other storage devices with backups at more than one locale. When the cloud as a utility for storage was introduced in 2006 by AWS, it was termed Simple Storage Service (S3).

S3 and other cloud "storage services" are the most familiar to surgeons and non-computer scientists. The idea of storing files "in the cloud" and accessing them from anywhere has become quite commonplace for end users. Today, most use a variety of cloud-based platforms for this purpose – Dropbox, iCloud, and OneDrive are just a few examples. While globally accessible files, multimedia, and photographic storage provide a valuable, highly secure, and near-limitless resource for machine learning (ML) and deep learning (DL) – including for medical robotics – it is not in and of itself sufficient, since ML and DL require compute capability, not simply hard drives packed with data.

The Advent of Modern Cloud Computing

In 2007, a year after the introduction of S3, AWS launched Elastic Compute Cloud (EC2), which was the start of cloud computing and *computing as a service* as suggested by McCarthy. In simple terms, this allowed software developers to login to the cloud over the Internet and use one, two, three, or *many computers at once.* Before cloud computing, an essential step in providing an Internet-based computing framework would require physical deployment of servers in a datacenter and establishing wired connections for them to the Internet. The advent of services like EC2 allowed deployment of computers into the cloud in either a point-and-click or programmatic manner, which was much more efficient than the traditional approach. With EC2, engineers could deploy an arbitrary number of computers or EC2 "instances" (i.e., for our purposes, an *instance* can simply be thought of as a *cloud computer*). This effectively allowed them to be *scalable* and thus *tailored to the level of service demand.* The concept of having an on-demand computer in the cloud that could just be instantiated at will was thus an important step forward for computer science.

Instances come in many shapes and sizes. Some have just a single processor, while others might have dozens. Some may include graphics processing units (GPUs) which can have thousands of small processors each, or they may include hardware that is programmable. *Both of these can be used to accelerate certain types of compute-intensive tasks.* In cloud computing, a set of instances all work together to provide a *service* (a term used frequently in this chapter). So, just as the web is comprised of interlinked web pages, the cloud is comprised of interlinked *services* that communicate with one another via the Internet. Some of these services render the web pages that we are used to seeing, while others only "talk to" other services, or to end-user devices, such as mobile phones.

EC2 and other cloud computing services essentially provide a network of low-cost computers (tens of thousands of them) organized into very large, warehouse-sized datacenters located in undisclosed sites at strategic regions. Typically, these datacenters are positioned near dense population centers. For example, AWS, the world's largest cloud service provider (maintaining 34% of the global infrastructure), has datacenters located in northern Virginia, in close proximity to major North American cities. In addition, data storage facilities (housing an array of hard drives) are also configured similarly. The cloud represents the network of these computers within datacenters and has special interconnections that allow them to be accessed remotely. In this fashion, one can access and use computers at one's discretion (for a fee) [3, 4].

Using cloud computers, or instances, for the purpose of computing is analogous to renting a car in many ways in that the user is not responsible for the maintenance of the vehicle, can borrow it for a preset period of time for a preset monetary amount, and return it when it is no longer needed. In this way, the cloud provides computing as a utility. But with the abundance of computers and their relative low cost, why would anyone need to "borrow" computers? What, possibly, could be the advantage of such a framework? The answer to these questions lies in the advantages of cloud computing. In brief, such an approach enables the cloud to (a) be elastic, or scalable in terms of number of processors and machines used simultaneously for a given task; (b) provide near infinite storage; and (c) the ability to potentially obtain unbounded virtual processing speeds.

The Cloud as a Computing Platform: Advantages

- Near infinite storage
- Scalable and elastic computing
- Ability to perform distributed computing
- Ability to perform calculations that require a large degree of computational power
- Secure system
- Low probability of information loss
- Does not require space-occupying hardware
- Globally accessible
- Upgraded and maintained by cloud service provider

The cloud as a computing utility is not direclty utilized by everyday persons (and certainly not surgeons) but is crucial to today's modern programmer, computer scientist, and those actively developing AI and ML on a global scale.

Cloud computing, because of its powerful infrastructure and practically infinite capacity, has effectively replaced mainframe computing; today, almost every major industry is driven by the cloud as centralized mainframes have been largely abandoned. Cloud computing has transformed software development and, in turn, the web itself. At its simplest level, it can be seen as a paradigm for how to structure, deploy, monitor, and manage arbitrary Internet services or applications. A core tenant of cloud computing is that compute and disk resources are essentially infinite for a very wide class of problems, and that they are typically only constrained by budgets. Another core tenant is that software engineers, via remote access to datacenters, maintain complete control of cloud-computing machinery within any given compute cluster. Thus, there is no loss of control or versatility within the cloud computing construct.

Offloading Computational Work to the Cloud

An important concept in cloud computing is the ability to offload computation-intensive tasks onto the cloud. Before we understand how the cloud can be applied to surgery and robotics in the operating theater, it is first important to really understand this principle. For this, let us consider an example from everyday life. Such an example is the use of app-based GPS navigation to determine automotive routes. While the best route and sometimes alternate routes can be found in seconds, how exactly does this happen? Optimal route determination can be complex, involving computation based on Dijkstra's algorithm [5–8], historical traffic data for the given geography, as well as broadband cellular, real-time traffic patterns from drivers on common roadways [9]. Thus, determining the shortest route requires computational power, mapping, and traffic data which far exceeds the capabilities of our handheld mobile devices. To deliver the route computation, mobile phones serve as a relay to cloud computers. In this infrastructure, the difficult computing is offloaded to the cloud, and the calculated route information is relayed to cellular phones for instant navigation, corrected for traffic patterns in real time. Because of the elastic and scalable nature of the cloud, the computed routes of multiple simultaneous users can be managed without difficulty. It was the use of the cloud that allowed phone-based navigation to become a useful alternative to modular and built-in automotive navigation systems, which required the storage of (often outdated) maps on CD devices and other bulky hardware. Hence, the principle of cloud-based automotive navigation provides a good paradigm for understanding how the cloud can be applied towards other fields, including surgical robotic systems.

Principles and Architecture of the Cloud

Consider a cloud-based service that just serves static web pages for a very busy site. A typical way this service would be implemented in the cloud would be to use a set number of computing instances (N), which typically range $1 \leq N \leq 500$. Cloud-based compute instances generally operate in conjunction with a *load balancer*. A load balancer is a simple, yet highly reliable device that fans incoming requests out to the instances behind it for processing (Fig. 4.1). This architecture is useful because it is the only externally visible presence of the service and it allows computer programmers to add and remove computing instances transparently to the outside world (for example, to dynamically scale any given service to meet user demand).

To view a web page, a user might specify the URL http://lb on their browser, representing the domain name or IP address that the load balancer has been configured with. The terminal's browser application would then request the main page from the load balancer which would forward that request onto one of the instances in a round-robin fashion. This instance could read the site's homepage content from its local disk and forward it back to the terminal through the load balancer for rendering in the browser. An architecture, as depicted in Fig. 4.1, can scale to considerably high levels because each request to fetch a web page by a user can be processed by any of the instances, and in fact each instance can typically process hundreds of such requests concurrently. Load balancers today can handle on the order of 500,000 requests per second, but even that is not an upper bound, because multiple load balancers can be used in tandem to handle tens of millions of requests per second. Services like this are designed so that regardless of which instance a load balancer selects to process a request, the results the user sees will be the same. In this way, if an instance fails while processing a request, it can be retried through the loadbalancer with the expectation that it will succeed, thus resulting in high service availability.

Cloud-based services usually perform functions that are more sophisticated than rendering static web pages, but their fundamental structure usually does not vary from that depicted in Fig. 4.1. Sophisticated services are usually

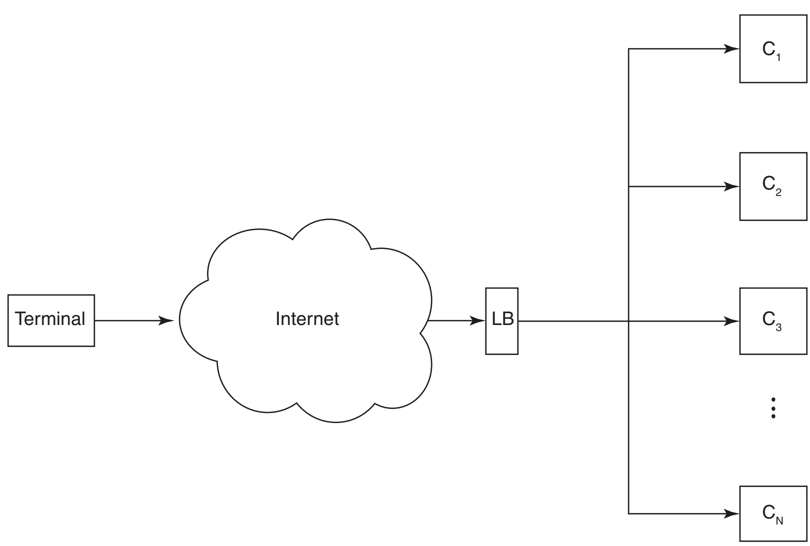

Fig. 4.1 The general framework for a cloud computing service is shown. Here, a "terminal," which represents any end user computer interface with Internet access can be used as a gateway to the cloud. The cloud service is composed of *numerous* computers (C_1, C_2, C_3 …C_N). A load balancer (LB) distributes or triages computational workload across the $_N$ instances, improving the efficiency of computing and allowing for the cloud to be scaled to meet demands. An important concept relating to cloud computing is that *multiple instances can be used simultaneously,* thus linearly increasing computational power

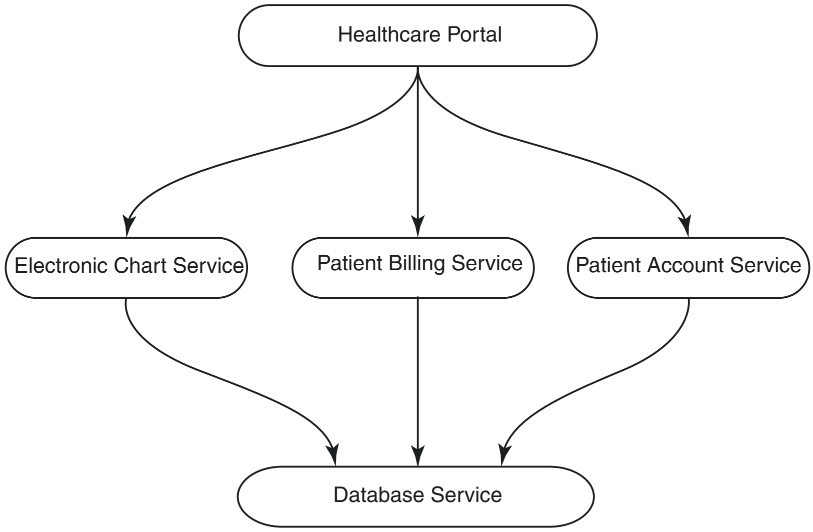

Fig. 4.2 In this diagram, a cloud-based model for a basic healthcare portal (electronic medical record system) is shown for purposes of illustration. In this example, patient accounts, patient billing, and physician charting all represent separate aspects, or services, which make up the healthcare portal in the cloud. The combination of these services creates a composite service which contains all of the essential component of the healthcare portal

created through *service composition.* That is, to perform a function, one service will typically call one or more other service(s) which, in turn, may call other services to complete a given task. To help us understand this in relation to medicine, let us envision a healthcare portal or electronic medical record (EMR) service as shown in Fig. 4.2. Here, the main healthcare portal service would be primarily responsible for rendering the portal's web pages. It might call a patient account service for verifying login credentials, an electronic charting service for showing test results, and a patient billing service for displaying billing history.

Commercial cloud-based services are deployed in multiple regions. The general topology is illustrated in Fig. 4.3. This is useful because GeoDNS (which essentially routes cloud and Internet traffic based on geographic location) [10] can be used to seamlessly route requests to the datacenter that is closest to the end user, resulting in much more responsive user experience. Without this architecture, network delays can be in the hundreds of milliseconds - over an order of magnitude higher than what is otherwise achievable.

The Cloud as a Workaround for Moore's Law

In 1965, Gordon Moore, one of the founders of Intel, correctly predicted that computational speed would continue to increase exponentially, and this would be matched by a dramatic fall in cost [11–14]. Specifically, Moore predicted a doubling of computational speed every two years by doubling the number of transistors on a computer circuit board, as expressed by the following formula:

$$n_b = n_a 2^{\left((y_b - y_a)/2\right)}$$

where Y_b represents any given future year and n_b number of transistors (or equivalent computing power) for that year, relative to the current year (Y_a) and current computing power n_a. However, there exist fundamental limits to Moore's law [15–18]. In the words of Stephen Hawking, those fundamental limits are defined by the atomic nature of matter itself and by the speed of light. In 2007, Gordon Moore also stated that his law would reach a boundary – a fundamental limit beyond which further processing speed and computational doubling would

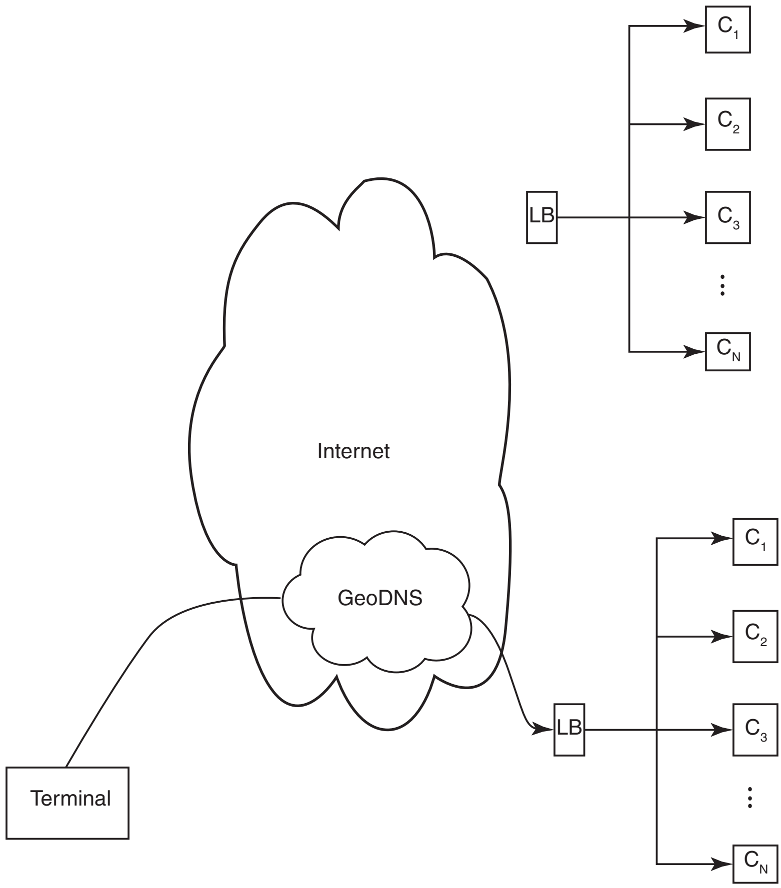

Fig. 4.3 The cloud operates best when the datacenters housing cloud computing instances are in geographic proximity to the end user (terminal). To help route users to the closest datacenter, a GeoDNS is integrated into the cloud. GeoDNS and load balancers work together to improve the computing efficiency of the cloud and help it work seamlessly with end users by limiting network-related delays

end. This can be mathematically demonstrated based on the laws of physics. Specifically, the Compton wavelength [19], λc, can be defined as follows:

$$\lambda c = \left(\frac{h}{m_e c} \right)$$

where h is Plank's constant (6.63 X 10^{-34} J s) divided by the mass, m_e, of the electron multiplied by the speed of light, c. Thus, the Compton wavelength λ_c represents a fundamental limit to measuring the smallest particle of matter and, in quantum computing, the smallest "quantum" bit of data (see next chapter). Since the speed of light and electron mass are known and because the yearly doubling of computing speed can be modeled using Moore's law ($n_b = n_a 2^{[(Yb-Ya)/2]}$), the point in time at which the doubling of computer speed will plateau can be determined. JR Powel has calculated that a limit to Moore's law will approach its limit by the year 2036 [20]. At that time, Powel predicts that the absolute physical limit of computational speed will have been realized. However, cloud computing could provide a workaround for the absolute limit to Moore's law [21–23]. As will be discussed in detail later, through distributed computing and cloud networked computers, even if this limit is reached, one can still achieve *virtual* computing speeds well in excess of any desktop computer today. *In this sense, cloud computing provides a critical pathway that works around the limit of Moore's law and the most practical framework for modern machine learning.*

Targets for the Cloud: Machine Learning and Vision

Artificial Intelligence (AI) has not evolved as swiftly as predicted in the era of mainframes [24, 25], probably because the transition had to be made from algorithm-based logical programming to those which utilize the principles of machine and deep learning (ML and DL) [26–29]. In computer science, ML deals with a machine's ability to recognize patterns based on datasets, typically referred to as *training data.* Unlike traditional computer algorithms which operate based on executing sets of instructions and syllogisms, ML trains machines by *examples* – lots of them [30, 31]. Human cognition is similar, but humans require far fewer examples to learn to recognize any specific item or object – as the human brain is better than today's machines at using small bits of data to abstract information. For example, a young child can recognize the difference between a bird and an airplane after seeing just a few of each, but a machine will need to learn by interpreting images from a spectrum of various planes and birds. For example, a machine would need to "see" (digitally interpret based on features) large planes, propeller planes, jet planes, etc., before it can recognize and label all of them as "planes" and especially to be able to tell the difference between a plane and bird. This is why ML requires a vast database to draw from before being able to make distinctions. In ML, the specific item that is digitally important for identifying an object is known as a *feature* (e.g., the wing and engine of an airplane are "features"), while the categorization of the object into a class based on the features it posesses is referred to as *labling.*

While we used birds and planes as an example, the same principles could be applied to anatomic targets. In clinical medicine, perhaps one of the best applications of ML/DL relates to image recognition. Specifically, dermal pathology with machines using convolutional neural networks (ConvNets, see Chap. 31) allows for the ability to classify skin cancer with the same level of competence as an experienced dermatologists [32]. *In the field of robotics in surgery, next-generation systems could utilize ML with the cloud as a platform for this and apply examples from surgical video and photo libraries stored in the cloud which can be accessed globally.* One can start to envision how ML could recognize a variety of key anatomic structures (such as the superior mesenteric artery, the recurrent laryngeal nerve, the common bile duct, or ureter) based on specific features and perhaps label such targets to help diminish the incidence of operative injury and thereby enhance patient safety.

By coupling cloud computing with ML, next-generation surgical robots could have improved capability, enhanced vision systems, and target tracking. The process of position orientation and tracking with respect to known (machine-learned) features is often referred to as visual odometry [33]. This approach relies on ML and the ability to interpret the visual field (by recognizing features) and then appropriately reacting to the given environment. An example of visual odometry is how it is used in the maneuvering of planetary rovers – namely, Mars *Curiosity* [34]. Visual odometry allows a system, such as *Curiosity,* to be autonomous, so long as it is able to recognize key features and translate them into labels. This would allow it to autonomously avoid hazardous terrain using various approaches to computer vision, including simultaneous localization and mapping (SLAM) and related algorithms [35–41]. Some robotic household vacuum systems operate by visual odometry as well [42]. In the field of medicine, visual SLAM has been applied towards the development of endoscopic capsule robotics [43, 44] and surface reconstruction for abdominal minimally invasive surgery [45, 46].

Cloud Robotics for Surgical Applications

Robotics in surgery is evolving rapidly, with a multitude of competing platforms poised to launch into the surgical arena by 2021 [47]. Such systems are being designed to solve problems for today's surgeons and healthcare systems. Operative efficiency could be improved [48–50], for example, by reducing the requirement of a bedside assistant – which is an achievable goal [51]. Tomorrow's surgical robots will provide an information and data-rich environment for surgeons that could theoretically improve the quality of surgery for complex cases [52–54] – especially for visual structure recognition during stepwise operative procedures [55].

Robotic automation in surgery is currently in development. An example of this included the emergence of automated robotic suturing – which has been demonstrated to be feasible with the smart tissue anastomosis robot (STAR) [56]. STAR uses AI in conjunction with visual and haptic sensors to complete surgical tasks and even has been shown to outperform surgeons on specific tasks based on quantitative analysis [53, 56, 57]. In order to maximize the potential of emerging systems such as STAR, however, a new approach to computing and processing will be needed. Cloud computing could provide the ideal framework, as it offsets the limitations of onboard computers.

Disadvantages of Onboard Robotic Computing in the Operating Theater

- Requires physical space and weight that may restrict device operation.
- Software management (upgrades) must be performed for each individual robot.
- Increases the per-unit cost of the device substantially.
- Prevents centralized robotic machine learning (each robot is independent of others).
- Does not allow for a method of sharing learned information among robots in different locales.

As discussed previously, central to the concept of cloud robotics is the ability to offload computing onto the cloud [58–65]. Importantly, this concept can also be coupled with robotics. The idea of "remote-brained" robotics probably emerged at the turn of the twenty-first century and predates the modern cloud by about 6 years [66, 67]. Cloud computing underlies globally networked robotic systems in a variety of nonsurgical applications – perhaps most notable among them are RoboEarth [68] and the da Vinci Project [69]. Today's cloud framework could support medical robotic computing, but medical robotic applications would essentially be part of a *PaaS* (platform as a service) model [70]. The central advantage of cloud-based robotics for surgical systems is global access to computer processing and storage over networks with load balancing, where workloads are distributed based on available cloud computing resources [70]. *In this construct, surgical robots with ML capability could share learned information, because they share a common brain* [62, 71].

Suppose, in an example, that surgical robot (A) in location (X) learns to recognize a specific anatomic structure or to perform a specific task, while surgical robot (B) in location (Y) learns to recognize a separate anatomic structure or to perform a separate task. Over time, both robot (A) and robot (B) master each of these objectives. Since the robotic systems share a common brain in the cloud (Fig. 4.4), effectively robot (A) masters robot (B)'s tasks and vice versa. In such a model, *adding more surgical robots (n) increases the learning capacity of the central-brain, cloud-based system, which exhibits an enhanced longitudinal effect (the cloud brain is enriched by the collective surgical robotic experience over time).*

As an analogy for surgeons, suppose that humans had a common brain like that of cloud robotic computing. Instead of robots learning, imagine four medical students who matched into four specialties – neurosurgery, urology, ophthalmology, and pathology. After completing residency, each will be adept in her/his field, but, because there is a common brain, each physician has now mastered *all four specialties*. It would be like waking up one day and suddenly being skilled at performing brain surgery, although you may have only actually completed a pathology

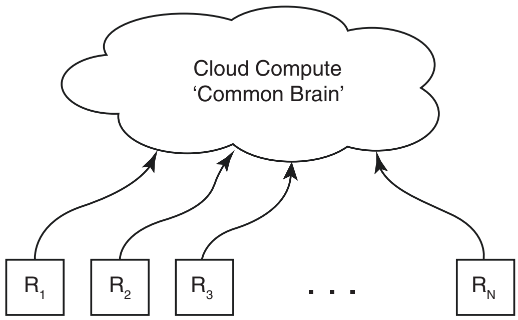

Fig. 4.4 Central to the vision of cloud robotic surgery is the concept of a common compute, cloud-based "brain." For any surgical robot, R_1, R_2, R_3 … R_N, machine learning is maintained centrally. There are important advantages to this approach. First, for every independently learned task of any single robot, all other robots in the same cloud network of robots automatically learn the same task. Second, because of the common brain framework, the more robots learning surgical tasks over any given period of time, the greater the collective learning of the cloud robot, and this learning is conserved over time. Third, offloading vast computational workloads onto the cloud reduces individual robot complexity and, at the same time, allows access to an extremely powerful computing framework capable of handling the high demands of ML required for next-generation surgical robots

residency! Thus, with cloud-centric robotics and cloud-based machine learning, *the more robots there are learning various types of surgical tasks, the greater the collective learning and experience of the common brain system. This underscores the potential power of cloud-based computing systems.* There are other key reasons why cloud-based computing could provide the basis for next-generation robots and digital surgery itself:

Advantages of Cloud Computing for Medical Robots

- The medical robot's computing becomes centralized (common compute brain).
- Minimization of hardware footprint in the operating theater as most compute resources are housed in the cloud.
- Software and system operations are managed by a third party (cloud service provider).
- Storage of files and data is virtually infinite.
- Infrastructure is suitable for ML and AI due to scalable capacity and the ability to utilize distributive computing (see later).
- Information can be shared from one robotic system to another regardless of geographic locale.
- ML developed on one device is automatically known by all devices on the platform via the cloud network.
- By off-loading the computational work load onto the cloud, the cost of the robot decreases as computing systems necessary for ML and AI become cloud based.
- Computers in surgery become an operating expense, rather than capital expense (pay per use).
- Allows for bidirectional flow of data between multiple robots and their cloud computing environment.
- Ability to share learning among robots and operating room devices (collective learning).
- Allows learnt information to be shared longitudinally, over time.

With this background into the cloud, we will now take a much closer look at how cloud-based computing technology can be used in surgical environments. We will also examine how the idea of parallelizing problems via cloud-distributed computing can provide an invaluable resource for machine learning. Later, learning curves for cloud-based computers will also be illustrated.

Cloud Surgery

Imagine the operating theater of the future equipped with cloud-based "black box" data-centric recorders [72–75]. While these can be a valuable tool to improve safety, they can also be utilized in a more global fashion, whereby data and various metrics are recorded, stored, and analyzed via the cloud. With such an infrastructure, it would be possible to cloud-connect operating theaters and perform analysis on a large scale. In this manner, various data inputs for each operation could be auto-captured in an electronic surgical record (ESR) as a kind of analogue to the electronic medical record (EMR). The ESR could be managed via the cloud and thus be accessible to various stakeholders from surgeons to research scientists, to hospitals, and to governmental administrations. While black boxes would capture individual operative case proceedings, a cloud-centric ESR would capture a collective whole allowing improved ML and analysis of big data [76]. Such metrics from the ESR could be informative and may be applied to tele-mentoring.

Electronic Surgical Record (ESR)

A List of Examples and Uses with Cloud-Based Infrastructure

1. *Comparative Analysis.* Example: A surgeon can query her/his cholecystectomy case time against national or international times and a percentile score could be computed.
2. *Operative Databases and Metrics.* Example: The number of minutes spent draping and docking a da Vinci Xi robotic cart for all robotic right hemicolectomies in a given state, country, or continent can be known and analyzed.
3. *Longitudinal Operative Case Analysis.* Example: The number of laparoscopic pancreatectomies being performed on a given day, month, or year can be instantly known and tracked over time.
4. *Case Metrics and Variances.* Example: Average urine output, blood loss, oxygenation, and mean arterial pressure for all right upper lobectomies could be computed, compared, and analyzed – comparing the measurable values against those observed in a department, region, nation, or continent. Sentinel events could be registered and shared in real time, improving the awareness of potential operative risks, especially with newly implemented operations.
5. *Real-Time Regional and Global Operative Logs.* Example: Relationship of time of day for any operation can be known. For example, at any given time, what is the total number of cesarean sections being performed in Paris, France? What is the trend by month and day of the week? Such information can help budget staffing and operative services.
6. *Operative Service Supply and Demand Analysis.* Example: Determining the trend in the number of bypass grafting operations performed in a given city over time, to predict growth and ascertain overall surgeon supply and demand for any given hospital or region.
7. *Surgeon Logbook Digitization.* Example: Automatic logbooks, whereby a surgeon tracks their volume and is able to compare this to specialists in the same field. For example, an ENT surgeon may compare his/her number of tonsillectomies performed in the past year to the number performed by ENTs with the same number of years in practice by city, region, or country. This could be automatically registered into a cloud-centric logging system.
8. *Surgeon Performance Assessment.* Example: Creation of factual data could develop verifiable score cards for surgeons that assign a percentile for case time, blood loss, approach used, etc. For example, Surgeon Jones has a mean operating time of 34 min for a right hemicolectomy, which is in the 98%-tile for the nation in 2019; he converts to open 3% of the time, which is in the 96%-tile in 2019.
9. *Feature-Searchable Video Fields.* Example: Via cloud access and storage, a surgeon could query the system to view all videos which capture (tagged with) a specific element or feature for review and analysis and educational purposes, for example, videos of all common bile duct injuries.
10. *Global Surgical Pathology Data Repository.* Example: If pathology systems are linked to the ESR via the cloud, that pathologic data could be incorporated; much as the SEERS (Surveillance, Epidemiology, and End Results) databases are used today, only this information could be instantly known. For example, how many T2 rectal adenocarcinomas were resected in the state of California today? Which country has the highest rate of lower extremity sarcoma resections?

11. *Anatomic Video Library for Machine Learning (ML).* Example: Modern, cloud-based medical robots use ML to identify key anatomic structures and share this information via the cloud. In a construct whereby robots share a common brain (e.g., cloud robotic surgery), a surgical robot being used, for example, to perform a sigmoid colectomy has just determined the features necessary to identify (and thus label) the left ureter to prevent it from being injured. Now, this information is immediately known among all robots in the same cloud-based model, regardless of geographic region.

Distributed Cloud Computing, Amdahl's Law, and Speedup

Recall from our previous analogy that using cloud computer(s) is like renting a car – or a fleet of cars. Software engineers can access the cloud via secure servers and "rent" as many computers as they like. The more they rent, the more computational power becomes available. In this way, programmers are able to compute various problems which demand a heavy CPU workload via the cloud. Although the computers that are used in datacenters are typically only moderately powered machines that actually fail at a predictable rate, software engineers still prefer to use them because they can be linked together for increased computational power.

It is important to understand that distributed computing is integral to modern cloud computing [77–79], although it predates the cloud by decades. Distributed computing is the process of dividing computational work among separate machines.

To understand how distributed computing works, imagine having a very complex problem to solve, one that would require a computer several hours to determine the solution, even with high processing speeds. A software engineer can write the program in such a way as to distribute the computation (required to arrive at a solution) among different machines. Thus, the more machines there are working to solve a problem, the faster the solution will be obtained; hence, distributed computing is a method to increase a machine's virtual computational speed. Remember that cloud computing is scalable, so access to multiple computers is possible simultaneously due to this intrinsic property [80–82]. Distributed cloud computing architecture is a structural paradigm fundamental to the cloud. In most cases, the "units of work" are very small, so the speed gains achievable with distributed computing are not always evident. However, as the complexity of the problem increases, the improved computing speed, termed *speedup*, can be substantial.

To appreciate the power of distributed computing, we will consider its use in the context of computer graphics, specifically in *ray tracing*. Ray tracing is a graphics rendering technique that analyzes reflections, the observer's point of view, and light source directionality to produce a highly photorealistic digital image. It is very computationally intensive since the path light taken from each pixel in the image must be analyzed to see which objects in the scene it intersects and, for reflective objects, which *other* objects the reflection of the light beam intersects. Rendering a ray-traced image for a complex scene with many objects and light sources can take hours, but it is a problem that is highly *parallelizable*. We can do this by having a set of computers that each render some portion of the target image and just "glue together" their results. For example, in the cloud, we can render a ray tracing scene almost 4X faster by having each of four instances render one quadrant of the image (Fig. 4.5). Note that the time needed to describe the scene to each of the instances and to stitch the completed visual scene together is negligible compared to the image rendering time. Via the cloud, one could use the following hypothetical model to complete the distributed computing task of ray tracing. For example, consider the *m5.xlarge* instance from AWS, which is a quad-core architecture. Now, assume that 500 *m5.xlarge* instances are configured as a service to render a ray-traced image. Since each CPU of the *m5.xlarge* instance has a clock speed of 3.1GHz, one can calculate the virtual clock speed as follows:

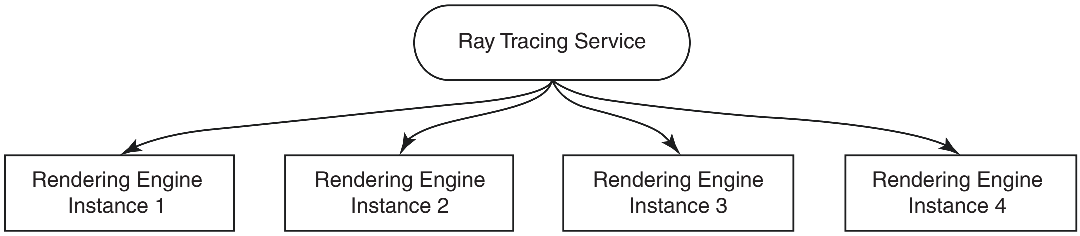

Fig. 4.5 Here, the cloud-based framework for a ray tracing service is depicted. Ray tracing, which is computationally intensive, is also highly parallelizable. Thus, the time required to complete any specific digital ray tracing can be substantially reduced. Later, we shall see that the problem-solving "speedup" can be calculated based on Amdahl's law. In this example, the ray tracing has been distributed to four instances in the cloud which can reduce the time needed to complete the task and render the digital image. This example highlights how distributing a problem across multiple instances in the cloud can increase computational power

$$\{\text{No. of } (m5.\text{xlarge}) \text{ instances}\} \times \{\text{Clock Speed}\} \times \{\text{No. of Cores}\} = \text{Virtual Clock Speed}$$

or

$$\{500\} \times \{3.1\} \times \{4\} = 6{,}200\,\text{GHz}$$

Thus, the cloud-based distributing computing speed is, in this example, over three orders of magnitude faster than the fastest commercially available processors today.

The limit to the speedup we can achieve on such problems is dictated by the unparallelizable part of the problem as well as the number of "computing units" that the problem can be disturbed across. For the cloud, these computing units can be thought of as the number of instances, factoring in the number of CPUs per instance. This number can be defined as N. For example, for a system of 2 instances with 4 CPUs per instance, N is as follows:

$$N = \{2\,\text{instances}\} \times \{4\,\text{CPUs}\} = 8$$

If the percentage a problem amenable to parallelization is p, then, according to *Amdahl's law* [83], the speedup (S) would be given by the following expression:

$$S = \frac{1}{(1-p) + \frac{p}{N}}$$

where S is the total speedup. So if $p = 99.95\%$ (i.e., all but 0.05% of the problem can be processed in parallel) and $N = 4$, then:

$$S = \frac{1}{(1-.9995) + \left(\frac{.9995}{4}\right)} = \frac{1}{(0.0005) + (0.2499)} = \frac{1}{0.2504} = 3.99361$$

In this example, the speedup expected would be ~4×. *Thus, based on Amdahl's law, the more any given problem can be parallelized, the greater the speedup.*

Now, let us suppose a cloud-based computing system with a limitless number of instances. As $N \to \infty$, and if one assumes that a problem can be entirely parallelized ($p = 1.0$), then an upper bound of speedup would become infinite, as $S \to \infty$:

$$S = \frac{1}{(1-1)+\frac{1}{\infty}} = \frac{1}{(0)+\frac{1}{\infty}} = \frac{1}{\frac{1}{\infty}} = \infty$$

More generally, when $p = 1,\ S = N$, speedup becomes dependent upon the number of processors which can be used to solve any given problem, and this can be shown as follows:

$$S = \frac{1}{(1-1)+\frac{1}{N}} = \frac{1}{(0)+\frac{1}{N}} = \frac{1}{\frac{1}{N}} = N$$

As $N \to \infty$, the maximum achievable speedup can be expressed as follows ($0 \le p \ge 1$):

$$\lim_{N\to\infty} S = \frac{1}{1-p}$$

This defines a speedup limit that is dependent on the portion of the problem that can be parallelized. We can visually understand how speedup varies based on p, as depicted in Fig. 4.6, where speedup is given for three arbitrary p values, 0.9, 0.8, and 0.4 (note: due to practical limitations, $p \neq 1$, since computational problems cannot typically be 100% parallelized).

What this tells us is that the more a problem can be parallelized, and the greater the number of computers which can be used to solve the problem in a distributed fashion, the greater the speedup. Since the cloud places thousands of computers at our disposal, it provides the perfect framework to create dramatic increases in com-

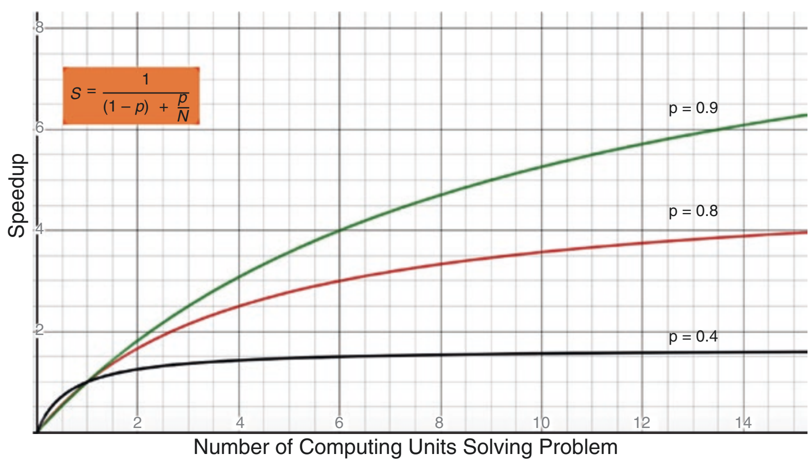

Fig. 4.6 Amdahl's law, in computer science, mathematically predicts the speedup for any given problem and is given by the expression $S = \frac{1}{(1-p)+\frac{p}{N}}$ where S represents the total speedup, and p represents the parallelizable portion of any given problem. N represents the number of computers (CPUs) computing in a given cloud compute system. The graph demonstrates the speedup limitation by comparing three different problems that are 40% parallelizable ($p = 0.4$), 80% parallelizable ($p = 0.8$), and 90% parallelizable ($p = 0.9$). This demonstrates that the greater the portion of a problem which is amenable to parallelization, the greater the speedup

puting speeds, for complex problems that can be parallelized. This is why the cloud is often said to be infinite in terms of *computing power*. This can be seen as a clear advantage of combining the cloud with the architecture of distributed computing. In computer science, the ability to add more instances, to increase *N*, is known as *horizontal* scaling. In contrast, *vertical* scaling would involve using faster instances. Thus, the cloud, as a scalable computer, provides a virtual platform for solving complex problems that require high computing power, without leaving a bulky physical footprint [84, 85], further making this framework ideal for the limited space of operating theaters.

Variability in Human and Machine Learning

Just as surgeons exhibit differing learning ability and proficiency, so, too, do machines. In this section, we explore and try to understand some of these differences. Let us first examine surgeon learning. Human cognition and the proficiency-gain curve is sigmoidal (i.e., a logistic curve) and varies to some degree based on the surgeon's ability. This can be expressed as:

$$f(x) = \frac{1}{\left(\partial + \Delta e^{-x}\right)}$$

Here, *e* represents Euler's number (~2.71828) and ∂ represents a coefficient which correlates to surgeon skill and ability, approximating the total learning capacity for any give task or operation. Thus, learning along the proficiency-gain curve is variable among surgeons based on their inherent ability and aptitude (Fig. 4.7). The smaller the coefficient, ∂, the greater the learning ability of the surgeon and varies from 0.1 to 0.07 in this hypothetical model; Δ is also a surgeon-specific coefficient and represents the slope of the sigmoid curve, as a measurement of learning speed. Now, let us compare human or machine learning over time. How would machine learning differ from human (surgeon) learning? How would machine learning differ for systems that use a cloud-based, common brain versus machines that do not? A few

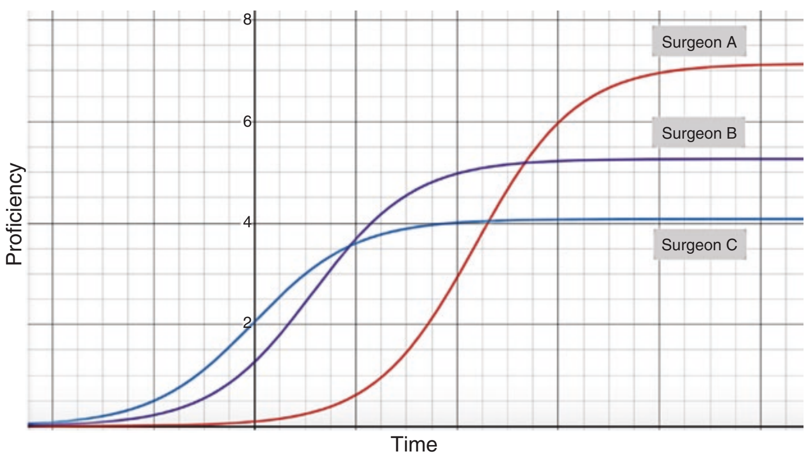

Fig. 4.7 In general, surgeon aptitude improves over time and is based on experience, but also on a surgeon's innate ability. The human proficiency-gain curve is a sigmoidal logistic curve and is here drawn to demonstrate variability among three hypothetical surgeons. Surgeon C learns at a faster rate than Surgeons B and A, but peaks along the proficiency-gain curve early. Surgeon B gains proficiency very similar to Surgeon C, but then reaches a lower plateau than Surgeon A. Finally, Surgeon A takes the longest to rise along the proficiency-gain curve, but eventually surpasses the other two surgeons. Just as surgeons exhibit different learning abilities, machine systems also share similar variances. Cloud-based systems may be able to achieve machine learning capability that significantly exceeds the ability of conventional computer systems

important suppositions need to be made before we can understand these relationships. First, we will assume that cloud computing capacity is near infinite. Second, theoretically, the number of cloud-connected robots, capable of machine learning activity, has no upper bound (R_1, R_2, $R_3 \ldots R_{n+1}$). And third, the number of machine-learnable tasks or events related to the field of all surgery and anatomy is expanding and is likewise unbounded. In this model, one could envision a common-brained system which continues to expand and, with each incremental increase in the number of ML capable robots, will grow to orders of magnitude beyond non-cloud-based robots.

In a cloud-based surgical system with a common compute brain, incremental learning of a machine can be viewed as function of two covariates, specifically the number of surgical robotics (R) in operation (at either a single center or at multiple hospitals in separate geographic locations) and the number of procedures (*P*) each system performs over time. This implies that machine learning of a common brain increases based on the number of active surgical robots R and the number of procedures *P* for a given cloud system.

Network architecture can significantly impact overall machine learning ability. A cloud robotic approach could, as discussed, be particularly useful. Conceptually, this is a very different methodology for machine learning, because it implies that a cloud *common-brain surgical robotic system increases the collective learning as more robotic systems are added to the system. As each individual robot masters any given ML task, then all robots gain mastery of the same task.* Stated another way, the more robots there are learning, the greater the collective skill of each cloud-based robot. Therein lies the rationale for understanding the power and scalability of cloud robotics.

We can think about machine learning from a mathematical point of view. Suppose we have a single robot with ML capability. It is known that ML models improve as the number of training samples increase [86]. Often this improvement takes the shape of an inverse power-law curve [87–89], as follows:

$$\delta(t) = b - a(rt)^{-k}$$

where $\delta(t)$, or machine proficiency/skill, increases as a function of the number of operations over time rt, where r is the operation rate per unit of time, $k > 0$, $a > 0$, and b can be arbitrarily defined. Thus, for a single robot learning a single skill, the learning and proficiency can be illustrated in Fig. 4.8 (*for* $a = 1$; $b = 0.99$; $r = 1$; *and* $k = 0.50$). With cloud robots, we accumulate training samples for an operation at a rate N times higher than the single robot case. Consequently, skill would increase more sharply and would be expected to stay higher asymptotically since the total number of training samples would be higher. Figure 4.9 illustrates the relative difference in skill acquisition for 20 cloud robots. For multiple operations (i.e., multiple skills or learned robotic tasks), a single robot has $\frac{1}{20}$ the learning capacity at any given time, relative to $N = 20$ cloud-based robots. Mathematically, this can be expressed as follows:

$$\text{single robot}: \delta(t) = b - a(\lambda t)^{-k}$$

$$20\,\text{Cloud robots}: \delta(t) = b - a(20\lambda t)^{-k}$$

Here, λ represents the operation or learning rate for a single surgical robot. With multiple cloud robots, each one of which is learning a different operation, or type of procedure *P,* the *total* skill *S* (robotic ability for all operative tasks) will continue to increase with *P* and can be defined as:

$$S(t) = \sum_{P}^{i=1} \delta\mathrm{i}(t)$$

where $\delta\mathrm{i}(t)$ is the skill level at time t for procedure i. Thus, $S(t)$ is the sum of all robotic skills (i.e., machine learning) across *all* procedure types (*P*). This is possible, because cloud robots share a common brain. The difference in skill acquisition for $P = 1$ versus $P = 10$ is illustrated graphically in Fig. 4.10. If the number of robots in the system and types of procedures performed grow linearly over time and *P* is unbounded, mathematical modeling predicts that the learning of the machine will eclipse that of a human (Fig. 4.11).

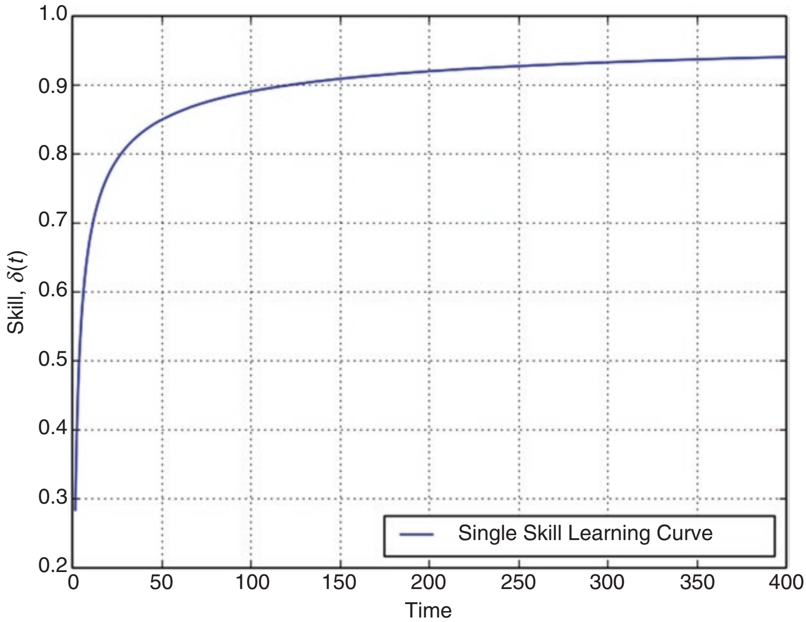

Fig. 4.8 Machine learning improves as a function of the number of training samples. Mathematically, this relationship can be expressed as $\delta(t) = b - a(rt)^{-k}$, where $\delta(t)$, or machine proficiency/skill, increases as a function of the number of operations over time. In this graph, the single robot learning a single skill is illustrated (*for* $a = 1$, $b = 0.99$, r=1, *and* $k = 0.50$). The graph takes on the shape of the inverse power-law curve and is quite typical for single machine learning

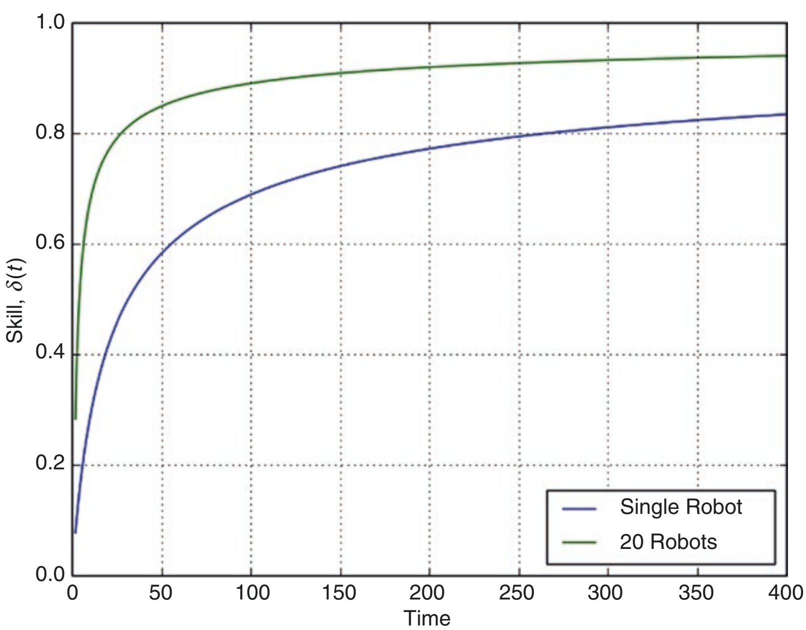

Fig. 4.9 If learning for a single machine or robot can be expressed as $\delta(t) = b - a(\lambda t)^{-k}$, then for 20 cloud-connected robots, the graph would exhibit a higher plateau and would be expressed by $\delta(t) = b - a(20\lambda t)^{-k}$. This illustrates the asymptotic increase in the rate of ML for multiple (in this example, 20) cloud-connected robots versus ML for a single conventional robot. Here, λ represents the operation or learning rate for a single robot. In this example, $a = 1$, $b = 0.99$, and $k = 0.5$

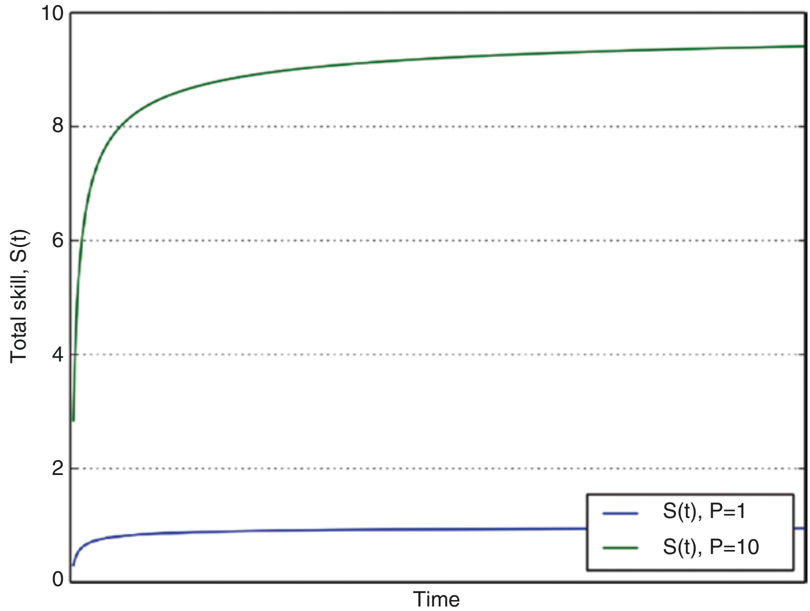

Fig. 4.10 The overall learning potential of a cloud robotic system is dependent on the number of procedures (*P*) which a robot is able to learn. This graph illustrates the relative difference in overall learning for a robot that is set to learn only a single procedure ($P = 1$), versus a robot, or system of robots, which is able to learn ten procedures ($P = 10$). This can be expressed as $S(t) = \sum_{P}^{i=1} \delta i(t)$, whereby $\delta i(t)$ is the skill level at time *t* for procedure *i*. Thus, $S(t)$ is the sum of all machine learning across *all* procedure types (*P*)

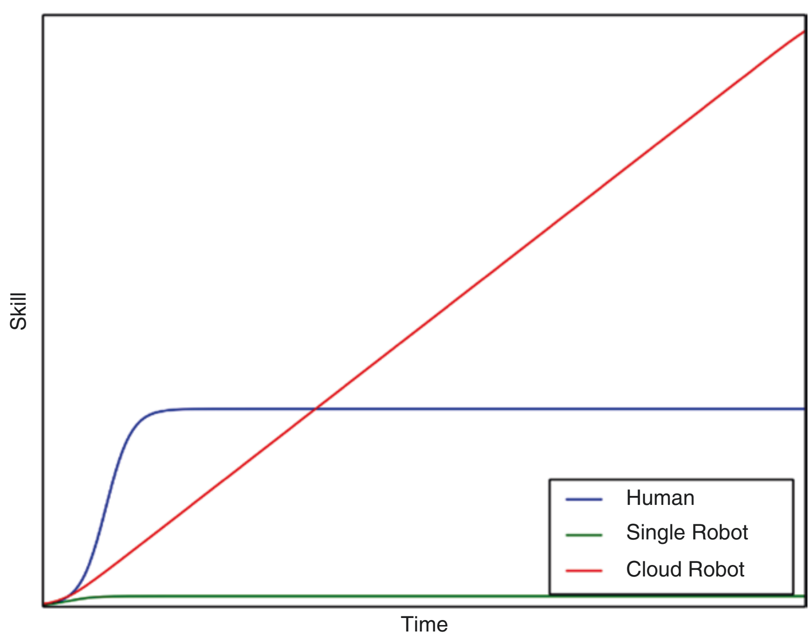

Fig. 4.11 Projected models illustrate different learning curves for a human, a single robotic system, and a cloud robotic system. For a single robotic system and a single learnable task, learning plateaus early and the overall learning is finite. For any surgeon, the learning of all procedures increases over time and is modeled based on a proficiency-gain curve which is fundamentally sigmoidal. Cloud robots exhibit the ability to learn via a common compute brain, and if one assumes that the number of robots learning procedures continues to increase, then there will be no upper bound to the machine learning capability

A Paradigm for Cloud Robotic Surgery

In this section, a service-oriented architecture [90] to realize a cloud surgical solution is presented in theory. Assume there exists a common cloud robotic surgical platform that is physically capable of performing any operation with varying levels of autonomy. Such a system could be designed such that there are two distinct modes: training mode and operating mode. In training mode, a surgeon manually delineates the steps of the procedure – annotating structures in the field of view. During the operation, all input streams are recorded and transmitted to a training data capture service in the cloud as a type of ESR. With *N* such robots (*R*), the overall architecture of the system would appear as depicted in Fig. 4.12.

In operating mode, the surgical robot is provided with information regarding the operation being performed and patient-specific data. Next, an operating skill service in the cloud downloads the ML models (i.e., neural networks) and configuration information necessary to drive the robot and assist the surgeon in performing the operation with variable autonomy, thereby augmenting the perception of complex surgical fields. The corresponding cloud architecture for this is illustrated in Fig. 4.13.

In this framework there exists a key service which is responsible for generating ML models (i.e., surgical skills) and storing them for use by robots using a *skill storage service.* In particular, for each operation type and, on a regular basis, it builds an ML model and stores it in the skill storage service. The model is built by querying the training data storage service for training samples for the operation in question then using the appropriate ML algorithms to generate the actual model(s) for each step of the surgery or for a given surgical task. Intuitively, we can think of this as follows: Given 1000 training datasets for any operation which can be decomposed into video definable steps (such as for laparoscopic cholecystectomy), the *skill generation service* would analyze the first 800 examples and then use the model created to manipulate controls in simulation for the next 200 training examples. Next, the *skill generation service* would find the model(s) that produce(s) the minimum error between the

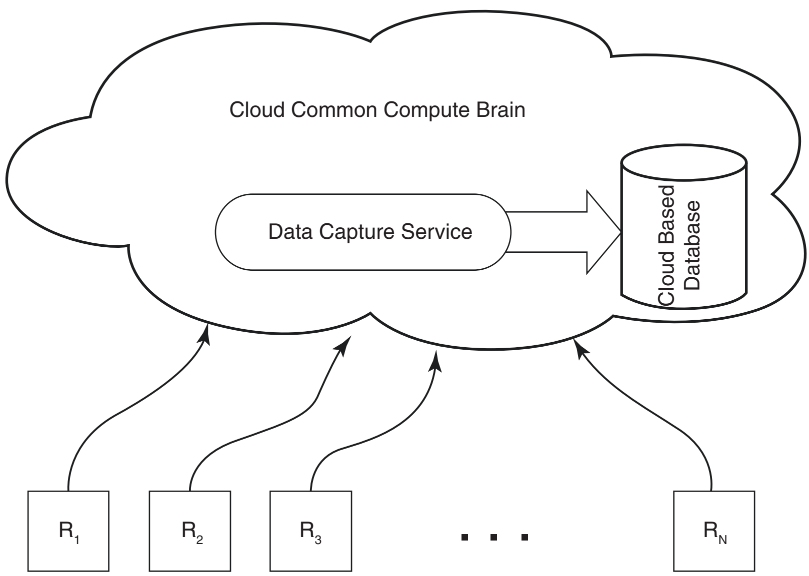

Fig. 4.12 Cloud-based robotics are elastic and thus highly scalable to the *N* number of robots in a given system. As illustrated, robots (R) are trained on various operating procedures. This data is then captured in the common cloud, allowing it to be shared and accessed by any given robot at any time. Information is uploaded to a data capture service where the data can be both stored and analyzed and maintained in a cloud database. This provides an ideal framework for AI and ML in surgery

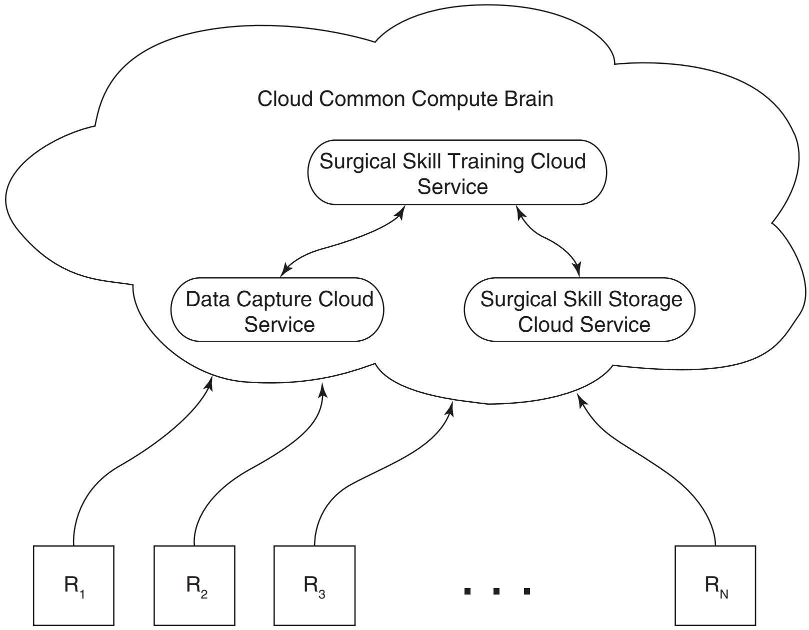

Fig. 4.13 Within a common compute brain shared among all surgical robots, services for machine learning can include a service for data capture and surgical skill storage. This would be part of a larger, adaptive service, the surgical skill cloud training service. Fundamental to this architecture is the offloading of computational work onto to the cloud and, at the same time, centralizing computing so that it is globally available to any machine and to any digital surgical system

surgeon's known control inputs (or decision points) and the computer-generated ones – storing the best model for later use.

Conclusions

The cloud is well suited for high-scale computational tasks necessary for the integration of AI and ML into tomorrow's surgical suite. It provides a powerful framework capable of supporting next-generation robots in operating theaters and will more generally help expand the role of AI and ML in medicine and surgery. The near infinite capacity for data storage and computation and the ability to link surgical robots with a common brain achieves a collective learning which exceeds the ability of conventional systems. Thus, the cloud can be viewed as a gateway to digital surgery.

References

1. Jadeja Y, Modi K. Cloud computing-concepts, architecture and challenges. International conference on computing, electronics and electrical technologies (ICCEET). IEEE; 2012. p. 877–80.
2. Regalado A. Who coined 'cloud computing'? Technol Rev. 2011;31.
3. Erl T, Puttini R, Mahmood Z. Cloud computing: concepts, technology & architecture. Westford, MA, USA: Pearson Education; 2013.
4. Qian L, Luo Z, Du Y, Guo L. Cloud computing: an overview. In: IEEE international conference on cloud computing. Berlin, Heidelberg: Springer; 2009. p. 626–31.
5. Dijkstra EW. A note on two problems in connexion with graphs. Numer Math. 1959;1(1):269–71.
6. Duckham M, Kulik L. "Simplest" paths: automated route selection for navigation. In: International conference on spatial information theory. Berlin, Heidelberg: Springer; 2003. p. 169–85.
7. Nazari S, Meybodi MR, Salehigh MA, Taghipour S. An advanced algorithm for finding shortest path in car navigation system. In: 2008 first international conference on intelligent networks and intelligent systems. New York City, NY, USA: IEEE; 2008. p. 671–4.
8. Wang H, Yu Y, Yuan Q. Application of Dijkstra algorithm in robot path-planning. In: 2011 second international conference on mechanic automation and control engineering. New York City, NY, USA: IEEE; 2011. p. 1067–9.
9. Paul U, Subramanian AP, Buddhikot MM, Das SR. Understanding traffic dynamics in cellular data networks. In: 2011 Proceedings IEEE INFOCOM. New York City, NY, USA:IEEE; 2011. p. 882–90.
10. Hawley J. GeoDNS—geographically-aware, protocol-agnostic load balancing at the DNS level. In: Proceedings of the linux symposium. p. 123–30. https://www.linuxsecrets.com/kdocs/ols/2009/ols2009-pages-123-130.pdf.
11. Moore G. Moore's law. Electronics Magazine. 1965;38(8):114.
12. Mack CA. Fifty years of Moore's law. IEEE Trans Semicond Manuf. 2011;24(2):202–7.

13. Schaller RR. Moore's law: past, present and future. IEEE Spectr. 1997;34(6):52–9.
14. Keyes RW. The impact of Moore's law. IEEE Solid-State Circuits Soc Newsletter. 2006;11(3):25–7.
15. Waldrop MM. The chips are down for Moore's law. Nature News. 2016;530(7589):144.
16. Lundstrom M. Moore's law forever? Science. 2003;299(5604):210–1.
17. Kish LB. End of Moore's law: thermal (noise) death of integration in micro and nano electronics. Phys Lett A. 2002;305(3–4):144–9.
18. Borkar S. Obeying Moore's law beyond 0.18 micron [microprocessor design]. In: Proceedings of 13th annual IEEE international ASIC/SOC conference (Cat. No. 00TH8541). New York City, NY, US: IEEE; 2000. p. 26–31.
19. Compton AH. A quantum theory of the scattering of X-rays by light elements. Phys Rev. 1923; 21(5):483.
20. Powell JR. The quantum limit to Moore's law. Proc IEEE. 2008;96(8):1247–8.
21. Theis TN, Wong HS. The end of Moore's law: a new beginning for information technology. Comput Sci Eng. 2017;19(2):41.
22. Roberts LG. Beyond Moore's law: internet growth trends. Computer. 2000;33(1):117–9.
23. Meindl JD. Beyond Moore's law: the interconnect era. Comput Sci Eng. 2003;5(1):20–4.
24. Schwartz WB. Medicine and the computer. The promise and problems of change. N Engl J Med. 1970;283(23):1257–64.
25. Schwartz WB, Patil RS, Szolovits P. Artificial intelligence in medicine. Where do we stand? N Engl J Med. 1987;316(11):685–8.
26. Topol EJ. High-performance medicine: the convergence of human and artificial intelligence. Nat Med. 2019;25(1):44.
27. LeCun Y, Bengio Y, Hinton G. Deep learning. Nature. 2015;521(7553):436–44. https://doi.org/10.1038/nature14539.
28. Hinton G. Deep learning-A technology with the potential to transform health care. JAMA. 2018;320(11):1101–2. https://doi.org/10.1001/jama.2018.11100.
29. Beam AL, Kohane IS. Big data and machine learning in health care. JAMA. 2018;319(13):1317–8. https://doi.org/10.1001/jama.2017.18391.
30. Rajkomar A, Dean J, Kohane I. Machine learning in medicine. N Engl J Med. 2019;380(14):1347–58. https://doi.org/10.1056/NEJMra1814259.
31. Ferrucci D, Brown E, Chu-Carroll J, Fan J, Gondek D, Kalyanpur AA, Lally A, Murdock JW, Nyberg E, Prager J, Schlaefer N. Building Watson: an overview of the DeepQA project. AI Mag. 2010;31(3):59–79.
32. Esteva A, Kuprel B, Novoa RA, Ko J, Swetter SM, Blau HM, Thrun S. Dermatologist-level classification of skin cancer with deep neural networks. Nature. 2017;542(7639):115–8. https://doi.org/10.1038/nature21056. Epub 2017 Jan 25.
33. Nistér D, Naroditsky O, Bergen J. Visual odometry. In: Proceedings of the 2004 IEEE computer society conference on computer vision and pattern recognition, 2004. CVPR 2004, vol. 1. New York City, NY, USA: IEEE; 2004. p. I.
34. Howard TM, Morfopoulos A, Morrison J, Kuwata Y, Villalpando C, Matthies L, McHenry M. Enabling continuous planetary rover navigation through FPGA stereo and visual odometry. In: 2012 IEEE aerospace conference: IEEE; 2012. p. 1–9.
35. Bojarski M, Del Testa D, Dworakowski D, Firner B, Flepp B, Goyal P, Jackel LD, Monfort M, Muller U, Zhang J, Zhang X. End to end learning for self-driving cars. arXiv preprint arXiv:1604.07316. 2016.
36. Dissanayake MG, Newman P, Clark S, Durrant-Whyte HF, Csorba M. A solution to the simultaneous localization and map building (SLAM) problem. IEEE Trans Robot Autom. 2001;17(3):229–41.
37. Guivant JE, Nebot EM. Optimization of the simultaneous localization and map-building algorithm for real-time implementation. IEEE Trans Robot Autom. 2001;17(3):242–57.
38. Leonard JJ, Durrant-Whyte HF. Simultaneous map building and localization for an autonomous mobile robot. In: Proceedings IROS'91: IEEE/RSJ international workshop on intelligent robots and systems' 91: IEEE; 1991. p. 1442–7.
39. Montemerlo M, Thrun S, Koller D, Wegbreit B. FastSLAM: A factored solution to the simultaneous localization and mapping problem. AAAI/IAAI. 2002;593–8.
40. Newcombe RA, Izadi S, Hilliges O, Molyneaux D, Kim D, Davison AJ, Kohli P, Shotton J, Hodges S, Fitzgibbon AW. Kinectfusion: real-time dense surface mapping and tracking. In: ISMAR. Vol. 11, No. 2011. New York City, NY, USA: IEEE; 2011. p. 127–36.
41. Newcombe RA, Lovegrove SJ, Davison AJ. DTAM: dense tracking and mapping in real-time. In: 2011 international conference on computer vision. New York City, NY, USA: IEEE; 2011. p. 2320–7.
42. Yamamoto Y, Pirjanian P, Munich M, DiBernardo E, Goncalves L, Ostrowski J, Karlsson N. Optical sensing for robot perception and localization. In: IEEE workshop on advanced robotics and its social impacts, 2005. New York City, NY, USA: IEEE; 2005. p. 14–7.
43. Turan M, Almalioglu Y, Konukoglu E, Sitti M. A deep learning based 6 degree-of-freedom localization method for endoscopic capsule robots. arXiv preprint arXiv:1705.05435. 2017.
44. Turan M, Almalioglu Y, Araujo H, Konukoglu E, Sitti M. A non-rigid map fusion-based direct slam method for endoscopic capsule robots. Int J Intelligent Robot Appl. 2017;1(4):399–409.
45. Lin B. Visual SLAM and surface reconstruction for abdominal minimally invasive surgery. 2015. Graduate Theses and Dissertations. https://scholarcommons.usf.edu/etd/5849.
46. Lin B, Sun Y, Qian X, Goldgof D, Gitlin R, You Y. Video-based 3D reconstruction, laparoscope localization and deformation recovery for abdominal minimally invasive surgery: a survey. Int J Med Robot Comput Assist Surg. 2016;12(2):158–78.

47. Peters BS, Armijo PR, Krause C, Choudhury SA, Oleynikov D. Review of emerging surgical robotic technology. Surg Endosc. 2018;32(4):1636–55.
48. Atallah S, Parra-Davila E, Melani AGF. Assessment of the Versius surgical robotic system for dual-field synchronous transanal total mesorectal excision (taTME) in a preclinical model: will tomorrow's surgical robots promise newfound options? Tech Coloproctol. 2019;23(5):471–7. https://doi.org/10.1007/s10151-019-01992-1. Epub 2019 May 8.
49. Wu C. Towards linear-time incremental structure from motion. In: 2013 international conference on 3D vision-3DV 2013. New York City, NY, USA: IEEE; 2013. p. 127–34.
50. Burschka D, Li M, Ishii M, Taylor RH, Hager GD. Scale-invariant registration of monocular endoscopic images to CT-scans for sinus surgery. Med Image Anal. 2005;9(5):413–26.
51. Chen PD, Hu RH, Liang JT, Huang CS, Wu YM. Toward a fully robotic surgery: performing robotic major liver resection with no table-side surgeon. Int J Med Robot. 2019;15(2):e1985. https://doi.org/10.1002/rcs.1985. Epub 2019 Feb 17.
52. Panesar S, Cagle Y, Chander D, Morey J, Fernandez-Miranda J, Kliot M. Artificial intelligence and the future of surgical robotics. Ann Surg. 2019;270(2):223–6. https://doi.org/10.1097/SLA.0000000000003262.
53. Hashimoto DA, Rosman G, Rus D, Meireles OR. Artificial intelligence in surgery: promises and perils. Ann Surg. 2018;268(1):70–6. https://doi.org/10.1097/SLA.0000000000002693.
54. Mezger U, Jendrewski C, Bartels M. Navigation in surgery. Langenbeck's Arch Surg. 2013;398:501–14.
55. Hashimoto DA, Rosman G, Witkowski ER, Stafford C, Navarette-Welton AJ, Rattner DW, Lillemoe KD, Rus DL, Meireles OR. Computer vision analysis of intraoperative video: automated recognition of operative steps in laparoscopic sleeve gastrectomy. Ann Surg. 2019; https://doi.org/10.1097/SLA.0000000000003460. [Epub ahead of print].
56. Leonard S, Wu KL, Kim Y, Krieger A, Kim PC. Smart tissue anastomosis robot (STAR): A vision-guided robotics system for laparoscopic suturing. IEEE Trans Biomed Eng. 2014;61(4):1305–17.
57. Shademan A, Decker RS, Opfermann JD, Leonard S, Krieger A, Kim PC. Supervised autonomous robotic soft tissue surgery. Sci Transl Med. 2016;8(337):337ra64. https://doi.org/10.1126/scitranslmed.aad9398.
58. Hu G, Tay WP, Wen Y. Cloud robotics: architecture, challenges and applications. IEEE Netw. 2012;26(3):21–8.
59. Kehoe B, Patil S, Abbeel P, Goldberg K. A survey of research on cloud robotics and automation. IEEE Trans Autom Sci Eng. 2015;12(2):398–409.
60. Goldberg K, Kehoe B. Cloud robotics and automation: a survey of related work. EECS Department, University of California, Berkeley, Tech. Rep. UCB/EECS-2013-5; 2013.
61. Wan J, Tang S, Yan H, Li D, Wang S, Vasilakos AV. Cloud robotics: current status and open issues. IEEE Access. 2016;4:2797–807.
62. Quintas J, Menezes P, Dias J. Cloud robotics: towards context aware robotic networks. In: International conference on robotics; 2011. p. 420–7. Available online at: https://home.isr.uc.pt/~jorge/wp-content/uploads/OP242.pdf.
63. Kamei K, Nishio S, Hagita N, Sato M. Cloud networked robotics. IEEE Netw. 2012;26(3):28–34.
64. Turnbull L, Samanta B. Cloud robotics: formation control of a multi robot system utilizing cloud infrastructure. In: 2013 Proceedings of IEEE Southeastcon. New York City, NY, USA: IEEE; 2013. p. 1–4.
65. Du Z, He L, Chen Y, Xiao Y, Gao P, Wang T. Robot cloud: bridging the power of robotics and cloud computing. Futur Gener Comput Syst. 2017;74:337–48.
66. Goldberg K, Siegwart R, editors. Beyond Webcams: an introduction to online robots. Cambridge, MA, USA: MIT Press; 2002.
67. Inaba M, Kagami S, Kanehiro F, Hoshino Y, Inoue H. A platform for robotics research based on the remote-brained robot approach. Int J Robot Res. 2000;19(10):933–54.
68. Waibel M, Beetz M, Civera J, d'Andrea R, Elfring J, Galvez-Lopez D, Häussermann K, Janssen R, Montiel JM, Perzylo A, Schiessle B. Roboearth-a world wide web for robots. IEEE Robotics Automation Magazine (RAM), Special Issue Towards a WWW for Robots. 2011;18(2):69–82.
69. Arumugam R, Enti VR, Bingbing L, Xiaojun W, Baskaran K, Kong FF, Kumar AS, Meng KD, Kit GW. DAvinCi: A cloud computing framework for service robots. In: 2010 IEEE international conference on robotics and automation. New York City, NY, USA: IEEE; 2010. p. 3084–9.
70. Mohanarajah G, Hunziker D, D'Andrea R, Waibel M. Rapyuta: A cloud robotics platform. IEEE Trans Autom Sci Eng. 2014;12(2):481–93.
71. Aguiar RL, Gomes D, Barraca JP, Lau N. Cloud thinking as an intelligent infrastructure for mobile robotics. Wirel Pers Commun. 2014;76(2):231–44.
72. Goldenberg MG, Jung J, Grantcharov TP. Using data to enhance performance and improve quality and safety in surgery. JAMA Surg. 2017;152(10):972–3. https://doi.org/10.1001/jamasurg.2017.2888.
73. Grantcharov TP, Yang KL, inventors; Surgical Safety Technologies Inc, Assignee. Operating room blackbox device, system, method and computer readable medium for event and error prediction. United States patent application US 15/561,877. 2018.
74. Gambadauro P, Magos A. Surgical videos for accident analysis, performance improvement, and complication prevention: time for a surgical black box? Surg Innov. 2012;19(1):76–80.
75. Guerlain S, Adams RB, Turrentine FB, Shin T, Guo H, Collins SR, Calland JF. Assessing team performance in the operating room: development and use of a "black-box" recorder and other tools for the intraoperative environment. J Am Coll Surg. 2005;200(1):29–37.
76. Murdoch TB, Detsky AS. The inevitable application of big data to health care. JAMA. 2013;309(13):1351–2.

77. Dikaiakos MD, Katsaros D, Mehra P, Pallis G, Vakali A. Cloud computing: distributed internet computing for IT and scientific research. IEEE Internet Comput. 2009;13(5):10–3.
78. Nickolov P, Armijo B, Miloushev V, Inventors; CA Inc, Assignee. Globally distributed utility computing cloud. United States patent US 9,578,088. 2017.
79. Strom N. Scalable distributed DNN training using commodity GPU cloud computing. In: Sixteenth annual conference of the International Speech Communication Association. 2015. Available online at: https://www.isca-speech.org/archive/interspeech_2015/papers/i15_1488.pdf.
80. Skala K, Davidovic D, Afgan E, Sovic I, Sojat Z. Scalable distributed computing hierarchy: cloud, fog and dew computing. Open J Cloud Computing (OJCC). 2015;2(1):16–24.
81. Jonas E, Pu Q, Venkataraman S, Stoica I, Recht B. Occupy the cloud: distributed computing for the 99%. In: Proceedings of the 2017 symposium on cloud computing. New York, NY,USA: ACM; 2017. p. 445–51.
82. Zhang Q, Cheng L, Boutaba R. Cloud computing: state-of-the-art and research challenges. J Internet Services Appl. 2010;1(1):7–18.
83. Amdahl GM. Validity of the single processor approach to achieving large scale computing capabilities. In: Proceedings of the April 18–20, 1967, spring joint computer conference. New York, NY,USA: ACM; 1967. p. 483–5.
84. JoSEP AD, KAtz R, KonWinSKi A, Gunho LE, Patterson D, Rabkin A. A view of cloud computing. Communications ACM. 2010;53(4):50–8.
85. Vecchiola C, Pandey S, Buyya R. High-performance cloud computing: a view of scientific applications. In: 2009 10th international symposium on pervasive systems, algorithms, and networks. New York, NY, USA: IEEE; 2009. p. 4–16.
86. Banko M, Brill E. Scaling to very very large corpora for natural language disambiguation. In: Proceedings of the 39th annual meeting on association for computational linguistics. Stroudsburg,PA,USA: Association for Computational Linguistics; 2001. p. 26–33.
87. Mukherjee S, Tamayo P, Rogers S, Rifkin R, Engle A, Campbell C, Golub TR, Mesirov JP. Estimating dataset size requirements for classifying DNA microarray data. J Comput Biol. 2003;10(2):119–42.
88. Hwang EJ, Jung JY, Lee SK, Lee SE, Jee WH. Machine learning for diagnosis of hematologic diseases in magnetic resonance imaging of lumbar spines. Sci Rep. 2019;9(1):6046.
89. Johnson M, Anderson P, Dras M, Steedman M. Predicting accuracy on large datasets from smaller pilot data. In: Proceedings of the 56th annual meeting of the Association for Computational Linguistics, vol. 2: Short Papers; 2018. p. 450–5. Available online at: https://www.aclweb.org/anthology/P18-2072.pdf.
90. Seth A, Singla AR, Aggarwal H. Service oriented architecture adoption trends: a critical survey. In: International conference on contemporary computing. Berlin, Heidelberg: Springer; 2012. p. 164–75.
91. Stépán G. Instability caused by delay in robot systems. Periodica Polytechnica Mech Eng. 1989;33(1–2):37–44.
92. Buzurovic I, Debeljkovic DL, Misic V, Simeunovic G. Stability of the robotic system with time delay in open kinematic chain configuration. Acta Polytechnica Hungarica. 2014;11(8):45–64.
93. Behnke S, Egorova A, Gloye A, Rojas R, Simon M. Predicting away robot control latency. In: Robot soccer world cup. Berlin, Heidelberg: Springer; 2003. p. 712–9.

5 Quantum Theory and Computing for Surgeons

Sam Atallah and Asa B. Atallah

Introduction to Quantum Mechanics

What we observe is not nature itself, but nature exposed to our method of questioning

Werner Heisenberg
W. Heisenberg (1901–1976) was awarded the Nobel Prize in physics in 1932 for his work on quantum mechanics published in 1925, when he was 24 years old.

In this chapter, we present some of the fundamental principles of quantum physics, intended for practicing surgeons and non-physicists. It will provide a foundation for understanding of quantum computing. Many of the inherent concepts known to us from Newtonian and classical mechanics differ in the field of quantum mechanics [1–5]. For example, in classical physics, everything in our observable universe is composed of either matter or waves. However, in the quantum universe, it is known that particles can exhibit wavelike behavior. Moreover, particles and waves are not mutually exclusive. Thus, waves can behave as particles – discrete packets of light (i.e., photons), as demonstrated prior to the era of quantum mechanics in the early 1900s by Einstein with the photoelectric effect [6]. Conversely, particles can behave as waves (not meaning particles can move in a wavelike pattern, but rather *be* a wave). Quantum theory predicts that everything in our universe can be modeled as "both matter and wave" in a superposition of states, as demonstrated by the Davisson-Germer double-slit experiment (Fig. 5.1) [7]. The "electron as a wave" behavior would later be shown to be dependent on whether or not (and how) the system was being observed, which remains one of the most puzzling enigmas of quantum physics to this day [8–11].

In quantum physics, the wave-matter relationship can be expressed by the de Broglie wavelength. This is precisely the same as the Compton wavelength λc [12] for light discussed in the previous chapter, except it is defined for an electron, λe [13], and can be expressed as a wavelength $\lambda e = \frac{h}{p}$ where again h is Planck's constant and p is the momentum of the electron (the same equation is applied for light, but since photons have no rest mass, there is another, more complex expression for determining momentum when traveling near the speed of light, that is beyond the scope of this discussion). In simple terms, this tells us not only that an electron behaves as a wave (as demonstrated by the double-slit experiment) but also that it behaves as a wave with a discrete and measurable wavelength. Thus, electrons are both matter and wave and, in the realm of quantum mechanics, exist in a superposition of states.

S. Atallah (✉)
College of Medicine, University of Central Florida, Orlando, FL, USA
e-mail: atallah@post.harvard.edu

A. B. Atallah
Apple Inc., Los Gatos, CA, USA

S. Atallah (ed.), *Digital Surgery*, https://doi.org/10.1007/978-3-030-49100-0_5

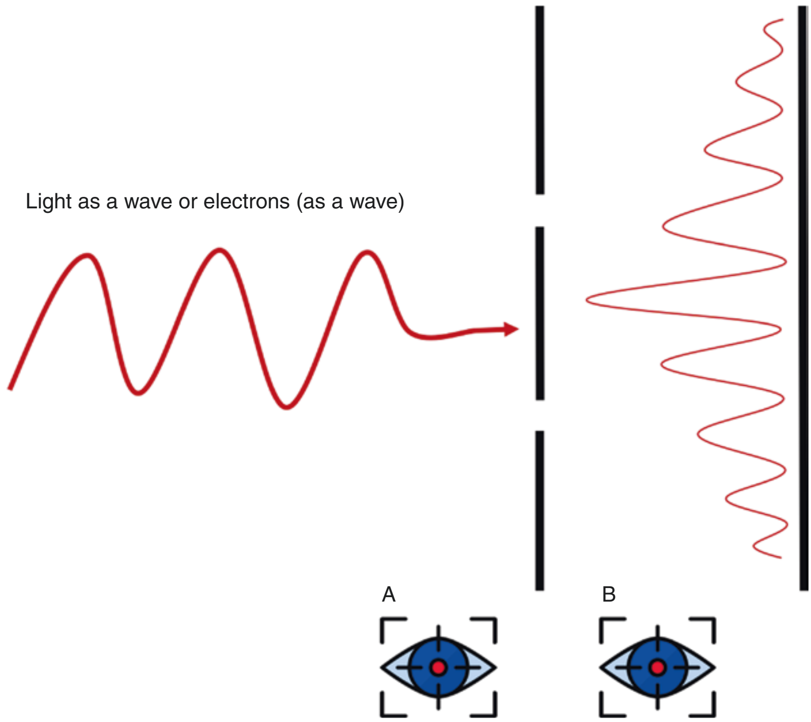

Fig. 5.1 The double-slit experiment is one of the most fundamental experiments to the understanding of quantum mechanics and particle behavior. Here, light (an electromagnetic wave) or electrons (particles) are directed toward the double slits, as shown, using either a light source or an electron gun. Since light is a wave, when it passes through the two slits, it creates an interference pattern. In classical physics, any wave (ocean waves, etc.) will create the same pattern when passing through two slits. Particles, however, are predicted to create no interference pattern, and rather just two discrete bands – correlating with the position of the two slits. However, electrons, instead of exhibiting particle-like behavior, act as a wave and create an interference pattern on the screen. This ability of particles to behave as a wave sometimes and as a particle at other times represents a superposition of states that underlies a core principle of quantum mechanics. Another important principle in quantum physics is that the very act of observing or measuring a system affects the outcome. In this double-slit experiment, for example, if an observer (A) attempts to "see" which slit the electrons are going through, the electrons revert back to behaving as particles, and two discrete bands appear on the screen, not an interference pattern. Even if one tries to observe the electrons *after* they pass through the double slits (Observer B), the interference pattern will be replaced by two bands as the electrons revert to behaving as particles, as if they "know they are being watched," and when they are being watched, we only observe particle-like behavior. This remains a perplexing property in quantum mechanics that scientists still do not fully understand

Quantum Spin and Superposition

From particle physics, it is known that atoms and electrons possess tiny magnetic fields, and this creates an orientation equitable to the north and south poles of two traditional magnets. This is called "spin" in quantum physics, and is not totally unfamiliar to medical scientists and physicians since it is the basis of magnetic resonance imaging (MRI), developed in 1947 by Felix Bloch and Edward Mills Purcell, which manipulates the hydrogen proton spin orientation in living tissue to derive useful data [14, 15]. In essence, atomic spin controlled by magnetic fields and radio waves is used to determine the nature of tissue, for the purpose of medical imaging without subjecting patients to harmful, ionizing radiation. Particle spin is fundamental to quantum mechanics and quantum computing as well.

In 1924, the spin properties of matter were first explored in the context of quantum physics. That year, Stern and Gerlach performed a landmark study on the atomic spin: Today, it is known as the Stern-Gerlach experiment [16, 17]. They used silver (Ag) atoms, which have 47 electrons, with only one in the outermost orbital according to the Bohr atomic model [18]. While the other electrons in orbit around the nucleus cancel their magnetic fields, the outer electron does not, which creates a small magnetic field. Thus, Ag atoms become tiny magnets with north and south poles. At the time of the experiment, very little was understood about atomic and electron magnetic fields, but as we will see later, this turns out to be a fundamental part of quantum computing because it allows particles to be used as bits of information. In the Stern-Gerlach experiment, Ag atoms were delivered as a beam between two magnets, as shown in Fig. 5.2. The position of the Ag atoms could then be detected on a screen. The south magnet was stronger than the north magnet; this essentially allowed the Ag atoms to be deflected by the magnetic field and thus spread out vertically along the detection screen. If the Ag atom has a north "up" spin, then it should be attracted to the south magnet, since it is stronger, and if an Ag atom has south "up" spin, the atom will be drawn more toward the north magnet because the repulsion of the south magnet is stronger.

But what about all of the atoms that are in some other random orientation? For example, what if the atom's north-south orientation was in some other direction (e.g., sideways)? Then, one would predict that it would fall in the center of

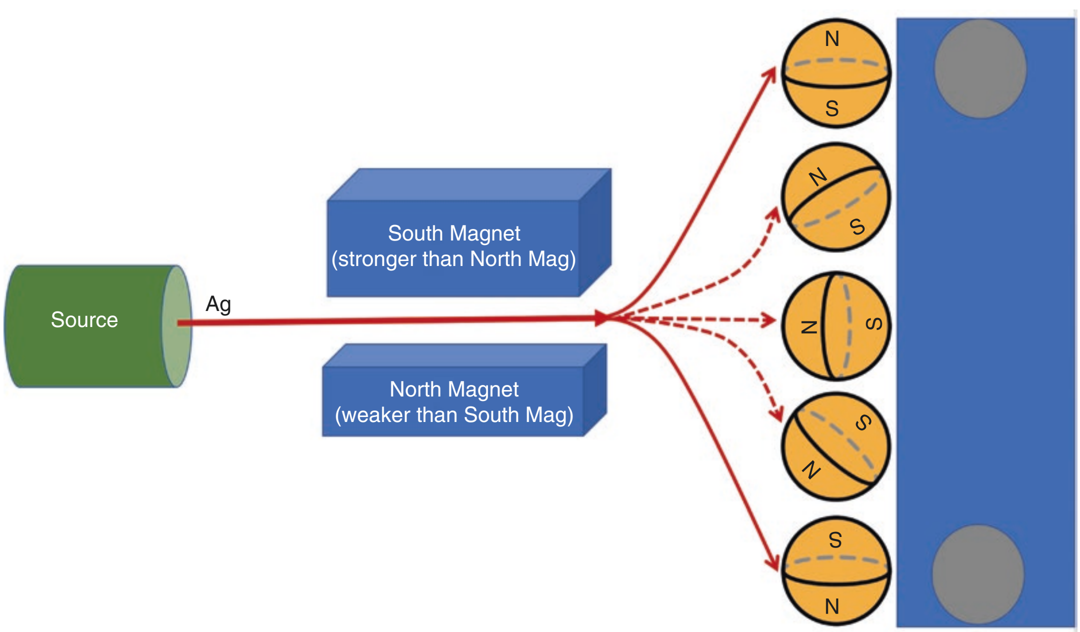

Fig. 5.2 The Stern-Gerlach experiment is illustrated. Silver atoms (Ag) are delivered as a beam between two magnets: a north and a relatively stronger, south magnet. Because Ag behaves as a tiny magnet itself, if the north pole of Ag is facing toward the (stronger) south pole, it is drawn to the far upper end of the screen, where it is recorded. If the Ag atom is oriented such that its south pole is facing the south magnet, then it is repelled more by the stronger south magnet, allowing it to be deflected toward the bottom of the screen. It was assumed that for every other orientation of Ag (where the north and south poles are not precisely up or down), the atoms would deflect to varying degrees to create a line along the detection screen (dashed red arrows). But this was not at all what was observed. Instead, Stern and Gerlach observed that only two points were found on the measuring screen. That is, the Ag atoms either behaved as north up or north down (spin up or spin down). This meant that atomic particles are quantized. In other words, quantum spin resolves to either up or down relative to the direction of measurement. This principle is fundamental to quantum theory and computing

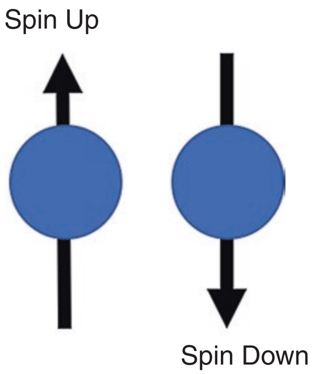

Fig. 5.3 Electrons and other quanta have a random chance of being measured in either the spin-up or spin-down position. While they may exist in a superposition of states prior to measurement, upon measuring their spin, they will resolve to either spin up or spin down (and nothing in between) relative to the direction of measurement. The ability to quantize or resolve particle spin to just two values (i.e., either up or down) means they can be used in a similar fashion to binary computer code, where data is either 0 or 1

the screen, and for every possible spin "direction" of the atom, a line should be created between the north *up* and north *down* ends. But this is not what was observed. Instead, Stern and Gerlach found only two dots on the screen – because the atom spin was *either* measured to be up or measured down – and nothing between the two. Thus, atomic spin is *quantized* (Fig. 5.3). It does not give a range of possibilities, but rather just two options: spin up or spin down. *The quantized nature of this output – upon measurement and relative to the direction of measurement – underlies the principle of quantum computing.*

There are a few additional findings that have been summarized from this and various other experiments. First, the probability of spin up or spin down for any given particle is completely random. Second, whether particle spin is up or down is not known *until it is measured.* Third, subsequent measurements may affect the particle's spin state. The latter is somewhat odd and altogether differs from classical physics. In quantum mechanics, if a particle's spin is found to be up, and you measure it again in the exact same way (method 1), it will have a 100% chance of being spin up, but if you measure it in another way (method 2), it may or not be spin up, as the measurement itself could affect the spin orientation. Now, if you go back and try and measure spin as you did before (method 1), you find that the outcome has returned to being random (50–50 probability of spin up). That is, somehow, *the actual act of measuring spin appears to impact the outcome* and thus the spin orientation.

For practicing surgeons, let's use an example to help clarify this point. Let's suppose we are measuring the quality of a surgical specimen, such as the quality of the mesorectal envelope after radical resection for rectal cancer. We ask Pathologist A to grade the specimen, and she states it is complete (intact mesorectal envelope). We ask her again, and she gives us the same answer: the specimen is intact. No matter how many times we ask Pathologist A to give us the specimen grade, it is always the same. Now, after we have had the grading by Pathologist A, we ask Pathologist B to measure the quality of resection, and he states that it is not completely intact, as there is a defect in the envelope. Imagine that we give the specimen back to Pathologist A, and now that she is shown the defect, she changes her mind and regrades the specimen as not intact. Thus, by changing how we measure something (in this case, which pathologist), we impact the outcome of the specimen grading, and this can affect (subsequently) the original grading by the first pathologist. This is essentially what we observe in quantum measurements. Although Stern and Gerlach used sliver atoms in their experiment, the same would apply for electrons, which also exhibit the same magnetic field and the same quantized spin values (i.e., spin up or spin down), allowing them to be useful for quantum computing. This will be addressed further in a later section.

Quantum Entanglement

Quantum entanglement [19–21] is an important part of quantum physics, and it represents a special relationship between certain particles. Entanglement has no correlate in classical physics [22]. When two quantum particles are entangled, a measurement of one particle predicts the measurement of the other particle. So, if an electron, for example, is measured to be spin up, then an entangled second electron will always be found to be spin down when measured, regardless of the physical distance that separates the two. To help us understand quantum entanglement, we will use a thought experiment from our more familiar world. Let us suppose that two quantum-entangled particles (electrons) are represented by two identical coins. Let us place each coin into identical boxes. Imagine that you take one of them and travel on a plane to the opposite side of the Earth, and I stay holding mine, right where I am. At a predetermined time, you and I will throw our coins out of their boxes and onto the ground. I will throw mine down first; then, it's your turn. If my coin lands on heads, then, due to quantum entanglement, I automatically know your coin has landed on tails. Likewise, you, although thousands of miles away from me, instantly know that since your coin landed on tails, mine has landed on heads. It does not matter how much distance separates the two entangled particles – the same would hold true if they were on opposite sides of the galaxy. As strange as this may seem, this "teleportation of information" is a proven property of quantum mechanics. It has also been elegantly proven by John S. Bell (and others) [23] that this is not a predetermined outcome that is "fixed ahead of time." That is, there is no communication medium between the two particles at a distance. Also note that the measurement of the first coin landing (heads or tails) is *completely random* since it has a 50–50 probability of landing or either side [24, 25]. Einstein had previously referred to this as "spooky action at a distance," and that quanta must possess some "hidden variables" that cause entanglement [26] (later disproven by Bell).

Quantum particle entanglement is an important reason for why quantum computing differs from classical computing, and it also underlies the principle of quantum teleportation [27–29]. Entangled qubits (discussed next) create associations that do not otherwise exist in classical computing, and this can help achieve calculation shortcuts that otherwise are not possible with conventional computational algorithms. Most notable of these quantum algorithms were ones developed by Shor and Grover [30–39].

Quantum Computing

With this background, we can begin to understand quantum computing [40–42]. While quantum physics was developed in the 1920s by a group of physicists (esp. E Schrodinger and W Heisenberg) [2, 5], the idea of quantum computing did not emerge until the mid-1980s, and mostly to the credit of R Feynman [43] and D Deutsch [44]. Quantum computing is a complex yet experimental approach that differs considerably from classical computing in methodology (Table 5.1). Classical computing is based on bits (BInary digiTS) of information that are either 0 or 1, representing whether a micro-transistor is in the ON or OFF state. Transistors can be either on or off (1 or 0), but, of course, cannot exist in both states at once. In quantum computing, however, 0 and 1 are determined by the measurement of particle spin. Such a unit of computing is known as a *quantum bit*, or *qubit*, and represents the north

Table 5.1 Classical versus quantum computing

Classical computing	Quantum computing
Binary output (0/1)	Binary output (0/1)
Unit of measurement: bit	Unit of measurement: qubit
One bit: either 0 or 1	One qubit: a superposition of 0 and 1
0 or 1: transistor on or off	0 or 1: particle (electron) spin $\|\uparrow\rangle$ or spin $\|\downarrow\rangle$
Only one type of computing	Different types of computing (quantum gate, annealing, universal)
Uses algorithms in a stepwise method to solve problems	Can solve entire problems at once
Stable system, not affected by environment	Highly vulnerable to external environment
Internet accessible	Internet accessible
Can be cloud-based	Can be cloud-based

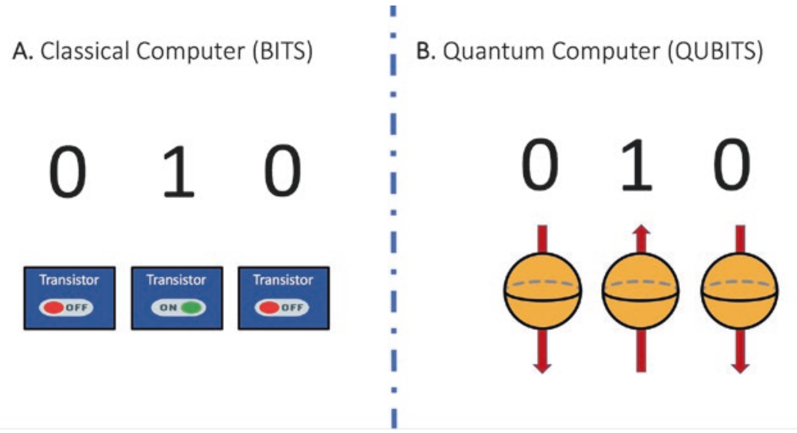

Fig. 5.4 Classical versus quantum computing. With classical computing, all data is represented using binary code. Specifically, bits of information (either 0 or 1) are determined by the on/off state of a micro-transistor. If the transistor is off, this represents a binary code of 0, and if it is on, it represents a binary code of 1. Quantum computing can also be reduced to binary code in this sense. However, rather than using manufactured transistors, quantum computers utilize natural atomic particles, such as electrons. This is because electrons, upon measurement, produce binary outcomes – that is, they are either measured to be spin |↑⟩ or spin |↓⟩. Thus, |↑⟩ can represent 1, and |↓⟩ can represent 0, making computation possible (sometimes, this is expressed as |1⟩ and |0⟩). When quantum spin in used in this manner, it represents data. The analogue of the classical bit (1,0), in quantum computing, is the qubit (|1⟩, |0⟩)

versus south "spin" of an electron (or any other atomic particle). From linear algebra, spin *up* is denoted as the vector |↑⟩, and spin *down* can be expressed as |↓⟩. So, an electron with spin |↑⟩ represents 1, while electron with spin |↓⟩ represents 0. Hence, quantum computers use *natural particles* (as opposed to manmade transistors) as the basic computational unit (Fig. 5.4). By using electrons – the smallest particle in the atomic model – quantum computers are quite literally able to function on an atomic scale. Think of this as having an ON/OFF transistor the size of an electron. While this atomic scale is an advantage which can help lengthen the time before Moore's law reaches its limit, there is something far more important. Specifically, it is the ability for such a system to exhibit (a) a superposition of states and (b) quantum entanglement, that quantum computing can be exploited in ways not possible with classical computing systems (Fig. 5.5). In quantum computing, the basic unit of computation (an electron) exists in a superposition of states (0 →1) until the point of measurement. That is, qubits can be both 0 and 1 simultaneously. In addition, matter in quantum physics is probabilistic (i.e., it behaves with uncertainty; thus, we do not know if the outcome will be 0 or 1, *until* we measure it). Note that a superposition of states is a recurrent theme in quantum mechanics, as we saw with the double-slit experiment where an electron is both a particle and a wave, with a specific and definable de Broglie wavelength.

But how exactly is having a superposition of states important, and what makes this feature powerful in quantum computing? The answer is that qubits (in a superimposed state) increase exponentially the amount of information each qubit can hold. With 1-qubit, there can be two states; with 2-qubits, four states; with 3-qubits, eight superimposed states; and so on. In other words, for each classical bit of information (0 or 1), there exist *two* qubits of information, or more generally 2^n, where n = the number of qubits in the quantum computer or circuit (Fig. 5.6). The possible combinations for each quantum computing system could also be expressed as a matrix as follows:

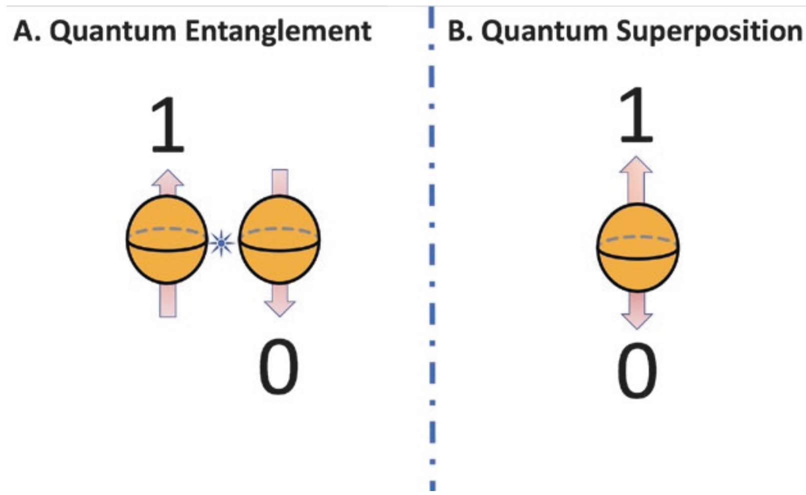

Fig. 5.5 (**a**) Quantum entanglement and (**b**) quantum superposition of states are two of the most important aspects of quantum computing that provide a powerful framework which allows quantum computers to carry out some types of computations more efficiently than classical computing systems. (**a**) Quantum entanglement for two entangled particles is illustrated. It implies that when the measured outcome (e.g., spin orientation) of one particle is determined, then this automatically predicts the outcome of the entangled particle. Thus, if one electron is spin $|\uparrow\rangle$, then the entangled second electron will be spin $|\downarrow\rangle$ upon measurement. In classical computing, with man-made transistors, there is no ability for one classical bit to affect another bit in this manner. (**b**) Quantum superposition is another important factor which defines the uniqueness of quantum computing. While a qubit will resolve to either spin $|\uparrow\rangle$ or $|\downarrow\rangle$, until the point of measurement, they are in a superposition of states (that means the qubit is both spin up and spin down simultaneously). This increases the possible states any given qubit can exist in, making for more possible combinations of 1s and 0s within any given quantum computing system (see Fig. 5.6)

$$3-\text{qubit computer}: \mathbf{2^3}\,\text{expressed as}\begin{bmatrix} 0 & 0 & 1 & 1 & 0 & 1 & 0 & 1 \\ 0 & 1 & 0 & 1 & 1 & 0 & 0 & 1 \\ 1 & 0 & 0 & 0 & 1 & 1 & 0 & 1 \end{bmatrix} = 8\,\text{possible states}$$

$$\text{Same data expressed as particle spin}\begin{bmatrix} \downarrow & \downarrow & - & - & \downarrow & - & \downarrow & - \\ \downarrow & - & \downarrow & - & - & \downarrow & \downarrow & - \\ - & \downarrow & \downarrow & \downarrow & - & - & \downarrow & - \end{bmatrix} = 8\,\text{possible states}$$

Due to this exponential characteristic, if a controllable 300-qubit quantum computer was developed, it would have 2^{300} possibilities (2.037×10^{90}) – which is more than the number of all particles in the observable universe (known as the Eddington number, approximately 10^{86}). This allows each unit of computation to exist in an enriched set of states, something which can aid scientists in finding solutions to problems which pose exponential potential solutions – including problem sets unique to surgery and robotic systems.

Quantum computers can solve *some* types of problems considerably faster than classical computers as well. For example, determining the prime factors of a large number – such as a 2100-

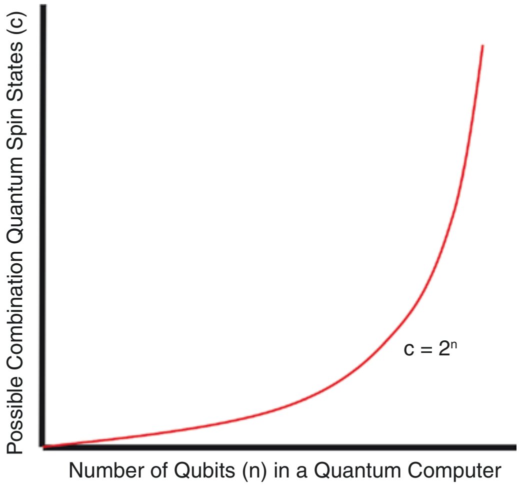

Fig. 5.6 With classical computing, each bit of information holds one and only one value. For example, a bit can either be 1 or 0. With quantum computing, however, each qubit represents a superposition of states (a qubit is both 1 *and* 0 (i.e., spin |↑⟩ *and* spin |↓⟩), until it is measured at which point it resolves to one or the other. This means that for every qubit, there are $\mathbf{2^n}$ possibilities, defined as ***C***. For example, for 2-qubits, the combination possibilities are four – 00, 01, 10, and 11, or 2^2. In contrast, for classical computers, 2 bits of information are just 2 bits of data, and there are no combination possibilities, because there is no superposition of states in classical computing. The graph demonstrates the exponential implication. If one were to consider a 300-qubit quantum gate computer, this would represent a system with 2^{300} possible combinations, which is more than there are particles in the observable universe

bit number – would take millions of years for a traditional computer to solve, but a quantum computer could solve this problem in just minutes. This is because quantum computers have the ability to reduce the number of steps required to determine the computation (not because they are intrinsically faster at computing). Recently, Arute et al. demonstrated quantum supremacy using a programmable superconducting 53-quibit system. In their analysis, what would take their quantum computer 200 seconds to complete would have taken a conventional supercomputer 10,000 years [45]. Thus, this modality of computing could be highly useful for problems in which the number of possible answers is exceedingly large, such as the possible configuration of atoms within a large molecule, or where solutions are based on factorials. For example, for computing the solution to a problem whose possibilities are one hundred factorial, i.e., 100! (100 × 99 × 98 × 97…), in general, quantum computing would probably be best suited for such a calculation.

It is important to understand that quantum computing is not a replacement for classical computing and that its actual computing speed is not necessarily faster. However, when presented with a problem that requires multiple complex executions to solve, quantum computing can exponentially shorten the number of calculations necessary to arrive at a solution. Thus, for special problems, quantum computing will have an incredibly important role, and this may include a role in the operating theater and for surgical robotics. Today, we are just beginning to understand the power of this new kind of computing. If we were to use an analogy to transportation, its current stage of development is akin to having a working jet engine in a laboratory, but the technology is years away from placing such engines on jets capable of flight.

Quantum computer design is complex, and there is more than one approach – quantum gate model computing [46, 47] and quantum annealing [48, 49] are two examples. They use electrons or atoms (qubits) which exhibit spin derived from what is known as a superconducting Josephson junction [50–52] (cooled to 0.015 Kelvin, which is colder than the temperature of outer space, 2.7 K, or −270.45 °C). Such a system is then coupled to a microwave resonator; other configuration and approaches including the use of superconducting niobium have also been used. As seemingly unimaginable and theoretical quantum computing may seem, today, there are actually operational systems which are accessible via cloud networking. The IBM Q System One (a quantum gate model computer) was launched in 2016 and is available to anyone with Internet access via the URL: http://ibm.biz/qx-introduction. The IBM Q has two 5-qubit quantum processors and a 16-qubit processor which allows end users to construct quantum computing “circuits” (Fig. 5.7). D-Wave has developed a cloud-accessible quantum annealing computer with 2000-qubits; it is web accessible at https://cloud.

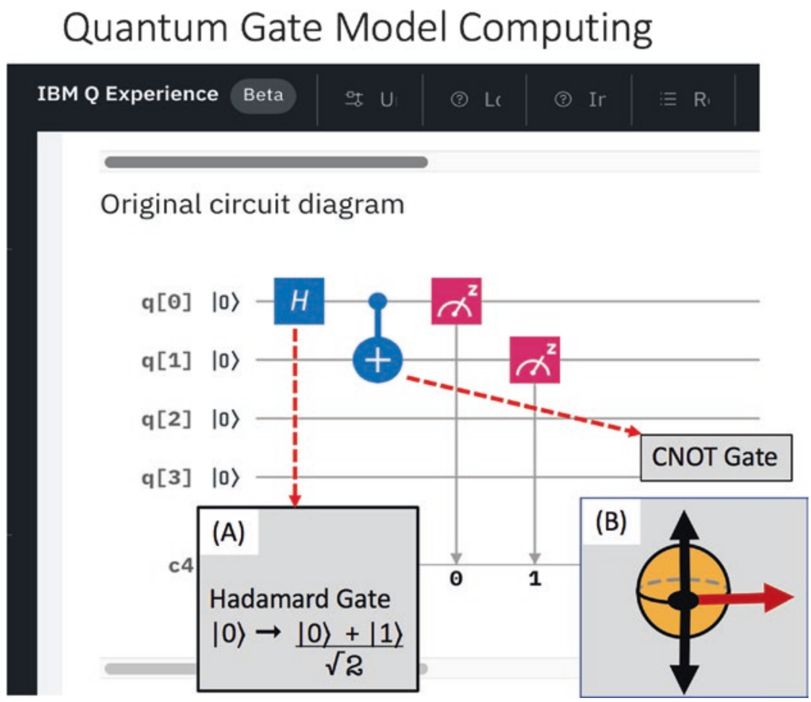

Fig. 5.7 Cloud-based quantum gate computing. The graphic user interface for creating quantum circuits on the IBM Q cloud-accessible quantum computer is shown. This computer has four qubits that start in the lower-energy spin-down |0⟩ state (same as |↓⟩) and are denoted as q[0], q[1], q[2], and q[3] on the circuit diagram. In this simple system, the first qubit q[0] is in the |0⟩, and a so-called "H" (Hadamard) quantum gate is applied, which, via the linear algebraic equation shown in *inset* (**a**), effectively causes the spin to be oriented orthogonally |→⟩ relative to the direction of measurement (as denoted by the *red arrow* on the electron spin model, *inset* (**b**)). Recall from the Stern-Gerlach experiment that spin values are quantized and thus must resolve to either |↑⟩ or |↓⟩ upon measurement (i.e., 0 or 1). Due to quantum randomness, the true probability of measuring |0⟩ or |1⟩ spin is 50–50 after the application of the Hadamard gate. In the second qubit, q[1], what is known as a controlled-NOT (C-NOT) quantum logic gate has been applied to the circuit in such a way that it becomes entangled with the qubit q[0]. With the two qubits q[0] and q[1] entangled, we would expect the spin to be opposite – for example, if q[0] is|↓⟩, then q[1] is |↑⟩. However, the effect of the CNOT gate is to flip the spin of q[1] so that it is the same as q[0]; thus, the expected outcomes would be q[0] and q[1]: |↑⟩ and |↑⟩. This relationship of two qubits represents a special condition called a Bell state, which is an example of maximal quantum entanglement of two qubits, often mathematically expressed as ⟨Φ|Φ⟩

dwavesys.com. One of the most important challenges for quantum computing is to control qubits so they can be accurately measured and to create a stable system, as quantum computers are highly sensitive to the external environment.

Utilizing an in-house quantum computer for AI and ML for surgical robots would be cost-prohibitive and impractical for a multitude of reasons, including the requirement to supercool and maintain such systems – although the possibility of superconductivity near room temperature has recently been successfully demonstrated (with limitations) [53]. Today, quantum computers must be maintained at specialized facilities, and their physical usage in operating theaters is not realistic or likely. However, via the cloud, access becomes achievable, and one can envision quantum cloud computing whereby a centralized system is maintained at a specialized facility yet accessed for computing via the Internet in the same manner that cloud computing is performed with commodity computers today, and just as the IBM Q is accessed (Fig. 5.8).

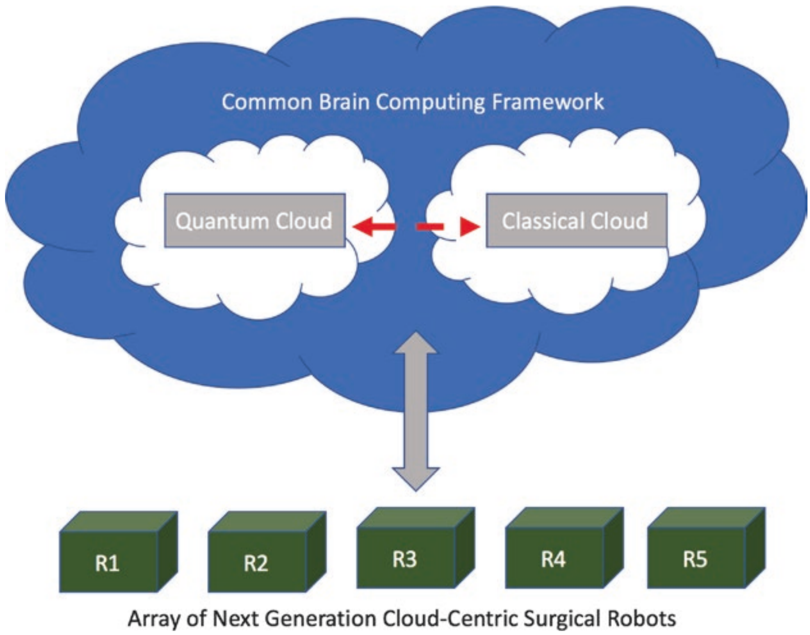

Fig. 5.8 A future framework for digital surgery may include a cloud-based interface with both classical and quantum computers interlinked. In this schematic diagram, robotic operative systems with machine and deep learning capability would possess varying degrees of autonomy and will offload high-demand computational workloads onto the cloud. Surgical robots could be interlinked via centralized, cloud-based computing, with vast data sets, essential for machine and deep learning, stored in the cloud. Because quantum computing is not considered to be a replacement but instead an adjunct to classical computing, such a design would utilize both quantum and classical computing within the cloud infrastructure

Quantum Robotics and Possible Applications for Surgery

The ability to develop functional quantum robots is already underway [54–59], and such technology could soon be translated into applications for next-generation surgical robots. This could allow quantum robots to solve certain kinds of problems more efficiently (such as determining the optimal position and trajectory of robotic devices in relation to target anatomy). It has been demonstrated mathematically that quantum robots can likely learn more efficiently. In complexity and computer science theory, Landau's symbol, O, represents the rate of growth of any given function. Ordinarily, problems related to search are defined as *Order N*, or $O(N)$, but Grover has demonstrated that quantum computing can reduce the complexity of this to $O\sqrt{N}$) [32]. Extrapolating from this, one can consider how the Grover algorithm can reduce complex operations, such as robotic navigation within a given space (potentially including for robotic navigation of anatomic and surgical targets). It has been shown by Dong et al. that quantum robots can be designed to take, for example, unstructured search problems N, from a quadratic relationship used with classical systems, $O(N^2)$ and reduce the problem set to $O\left(N\sqrt{N}\right)$ which effectively makes the learning control algorithm of quantum robots considerably more efficient, since the exponential complexity of classical computing systems is reduced [57] (Fig. 5.9). This occurs essentially because quantum computers and robots have more parallel processing power [57–59]. While quantum robotics remains theoretical, remote-brained (cloud-based) surgical robots with varying degrees of autonomous learning could be introduced over the next 10–15 years. Such systems would be more capable of solving certain types of complex problems quickly and would provide a framework for next-generation machine and deep learning of surgical robots – ultimately enhancing interpretation of surgical fields and operative environments.

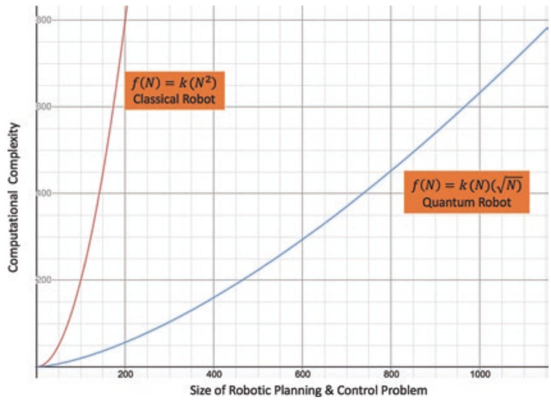

Fig. 5.9 Comparative models depicting the difference in computational (time) complexity between classical robots and quantum robots. Grover's algorithm on quantum computing effectively states that for specific types of problems (e.g., such as a search for a specific target or object) can be reduced from $O(N)$ to $O\sqrt{N}$ [32]. But for robotic navigation, for example, the complexity is more involved because the robot state (i.e., position relative to the target) must also be considered. For classical computer-based robotic systems, this relationship has been defined to be $O(N^2)$, and correspondingly, it can be simplified to $O\left(N\sqrt{N}\right)$ under the framework of quantum robotics [57]. In this graph, $f(N)$ represents y-axis values, and k is an arbitrary coefficient (in this example, $k = 0.02$). The X and Y axes are set to arbitrary scales and are for purposes of illustration only. The two equations and graphs for (a) classical and (b) quantum robotics are shown. This delineates how, as the nature (scope and size) of any given problem increases (for example, the scope and size of the search area for target anatomy), the complexity of the problem increases *much less* for a quantum robot when compared to a classical robot. Since computation complexity is a proxy for computational time, this demonstrates that quantum robotic platforms can perform search and navigation tasks much more efficiently than their classical robotic counterparts. This may apply to a variety of search-related robotic "planning and control" functions, including autonomous navigation. In the future, this may include surgical applications

References

1. Murdoch TB, Detsky AS. The inevitable application of big data to health care. JAMA. 2013;309(13):1351–2.
2. Schrödinger E. Quantisierung als eigenwertproblem. Ann Phys. 1926;385(13):437–90.
3. Heisenberg W. The physical principles of the quantum theory. Mineola, New York, USA: Courier Corporation; 1949.
4. Kramers HA, Heisenberg W. Über die streuung von strahlung durch atome. Zeitschrift für Physik A Hadrons and Nuclei. 1925;31(1):681–708.
5. Heisenberg W. Über den anschaulichen Inhalt der quantentheoretischen Kinematik und Mechanik. Z Phys. 1927;43:172–98.
6. Millikan RA. Einstein's photoelectric equation and contact electromotive force. Phys Rev. 1916;7(1):18.
7. Davisson C, Germer LH. Diffraction of electrons by a crystal of nickel. Phys Rev. 1927;30(6):705.
8. Wheeler JA. The "past" and the "delayed-choice" double-slit experiment. In: Mathematical foundations of quantum theory. New York, New York, USA: Academic Press, Inc.; 1978. p. 9–48.
9. Jacques V, Wu E, Grosshans F, Treussart F, Grangier P, Aspect A, Roch JF. Experimental realization of Wheeler's delayed-choice gedanken experiment. Science. 2007;315(5814):966–8.
10. Walborn SP, Cunha MT, Pádua S, Monken CH. Double-slit quantum eraser. Phys Rev A. 2002;65(3):033818.
11. Kim YH, Yu R, Kulik SP, Shih Y, Scully MO. Delayed "choice" quantum eraser. Phys Rev Lett. 2000;84(1):1.
12. Compton AH. A quantum theory of the scattering of X-rays by light elements. Phys Rev. 1923;21(5):483.
13. De Broglie L. Waves and quanta. Nature. 1923;112(2815):540.
14. Bloch F. Nuclear induction. Phys Rev. 1946;70(7–8):460.
15. Purcell EM, Torrey HC, Pound RV. Resonance absorption by nuclear magnetic moments in a solid. Phys Rev. 1946;69(1–2):37.
16. Gerlach W, Stern O. über die richtungsquantelung im magnetfeld. Ann Phys. 1924;379(16):673–99.
17. Rosen N, Zener C. Double Stern-Gerlach experiment and related collision phenomena. Phys Rev. 1932;40(4):502.
18. Bohr N. The structure of the atom. Nature. 1923;112(2801):29.
19. Bengtsson I, Życzkowski K. Geometry of quantum states: an introduction to quantum entanglement. Cambridge, United Kingdom: Cambridge university press; 2017. 2017.
20. Laflorencie N. Quantum entanglement in condensed matter systems. Phys Rep. 2016 Aug 3;646:1–59.
21. Streltsov A. Quantum entanglement. In: Quantum correlations beyond entanglement. Cham: Springer; 2015. p. 11–6.

22. Bernhardt C. Quantum computing for everyone. Cambridge, MA, USA: MIT Press; 2019.
23. Bell JS. On the einstein podolsky rosen paradox. Physics Physique Fizika. 1964;1(3):195.
24. Erber T, Putterman S. Randomness in quantum mechanics—nature's ultimate cryptogram? Nature. 1985;318(6041):41.
25. Dürr D, Goldstein S, Zanghi N. Quantum mechanics, randomness, and deterministic reality. Phys Lett A. 1992;172(1–2):6–12.
26. Einstein A, Podolsky B, Rosen N. Can quantum-mechanical description of physical reality be considered complete? Phys Rev. 1935;47(10):777.
27. Kohn W, Luttinger JM. Quantum theory of electrical transport phenomena. Phys Rev. 1957;108(3):590.
28. Bouwmeester D, Pan JW, Mattle K, Eibl M, Weinfurter H, Zeilinger A. Experimental quantum teleportation. Nature. 1997;390(6660):575.
29. Ren JG, Xu P, Yong HL, Zhang L, Liao SK, Yin J, Liu WY, Cai WQ, Yang M, Li L, Yang KX. Ground-to-satellite quantum teleportation. Nature. 2017;549(7670):70.
30. Shor PW. Polynomial-time algorithms for prime factorization and discrete logarithms on a quantum computer. SIAM Rev. 1999;41(2):303–32.
31. Shor PW. Algorithms for quantum computation: discrete logarithms and factoring. In: Proceedings 35th annual symposium on foundations of computer science. Philadelphia, PA, USA: IEEE; 1994. p. 124–34.
32. Grover LK. A fast quantum mechanical algorithm for database search. arXiv preprint quant-ph/9605043. 1996.
33. Grover LK. Quantum mechanics helps in searching for a needle in a haystack. Phys Rev Lett. 1997;79(2):325.
34. Zidan M, Abdel-Aty AH, El-shafei M, Feraig M, Al-Sbou Y, Eleuch H, Abdel-Aty M. Quantum classification algorithm based on competitive learning neural network and entanglement measure. Appl Sci. 2019;9(7):1277.
35. Zidan M, Abdel-Aty AH, Younes A, Zanaty EA, El-khayat I, Abdel-Aty M. A novel algorithm based on entanglement measurement for improving speed of quantum algorithms. Appl Math. 2018;12(1):265–9.
36. Zalka C. Grover's quantum searching algorithm is optimal. Phys Rev A. 1999;60(4):2746.
37. Vandersypen LM, Steffen M, Breyta G, Yannoni CS, Sherwood MH, Chuang IL. Experimental realization of Shor's quantum factoring algorithm using nuclear magnetic resonance. Nature. 2001;414(6866):883.
38. Bennett CH, Shor PW. Quantum information theory. IEEE Trans Inf Theory. 1998;44(6):2724–42.
39. Lanyon BP, Weinhold TJ, Langford NK, Barbieri M, James DF, Gilchrist A, White AG. Experimental demonstration of a compiled version of Shor's algorithm with quantum entanglement. Phys Rev Lett. 2007;99(25):250505.
40. Leuenberger MN, Loss D. Quantum computing in molecular magnets. Nature. 2001;410(6830):789.
41. Steane A. Quantum computing. Rep Prog Phys. 1998;61(2):117.
42. Walther P, Resch KJ, Rudolph T, Schenck E, Weinfurter H, Vedral V, Aspelmeyer M, Zeilinger A. Experimental one-way quantum computing. Nature. 2005;434(7030):169.
43. Feynman RP. Quantum mechanical computers. Optics News. 1985;11(2):11–20.
44. Deutsch D. Quantum theory, the church–Turing principle and the universal quantum computer. Proc Royal Soc Lond A Math Phys Sci. 1985;400(1818):97–117.
45. Arute F, Arya K, Babbush R, Bacon D, Bardin JC, Barends R, Biswas R, Boixo S, Brandao FG, Buell DA, Burkett B. Quantum supremacy using a programmable superconducting processor. Nature. 2019;574(7779):505–10.
46. Barenco A, Bennett CH, Cleve R, DiVincenzo DP, Margolus N, Shor P, Sleator T, Smolin JA, Weinfurter H. Elementary gates for quantum computation. Phys Rev A. 1995;52(5):3457.
47. Monroe C, Meekhof DM, King BE, Itano WM, Wineland DJ. Demonstration of a fundamental quantum logic gate. Phys Rev Lett. 1995;75(25):4714.
48. Bunyk PI, Hoskinson EM, Johnson MW, Tolkacheva E, Altomare F, Berkley AJ, Harris R, Hilton JP, Lanting T, Przybysz AJ, Whittaker J. Architectural considerations in the design of a superconducting quantum annealing processor. IEEE Trans Appl Supercond. 2014;24(4):1–0.
49. Finnila AB, Gomez MA, Sebenik C, Stenson C, Doll JD. Quantum annealing: a new method for minimizing multidimensional functions. Chem Phys Lett. 1994;219(5–6):343–8.
50. Josephson BD. Possible new effects in superconductive tunnelling. Phys Lett. 1962;1(7):251–3.
51. Makhlin Y, Scöhn G, Shnirman A. Josephson-junction qubits with controlled couplings. Nature. 1999;398(6725):305.
52. Cataliotti FS, Burger S, Fort C, Maddaloni P, Minardi F, Trombettoni A, Smerzi A, Inguscio M. Josephson junction arrays with Bose-Einstein condensates. Science. 2001;293(5531):843–6.
53. Hamlin JJ. Superconductivity near room temperature. Nature. 2019;569(7757):491–2.
54. Benioff P. Quantum robots and environments. Phys Rev A. 1998;58(2):893.
55. Benioff P. Some foundational aspects of quantum computers and quantum robots. Superlattice Microst. 1998;23(3–4):407–17.
56. Benioff P. Quantum robots. Feynman Comput. 2018;8:155–75.
57. Dong D, Chen C, Zhang C, Chen Z. Quantum robot: structure, algorithms and applications. Robotica. 2006;24(4):513–21.
58. Mahanti S, Das S, Behera BK, Panigrahi PK. Quantum robots can fly; play games: an IBM quantum experience. Quantum Inf Process. 2019;18(7):219.
59. Kagan E, Ben-Gal I. Navigation of quantum-controlled mobile robots. In: Recent advances in mobile robotics. London, UK: IntechOpen; 2011.

6 5G Networks, Haptic Codecs, and the Operating Theatre

Mischa Dohler

Introduction

The Internet has evolved over many generations: The first and "original" Internet, a virtually infinite network of computers, was a paradigm change and went on to define the global economies of the late twentieth century. After that Internet came the *Mobile Internet,* connecting billions of smartphones and laptops and yet again redefining entire segments of the economy in the first decade of the twenty-first century. Today, we see the emergence of the *Internet of Things* (IoT), soon to connect billions of objects, and it is already starting to redefine various global economies over the next decades.

Underpinned by zero-delay data transmission paradigms in the network and the *Tactile Internet* at the wireless edge, the aforementioned embodiments of the Internet will be dwarfed by the emergence of two new Internet families: (i) *industrial local area networks* with focus on manufacturing efficiencies ("Industry 4.0") and (ii) the *Internet of Skills* with focus on human skills ("Human 4.0").

The focus of this chapter is the *Internet of Skills,* which enables the delivery of *physical experiences* – such as touching or moving an object – *remotely*. This will revolutionize operations and servicing capabilities for industries, and it will revolutionize the way we teach, learn, and interact with our surroundings. The *Internet of Skills* will be an enabler for skillset delivery – thus, a very timely technology for service-driven economies around the world.

The potential global impact of this creation would be instrumental in conquering some of the world's biggest challenges. The *Internet of Skills* – having reached widespread adoption or being deployed at needs – will enable important disaster operation applications, such as telesurgery and telemedicine for patients in need (e.g. applicable in Ebola-afflicted locales); remote education (e.g. a child in war-torn Gaza is taught painting); and industrial remote decommissioning and servicing capabilities (e.g. the remote reparation of a broken car in Africa); among other important applications.

Take the example of the United Nation's response to the Ebola pandemic, which was, in part, as follows: We are confident that some of the basic and frequent manual operations like spraying antiseptics on equipment and healthcare workers and communicating with patients through gestures, pictures, or animations can be done using commercially available light tactile robots. Medical experts will move the hands and grippers of an exact replica of the remote robot to send commands and receive feedback via the *Internet of Skills.* This will allow aid workers and medical experts to contribute to the Ebola response operation without endangering their

M. Dohler (✉)
Department of Engineering, King's College London, London, UK
e-mail: Mischa.dohler@kcl.ac.uk

S. Atallah (ed.), *Digital Surgery*, https://doi.org/10.1007/978-3-030-49100-0_6

own lives or risking viral spread to other geographic regions. The same measures could be used to curtail the spread of the COVID-19.

Let us consider another example of remote servicing. Operational costs are one of the largest expenditure items for industries to date, with inefficiencies due to the *suboptimal* skill being one of the largest contributors. The *Internet of Skills* will allow matching specific needs in one physical location with the best skill in another location. Automobiles and airplanes requiring maintenance can thus be serviced remotely, industrial plants inspected and repaired, and high-value manufacturing supervised – all in a significantly more efficient and effective manner, with a minimized carbon footprint. *The Internet of Skills will thus be an enabler for remote skillset delivery and thereby democratize labour in the same way as the Internet has democratized knowledge.*

The aim of this chapter is to introduce the technical challenges encountered when designing and building the first iterations of the *Internet of Skills* and how it can be meaningfully applied in the context of robotic operating theatres. To this end, the chapter is organized as follows. In the subsequent section, an overview of the technical design challenges is provided. Thereupon, the important components are carefully explored – such as emerging 5G networks, artificial intelligence (AI), and standardized haptic codecs. The chapter concludes by discussing applications in the context of medical interventions and future frameworks.

The Internet of Skills

In this section, the design approach taken for the Internet of Skills is outlined, as are the technical challenges and limitations.

Design Approach

Whilst *haptic communication* has been in existence for some time [1] and the communications principles of the zero-delay Internet/Tactile Internet have been previously established [1–6], the design of an *Internet of Skills* requires a ground-breaking, cross-disciplinary approach. Specifically, it will require combining electrical engineering (communications, networking), with key aspects of computer science (artificial intelligence, data science), and will mechanical engineering (kinesthetic robotics, tactile sensors).

To accelerate the design of the new *Internet of Skills,* it is prudent to borrow insights and lessons learned from the development of today's Internet. The Internet took several decades of innovation to transit from a heavily proprietary paradigm to today's standardized Internet enabling economies of scale. Two important developments are noteworthy:

1. *IP networks:* The first is the development of Internet protocol (IP) networks where devices communicate with each other using a *single standardized "language"*, the IPv4 or now IPv6 protocol. As long as a device is able to "speak IP", it can communicate with any other device, no matter how large or small, far or close. As a result, today an IP-enabled nanosensor can be connected to a supercomputer on the opposite side of the planet.
2. *Video/audio codecs:* The second major development was the introduction of standardized *encoders and decoders* (in short, "codecs") of audio and video signals that not only allowed transmission bandwidth to be conserved, but also catered for a rich supply of device and software manufacturers. As a result, users can record a video on any smartphone, allowing it to be viewed on any device (e.g. laptop) regardless of the manufacturer, due to codec standards.

Both IP networks and codecs provide important costs reductions and hence the ability to *scale* the network globally to the point where, today, it forms the digital fabric of society. The aforementioned transition is exemplified in Fig. 6.1, where the top half depicts the Internet's more classical transition and the lower half shows the pathway required towards the design of the *Internet of Skills.*

Indeed, when it comes to the *Internet of Skills*, the necessary elements and constituents already exist – just as building blocks were present 50 years ago at the birth of the Internet. At that time, video-enabled devices worked only across the same vendor's devices and had quite prohibitive costs. In 2020, robotic, master-slave surgical systems allow for local or remote robotic surgery, but still such systems can only be linked across the *same* vendor's devices (da Vinci to da Vinci ®). Furthermore, this is quite expensive. Previously, there were weak and unstable networks with frequent outages. Today, we have networks which are much better – but still not at the reliability and latency level to support a remote robotic surgery between two hospitals. The key is to define the foundational blocks in integrated end-to-end low-latency networking and haptic codec design to enable a similar transformation from today's proprietary and costly haptic-edge technologies to a truly global, standardized, and scalable *Internet of Skills*.

Design Challenges

This transition does have significant design challenges which must first be solved. To start with, the network has to have the following characteristics: (i) ensure *ultra-reliability*, since many remotely executed tasks are critical; (ii) provide *negligible latency*, since the transmission of kinesthetic (movement) data requires closed control loops to support action / reaction with long delays yielding system instabilities; and (iii) rely on *cheap edge technologies* to enable true scale. Illustrated in Fig. 6.2, major research and innovation within three major technology and scientific areas is required: (1) communications networks, (2) artificial edge intelligence, and (3) standardized haptic codecs.

Networks must provide an infrastructure that minimizes transmission delays, resulting in a reliable and robust wireless communication system. End-to-end path reservation, through network slicing, enabled by software-defined networking (SDN) technologies, will be integral to the success

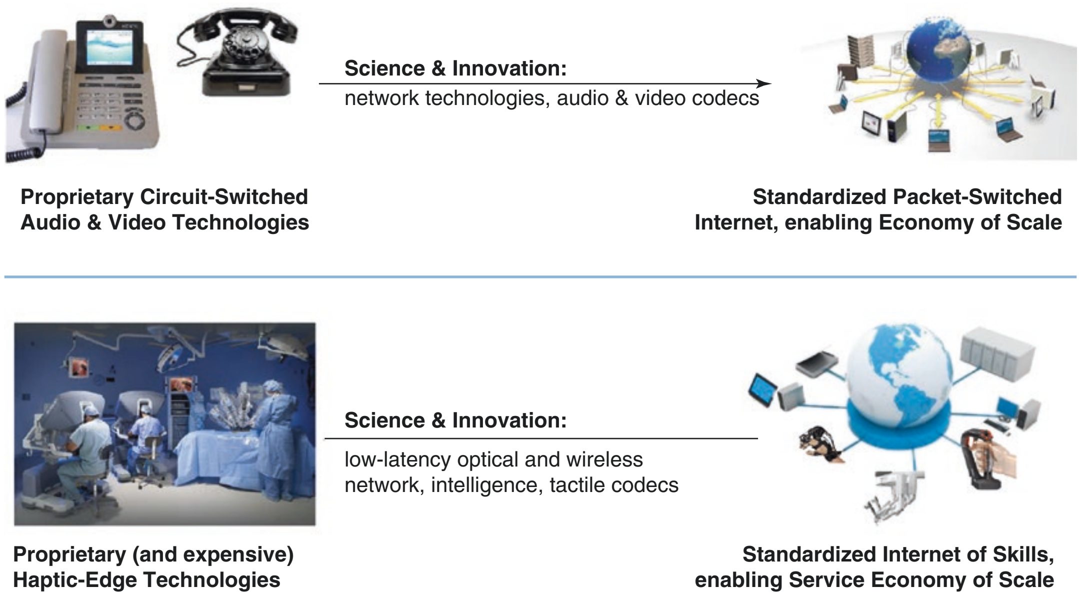

Fig. 6.1 Top: Visualisation of the fundamental transformation from a proprietary intranet to a scalable Internet. Bottom: The foundational blocks of an "internetization" of the haptic paradigm, i.e. enabling the transformation from today's very expensive haptic edge technologies to a standardized Internet of Skills. (Bottom left photograph ©2016 Intuitive Surgical, Inc., used with permission. From: Dohler et al. [7]. Reprinted with permission from IEEE)

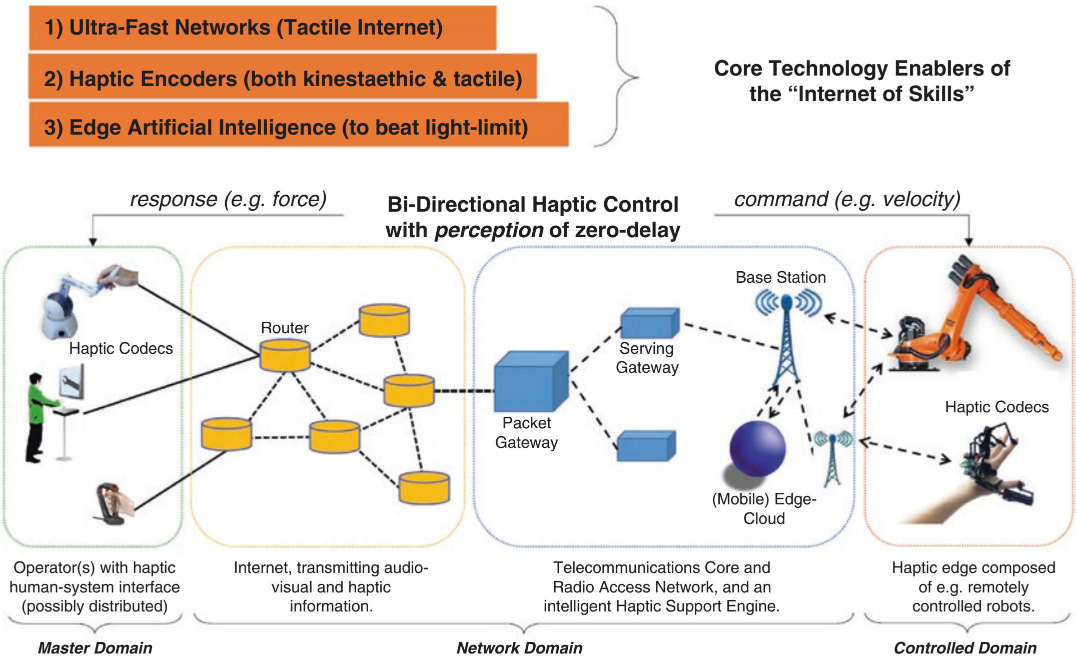

Fig. 6.2 High-level architecture of the Internet of Skills and required building blocks. (From: Dohler et al. [7]. Reprinted with permission from IEEE)

of such next-generation networks. Furthermore, the *Tactile Internet* will be instrumental in guaranteeing minimal delay and maximal robustness over the wireless edge. Fundamental architecture changes are required to enable low delay, along with many other networking transformations, as discussed in a subsequent section.

AI, together with networks, plays an instrumental role in giving the perception of zero-latency networks. Indeed, one could consider model-mediated teleoperation systems whereby AI is able to predict movement on the remote end, thus giving enough time for the signal to reach its target, irrespective of geographical divide. *Haptic control loops* typically require a delay of 1–10 ms – which translates to 100–1000 km range under typical networking conditions. This range can be extended by a model-mediated approach to the tens of thousands of kilometres needed to provide acceptable service worldwide. Haptic codecs will enable scale in the future, as it will avoid vendor "lock-ins". Here, we envisage the combination of tactile (touch) and kinesthetic (movement) information into the already available modalities of video and audio. Progress and developments in this field are discussed in a subsequent section.

Another open challenge is in the area of robotics, including for surgical applications. To enable an era of the man-machine interface where the *Internet of Skills augments* human skills, much more emphasis needs to be given to *soft robotics*. The challenge is to design robotic structures which can exhort force and which are fully controllable whilst being soft — in part or entirely.

Technical Enablers of the Internet of Skills

5G End-to-End Slicing

The telco system is roughly structured in three parts:

1. *Wireless radio channel:* It connects the mobile phone, a.k.a. end-user equipment (UE), with the base station, a larger antenna system often

installed at elevation, such as on building rooftops.

2. *Radio access network:* The base station antennas need to be connected between themselves using fibre or another wireless system (often visible through smaller round antenna dishes which enable these connections). All connected base stations form a network, which is referred to as the radio access network (RAN). This is vital in ensuring handovers, i.e. the ability of one base station to hand over a call to another base station without breaking the connection.
3. *Core and transport networks:* The last segment constitutes the transport network and connects rooftop base stations with the wider Internet, or another operator, or another base station of the same telco operator. The infrastructure here is vast, as it is in essence a telco-owned "private Internet", which stretches throughout the entire country and which only has a few gateways to the wider Internet. The algorithmic and software framework which controls the entire end-to-end infrastructure is called the *core network.*

For 2G, 3G, and 4G networks, above telco constituents were hard-coded and delivered in purpose-made hardware, making the infrastructure *inflexible and expensive*. A very important development within 5G networks is the ability to be *much more flexible.* This design revolution is underpinned by the following developments:

- *Hardware-software separation:* Within the 5G system, software and hardware are becoming increasingly separated from each other. This means that 5G features are *virtualized in software* and delivered over commodity hardware, where it runs on virtual machines (known as containers). *Such a decoupling is important as it enables each ecosystem to innovate independently and at their respective pace.* It has proven very successful in the computing industry, where hardware (computer), middleware (operating system), and software (applications) are developed *independently.*
- *Atomization of functionalities:* We now observe a much stronger atomization of functionalities within the software, based upon a clear separation between *data* and *control plane,* where the former carries user traffic and the latter control traffic. The clear separation of software functionalities allows one to potentially replace certain functionalities much quicker with more advanced embodiments. *Therefore, incremental improvements of the technology can now occur more easily and within months, rather than having to change physical devices or firmware which traditionally takes years.*
- *Virtualization and orchestration:* The atomized software components are much easier to virtualize, then arrange, and physically place, as needed. For instance, software functions responsible for mobility management (such as handovers) can be placed at the very edge of the network (i.e. close to the rooftop antennas) for mobile users driving or walking; the same functions can be hosted much more cost-efficiently in a central cloud server for slowly moving users, such as people in coffee shops watching a streaming video or other content. Finally, the functions can be omitted altogether for the Internet of Things applications – such as robotic surgery, since those devices are stationary. Advanced functionalities can thus be moved *flexibly,* resources instantiated in a moment, and services delivered at scale. All of these require suitable control which is handled by a functionality referred to as *orchestrator.*
- *Open source:* Another critical development is the move towards the use of *open-source hardware and software.* Apart from being more cost-efficient, open-source leverages the collective intelligence by the community designing the solution and is thus also much more scrutinized from a security and stability point of view. The most prominent initiative is the Open-RAN (O-RAN) alliance which counts on several high-profile vendors and operators.
- *(Super-)convergence:* Given the high flexibility of current network systems, 5G will enable

> a convergence between various wireless technologies, including 4G/3G/2G and Wi-Fi, as well as fibre technologies. *Such a "super-convergence" between very different systems allows for much greater reliability and performance.*

These substantial design refinements will provide a foundation for new waves of innovation within the telecommunications architecture. As related to the advent of digital surgery, this will provide a framework for next-generation services such as the provisioning of robotic telesurgery across different geographies.

More technically, the 5G telco ecosystem manifests several advanced features and capabilities. First, it provides an order of magnitude improvement on key performance indicators (KPIs). This is illustrated in Fig. 6.3, with KPIs highlighted in the table. We observe an increase of an average experienced data rate from 10Mbps in 4G to 100Mbps in 5G, latency decreases from 10 ms to 1 ms, and the amount of devices which can be connected increases from 1000 devices/km^2 to >1,000,000 devices/km^2. The three important use cases these KPIs will be able to support are summarized in Fig. 6.4. They will rely on significantly higher data rates (enhanced mobile broadband, eMBB), an increased number of *Internet of Things* devices (massive machine-type communications, mMTC), and critical service capabilities (ultra-reliable and low-latency communications, URLLC).

In terms of technical capabilities and features, the following are important and worth highlighting:

- *5G spectrum:* To be able to deliver KPIs, a substantially new spectrum needs to be made available globally. Although each country differs in the exact band allocations, the spectral areas new to 5G are the three "pioneering bands", as illustrated in Fig. 6.5. The first is the sub-GHz band ~700 MHz, typically occupying where analogue television signal bands were (before the transition to digital); this band provides low capacity but great coverage (range). The second is ~3.5GHz band which provides great capacity and very good coverage. The third is a millimetric wave, i.e. any frequencies in the range of 24GHz and higher, whilst giving close-range coverage only the capacity is outstanding. 5G thus constitutes a heterogeneous mix of these bands, which – as a whole – allows providing the required services.
- *5G radio capabilities:* Apart from the challenges of providing radio hardware able to

Parameter	IMT-Advanced (4G)	IMT-2020 (5G)
Peak data rate	DL: 1Gbps UL: 0.5Gbps	DL: 20Gbps UL: 10Gbps
User experienced data rate	10Mbps	100Mbps
Peak spectra efficiency	DL: 15bps/Hz UL: 6.75bps/Hz	DL: 30bps/Hz UL: 15bps/Hz
Mobility	350km/h	500km/h
User Plane latency	10ms	1ms
Connection density	1 000 devices/km^2	1 000 000 devices/km^2
Energy consumption	1 (normalized)	1/10x of 4G
Mobile data volume	0.01Tb/s/km^2	10Tb/s/km^2

Fig. 6.3 Important 5G key performance indicators and how they compare to 4G. (Source: ITU and 5G-Courses.com)

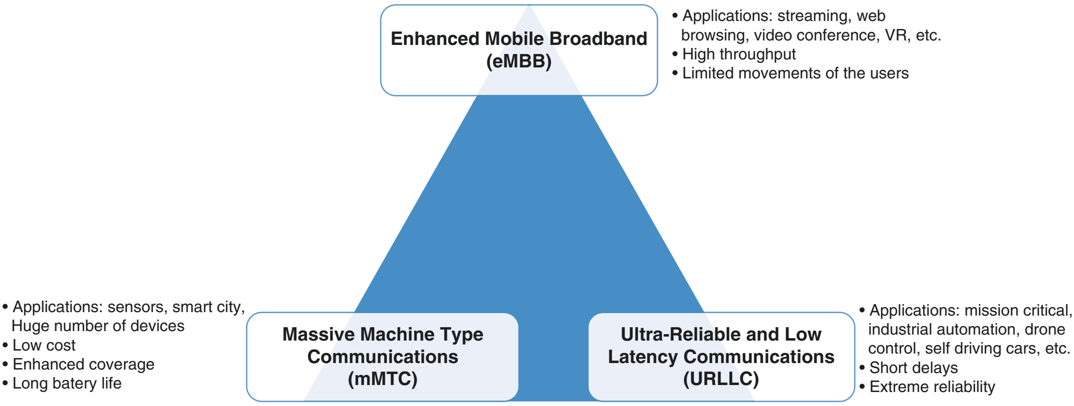

Fig. 6.4 The most important 5G use cases underpinned by higher data rates, more IoT devices, and ability to support critical services. (Source: ITU and 5G-Courses.com)

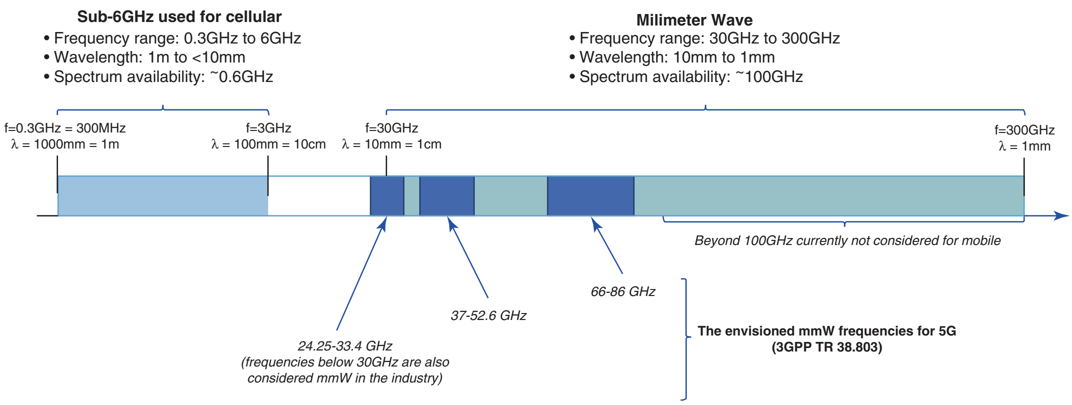

Fig. 6.5 The spectrum regions new to 5G: sub-1GHz, around 3.5GHz, and above 24GHz. (Source: 5G-Courses.com)

communicate over wider bands and at higher frequencies, *the most disruptive element in 5G is massive multiple-input multiple-output (massive MIMO, or MMIMO)*. MIMO is being used extensively today in 4G, where the more elements are available the more data can be transmitted. Today in 4G, mobile phones have three to six antenna elements available in the back of the phone and three to six antenna elements in the base stations positioned on building rooftops. In 5G, the number of antenna elements in mobile phones is slightly augmented, but the antenna elements in base stations will be *substantially* increased in number. Currently, this number is around 100 but is expected to increase to 1000 or even more. As a result, much more data can be transmitted, and beams can be generated with higher precision; this is illustrated in Fig. 6.6.

- *Cloud RAN and functional split:* Virtualization in the context of the access network has achieved maturity in standardization bodies [8–10]. Prior to 5G, processing of the radio signal was conducted at the base station. The economics of scale, however, suggests that several base stations should utilize a *single processing server farm*, which could be placed in a basement of a given building. That separation of radio elements from the processing by means of a cloud infrastructure is referred to as *Cloud RAN* (C-RAN). How exactly the split of processing is done is an open choice at implementation as long as it obeys the configuration

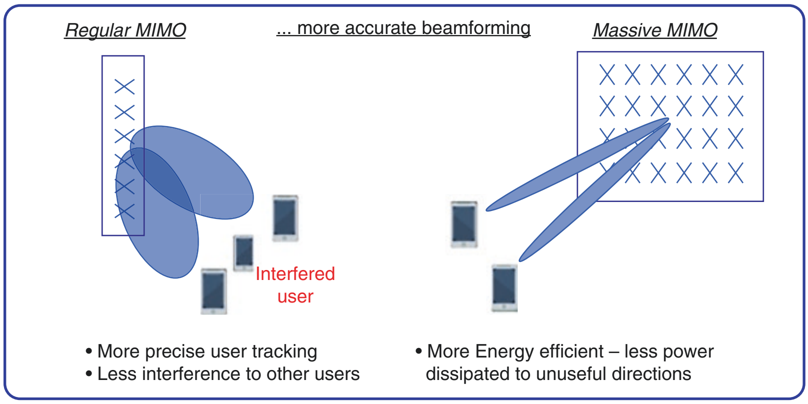

Fig. 6.6 Transition from regular MIMO in 4G to really sophisticated massive MIMO in 5G. (Source: 5G-Courses.com)

protocols established by the 5G standards body, the 3GPP.

- *Virtualized core network:* Virtualization of core network functions allows more flexible deployments which can address some of the KPIs required for 5G, thereby paving the way towards a service-oriented core. Specifically, 3GPP considers a more modular core network architecture for 5G [11], where the control and user plane functions are completely decoupled and communicate with each other through new interfaces. When control and user plane functions are separated, the user plane, which operates at a more stringent time scale than the control plane, can reside closer to the edge as a local breakout for content and service provisioning. Such a deployment allows the decentralization of services and distribution of content caching across the network – which addresses both latency and congestion in the transport network.
- *Software-defined networking (SDN):* The routers and switches in the core network are also being "softwarized", i.e. congestion can be handled much better at scale and also specific IP packets labelled as a high priority can be ushered through without queuing delays. These decisions are being taken by SDN controllers, which rely on information provided by the infrastructure and orchestrators. Overall, the quality of service (QoS) in the network can be significantly improved using modern SDN technologies.
- *Network function virtualization (NFV) and orchestration:* Since the inclusion of the NFV framework, all network functions included in the communications systems are a combination of physical elements (such as antennas) and software that runs in cloud infrastructures. Illustrated in Fig. 6.7, *cloud and virtualization technologies are therefore a critical tool to allow a dynamic deployment and management of these virtualized network functions* [10]. In order to achieve successful deployment and management, the NFV architecture includes the Virtual Infrastructure Management (VIM) component, which controls the NFV Infrastructure, i.e. the totality of all hardware and software components that build the environment where VNFs are deployed. The telecommunications community has recognized the potential of OpenStack, and it is well established as a viable platform for NFV [12]. The Management and Orchestration (MANO) component is addressed via Open Source MANO (OSM), a software stack that enables the orchestration, synchronization, and lifetime management of VNFs or network services. OSM facilitates a *plugin framework* to use a variety of different software solutions as well as the inclusion of in-house, ready-to-use resource orchestration and VIMs [10].
- *Service slicing:* The technical transformations herein allow for a flexible 5G architecture, where features are enabled in software on demand. Illustrated in Fig. 6.8, the mobility management function is not being used for the IoT slice (bottom), at the mobile edge for the highly mobile car application (middle), and is in the central core cloud for the slowly-moving broadband user (top).

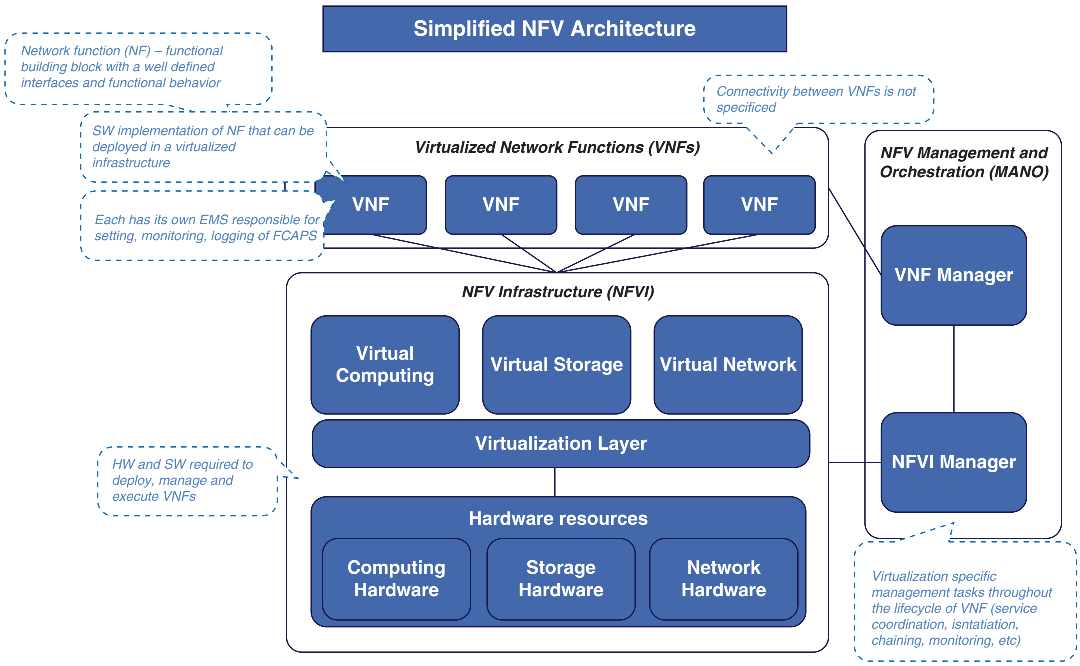

Fig. 6.7 Completely virtualized infrastructure approach in 5G, mimicking modern computing systems. (Source: 5G-Courses.com)

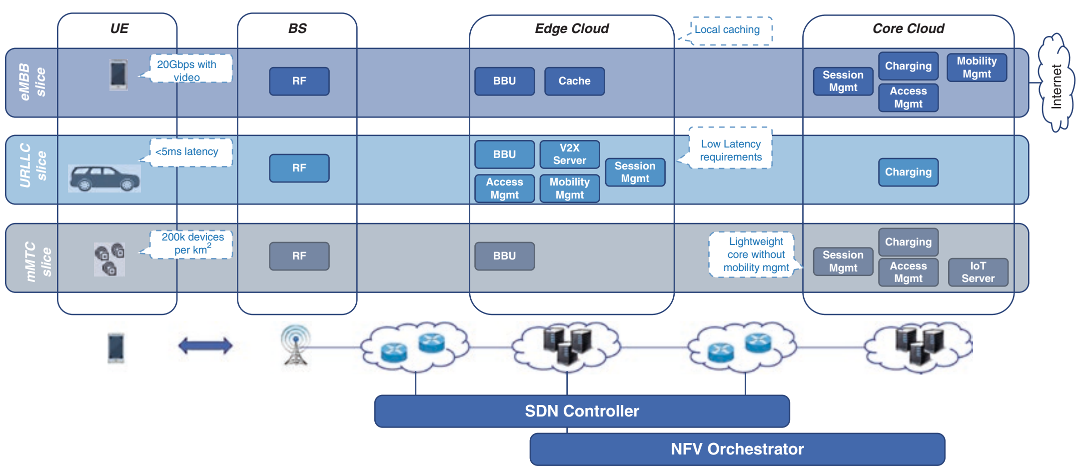

Fig. 6.8 5G's slicing capabilities, i.e. being able to offer different software features for different applications. (Source: 5G-Courses.com)

AI and Digital Twinning

A major impediment to ultra-low-latency connectivity across geographies is the finite speed of light. Whilst the advances on hardware, protocols, and architecture are paramount in diminishing end-to-end delays, the ultimate limit is set by this upper boundary. As breaking the laws of physics is not an option, other – more sophisticated – techniques need to be invoked to facilitate the required paradigm shift. This could be provided by unprecedented *edge artificial intelligence (AI) engines* which are cached and then executed in real time, close to the skill experience. Two of the most important components are:

- *Edge-cloud content caching:* With cloud computing technology, the *Internet of Skills* application content needs to be loaded, or ported. A typical example would be an AI algorithm (see below) which is tailored to work in the context of, for example, remote surgery. These advanced caching techniques and user-oriented traffic management approaches at the edge of the network improve network performance by decongestion of the core network and reduction of end-to-end latency – the latter is particularly important to the *Internet of Skills.* Significant work has been conducted on optimum edge-cloud caching policies [13]. With these advocated approaches, peak traffic demands are substantially reduced by intelligently serving predictable user and application demands via caching at base stations and users' devices. Whilst the advocated approach pertains to rather long-term windows and file structures, it forms the foundation for predictive *Internet of Skills* caching.
- *Artificial intelligence engines:* The AI algorithms predict the haptic/tactile experience – i.e. *acceleration of movement* on one end and the *force feedback* on the other. That allows for the spatial decoupling of the active and reactive ends of the *Internet of Skills*, since the tactile experience is virtually emulated on either end. *This, in turn, allows a much wider geographic separation between the tactile ends, beyond the 10 ms-at-speed-of-light-limit.* The algorithmic framework is currently based on simple linear regression algorithms which are able to predict movement and reaction over tens of milliseconds. The reason for this is mainly because our skillset driven actions are fairly repetitive and exhibit strong patterns across the six degrees of freedom. As illustrated in Fig. 6.9, when the predicted action/reaction deviates from the real one by a certain amount ε, then the coefficients are updated and transmitted to the other end allowing for corrections to be put in place, before damage is done at, e.g. a deviation of δ. More sophisticated algorithms have become available. For example, Sakr et al. [14] employed a prediction method for three-dimensional position and force data by means of an advanced first-order autoregressive (AR) model. After an initialization and training process, the adaptive coefficients of the model are computed for the predicted values to be produced. The algorithm then decides if the training values need to be updated either from the predicted data or the current real data.

Stabilizing both ends of the system allows the creation of *Digital Twins,* an emerging capability which *visualizes the exact spatial context from a remote end.* It could be adapted for surgical use in the future – for example, by allowing a surgeon to have improved contextual awareness during telerobotic operation. Illustrated in Fig. 6.10, such an approach is enabled by model-mediated teleoperation systems which is able to stabilize the end-to-end system with

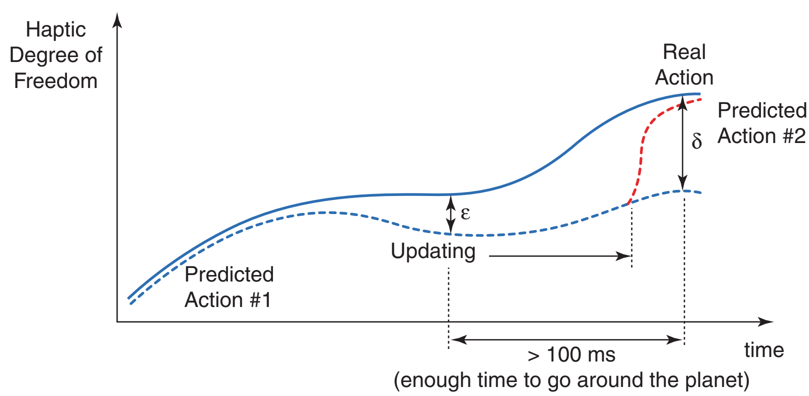

Fig. 6.9 Illustration of how predictive edge AI gives the perception of a 1 ms delay, whilst the actual latency due to communications can be much larger. (From: Simsek et al. [5]. Reprinted with permission from IEEE)

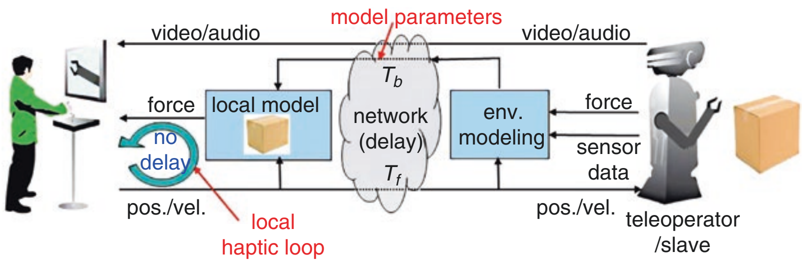

Fig. 6.10 Model-mediated teleoperation system approach in providing digital twinning across far geographies in real time. (Courtesy of Prof Eckehard Steinbach, TU Munich)

latencies in excess of 100 ms (thus covering a geographic range spanning from 20,000 to 30,000 kilometres).

Haptic Codecs

With the consolidation of multimedia technologies, high-quality audio-visual communication makes users feel present remotely to some extent. However, physical interaction and a strong sense of immersion remain deficient to date, possibly because humans rely heavily on haptic interaction within the environment of everyday life [15]. The addition of haptic perception has proven to significantly increase the degree of immersion for distant communications [16]. Haptic perception relies on two different human receptors that are kinesthetic and tactile. The former refers to the physical movement/activation of muscles and joints, whilst the latter includes sensing pressure, temperature, texture, and qualities of touch. Design and development of (proprietary) codecs for kinesthetic data have been well studied using different compression approaches such as *sampling and quantization* technologies, *perceptual deadband* (PD), and *predictive coding* [17].

It is instrumental to understand the *mechanoreceptors* that are responsible for *human tactile perception,* which are summarized in Table 6.1 and of use as follows [18]:

Table 6.1 Function, applications, and respective frequency ranges of four types of mechanoreceptors

	Merkel cell	Ruffini ending	Meissner corpuscle	Pacinian corpuscle
Best stimulus	Pressure, edges, corner, points	Stretch	Lateral motion	High-frequency vibration
Example	Reading braille	Holding large objects	Sensing slippage of objects	Sensing texture
Freq. range (Hz)	0–100	/	1–300	5–1000
Most sensitive freq. (Hz)	5	/	50	200

- *Object identification:* The human haptic perception system relies on kinesthetic as well as tactile sensory information in the interaction with objects. Humans typically perform various types of exploration patterns to identify unknown objects. Humans *lift objects* to estimate their weight. *Static touch* is used to identify the thermal conductance through the bare finger. *Pressing* upon the material reveals information about its stiffness. Finally, *arbitrary sliding motions* allow for the perception of the fine roughness, also known as *haptic texture,* and the friction properties of the object surface.
- *Tactile dimensions:* Five major tactile dimensions have been identified [18, 19]: *friction* between a bare finger and a surface forces the human to apply a specific lateral force during sliding motions, *hardness perception* results from specific exploration patterns such as tapping on an object surface, *warmth conductivity* which is perceived by the thermal receptors in the human skin, and finally determination of *macroscopic roughness* and *microscopic roughness.*

The biggest challenge has been to standardize touch perception into a haptic codec which can be used by different vendors at low cost. This has been a central to the *IEEE P1918 Tactile Internet*

(TI) Standardization Initiative. As outlined in detail by Holland et al. [20], the IEEE 1918.1 TI Standards WG [15] was formulated initially out of the IEEE ComSoc Standards Development Board (COM/SDB) 5G Rapid Reaction Standardization Initiative (RRSI), as a collaborative effort between King's College London and Technical University of Dresden. The scope of the baseline standard is to define a framework for the emerging *low-latency TI,* including descriptions of its application scenarios, definitions and terminology, necessary functions involved, and technical assumptions. This includes the definition of a reference model and architecture, comprising the detailing of common architectural entities, interfaces between those entities, and the definition and mapping of functions to those entities. The structure, including on-going work packages, is shown in Fig. 6.11.

The focus of IEEE 1918.1.1 is to define haptic codecs (HCs) addressing application scenarios with humans in the loop, including remote control. The mission is to define perceptual data reduction algorithms for closed-loop (kinesthetic information exchange through muscle movement) and open-loop (tactile information exchange through touch) communication. The codecs are designed such that they can be combined with stabilizing control and local communication architectures as discussed above. The standard also aims to specify mechanisms and protocols for the exchange of capabilities among haptic devices – e.g. defining the workspace, the number of degrees of freedom of equipment, the amplitude range of each, and temporal and spatial resolution [20].

The standards group has now assessed the requirements for all types of codecs it is considering which are summarized in [18]. It was decided to split the work into two types of codecs based on their underlying requirements: kinaesthetic (closed loop) and tactile (open loop), and the structure of the standards streams is shown in Fig. 6.12 and explained in more detail below:

- *Kinesthetic codec (KC) (Part I):* This pertains to a codec for kinesthetic information, which consists of 3-D position, velocity, force, and torque data. The data is captured by respective sensors and exchanged between different *kin-*

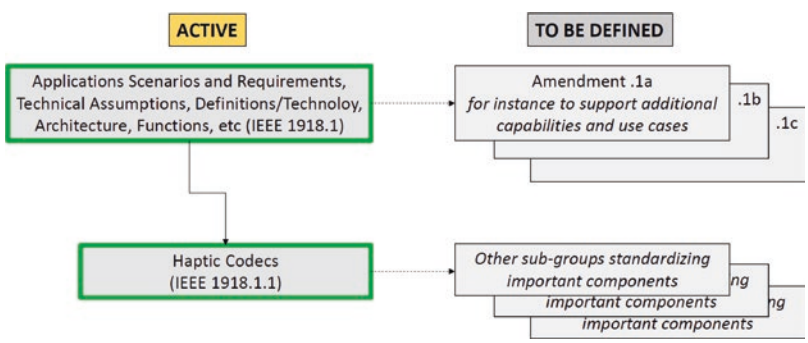

Fig. 6.11 The working groups and its baseline standard as a foundation for further standards. Note that IEEE 1918.1 and IEEE 1918.1.1 are already initiated. (Data from Holland et al. [20])

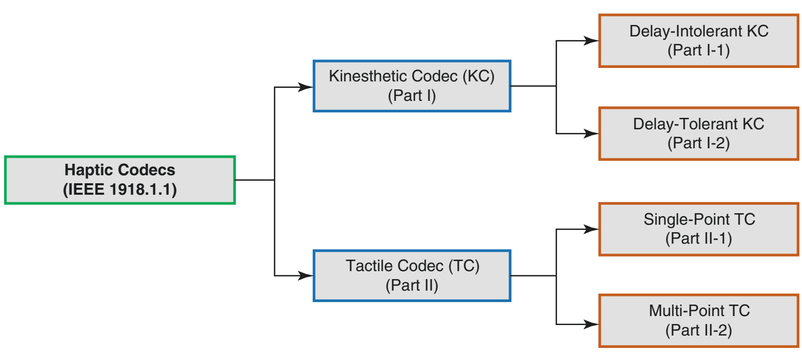

Fig. 6.12 The IEEE P1918.1.1 standardization streams, splitting into closed-loop kinesthetic codecs and open-loop tactile codecs. (Data from Holland et al. [20])

esthetic nodes for teleoperation. The main objective is to reduce the update rate whilst maintaining a high quality of experience (QoE), where we need to distinguish between two cases:
  - *No communication delay (delay-intolerant):* In that case, the codec does not require a control mechanism to stabilize the physical interaction as discussed above.
  - *With communication delay (delay-tolerant):* In the presence of communication delay (typically above 5–10 ms), *a stabilizing control mechanism needs to be deployed*. The standards work established that – whilst it is possible to separate the codec from the control approach – there are significant benefits for tightly coupling both.
- *Tactile codec (TC) (Part II):* Open-loop interaction in this context means that in particular, the delay requirements are fairly relaxed to the order of 10–100 ms. This, as suggested by Holland et al. [20], opens the opportunity for codecs that cannot be used in the KC design. Examples thereof are *block-based processing* or *frequency-domain models* of human tactile perception. Although the tactile modality consists of several submodalities (hardness, thermal conductivity, friction, micro-roughness, and macro-roughness), the task group commenced standards work with vibro-tactile signals which pertain to micro-roughness and friction [21, 22]. Tactile interaction can be a *point interaction* (single point) or *surface interaction* (sampled multipoint):
  - *Single-point TC (Part II-1):* The input is a one-dimensional vibro-tactile signal (e.g. 100 Hz, 32bits). The codec splits the vibro-tactile signal into small segments and encodes these segments independently [20]. A model of vibro-tactile perception ought to be used to hide coding artefacts below perceptual thresholds. In this sense, this coding process shares many similarities with speech/audio coding [22].
  - *Multipoint TC (Part II-2):* Multipoint tactile coding addresses the simultaneous stimulations of the human skin at the surface *from several points,* which will lead to more realistic (area-based) experiences. From a codec perspective, additionally to *temporal correlation* in the vibro-tactile signal, now, the inter-channel or *spatial correlation* should be used for maximum compression performance.

The standardization of the two codec families is an open and ongoing process; its importance is equitable to the standardization on other files requiring human perception, such as audio files (e.g. mp3), photograph files (e.g. JPEG), and video files (e.g. MPEG).

Application to the Operating Theatre

Challenges for Minimally Invasive Surgery and Robotics in Surgery

Robotic surgery is a type of minimally invasive surgery which is now fairly well established. It has proven benefits over traditional surgery, with reduced incision size and diminished blood loss – both significantly decrease risks of infection as well as hospital length of stay. Laparoscopy offers the same advantages, *but does not provide a paradigm for scalability*. For this, the robotic platform is best suited. However, improvements are required to enable true scale across markets and hospitals globally [23]:

- *Haptic feedback:* Surgeons rely heavily on their sense of touch and the force exerted on human tissues, surgical instruments, and sutures to differentiate critical structures; this enables them to prevent intraoperative complications by inadvertently damaging surrounding tissues [24]. Thus, the loss of both kinesthetic and cutaneous haptic feedback is an important shortcoming which – once overcome – would allow for much more complex interventions to be performed with a higher level of patient safety.
- *Telesurgery:* Whilst prototype telesurgery trials have been conducted (see below), spatially

distributed systems with the surgeon and the patient in different locations are not yet practical. Overcoming this challenge, however, would allow for a much more efficient use of surgical skills across countries.

- *Deployment and operational costs:* The systems are extremely expensive and thus not affordable at scale. *It is well known that a decrease in cost by 10 times leads to an exponential market penetration well beyond 10 times.* The aim thus should be to reduce the cost of such equipment by an order of magnitude.

These challenges can be addressed by using the aforementioned *Internet of Skills* and its technology capabilities [23]. Notably, any future system is underpinned by ultra-sensitive miniaturized sensors which will be inserted through laparoscopic or robotic trocars into a patient's body cavity that are able to provide the surgeon with precise haptic feedback. Furthermore, ultra-reliable and low-latency 5G communications networks will be able to provide signal round-trip times of less than 10 ms, enabling fully immersive surgery experiences including visual, audio, and haptic information. And finally, *standardized haptic interfaces* will prevent vendor lock-in and thus lower costs to hospitals and society, allowing for widespread implementation.

Future embodiments of telesurgery systems could allow for multiple operating surgeons to intervene at the same time, for the same patient – all from different hospitals regardless of location. In an even more advanced embodiment, local or remote AI could be used for human-assisted autonomous surgery. The virtualized skills approach of the *Internet of Skills* would allow different domain specialists – whether human or machine – to operate at the same time and on the same patient cooperatively, thus reducing operative time and healthcare costs.

Past and Modern Teleoperations

Telesurgery is not new; however, the implementation using a public and yet extremely reliable and low-latency Internet is new. The first telesurgery operation was performed in mid-2001 between Strasbourg in France and New York City, USA. The distance of about 6500 km (ca. 4000 miles) was covered using expensive dedicated fibre. The surgical system was provided by the ZEUS robotic system (subsequently purchased by Intuitive Surgical, Sunnyvale, CA, USA). The 2-hour laparoscopic cholecystectomy operation was conducted on a 69-year-old female patient, who later recovered uneventfully [25]. Thereupon, further trials were conducted such as by Prof Prokar Dasgupta, King's College London, between London and Stockholm, and also in 2008 using a Da Vinci (Intuitive Surgical, Sunnyvale, CA, USA) system.

All studies concluded that, in principle, telesurgery is feasible, yet not surprisingly, most of the practically tested systems reported the most significant shortcoming to be related to network latency. In-depth studies [26] have concluded that latencies should be less than 100 ms for the system to be useable, and *latencies above 300 ms produce serious inaccuracies during the medical intervention with potentially catastrophic effects.* That is further amplified with emerging haptic feedback systems, thus requiring even more stringent latency budgets. Other major issues pertained to cost and network stability. In one example, 40 engineers had to be used to ensure the stability of the connection. Launching the 5G public networking infrastructure and the emerging *Internet of Skills*, researchers (including the author) at King's College London have been able to demonstrate the viability of telesurgery overcoming these challenges [27, 28].

A first commercial (preclinical) trial has been conducted early 2019 by surgeons in China using 5G networking technology. As reported, a surgeon in Fujian, China, used an ultra-reliable and very performant 5G system to control robotic arms in a remote location several miles away. The surgeon operated on the liver of a laboratory test animal and experienced an extremely low latency [29]. Over the coming years, we hope to see an increasing use of telesurgery using the emerging 5G infrastructure.

Other Medical Applications

The application of telesurgery using 5G and the *Internet of Skills* is just one of many medical use scenarios which can be executed using this new technology platform. Other applications include the usage of advanced 5G technology in ambulances so that skilled doctors can intervene quicker and so that treatment can be more appropriately delivered in the pre-hospital setting. Another application could involve the use of 5G-connected drones to supply medicine to remote areas expeditiously before paramedics and other first responders arrive on the scene.

Lastly, one of the most exciting applications being explored at King's College London is the design of a 5G-enabled Internet of Skills application for *tele-colonoscopy* [30]. The rationale is that colon cancer is difficult to detect by those not skilled at performing colonoscopy, thus leading to numerous deaths due to non-detection, secondary to a lack of clinical expertise. Rural and remote areas are particularly affected. Led by Dr. Hongbin Liu, a system is being designed which allows remote colonoscopy to be conducted from main hospitals in China into rural areas using 5G and performant fibre. Furthermore, Dr. Liu pioneered novel sensing and soft-robotics technologies, all of which form part of the solution's portfolio. If successful, tele-colonoscopy could be an important and potentially life-saving application of 5G networks; ultimately, democratizing skills the same way as the Internet has democratized information.

Acknowledgements The material of this chapter would now have been possible without the years-long collaboration and input from Prof Prokar Dasgupta, Dr. Toktam Mahmoodi, Dr. Hongbin Liu, Prof Eckehard Steinbach, Xun Liu, and Sandra Kim.

References

1. Fettweis G, Boche H, Steinbach E, et al. The tactile internet. ITU-T Technology Watch Report. 2014; http://bit.ly/1BvAhlr.
2. Dohler M, Fettweis G. The tactile internet – IoT, 5G and cloud on steroids. Telefonica Guest Blog Post, 30 October 2014, >200k views; http://bit.ly/1BpOG3H.
3. Fettweis G. The tactile internet: applications and challenges. IEEE Vehicular Technology Magazine. 2014;9(1); http://bit.ly/1wXjwks.
4. Aijaz A, Dohler M, Aghvami AH, Friderikos V, Frodigh M. Realizing the Tactile Internet: Haptic Communications over Next Generation 5G Cellular Networks, in IEEE Wireless Communications. 2017;24(2):82–9. https://doi.org/10.1109/MWC.2016.1500157RP.
5. Simsek M, Aijaz A, Dohler M, Sachs J, Fettweis G. 5G-Enabled Tactile Internet, in IEEE Journal on Selected Areas in Communications. 2016;34(3):460–73. https://doi.org/10.1109/JSAC.2016.2525398.
6. An internet of skills, where robotics meets AI and the tactile internet. Plenary Keynote at IEEE ICC 2016, 26 May 2016, Kuala Lumpur, [PDF].
7. Dohler M, et al. Internet of skills, where robotics meets AI, 5G and the tactile internet. EuCNC. 2017.
8. Mountaser G, Rosas ML, Mahmoodi T, Dohler M. On the feasibility of MAC and PHY split in cloud RAN. 2017 IEEE Wireless Communications and Networking Conference (WCNC). San Francisco; 2017. p. 1–6. https://doi.org/10.1109/WCNC.2017.7925770.
9. 3GPP TR38.801, Study on new radio access technology: radio access architecture and interfaces. Release 14 Mar 2017.
10. Quintana-Ramirez I, Tsiopoulos A, Lema MA, Sardis F, Sequeira L, Arias J, Raman A, Azam A, Dohler M. The making of 5G – building an end-to-end 5G-enabled system. IEEE Communications Standards Magazine. Accepted 10 Aug 2018.
11. 3GPP TR23.501, System architecture for 5G. Release 15 Dec 2017.
12. OpenStack Foundation Report. Accelerating NFV delivery with OpenStack. White Paper. 2016. [Online] Available at: https://www.openstack.org/telecoms-and-nfv/.
13. Bastug E, Bennis M, Debbah M. Living on the edge: the role of proactive caching in 5G wireless networks. Communications Mag IEEE. 2014;52(8):82–9.
14. Sakr N, Georganas N, Zhao J, Shen X. Motion and force prediction in haptic media. In: Multimedia and expo, 2007 IEEE international conference on, July 2007. p. 2242–5.
15. MacLean KE. Haptic interaction design for everyday interfaces. Rev Human Factors Ergonomics. 2008;4(1):149–94.
16. Steinbach E, et al. Haptic communications. Proc IEEE. 2012;100(4):937–56.
17. Steinbach E, Hirche S, Kammerl J, Vittorias I, Chaudhari R. Haptic data compression and communication. IEEE Signal Process Mag. 2011;28(1):87–96.
18. Steinbach E, Strese M, Eid M, Liu X, Bhardwaj A, Liu Q, Al-Ja'afreh M, Mahmoodi T, Hassen R, El Saddik A, et al. Haptic codecs for the tactile internet. Proc IEEE. 2018;107(2):447–70.
19. Okamoto S, Nagano H, Yamada Y. Psychophysical dimensions of tactile perception of textures. IEEE Trans Haptics. 2013;6(1):81–93.

20. Holland O, Steinbach E, Prasad RV, Liu Q, Dawy Z, Aijaz A, Pappas N, Chandra K, Rao VS, Oteafy S, et al. The IEEE 1918.1 "tactile internet" standards working group and its standards. Proc IEEE. 2019;107(2):256–79.
21. Liu X, Dohler M. A data-driven approach to vibrotactile data compression. IEEE SiPS 2019, IEEE international workshop on signal processing systems, Nanjing, 20–23 Oct 2019.
22. Liu X, Dohler M, Mahmoodi T, Liu H. Challenges and opportunities for designing tactile codecs from audio codecs. EuCNC; 2017.
23. Kim S, Dohler M, Dasgupta P. The internet of skills: the use of 5th generation telecommunications, Haptics, and artificial intelligence in robotic surgery. BJU Int. 2018;122(3):356–8. https://doi.org/10.1111/bju.14388. Epub 10 June 2018.
24. Okamura AM. Haptic feedback in robot-assisted minimally invasive surgery. Curr Opin Urol. 2009;1:102–7.
25. Choi PJ, Oskouian RJ, Tubbs RS. Telesurgery: past, present, and future. Cureus. 2018;10(5):e2716.
26. Xu S, Perez M, Yang K, Perrenot C, Felblinger J, Hubert J. Determination of the latency effects on surgical performance and the acceptable latency levels in telesurgery using the dV-trainer((R)) simulator. Surg Endosc. 2014;28:2569–76.
27. Can connected health be the lifeblood of 5G? Mobile World Congress 2017; last accessed Q4 2019: https://www.mobileworldlive.com/blog/blog-can-connected-health-be-the-lifeblood-of-5g/.
28. Ericsson and King's College London give tactile robotic surgery the finger with 5G. Fierce Wireless. June 2016; last accessed Q4 2019.: https://www.fiercewireless.com/europe/ericsson-applies-5g-to-robotic-surgeon-s-finger.
29. Surgeon performs world's first remote operation using '5G surgery' on animal in China. Independent, 17 January 2019; last accessed Q4 2019: https://www.independent.co.uk/life-style/gadgets-and-tech/news/5g-surgery-china-robotic-operation-a8732861.html.
30. 5G future: a world of remote colonoscopies. Financial Times, 28 March 2018; last accessed Q4 2019.: https://www.ft.com/video/ecce7b44-fd92-4073-915b-36b7a537fc60.

7 Haptics and Vision Systems for Surgical Robots

Marco Ferrara and Mark K. Soliman

Abbreviations

3D	Three dimensional
AR	Augmented reality
HD	High definition
SD	Standard definition
UHD	Ultra-high definition
VR	Virtual reality

Introduction

Although one tends to think of robotic surgery as a recent development, the first documented surgical robot, the PUMA, was introduced in the 1980s. Modern-day robotic systems have evolved substantially from these origins due to incremental improvements in the various technologies involved in the functioning of the robotic systems. In 2000, the da Vinci Surgery System (Intuitive Surgical Inc., Sunnyvale, CA) was introduced, which launched surgical robotics into the mainstream and vastly expanded their potential uses. Until recently, this was the only FDA-approved robotic surgery system, and thus, the majority of robotic advances have been focused on this system. Today, there are numerous competing companies, both large and small, that are developing innovative surgical robots to further improve the ability of surgeons to care for their patients. The ultimate goal of these varied platforms is to not only replicate the tools innate to the operating surgeon but also expand upon them as well. This comes in many forms, from improved ergonomics to providing access to anatomic targets that are otherwise out of reach with conventional laparoscopy and robotics.

One of the areas which has already proven utility and holds some of the greatest promise for the future is the enhanced visualization afforded to the surgeon when operating robotically. Alternatively, an area that has somewhat lagged behind in development and remains a limiting factor in the fidelity of robotic surgery is the incorporation of haptic feedback into the robotic systems.

Haptic Feedback in Robotic Surgery

The advent of robotic surgery brought with it the promise of not only simulating innate human dexterity and vision but also augmenting the surgeon's overall ability and performance. The visual aspect of the current robotic systems has attained these heights and will continue to evolve over time. However, to truly attain the promise of simulating and enhancing surgery through the aid of a robot, incorporating haptic feedback is paramount. However, this is quite challenging, since

M. Ferrara (✉) · M. K. Soliman
Department of Colon and Rectal Surgery, Colon and Rectal Clinic of Orlando, Orlando, FL, USA
e-mail: mferrara@crcorlando.com

S. Atallah (ed.), *Digital Surgery*, https://doi.org/10.1007/978-3-030-49100-0_7

no currently designed surgical instrument is able to replicate the efficacy of the discerning hands of a well-trained surgeon. The assessment of texture, temperature, turgor, and countless other haptic cues aids a surgeon in assessing the structural integrity and identification of important anatomy during operation. The human hand alone contains a multitude of functionally distinct tactile nerve endings, each of which aids in discerning texture, temperature, and many other tissue characteristics that determine how to appropriately manipulate a given object [1].

Although not equivalent to direct palpation of tissue, tactile feedback with laparoscopic instruments allows rudimentary assessment of tissue resistance and tension. The investigation into incorporating more informative haptic feedback has been explored for laparoscopy, with the testing and development of several systems aimed at improving surgeon feedback [2]. Despite the ingenuity and potential, this has not been widely adopted. One notable exception to this is the Senhance® Surgical System (TransEnterix Surgical Inc., Morrisville, NC, USA). This platform includes haptic feedback along with precision dissection at lower costs than conventional robotic platforms. Although not in widespread use, initial reports of its performance and patient outcomes have been promising, though further study is needed [3, 4] (Fig. 7.1).

Haptic integration into robotic systems presents a further challenge, as the surgeon is often remote from the instrument being manipulated. Myriad technological and logistical hurdles that exist for implementation of haptic feedback in robotic surgery have forced many investigations into these technologies to remain in the design and development phase – without progressing to clinical use [5]. In addition, some have reported difficulty with integrating haptic force feedback without leading to potentially disrupting oscillations in the robotic system [6]. This has led to alternate paths for enhancing tactile feedback, one of which is *sensory substitution*. This involves translating forces via stimulation of other senses, such as auditory or visual. However, this has generally been found to be inferior to unaltered force feedback [7].

Haptic Feedback and Surgical Training

The importance of tactile feedback in the development of surgical skills in trainees cannot be understated. As the role of virtual reality has blossomed in surgery, this truism has been validated and tested. A recent systemic review by Rangarajan et al. demonstrated that for surgical tasks and activities, simulation with haptic feed-

Fig. 7.1 The Senhance® Surgical System (TransEnterix Surgical Inc., Morrisville, NC, USA). (©2020 TransEnterix Surgical, Inc. All rights reserved. Senhance is a registered trademark of TransEnterix. Image publicly available on https://www.senhance.com/us/digital-laparoscopy)

back leads to an improved sense of realism and led to a reduced learning curve for trainees when compared to simulators without haptic feedback [8]. Several other studies have shown that haptic feedback is integral in skill acquisition for surgical trainees [9, 10] One of the limitations of applying haptic feedback is that, as a relatively new technology, the initial products tend to be cumbersome and difficult to integrate – particularly when working in narrow spaces, as is often the case in robotic surgery. However, this is an area of active research as improvements in technology will allow for smaller and more discreet systems to grant the sensing and transmission of haptic information.

Clinical Implications of Haptic Feedback

One of the primary concerns with the lack of tactile sensation with robotic platforms is the potential for tissue trauma due to often unidentified excessive grasping and shearing forces from robotic effector arms. A specific task in which the incorporation of force sensation has great potential is in the handling of suture material. Most surgeons who have attempted robotic suturing have experienced inadvertent fraying or breakage of suture material. Even more so than handling suture, the tying of knots robotically requires practice and close attention to visual cues in order to avoid suture breakage. This can be frustrating, adding significant time to the operation. However, reliance on visual cues is imperfect and can also be dependent on image quality [11]. To mitigate this, multiple haptic sensors have been utilized specifically to avoid suture trauma. One of the difficulties in transmitting usable tactile information when performing a complex maneuver such as suturing is that the surgeon is often pulling the suture material in *multiple* directions. *This makes the use of uniaxial sensors of limited utility* [12]. The development of biaxial shear sensing along with haptic feedback has been used in order to alert a surgeon when undue tension is being applied to suture material. A recent study by Dai et al. tested such a system and showed a 59% reduction in suture breakage while reducing the overall mean force application by 25% [13]. A similar study by Abiri et al. utilized a multimodal pneumatic system which incorporated various tactile facets in order to allow more delicate tissue handling. This study similarly found that integration of this system led to significant force reduction and a theoretical decrease in tissue trauma [14]. Future integration of this technology also requires recognition of the different tensile strengths of suture material, as this can vary widely [15]. The potential complications from poorly tied knots or damaged suture material are myriad, and one's standards for quality of such a basic tenet of surgery should not be lessened to accommodate any surgical platform.

As surgeons gain experience with robotic surgery, many learn to use visual cues to guide their movements. Thus, haptic feedback may be of limited utility for those at the expert level. In fact, this is one area where the improved optics afforded by the surgical robot can help compensate for the loss of the sense of touch. In a study by Reiley et al., visual cues to aid with force feedback led to improved performance in novice surgeons while not significantly impacting surgeons with pre-existing experience with the da Vinci robotic system [16]. The possibility of real-time incorporation of suture strain evaluation by interpreting visual cues has also been explored [11].

Cutaneous Feedback

While the integration of force tension continues to present a significant challenge in robotic surgery, the replication of *cutaneous feedback,* as is experienced by the surgeon's fingertips, is perhaps an even greater challenge to capture. This focuses on the replication of the senses of direction, location, and intensity (as well as others parameters), as would be detected on the surgeon's fingertips. Utilization of cutaneous feedback has been found to supply the surgeon with tactile information without the negative potential effect of causing the destabilization of the robotic system [7]. Multiple different technologies have been developed and adapted to replicate cutaneous feedback. Many of the earlier methods relied upon pneumatic mechanisms to relay tactile feedback [17]. One technology that has been developed and tested to replicate this is the SynTouch BioTac sensor. This system utilizes sensors to replicate deformation, temperature, and internal fluid pressure. These data are then transferred to the operating surgeon's fingers to allow for cutaneous feedback of tissue. Although the current iteration is bulky and not currently practical for surgery, further advances in this technology could eventually lead to its adaptation [18].

Vision Systems in Robotic Surgery

One of the primary and immediate improvements afforded by not only robotic but all modalities of video-assisted surgery has been the ability to improve upon visualization of critical structures when operating in difficult areas. As video technology has improved, the possible implementations and enhancements to the performance of surgery have as well. While many surgeons already enjoy access to improved optics when operating robotically, the field itself is relatively young and ripe with the potential for further integration of advanced visual systems to lead to safer, more accurate surgery which ultimately improves the quality of patient care.

High-Definition Vision Systems

The advancements in vision projection technology have been mostly driven by consumer demand for high-resolution television and computer screens. However, those advances can then be applied to a broad range of areas, including medicine and surgery in particular. Unfortunately, there is no universal standard in terms of quality of optics utilized in operating rooms, and many still utilize standard-definition (SD) technology. High-definition (HD) technology has become more widespread and can offer a significant advantage in terms of resolution, providing up to 1920 × 1080 pixels. Although not as widespread, 4K HD vision systems, which depict video in 3840 × 2160 pixel resolution, have been in use in operating theaters for several years, first being applied in orthopedic surgery. Today, most surgical vision system vendors offer a 4K platform. While the adaptation of 4K visual systems has not yet become widespread, even in advanced centers, already there are 8K systems being evaluated. 8K technology allows for 7680 × 4320 pixels to be displayed, significantly improving upon the standard 2K HD technology widely used in operating rooms in North America and Europe. While many surgeons currently utilizing standard HD and even SD technology are facile and able to expertly perform complex operations in this manner, one could argue that supplying the experienced surgeon with more information, in this case, *pixels*, will lead to further improvement of technique and quality of surgical care rendered. *To put this in perspective, when compared to standard definition, 4K offers almost 30 times the pixels, while 8K increases the pixels by a factor of one hundred* (Table 7.1).

Ohigashi et al. reported their experience with three cases of colon resections for cancer utilizing an 8K UHD endoscope. They reported improved visualization, allowing enhanced ability to identify and preserve the autonomic nerves during dissection [19]. At this level of definition, it is often reported that the stereoscopic vision is improved to project a more realistic three-dimensional vision without necessarily incorporating specific technologies to project in 3D. As with many new technologies, the first iteration is heavier and occupies considerable space, due to the increased onboard processors required for a higher-definition camera. With time and further

Table 7.1 Commonly used screen resolutions with respective pixel counts

Resolution	Measurements (pixels)	Pixel count
480p (SD)	640 × 480	307,000
720p (HD)	1280 × 720	921,600
1080p (Full HD)	1920 × 1080	2,073,600
4k (Ultra HD)	3840 × 2160	8,294,400
8k (Ultra HD)	7680 × 4320	33,177,600

improvements in technology, this is predicted to improve, making it more practical for the operating theater. Notwithstanding, there may be a limit to the added value gained by increasing the video quality, beyond which appreciable gains are diminished. One could also argue that at the "close" view-finder distance from the monitor being utilized in da Vinci robotic surgery, the actual perceptible differences to the surgeon would be minute when the image definition is further enhanced.

Current iterations of the da Vinci robotic system utilize 3DHD vision, which allows for accurate dissection and recognition of minute anatomic details. The addition of an integrated Firefly® infrared camera has further enabled surgeons to identify critical structures in order to avoid inadvertent injury and to assess tissue perfusion. This technology utilizes near-infrared fluorescence (NIRF) and allows the identification of tissue perfusion when utilized with indocyanine green. This is often particularly useful when a patient's anatomy may be altered, such as in reoperative surgery or when neoadjuvant radiation therapy has been administered. Future uses of this technology include the potential identification of lymph nodes for more precise oncologic resection [20]. Recent advances in imaging technology have allowed for the identification of structures based on autofluorescence, obviating the need for administration of a fluorescent agent and allowing more uninterrupted evaluation of structures during surgery [21]. Particularly useful in pelvic surgery, the use of infrared lighted ureteral stents can aid in the identification and preservation of these structures during surgical dissection (Fig. 7.2).

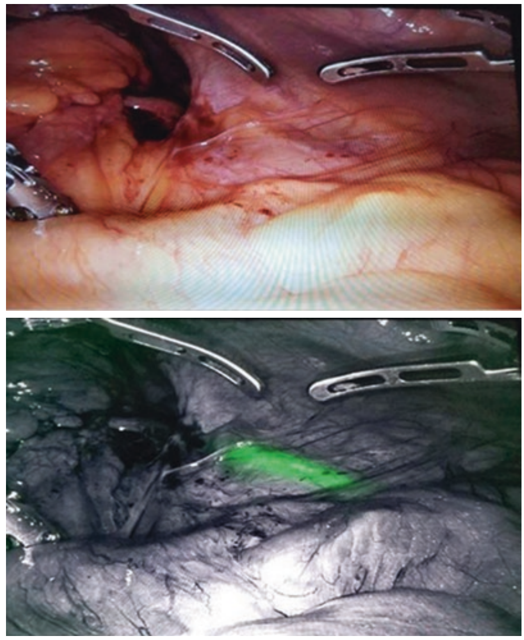

Fig. 7.2 Immunofluorescence of the ureter as seen on Firefly® during da Vinci robotic surgery. (Photo courtesy of Dr. Avery Walker)

Augmented Reality

Augmented reality (AR) is an exciting technology that has begun to become more prevalent and is particularly important to the development of digital surgery. The potential applications are clear, and many systems have been developed for use in different surgical fields. The value of AR, as related to surgery, is probably best suited for relatively static anatomical structures, such as the brain, retroperitoneal structures, or bones [22–24]. The nature of these organs leads them to accurate representation intraoperatively, as most AR systems integrate preoperative imaging to display important structures to the operating surgeon. The use of AR in the performance of robotic nephrectomy has been well-described with promising results [25]. Future uses of AR segue beyond the overlay of structures and even assist surgeons by avoiding hazardous areas and redirect dissection in the event an incorrect plane is entered. The utilization of AR in robotic surgical training has led to the development of several different systems focused on reproducing accurate anatomic models with integrated guidance for surgical education.

Beyond the identification of structures during surgery, AR technologies can be utilized to enable real-time feedback for surgeons from colleagues without geographic restrictions. This has the potential to revolutionize the quality of surgical care worldwide, particularly in areas with poor access to surgical expertise. The excitement toward this and other potential uses of AR in surgery led to a seminal TED talk by the plastic surgeon and founder of the company Proximie, Nadine Hachach-Haram, in 2017 [26]. With the democratization of data and the increased accessibility afforded by communication technologies, the ability to share expert opinions in real time regardless of geographic constraints is becoming less science fiction and more reality.

Virtual Reality

Virtual reality (VR) is another technology that is already widely used, particularly for the acquisition of rudimentary robotic skills by surgeons. The most commonly used is the da Vinci Skills Simulator, which allows the surgeon to practice various maneuvers and manipulations in a virtual space [27]. Other virtual training platforms include the RobotiX Mentor (Simbionix USA Inc., Cleveland, OH), Robotic Surgical Simulator (RoSS; Simulated Surgical Systems, LLC, Williamsville, NY), and the Mimic dV-Trainer (Mimic Technologies, Inc., Seattle, WA) [28]. It has been well-established that structured robotic training utilizing practice within the virtual realm leads to increased efficiency in real-time surgical technique [29–32]. As this technology continues to mature and incorporates more realistic physics engines and software, it will become more feasible to allow surgeons to "practice" specific cases in a virtual reality environment prior to embarking upon the actual operation. This could be utilized to aid in the identification of aberrant anatomy and even help with the development of innovative new techniques to tackle difficult surgical situations.

Summary

Robotic surgery has enhanced the ability of surgeons to perform complex operations, benefitting both the patient and the surgeon. The goal of robotic surgery is to not only replicate the innate senses of the surgeon but also expand upon them as well. The continued development of this field has brought together the disciplines of medicine, bioengineering, computer programming, and many others. As these individual fields and technologies continue to advance, the possibilities for synergistic collaboration will continue to expand into new and often unexpected directions. As these advances bring increased fidelity and decreased costs to robotic surgery, the adoption and utility of this field will continue to grow.

References

1. Johansson RS, Flanagan JR. Coding and use of tactile signals from the fingertips in object manipulation tasks. Nat Rev Neurosci. 2009;10(5):345–59.
2. Tholey G, Desai JP, Castellanos AE. Force feedback plays a significant role in minimally invasive surgery: results and analysis. Ann Surg. 2005;241(1):102–9.
3. Samalavicius NE, Janusonis V, Siaulys R, Jasėnas M, Deduchovas O, Venckus R, et al. Robotic surgery using Senhance(®) robotic platform: single center experience with first 100 cases. J Robot Surg. 2019;12. doi: [Epub ahead of print].
4. deBeche-Adams T, Eubanks WS, de la Fuente SG. Early experience with the Senhance®-laparoscopic/robotic platform in the US. J Robot Surg. 2019;13(2):357–9.
5. Amirabdollahian F, Livatino S, Vahedi B, Gudipati R, Sheen P, Gawrie-Mohan S, et al. Prevalence of haptic feedback in robot-mediated surgery: a systematic review of literature. J Robot Surg. 2018;12(1):11–25.
6. Diolaiti N, Niemeyer G, Barbagli F, Salisbury JK. Stability of haptic rendering: discretization, quantization, time delay, and coulomb effects. IEEE Trans Robotics. 2006;22(2):256–68.
7. Meli L, Pacchierotti C, Prattichizzo D. Sensory subtraction in robot-assisted surgery: fingertip skin deformation feedback to ensure safety and improve transparency in bimanual haptic interaction. IEEE Trans Biomed Eng. 2014;61(4):1318–27.
8. Rangarajan K, Davis H, Pucher PH. Systematic review of virtual haptics in Surgical simulation: a valid educational tool? J Surg Educ. 2019;26. [Epub ahead of print].
9. Cao CGL, Zhou M, Jones DB, Schwaitzberg SD. Can surgeons think and operate with haptics at the same time? J Gastrointest Surg. 2007;11(11):1564–9.
10. Rodrigues SP, Horeman T, Sam P, Dankelman J, van den Dobbelsteen JJ, Jansen FW. Influence of visual force feedback on tissue handling in minimally invasive surgery. Br J Surg. 2014;101(13):1766–73.
11. Martell J, Elmer T, Gopalsami N, Park YS. Visual measurement of suture strain for robotic surgery. Comput Math Methods Med. 2011;2011:879086.

12. Abiri A, Askari SJ, Tao A, Juo YY, Dai Y, Pensa J, et al. Suture breakage warning system for robotic surgery. IEEE Trans Biomed Eng. 2019;66(4):1165–71.
13. Dai Y, Abiri A, Pensa J, Liu S, Paydar O, Sohn H, et al. Biaxial sensing suture breakage warning system for robotic surgery. Biomed Microdevices. 2019;21(1):10.
14. Abiri A, Pensa J, Tao A, Ma J, Juo YY, Askari SJ, et al. Multi-modal haptic feedback for grip force reduction in robotic surgery. Sci Rep. 2019;9(1):5016.
15. Abiri A, Paydar O, Tao A, LaRocca M, Liu K, Genovese B, et al. Tensile strength and failure load of sutures for robotic surgery. Surg Endosc. 2017;31(8):3258–70.
16. Reiley CE, Akinbiyi T, Burschka D, Chang DC, Okamura AM, Yuh DD. Effects of visual force feedback on robot-assisted surgical task performance. J Thorac Cardiovasc Surg. 2008;135(1):196–202.
17. Li M, Luo S, Seneviratne LD, Nanayakkara T, Althoefer K, Dasgupta P. Haptics for multi-fingered palpation. IEEE international conference on systems, man, and cybernetics. IEEE. Manchester. 2013. p. 4184–9.
18. Pacchierotti C, Prattichizzo D, Kuchenbecker KJ. Cutaneous feedback of fingertip deformation and vibration for palpation in robotic surgery. IEEE Trans Biomed Eng. 2016;63(2):278–87.
19. Ohigashi S, Taketa T, Shimada G, Kubota K, Sunagawa H, Kishida A. Fruitful first experience with an 8K ultra-high-definition endoscope for laparoscopic colorectal surgery. Asian J Endosc Surg. 2019;12(3):362–5.
20. Daskalaki D, Aguilera F, Patton K, Giulianotti PC. Fluorescence in robotic surgery. J Surg Oncol. 2015;112(3):250–6.
21. Gorpas D, Phipps J, Bec J, Ma D, Dochow S, Yankelevich D, et al. Autofluorescence lifetime augmented reality as a means for real-time robotic surgery guidance in human patients. Sci Rep. 2019;9(1):1187.
22. Guha D, Alotaibi NM, Nguyen N, Gupta S, McFaul C, Yang VXD. Augmented reality in neurosurgery: a review of current concepts and emerging applications. Can J Neurol Sci. 2017;44(3):235–45.
23. Lee C, Wong GKC. Virtual reality and augmented reality in the management of intracranial tumors: a review. J Clin Neurosci. 2019;62:14–20.
24. Burström G, Nachabe R, Persson O, Edström E, Elmi TA. Augmented and virtual reality instrument tracking for minimally invasive spine surgery: a feasibility and accuracy study. Spine (Phila Pa 1976). 2019;44(15):1097–104.
25. Hughes-Hallett A, Mayer EK, Marcus HJ, Cundy TP, Pratt PJ, Darzi AW, et al. Augmented reality partial nephrectomy: examining the current status and future perspectives. Urology. 2014;83(2):266–73.
26. Hachach HN. How augmented reality could change the future of surgery. Presented at TEDWomen. 2017. https://www.ted.com/talks/nadine_hachach_haram_how_augmented_reality_could_change_the_future_of_surgery?language=en.
27. Intuitive Surgical. da Vinci skills simulator. http://www.intuitivesurgical.com/products/skills_simulator/. Accessed Oct 2019.
28. Julian D, Tanaka A, Mattingly P, Truong M, Perez M, Smith R. A comparative analysis and guide to virtual reality robotic surgical simulators. Int J Med Robot. 2018;14(1):e1874.
29. Schreuder HW, Persson JE, Wolswijk RG, Ihse I, Schijven MP, Verheijen RH. Validation of a novel virtual reality simulator for robotic surgery. ScientificWorldJournal. 2014;2014:507076.
30. Ruparel RK, Taylor AS, Patel J, Patel VR, Heckman MG, Rawal B, et al. Assessment of virtual reality robotic simulation performance by urology resident trainees. J Surg Educ. 2014;71(3):302–8.
31. Alzahrani T, Haddad R, Alkhayal A, Delisle J, Drudi L, Gotlieb W, et al. Validation of the da Vinci Surgical skill simulator across three surgical disciplines: a pilot study. Can Urol Assoc J. 2013;7(7–8):e520–9.
32. Kumar A, Smith R, Patel VR. Current status of robotic simulators in acquisition of robotic surgical skills. Curr Opin Urol. 2015;25(2):168–74.

8 Digital and 3D Printed Models for Surgical Planning

Jordan Fletcher and Danilo Miskovic

Introduction

3D visualization and printing techniques have been met with great enthusiasm by the surgical community; they potentially provide significant benefits in a wide range of clinical applications, particularly in preoperative planning [1, 2]. Preoperative planning is considered a crucial aspect of safe and effective surgery. We can broadly define preoperative planning as any activity aimed at understanding a patient's anatomy or pathology in order to inform clinical decision-making and determine an appropriate operative strategy [3]. This can involve attempts to understand specific structural relationships, preoperative rehearsal, simulation, judgments of feasibility for a given procedure (e.g., tumor resectability), physiological modeling, or implant placement/design [4, 5]. It can encompass a diverse range of activities that occur at the level of the individual surgeon or as part of a more formalized process such as multidisciplinary team (MDT) meetings.

Medical imaging plays a major role in surgical planning. Currently, clinical decisions are made after 2D imaging modalities such as plain radiographs, computed tomography (CT), or magnetic resonance imaging (MRI) are reviewed by the surgeon and/or radiologist. However, extracting the relevant 3D anatomical relationships from 2D images in order to apply them intraoperatively can be difficult even for experienced practitioners. Intuitively, 3D reconstructions appear to have an advantage over traditional 2D images. Consequently, the interest of 3D visualization techniques in surgical specialties has increased in recent years [6].

Anatomically accurate 3D virtual models can be reconstructed from standard 2D Digital Imaging and Communications in Medicine (DICOM) data sets through a variety of methods [2]. Such virtual models can subsequently be printed as physical objects through a process termed *additive manufacturing* – more commonly known as 3D printing. Although there are various methods of 3D printing available, each relies on the principle of sequentially laying 2D layers of material in order to construct a 3D structure.

Advances in technology have facilitated dissemination of 3D modeling. Easier access to cheaper computer processing power in conjunction with the proliferation of open-source imaging and computer graphics software has made it possible to generate anatomical models on a personal computer [7]. Similarly, development of low-cost 3D desktop printers has enabled use outside industrial manufacturing. After initial pioneering work performed by oral maxillofacial and congenital cardiac surgeons [8, 9], the majority of surgical specialties have now utilized 3D

J. Fletcher (✉) · D. Miskovic
Department of Colorectal Surgery, St. Marks Hospital, London, UK
e-mail: jordan.fletcher@nhs.net

S. Atallah (ed.), *Digital Surgery*, https://doi.org/10.1007/978-3-030-49100-0_8

visualization to plan and perform a diverse range of procedures [10].

Early research suggests 3D visualization may result in improved anatomical understanding [11, 12]. This may be particularly evident in cases involving highly variable, complex structural relationships [13, 14]. Proponents hope 3D models may facilitate more tailored procedures, reduce errors and complications, and ultimately improve patient outcomes [1]. Beyond pure anatomical visualization, 3D modeling could facilitate new methods of interacting with imaging data for preoperative preparation. 3D models can enable patient-specific virtual simulations and computer-aided design (CAD) of custom implants and serve as the substrate for augmented reality (AR)-enhanced navigation [15–17].

Despite initial optimism, the extent to which 3D models influence preoperative decision-making and their relative effectiveness has yet to be established. Furthermore, the ideal user (novice versus expert), specific indications, optimal user interface, and even evaluation methodology remain unknown. In this chapter, we will provide an overview of 3D reconstruction methods along with current 3D printing technology. We will outline how these techniques have been used for preoperative planning across surgical specialties to date and highlight research priorities going forward.

Methods of Generating 3D Virtual Reconstructions

Segmentation

Image segmentation is a fundamental step in 3D surface-rendered model production. *Segmentation* refers to the process by which unique labels are applied to imaging data in order to identify anatomical or pathological structures of interest [18]. This can be manual or automated to varying degrees – at present the majority of approaches require some user input.

Manual segmentation is the simplest method. The user (typically radiologist) will manually highlight or outline relevant structures slice by slice. This can be performed with a simple mouse-controlled cursor; however, specialized devices like tablet/digital pens are preferable.

One of the principle advantages is flexibility. Manual segmentation is always applicable, even if structures are difficult to delineate owing to artifact or poor-quality imaging. However, manual segmentation can be extremely time-consuming and lacks precision or reproducibility owing to individual interpretation of scan data. Despite these drawbacks, manual segmentation is widely employed due to its ease of implementation and availability of multiple open-source software solutions.

Several different algorithmic approaches have been implemented for segmentation. A detailed discussion of this complex area is beyond the scope of this chapter. However, we provide an overview of key techniques:

Thresholding

A straightforward and fast method is termed *thresholding*. The user sets a global or upper and lower threshold for Hounsfield intensity generating a binary segmentation. Pixels are classified as either belonging to the target structure or else marked as background. This method can be extremely effective for high-intensity structures such as bone [19].

Edge-Based Segmentation

Edge-based segmentation relies on discontinuities in the image data, usually signified by rapid changes in pixel signal intensity between two different structures [19].

Region-Based Segmentation

Region-based segmentation is based on the concept of homogeneity. A target structure is assumed to possess similar pixels clustered together. With the *seed point method*, the user identifies seed points within a target structure, and a region of homogenous pixels of similar intensities is then grown iteratively. Region-growing approaches are typically used for contrast-enhanced vascular structures [18].

Atlas-Based Segmentation

In *atlas-based segmentation*, the geometry and features of organs, blood vessels, and soft tissues are compiled as an atlas. Large databases of images can be constructed, providing a rich compendium of anatomical variation within a population. Statistical shape models (SSMs) form the basis of atlas-based segmentation. SSMs iteratively deform to fit the target of new structures with shapes that are derived from the atlas training set of labeled data. Although conceptually simple, the implementation can be computationally demanding and time-consuming [18, 20].

Automatic Segmentation

Fully *automated segmentation* remains a highly desirable goal, because of the time constraints imposed by modern medicine. With "one click," the whole task would be implemented accurately and reliably from start to finish. Despite the number of algorithmic segmentation methods (as outlined above), there remains no universal algorithm for every form of medical imaging. It is likely such an approach is unrealistic owing to the wide variation in imaging modalities, anatomical relationships, pathological processes, and biological diversity we encounter in medical imaging. Requirements of brain imaging, for example, would differ significantly from abdominal imaging.

Furthermore, automated solutions must factor in problems common to all imaging modalities, such as partial volume effect (loss of activity in small structures due to limited resolution of imaging system), imaging artifact (e.g., motion, ring, intensity inhomogeneity), and signal noise.

Key requirements of automatic segmentation include:

1. *Accuracy*: Relevant structures should be correctly identified and delineated precisely if results are to be used in clinical decision-making
2. *Speed*: Results should be sufficiently quick to enable integration into current clinical workflows
3. *Reproducibility*: Results should be similar for different users analyzing the same data
4. *Robustness*: Methods should be applicable in a wide range of scenarios [21].

Recent research has demonstrated that *convolutional neural networks* (a subset of machine learning) may help solve the automatic segmentation problem. Briefly, convolutional neural networks (CNNs) take inspiration from the animal visual cortex processing data in a grid pattern to adaptively learn spatial patterns in a hierarchical fashion from low- to high-level features [22]. Investigators from around the world have successfully applied the technique to multiple segmentation problems including brain and abdominal segmentation [23, 24]. CNNs represent a form of *supervised learning* – meaning they require large training data sets of labeled scan data.

Rendering Methods for 3D Virtual Models

We can broadly divide 3D virtual visualization into two main categories:

1. *Surface-rendered models*
2. *Volumetrically rendered models*

Surface Rendering Techniques

Surface-rendered models are based on indirect polygonal mesh representations derived from the results of segmentation. For this reason, it is alternatively known as indirect volume visualization, as the surface mesh representation is not the original data set itself.

Through segmentation, we classify each pixel of imaging data as belonging to a certain piece of anatomy. Results of this labeling are stacked sequentially, slice by slice, and used by segmentation software to reconstruct the 3D surface geometry. This can subsequently be exported as a polygonal surface mesh for further editing and processing (Fig. 8.1).

The basic unit of a mesh is a vertex, which describes a position in three-dimensional space. Two vertices joined by a straight line form an edge. A polygon is defined by three (triangle) or four (quad) vertices joined by the corresponding

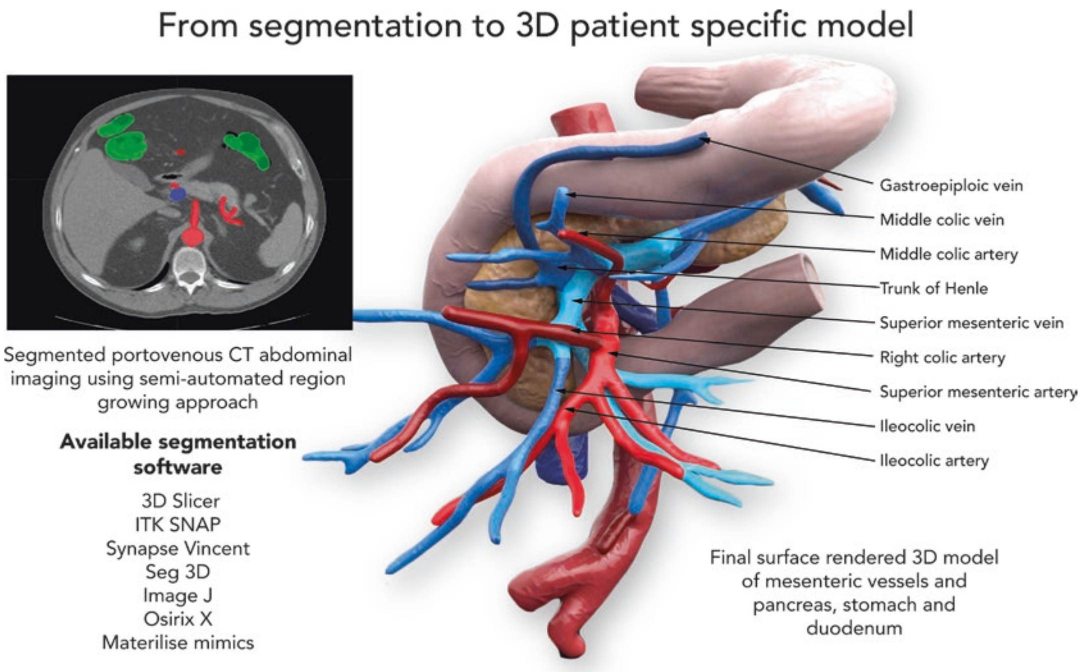

Fig. 8.1 From image segmentation to surface-rendered model – surface-rendered model of mesenteric vascular anatomy derived from CT imaging

number of edges in Euclidean space. Polygonal modeling is an approach for representing three-dimensional objects by approximating their surface structure using multiple polygons (Fig. 8.2).

Surface extraction methods typically rely on binary decisions – for example, whether or not a given pixel in an image slice belongs to the surface. This is appropriate for structures with distinct surfaces, such as bone/ teeth. However, this can produce misleading results when considering non-homogeneous data sets (e.g., abdominal or pelvic imaging), where structures have indistinct boundaries. It is common to see a "staircase" or "stepping" effect especially as the distance between imaging slices increases (this is especially evident with MRI imaging). Most models produced with this workflow therefore require some processing.

Original advantages such as faster render times, a consequence of reduced memory requirements in comparison to volume-rendered models, are less relevant today – due to advances in the capacity of graphical processing units (GPUs). However, surface rendering continues to be an important technique in medical visualization with other potential advantages being as follows:

1. Simplicity of interactive visualization on web or mobile platforms, due to lower memory requirements
2. Surface mesh models are required for 3D printing (see below)
3. Biomedical virtual simulation using computer game engines requires surface mesh models. Producing deformable models with physical properties that can be "digitally dissected" requires surface mesh objects.
4. The majority of commercial computer graphics software works with surface meshes allowing for advanced model manipulation techniques to be applied (e.g., digital sculpting, division of structures, colorization and transparency, realistic texturing of organs).

Volumetric Rendering

Volumetric rendering, also termed *direct volume visualization*, represents the original data set without the requirement of the intermediate rep-

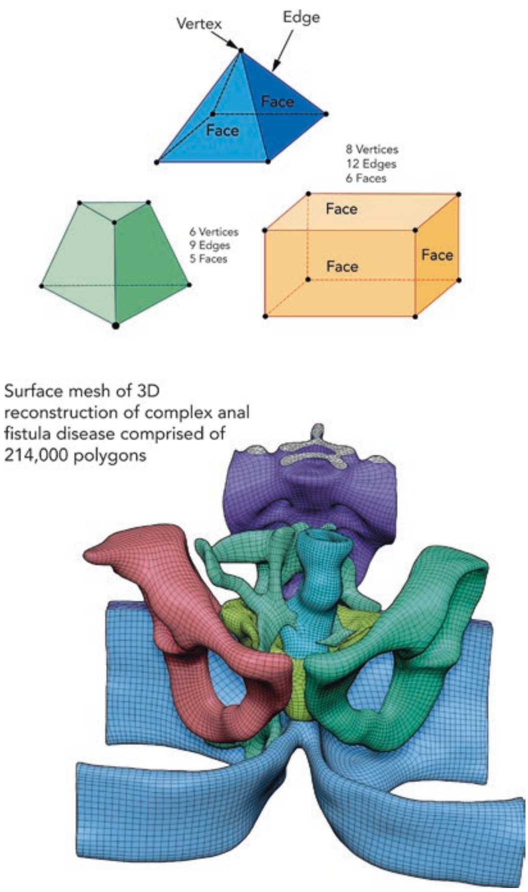

Fig. 8.2 Surface-rendered polygon 3D models composed of vertices, edges, and faces

resentation. Data is visualized as sampled functions of the 3D volume data that are projected as semitransparent volumes onto the 2D viewing plane (Fig. 8.3).

Without the requirement of segmentation, the method preserves all information contained in the image volume. By classifying the values of the contributing structures of the volume and assigning visual properties such as color and transparency, surfaces can be discerned in the rendered image.

3D Printing

The rapid development of 3D printing technology in recent years has created new possibilities in surgical planning and education. Dramatic reductions in cost along with improvements in the accuracy have facilitated production of patient-specific anatomical printed models.

3D printing or additive manufacturing with rapid prototyping was originally described in the 1980s and is based on the principle of sequentially layering material in order to construct a physical object. Each layer of material will be of equal thickness which varies between machines and techniques – the smaller the layer height, the greater the accuracy or resolution of the model.

The first steps in creating a 3D printed model from DICOM data are synonymous with the process outlined above for creating a 3D surface mesh. The area of interest must be segmented and subsequently exported as a stereolithography (STL) file – the most widely used file format in 3D printing. However, the raw segmented mesh data will likely need processing in order to be optimized for 3D printing.

Basic smoothing algorithms can be applied to the model to correct minor surface irregularities (e.g., secondary to the “stepping” artifact). A side effect of smoothing can be a loss of resolution. Care must be taken to not grossly distort the original anatomy. More advanced techniques can be used to divide objects into separate components, complete incomplete mesh structures, and perform “digital sculpting.” Such manipulations can be achieved with most commercially available computer graphics modeling software – however, this requires a degree of expertise, with a steep learning curve commonly observed for novices.

3D Printing Methods

There are three main methods of 3D printing commonly used:

1. Material extrusion
   - Fused deposition modeling (FDM)
   - Fused filament fabrication (FFF)
2. Powder solidification
   - Selective laser sintering (SLS)
   - Binder Jetting (BJ)
3. Photosolidification

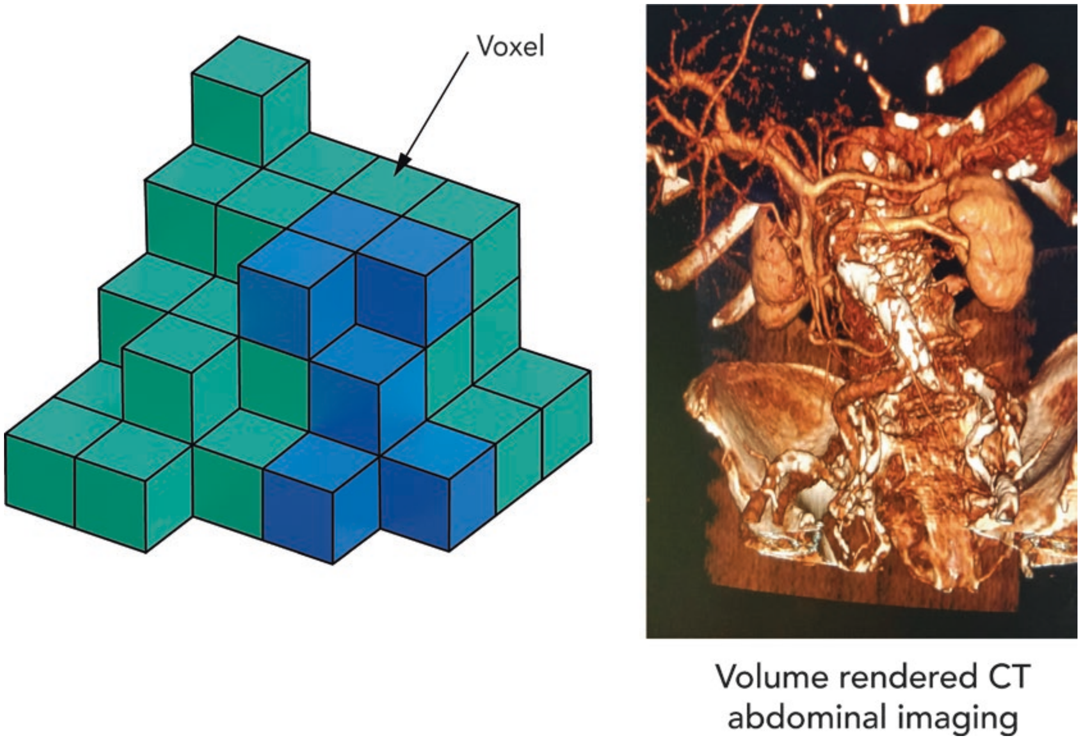

Fig. 8.3 Volume-rendered models. Each voxel represents a point on a regular three-dimensional grid. Their positions/coordinates are not explicitly encoded in their values but are instead inferred from their position to other voxels. In order to render a 2D project of the 3D data set, a camera is defined relative to the volume, and each voxel is defined using an RGBA (red, green, blue, and alpha) transfer function

- Stereolithography (SLA)
- Polyjet (PJ)
- Digital light processing (DLA)

Material extrusion is the most common technique utilized by commercially available desktop 3D printers. Material extrusion printers require a continuous filament of "thermoplastic" which is extruded through a heated nozzle. The printer head is precisely moved under computer control using stepper motors, depositing filament on the horizontal plane, one layer at a time to define the printed shape (Fig. 8.4). They are widely used due to their low cost and ease of setup. However, drawbacks include slow print times, a relative lack of precision (in comparison to other methods), and reliability issues which may limit their clinical utility [6].

Powder solidification techniques, such as SLS and BJ, solidify powdered materials. SLS uses a laser to sinter a bed of powder (form a mass solid by applying heat and pressure, without melting to the point of liquefaction). When the layer is solidified, the build plate lowers and a new layer of powder is added, and the process is then repeated (Fig. 8.5). No support materials are required as the powder bed acts as support. *Binder jetting* similarly uses a powder bed build plate but instead uses a precisely sprayed liquid binder for solidification [25].

Photosolidification uses an ultraviolet light laser controlled with lenses and mirrors in order to cure a VAT of photocurable liquid resin. The build platform is typically inverted and moved up as each layer of the object is fabricated in the familiar layer-by-layer fashion (Fig. 8.6). Photosolidification can rapidly produce highly accurate models of incredible intricacy (ideally suited for printing lattice-like vascular structures). Care needs to be taken to ensure the proper handling of resin which can cause severe contact dermatitis.

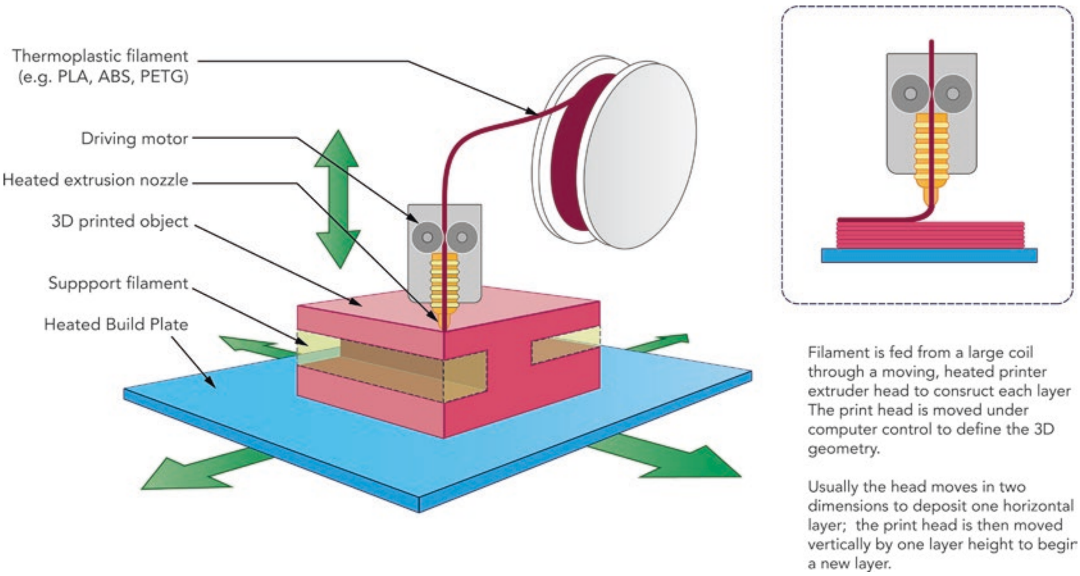

Fig. 8.4 Material extrusion 3D printing

Fig. 8.5 Powder solidification 3D printing. A high-powered laser is used to sinter (fuse) particles of material (plastic, glass, metal). After each layer is produced, the powered bed is lowered, and the roller is used to add new layer of material on top, and the process is repeated

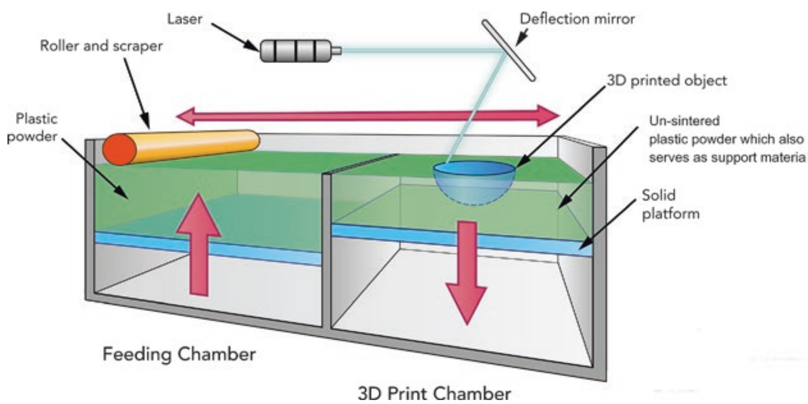

When printing patient models for 3D anatomy, several considerations should be kept in mind. With each method, a degree of technical knowledge is required in order to troubleshoot common mechanical or print errors. This would likely require a dedicated technician or department if printing is to be used in a clinical setting as part of routine care processes [25].

Computer-Assisted Surgery

Computer-assisted surgery (CAS) aims to improve the outcomes and safety of surgical interventions by utilizing digital technologies for preoperative planning and intraoperative navigation. 3D patient-specific models form an integral aspect of CAS. As discussed above, the workflow begins with image acquisition, followed by higher order processing (segmentation and rendering, etc.) in order to prepare for the visualization stage. It is during this phase that surgical planning occurs as the surgeon interacts with the virtual/physical model in order to gain an appreciation of the specific anatomy and potentially rehearse aspects of the surgery and model outcomes.

This interaction is highly variable in terms of the specific hardware, user interface, type of software utilized, and the planning activity under-

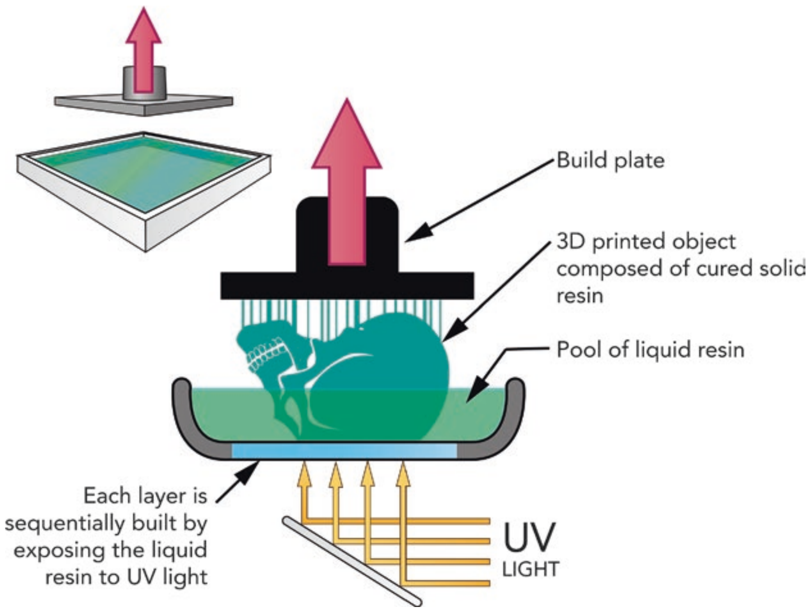

Fig. 8.6 Photosolidification 3D printing

taken. While 2D screen interfaces constitute the principal method of interacting with virtual models, developments in both virtual and augmented realities have allowed for new innovative interface mechanisms.

The resulting plan is subsequently transferred into the operating room. This can be *implicit*, through a mental representation of the case derived from interaction with the model, or *explicit*, through the use of image-guided surgery or mechanical guides (e.g., patient-specific 3D printed cutting guides). The distinction between planning and navigation is increasingly blurred as 3D models are utilized in theater to aid intraoperative navigation through real-time augmented reality interfaces in which the digital image is overlaid onto the operative view. Images can be static, or they can utilize advanced tracking techniques in order to deform the model in synchronicity with real-world tissue manipulations.

3D models have been used in a wide array of planning applications. We can categorize activities of surgical planning into the following general tasks:

1. Improving spatial understanding anatomy and pathology
2. Patient-specific simulation – task rehearsal versus outcome-oriented modeling
3. Resection planning (usually in the context of oncological surgery)
4. Reconstruction planning
5. Implant placement/design

3D and Anatomical Understanding

Anatomical understanding is the baseline requirement on which all surgical procedures are planned and performed. An improved spatial understanding of a patient's anatomy and pathology is a commonly cited advantage of 3D visualization. The task of mentally reconstructing complex structures from 2D imaging slice can be difficult, even for experienced surgeons.

Several authors have examined the effect of 3D virtual models on undergraduate anatomical knowledge acquisition. Azer et al. performed a systematic review on the impact of 3D anatomy models on learning. Of the 30 studies, 60% were randomized controlled trials and the remaining 40% non-randomized comparative studies. 60% utilized objective outcome measures (OSCE, written exam) as opposed to 40% in which subjective ratings were used [26]. Definitive conclusions from these studies are difficult owing to the heterogeneity of methods used and lack of validation for the given outcome measures. Students generally had a preference for 3D visualization techniques over traditional teaching methods [26]. However, not all studies demonstrated the superiority 3D in comparison to other teaching methods. An important observation of this work was to recognize that multiple factors interact to influence the effectiveness of 3D models on learning. These include 3D model and interface design, cognitive load and task complexity, factors related to the learner (e.g., innate visual-spatial ability), and integration of 3D tools into a wider curriculum.

Few authors have compared the effectiveness of virtual and printed models. Kong et al. found that both virtual and printed models enabled superior understanding of hepatic segment anatomy in comparison to traditional atlas-based training but found no difference between the two 3D groups [27].

Relatively fewer studies have evaluated the effect of 3D models on surgeon anatomical understanding. Awan et al. found the use of 3D printed models of acetabular fractures during a formal training program improved radiology trainee's short-term ability to identify fracture subtypes [28]. Yang et al. evaluated the effect of 3D printed models on the understanding of a retroperitoneal tumor anatomy for medical students, trainees, and consultant (attending) surgeons. When asked to identify three vascular structures, 3D printed and virtual models both demonstrated superiority over MDCT (83.33, 73.33, and 46.67%, respectively, $P = 0.007$), with maximum benefit derived from student group [14].

3D visualization techniques are thought to be of maximum benefit when considering complex variable anatomy. Cromeens et al. tested the ability of pediatric surgeons ($n = 21$) to identify anatomy, understand point-to-point measurements, and the shape and scale in pygopagus twins using conventional CT versus virtual reconstructions versus 3D printed models. 3D printed models statistically increased understanding of shape, scale, and anatomy in a significantly quicker time in comparison to MDCT [13].

Patient-Specific Simulation

We can broadly classify simulation using 3D patient-specific modeling into two groups: (a) *process simulation* and (b) *outcome simulation*. In *process simulation*, the model is used either virtually or physically to recreate the entire procedure or steps of the procedure. *Outcome simulation* attempts to predict operative outcomes and impact of surgery for patients. This can include predictions on the aesthetic appearance post-reconstruction, blood flow, or organ function [21].

Process Simulation

Surgical education has undergone a paradigm shift in recent decades as learning has transitioned from the operating theater to the simulation lab. Reduced operative volume, the need for competency-based curriculum, and patient safety concerns have accelerated this transition. Surgical simulation enables trainees to practice and rehearse skills in a safe environment. This may be especially important for complex, infrequently performed procedures.

Simulation can encompass a wide range of techniques and activities; however, perhaps one drawback of existing training models is their generic nature that lacks the anatomical variation found in real patients [29, 30]. 3D modeling has opened the possibility of patient-specific rehearsal. Imaging data can now be used to generate virtual and physical models in which a trainee or surgeon can perform key operative steps before carrying out the actual operation on a real patient. When considering the link between deliberate practice and expert performance in a wide range of fields such as sports, board games, and music, patient-specific rehearsal offers great promise in improving operative performance and safety [31, 32].

3D Printing and Simulation

The ability to print accurate scale models of bony anatomy (Fig. 8.7) has enabled surgeons from a variety of specialties to rehearse aspects of trauma and reconstructive surgery. Surgeons have used these printed models to design and perform osteotomies, prebend, and apply osteosynthesis implants. Head and neck surgeons have used such methods extensively to simulate complicated mandibular and other complex facial reconstructions [33–35]. Authors commonly cite reduced operative times, improved accuracy, and superior aesthetic results as the key benefits [8].

The hard materials used by the majority of 3D printers limit their use for simulation of procedures involving soft organs. However, soft flexible materials can now be printed, and hard 3D prints can be used to make silicone molds for traditional casting techniques.

Coelho et al. recently developed a 3D printed model with multiple materials of varying consistencies and resistances for planning frontoethmoidal meningoencephalocele surgical correction. Aside from reducing operative time by an estimated 29%, the model facilitated multidisciplinary discussion between neurosurgeon and plastic surgeons allowing alterations of the previously defined plan [36].

Initial feasibility studies for simulating nephrectomies with patient-specific 3D printed models have been undertaken. Glybochko et al. evaluated patient-specific silicone models for five patients with renal cell carcinoma. Surgeons rated the models highly for fidelity, and, subjectively, the models enabled better evaluation of the tumor anatomy [37]. Von Rundstedt et al. similarly generated patient-specific soft models for preoperative rehearsal for ten patients with complex renal tumor anatomy. Construct validity was demonstrated by similar enucleation times and resected tissue volumes between the model and actual tumors. Authors felt such rehearsals impacted their operative approach as difficulties encountered during the simulation *significantly altered the approach to the tumor in several cases* [15]. Cheung et al. used a three-stage production process to develop and validate a pediatric laparoscopic pyeloplasty. 3D organs based on imaging data were used to create 3D printed molds for subsequent silicone casting. During initial validation at the Canadian Urological Association, both trainee and expert users rated the models 4.75 (out of 5) for overall impression, 4.50 for realism, and 4.38 for handling [38]. Although promising, these early studies lack any clear objective assessment of utility or transferability into theater. Further drawbacks relate the time and expense incurred, with models taking up to 5 days and \$450–\$1000 to produce.

Fig. 8.7 1:1 scale FDM 3D printed sacrum derived from CT data (print material PLA, print time 34 h)

Virtual Patient-Specific Simulation

Given the material cost and infrastructure required for physical model production, virtual simulation is desirable. However, generating patient-specific realistic procedural simulations based on imaging-derived 3D models remains a significant challenge.

Models must undergo complex post-segmentation processing in order to be optimized for a game engine – the software development environment used in video game development that enables realistic rendering and physics to be applied to 3D models.

Creating deformable models with real-world physical properties that the user can interact with and dissect would not only be costly and time-consuming but also require a team with advanced computer programming knowledge [39].

Currently, only a handful of early feasibility studies are available. Rai et al. utilized Mimics (Leuven, Belgium) 3D virtual simulation environment in order to simulate three partial nephrectomy cases using CT reconstructed models [16]. Other preliminary studies by head and neck surgeons developed a virtual surgical environment for simulating ten endoscopic skull base procedures, demonstrating sufficient realism to allow patient-specific rehearsal [40]. Despite the obvious difficulties posed by virtual patient-specific simulation, the potential benefits for surgical training and patient safety are enormous and should therefore be a research priority in surgical education and training moving forward.

Outcome Simulation

Outcome simulation attempts to predict the result of surgery. We encounter four main types of outcome simulations in the literature: aesthetic, motion, blood flow, and structural. As discussed in further detail below, aesthetic outcomes are especially important in plastic and oral maxillofacial surgery. Computer modeling using finite element methods can accurately predict the soft tissue changes following bony reconstruction of the mandible and hence the resulting facial appearance [41]. The anticipated range of motion can similarly be modeled after orthopedic implants. This can facilitate decision-making, as real-time feedback is provided as different implants and placements are virtually trialed [42].

With virtual stenting, postoperative blood flow patterns can be modeled. This can be crucial when planning interventional procedures, e.g., aneurysm repair. The pressure and wall stress following stent placement can be predicted, meaning placement can be optimized [21]. Orthopedic surgeons use algorithmic approaches to predict the structural integrity of an implant and anatomic embedding. Surgeons can now visualize the forces and stresses on implants in order to optimize configurations [43].

Resection Planning

Achieving R0 (tumor-free) resection margins is the primary objective of curative oncological surgery and is one of the most important predictors of long-term survival [44].

Surgical planning involves interpretation of 2D CT/MRI imaging in order to mentally reconstruct the tumor anatomy and relationships to surrounding structures. 3D modeling may be especially beneficial when planning complex resections, given the potential for improved anatomical understanding that may subsequently impact decision-making and operative performance. One of the challenges of this surgery lies in removing sufficient tissue to ensure tumor-free margins while preserving enough tissue to avoid post-resection liver failure. Identification of vascular tributaries is fundamental aspect of plan in order to preserve healthy liver. Hepatobiliary surgeons have used 3D reconstructions in planning liver resections for primary and secondary liver cancer [45].

Tian et al. virtually simulated resection of tumors, demonstrating accurate predicted values for the specimen volume and surgical margins using the technique [46]. Wang et al. examined the effect of 3D visualization and virtual resection on surgical planning in comparison to 2D imaging on 305 consecutive patients undergoing hepatectomy. 3D visualization was found to alter the intended surgical plan for complex hepatectomy patients in 49/131 cases; *notably, 15 patients deemed unresectable based on 2D DICOM data were reconsidered operable.* The virtual resection volumes similarly correlated with the eventual specimen volume [47].

Virtual 3D analysis of hepatic tumors enabled accurate identification of tumor-bearing vasculature and perfusion areas essential for anatomical segmentectomy. Furthermore, by combining perfusion data with virtual resections, surgeons can automatically be provided with resection volumes, functional liver reserve, and dysfunction volumes, all critical information when planning the feasibility of hepatectomy. However, not all studies demonstrated 3D had any benefit. For example, Andert et al. found no difference between the R0 resection rates for hilar cholangiocarcinoma for 3D (n = 17) versus non-3D (n = 16) planning methods [48].

Video-assisted thoracotomy (VATS) lobectomy is a lesion-oriented procedure requiring a clear understanding of the pathology in relation to the complex distribution of blood vessels and bronchi. Consequently, thoracic surgeons have utilized 3D reconstructions for planning minimally invasive pulmonary resections [49, 50].

Similar preliminary work has been conducted in planning partial nephrectomy for renal cell carcinoma, complete mesocolic excision for colonic cancer [12], and complex sarcoma resections [51]. While 3D was considered to be useful and beneficial to operative performance, these studies are characterized by subjective findings lacking comparators, thus precluding any firm conclusions. At St. Mark's Hospital (London, UK), we have performed initial feasibility work assessing 3D reconstructions for planning locally advanced rectal cancer exenterative surgery (Fig. 8.8).

Reconstruction

Oral maxillofacial surgery (OMFS) serves as one of the best examples of using 3D modeling for planning reconstructive surgery. OMFS primarily deals with the reconstruction of the bones of the facial area following trauma or to correct congenital malformations [52]. Not only is craniofacial anatomy geometrically complex, but deformities are also exceptionally visible and carry a considerable psychosocial burden for patients. The precision and aesthetic requirements of procedures are therefore particularly

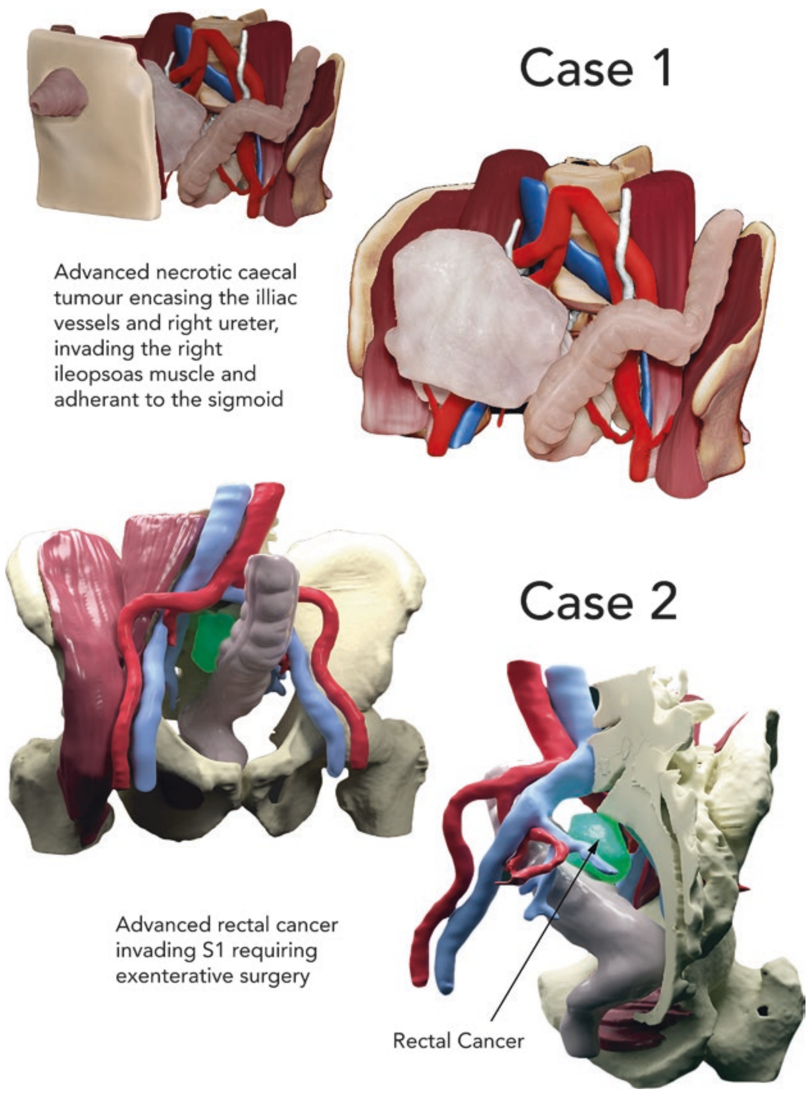

Fig. 8.8 3D surface-rendered reconstructions of two complex colorectal cancer patients requiring exenterative surgery

stringent. 3D imaging potentially has its biggest impact where correction of defects is essential for functional and cosmetic outcomes.

3D visualization techniques have been used not only to improve understanding of the deformity but to also accurately plan osteotomies, virtually/physically rehearse reconstructive techniques [52], accurately model the soft tissue postoperative appearances [53], and 3D print patient-specific cutting guides and custom implants [54]. Such measures have enabled quicker surgery with improved precision and aesthetic outcomes [55, 56].

In facial trauma, the spatial localization of bone fragments is essential in restoring the shape of the face and normal bite. 3D CT enables planning symmetrical corrections along with placement of implants. Several studies have demonstrated the value of 3D CT visualization in the treatment of displaced complex midfacial and mandibular fractures [54, 57, 58].

3D has also demonstrated value in the evaluation and treatment of craniofacial clefts, synostoses, and other asymmetries. In craniosynostosis – a condition in which the cranial suture closes prematurely changing the growth pattern of the skull – 3D CT is more likely to reveal subtle asymmetries and result in more accurate classification of abnormal suture lines [59]. 3D printing also provides a useful means of simulating surgery, particularly through planning and performing osteotomy sites.

In one review, Lin et al. identified 78 studies in the past decade that have employed 3D printing to transfer virtual planning to actual orthognathic reconstructions (methods include occlusal splints, osteotomy guides, repositioning guides, fixation plates/implants, spacers, and 3D models) [60]. The majority of studies were prospective case series ranging between 1 and 150 patients (with a median of 10) using accuracy as primary outcome measures.

Significantly fewer randomized controlled trials have been undertaken. Ayoub et al. compared computer-assisted mandibular reconstruction with vascularized iliac crest bone grafts with conventional surgery with a total of 20 patients randomized into each group. Computer-assisted surgery reduced the transplant ischemia time and reduced the donor site defect size [61].

Discussion

3D modeling is an emerging technology that will likely gain increased prominence within surgical workflows in the next decade. Patient-specific modeling offers not only the potential for improving anatomical understanding but also novel ways of interacting with imaging data. Proponents hope the use of such models will facilitate the delivery of precision medicine and result in safer, faster surgery with better outcomes.

However, the effectiveness of 3D virtual or printed models remains to be definitively established. Considerable technical challenges remain if 3D modeling is to be integrated into routine care. The surgical community will likely need to partner with industry if model production is to be automated.

We have yet to elucidate the ideal user (novice versus expert), specific indications, optimum design, and interface features. The majority of the current literature consists of small-scale feasibility studies in which only subjective measures of utility are employed. Future research must address these questions and establish adequate methodology in order to validate 3D modeling as an effective adjunct to preoperative planning.

References

1. Martelli N, Serrano C, Van Den Brink H, Pineau J, Prognon P, Borget I, El Batti S. Advantages and disadvantages of 3-dimensional printing in surgery: a systematic review. Surg (United States). 2016;159:1485–500.
2. Bücking TM, Hill ER, Robertson JL, Maneas E, Plumb AA, Nikitichev DI. From medical imaging data to 3D printed anatomical models. PLoS One. 2017;12:1–10.
3. Salb T, Weyrich T, Dillmann R. Preoperative planning and training simulation for risk reducing surgery. Proc Int Train Educ Conf. 1999;1–8.
4. Fadero PE, Shah M. Three dimensional (3D) modeling and surgical planning in trauma and orthopaedics. Surgeon. 2014;12:328–33.

5. Okuda Y, Taura K, Seo S, Yasuchika K, Nitta T, Ogawa K, Hatano E, Uemoto S. Usefulness of operative planning based on 3-dimensional CT cholangiography for biliary malignancies. Surgery. 2015;158:1261–71.
6. Hodgdon T, Danrad R, Patel MJ, et al. Logistics of three-dimensional printing: primer for radiologists. Acad Radiol. 2018;25:40–51.
7. Ballard D, Trace A, Ali A, Hodgdon T, Zygmont M, DeBenedectis C, Smith S, Richardson M, Patel M, Decker S. Clinical applications of 3D printing: primer for radiologists. Acad Radiol. 2018;25:52–65.
8. Crafts TD, Ellsperman SE, Wannemuehler TJ, Bellicchi TD, Shipchandler TZ, Mantravadi AV. Three-dimensional printing and its applications in otorhinolaryngology–head and neck surgery. Otolaryngol Head Neck Surg. 2017;156:999–1010.
9. Lau I, Sun Z. Three-dimensional printing in congenital heart disease: a systematic review. J Med Radiat Sci. 2018;65:226–36.
10. Soon DSC, Chae MP, Pilgrim CHC, Matthew W, Spychal RT, Hunter-smith DJ. 3D haptic modeling for preoperative planning of hepatic resection : a systematic review. Ann Med Surg. 2016;10:1–7.
11. Javan R, Herrin D, Tangestanipoor A. Understanding spatially complex segmental and branch anatomy using 3D printing: liver, lung, prostate, coronary arteries, and circle of Willis. Acad Radiol. 2016;23:1183–9.
12. Luzon JA, Andersen BT, Stimec BV, Fasel JHD, Bakka AO, Kazaryan AM, Ignjatovic D. Implementation of 3D printed superior mesenteric vascular models for surgical planning and/or navigation in right colectomy with extended D3 mesenterectomy: comparison of virtual and physical models to the anatomy found at surgery. Surg Endosc. 2018;32:567–75.
13. Cromeens BP, Ray WC, Hoehne B, Abayneh F, Adler B, Besner GE. Facilitating surgeon understanding of complex anatomy using a three-dimensional printed model. J Surg Res. 2017;216:18–25.
14. Yang T, Lin S, Tan T, Yang J, Pan J, Hu C, Li J, Zou Y. Impact of 3D printing technology on comprehension of surgical anatomy of retroperitoneal tumor. World J Surg. 2018;42:2339–43.
15. von Rundstedt FC, Scovell JM, Agrawal S, Zaneveld J, Link RE. Utility of patient-specific silicone renal models for planning and rehearsal of complex tumour resections prior to robot-assisted laparoscopic partial nephrectomy. BJU Int. 2017;119:598–604.
16. Rai A, Scovell JM, Xu A, Balasubramanian A, Siller R, Kohn T, Moon Y, Yadav N, Link RE. Patient-specific virtual simulation - a state of the art approach to teach renal tumor localization. Urology. 2018;120:42–8. https://doi.org/10.1016/j.urology.2018.04.043.
17. Khor WS, Baker B, Amin K, Chan A, Patel K, Wong J. Augmented and virtual reality in surgery—the digital surgical environment: applications, limitations and legal pitfalls. Ann Transl Med. 2016;4:454.
18. Paragios N, Duncan J. Handbook of biomedical imaging. Handb Biomed Imaging. 2015. https://doi.org/10.1007/978-0-387-09749-7.
19. Sharma N, Aggarwal LM. Automated medical image segmentation techniques. J Med Phys. 2010;35:3–14.
20. Kaur D, Kaur Y. Various image segmentation techniques: a review. Int J Comput Sci Mob Comput. 2014;3:809–14, date accessed: 18/05/2016.
21. Preim B, Botha CP. Visual computing for medicine. 2nd ed. New York: Morgan Kaufmann; 2014.
22. Yamashita R, Nishio M, Do RKG, Togashi K. Convolutional neural networks: an overview and application in radiology. Insights Imaging. 2018;9:611–29.
23. Hu P, Wu F, Peng J, Bao Y, Chen F, Kong D. Automatic abdominal multi-organ segmentation using deep convolutional neural network and time-implicit level sets. Int J Comput Assist Radiol Surg. 2017;12:399–411.
24. Trebeschi S, Van Griethuysen JJM, Lambregts DMJ, Lahaye MJ, Parmer C, Bakers FCH, Peters NHGM, Beets-Tan RGH, Aerts HJWL. Deep learning for fully-automated localization and segmentation of rectal cancer on multiparametric MR. Sci Rep. 2017;7:1–9.
25. Garcia J, Yang Z, Mongrain R, Leask RL, Lachapelle K. 3D printing materials and their use in medical education: a review of current technology and trends for the future. BMJ Simul Technol Enhanc Learn bmjstel-2017-000234. 2017.
26. Azer SA, Azer S. 3D anatomy models and impact on learning: a review of the quality of the literature. Heal Prof Educ. 2016;2:80–98.
27. Kong X, Nie L, Zhang H, Wang Z, Ye Q, Tang L, Li J, Huang W. Do three-dimensional visualization and three-dimensional printing improve hepatic segment anatomy teaching? a randomized controlled study. J Surg Educ. 2016;73:264–9.
28. Awan OA, Sheth M, Sullivan I, Hussain J, Jonnalagadda P, Ling S, Ali S. Efficacy of 3D printed models on resident learning and understanding of common acetabular fracturers. Acad Radiol. 2018;26:130.
29. Kneebone R. Evaluating clinical simulations for learning procedural skills: a theory-based approach. Acad Med. 2005;80:549–53.
30. Reznick RK. Surgical simulation. Ann Surg. 2005;242:640–1.
31. Ericsson KA. Deliberate practice and the acquisition and maintenance of expert performance in medicine and related domains. Acad Med. 2004;79:70–81.
32. Crochet P, Aggarwal R, Dubb SS, Ziprin P, Rajaretnam N, Grantcharov T, Ericsson KA, Darzi A. Deliberate practice on a virtual reality laparoscopic simulator enhances the quality of surgical technical skills. Ann Surg. 2011;253:1216–22.
33. Fan B, Chen H, Sun YJ, Wang BF, Che L, Liu SY, Li GY. Clinical effects of 3-D printing-assisted personalized reconstructive surgery for blowout orbital fractures. Graefes Arch Clin Exp Ophthalmol. 2017;255:2051–7.
34. Ciocca L, Mazzoni S, Fantini M, Persiani F, Marchetti C, Scotti R, Cam CAD. CAD / CAM guided secondary mandibular reconstruction of a discontinuity defect

after ablative cancer surgery. J Cranio Maxillofacial Surg. 2012;40:e511–5.
35. Zheng W, Su J, Cai L, Lou Y, Wang J, Guo X, Tang J, Chen H. Application of 3D-printing technology in the treatment of humeral intercondylar fractures. Orthop Traumatol Surg Res. 2018;104:83–8.
36. Coelho G, Chaves TMF, Goes AF, Del Massa EC, Moraes O, Yoshida M. Multimaterial 3D printing preoperative planning for frontoethmoidal meningoencephalocele surgery. Childs Nerv Syst. 2018;34:749–56.
37. Glybochko PV, Rapoport LM, Alyaev YG, Sirota ES, Bezrukov EA, Fiev DN, Byadretdinov IS, Bukatov MD, Letunovskiy AV, Korolev DO. Multiple application of three-dimensional soft kidney models with localized kidney cancer: a pilot study. Urologia. 2018;85:99–105.
38. Cheung CL, Looi T, Lendvay TS, Drake JM, Farhat WA. Use of 3-dimensional printing technology and silicone modeling in surgical simulation: development and face validation in pediatric laparoscopic pyeloplasty. J Surg Educ. 2014;71:762–7.
39. Zhang J, Chang J, Yang X, Zhang JJ. Virtual reality surgery simulation: a survey on patient specific solution. Lect Notes Comput Sci. 2017:220–33.
40. Bin WT, Hwang P, Lim JH, Cho SW, Paek SH, Losorelli S, Vaisbuch Y, Chan S, Salisbury K, Blevins NH. Early experience with a patient-specific virtual surgical simulation for rehearsal of endoscopic skull-base surgery. Int Forum Allergy Rhinol. 2018;8:54–63.
41. Westermark A, Zachow S, Eppley BL. Three-dimensional osteotomy planning in maxillofacial surgery including soft tissue prediction. J Craniofac Surg. 2005;16:100–4.
42. Digioia AM, Jaramaz B, Nikou C, Labarca RS, Moody JE, Colgan BD. Surgical navigation for total hip replacement with the use of HipNav. Oper Tech Orthop. 2000;10:3–8.
43. Dick C, Georgii J, Burgkart R, Westermann R. Stress tensor field visualization for implant planning in orthopedics. IEEE Trans Vis Comput Graph. 2009;15:1399–406.
44. Shaikh I, Holloway I, Aston W, Littler S, Burling D, Antoniou A, Jenkins JT. High subcortical sacrectomy: a novel approach to facilitate complete resection of locally advanced and recurrent rectal cancer with high (S1-S2) sacral extension. Color Dis. 2016;18:386–92.
45. Xiang N, Fang C, Fan Y, Yang J, Zeng N, Liu J, Zhu W. Application of liver three-dimensional printing in hepatectomy for complex massive hepatocarcinoma with rare variations of portal vein: preliminary experience. Int J Clin Exp Med. 2015;8:18873–8.
46. Tian F, Wu J-X, Rong W-Q, et al. Three-dimensional morphometric analysis for hepatectomy of centrally located hepatocellular carcinoma: a pilot study. World J Gastroenterol. 2015;21:4607–19.
47. Wang X-D, Wang H-G, Shi J, Duan W-D, Luo Y, Ji W-B, Zhang N, Dong J-H. Traditional surgical planning of liver surgery is modified by 3D interactive quantitative surgical planning approach: a single-center experience with 305 patients. Hepatobiliary Pancreat Dis Int. 2017;16:271–8.
48. Andert A, Bruners P, Heidenhain C, Ulmer F, Klink CD, Alizai PH, Kuhl C, Neumann UP, Binnebosel M. Impact of preoperative three-dimensional computed tomography cholangiography on postoperative resection margin status in patients operated due to hilar cholangiocarcinoma. Gastroenterol Res Pract. 2017;2017:1947023.
49. Iwano S, Usami N, Yokoi K, Naganawa S. Segmentectomy simulation using a virtual three-dimensional safety margin. Ann Thorac Surg. 2012;93:e37–9.
50. Kanzaki M, Kikkawa T, Shimizu T, Maeda H, Wachi N, Isaka T, Murasugi M, Onuki T. Presurgical planning using a three-dimensional pulmonary model of the actual anatomy of patient with primary lung cancer. Thorac Cardiovasc Surg. 2013;61:144–50.
51. Jentzsch T, Vlachopoulos L, Fürnstahl P, Müller DA, Fuchs B. Tumor resection at the pelvis using three-dimensional planning and patient-specific instruments: a case series. World J Surg Oncol. 2016;14:1–12.
52. Herlin C, Charles J, Bigorre M, Cheikh H, Captier G. Computer-assisted midface reconstruction in Treacher Collins syndrome part 1. Skelet Reconstr. 2013;41:670–5.
53. Van Hemelen G, Van Genechten M, Renier L, Desmedt M, Verbruggen E, Nadjmi N. Three-dimensional virtual planning in orthognathic surgery enhances the accuracy of soft tissue prediction. J Craniomaxillofac Surg. 2015;43:918–25.
54. Day KM, Gabrick KS, Sargent LA. Applications of computer technology in complex craniofacial reconstruction. Plast Reconstr Surgy Glob Open. 2018;6:e1655.
55. Ciocca L, Mazzoni S, Fantini M, Persiani F, Marchetti C, Scotti R. CAD/CAM guided secondary mandibular reconstruction of a discontinuity defect after ablative cancer surgery. J Cranio Maxillofacial Surg. 2012;40:e511–5.
56. Chin SJ, Wilde F, Neuhaus M, Schramm A, Gellrich NC, Rana M. Accuracy of virtual surgical planning of orthognathic surgery with aid of CAD/CAM fabricated surgical splint—a novel 3D analyzing algorithm. J Cranio-Maxillofacial Surg. 2017;45:1962–70.
57. Lo Casto A, Priolo G, Garufi A, Purpura P, Salerno S, La Tona G. Imaging evaluation of facial complex strut fractures. Semin Ultrasound, CT MRI. 2012;33:396–409.
58. Hanasono MM, Jacob RF, Bidaut L, Robb GL, Skoracki RJ. Midfacial reconstruction using virtual planning, rapid prototype modeling, and stereotactic navigation. Plast Reconstr Surg. 2010;126:2002–6.
59. Strumas N, Antonyshyn O, Caldwell CB, Mainprize J. Multimodality imaging for precise localization of craniofacial osteomyelitis. J Craniofac Surg. 2003;14:215–9.

60. Lin HH, Lonic D, Lo LJ. 3D printing in orthognathic surgery – a literature review. J Formos Med Assoc. 2018;117:547–58.
61. Ayoub N, Ghassemi A, Rana M, Gerressen M, Riediger D, Hölzle F, Modabber A. Evaluation of computer-assisted mandibular reconstruction with vascularized iliac crest bone graft compared to conventional surgery: a randomized prospective clinical trial. Trials. 2014; https://doi.org/10.1186/1745-6215-15-114.

9 Realistic Organ Models for Simulation and Training

Pratik M. S. Gurung and Ahmed E. Ghazi

Abbreviations

3D	Three dimensional
CAD	Computer-aided design
cm	Centimeter
CT	Computed tomography
DICOM	Digital imaging and communication in medicine
EBL	Estimated blood loss
GEARS	Global evaluative assessments scores
MIPN	Minimally invasive partial nephrectomy
mm	Millimeter
N	Newton
OR	Operating room
PCS	Pelvicalyceal system
PSM	Positive surgical margin
PVA	Polyvinyl alcohol
RAPN	Robot-assisted partial nephrectomy
RMSE	Root mean square error
STL	Stereolithographic
WIT	Warm ischemia time

P. M. S. Gurung
Department of Urology, University of Rochester, Rochester, NY, USA

A. E. Ghazi (✉)
Department of Urology, University of Rochester, Rochester, NY, USA

Simulation Innovation Laboratory, University of Rochester, Department of Urology, Rochester, NY, USA
e-mail: ahmed_ghazi@urmc.rochester.edu

Introduction

Simulation training has an important emerging role in optimizing the technical as well as non-technical skills of surgical trainees in most specialties, including urology [1]. In the current healthcare systems worldwide, with the competing demands of producing competent surgeons in a time-efficient manner on the one hand and ensuring patient safety on the other, simulation training can move the learning curve of the trainee surgeon away from the patient in the operating room to a more controlled environment in the simulation room [2]. Indeed, simulation training, delivered in a structured format, within prescribed surgical curricula, has been recommended by most training program directors [3]. Moreover, advances in technologies, such as the expanding applications of robotic platforms, necessitates updated, dynamic, and sophisticated surgical simulation training to be incorporated into such surgical curricula [4].

With respect to organ models for use in simulation platforms, the utopian ideal would be high-fidelity models which can be utilized to recreate the most critical steps of the operation, customized to the specific patient. Cadaveric and live animal models, although allowing a realistic procedural experience, are significantly limited, for routine and wide-scale use in surgical curricula, due to a variety of factors – such as cost, availability, potential for transferrable diseases, and ethical concerns [5]. Even allowing for these

S. Atallah (ed.), *Digital Surgery*, https://doi.org/10.1007/978-3-030-49100-0_9

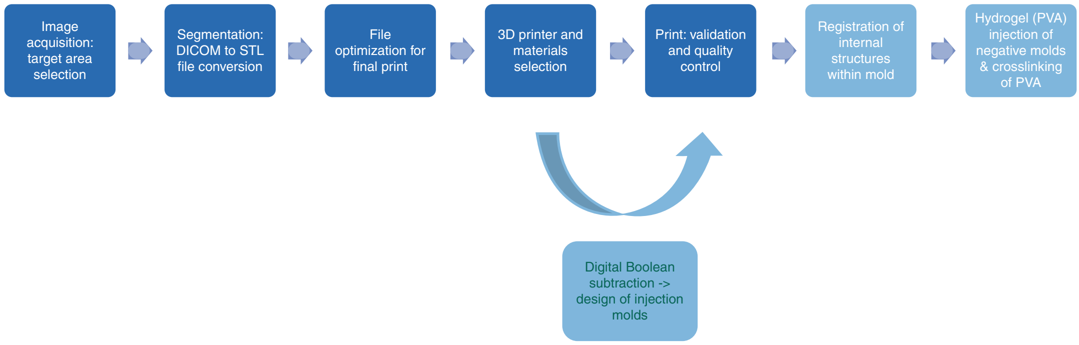

Fig. 9.1 Steps in 3D printing workflow (modified from [8]), with our modifications for the fabrication of soft realistic hydrogel organs

limitations, such animal or cadaveric models do not provide operative exposure to *specific* anatomical variations (e.g., vascular anatomy) and/or *specific* pathologies (e.g., tumor size, location) which are important for achieving a higher level of proficiency [6]. In this context, artificially elaborated organ model platforms, which not only replicate the morphological architecture and mechanical texture of actual human organs but also enable dynamic and functional immersion during simulation (e.g., bleeding during partial nephrectomy during robotic simulation or urine leak during percutaneous nephrolithotomy), may add considerable value to the simulation training experience. Such immersive and high-fidelity simulation training, in turn, may translate to an improved learning curve for trainees, better performance (even in experienced surgeons beyond their learning curve when tackling complex cases), and ultimately better surgical outcomes for the individual patient. In this chapter, the urologic system is used as a paradigm, but the same principles could be applied to other target anatomy and organ systems.

Combining Technologies: 3D Printing and Hydrogel Casting

Three-dimensional (3D) printing is a process which enables the creation of a three-dimensional solid object from a digital model of that object. Since the introduction of stereolithographic (STL) systems in the 1980s, 3D printing technology has rapidly expanded, and the growth of medical 3D printing has been particularly important [7]. Essentially, medical 3D printing involves five technical steps (Fig. 9.1) [8].

The first step requires the selection of the target organ (e.g., kidney, prostate) based on the available acquired imaging (e.g., computed tomography, magnetic resonance imaging). The selected target images are then "segmented" from digital imaging and communication in medicine (DICOM) to STL file format. The segmented files are optimized and sent to a selected 3D printer with the selected materials. The printer then produces the object, using appropriately selected materials, from the base layer sequentially into a series of top layers. In the end, the selected patient-specific organ model is created.

In general medical use, the majority of printed models are made of hard materials. While such models are useful to understand anatomical pathology for the surgeon and the patient, they do not allow simulated practice due to their limited material resemblance to tissues and low fidelity in haptic feedback and dynamic interactions. Hence, materials with the appropriate biomechanical properties are required to create an organ model (e.g., prostate gland, kidney). Furthermore, combinations or permutations of such materials may be required to attempt to replicate the differing physical properties of the different structures within the organ (e.g., artery, vein, and collecting system within the kidney). Moreover, such models may be incorporated into a high-fidelity simulation platform (e.g., bleeding from a renal vein or urine leak from the collecting system if such structures are inadvertently violated during a partial nephrectomy simulation). In this regard, polyvinyl alcohol (PVA), a biocompatible and inexpensive hydrogel polymer, can be adapted to mimic human tissues in the fabrication process of the organ model [9]. PVA can be altered to replicate the variable mechanical properties of different tissues such as tissue parenchyma, blood vessels, tumors, and fat by varying PVA concentration and the number of processing (freeze/thaw) cycles that form polymeric bonds. The desired concentration is obtained by heating commercially available PVA powder and varying amounts of water. The result is a relatively viscous gel that is shelf-stable and cost-effective (currently costing approximately $1 per liter). The freezing process is completed at −20 °C, and thawing is completed at 23 °C for varying times depending on the size of the object. The phase change property of PVA is also critical for the fabrication process whereby the induction of cross-links, through successive freeze/thaw cycles, polymerizes it from an injectable gel into a progressively stiffer and more solid texture that maintains its shape. To configure this PVA hydrogel into the geometry of a patient's specific anatomy, combinations of additive and subtractive methods are utilized.

Realistic Organ Models in Urology: Kidney – Partial Nephrectomy

In urology, there are a number of realistic organ models in development and validation. Upper tract models include kidney models for partial nephrectomy (PN) or percutaneous nephrolithotomy (PCNL). Lower tract organ models include those of the prostate for radical nephrectomy and bladder for radical cystectomy – generally for use in minimally invasive surgical platforms (e.g., robot-assisted radical prostatectomy and robot-assisted radical cystectomy). Herein, using a kidney model optimized for partial nephrectomy as an illustrative example, the salient aspects of the rationale, methods of creation, and methods of validation of a PVA hydrogel model, for use as a full immersion surgical simulation platform, are summarized. In this chapter, we have provided details of our operating protocols for experiments, experimental data, and observational experiences enabling readers to follow and/or replicate our work.

Rationale

As opposed to radical nephrectomy, which involves the removal of the whole kidney, minimally invasive partial nephrectomy (MIPN), performed either laparoscopically or robotically (robot-assisted partial nephrectomy, RAPN), attempts to preserve nephrons during the definitive surgical treatment of small renal masses (SRMs) which are concerning for cancer. Although MIPN, in particular RAPN, is increasingly popular worldwide, there are some technical barriers to its widespread adoption owing to factors which impact on the learning curve of those seeking proficiency. These include the need to appreciate the 3D spatial configuration of the tumor within the kidney in order to minimize positive surgical margins or entry into the collecting system; the advanced technical skills required to minimize ischemia during selective or nonselective arterial clamping, tumor resection, and renorrhaphy; and handling of tissues with limited haptic feedback compared to open surgery. In this context, a simulation platform, which incorporates a realistic patient-specific 3D kidney model, allows rehearsal of the MIPN prior to the actual case.

Method of Model Creation

Each patient-specific model starts by importing DICOM files from a CT scan of a patient with a renal tumor scheduled for a MIPN, into a medical image processing software (e.g., Mimics, Belgium). Segmentation is completed for each component of the patient's kidney including the parenchyma, tumor, inferior vena cava and renal vein, abdominal aorta and renal artery, and urinary drainage system (Fig. 9.2a). Most structures

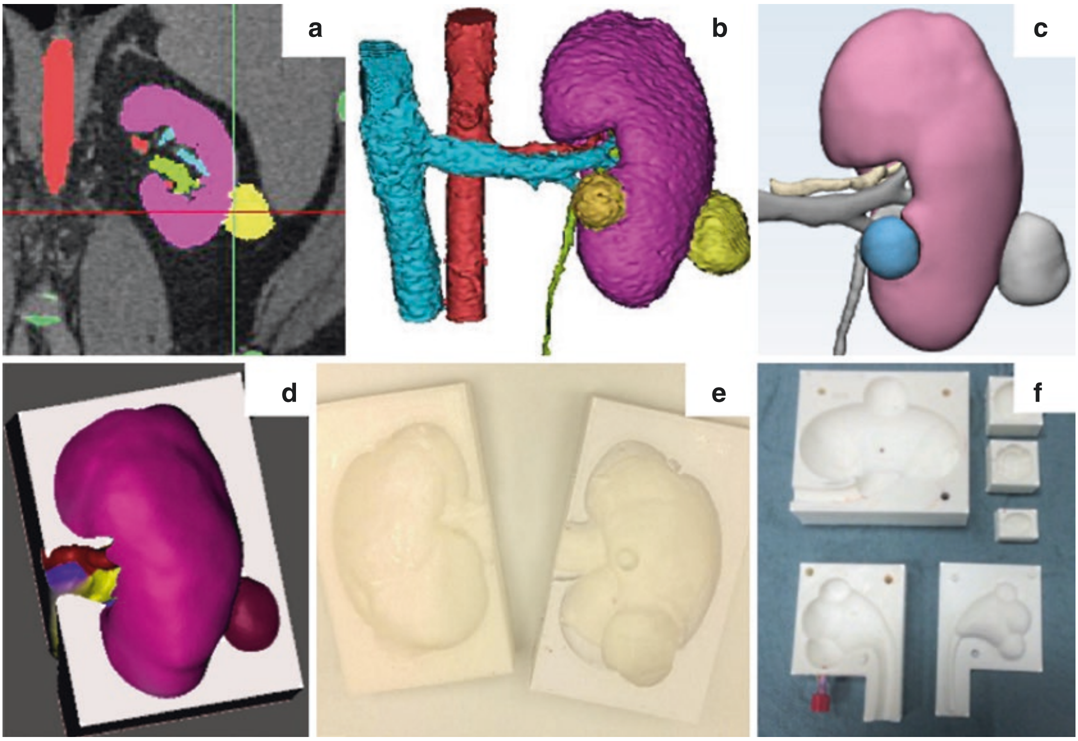

Fig. 9.2 (**a**) Segmentation of patient's DICOM images; (**b**) resulting 3D mesh; (**c**) CAD after repairs and smoothing in 3-matic; (**d**) Boolean subtraction to form mold for kidney; (**e**) injection mold for kidney printed in PLA with registration points for hilar plug and tumor; (**f**) kidney, tumor, and hilar molds

are amenable to being isolated with "thresholding" and "region-growing" tools. Multiple slide edits are used to increase the accuracy of the segmentation for non-contrasted structures. Each component is then converted to a 3D mesh (Fig. 9.2b) and imported into the medical image processing software to form a computer-aided design (CAD) model of the patient's anatomy. Each structure is wrapped and corrections are made following recommendations from the "fix wizard" (Fig. 9.2c). To recreate both anatomical and functional aspects of the patient's kidney using PVA hydrogel, the patient's CAD is then converted into an "injection mold" by using a Boolean difference operation to create a cavity of the same shape (Fig. 9.2d). PVA is injected into these molds and once processed will retain the cavity geometry representative of the patient's anatomy (Fig. 9.2e). The three main injection molds are of the tumor, kidney, and renal hilum (Fig. 9.2f). Once all injection molds are designed, they are printed in hard plastic (PLA) on a 3D printer (e.g., Fusion3 Design; Greensboro, NC).

To incorporate the functionality of the model in terms of bleeding and urine leakage, the hilar structures (arterial, venous, and calyx urinary systems) are printed using dissolvable PVA filament using a FlashForge Creator Pro and coated with processed PVA (Fig. 9.3a). Once the layers are solidified, the inner PVA filament is dissolved in water to create a hollow, watertight vascular and urinary system (Fig. 9.3b). All these structures are then registered into the hilar mold and surrounded by PVA to mimic fat, which will form the hilar plug. Simultaneously, the tumor mold is also injected with PVA hydrogel mixed with silica powder or iodinated contrast to mimic the acoustic appearance of these tissues under ultrasonography and X-ray imaging. The final injection mold will form the kidney, encasing the preformed tumor and hilar plug to form a single entity (Fig. 9.3c). This mold is then injected with

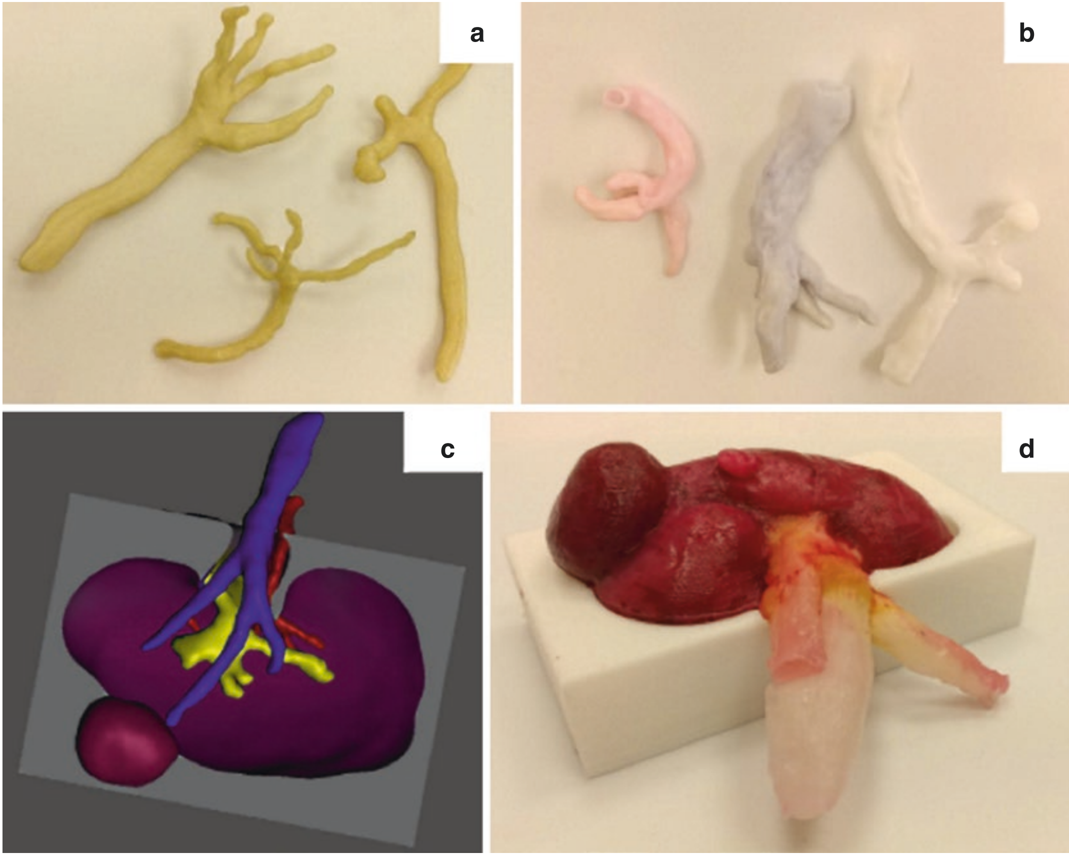

Fig. 9.3 (**a**) PVA prints of the renal artery, renal vein, and calyx. (**b**) Following our processing technique to fabricate hollow vascular structures. (**c**) Positioning of hilar structures and tumor in kidney mold (CAD). (**d**) Kidney phantom arranged in mold

PVA previously tested to replicate the mechanical properties of human kidneys (discussed below). The result is a kidney phantom that replicates the patient anatomy (Fig. 9.3d).

Methods of Model Validation

There are various levels of validation that are desirable for the model generated. Firstly, realistic surgical simulation requires that the synthetic organs demonstrate lifelike mechanical characteristics. As a substitute for human kidneys, porcine tissues have been widely used due to their greater availability, decreased biohazard concerns, and similarity of properties to human tissue. Porcine kidneys, ex vivo, have been demonstrated to closely match the material properties of human kidneys sufficiently enough to be used as a surrogate [10, 11]. Guided by this work, we tested fresh porcine kidney specimens to model the mechanical properties of the PVA hydrogel used in our models. Compression testing was completed in order to determine the concentration of PVA hydrogel that best replicates the properties of the porcine kidney. Porcine kidneys were obtained within 24 hours after death and kept at 4 °C until testing. Samples were carefully cut out of the cortex into cubes taking care to exclude the medulla. Forty samples were harvested. Four different conditions of PVA were prepared by varying combinations of concentrations and freeze/thaw cycles. The samples were prepared in blocks that are the size of average

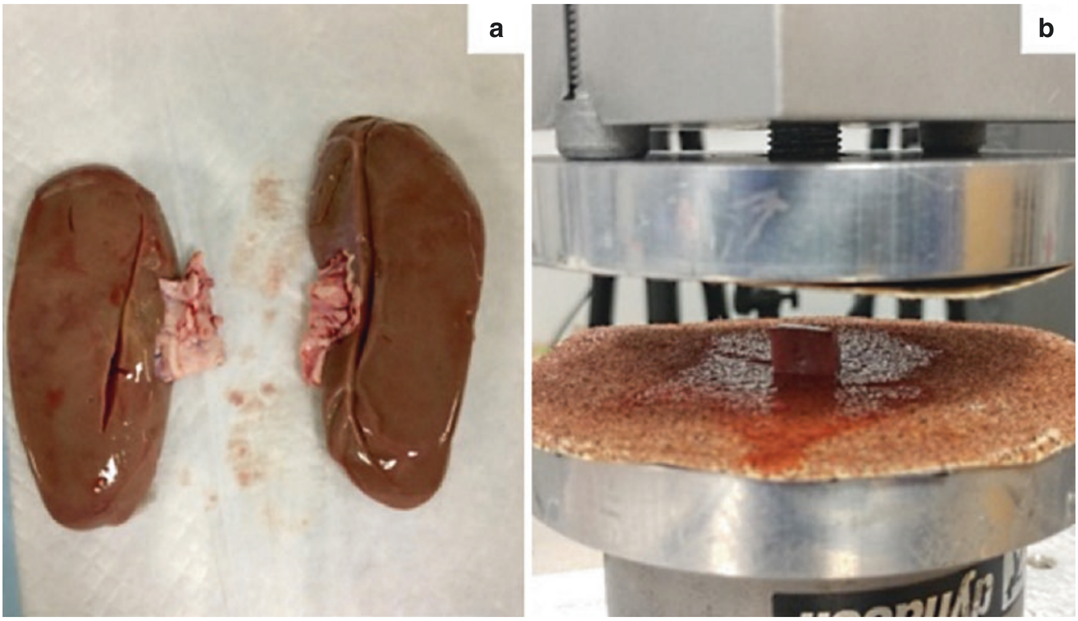

Fig. 9.4 Compression testing: (**a**) porcine kidney; (**b**) cortex sample during compression testing

kidneys. Each sample was placed in a −20 °C freezer for 16 hours and then thawed at 23 °C for 8 hours for as many cycles as prescribed. Ten cubes of each condition were cut from the blocks and measured 10.14 (± 0.659) mm in length and width and 9.966 (± 0.725) mm in height over all samples harvested. Samples were placed on sandpaper-covered test plates in order to create a no-slip boundary, and excess fluids were removed between tests (Fig. 9.4a). An Instron ElectroPulsTM E10000 Linear-Torsion All-Electric Dynamic Test Instrument (Instron Corp, Norwood, MA) with a 1000 N load cell was used, and data acquisition and testing protocol were handled by Bluehill software (Instron Corp, Norwood, MA). Porcine samples were compressed along their heights, corresponding with the radial vector, at a rate of 10 mm/min. PVA samples were compressed along their heights without preference to orientation at a rate of 10 mm/min (Fig. 9.4b). The test ended after failure or if a force of 1 MPa was reached.

Strain was calculated as a percent change in height (mm/mm). Stress was calculated as force measured (N) over the initial cross-sectional area (mm^2). Figure 9.5 displays the average stress

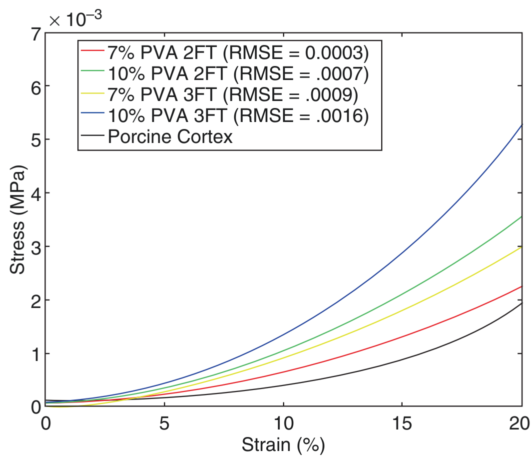

Fig. 9.5 Stress-strain relationship of porcine kidney cortex (black) and four different conditions of PVA under uniaxial compression; FT (freeze/thaw); MPa (megapascals)

experienced over low strains relevant to those applied during surgery for each of the PVA conditions and cortex samples. The root mean square error (RMSE) was calculated between each curve representing a PVA condition to the porcine cortex in order to establish which condition best replicated that of the porcine cortex. Results are displayed in Fig. 9.5. Preliminary mechanical testing data showed that the stress-strain relationship for PVA at a concentration of 7% after two processing cycles produced the lowest RMSE (0.0003) compared to porcine tissue. This assessment would serve as the basis for replicating the mechanical properties of human kidney tissue.

Secondly, with respect to validity, the models generated need to be validated for anatomical accuracy. To authenticate their anatomical accuracy, the patient-specific PVA kidney phantoms are reimaged using a CT scanner, at a spatial resolution of 3 mm after backfilling the calyx, artery, and vein within the kidney with iodinated contrast. A similar process of segmentation and surface reconstruction is performed using the models' DICOM images to generate duplicate sets of CAD files one from the patients' original scan and the other from the PVA replica. The separate CAD files from the patient's original imaging and the matching PVA kidney phantom are then overlaid. A detailed quantitative error analysis, with multiple iterations in order to minimize the discrepancies between the image overlays, is performed using the part comparison tool in the analysis module of the medical image processing software (e.g., Mimics 3-matic, Belgium). A visual representation of the discrepancies between the model and patient is displayed over the surface of the CAD of the model in millimeters. An example of the resulting visual analysis is shown in Fig. 9.6.

Finally, validation of surgical simulation to resemble live surgical cases needs to be performed. In order to recreate the entire operative experience, a full procedural rehearsal platform containing the patient-specific kidney model,

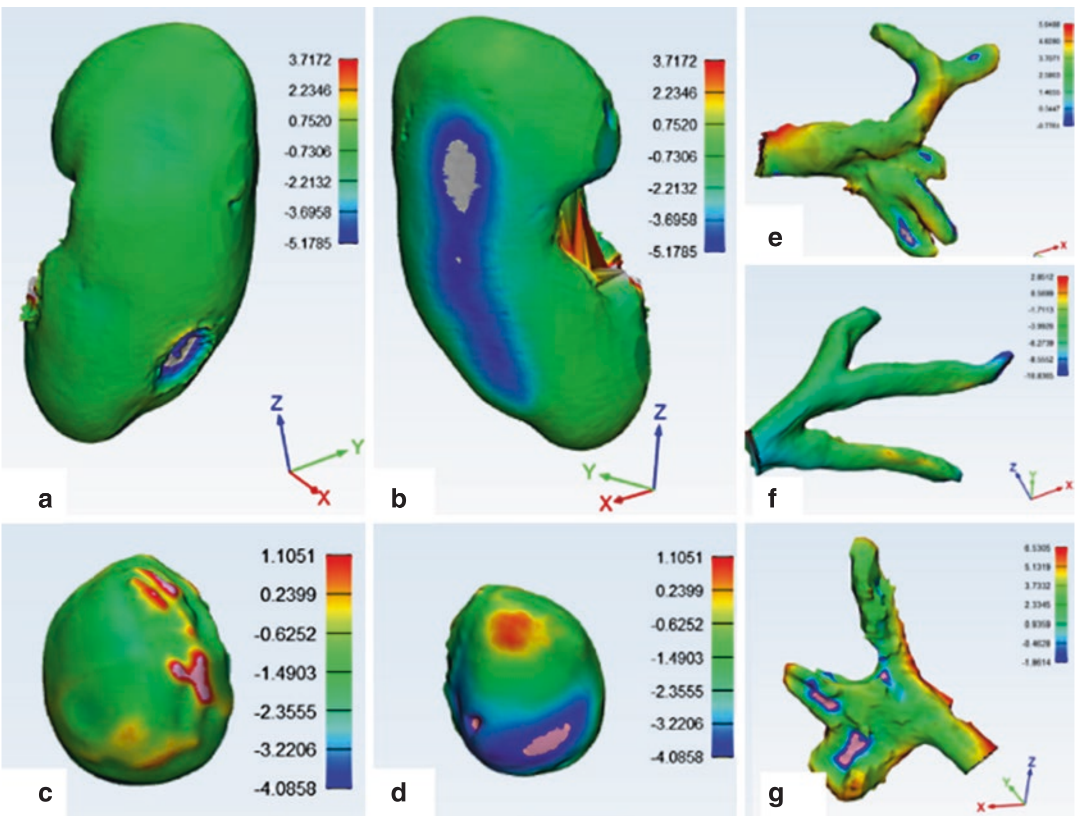

Fig. 9.6 Analysis using part comparison tool displaying distance (mm) of the model from the patient kidney, (**a**) anterior view of the kidney; (**b**) posterior view of the kidney; (**c**) anterior view of the tumor; (**d**) posterior view of the tumor, (**e**) artery, (**f**) vein, and (**g**) calyx

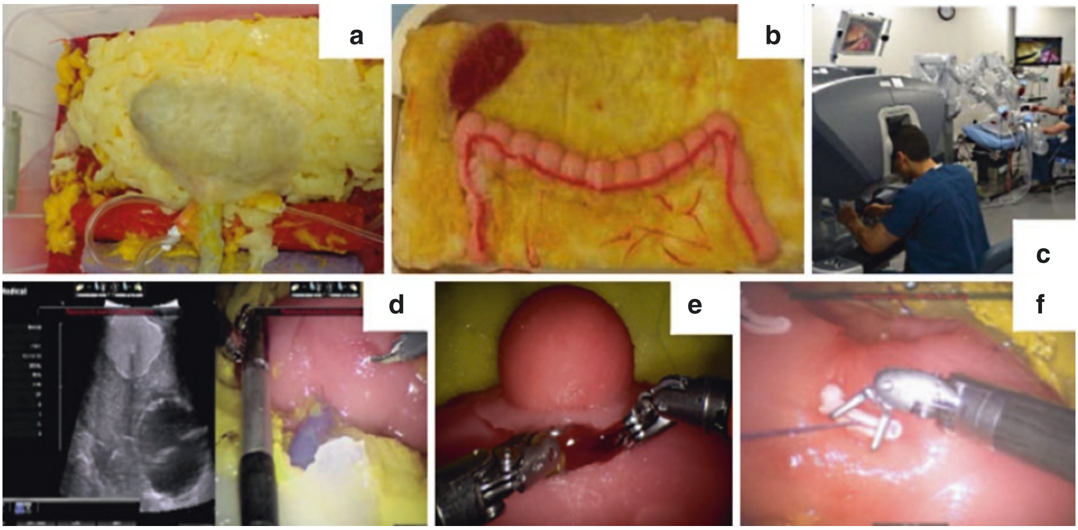

Fig. 9.7 (**a**) Kidney phantom laying on a fabricated posterior abdominal muscular wall, surrounded by fat and with the major vessels in the midline. (**b**) Completed model prior to rehearsal with added fat, descending colon, and spleen. (**c**) Rehearsal in progress in a mock operating room. (**d**) Left: Intraoperative ultrasound image. Right: Ultrasound probe used to identify tumor borders during simulation. (**e**) Excision of a tumor with functional bleeding. (**f**) Closure of the parenchymal defect

along with the relevant generic surrounding structures such as the bowel, liver, or spleen, is fabricated and added one at a time within a custom abdominal trainer (Fig. 9.7a, b). The trainer is further covered in a generic outer abdominal wall model so that incisions and trocar access can be performed in order to recreate the relevant steps of surgery (e.g., placements of ports and docking of the robotic arms, as seen in the background of Fig. 9.7c). Rehearsals of the main surgical steps, with respect to the patient-specific partial nephrectomy, can then be performed (e.g., robot-assisted partial nephrectomy, as seen in Fig. 9.7c–f). Emphasis is placed not only on rehearsing the sequential steps of the actual surgery, from incision to specimen retrieval, but also on precision and efficiency with respect to identifying the correct tissue planes, avoiding collateral damage to adjacent structures, resecting the tumor, and repairing the parenchymal defect. In this respect, metrics such as operating room (OR) time, estimated blood loss (EBL), clamping time or warm ischemia time (WIT), entry into the collecting system, and positive surgical margins (PSM) can be collected. Such metrics from the simulated case can be compared against the readouts for the actual surgical case. Moreover, quality of outcome metrics, such as perioperative complications and length of hospital stay, can also be collected for the surgical cases. Additionally, the multi-metric validity of these models can be demonstrated through their ability to differentiate experts and novices (Fig. 9.7). As such, these models have been demonstrated to exhibit face, content, construct, and concurrent validity [12–14].

To validate our simulation platform, DICOM files, from a CT scan of a patient with a single renal artery and moderate tumor complexity (4.2 cm in size, partially exophytic, close proximity of the PCS, and a RENAL nephrometry score of 7x) scheduled for a RAPN, were imported and utilized to fabricate a kidney phantom. Individual components (kidneys with incorporated vasculature and pelvicalyceal system (PCS), Gerota's fascia, surrounding fat layers, peritoneum, partial colon segment, and abdominal wall) were then assembled in anatomic orientation and subjected to final processing for organ cohesion to create the simulation platform for RAPN. Following institutional research review board (IRB) approval, 43 participants (16 experts with >150 upper-tract robotic cases and 27 novices with >10 but <50 robotic upper-tract cases) in 2 academic institutions were recruited. Experts were defined as per Larcher et al. [15]. Using the da Vinci robotic platform (Intuitive Surgical, CA, USA), participants performed all steps of a partial nephrectomy (Fig. 9.7). All participants received the same instructions prior to surgery and were encouraged to treat the procedure as a live case with an experienced bedside assistant. Differences in performances, among the two groups, were calculated by comparing procedure-specific metrics incorporated into our models. Warm ischemia time (WIT) was calculated as in live surgery. The fabricated vasculature was perfused with a combination of red saline and glycerine to simulate blood viscosity [16]. Estimated blood loss (EBL) was calculated by measuring the artificial blood in the suction at the end of the simulation. Positive surgical margins (PSM) were ascertained by an inspection of the specimen. Third-party validations (C-SATS) of tumor resection and renorraphy were completed after reviewing recovered videos using the validated Global Evaluative Assessment of Robotic Skills (GEARS) [17]. Significant differences were observed, between experts and novices, with respect to WIT, EBL, PSM, and GEARS (all p values <0.001) (Fig. 9.8). Moreover, whereas there were no major complications in the expert group, six major intraoperative complications were reported in the novice group which included two renal vein injuries, two renal artery injuries, and two ureteric transections.

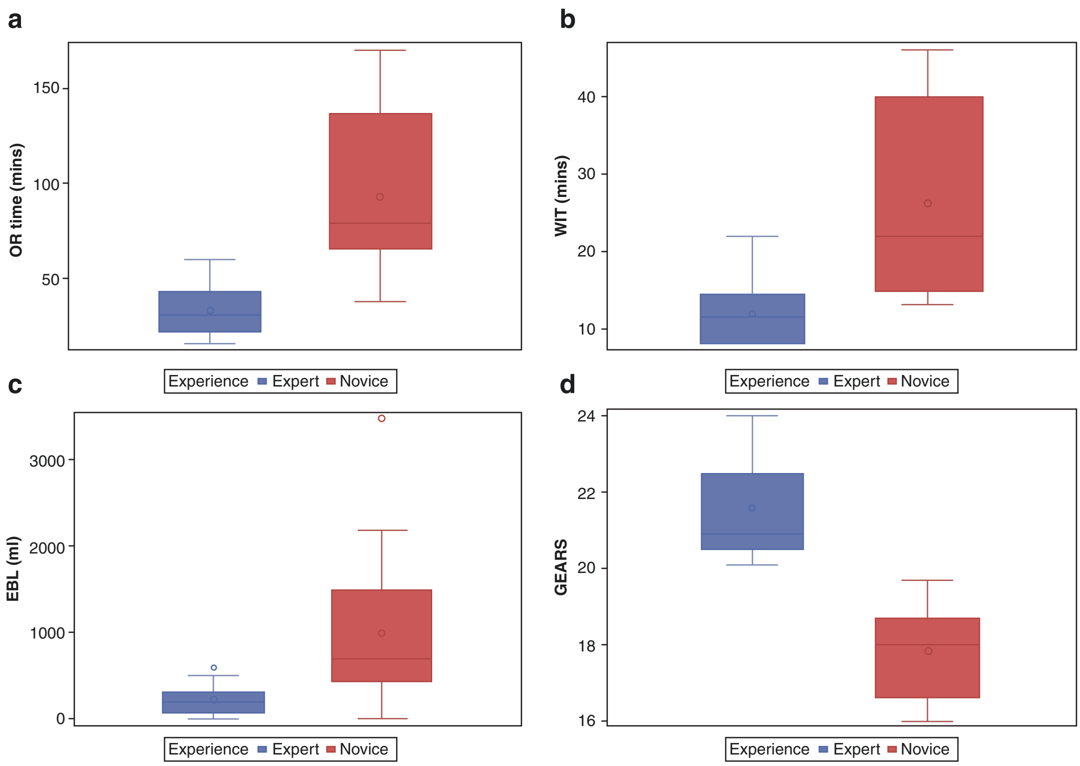

Fig. 9.8 Differentiation between experts and novices during robotic partial nephrectomy simulation using realistic organ models. (**a**) Operating room (OR) time is significantly lower in experts, (**b**) warm ischemia time (WIT) is significantly lower in experts, (**c**) estimated blood loss (EBL) is significantly lower in experts, (**d**) global evaluative assessments scores (GEARS) are significantly higher in experts

Conclusions

Using robot-assisted partial nephrectomy as an illustrative example, it is evident that realistic organ models can be created with the overarching goal of improving surgical training and, ultimately, surgical outcomes. As the creation and use of such organ models become increasingly common within various simulation platforms, it is important that literature pertaining to their methodology and validation become robustly assessed so as to be able to replicate and standardize reported protocols.

References

1. Rashid P, Gianduzzo TR. Urology technical and non-technical skills development: the emerging role of simulation. BJU Int. 2016;117(Suppl 4):9–16.
2. Cox T, Seymour N, Stefanidis D. Moving the needle: simulation's impact on patient outcomes. Surg Clin North Am. 2015;95(4):827–38.
3. Kamel M, et al. Simulation-based training in urology residency programmes in the USA: results of a nationwide survey. Arab J Urol. 2018;16(4):446–52.
4. Aydin A, et al. Simulation-based training and assessment in urological surgery. Nat Rev Urol. 2016;13(9):503–19.
5. Van Bruwaene S, et al. Porcine cadaver organ or virtual-reality simulation training for laparoscopic cholecystectomy: a randomized, controlled trial. J Surg Educ. 2015;72(3):483–90.
6. Ericsson KA. Deliberate practice and the acquisition and maintenance of expert performance in medicine and related domains. Acad Med. 2004;79(10 Suppl):S70–81.
7. Garcia J, et al. 3D printing materials and their use in medical education: a review of current technology and trends for the future. BMJ Simul Technol Enhanc Learn. 2018;4(1):27–40.
8. Aimar A, Palermo A, Innocenti B. The role of 3D printing in medical applications: a state of the art. J Healthc Eng. 2019;2019:5340616.
9. Li P, et al. Biomaterial characteristics and application of silicone rubber and PVA hydrogels mimicked in organ groups for prostate brachytherapy. J Mech Behav Biomed Mater. 2015;49:220–34.
10. Snedeker JG, et al. Strain energy density as a rupture criterion for the kidney: impact tests on porcine organs, finite element simulation, and a baseline comparison between human and porcine tissues. J Biomech. 2005;38(5):993–1001.
11. Umale S, et al. Experimental mechanical characterization of abdominal organs: liver, kidney & spleen. J Mech Behav Biomed Mater. 2013;17:22–33.
12. Ghazi A, et al. Simulated inanimate model for physical learning experience (simple) for robotic partial nephrectomy using a 3-d printed kidney model. J Urol. 2015;193(4):e778.
13. Candela B, et al. Concurrent validity of a simulated inanimate model for physical learning experience in partial nephrectomy (SIMPLE-PN). J Urol. 2016;4:e220.
14. von Rundstedt FC, et al. Utility of patient-specific silicone renal models for planning and rehearsal of complex tumour resections prior to robot-assisted laparoscopic partial nephrectomy. BJU Int. 2017;119(4):598–604.
15. Larcher A, et al. The learning curve for robot-assisted partial nephrectomy: impact of surgical experience on perioperative outcomes. Eur Urol. 2019;75(2):253–6.
16. Boes S, et al. Control of the fluid viscosity in a mock circulation. Artif Organs. 2018;42(1):68–77.
17. Kowalewski TM, et al. Crowd-sourced assessment of technical skills for validation of basic laparoscopic urologic skills tasks. J Urol. 2016;195(6):1859–65.

10 The Challenge of Augmented Reality in Surgery

P. J. "Eddie" Edwards, Manish Chand, Manuel Birlo, and Danail Stoyanov

Introduction

Imaging has revolutionized surgery over the last 50 years. Diagnostic imaging is a key tool for deciding to perform surgery during disease management; intraoperative imaging is one of the primary drivers for minimally invasive surgery (MIS), and postoperative imaging enables effective follow-up and patient monitoring. However, notably, there is still relatively little interchange of information or imaging modality fusion between these different clinical pathway stages [1].

Preoperative imaging provides three-dimensional (3D) digitization of internal patient anatomy and pathology which can be segmented and converted to surfaces in order to be displayed as a virtual model. The idea of presenting this model directly overlaid on the surgeon's view of the surgical site during procedures has been around for several decades, with solutions being proposed in the neurosurgical microscope as early as 1982 [2] and in head-mounted displays in 1996 [3]. Since these early beginnings, there has been a steady increase in research interest around both the technology and the clinical translation of such systems. An excellent overview of the current state of the art in terms of the technology is provided by the book by Peters et al. [4] and recent reviews on the topic [5, 6].

Augmented reality (AR) devices can be broadly split into two groups – video-based AR and optical see-through AR (Fig. 10.1). Literature around the former is dominated by efforts in MIS and laparoscopic procedures, which are very amenable to AR when performed either with handheld instrumentation [5] or with robotic systems such as the da Vinci® Surgical System (Intuitive Surgical Inc., CA) [7].

Optical see-through AR, which began with surgical microscope systems, has had a resurgence of interest due to the prevalence of wearable AR head-mounted displays, such as the Microsoft HoloLens™, but recent studies still suggest that more work is needed, especially in hardware to make the technology more effectively applicable to surgery [8].

Though the idea that an overlay combining information from different imaging modalities should provide direct and ergonomic visualization seems reasonable, such AR visualizations have not yet made it into mainstream clinical practice. Indeed, while there have been many initial demonstrations of AR guidance, in the laboratory and in the operating room (OR), there have been only a few attempts to investigate clinical effectiveness of the systems developed. In such cases, the clinical utility of direct overlay on the surgical view is often not clear or not proven, and there have been very few examples of successful products incorporating AR.

P. J. E. Edwards (✉) · M. Birlo · D. Stoyanov
Computer Science/WEISS, University College London, London, UK
e-mail: eddie.edwards@ucl.ac.uk

M. Chand
Surgery and Interventional Sciences, University College London, London, UK

S. Atallah (ed.), *Digital Surgery*, https://doi.org/10.1007/978-3-030-49100-0_10

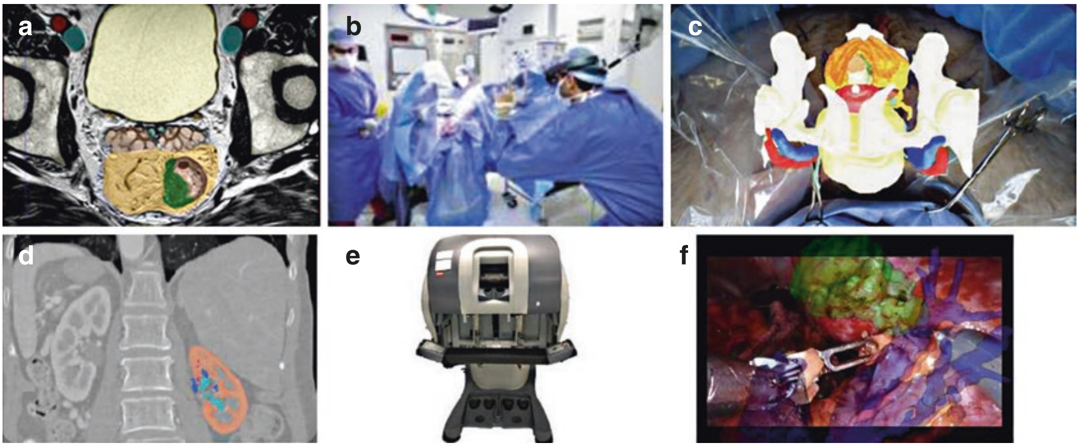

Fig. 10.1 Augmented reality devices in surgical applications. In the top row, we have an optical see-through AR example, showing segmented preoperative MRI (**a**), the head-mounted display (Microsoft HoloLens™) in colorectal surgery (**b**) and the surgeon's view with overlay (**c**). Below is a video see-through example, showing preoperative segmented CT (**d**), the da Vinci robot console (**e**) and overlay of the kidney model through the console during partial nephrectomy (**f**)

This book chapter provides a critique of existing AR methods or application studies described in the literature using relevant examples. The aim is not to provide a comprehensive review, but rather to give an indication of the clinical areas in which AR has been proposed, to begin to explain the lack of clinical systems and to provide some clear guidelines to those intending to pursue research in this area.

We start by describing the two broad categories of AR, video see-through and optical see-through, within a historical context of the field. We then go on to examine the components that make up an AR system, in each case examining aspects of this component that may provide barriers to introduction in the clinic (Fig. 10.2). Finally, we make the case for increased research in human perception and effect on performance in the virtual and lab settings, as well as task-focused applications in the operating room. With the ready availability and increasing quality of visualization devices, it seems likely that interest in this area will continue to increase. We hope this chapter is helpful in informing and guiding researchers in this field towards clinically effective products.

Historical Context

AR guidance of surgery was first proposed in 1982 by Kelly et al. [2], who overlaid tumour outlines from CT into the view of a surgical microscope attached to a stereotactic frame. A few years later, Roberts et al. took this further by incorporating an ultrasonic tracking system [9]. Despite significant errors of >5 cm, these efforts are considered to be the beginning of frameless stereotaxy in neurosurgery, which is now more commonly called image-guided surgery and is routinely used for the treatment of conditions in the brain [4].

AR overlay in the surgical microscope became part of the Zeiss MKM robotic microscope system, providing similar views to those originally proposed by Kelly et al. [2]. Augmented reality representation providing 3D visualization of preoperative imaging models was also proposed within the surgical microscope for ENT and neurosurgery [10]. Such augmented views are now available in surgical microscope products including the Zeiss Kinevo® 900 and the Leica ARveo in conjunction with image guidance systems such as Brainlab's neurosurgical microscope navigation product [11].

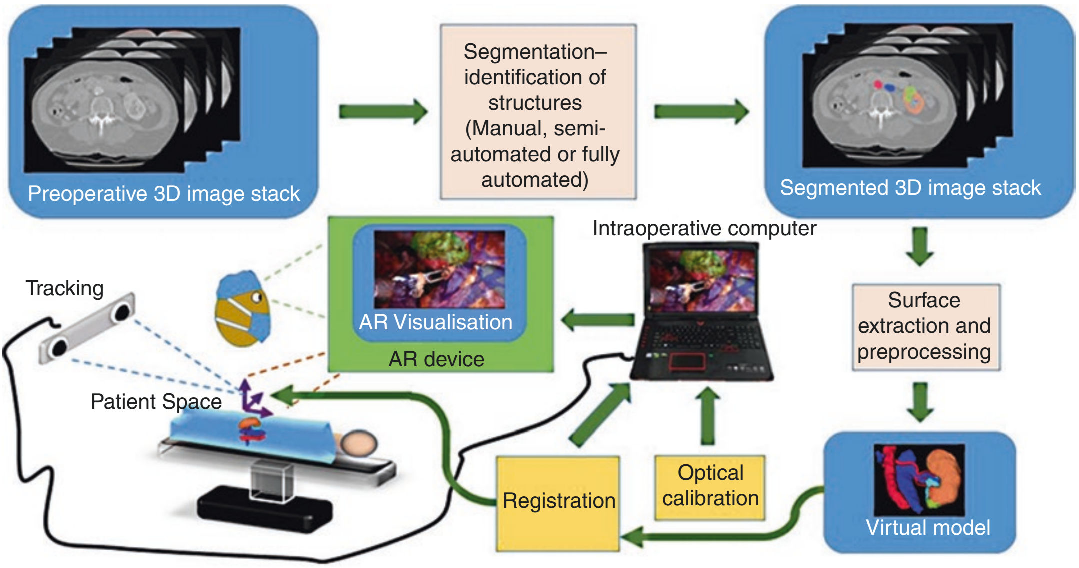

Fig. 10.2 Schematic of the system layout for AR, showing how the different technical components of an AR system that we describe in the chapter are connected

Such microscope-based systems are examples of optical see-through (OST) AR, in which the overlaid information is projected onto the optical view using a half-silvered mirror. The structure of an OST-AR system is shown in Fig. 10.3. In addition to custom solutions such as the PerkStation for needle guidance [12], there has been a resurgence of interest in OST-AR with the introduction of commercial head-mounted devices such as the Microsoft HoloLens 2™ (www. microsoft.com/en-us/hololens) and the Magic Leap One™ (www.magicleap. com).

In contrast to optical see-through systems, Fuchs et al. developed a camera-based head-mounted display system for guidance of breast and tumour biopsy in 1996 [3]. The system combined a virtual reality (VR) headset linked to calibrated stereo video cameras and was able to show the ultrasound image visualized coming physically out from the end of the probe. This initial system was further developed for breast tumour aspiration a couple of years later and demonstrated on phantoms and in four clinical cases [13]. This was the first video AR device for surgical guidance. A schematic showing how video AR is achieved is shown in Fig. 10.4, where the virtual and real views are mixed on the computer and then displayed to the surgeon.

The more recent literature for video-based surgical AR is dominated by the da Vinci Surgical System (Intuitive Surgical Inc., CA, USA). The robot was originally developed for cardiac procedures, specifically to perform totally endoscopic coronary artery bypass (TECAB), and AR has been proposed for such operations using a 4D cardiac CT model [14]. This was extended to potentially compensate for cardiac motion using dynamic information from the video feed and finite element modelling [7]. However, cost-effectiveness was not readily demonstrated for TECAB, and clinical focus for the robot has shifted to urology, with prostatectomy and partial nephrectomy becoming commonly performed procedures, as well as gynaecological surgery like robotic hysterectomy. Accordingly, AR focus shifted towards these application areas [15].

A recent comprehensive review of AR in robot-assisted surgery is provided by Qian et al. [16]. Despite taking into account 93 relevant papers over 19 years of research, they state that the field of AR in robotic-assisted surgery is not yet mature and clinical effectiveness remains to be proven. This conclusion is reiterated by a systematic review of AR in urological procedures [17]. The automatic provision of segmentation

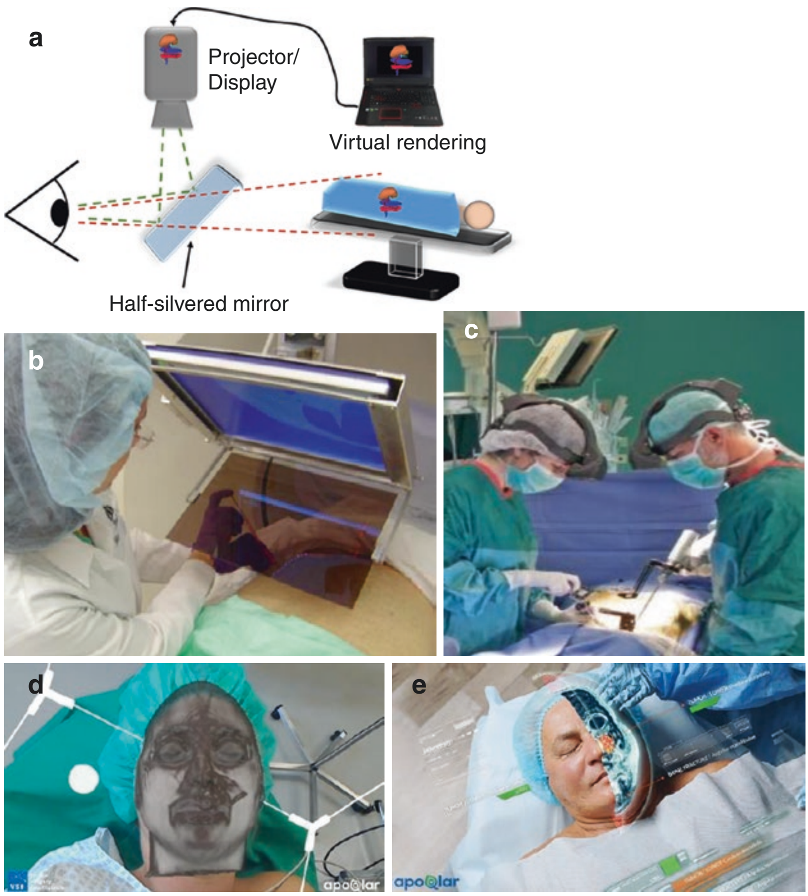

Fig. 10.3 The layout for an optical see-through (OST) AR system (**a**). A purely virtual view is overlaid on the surgeon's direct optical view using a half-silvered mirror. Examples include the PerkStation for CT needle guidance (**b**) (Image courtesy of Worcester Polytechnic Institute) and the Augmedics XVision system for spinal surgery (**c**) (Image courtesy of Augmedics). The VSI overlay system from apoQlar (https://apoqlar.com/) uses facial surface alignment to guide sinus surgery using the HoloLens™ (**d**, **e**). (Image courtesy of apoQlar GmbH)

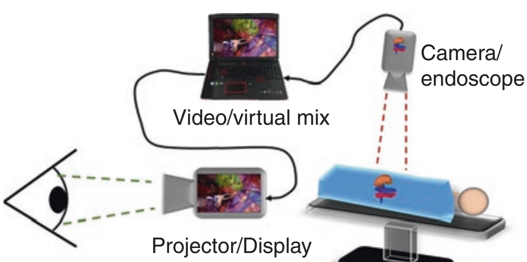

Fig. 10.4 Video-based AR systems. A video camera takes a live image of the patient, which is mixed with a virtual view on a computer before being displayed to the surgeon

services for renal cancer is provided by companies such as Innersight Labs Ltd. (https://www.innersightlabs.com), Visible Patient (visiblepatient.com), Ceevra Inc. (https://ceevra.com) and Intuitive Surgical Inc. (intuitive.com) through their da Vinci Iris app. These products should enable much greater use of AR in the OR and lead towards a clearer understanding of the clinical effectiveness and best modes of operation for robotic AR surgical guidance.

In addition to robotic procedures, video-based AR has been proposed for non-robotic laparoscopic procedures (Fig. 10.5). Providing guidance during laparoscopic liver resection has attracted significant effort from both research [18, 20] and industry [21]. In laparoscopic gynaecology, Bartoli et al. have proposed an AR system for surgery of the uterus [22]. Neurosurgery, with the desire for accuracy and comparatively rigid anatomy encased within the cranium, is a well-suited candidate for image guidance, and Meola et al. provide a comprehensive review of this area [23].

A Google Scholar search for "augmented reality and surgery" produces the graph in Fig. 10.6. The increase in research interest in AR is clear,

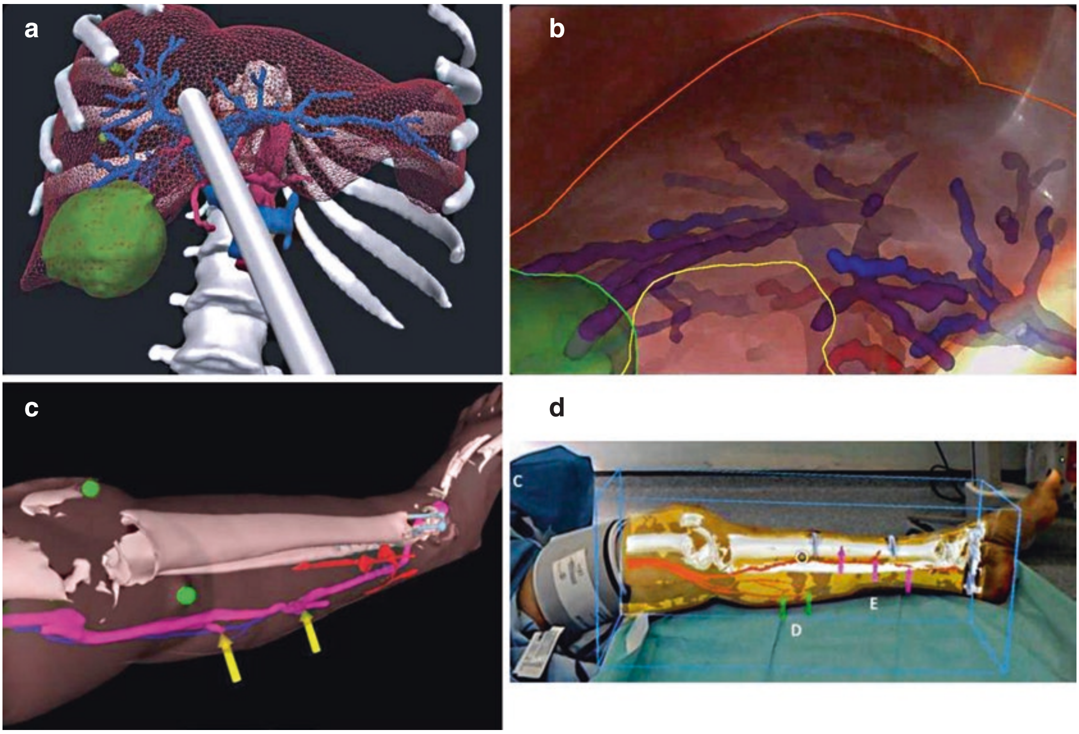

Fig. 10.5 Registration of virtual and augmented views. The SmartLiver system [18] showing a rendering of the endoscope position relative to the patient anatomy (**a**) and the liver outline, underlying vessels and lesion from CT overlaid on the endoscopic view (**b**). Alignment is achieved with surface matching. The orthopaedic guidance system of Pratt et al. [19] uses manual alignment to overlay a virtual view of bones and blood vessels (**c**) on the surgeon's view of the patient using the HoloLens™ (**d**). (From Pratt et al. [19]. Open Access article under the Creative Commons Attribution 4.0 International License)

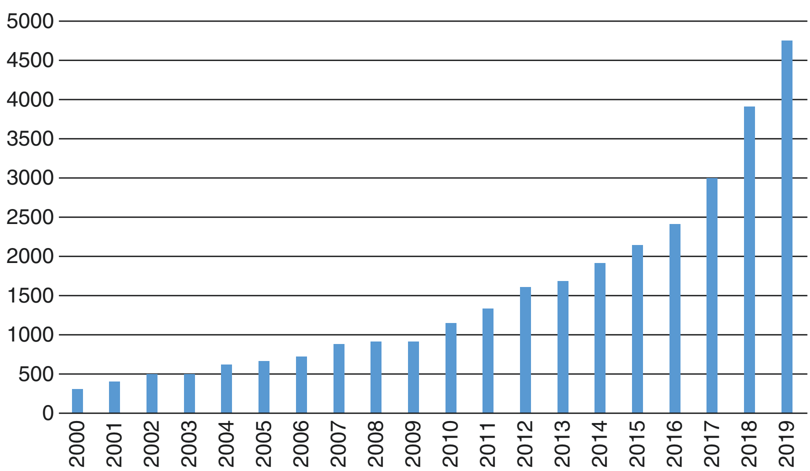

Fig. 10.6 Google Scholar search results for "augmented reality" and "surgery" in the last 20 years

with almost 5000 papers in 2019, and the trend is still upwards. This significant research effort has not yet been matched by AR products becoming commonplace in the operating room though there are indications that such systems may not be in the distant future. For example, Philips and Microsoft recently announced a collaboration to develop AR solutions for the operating room combining imaging technology and the HoloLens™ platform [24]. The VSI solution from apoQlar GmbH offers integration of care into the augmented view, including facial surface alignment for AR guidance of sinus surgery (see Fig. 10.3d, e). The Scopis system also provides AR visualization for endoscopic sinus surgery (https://navigation. scopis.com/tgs). It is likely that interest in AR for surgical applications will continue to grow.

In the remainder of this chapter, we consider the stages required to produce accurately aligned AR – preoperative model construction, calibration, registration, tracking and visualization. In each instance, we consider how it is achieved, what research problems remain and whether these problems are likely to be a reason for the lack of clinical uptake of AR.

Preoperative Patient Data Acquisition and Model Construction

An example segmentation of a CT scan can be seen in Fig. 10.7. The blood vessels supplying the kidney are segmented along with the lesion itself and the ureter. This model is intended for guidance of robotic-assisted partial nephrectomy. Identifying the relevant anatomy and physiology has traditionally been achieved by marking structures either by hand or in a semi-automated fashion in each of the image slices. A number of free

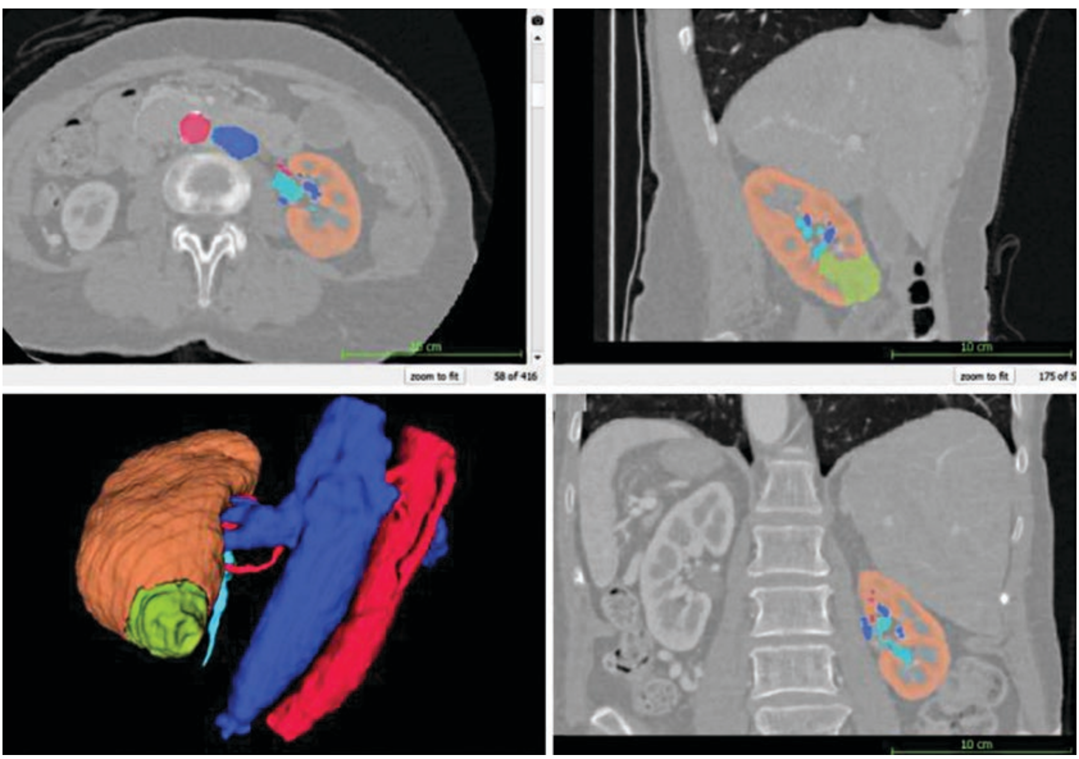

Fig. 10.7 Example CT segmentation of a kidney tumour. Voxels are labelled in the three orthogonal cuts, and a 3D rendered model is constructed (bottom left). Blood vessels, ureter, kidney, and lesion are visible. (Model courtesy of Innersight Labs Ltd. displayed in ITKSnap)

or open-source packages are available to help with this process, including Slicer (https://www.slicer.org/), ITKSnap (http://www.itksnap.org/), Osirix (https://www.osirix-viewer.com/) and ImageJ (https://imagej.net/). These packages are helpful, but not quite ready for routine clinical use to generate anatomical models for AR visualization. The main additions needed to such software packages are greater automation of segmentation to alleviate the time needed for clinicians to generate the AR model and also customization for specific organs and modalities to ensure high fidelity models are generated across different surgical specialties.

The research area of image segmentation is substantial and is becoming more mature as automated identification of structures is improving using deep learning [25]. The image shown in Fig. 10.7 depicts a model from Innersight Labs Ltd. Such services or automated segmentations, though currently focused on the kidney, will hopefully become more readily available in other clinical application areas.

AR surgical guidance provided by preoperative 3D imaging firstly requires that preoperative imaging is able to provide information that is useful to the surgery being performed. Deep learning is leading towards automated segmentation of images that is approaching the performance of expert radiologists [25]. However, despite its great promise and considerable research effort, automated segmentation methods have not yet made in into regular clinical practice. This presents a significant challenge to the surgical workflow for AR guidance. The other question is whether preoperative imaging provides the desired information and also whether the anatomical and pathological structures can be readily identified in the scans. Taking examples from robotic procedures, in partial nephrectomy the models obtained from CT and CT angiography provide the general shape of the kidney and the structure of the feeding arteries that must be clamped before lesion removal. The tumour itself can also be seen, though the accuracy with which the tumour boundary can be delineated in the parenchyma has not yet been established. The CT model may speed up the process of vessel identification and could also help in tumour delineation in conjunction with laparoscopic ultrasound [26].

For radical prostatectomy the principal structure of interest is the neurovascular bundle, since preservation of the nerves and blood vessels will result in improved postoperative function. But this structure is not readily and accurately found in preoperative imaging, which makes the case for AR guidance less clear for this procedure [15]. With the adoption of new imaging agents or hybrid imaging techniques like PET-MRI this issue may be alleviated. This is a key criterion for successful future applications of AR. *One must consider whether preoperative imaging can provide the relevant critical information that can help guide surgery.* This is the first consideration that should be taken into account when proposing AR in any new clinical specialization.

Optical Calibration

Calibration is a key component of the software for AR systems allowing the transformation of information between the different coordinate frames of the environment, sensors and the AR model. The standard procedure is to calibrate the surgical camera to establish correspondence between 3D space of the surgical site and the video image from the camera sensor. There are standard implementations in OpenCV and MatLab that tend to be used [27, 28]. For video see-through, the methods for calibration are well-established and most studies suggest that registration is a larger source of error [29] but perhaps new constraints that incorporate the position of the trocar point can reduce error [30].

Calibration for OST devices such as the HoloLens™ is more complex. In the case of the HoloLens™, sensors on the device create a model of the room and objects are placed within this coordinate system. In order to anchor an object to a specific location in the room, optical tracking markers have been proposed, such as the ARToolkit markers or the image-based tracking provided by Vuforia [31]. Such methods perform tracking through the same sensors as those used for head tracking; calibration should be straightforward or even unnecessary. However, one must rely on the manufacturer's calibration to the individual user's vision. In addition to single-user calibrations, it is possible to have multiple users, each wearing a HoloLens™, to interact together by viewing the same object in the same place anchored to a reference frame in the room. There remains a paucity of data examining the accuracy of this and while this is great for collaborative working, we are not aware of this aspect of the HoloLens™ being used for surgery guidance. The spinal surgery guidance system from Augmedics (https://www.augmedics.com/) enables collaborative AR guidance using their customized visualization system (see Fig. 10.3c).

Registration of the Preoperative Model to the Patient

In order to align the preoperative imaging model to an AR view, it is first necessary to align the imaging model to the physical space of the surgical site or patient. This may be achieved with markers, either passive or active, and these can be either fixed to the anatomy (e.g. bone implanted) or attached using adhesives. Fiducial markers allow a straightforward calculation of the transformation between the different coordinate frames if they can be reliably detected, but practically such systems can suffer from occlusions or line of sight problems even in commercially available navigation systems such as Brainlab's surgery products (https://www.brainlab.com/surgery-products/) and the StealthStation™ from Medtronic [32].

Markerless registration algorithms to align the surgical video feed to preoperative models have been the topic of many research systems and papers [18, 22, 33–35]. Despite great process in such technology and advances in all aspects of the required algorithms – real-time performance, biomechanical deformation and realism, accuracy and robustness – fully automatic clinical solutions are still not readily available. *This aspect of AR is crucial because registration accuracy may be a key factor in the lack of uptake of AR.* In their critical systematic review of the literature for urological procedures, Bertolo et al. identify registration accuracy as the major limitation of AR [17].

However, even with perfect registration demonstrated in a virtual system, AR may not be the most effective visualization. Dilley et al. compared AR with nearby virtual rendering and no guidance, finding that nearby virtual rendering was more effective than AR and no guidance [36]. This suggests that accurate registration is not the sole cause of AR's limitations.

Tracking

Live tracking and update of the image as the surgeon's view changes is required for accurate AR as the scene and the observer change their relationship. In the case of robot-assisted procedures, the camera motion can potentially be provided by the robot kinematics although correction is likely needed because error propagates between the robot encoder coordinates and the camera frame [30]. For non-robotic MIS, an external tracker is usually attached to the proximal end of the laparoscope and used to estimate the camera motion [18]. However, for optical tracking, it has been recognized that the distance between the tracker and the camera position can cause significant errors. This has led to interest in improving tracking using the endoscope visual view [37–39] and potentially mapping the entire surgical scene at the same time in structure from motion (SfM) or simultaneous localization and mapping (SLAM) frameworks [40, 41].

Poor tracking may be problematic for guidance accuracy because a registered AR model may drift out of alignment. The relatively slow movement of the camera in robotic procedures make this less of an issue, and the robot also provides camera positional information from the kinematics of the system. Even with handheld laparoscopic surgery, the camera tends to be held reasonably steady.

With head-mounted displays, even a relatively small amount of lag can cause a lack of comfort or even nausea. One of the main advantages of the HoloLens™ is that substantial R&D has gone into improving accuracy and reducing latency in the head tracking and positional mapping of the environment to alleviate this precise problem.

Intraoperative Visualization

Having calibrated the optics and aligned the model correctly to the patient, it remains to decide on the most effective visualization for AR during surgery. In minimally invasive surgery where direct access or visualization of the anatomy is not possible or in microsurgery, the inherent use of a display facilitates AR visualization. In open surgery or orthopaedics, an AR display needs to be incorporated into the process (see Figs. 10.3c and 10.5c, d). In addition to the display, a number of additional considerations are important for surgical AR displays including fidelity of depth visualization and minimization of the information presented to avoid overload [42, 43]. Overall, it appears that visualization and issues surrounding perception and interaction are in fact the biggest issues facing AR surgical guidance [44]. Below, we discuss in a little more detail some of the challenges.

Depth Perception

Even with correct alignment and well-calibrated stereo views or other means of 3D scene mapping, there are remaining issues of depth perception that have been investigated in the general field of human vision [45]. This is also recognized as a significant problem in surgical applications [46]. In general, the perceived relative depths of the real and virtual objects become distorted as they approach the same depth, *an effect known as depth contrast.* This is an area that deserves more attention, as the direction of the distortion has been observed differently in different experiments [45, 47]. It is possible some of these effects can be reduced or perhaps alleviated entirely with the correct level of mixing, adjustment of visual parameters such as spatial frequency or colour and incorporation of other visual cues such as motion. Techniques such as inverse realism have also been proposed to help make the real surface look transparent in video-based AR, where the real surface can be partially blacked out to make perception of underlying structures more natural [48, 49]

Fatigue

It has been recognized in both virtual and augmented displays that, over a period of time, the use of the device may cause fatigue or a lack of comfort in the user. Symptoms such as tiredness, dizziness or even nausea have been reported [50, 51]. The cause has not been fully established, but it has been suggested that lag between head motion and movement of the virtual scene could be a factor as well as inconsistency between the focus and convergence of binocular vision [52]. Issues that occur for virtual reality displays are equally a problem for AR and can be attributed to the display resolution, refresh rate, brightness and other characteristics [53]. Efforts from the VR community to alleviate fatigue in wearable consumer systems for gaming may provide useful ideas to address this in surgery. Examples include a dynamic depth-of-field [54] and focal surface displays [55].

Visual Clutter

Possibly the biggest challenge for AR as a method of surgical guidance is that it adds clutter to the scene. The visualization in Fig. 10.8 demonstrates the problem, where the tools are obscured by the solid AR view. This issue is specifically documented by Dixon et al. [56] and Hughes-Hallet et al. [57] and is also recognized in Qian's review of robotic AR, where they suggest that methods such as activation-on-demand can be used to reduce visual clutter [16].

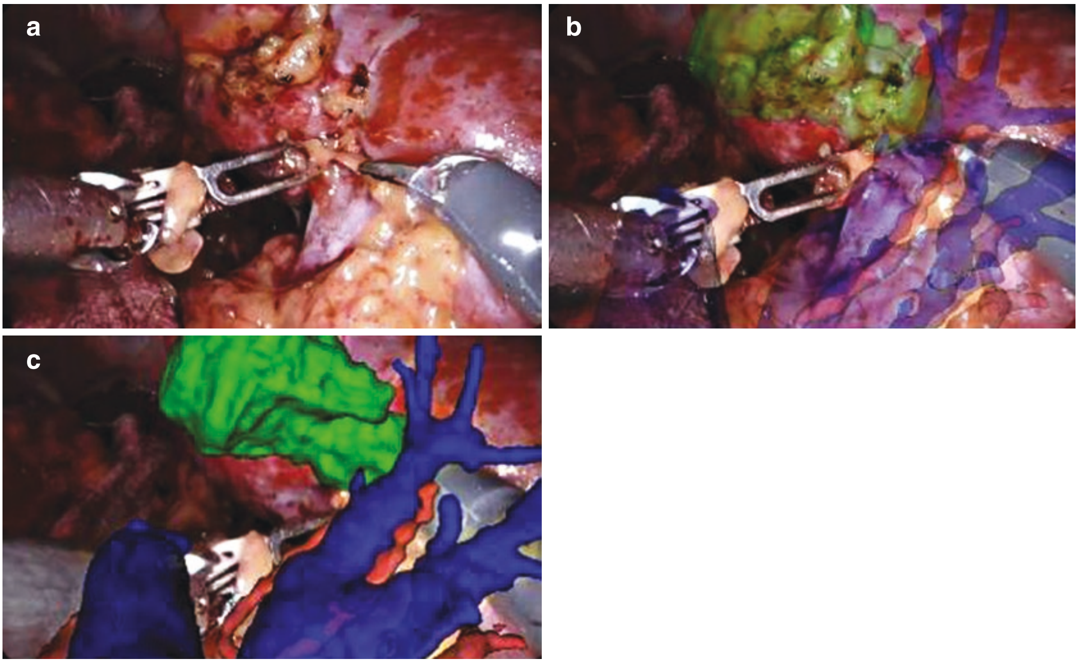

Fig. 10.8 A scene from a robotic-assisted partial nephrectomy with no overlay (**a**), transparent overlay (**b**) and solid overlay (**c**), using the CT model from Fig. 10.7. The figure underlines the need to provide appropriate mixing of the virtual and real so as not to obscure or distract from the surgeon's view

Future Directions

AR Display Technology

In the MIS or microsurgery setting, the display of fused information is naturally accommodated by the inherent presence of a digital monitor showing the surgical camera feed. However, displays are a major technological area for further development to allow AR in other procedures or where a surgical camera is not present. See-through mirror displays or video see-through displays could be brought in to enable visual information overlay [58]. These could be enhanced through different display technologies to support, for example, better depth perception without immersive consoles using autostereoscopic displays or visualization directly on the patient through a projection of information onto the surgical site [59].

Interventional Imaging

It is possible to augment views other than the optical view of the patient in procedures where different energy levels are used to image the anatomy. This is particularly relevant in endovascular surgery or interventional radiology where fluoroscopy is used to see the internal anatomy. Overlays of information from CT onto the fluoroscopic image can guide treatment in a range of procedures supporting better stent placement or valve replacement and meanwhile reducing the time taken for the procedure and thus the radiation dose. Figure 10.9 shows the overlay of preoperative CT accurately aligned to the fluoroscopic view using the Cydar EV system (https://www.cydarmedical.com/product). Live deformation is performed in the cloud to provide accurate and reliable alignment. This is an example of a system where live radiological images can be augmented using preoperative models.

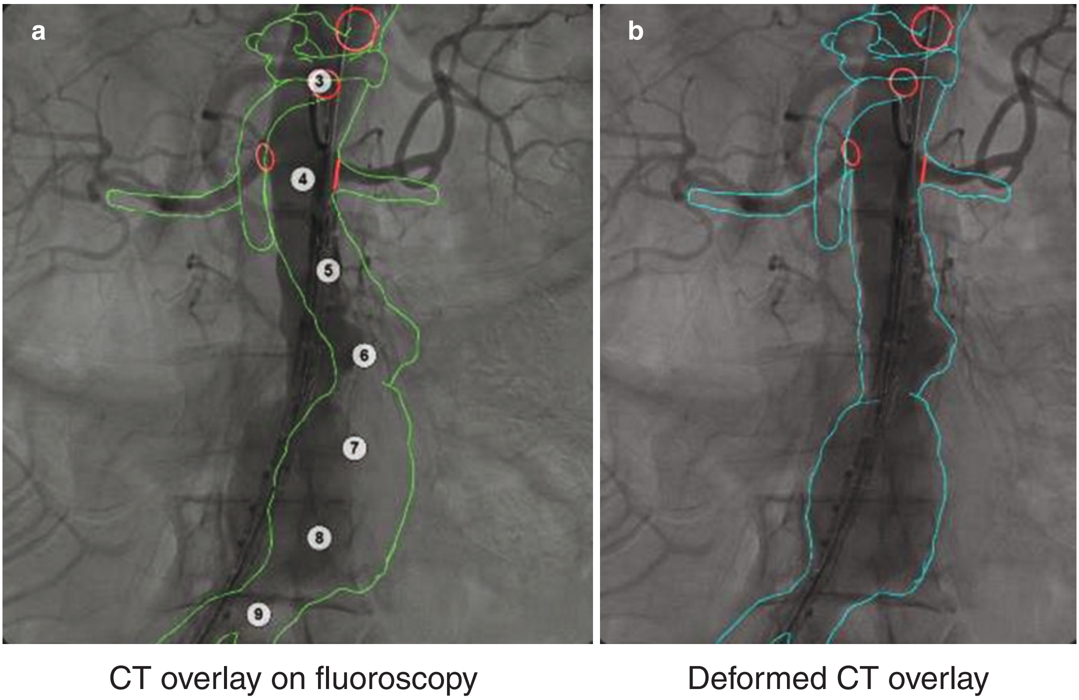

Fig. 10.9 The Cydar system, showing a CT model overlaid on X-ray for the guidance of interventional procedures. The CT model is first aligned rigidly (**a**) and then deformed to match the therapeutic position of the patient (**b**). The alignment allows correct identification of vessels and reduces X-ray dose and clinical errors. (Images reproduced with permission from cydarmedical.com)

Live imaging can also be used to augment the endoscopic view. Examples of this include the da Vinci Firefly fluorescence imaging seen in Fig. 10.10. Fluorescence imaging can provide live visualization of metabolism, showing the location of blood vessels or cancerous tissue [60, 61]. Blood vessels may also be identified by analytic methods such as video amplification [62]. The use of such live imaging modalities alleviates the need for model registration, and it is likely that these methods will have a significant role in future surgical practice. But it will still be important to develop systems that can optimize the displayed information by making use of all relevant contrasts of specific structures that are available across the different modalities.

Conclusions and Recommendations

In this chapter, we have outlined the methods and applications employed to achieve AR for surgical guidance and navigation. Although there have been some systems that have demonstrated potential clinical advantages of using AR in small numbers of cases, there are clearly challenges that remain both in the underpinning technology and in clinical translation to fit AR with current clinical processes. It should be added that a significant proportion of the papers in the graph shown in Fig. 10.6 details attempts to address some of the technical or algorithmic challenges in AR visualization or registration. Yet few papers address in detail the clinical practicalities and possible barriers in underpinning technology such as in medical image segmentation and preprocessing which, despite tremendous advances, is still not routinely available for all anatomical regions. Other technical challenges remain, such as in the level of maturity of wearable AR devices and their restricted applicability to surgery [44].

We suggest that there is a need to perform experiments in the laboratory to establish the utility of AR for specific tasks. Figure 10.11a–d shows a very stylized kidney phantom. Such models can be produced relatively cheaply and

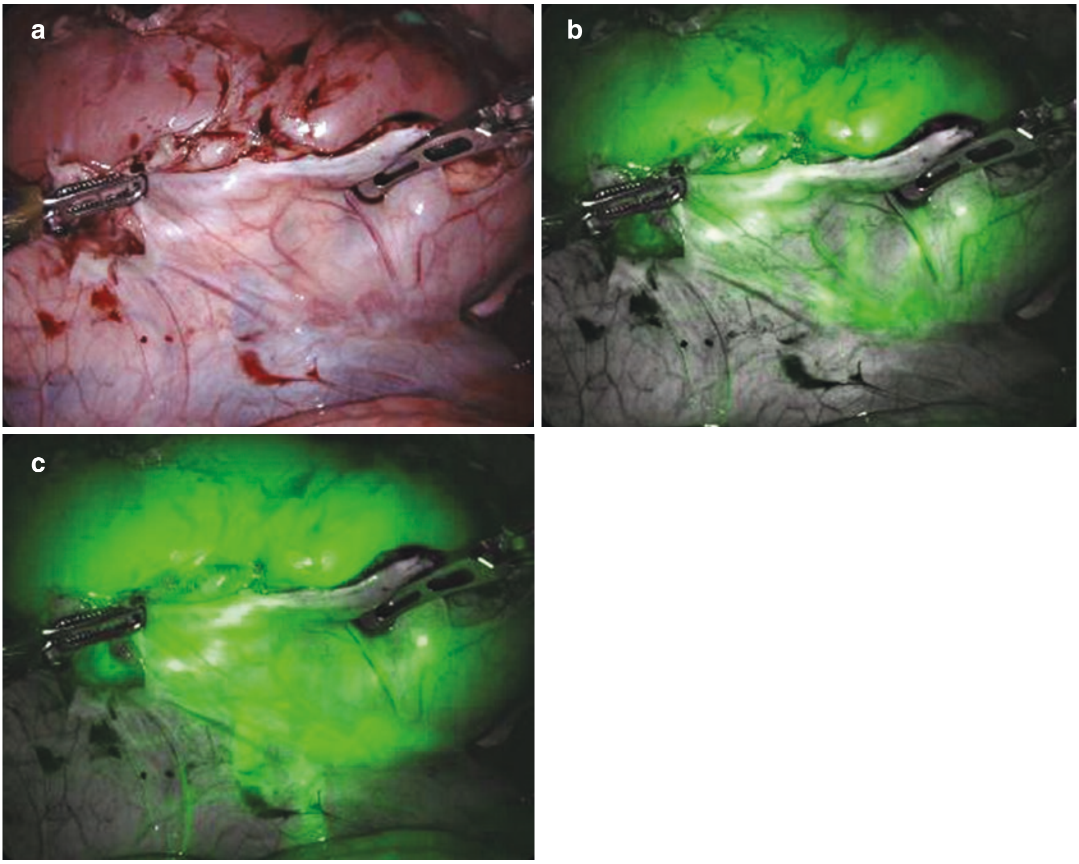

Fig. 10.10 Images from the Firefly system, showing the endoscopic view (**a**), and overlays of live fluorescence imaging with different thresholds (**b, c**) which can provide a view of blood vessels or tumour metabolism directly on the surgeon's view. Such live views alleviate the need for registration

incorporated into a training curriculum, allowing a significant number of experiments to establish the effectiveness of AR visualization without posing a risk to patients. The phantom shown here is not realistic, but may be sufficient to show whether AR can improve outcomes such as surgical margins in the laboratory setting.

There may also be a case for incorporating much more realistic phantoms (Fig. 10.11e) into the surgical training curriculum in the future, enabling trainees to practice in a realistic setting without risk to patients [63]. Such a platform would also allow safe investigation of the effect of AR visualization on surgical training and practice.

When considering AR as visualization methodology for any particular surgical application, we recommend considering the following issues:

- What is the real clinical problem being addressed, and is AR the most appropriate technology to tackle it?
- Is the underlying data needed available? For example, are the structures of interest seen in MRI or CT, and are they of sufficient resolution?
- Is clinical workflow, for example, preprocessing of the data, suitable, and who will prepare models prior to surgery?
- How is AR likely to help? Accuracy? Speed? Reduction of errors? Decision-making?
- What visualization strategy is the most appropriate? Side-by-side? Mixed? OST or video AR?
- Aim to demonstrate improved performance in a virtual or phantom environment.

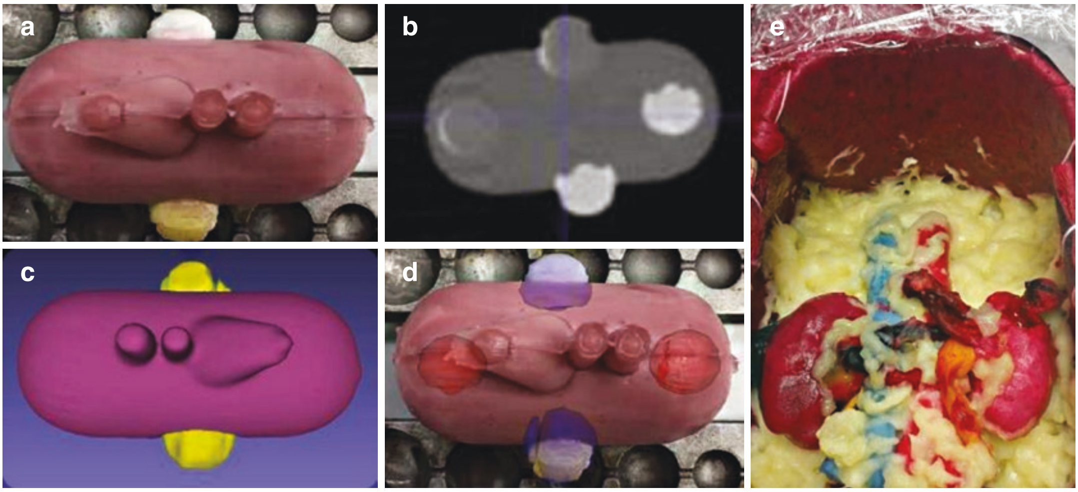

Fig. 10.11 A stylized kidney phantom, showing the phantom (**a**), CT scan (**b**), virtual model (**c**) and AR overlay (**d**). Though the phantom is not anatomically realistic, it can be readily manufactured to enable experiments in the lab that can demonstrate the accuracy of lesion extraction with different visualizations. Anatomically and physically more accurate phantoms (**e**) can enable realistic and safe surgical rehearsal of AR systems. (Image courtesy of Ahmed Ghazi, Simulation Innovation Laboratory)

- When should AR visualization be provided (which sections of the procedure, only on-demand)?

With a focus on finding the appropriate visualization to produce proven improvements in performance and decision-making for specific surgical tasks, we believe that AR will find its correct place in surgery, and improved outcomes for patients will result. Significant research effort will still be required to achieve this goal, and it is likely that the effort in this area will continue to grow, taking advantage of continued improvements in surgical AR technology including both hardware and software. We hope this chapter helps to guide those working in this field towards measurable improvements in surgical performance and clinical outcomes.

References

1. Maier-Hein L, Vedula SS, Speidel S, Navab N, Kikinis R, Park A, Eisenmann M, Feussner H, Forestier G, Giannarou S. Surgical data science for next-generation interventions. Nat Biomed Eng. 2017;1(9):691–6.
2. Kelly PJ Jr, Alker GJ, Goerss S. Computer-assisted Stereotactic Laser Microsurgery for the Treatment of Intracranial Neoplasms. Neurosurgery. 10(3):324–31, 03 1982.
3. Fuchs H, State A, Pisano ED, Garrett WF, Hirota G, Livingston M, Whitton MC, Pizer SM. Towards performing ultrasound-guided needle biopsies from within a head-mounted display. In: Hohne KH, Kikinis R, editors. Visualization in biomedical computing. Berlin: Springer; 1996. p. 591–600.
4. Peters TM, Linte CA, Yaniv Z, Williams J. Mixed and augmented reality in medicine. Boca Raton: CRC Press; 2018.
5. Bernhardt S, Nicolau SA, Soler L, Doignon C. The status of augmented reality in laparoscopic surgery as of 2016. Med Image Anal. 2017;37:66–90.
6. Ferrari FCV, Klinker G. Augmented reality in healthcare. J Health Eng. 2020.
7. Pratt P, Stoyanov D, Visentini-Scarzanella M, Yang GZ. Dynamic guidance for robotic surgery using image-constrained biomechanical models. In international conference on medical image computing and computer-assisted intervention. Springer; 2010. p. 77–85.
8. Condino S, Carbone M, Piazza R, Ferrari M, Ferrari V. Perceptual limits of optical see-through visors for augmented reality guidance of manual tasks. IEEE Trans Biomed Eng. 2020;67(2):411–9.
9. Roberts DW, Strohbehn JW, Hatch JF, Murray W, Kettenberger H. A frameless stereotaxic integration of computerized tomographic imaging and the operating microscope. J Neurosurg. 1986;65(4):545–9.

10. Edwards PJ, King AP, Maurer CR, De Cunha DA, Hawkes DJ, Hill DLG, Gaston RP, Fenlon MR, Jusczyzck A, Strong AJ. Design and evaluation of a system for microscope-assisted guided interventions (magi). IEEE Trans Med Imaging. 2000;19(11):1082–93.
11. Brainlab AG. Microscope navigation. https://www.brainlab.com/surgery-products/overview-neurosurgery-products/microscope-navigation/. 2020. Online; accessed 19 Feb 2020.
12. Vikal S, Paweena U, Carrino JA, Iordachita I, Fischer GS, Fichtinger G. Perk station—percutaneous surgery training and performance measurement platform. Comput Med Imaging Graph. 2010;34(1):19–32.
13. Pisano ED, Fuchs H, Livingston MA, Hirota G, Garrett WF, Whitton MC. Augmented reality applied to ultrasound-guided breast cyst aspiration. Breast Dis. 1998;10(3–4):221–30.
14. Figl M, Rueckert D, Hawkes D, Casula R, Hu M, Pedro O, Zhang DP, Penney G, Bello F, Edwards P. Image guidance for robotic minimally invasive coronary artery bypass. Comput Med Imaging Graph. 2010;34(1):61–8.
15. Sridhar AN, Hughes-Hallett A, Maye EK, Pratt PJ, Edwards PJ, Yang GZ, Darzi AW, Vale JA. Image-guided robotic interventions for prostate cancer. Nat Rev Urol. 2013;10:452–62.
16. Qian L, Wu JY, DiMaio S, Navab N, Kazanzides P. A review of augmented reality in robotic-assisted surgery. IEEE Trans Med Robot Bionics. 2019;2:1.
17. Riccardo Bertolo, Andrew Hung, Francesco Porpiglia, Pierluigi Bove, Mary Schleicher, and Prokar Dasgupta. Systematic review of augmented reality in urological interventions: the evidences of an impact on surgical outcomes are yet to come. World J Urol, 2019; 1–10.
18. Thompson S, Schneider C, Bosi M, Gurusamy K, Ourselin S, Davidson B, Hawkes D, Clarkson MJ. In vivo estimation of target registration errors during augmented reality laparoscopic surgery. Int J Comp Assist Radiol Surg. 2018;13(6):865–74.
19. Pratt P, Ives M, Lawton G, Simmons J, Radev N, Spyropoulou L, Amiras D. Through the hololens™ looking glass: augmented reality for extremity reconstruction surgery using 3D vascular models with perforating vessels. Eur Radiol Exp. 2018;2(1):2.
20. Ozgur E, Lafont A, Bartoli A. Visualizing in-organ tumors in augmented monocular laparoscopy. In IEEE international symposium on mixed and augmented reality, ISMAR 2017 Adjunct, Nantes, France, October 9–13, 2017. IEEE Comput Soc; 2017. p. 46–51.
21. Lachenmayer A, Tinguely P, Maurer MH, Frehner L, Knopfli M, Peterhans M, Weber S, Dufour J-F, Candinas D, Banz V. Stereotactic image-guided microwave ablation of hepatocellular carcinoma using a computer-assisted navigation system. Liver Int. 2019;39(10):1975–85.
22. Collins T, Pizarro D, Bartoli A, Canis M, Bourdel N. Computer-assisted laparoscopic myomectomy by augmenting the uterus with pre-operative MRI data. In 2014 IEEE International Symposium on Mixed and Augmented Reality (ISMAR). IEEE; 2014. p. 243–8.
23. Meola A, Cutolo F, Carbone M, Cagnazzo F, Ferrari M, Ferrari V. Augmented reality in neurosurgery: a systematic review. Neurosurg Rev. 2017;40(4):537–48.
24. Philips and Microsoft. Hololens navigation. https://www.philips.com/aw/about/news/archive/standard/news/press/2019/20190224-philipsshowcases-unique-augmented-reality-concept-for-image-guided-minimallyinvasive-therapies-developed-with-microsoft.html, 2019. Online; accessed 19 Feb 2020.
25. Hesamian MH, Jia W, He X, Kennedy P. Deep learning techniques for medical image segmentation: Achievements and challenges. J Digital Imaging. 2019;32(4):582–96.
26. Hughes-Hallett A, Pratt P, Mayer E, Di Marco A, Yang G-Z, Vale J, Darzi A. Intraoperative Ultrasound Overlay in Robot-assisted Partial Nephrectomy: First Clinical Experience. Eur Urol. 2014;65(3):671–2.
27. Bouguet JY. Matlab camera calibration toolbox. Caltech Technical Report. 2000.
28. Zhang Z. A flexible new technique for camera calibration. IEEE Trans Pattern Anal Mach Intell. 2000;22(11):1330–4.
29. Thompson S, Stoyanov D, Schneider C, Gurusamy K, Ourselin S, Davidson B, Hawkes D, Clarkson MJ. Hand–eye calibration for rigid laparoscopes using an invariant point. Int J Comput Assist Radiol Surg. 2016;11(6):1071–80.
30. Pachtrachai K, Vasconcelos F, Dwyer G, Hailes S, Stoyanov D. Hand-eye calibration with a remote centre of motion. IEEE Robot Autom Lett. 2019;4(4):3121–8.
31. Frantz T, Jansen B, Duerinck J, Vandemeulebroucke J. Augmenting microsoft's hololens with vuforia tracking for neuronavigation. Healthcare Technol Lett. 2018;5(5):221–5.
32. Medtronic. Stealthstation™. https://www.medtronic.com/us-en/healthcare-professionals/products/neurological/surgical-navigation-systems/stealthstation.html, 2020. Online; accessed 21 Feb 2020.
33. Haouchine N, Stoyanov D, Roy F, Cotin S. Dejavu: Intra-operative simulation for surgical gesture rehearsal. In international conference on medical image computing and computer-assisted intervention. Springer; 2017. p. 523–531.
34. Ozgur E, Koo B, Le Roy B, Buc E, Bartoli A. Preoperative liver registration for augmented monocular laparoscopy using backward-forward biomechanical simulation. Int J Comput Assist Radiol Surg. 2018;13(10):1629–40.
35. Modrzejewski R, Collins T, Bartoli A, Hostettler A, Marescaux J. Soft-body registration of pre-operative 3D models to intra-operative rgbd partial body scans. In international conference on medical image computing and computer-assisted intervention. Springer; 2018. p. 39–46.
36. Dilley JWR, Hughes-Hallett A, Pratt PJ, Pucher PH, Camara M, Darzi AW, Mayer EK. Perfect registration leads to imperfect performance: A randomized trial of

multimodal intraoperative image guidance. Ann Surg. 2019;269(2):236–42.
37. Chang PL, Handa A, Davison AJ, Stoyanov D. Robust real-time visual odometry for stereo endoscopy using dense quadrifocal tracking. In international conference on information processing in computer-assisted interventions. Springer; 2014. p. 11–20.
38. Allan M, Thompson S, Clarkson MJ, Ourselin S, Hawkes DJ, Kelly J, Stoyanov D. 2D–3D pose tracking of rigid instruments in minimally invasive surgery. In international conference on information processing in computer-assisted interventions. Springer; 2014. p. 1–10.
39. Vasconcelos F, Mazomenos EB, Kelly JD, Stoyanov D. RCM-SLAM: visual localisation and mapping under remote centre of motion constraints. In international conference on robotics and automation, ICRA 2019. Montreal, QC, Canada, May 20–24, 2019. IEEE, 2019. p. 9278–84.
40. Lamarca J, Parashar S, Bartoli A, Montiel JMM. Defslam: Tracking and mapping of deforming scenes from monocular sequences. CoRR, abs/1908.08918. 2019.
41. Mahmoud N, Collins T, Hostettler A, Soler L, Doignon C, Montiel JMM. Live tracking and dense reconstruction for handheld monocular endoscopy. IEEE Trans Med Imaging. 2019;38(1):79–89.
42. Stoyanov D, Mylonas GP, Lerotic M, Chung AJ, Yang G. Intra-operative visualizations: perceptual fidelity and human factors. J Disp Technol. 2008;4(4):491–501.
43. Stoyanov D, ElHelw M, Lo BP, Chung A, Bello F, Yang GZ. Current issues of photorealistic rendering for virtual and augmented reality in minimally invasive surgery. In proceedings on seventh international conference on information visualization, 2003. IV 2003. IEEE; 2003 p. 350–8.
44. Cutolo F, Fida B, Cattari N, Ferrari V. Software framework for customized augmented reality headsets in medicine. IEEE Access. 2020;8:706–20.
45. Kruijff E, Swan JE, Feiner S. Perceptual issues in augmented reality revisited. In 2010 IEEE international symposium on mixed and augmented reality. IEEE; 2010. p. 3–12.
46. Sielhorst T, Bichlmeier C, Heining SM, Navab N. Depth perception–a major issue in medical ar: evaluation study by twenty surgeons. In international conference on medical image computing and computer-assisted intervention. Springer; 2006. p. 364–372.
47. Edwards PJ, Johnson LG, Hawkes DJ, Fenlon MR, Strong AJ, Gleeson MJ. Clinical experience and perception in stereo augmented reality surgical navigation. In international workshop on medical imaging and virtual reality. Springer; 2004. p. 369–376.
48. Bichlmeier C, Wimmer F, Heining SM, Navab N. Contextual anatomic mimesis hybrid in-situ visualization method for improving multi-sensory depth perception in medical augmented reality. In 2007 6th IEEE and ACM international symposium on mixed and augmented reality. IEEE; 2007. p. 129–138.
49. Lerotic M, Chung AJ, Mylonas G, Yang GZ. Pq-space based non-photorealistic rendering for augmented reality. In international conference on medical image computing and computer-assisted intervention. Springer; 2007. p. 102–9.
50. Hettinger LJ, Riccio GE. Visually induced motion sickness in virtual environments. Presence Teleop Virtual Environ. 1992;1(3):306–10.
51. Lambooij MTM, IJsselsteijn WA, Heynderickx I.Visual discomfort in stereoscopic displays: a review. In stereoscopic displays and virtual reality systems XIV, vol. 6490. International Society for Optics and Photonics. 2007. p. 64900I.
52. Hoffman DM, Girshick AR, Akeley K, Banks MS. Vergence–accommodation conflicts hinder visual performance and cause visual fatigue. J Vis. 2008;8(3):33.
53. McIntire JP, Havig PR, Geiselman EE. Stereoscopic 3D displays and human performance: a comprehensive review. Displays. 2014;35(1):18–26.
54. Carnegie K, Rhee T. Reducing visual discomfort with hmds using dynamic depth of field. IEEE Comput Graph Appl. 2015;35(5):34–41.
55. Matsuda N, Fix A, Lanman D. Focal surface displays. ACM Transactions on Graphics (TOG). 2017;36(4):1–14.
56. Dixon BJ, Daly MJ, Chan H, Vescan AD, Witterick IJ, Irish JC. Surgeons blinded by enhanced navigation: the effect of augmented reality on attention. Surg Endosc. 2013;27(2):454–61.
57. Hughes-Hallett A, Mayer EK, Marcus HJ, Pratt P, Mason S, Darzi AW, Vale JA. Inattention blindness in surgery. Surg Endosc. 2015;29(11):3184–9.
58. Fraunhofer MEVIS. Liver operation app. http://www.fraunhofer.jp/content/dam/japan/en/documents/News/ News/Liveroperationapp.pdf, 2020. Online; accessed 19 Feb 2020.
59. Medical Futurist. Vein scanners. https://medicalfuturist.com/vein-scanners-examples-for-disruption/. 2016. Online; accessed 19 Feb 2020.
60. Vahrmeijer AL, Hutteman M, Van Der Vorst JR, Van De Velde CJH, Frangioni JV. Image-guided cancer surgery using near-infrared fluorescence. Nat Rev Clin Oncol. 2013;10(9):507.
61. Keller DS, Ishizawa T, Cohen R, Chand M. Indocyanine green fluorescence imaging in colorectal surgery: overview, applications, and future directions. Lancet Gastroenterol Hepatol. 2017;2(10):757–66.
62. Janatka M, Sridhar A, Kelly J, Stoyanov D. Higher order of motion magnification for vessel localisation in surgical video. In international conference on medical image computing and computer-assisted intervention. Springer; 2018. p. 307–14.
63. Ghazi A, Campbell T, Melnyk R, Feng C, Andrusco A, Stone J, Erturk E. Validation of a full-immersion simulation platform for percutaneous nephrolithotomy using three-dimensional printing technology. J Endourol. 2017;31(12):1314–20.

11 Navigation and Image-Guided Surgery

Arthur Randolph Wijsmuller,
Luis Gustavo Capochin Romagnolo,
Esther Consten,
Armando Errando Franchini Melani,
and Jacques Marescaux

Introduction

At the present time, computer-assisted navigated surgery is defined as a surgical procedure with real-time continuous tracking of the patient and displaying of the tip of a surgical device in relation to the patient on radiographic images that were made pre- or intraoperatively. Stereotactic navigation was developed by neurosurgeons who integrated medical imaging and stereotaxy to minimize invasiveness and radiation exposure for the surgeon and ancillary personnel while optimizing the accuracy and safety of the procedure [1]. After the advent of computed tomography (CT) in the late 1970s, the stereotactic biopsy was developed by the joining of CT to a stereotactic frame [2, 3]. Stereotactic surgery without the application of a frame (frameless stereotaxy) became possible with the development of new techniques for neuronavigation [4, 5].

Stereotactic navigation functions quite similarly to a navigation system in a car. Both systems determine and track the position of an instrument or a car in relation to a patient or the earth, respectively. However, the type of localization technology differs. A stereotactic navigation system does not localize via triangulation similarly to a global positioning system with the help of several satellites. It has different systems to track the position of the patient and the tip of an instrument or device. The most widely used tracking system works optically and uses a stereoscopic infrared camera that localizes and tracks reflective marker spheres that are fixed to the patient and to the operating instrument (which is free to move). Navigation is performed on the basis of pre- or intraoperative radiographic images that are uploaded to and processed by a computer-based image processing module. In this way, the operator can verify the position of the tip of an instrument or device on imaging in a transverse, coronal, and sagittal direction – or in a 3D model based on a reconstruction of these images. Stereotactic navigation is reported to increase safety and to minimize the invasiveness of surgical procedures by acting as a real-time guidance tool during the operation using tracked

A. R. Wijsmuller (✉)
Department of Surgery, University Medical Center Groningen, Groningen, The Netherlands
e-mail: a.r.wijsmuller@umcg.nl

L. G. C. Romagnolo
Surgical Oncologic of Colon and Rectal, Barretos Cancer Hospital/IRCAD Latin America, Barretos, Sao Paulo, Brazil

E. Consten
Department of Surgery, University Medical Center Groningen, Meander Medical Centre, Groningen, The Netherlands

A. E. F. Melani
Department of Surgery, IRCAD Latin America/ Americas Medical Service, Rio de Janeiro, Brazil

J. Marescaux
Research Institute Against Digestive Cancers (IRCAD), Institute of Image-Guided Surgery (IHU Strasbourg), Strasbourg, France

S. Atallah (ed.), *Digital Surgery*, https://doi.org/10.1007/978-3-030-49100-0_11

surgical instruments in conjunction with preoperative images. It helps the surgeon to identify critical anatomical structures, which should be either targeted or avoided. These systems are currently mainly used in cranial surgery, skull base surgery, and vertebral surgery, and they have proven to be an essential adjunct to surgical procedures where anatomical landmarks are obscured and cannot be used for topographic orientation [6].

Advancements in the field of stereotactic navigation have facilitated its application into a wider range of indications including minimally invasive pelvic visceral surgery. The first reports of the performance of optical-based stereotactic navigation for minimally invasive visceral surgery were published by Atallah et al. in 2015 [7, 8]. Navigated-surgery was performed by the calibration of the tip of an endoscopic instrument. The pelvis was chosen for pioneering in the field of minimally invasive visceral surgery since anatomical structures at risk during, for example, rectal surgery are largely fixed retroperitoneally. Therefore, they seem to be less affected by pneumoperitoneum and respiratory movements as compared to upper abdominal organs. Nijkamp et al. performed electromagnetic-based stereotactic navigation during open pelvic surgery during 33 cancer resections and reported a radical resection in all but one patient concluding that the system was safe and technique feasible [9]. The challenges associated with stereotactic visceral pelvic navigation were recently assessed by a study investigating the potential differences in patient anatomy between intraoperative lithotomy and preoperative supine position for imaging [10]. It seems that, when several aspects related to patient setup are taken into account, minimally invasive pelvic stereotactic navigation can be performed with accuracy.

Types of Frameless Navigation Systems

The navigations systems which are currently used for frameless stereotactic navigation use different techniques to track the position of the patient and the tip of a surgical instrument: they are optical-, electromagnetic-, and ultrasonic-based. The most widely used system is based on passive optical tracking. It uses a stereoscopic infrared-emitting source connected to a stereoscopic camera that detects infrared light which is reflected by marker spheres affixed to a patient tracker and an instrument tracker. An active optical tracking system uses active infrared light-emitting diodes on the patient and instrument. An electromagnetic-based navigation system uses a low-frequency magnetic field induced by a magnetic source fixed to or near the patient to detect the spatial position of a small magnetic field sensor (fixed to an instrument). An ultrasonic-based navigation system works in the same way but with ultrasound transmission instead of an electromagnetic field. However, these latter two systems have been used to a lesser extent because reported accuracy seems inconsistent; however, some investigators have reported acceptable accuracy [9, 11].

Equipment and Operative Setup Optical Navigation

Given the widespread use of the optical navigation system and the experience of some of the authors of this chapter in this area, optical navigation is addressed in detail. The rationale for the application of stereotactic navigation to rectal surgery lies in the poor oncological outcome after surgery for locally advanced and recurrent rectal cancer. The current rate of irradical resections is unacceptably high with around up to a quarter of resections in locally advanced and more than half of the resections in recurrent rectal cancer patients being irradical [12, 13]. Additionally, long-term morbidity associated with the surgical procedure is high and is suggested to mainly originate from nerve injury-related disorders such as urogenital and bowel dysfunctions [14–16]. Outcomes can be improved by a better recognition of anatomical dissection planes, anatomical landmarks, and the dissection margin to the tumor to optimize resection margins and to minimize iatrogenic nerve damage. Recently, the performance of stereotactic navigation for minimally invasive transanal and abdominal rectal surgery has been reported [7, 8, 17]. Additionally, critical challenges related to soft-tissue stereotactic pelvic navigation were assessed [10]. In this section, the required equipment and several aspects of the setup of minimally invasive stereotactic pelvic navigation are described.

The navigation systems rely on several major components:

- *A stereoscopic infrared-emitting optical system* – emits infrared light and determines the position of an instrument and the pelvis of the patient in the operation room (OR) by detecting infrared light which is reflected by marker spheres affixed to a patient tracker and an instrument tracker (Fig. 11.1).
- *A patient tracker* – is fixed to the patient or operating table and has marker spheres fixed to it for the continuous tracing of the patient by means of the optical system (Figs. 11.1 and 11.2).
- *An instrument tracker* – is fixed to an instrument and has marker spheres fixed to it for continuous tracing by means of the optical system (Fig. 11.3).
- *Skin fiducials* – at least six fiducials are fixed to the skin of the patient during CT scan just before the operation if registration is to be performed by paired-point matching. Initially in the OR, the position of the pelvis is determined by touching the center of these fiducials via a calibrated instrument with marker spheres attached to it (Fig. 11.2).
- *A computer platform* – matches the three-dimensional position of the patient to the CT scan by registration. The position of the tip of the instrument in the 3D image data set is depicted on a separate screen.
- *Merging software* – merges an MRI or CT scan which was performed well in advance and in which relevant anatomical structures and tumor were segmented, to the most recent CT scan with fiducials which was used to determine the position of the patient.

In optical-based stereotactic navigation, it is essential to obtain a perfect patient position registration in the operation room (OR) and image-to-patient registration by means of the infrared optical system. A computerized process is used to match the three-dimensional position of the patient in the OR to the preoperative images which will be used for navigation. There are several registrations methods to determine the exact position and orientation of the patient in the OR and to reference this position with the patient's radiographic images in the coronal, transverse, and sagittal plane:

- Paired-point matching
- New intraoperative 2D or 3D imaging
- Region contour matching

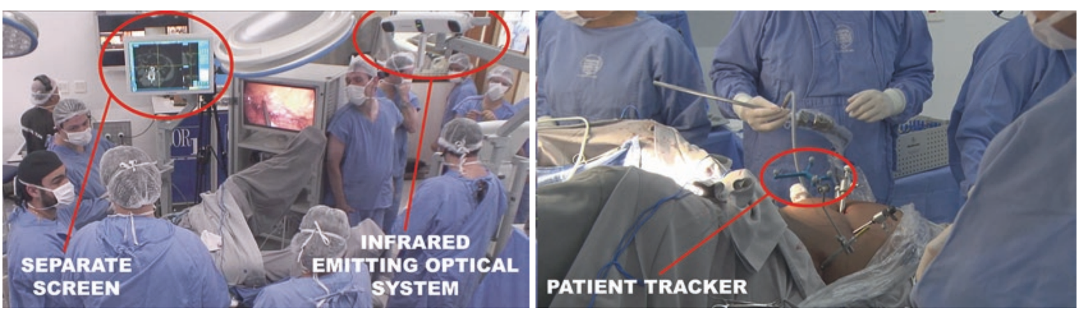

Fig. 11.1 A stereoscopic infrared-emitting optical system continuously tracks the patient and instrument by detecting infrared light which is reflected by marker spheres affixed to a patient tracker and an instrument tracker. On an additional screen which is connected to the navigation platform, the location of the tip of the instrument is displayed in the image data set. (From Romagnolo et al. [28]. Reprinted with permission from Springer Nature)

Fig. 11.2 Several fiducials are placed on the skin anteriorly to the pelvic area. After a CT scan has been made just preoperatively with these fiducials in situ, this image data set is uploaded to the navigation system. These sterile fiducials can then be changed for sterile skin markers after marking. Subsequently, the position of the patient in the OR can be determined via recognition and registration of the position of the fiducials/markers by using a calibrated instrument (with marker spheres fixed to it) of which the position of the tip is recognized by the infrared optical system. Additionally, the patient tracker (with marker spheres fixed to it) can be recognized which is fixed to the patient or OR table. (From Romagnolo et al. [28]. Reprinted with permission from Springer Nature)

Fig. 11.3 The tip of a surgical instrument can be tracked by means of an instrument tracker which is fixed to the instrument. It can be attached to an energy device or a regular surgical instrument. (From Romagnolo et al. [28]. Reprinted with permission from Springer Nature)

To perform paired-point registration, several skin reference points overlying the area of anatomical interest are marked by means of at least six to ten radiopaque fiducials in a nonlinear distribution during preoperative CT scanning, and these fiducials are left in place or changed for sterile fiducials intraoperatively [18]. In the studies published, 12–18 fiducials were placed on the skin anteriorly to the pelvic area to optimize the registration process [7, 8, 10, 17]. The more paired points registered over the area to be navigated, the more accurate the navigation will become. Subsequently, after uploading these preoperative CT scan images to the navigation system, the position of the patient in the operation room (OR) can be determined via recognition and registration of the position of the fiducials by using a calibrated instrument of which the position of the tip is recognized by the infrared optical system (Figs. 11.2 and 11.3). This is the only registration option, which has been described in the literature for stereotactic soft-tissue pelvic navigation [7, 8, 10].

Another method to register the position of the patient is by new, intraoperative 2D or 3D imaging by a compatible C-arm after fixing the patient reference to the patient. Two fluoroscopic shots with a compatible 2D C-arm and a separate registration device enable the surgeon to register and track the position of the patient. An intraoperative scan with a 3D C-arm that is calibrated to the navigation system enables the surgeon to register the position of the patient without the need for a separate registration device.

Finally, registration can be performed manually by a registration of the surface of the patient, usually a bone surface, with a calibrated instrument. By means of an autocorrecting algorithm, the navigation system matches the acquired points on the patient with the same points on the preoperative CT scan.

After this registration, the patient is tracked by means of optical markers on a patient tracker, which is fixed to the patient, for example, the patient's anterior superior iliac spine by Kirschner wires or a screw (Figs. 11.1 and 11.2). Surgical instruments are tracked by means of an instru-

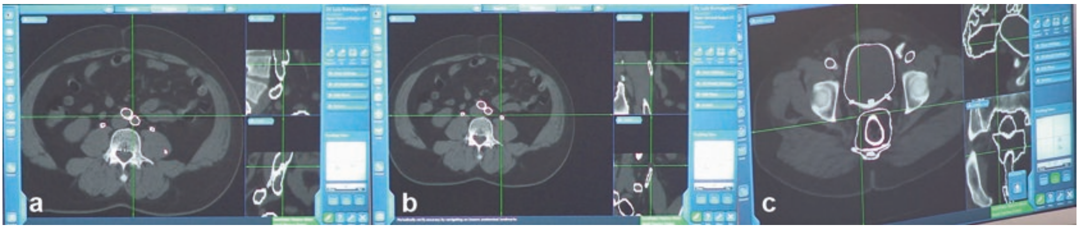

Fig. 11.4 The position of the tip of the surgical instrument is displayed in the image data set. Using an abdominal approach, the aortic bifurcation (**a**) and the left ureter are located (**b**). During a transanal endoscopic approach, the border of the mesorectum is located (**c**). (From Romagnolo et al. [28]. Reprinted with permission from Springer Nature)

ment tracker, which is fixed to the instrument allowing the position of the tip of the instrument to be determined, calibrated, and visualized in the navigation scans (Figs. 11.3 and 11.4).

Three surgical infrared optical navigation platforms were reported to have been used for stereotactic soft-tissue pelvic navigation (CURVE Navigation System, Brainlab, Feldkirchen, Germany; StealthStation ®S7 Surgical Navigation System, Medtronic Inc., Louisville, USA; Stryker Navigation, Kalamazoo, MI, USA;) [7, 10, 19]. All systems rely on a stereoscopic camera emitting infrared light, a computer platform, a patient tracker, and an instrument tracker.

Image Analysis

High-resolution CT and MRI data sets that are acquired preoperatively are uploaded to the navigation system. Most navigation systems are also equipped with software which facilitates the merging of different imaging modalities, for example, MRI with CT. By fusing soft-tissue MRI information with a registered CT scan, navigation can be performed on the basis of MRI imaging, and information of both imaging modalities can be used. Most modern navigation systems have a planning application through which relevant anatomy and target lesions can be delineated after which a 3D reconstruction can be made. On the basis of these delineations and 3D reconstruction, an operative plan, including surgical trajectory for resection, can be established, optimizing oncologic margins and minimizing surgical morbidity. This preoperative planning has a central role in the functioning of stereotactic navigation. Yet, preoperative planning on the basis of imaging acquired prior to surgery has its limitations, for example, in case of real-time geometric changes in anatomy and the target lesion itself during the course of surgery affecting the accuracy [20]. Advancements of imaging technology include the possibility of intraoperative MRI and CT scanning which visualizes changing geometry during the operation [20]. A randomized clinical trial investigating its use in the removal of gliomas compared to conventional microsurgery reported promising results with significantly more radical resection [20].

Limitations

Optical tracking is associated with high accuracy with an ability to track large volumes. However, compared to the other stereotactic navigation systems, limitations related to optical navigation include the need for maintaining a direct line of sight between the infrared camera of the navigation system and the patient and instrument tracker. This line of sight can be hampered (as is the case for navigated rectal cancer surgery through a transanal approach) by the patient's legs, morbid obesity, or the surgeon who is positioned between the patient's legs.

For electromagnetic-based navigation systems, a direct line of sight is not required. However, a variable stability for these electromagnetic fields has been reported that can be distorted through metallic objects [21]. Ultrasonic-based navigation systems have been used to a lesser extent because reported accuracy seems moderate [11].

Another limitation for stereotactic navigation in general is its reliance on preoperative images for accurate navigation. Real-time geometric changes in pelvic anatomy caused by tissue dissection and traction are known to affect the accuracy of stereotactic navigation. Additionally, imaging can be acquired days or weeks prior to an intervention during which neoplasms can progress and errors are introduced. Other factors which should be considered based on earlier studies on pelvic organ motion are the following: rectal and bladder volume should be equal during the scans which are used for registration/navigation, as well as intraoperatively. Consequently, the bladder should be emptied before scanning as well as intraoperatively via the placement of a catheter. The rectum should be emptied by means of an enema. The pelvic diaphragmatic muscle tension should be equal during the scans, as well as intraoperatively.

An analysis by the FDA into the accuracy of stereotactic navigation in 2017 revealed that some healthcare providers using stereotactic navigation systems experienced navigational errors leading to patient death, serious or life-threatening injuries, and inaccurate, aborted, or prolonged medical procedures [22]. In these cases, navigational accuracy errors were reported due to problems associated with navigation software/hardware, system complexity (including human factors), compatibility, anatomical complexity, registration and tracking, and medical image quality. However, despite these navigational accuracy errors, the FDA issued a communication to merely make healthcare providers aware of possible navigational accuracy errors while believing the overall benefits of using frameless stereotactic navigation systems continue to outweigh the risks.

Specific Pelvic Surgery-Related Navigation Challenges

Since anatomical structures at risk during rectal surgery are fixed retroperitoneally, they seem to be less affected by pneumoperitoneum and respiratory movements as compared to upper abdominal organs. However, pelvic surgery is associated with additional challenges as compared to surgical navigation in other fields, such as neurological and orthopedic surgery. Rectal surgery is performed in patients with variable degrees of lithotomy, a position which is different from the supine position used for the acquisition of preoperative imaging. This positional change could alter the patient anatomy and subsequently render stereotactic pelvic navigation using preoperative imaging inaccurate. Additionally, the motion of the skin reference points with their fiducial markers by means of positional change may hamper patient position registration in the operating room (OR) to begin with. To assess these challenges, a study was undertaken to determine the difference in patient anatomy, sacral tilt, and fiducial marker position between these different patient positions and to investigate the feasibility and optimal setup for stereotactic pelvic navigation [10]. Four consecutive human anatomical specimens were submitted to repeated CT scans in a supine and several degrees of lithotomy position. Patient anatomy, sacral tilt, and skin fiducial position were compared by means of an image computing platform. In two specimens, a 10° wedge was introduced to reduce the natural tilt of the sacrum during the shift from a supine to a lithotomy position. A simulation of laparoscopic and endoscopic transanal surgical procedures was performed to assess the accuracy of stereotactic navigation. A significant, supra-centimetric change in patient anatomy was noted between different patient positions. However, this observation was minimized through the application of a wedge. When switching from the supine to another position, sacral retroversion occurred irrespective of the use of a wedge. There was considerable skin fiducial motion between different positions. Accurate stereotactic navigation was obtained with the least registration error (1.9 mm) when the position of the anatomical specimen was registered in a supine position with straight legs, without a pneumoperitoneum, using a conventional CT scan with an identical specimen positioning.

The authors concluded that the change in patient anatomy is small during the sacral tilt induced by positional changes when using a 10° wedge, allowing for an accurate stereotactic surgical navigation when certain prerequisites are taken into account. The following aspects should be considered and included in the protocol for an optimal setup of point-merge stereotactic navigation in pelvic surgery. Patient position registration should be performed without a pneumoperitoneum in a patient position which is similar to the position during preoperative CT scanning with fiducials. This is because a changing patient position results in skin fiducial motion, hampering accurate patient position registration. A supine position with straight legs is the preferred position. The patient tracker should be fixed into the anterior superior iliac spine to integrate the change in the sacral tilt angle into the surgical navigation system since a change is expected to occur when switching positions. Finally, a forced sacral tilt seems to minimize the change in patient anatomy.

Additionally, it is expected that the combination of surgical navigation systems with platforms that facilitate robotic-assisted surgery might further improve the precision and accuracy of the navigation system. For that reason, the Monarch™ platform (Auris Health, Inc., Redwood City, CA, USA) was established developing a flexible robotic endoscope and combining this with electromagnetic stereotactic navigation to allow physicians to accurately access small and hard-to-reach lung nodules early for diagnosis and targeting treatment [25]. Preliminary data suggest this might be beneficial [26]. Another robotic platform guided by stereotactic navigation, Mazor X Stealth™ Edition system, was recently acquired by Medtronic [27]. These platforms are suggested to increase the accuracy of screw placement while minimizing radiation exposure during orthopedic spine operations [27]. Additionally, such a platform facilitates tool exchange while maintaining access to the planned surgical trajectory.

Future Directions in Stereotactic Navigation

Stereotactic navigation would be more effective when the tumor, relevant anatomical structures, and resection margins are highlighted. MRI is currently the most accurate tool for the depiction of a tumor, mesorectum, and the relationship of the tumor to the surrounding structures. A recent study in which pelvic nerves were manually delineated in 20 volunteers who were scanned with a 3-Tesla MRI reported that even pelvic nerves are usually visible on high-resolution MRI with dedicated scanning protocols [23]. The advances in medical software facilitating automatic three-dimensional reconstruction from CT scans when used by a radiological technician provide quite promising opportunities [24]. And all the more so because the merging software allows the surgeon to auto-merge the three-dimensional reconstructions with intraoperative 2D or 3D C-arm imaging which is used for the registration of the position of the patient.

Conclusions

The application of stereotactic navigation to several orthopedic and neurosurgical procedures has been reported to improve surgical accuracy. Studies also suggest an added value of its application to visceral pelvic procedures. With improved recognition of anatomical dissection planes, anatomical landmarks, and the dissection margins to the tumor, oncologic resection margins can be optimized, and iatrogenic injuries can be minimized. This is expected to improve functional and oncological outcomes. Additionally, the associated preoperative planning and determination of surgical trajectory is expected to play a major role in the improvements in the quality of surgery. The challenges related to optimal patient setup for minimally invasive stereotactic pelvic visceral navigation are currently being assessed in a prospective study. Surgical navigation systems are expected to improve the quality of surgery for locally advanced and recurrent rectal cancer as shown when used in other contexts.

References

1. Mezger U, Jendrewski C, Bartels M. Navigation in surgery. Langenbeck's Arch Surg. 2013;398(4):501–14.
2. Gildenberg PL. Stereotactic neurosurgery and computerized tomographic scanning. Appl Neurophysiol. 1983;46(1–4):170–9.
3. Heilbrun MP. Computed tomography-guided stereotactic systems. Clin Neurosurg. 1983;31:564–81.
4. Kitchen ND, Lemieux L, Thomas DG. Accuracy in frame-based and frameless stereotaxy. Stereotact Funct Neurosurg. 1993;61(4):195–206.
5. Benardete EA, Leonard MA, Weiner HL. Comparison of frameless stereotactic systems: accuracy, precision, and applications. Neurosurgery. 2001;49(6):1409–15; discussion 1415–6.
6. Wadley J, et al. Pre-operative planning and intra-operative guidance in modern neurosurgery: a review of 300 cases. Ann R Coll Surg Engl. 1999;81(4):217–25.
7. Atallah S, Martin-Perez B, Larach S. Image-guided real-time navigation for transanal total mesorectal excision: a pilot study. Tech Coloproctol. 2015;19(11):679–84.
8. Atallah S, Nassif G, Larach S. Stereotactic navigation for TAMIS-TME: opening the gateway to frameless, image-guided abdominal and pelvic surgery. Surg Endosc. 2015;29(1):207–11.
9. Nijkamp J, et al. Prospective study on image-guided navigation surgery for pelvic malignancies. J Surg Oncol. 2019;119(4):510–7.
10. Wijsmuller AR, et al. Advances in stereotactic navigation for pelvic surgery. Surg Endosc. 2018;32(6):2713–20.
11. Rana M, Eckardt AM. Chapter: Computer-Assisted Head and Neck Oncologic Surgery. In book: Contemporary Oral Oncology. 2017;279–96.
12. van Zoggel D, et al. Preliminary results of a cohort study of induction chemotherapy-based treatment for locally recurrent rectal cancer. Br J Surg. 2018;105(4):447–52.
13. Mariathasan AB, et al. Beyond total mesorectal excision in locally advanced rectal cancer with organ or pelvic side-wall involvement. Eur J Surg Oncol. 2018;44(8):1226–32.
14. Lange MM, et al. Urinary dysfunction after rectal cancer treatment is mainly caused by surgery. Br J Surg. 2008;95(8):1020–8.
15. Lange MM, et al. Risk factors for sexual dysfunction after rectal cancer treatment. Eur J Cancer. 2009;45(9):1578–88.
16. Wallner C, et al. Causes of fecal and urinary incontinence after total mesorectal excision for rectal cancer based on cadaveric surgery: a study from the Cooperative Clinical Investigators of the Dutch total mesorectal excision trial. J Clin Oncol. 2008;26(27):4466–72.
17. Kwak JM, et al. Stereotactic pelvic navigation with augmented reality for transanal total mesorectal excision. Dis Colon Rectum. 2019;62(1):123–9.
18. Citardi MJ, Batra PS. Image-guided sinus surgery: current concepts and technology. Otolaryngol Clin N Am. 2005;38(3):439–52.. vi
19. Kawada K, et al. Stereotactic navigation during laparoscopic surgery for locally recurrent rectal cancer. Tech Coloproctol. 2017;21(12):977–8.
20. Gasser T, et al. Intraoperative MRI and functional mapping. Acta Neurochir Suppl. 2011;109:61–5.
21. Metson R, Gliklich RE, Cosenza M. A comparison of image guidance systems for sinus surgery. Laryngoscope. 1998;108(8 Pt 1):1164–70.
22. FDA Safety Communication: Navigational Accuracy Errors Associated with Frameless Stereotaxic (Stereotactic) Navigation Systems. 2017. https://www.fda.gov/medicaldevices/safety/alertsandnotices/ucm563249.htm.
23. Wijsmuller AR, et al. A step towards stereotactic navigation during pelvic surgery: 3D nerve topography. Surg Endosc. 2018;32(8):3582–91.
24. Guerriero L, et al. Virtual reality exploration and planning for precision colorectal surgery. Dis Colon Rectum. 2018;61(6):719–23.
25. https://www.aurishealth.com/about, 2019.
26. Murgu SD. Robotic assisted-bronchoscopy: technical tips and lessons learned from the initial experience with sampling peripheral lung lesions. BMC Pulm Med. 2019;19(1):89.
27. Staub BN, Sadrameli SS. The use of robotics in minimally invasive spine surgery. J Spine Surg. 2019;5(Suppl 1):S31–40.
28. Romagnolo LGC, Wijsmuller AR, Melani AGF. Navigation for transanal total mesorectal excision. In: Atallah S, editor. Transanal minimally invasive surgery (TAMIS) and transanal total mesorectal excision (taTME). Cham.: Springer; 2019. p. 485–91.

12 Operating in the Near-Infrared Spectrum

Thomas George Barnes

Abbreviations

APER	Abdominoperineal excision of the rectum
CBD	Common bile duct
CHD	Common hepatic duct
CI	Confidence interval
CT	Computerised tomography
DSB	Distyrylbenzene
EMA	European Medicines Agency
EMG	Electromyography
FDA	Food and Drug Administration
GE	General Electric
HCC	Hepatocellular carcinoma
ICG	Indocyanine green
IMV	Inferior mesenteric vein
IOC	Intraoperative cholangiogram
IV	Intravenous
LAACA	Left accessory aberrant colic artery
MRI	Magnetic resonance imaging
NHS	National Health Service
NIR	Near infrared
OR	Odds ratio
PET	Positron emission tomography
RR	Relative risk
SD	Standard deviation
SLN	Sentinel lymph node
UTI	Urinary tract infection
VUJ	Vesicoureteric junction

T. G. Barnes (✉)
Department of Colorectal Surgery, Oxford University Hospitals NHS Foundation Trust, Nuffield Department of Surgery, University of Oxford, Oxford, UK
e-mail: tom.barnes@doctors.org.uk

Introduction

Near-infrared imaging is an evolving technology that is increasingly being used in operating theatres. NIR technology includes fluorescent dyes and NIR-emitting lighted stents. There are a number of applications that utilise NIR light and include critical anatomy delineation of the biliary tree, urological tract (namely, the ureter and urethra) and critical vessel and nerve identification. The most common use of NIR light is to assess perfusion of gastrointestinal anastomoses, with the most widely reported outcomes relating to colorectal surgery. In oncological surgery, lymphatic mapping, primary tumour and metastatic deposit identification have all shown promising potential using non-specific fluorescent dyes.

Ureteric Imaging

Damage to the ureters during surgery is a feared but uncommon complication amongst surgeons. The nature of injury includes laceration, crush injury, ligation and devascularisation resulting in either ischaemic necrosis or ischaemic strictures [1]. Less than 30% of ureteric injuries are identified intraoperatively [2, 3], and the clinical

S. Atallah (ed.), *Digital Surgery*, https://doi.org/10.1007/978-3-030-49100-0_12

sequelae of late identification include sepsis, renal failure, ureteral fistulas, urinoma and death [4]. Most ureteric injuries occur in patients without significant risk factors, but the incidence increases in patients with prior pelvic surgery, inflammatory processes including diverticular disease and inflammatory bowel disease, sepsis, large tumours, obesity, pelvic radiation and aberrant ureteric anatomy such as duplication and bifid ureters [5]. Gynaecological procedures account for the majority of ureteric injuries with colorectal surgery being the second most common cause. In colorectal surgery, the rate of injury has remained at ~0.07–1.70% despite the introduction of laparoscopic surgery [5–9]. Injury of the ureter occurs even in experienced hands, and the risk is highest during low anterior resection or abdominoperineal excision of the rectum (APER) [1]. Injury most commonly occurs during ligation of mesenteric vessels and dissection at the sacral promontory [1]. In addition to the devastating effects to the patient, ureteric injury contributes a substantial burden from additional treatment, increased length of stay and medicolegal costs.

Early identification of the ureter, maintaining the correct surgical plane and visualising the hallmark 'vermiculation' of the ureter to confirm its location are essential in reducing risk of ureteric injury [1]. During colorectal surgery, it is not always possible to clearly see the ureter, and it may take significant time to identify this critical structure during a difficult dissection. As well as identifying the ureter to protect it, it is a key landmark of left-sided resections indicating to the surgeon the correct dissection plane between Gerota's and Toldt's fascia [10]. Therefore, early identification may help the surgeon maintain the correct plane of dissection.

Ureteric Stents

Prophylactic ureteral stents are occasionally employed in cases to assist the surgeon in identifying the ureter. In addition to identification of ureteric location, stents potentially allow intraoperative identification of iatrogenic injury [2] – although there is a paucity of evidence surrounding ureteric stents for these purposes [11]. Ureteric stents proved a benefit in open surgery where they can be easily palpated, and the rigid plastic is distinguishable from any other structure in the anatomic environment. Despite this, ureteric injury is not completely mitigated with the use of a stent; numerous retrospective studies reporting on their use compared with unstented patients reveal unrecognised ureteric injuries [1, 2, 12, 13]. From the limited evidence available, one can conclude that stents are placed entirely under surgeon choice and only for cases where difficulty in identifying the ureter in complex cases, particularly diverticular disease, is predicted [1, 12]. Stent placement itself is not without morbidity and cost. There is an increased operating time and cost associated with placement. Extra staff are required including, in many cases, a urologist, radiographer and additional equipment for cystoscopy. Additional time for stent insertion reported in the literature varies from 5 to 55 minutes [2, 14, 15]. Cost of prophylactic stent placement is estimated by Bothwell et al. to exceed $2000 [16].

In addition to costs and time, ureteral stents can result in specific morbidity. Complications from stent insertion range from pain, urinary tract infection, urinary retention, haematuria, anuria/oliguria, which is often secondary to oedema of the vesicoureteric junction and may require stent re-insertion, and even ureteric perforation. Ureteric perforation is a rare complication and often follows a traumatic and failed catheterisation [16].

Over the last 10 years, the number of colorectal resections performed laparoscopically has increased with most patients now undergoing a minimally invasive approach. Standard ureteric stents are less useful in this situation as the ability to rely on tactile feedback is reduced, and the visual appearance of the stented ureter may not be enhanced. As a result, lighted ureteral catheters have been introduced (Fig. 12.1). In 1994, Senagore et al. were the first to report on a case series of 49 patients who had undergone lighted stent placement during laparoscopic colectomy; the authors reported visualisation of the emitted

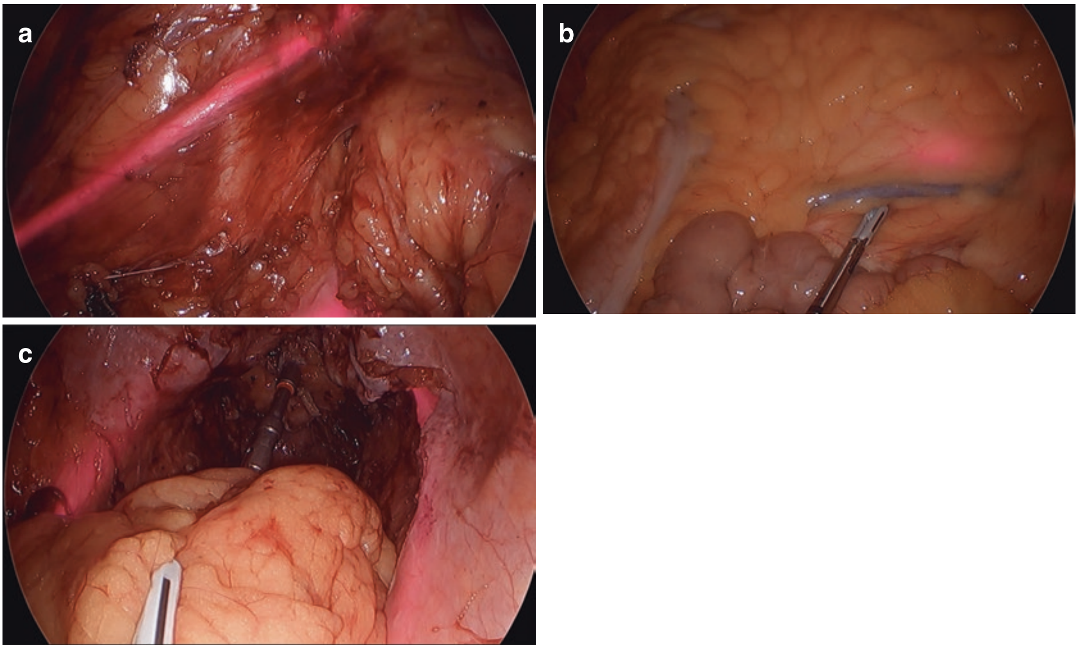

Fig. 12.1 (**a**) A lighted left ureteral stent is clearly visible in the near-infrared spectrum in a patient undergoing laparoscopic low anterior resection for distal rectal cancer. The ability to visualise the left ureter easily is an important aid to surgeons, especially when performing colorectal or gynaecological procedures; (**b**) even before mobilising the left colon, the red light of the NIR stent is visible, underscoring the value of its translucency as the stent can be seen deep to the descending colon mesentery lateral to the inferior mesenteric vein in this example; (**c**) bilateral ureteral stents are well delineated as a stapled anastomosis is being constructed laparoscopically. (Photographs courtesy of Sam Atallah MD, with permission)

light in 83% of cases [14]. The only other series reported in the literature by Boyan et al. describes their 5-year experience of using lighted stents in 402 patients; however, the authors had only reported on the rate of ureteric injuries (none in this series). Whether or not the stents improved ureteric visualisation was not examined [17]. Compared with white light, there is an obvious advantage of NIR lighted stents to allow increased tissue penetration of light and reduced background signal. While NIR lighted stents are most useful for colorectal surgery, they have also been described as an aid for safe retroperitoneal lymph node dissection [18].

Ureteric Fluorescence

The drawbacks outlined above have led to development of a solution providing improved ureteric visualisation that is fast, easy and reliable by using fluorescence. Over the last 10 years, a small number of institutions have investigated ureteric fluorescence with different fluorophores and techniques. Initially, indocyanine green (ICG) was explored as the potential fluorophore for this modality given that it has well-established safety profile and its approval status by the US Food and Drug Administration and the European Medicines Agency. However, as it is hepatically excreted, it has to be administered via retrograde injection. Case series have been reported for both urological [19–21] and gynaecological surgeries [22]. These fluorescent techniques provide good signal-to-background ratios but still require bladder instrumentation. While this is simpler than stent insertion, it would still come with potential risks of urinary tract infection and (rarely) injury. In addition, none of these studies report on the *duration* of ICG fluorescence nor signal-to-background ratios. Although there is a drawback of ureteric instrumentation, the advantage of

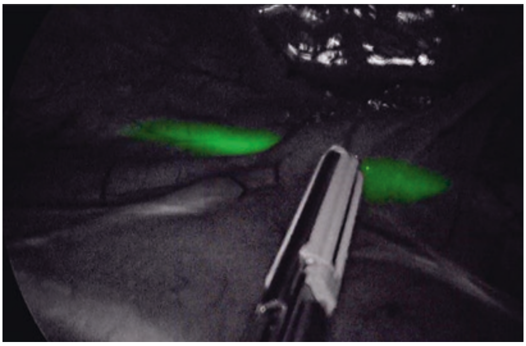

Fig. 12.2 A left ureter has been injected with ICG administered retrograde via cystoscopy, since it is undergoes hepatic clearance. Bio-fluorescence is a complex process which requires ICG to bind to protein. During laparoscopic left colectomy, the left ureter is visible (as in the example of the lighted NIR stent) deep to the mesentery because it, too, is translucent. For complex minimally invasive procedures, this provides an important landmark for the surgeon. (Photograph courtesy of Sam Atallah MD, with permission)

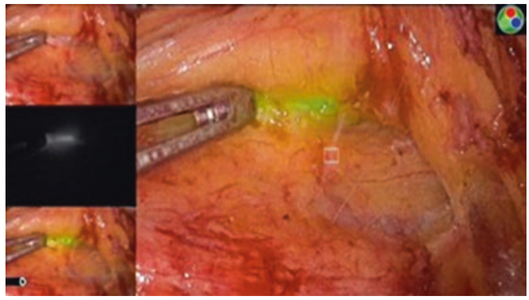

Fig. 12.3 Methylene blue, as an alternative to ICG, has been used to delineate the ureter

limited background signal could allow more precise identification (Fig. 12.2).

A number of alternative fluorophores to ICG have been explored in animals, including IR800CW-CA in rats and pigs [23, 24]. In the latter study by Tanaka et al. [23], it was demonstrated that with intraureteral injection of IR800CW-CA, the intraoperative ureteric injury could be identified by leakage of fluorescent contrast in the NIR visualisation mode. IR800CW-CA is a costly, manufactured carboxylated form of IR800CW and has since been abandoned for further development by its manufacturer LI-COR®. IRDye 800BK has been assessed in a first-in-man study for ureteric fluorescence during colorectal surgery by the author (TGB), and results are due to be published in late 2019.

Mahalingam and colleagues have developed UreterGlow which is a cyanine fluorophore, S0456 (λ_{ex} 800 nm, λ_{em} 830 nm), that has been coupled to glucosamine that cannot be released or metabolised in physiological conditions and is therefore extremely soluble and likely to pass through the kidney into the ureter [25]. Similarly, Cha et al. synthesised UL-766 [26] to be highly water soluble by using triethylene glycol chains. Both studies in mice and pigs seem to demonstrate reduced background signal in other organs while maintaining high signal in the ureter and kidneys.

Methylene blue was first explored for its NIR fluorescent properties and ureteric use by Matsui et al. in 2010 [27] in pigs following intravenous injection. This was subsequently demonstrated to be feasible in humans. The same group of investigators were the first to study low doses of methylene blue in patients undergoing abdominal surgery in which exposing the ureters was a planned step of the procedure [28]. The fluorescence device was an in-house manufactured mini-FLARE™ system that is not commercially in use. A similar study using an in-house device demonstrated that the ureters could fluoresce in patients ($n = 6$) undergoing laparoscopic surgery [29]. The dosing and timing of methylene blue has now been optimised to give signal-to-background ratios of up to 5 at a dose of 0.75 mg/kg given at approximately 10 minutes prior to the time at which ureteral identification is required [30]. An exemplary figure is shown in Fig. 12.3.

Urethral Identification Using NIR Guidance

The close proximity of the distal prostatic and membranous urethra to the anterior rectal wall and the perineal body make the pre-prostatic urethra at risk for injury during low rectal cancer surgery [31]. The incidence of urethral injury during transanal total mesorectal excision (taTME) was reported by Penna et al. to be 0.7%

in the first 720 voluntarily entered cases in the international taTME registry [32]. It is likely, however, that this complication is grossly under-reported with one reported case series of 30 patients having two urethral injuries [33] and, in another case series, one urethral injury in 50 cases [34]. In addition, urethral injury is a gender-specific complication, and thus reported incidence also includes females in the denominator. Incidence of urethral injury is likely to decrease as surgeons progress along the learning curve, and it has been advocated to undergo appropriate cadaver-based training as well as proctorship of the technique [31, 35]. Urethral injury during abdominoperineal resection (APR) is estimated to occur in 1.5–3.125% of cases and historically is not associated with sphincter-preserving surgery [36].

A number of strategies still in their exploratory phase have attempted to highlight the urethra in the NIR spectrum. These have included ICG [37, 38], IRDye 800BK [39] and NIR lighted stents [37, 40] both in cadaveric and in vivo work. Due to the low incidence of urethral injury, it is difficult to power a study that demonstrates a reduced injury rate using this technology.

Identification of the Biliary Tree

Laparoscopic cholecystectomy is one of the most commonly performed surgical procedures internationally. Common bile duct (CBD) injury during this procedure is one of the most serious complications having a devastating impact on the patient's quality of life and survival [41]. The most frequent biliary injury involves complete transection of the CBD when it is mistaken for the cystic duct [42]. During cholecystectomy, it is essential to visualise the critical view of safety where Calot's triangle is clearly delineated. Intraoperative cholangiography (IOC) has been used to assist surgeons in outlining the biliary anatomy, but this requires training and additional equipment, and IOC itself can cause ductal injury [43].

As previously mentioned, ICG binds to plasma proteins and is eventually excreted via the liver. This property has been utilised to visualise the bile ducts using fluorescence even before dissection of Calot's triangle (Fig. 12.4). First reports of fluorescence to identify the bile ducts used rolitetracycline and fluorescein as a proof of principle study, replaced over 10 years later with ICG [44]. Numerous studies have reported on the use of ICG fluorescence during cholecystectomy with a recent meta-analysis identifying 19 studies reporting on visualisation of the CBD and common hepatic duct (CHD) before and after Calot's dissection as well as four studies comparing ICG to IOC [45]. The CBD was visualised under fluorescence prior to Calot's dissection in 78.7% of cases where ICG was given. There was, however, no documented comparison to white light visualisation in these studies. In four studies, ICG was compared with IOC visualisation of ductal structures with moderate quality evidence that visualisation of the cystic duct (RR 1.16; 95% CI 1.00–1.35) and CBD (RR 1.00; 95% CI 0.97–1.03) but not the CHD (RR 0.76; 95% CI 0.58–1.01) is better with ICG compared to white light visualisation. A large proportion of these studies included patients with uncomplicated gallbladder disease, and it is likely that patients who have gallbladder disease complicated by cholecystitis will have a lower fluorescence intensity [46]. A larger multicentre randomised trial comparing ICG cholangiography with white light visualisation has completed and is due to report by 2020 (NCT02702843) [47].

Critical Vessel Identification

In addition to fluorescence of organ perfusion where intravenous ICG eventually reaches the micro-vasculature, this technique can be employed to visualise critical vessels during surgery. This use of fluorescence has only been reported in two studies. Schols et al. [48] first described this technique for using ICG as a repeated injection to identify the biliary vasculature, namely, the cystic artery which was successful in 87% of patients, although it was also seen clearly under white light. Finally, during esophagectomy, a report from Sarkaria and colleagues

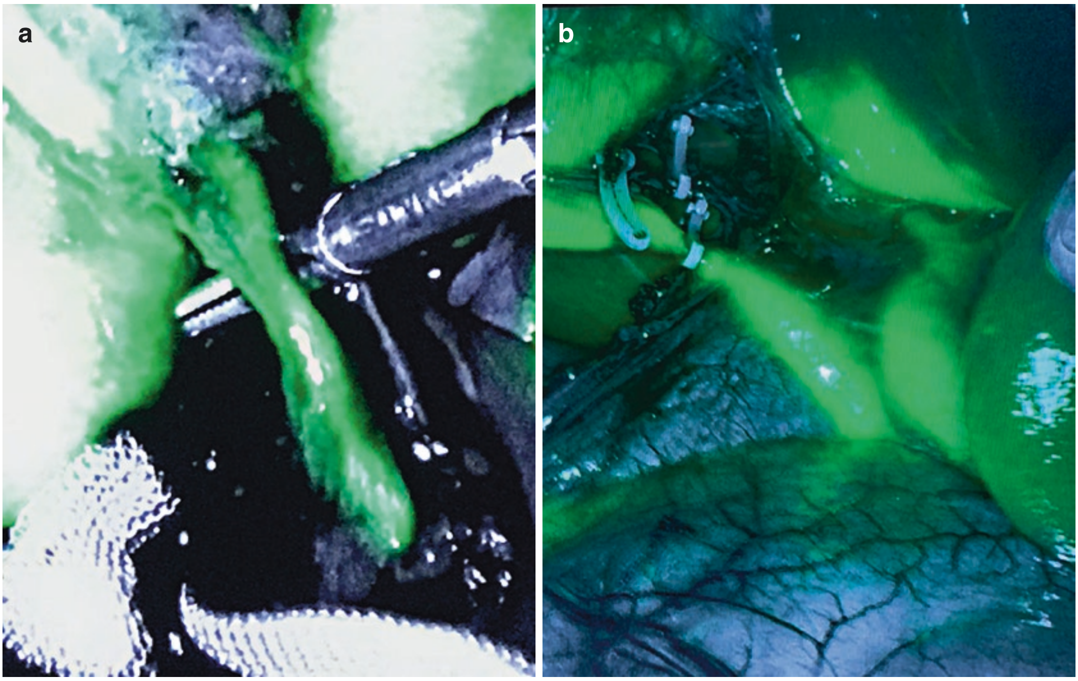

Fig. 12.4 (**a**) Systemic administration of ICG, because it undergoes hepatic excretion, allows for surgeons to visualise critical structures, such as the CBD, during laparoscopic cholecystectomy. Here, a laparoscopic dissector isolates a well-defined cystic duct, while in (**b**) FireFly technology, using the da Vinci Xi platform allows for delineation of the cystic duct and CBD. (Photographs are courtesy of Esteban Varela MD (with permission))

[49] demonstrated visualisation of the short gastric arteries, gastroepiploic arcade and unrecognised small communicating arteries aiding the gastric mobilisation. Although this was an incidental finding in a study primarily assessing conduit perfusion, vessel identification could help in numerous procedures.

Nerve Identification

During most surgical procedures, iatrogenic nerve injury can carry significant morbidity to patients leading to paralysis of muscle, paraesthesia, chronic pain and loss of organ function from autonomic nerve injury. A number of early technologies have been used to try and identify and preserve nerves at risk, including ultrasound, magnetic resonance imaging, computed tomography, positron emission tomography and electromyography – although these are difficult modalities to use in the typical operating room. Fluorescence is an upcoming technology for intraoperative nerve identification with NIR fluorophores being of most interest.

NIR nerve identification is broadly divided into non-specific agents and nerve-specific agents. The earliest of the non-specific agents are axonal transport agents which are traditionally used for histological examination of nerves and naturally made their way into fluorescence nerve identification. These include NeuroTrace, Fast Blue and Dio/Fast Dio [50]. These tracers are still being tested in animals and as yet are not in the NIR spectrum. As they do not cross the blood-brain barrier, they must be applied directly to the nerve. Other non-specific nerve agents are neurovascular dyes which remain in the intravascular space and highlight the vessels in the vasa nervorum, thereby providing proxy visualisation of nerves [50]. ICG has been used as a neurovascular dye in visualising the neurovascular bundles in robotic prostatectomy [51], the phrenic nerve during thymectomy [52] and the facial nerve during mastoid surgery [53]. While promising, the fluorescent signal only lasts a few seconds in these vessels and nerves before being redistributed to the surrounding tissues and would therefore require repeat administration.

Nerve-specific agents have gained much attention from pharmacological industry research and development. The aim is to specifically target nerve fibres and improve the surgeon's ability to detected nerves by minimising the background signal. The two targets of interest are myelin and the epineurium in peripheral nerves. Myelin targeting agents include distyrylbenzene (DSB) derivatives of which the GE Global Research Group has assessed sciatic nerve fluorescence in porcine models [54]. Unfortunately, translation into human is likely to be difficult as the current formulations contain products not suitable for human use [50]. Epineurium targeted compounds use lectins to target the glycan chains which form a major part of the connective tissue in peripheral nerves. This makes them extremely non-specific as these glycans are found in numerous surrounding tissues, namely, in lymphatic channels.

Although there is promise in fluorescent identification in nerves, these compounds are largely targeting peripheral nerves. As yet, autonomic nerves have not been assessed but remain important anatomic targets – particularly for pelvic surgery and esophago-gastric procedures.

Anastomosis Perfusion During Gastrointestinal Resections

For patients who undergo colorectal resection, a feared postoperative complication is anastomotic leak where healing of the anastomosis fails, causing leakage of colonic content, sepsis and potential multi-organ failure. In the literature, the risk of anastomotic leak is reported as being between 2.7% and 13.3% [55] with higher rates in rectal resection. Over the last 20 years, despite improvements in surgical technology, there has been no change in the leak rate [56]. There are numerous risk factors associated with an increased risk of anastomotic leak including age, male gender, malnutrition, smoking, preoperative chemotherapy and radiotherapy, advanced tumour stage, immunosuppression, blood loss and sepsis [57]. Notwithstanding, it is essential to have an adequate blood supply to allow the anastomosis to heal [58]. There has been an increasing use of fluorescence angiography to detect colonic ischemia near the anastomosis intraoperatively by using intravenous ICG. Traditionally, assessment of bowel perfusion during colorectal surgery includes inspection of the serosal colour, palpation of pulsating vessels in the mesentery and pulsatile bleeding at the divided artery [59]. While demonstration of pulsatile arterial bleeding at the cut edge of the bowel would obviate the need for further perfusion assessment, in clinical practice, there is often difficulty in determining this due to vasospasm and other factors, making the surgeon's ability to determine perfusion under white light highly subjective (Fig. 12.5).

The PILLAR II trial [60] enrolled 139 participants who underwent left-sided colonic resection and observed a leak rate of 1.4% with no leaks being observed in those where ICG angiography altered the surgical plan ($n = 11$). A recent meta-analysis of studies by Blanco-Colino et al. [61] examined the anastomotic leak rate in at least 30 days of follow-up in 1302 patients where 555 underwent ICG angiography and 747 underwent standard care. In the ICG group, a change to the planned anastomotic level was made in 7.4% of cases due to hypoperfusion identified on fluorescence imaging. On performing a subgroup analysis of the 956 cancer patients (382 ICG, 574 control), there was a significant decrease in leak rate in the ICG group (OR 0.34; CI 0.16–0.74; $p = 0.006$). Similar results were demonstrated in those undergoing rectal resection. In a larger study by Ris et al. not included in this meta-analysis, a leak rate of 2.6% for colorectal anastomoses and 3% following low anterior resection with 29 patients having an altered surgical plan following fluorescence angiography was observed [62]. Following these promising data, the first multicentre randomised trial for ICG fluorescence angiography in patients undergoing anterior resection is being conducted with results expected by 2020 [63].

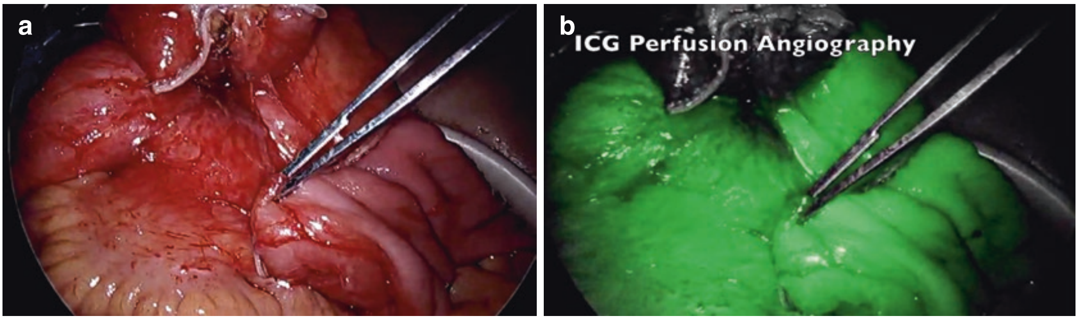

Fig. 12.5 (**a**) A stapled segment of small bowel (top) appears pink and quite viable under white light; (**b**) but under NIR, after ICG administration systemically, it is apparent there is no perfusion to this segment of bowel. Surgeons can use ICG as a method to assess perfusion in real time, providing an opportunity to improve the integrity of a planned anastomosis, especially in left-sided colorectal resections where blood supply of the conduit is almost completely predicated on a single vessel (the marginal artery). (Photographs courtesy of Sam Atallah MD, with permission)

This technique must use observation of fluorescence in either adjacent small bowel or proximal colon as a visual positive control. The current technology for anastomosis perfusion lacks quantification and the understanding of what is important in the interpretation of the fluorescent signal (e.g. time to signal, time to wash out, maximum signal) [62]. Such technology for quantification is already under evaluation where the aim is to give a 'cutoff' level where an anastomosis is less likely to heal [64].

Lymphatic Mapping

For curative resection of solid tumours, the two surgical principles are removing the cancer in its entirety (providing an R0 resection) and retrieving the draining lymph node basin. While there are few exceptions, in most instances, this approach is essential in providing the maximum recurrence-free survival to the patient. In addition, the draining lymph nodes provide essential pathological staging to guide further treatment. In some solid tumour malignancies, the concept of the sentinel lymph node (SLN) allows surgeons to stage and stratify patients into those requiring lymphadenectomy. In particular, for melanoma [65] and breast cancer surgery [66], lymph node mapping and SLN biopsy have become the standard of care.

The technique for SLN biopsy, in breast cancer, often involves injection of a visible blue dye (e.g. patent blue-V, isosulfan blue or methylene blue), a radioactive tracer with gamma probe detection or both, in the vicinity of the tumour, retroareolarly or periareolarly. During dissection for the SLN, the visible dye or radioactive tracer can then be identified positively in the first lymph node(s) in the lymphatic basin. Utilising these two techniques, the SLN detection is high, measuring on the order of 96–99.1% in large trials [67, 68] – note: it can be 10% lower with the use of a single technique [69]. The use of radioisotopes can provide difficulties for institutions with their handling, disposal, training and legislative requirements, which increase healthcare delivery costs. In most centres, it also is more cumbersome for patients since the injection takes place in the nuclear medicine department. With blue dyes, there is a risk of anaphylaxis and tattooing of the skin with their use. Thus, fluorescent SLN lymphatic mapping has been explored as a valid alternative to these modalities. When comparing ICG to blue dye alone, ICG is significantly better for SLN identification than blue dye (OR 18.37; 95% CI 8.63–39.10) as indicated by Ahmed et al. in a meta-analysis of 15 studies [70]. When compared with a radiocolloid, there is no consensus on which is superior [70, 71].

In colorectal cancer, the concept of SLN biopsy is less widely adopted because there is variability in the sensitivity of the SLN technique [72]. Therefore, all patients undergoing resection undergo en bloc mesenteric resection – even for T1 (except highly selected, histologically favourable rectal lesions) and T2 disease. This means that for the subset of patients who have early-stage, node-negative cancer, mesenteric resection provides no additional oncological benefit [73]. Thus, colorectal surgeons would like to be able to determine who does and who does not have lymph node metastatic disease and tailor the operation accordingly. However, applying SLN techniques here may be more challenging due to the phenomenon of 'skip metastases' where lymph nodes of aberrant drainage contain metastatic disease and thus the SLN biopsy would not identify these. The current evidence for fluorescence-guided SLN detection in colorectal cancer is limited by its heterogeneity in terms of technique, dose, equipment and timing as well as small patient numbers. Most importantly however, the published studies on this technique only report sensitivity and specificity based on positivity by histopathology which does not report its value in identifying a *negative* SLN. ICG is a non-specific dye, and thus reporting the sensitivity according to SLN positivity is perhaps a reasonable explanation for the varying results. Three well-conducted meta-analyses, although stating the technique as promising, fail to reach the same detection rates and quality of evidence seen in fluorescence-guided SLN biopsy for breast surgery [74–76].

Aside from SLN biopsy, lymphatic mapping with ICG can be used in colorectal surgery to identify the pattern of the lymph node basin and to recognise aberrant lymph node drainage allowing a tailored colorectal resection [77]. This is perhaps a more relevant question, with outcomes being visualisation of the lymphatic drainage, identification of aberrant lymph nodes and, ultimately, a potential change to mesenteric resection determined in real time. In particular, resection of some colorectal cancers, including the splenic flexure, is still not standardised due to difficulty in deciding on the appropriate mesenteric resection due to variation in the regional draining lymphatics from middle colic to left colic arteries [78]. Watanabe and colleagues have demonstrated a substantial variation in the lymphatic drainage of splenic flexural tumours with 38.7% of 31 patients having lymphatic drainage to the left accessory aberrant colic artery (LAACA), and of the 61.3% without the LAACA, 19.4% drained to the left branch of the middle colic, 25.8% to the left colic and 16.1% to the route of the IMV [79]. More work is required to optimise the dosing, timing and patient selection for fluorescence lymphatic mapping during colorectal cancer surgery.

Fluorescence Mapping of Disease Using Non-targeted Fluorophores

In the literature, there are a number of applications that utilise non-targeted NIR fluorophores. In resection of liver primary and secondary malignancy, ICG has been demonstrated as a potential non-specific tool to aid surgeons in determining the resection margin of these lesions. This technique was identified by Ishizawa and colleagues [80] who incidentally recognised that hepatocellular carcinomas (HCC) fluoresced strongly following IV administration of ICG. It is hypothesised that such lesions retain preoperatively injected ICG as a result of reduced biliary excretion in the cancerous tissue due to morphological obstruction in the surround biliary system. To date, a number of small studies have demonstrated the efficacy of ICG for liver cancer identification [80, 81]. Because ICG is not cancer-specific, false positives can be problematic and are reported to be as high as 40% [82]. Similar promising results have been seen in the detection of colorectal peritoneal metastases, although, as with liver lesions, this technique seems to lack specificity [75, 83]. Notwithstanding, colorectal lesions can be directly injected with ICG during colonoscopy, allowing them to be visible as a 'translucent tattoo' during minimally invasive surgery (Fig. 12.6).

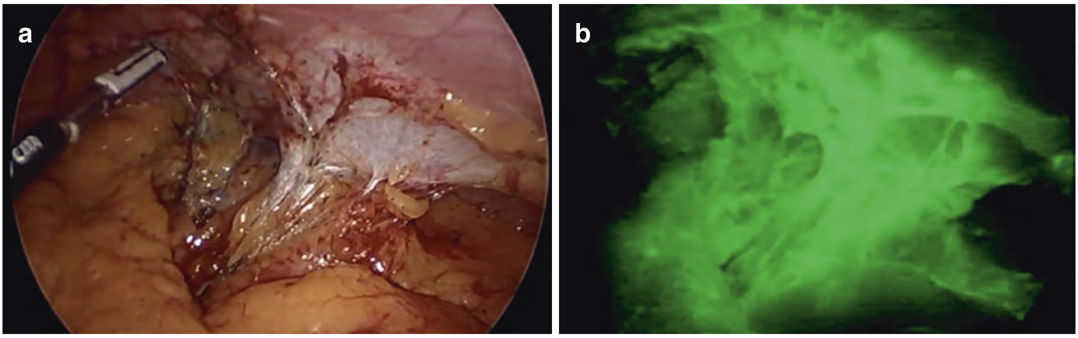

Fig. 12.6 (**a**) During laparoscopic colectomy, the target lesion was difficult to identify, due to the small size of the cancer, dense overlying omentum and adhesions from prior surgery. (**b**) Immediately prior to operation, a submucosal ICG tattoo was injected at the base of the splenic flexure cancer, allowing the surgeon to clearly localize and target the appropriate segment of large bowel. (Photographs courtesy of Sam Atallah MD, with permission)

Future Directions of NIR Imaging

NIR fluorophores have been experimented within this thesis. Fluorescence imaging in the *second* near-infrared window (NIR-II, 1000–1700 nm) is also possible and, some argue, more desirable than NIR-I (650–900 nm) owing to a reduction in photon scattering, diminished tissue autofluorescence and deeper tissue penetration improving imaging quality and signal-to-noise ratios [84–88]. Until recently, the only NIR-II fluorescent agents for in vivo imaging at present are inorganic including carbon nanotubes, quantum dots and nanoparticles. Toxicity concerns over these molecules have arisen as they have extremely long circulation times and are retained in the liver and spleen [89]. Organic fluorophores are much preferred for clinical imaging as they have a rapid metabolism and low toxicity; however, the design and manufacture of these are extremely difficult hence why organic NIR-II dye synthesis is further behind the inorganic dyes [85, 89]. Similarly, difficulties with constructing imaging equipment for the NIR-II window for in vivo use are costly and lengthy, and as a result, no commercial entities are developing such devices.

References

1. da Silva G, Boutros M, Wexner SD. Role of prophylactic ureteric stents in colorectal surgery. Asian J Endosc Surg. 2012;5(3):105–10.
2. Kyzer S, Gordon PH. The prophylactic use of ureteral catheters during colorectal operations. Am Surg. 1994;60(3):212–6.
3. Janssen PF, Brolmann HA, Huirne JA. Causes and prevention of laparoscopic ureter injuries: an analysis of 31 cases during laparoscopic hysterectomy in the Netherlands. Surg Endosc. 2013;27(3):946–56.
4. St Lezin MA, Stoller ML. Surgical ureteral injuries. Urology. 1991;38(6):497–506.
5. Delacroix SE Jr, Winters JC. Urinary tract injures: recognition and management. Clin Colon Rectal Surg. 2010;23(2):104–12.
6. Halabi WJ, Jafari MD, Nguyen VQ, Carmichael JC, Mills S, Pigazzi A, et al. Ureteral injuries in colorectal surgery: an analysis of trends, outcomes, and risk factors over a 10-year period in the United States. Dis Colon Rectum. 2014;57(2):179–86.
7. Mahendran HA, Praveen S, Ho C, Goh EH, Tan GH, Zuklifli MZ. Iatrogenic ureter injuries: eleven years experience in a tertiary hospital. Med J Malaysia. 2012;67(2):169–72.
8. Palaniappa NC, Telem DA, Ranasinghe NE, Divino CM. Incidence of iatrogenic ureteral injury after laparoscopic colectomy. Arch Surg. 2012;147(3):267–71.
9. Al-Awadi K, Kehinde EO, Al-Hunayan A, Al-Khayat A. Iatrogenic ureteric injuries: incidence, aetiological factors and the effect of early management on subsequent outcome. Int Urol Nephrol. 2005;37(2):235–41.

10. Tebala GD. The "left ureteral triangle" as an anatomic landmark for the identification of the left ureter in laparoscopic distal colectomies. Surg Laparosc Endosc Percutan Tech. 2016;26(5):e100–e2.
11. Nam YS, Wexner SD. Clinical value of prophylactic ureteral stent indwelling during laparoscopic colorectal surgery. J Korean Med Sci. 2002;17(5):633–5.
12. Coakley KM, Kasten KR, Sims SM, Prasad T, Heniford BT, Davis BR. Prophylactic ureteral catheters for colectomy: a national surgical quality improvement program-based analysis. Dis Colon Rectum. 2018;61(1):84–8.
13. Merola J, Arnold B, Luks V, Ibarra C, Resio B, Davis KA, et al. Prophylactic ureteral stent placement vs no ureteral stent placement during open colectomy. JAMA Surg. 2018;153(1):87–90.
14. Senagore AJ, Luchtefeld M. An initial experience with lighted ureteral catheters during laparoscopic colectomy. J Laparoendosc Surg. 1994;4(6):399–403.
15. Tsujinaka S, Wexner SD, DaSilva G, Sands DR, Weiss EG, Nogueras JJ, et al. Prophylactic ureteric catheters in laparoscopic colorectal surgery. Tech Coloproctol. 2008;12(1):45–50.
16. Bothwell WN, Bleicher RJ, Dent TL. Prophylactic ureteral catheterization in colon surgery. A five-year review. Dis Colon Rectum. 1994;37(4):330–4.
17. Boyan WP Jr, Lavy D, Dinallo A, Otero J, Roding A, Hanos D, et al. Lighted ureteral stents in laparoscopic colorectal surgery; a five-year experience. Ann Transl Med. 2017;5(3):44.
18. Kim K, Schwaitzberg S, Onel E. An infrared ureteral stent to aid in laparoscopic retroperitoneal lymph node dissection. J Urol. 2001;166(5):1815–6.
19. Lee Z, Moore B, Giusto L, Eun DD. Use of indocyanine green during robot-assisted ureteral reconstructions. Eur Urol. 2015;67(2):291–8.
20. Park H, Farnam RW. Novel use of indocyanine green for intraoperative, real-time localization of ureter during robot-assisted excision of endometriosis. J Minim Invasive Gynecol. 2015;22(6s):S69.
21. Lee Z, Simhan J, Parker DC, Reilly C, Llukani E, Lee DI, et al. Novel use of indocyanine green for intraoperative, real-time localization of ureteral stenosis during robot-assisted ureteroureterostomy. Urology. 2013;82(3):729–33.
22. Siddighi S, Yune JJ, Hardesty J. Indocyanine green for intraoperative localization of ureter. Am J Obstet Gynecol. 2014;211(4):436.e1–2.
23. Tanaka E, Ohnishi S, Laurence RG, Choi HS, Humblet V, Frangioni JV. Real-time intraoperative ureteral guidance using invisible near-infrared fluorescence. J Urol. 2007;178(5):2197–202.
24. Korb ML, Huh WK, Boone JD, Warram JM, Chung TK, de Boer E, et al. Laparoscopic fluorescent visualization of the ureter with intravenous IRDye800CW. J Minim Invasive Gynecol. 2015;22(5):799–806.
25. Mahalingam SM, Dip F, Castillo M, Roy M, Wexner SD, Rosenthal RJ, et al. Intraoperative ureter visualization using a novel near-infrared fluorescent dye. Mol Pharm. 2018;15(8):3442–7.
26. Cha J, Nani RR, Luciano MP, Kline G, Broch A, Kim K, et al. A chemically stable fluorescent marker of the ureter. Bioorg Med Chem Lett. 2018;28(16):2741–5.
27. Matsui A, Tanaka E, Choi HS, Kianzad V, Gioux S, Lomnes SJ, et al. Real-time, near-infrared, fluorescence-guided identification of the ureters using methylene blue. Surgery. 2010;148(1):78–86.
28. Verbeek FP, van der Vorst JR, Schaafsma BE, Swijnenburg RJ, Gaarenstroom KN, Elzevier HW, et al. Intraoperative near infrared fluorescence guided identification of the ureters using low dose methylene blue: a first in human experience. J Urol. 2013;190(2):574–9.
29. Yeung TM, Volpi D, Tullis ID, Nicholson GA, Buchs N, Cunningham C, et al. Identifying ureters in situ under fluorescence during laparoscopic and open colorectal surgery. Ann Surg. 2016;263(1):e1–2.
30. Barnes TG, Hompes R, Birks J, Mortensen NJ, Jones O, Lindsey I, et al. Methylene blue fluorescence of the ureter during colorectal surgery. Surg Endosc. 2018;32(9):4036–43.
31. Kneist W, Stelzner S, Aigner F, Fürst A, Wedel T. Urethral injury in body donor TaTME training. Coloproctology. 2017;39(3):179–83.
32. Penna M, Hompes R, Arnold S, Wynn G, Austin R, Warusavitarne J, et al. Transanal total mesorectal excision: international registry results of the first 720 cases. Ann Surg. 2016;266:111.
33. Rouanet P, Mourregot A, Azar CC, Carrere S, Gutowski M, Quenet F, et al. Transanal endoscopic proctectomy: an innovative procedure for difficult resection of rectal tumors in men with narrow pelvis. Dis Colon Rectum. 2013;56(4):408–15.
34. Burke JP, Martin-Perez B, Khan A, Nassif G, de Beche-Adams T, Larach SW, et al. Transanal total mesorectal excision for rectal cancer: early outcomes in 50 consecutive patients. Color Dis. 2016;18(6):570–7.
35. Simillis C, Hompes R, Penna M, Rasheed S, Tekkis PP. A systematic review of transanal total mesorectal excision: is this the future of rectal cancer surgery? Color Dis. 2016;18(1):19–36.
36. Atallah S, Mabardy A, Volpato AP, Chin T, Sneider J, Monson JRT. Surgery beyond the visible light spectrum: theoretical and applied methods for localization of the male urethra during transanal total mesorectal excision. Tech Coloproctol. 2017;21:413–24.
37. Atallah S, Mabardy A, Volpato AP, Chin T, Sneider J, Monson JRT. Surgery beyond the visible light spec-

trum: theoretical and applied methods for localization of the male urethra during transanal total mesorectal excision. Tech Coloproctol. 2017;21(6):413–24.
38. Barnes TG, Penna M, Hompes R, Cunningham C. Fluorescence to highlight the urethra: a human cadaveric study. Tech Coloproctol. 2017;21(6):439–44.
39. Barnes TG, Volpi D, Cunningham C, Vojnovic B, Hompes R. Improved urethral fluorescence during low rectal surgery: a new dye and a new method. Tech Coloproctol. 2018;22(2):115–9.
40. Nitta T, Tanaka K, Kataoka J, Ohta M, Ishii M, Ishibashi T, et al. Novel technique with the IRIS U kit to prevent urethral injury in patients undergoing transanal total mesorectal excision. Ann Med Surg (Lond). 2019;46:1–3.
41. Giger U, Ouaissi M, Schmitz SF, Krahenbuhl S, Krahenbuhl L. Bile duct injury and use of cholangiography during laparoscopic cholecystectomy. Br J Surg. 2011;98(3):391–6.
42. Branum G, Schmitt C, Baillie J, Suhocki P, Baker M, Davidoff A, et al. Management of major biliary complications after laparoscopic cholecystectomy. Ann Surg. 1993;217(5):532–40; discussion 40–1
43. Flum DR, Dellinger EP, Cheadle A, Chan L, Koepsell T. Intraoperative cholangiography and risk of common bile duct injury during cholecystectomy. JAMA. 2003;289(13):1639–44.
44. Ishizawa T, Bandai Y, Ijichi M, Kaneko J, Hasegawa K, Kokudo N. Fluorescent cholangiography illuminating the biliary tree during laparoscopic cholecystectomy. Br J Surg. 2010;97(9):1369–77.
45. Vlek SL, van Dam DA, Rubinstein SM, de Lange-de Klerk ESM, Schoonmade LJ, Tuynman JB, et al. Biliary tract visualization using near-infrared imaging with indocyanine green during laparoscopic cholecystectomy: results of a systematic review. Surg Endosc. 2017;31(7):2731–42.
46. van den Bos J, Wieringa FP, Bouvy ND, Stassen LPS. Optimizing the image of fluorescence cholangiography using ICG: a systematic review and ex vivo experiments. Surg Endosc. 2018;32:4820.
47. Clinicaltrials.gov. Fluorescent cholangiography vs white light for bile ducts identification 2018. Available from: https://clinicaltrials.gov/ct2/show/NCT02702843?term=ICG+cholangiography&rank=10.
48. Schols RM, Bouvy ND, van Dam RM, Masclee AA, Dejong CH, Stassen LP. Combined vascular and biliary fluorescence imaging in laparoscopic cholecystectomy. Surg Endosc. 2013;27(12):4511–7.
49. Sarkaria IS, Bains MS, Finley DJ, Adusumilli PS, Huang J, Rusch VW, et al. Intraoperative near-infrared fluorescence imaging as an adjunct to robotic-assisted minimally invasive esophagectomy. Innovations (Phila). 2014;9(5):391–3.
50. Walsh EM, Cole D, Tipirneni KE, Bland KI, Udayakumar N, Kasten BB, et al. Fluorescence imaging of nerves during surgery. Ann Surg. 2019;270(1):69–76.
51. Mangano MS, De Gobbi A, Beniamin F, Lamon C, Ciaccia M, Maccatrozzo L. Robot-assisted nerve-sparing radical prostatectomy using near-infrared fluorescence technology and indocyanine green: initial experience. Urologia. 2018;85(1):29–31.
52. Wagner OJ, Louie BE, Vallieres E, Aye RW, Farivar AS. Near-infrared fluorescence imaging can help identify the contralateral phrenic nerve during robotic thymectomy. Ann Thorac Surg. 2012;94(2):622–5.
53. Chen SC, Wang MC, Wang WH, Lee CC, Yang TF, Lin CF, et al. Fluorescence-assisted visualization of facial nerve during mastoidectomy: a novel technique for preventing iatrogenic facial paralysis. Auris Nasus Larynx. 2015;42(2):113–8.
54. Gibbs-Strauss SL, Nasr KA, Fish KM, Khullar O, Ashitate Y, Siclovan TM, et al. Nerve-highlighting fluorescent contrast agents for image-guided surgery. Mol Imaging. 2011;10(2):91–101.
55. Park JS, Huh JW, Park YA, Cho YB, Yun SH, Kim HC, et al. Risk factors of anastomotic leakage and long-term survival after colorectal surgery. Medicine (Baltimore). 2016;95(8):e2890.
56. Paun BC, Cassie S, MacLean AR, Dixon E, Buie WD. Postoperative complications following surgery for rectal cancer. Ann Surg. 2010;251(5):807–18.
57. McDermott FD, Heeney A, Kelly ME, Steele RJ, Carlson GL, Winter DC. Systematic review of preoperative, intraoperative and postoperative risk factors for colorectal anastomotic leaks. Br J Surg. 2015;102(5):462–79.
58. Rutegard M, Rutegard J. Anastomotic leakage in rectal cancer surgery: the role of blood perfusion. World J Gastrointest Surg. 2015;7(11):289–92.
59. Hirst NA, Tiernan JP, Millner PA, Jayne DG. Systematic review of methods to predict and detect anastomotic leakage in colorectal surgery. Color Dis. 2014;16(2):95–109.
60. Jafari MD, Wexner SD, Martz JE, McLemore EC, Margolin DA, Sherwinter DA, et al. Perfusion assessment in laparoscopic left-sided/anterior resection (PILLAR II): a multi-institutional study. J Am Coll Surg. 2015;220(1):82–92.e1.
61. Blanco-Colino R, Espin-Basany E. Intraoperative use of ICG fluorescence imaging to reduce the risk of anastomotic leakage in colorectal surgery: a systematic review and meta-analysis. Tech Coloproctol. 2018;22(1):15–23.
62. Ris F, Liot E, Buchs NC, Kraus R, Ismael G, Belfontali V, et al. Multicentre phase II trial of near-infrared imaging in elective colorectal surgery. Br J Surg. 2018;105(10):1359–67.
63. Armstrong G, Croft J, Corrigan N, Brown JM, Goh V, Quirke P, et al. IntAct: intra-operative fluorescence angiography to prevent anastomotic leak in rectal cancer surgery: a randomized controlled trial. Color Dis. 2018;20(8):O226–O34.
64. Diana M, Agnus V, Halvax P, Liu YY, Dallemagne B, Schlagowski AI, et al. Intraoperative fluorescence-based enhanced reality laparoscopic real-time imaging

to assess bowel perfusion at the anastomotic site in an experimental model. Br J Surg. 2015;102(2):e169–76.
65. Morton DL, Wen DR, Wong JH, Economou JS, Cagle LA, Storm FK, et al. Technical details of intraoperative lymphatic mapping for early stage melanoma. Arch Surg. 1992;127(4):392–9.
66. Giuliano AE, Kirgan DM, Guenther JM, Morton DL. Lymphatic mapping and sentinel lymphadenectomy for breast cancer. Ann Surg. 1994;220(3):391–8; discussion 8–401
67. Straver ME, Meijnen P, van Tienhoven G, van de Velde CJ, Mansel RE, Bogaerts J, et al. Sentinel node identification rate and nodal involvement in the EORTC 10981-22023 AMAROS trial. Ann Surg Oncol. 2010;17(7):1854–61.
68. Kuehn T, Bauerfeind I, Fehm T, Fleige B, Hausschild M, Helms G, et al. Sentinel-lymph-node biopsy in patients with breast cancer before and after neoadjuvant chemotherapy (SENTINA): a prospective, multicentre cohort study. Lancet Oncol. 2013;14(7):609–18.
69. Goyal A, Newcombe RG, Chhabra A, Mansel RE, Group AT. Factors affecting failed localisation and false-negative rates of sentinel node biopsy in breast cancer–results of the ALMANAC validation phase. Breast Cancer Res Treat. 2006;99(2):203–8.
70. Ahmed M, Purushotham AD, Douek M. Novel techniques for sentinel lymph node biopsy in breast cancer: a systematic review. Lancet Oncol. 2014;15(8):e351–62.
71. Qiu SQ, Zhang GJ, Jansen L, de Vries J, Schroder CP, de Vries EGE, et al. Evolution in sentinel lymph node biopsy in breast cancer. Crit Rev Oncol Hematol. 2018;123:83–94.
72. Tsioulias GJ, Wood TF, Morton DL, Bilchik AJ. Lymphatic mapping and focused analysis of sentinel lymph nodes upstage gastrointestinal neoplasms. Arch Surg. 2000;135(8):926–32.
73. Currie AC, Brigic A, Thomas-Gibson S, Suzuki N, Moorghen M, Jenkins JT, et al. A pilot study to assess near infrared laparoscopy with indocyanine green (ICG) for intraoperative sentinel lymph node mapping in early colon cancer. Eur J Surg Oncol. 2017;43(11):2044–51.
74. Yuasa Y, Seike J, Yoshida T, Takechi H, Yamai H, Yamamoto Y, et al. Sentinel lymph node biopsy using intraoperative indocyanine green fluorescence imaging navigated with preoperative CT lymphography for superficial esophageal cancer. Ann Surg Oncol. 2012;19(2):486–93.
75. Emile SH, Elfeki H, Shalaby M, Sakr A, Sileri P, Laurberg S, et al. Sensitivity and specificity of indocyanine green near-infrared fluorescence imaging in detection of metastatic lymph nodes in colorectal cancer: systematic review and meta-analysis. J Surg Oncol. 2017;116(6):730–40.
76. Liberale G, Bohlok A, Bormans A, Bouazza F, Galdon MG, El Nakadi I, et al. Indocyanine green fluorescence imaging for sentinel lymph node detection in colorectal cancer: a systematic review. Eur J Surg Oncol. 2018;44(9):1301–6.
77. Tuech JJ, Pessaux P, Regenet N, Bergamaschi R, Colson A. Sentinel lymph node mapping in colon cancer. Surg Endosc. 2004;18(12):1721–9.
78. Nakagoe T, Sawai T, Tsuji T, Jibiki M, Ohbatake M, Nanashima A, et al. Surgical treatment and subsequent outcome of patients with carcinoma of the splenic flexure. Surg Today. 2001;31(3):204–9.
79. Watanabe J, Ota M, Suwa Y, Ishibe A, Masui H, Nagahori K. Evaluation of lymph flow patterns in splenic flexural colon cancers using laparoscopic real-time indocyanine green fluorescence imaging. Int J Color Dis. 2017;32(2):201–7.
80. Ishizawa T, Fukushima N, Shibahara J, Masuda K, Tamura S, Aoki T, et al. Real-time identification of liver cancers by using indocyanine green fluorescent imaging. Cancer. 2009;115(11):2491–504.
81. Judy RP, Keating JJ, DeJesus EM, Jiang JX, Okusanya OT, Nie S, et al. Quantification of tumor fluorescence during intraoperative optical cancer imaging. Sci Rep. 2015;5:16208.
82. Abo T, Nanashima A, Tobinaga S, Hidaka S, Taura N, Takagi K, et al. Usefulness of intraoperative diagnosis of hepatic tumors located at the liver surface and hepatic segmental visualization using indocyanine green-photodynamic eye imaging. Eur J Surg Oncol. 2015;41(2):257–64.
83. Barabino G, Klein JP, Porcheron J, Grichine A, Coll JL, Cottier M. Intraoperative near-infrared fluorescence imaging using indocyanine green in colorectal carcinomatosis surgery: proof of concept. Eur J Surg Oncol. 2016;42(12):1931–7.
84. Diao S, Blackburn JL, Hong GS, Antaris AL, Chang JL, Wu JZ, et al. Fluorescence imaging in vivo at wavelengths beyond 1500 nm. Angewandte Chemie-Int Ed. 2015;54(49):14758–62.
85. Ding F, Chen S, Zhang W, Tu Y, Sun Y. UPAR targeted molecular imaging of cancers with small molecule-based probes. Bioorg Med Chem. 2017;25(20):5179–84.
86. Smith AM, Mancini MC, Nie SM. BIOIMAGING second window for in vivo imaging. Nat Nanotechnol. 2009;4(11):710–1.
87. Hong GS, Lee JC, Robinson JT, Raaz U, Xie LM, Huang NF, et al. Multifunctional in vivo vascular imaging using near-infrared II fluorescence. Nat Med. 2012;18(12):1841.
88. Zhang XD, Wang HS, Antaris A, Li LL, Diao S, Ma R, et al. In vivo vascular imaging of traumatic brain injury in the second near-infrared window. J Neurotrauma. 2016;33(13):A48-A.
89. Ding F, Zhan Y, Lu X, Sun Y. Recent advances in near-infrared II fluorophores for multifunctional biomedical imaging. Chem Sci. 2018;9(19):4370–80.

13 Fluorescence-Guided Resections: A Binary Approach to Surgery

Stephanie Schipmann and Walter Stummer

Abbreviations

5-ALA	5-Aminolevulinic acid
BBB	Blood-brain barrier
CCK2	Cholecystokinin-2
CEA	Carcinoembryonic antigen
EGFR	Epidermal growth factor receptor
EMA	European Medicines Agency
FDA	Food and Drug Administration
FGS	Fluorescence-guided surgery
FITC	Fluorescein isothiocyanate
GRPR	Gastrin-releasing peptide receptor
GTR	Gross total resection
HER	Human epidermal growth factor receptor
IGC	Indocyanine green
MB	Methylene blue
NIR	Near-infrared
NIR-PIT	Near-infrared photoimmunotherapy
OR	Operating room (OR)
PDT	Photodynamic therapy
PPIX	Protoporphyrin IX
PSMA	Prostate-specific membrane antigen
SWIG	Second window ICG
VEGF	Vascular epithelial growth factor

Introduction

Surgical resection is considered the primary treatment for many malignant tumors. In doing so, the aim of surgery is maximal safe tumor resection focusing at tumor-free margins, as it is a strong predictor for local tumor recurrence and correlates with survival in many cancers, such as breast cancer [1], head and neck cancer [2], colorectal cancer [3], bladder cancer [4], non-small cell lung cancer [5], and glioblastoma [6].

Visualization of the tumor and its margin is often challenging and relies on visual and tactile inspection, often being supported by intraoperative histopathological analysis of frozen section, a method which is time-consuming and has several limitations as a discrepancy with permanent pathological results [7]. Studies show that despite advances in preoperative imaging, there is still a tumor margin positivity rate of 5–21% across all cancers [8]. Especially in the field of neurosurgery, several conventional and non-optical imaging modalities, like intraoperative neuronavigation, CT, or MRI, all having in common that they are expensive, prolong surgical time, disrupt surgical workflow, require additional space in the operating room (OR), are not cancer-specific and not real-time, have emerged during the last decades, and play an important role in the management of malignant brain tumors [9, 10]. These methods mainly base on anatomical features and do not allow direct targeting of

S. Schipmann (✉) · W. Stummer
Department of Neurosurgery, University Hospital Münster, Münster, Germany
e-mail: stephanie.schipmann@ukmuenster.de

S. Atallah (ed.), *Digital Surgery*, https://doi.org/10.1007/978-3-030-49100-0_13

tumor cells.

For oncological surgeons, the ability to delineate between abnormal and normal tissue is of utmost importance in order to perform safe and effective surgery. Regarding this requirement, fluorescence-guided surgery (FGS) has been shown to be extremely helpful. It is based on the administration of optical imaging agents to patients during or prior to surgery that selectively accumulate in tumor tissue. The structures labeled by fluorescence can be detected during surgery and provide the surgeon with intraoperative visualization and delineation of pathological tissues.

Inducing fluorescence in pathological tissues has several advantages. Visualization is performed in real time, while the surgeon is operating. Thus, the surgeon no longer needs to interrupt surgery for using tools for reorientation. Not only is fluorescence used for detecting residual tumors, but also it changes the surgical strategy once fluorescence is encountered, e.g., allowing the surgeon to resect along the fluorescing edges of malignancy, rather than from the inside out. Optimally, as in 5-ALA, ambient and unequivocal information with normal illumination is rendered into simple, easily comprehended binary information.

The first description and use of FGS date back to the 1940s, when George E. Moore showed that brain tumors can be visualized by fluorescence after intravenous applications of fluorescein [11, 12].

Besides fluorescein, other fluorescent agents have been introduced into the field of surgery, such as indocyanine green (ICG) [13], methylene blue (MB) [14], and 5-aminolevulinic acid (5-ALA) [15], which is, to date, the only FDA-approved agent for intraoperative imaging. In addition, fluorescence-guided surgery has been developed not only in neurosurgery but also in several other surgical specialties for oncological and non-oncological indications as well since its initial description [16–18]. In this chapter, the different established fluorescent agents and newer methods with their applicability in surgery and their benefits and limitations will be discussed.

Indocyanine Green (ICG)

Indocyanine green (ICG) is a water-soluble tricarbocyanine that shows fluorescence in the near-infrared spectrum with peak emission at 780 nm and excitation at 810 nm. It is approved by the Food and Drug Administration (FDA) for ophthalmic angiography and determination of liver blood flow and cardiac function but has been used as an off-label device for several other indications, like uro-oncological surgery and vascular neurosurgery [13, 19–21].

After intravenous administration, ICG rapidly binds to albumin and can be visualized almost immediately. It has a rather short half-life of 150–180 seconds and is cleared by the liver [22]. ICG has a high toxic safety; only a low incidence of adverse side effects, such as anaphylactic shock, arrhythmia, and hypotension in 0.05% and mild symptoms as nausea or skin reactions in 0.2%, is described [13].

Nowadays, ICG has been widely and successfully used for sentinel lymph node mapping in various types of cancers, such as breast cancer [23–27], melanoma [28–30], head and neck cancer [28, 31–33], prostate cancer [34–36], lung cancer [37], gastric cancer [38, 39], colorectal cancer [40–42], and esophagus cancer [43, 44] as shown in Table 13.1. Using ICG for sentinel lymph node biopsy, the detection rates have been improved, and the procedure has become more accurate than with the use of methylene blue; particularly in detection of sentinel lymph nodes for breast cancer, a sensitivity between 95% and 100% has been described [28, 30, 45]. ICG lymphography can be also used for diagnosis and staging of chronic lymphedema, and it is helpful for intraoperative anatomical location of lymphatic pathways in case of planning a lymphovenous bypass [46].

In addition, ICG has been shown to be helpful in the imaging of tumor tissue when administered preoperatively, e.g., for the identification of small cancer nodules in pulmonary malignancies, lowering the rate of thoracotomies, and enabling surgeons to carry out precise resections with time-saving surgical techniques and less unnecessary intraoperative damage [47, 48]. Similar

Table 13.1 Overview of current applications of various fluorescent agents in surgery

Fluorescent agent	Indication/medical disorder	Type of surgery/benefit of fluorescent agent
Indocyanine green (ICG)	Breast cancer	Sentinel lymph node mapping [23, 24, 26, 27] Breast reconstruction (flap) – perfusion of flap [63, 64]
	Melanoma	Sentinel lymph node mapping [28–30]
	Head and neck cancer	Sentinel lymph node mapping [28, 31–33]
		Detection of malignant mucosal lesions (endoscopic tumor imaging) [57]
		Flap reconstruction – perfusion of flap [65]
	Lung cancer	Tumor imaging [48, 237–241]
		Flap reconstruction after anatomical lung resection- perfusion of flap [60]
		Sentinel lymph node mapping [37]
	Gastric cancer	Sentinel lymph node mapping [38, 39]
		Tumor imaging [242]
		Evaluation of invasivity of tumors [58]
	Colorectal cancer	Sentinel lymph node mapping [40–42]
		Detection of peritoneal metastases [49]
	Anal cancer	Sentinel lymph node mapping [243]
	Abdominal (oncological) surgery	Evaluation of intestinal anastomosis [76, 82–85]
	Esophagus cancer	Sentinel lymph node mapping [43, 44]
	Prostate cancer	Lymphography, sentinel lymph node mapping [34–36]
	Lymphedema	Lymphography [244, 245]
	Plastic-reconstructive surgery	Angiography – assessment of tissue and flap vascularization [62, 246–248]
	Cerebral aneurysm, arteriovenous malformations	Videoangiography or endoscopy for assessment of patency of vessels after clipping of an aneurysm [13, 66–72]
	Abdominal aortic aneurysm	Angiography for assessment of peripheral arterial perfusion [75]
	Coronary artery bypass surgery	Angiography for graft patency of coronary artery bypass [73, 126]
	Hepatocellular carcinoma	Detection of metastasis [249, 250]
		Identification of tumor mass/tumor imaging [50–52]
	Ovarian cancer	Identification of tumor mass/tumor imaging [53, 54]
	Malignant glioma	Identification of tumor mass/tumor imaging [55]
	Cerebral metastasis	Identification of tumor mass/tumor imaging [251]
	Meningioma	Identification of tumor mass/tumor imaging [252]
	Cholecystectomy	Cholangiography to determine biliary anatomy in laparoscopic cholecystectomy [76–78]
	Kidney, liver, pancreas transplantation	Assessment of perfusion of organs [79–81]
	Sellar lesions	Assessment of blood supply of adjacent structures, like optic nerves via fluorescence endoscopy [86]

(continued)

Table 13.1 (contnued)

Fluorescent agent	Indication/medical disorder	Type of surgery/benefit of fluorescent agent
5-Aminolevulinic acid (5-ALA)	Malignant glioma	Selective visualization of tumor and its infiltrating zone, improvement of extent of resection [6, 15, 92, 99–105, 253–256]
	Low-grade gliomas	Visualization of anaplastic foci within the tumor [107–110]
	Meningiomas	Imaging of tumor and bony infiltration [111–116, 257]
	Cerebral metastases	Imaging of tumor, potential prognostic factor for local recurrence and overall survival [106, 117, 118]
	Pediatric brain tumors, incl. ependymoma	Imaging of tumor [119, 122, 123]
	Intracranial lymphoma	Imaging of tumor, obtaining representative biopsy samples [124–126]
	Hemangioblastoma	Imaging of solid tumor [128, 129]
	Intracranial Germ cell tumors	Imaging of tumor [131]
	Subependymoma	Imaging of tumor [130]
	Prostate cancer	Imaging of tumor, assessing the presence of residual tumor in surgical margins [132–134]
	Bladder cancer	Imaging of tumor [135, 258]
	Basal cell carcinoma	Imaging of tumor and borders [259]
Fluorescein sodium	Fundus disorders in ophthalmology	Retinal angiography, detection of corneal abrasions [138]
	Malignant glioma	Tumor imaging, improving the extent of resection, background illumination [135, 138, 139, 143–146, 148, 149, 153, 154, 259]
	Cerebral metastases	Tumor imaging, improving the extent of resection [140, 155, 156]
	Meningioma	Tumor imaging, angiography and evaluation of surrounding vessels [157, 158]
	CNS lymphoma	Imaging of tumor, obtaining representative biopsy samples [140, 159]
	Cerebral aneurysms and vascular malformations	Fluorescence videoangiography to obtain anatomy and patency of adjacent vessels [160–162]
Methylene blue (MB)	Breast cancer	Near-infrared sentinel lymph node mapping [167]
		Tumor imaging [168]
	Thyroid surgery	Early identification and preservation of parathyroid glands during surgery Identification of parathyroid adenoma [171, 172]
	Pancreas tumor, incl. insulinoma	Tumor imaging [169, 170]
	Urology, abdominal surgery	Ureter mapping [173–175]

Folate	Ovarian cancer	Imaging of metastases (folate-FITC) [179, 180] Imaging of metastases (OTL38) [187]
	Lung cancer	Imaging of tumor (folate-FITC) [47, 181–183] Imaging of tumor (OTL38) [185, 186] Predina 2018
	Breast cancer	Imaging of tumor (folate-FITC) [179]
	Renal cancer	Imaging of tumor (OTL38) [188]
	Pituitary adenoma	Imaging of tumor (OTL38) [189, 190]
Tumor-specific monoclonal antibodies conjugated to fluorescently labeled dyes	Head and neck cancer	Imaging of tumor (cetuximab-IRDye800CW) [194, 260] Imaging of positive lymph nodes (cetuximab-IRDye800CW) [195] Imaging of tumor (panitumumab-IRDye800CW) [196, 260, 261]
	Breast cancer	Imaging of tumor (bevacizumab-IRDye800CW) [197] Imaging of tumor (LUM015) [210] Imaging of tumor and metastatic lymph nodes (AVB-620) [212]
	Colorectal cancer	Imaging of peritoneal metastases (bevacizumab-IRDye800CW) [203]
Peptide-based fluorescence-guided surgery	Glioma (high and low grade)	Imaging of tumor (tozuleristide – BLZ-100) [218]

results have been described for the detection of peritoneal metastases from colorectal cancer, where the use of ICG resulted in modification of the planned surgery in almost one-third of cases [49]. Apart from metastases, application of ICG can be beneficial in the detection of hepatocellular carcinoma [50–52] and ovarian cancer [53, 54]. A growing body of research has led to the utilization of ICG for resection of malignant gliomas as well, a technique referred to as second window ICG (SWIG). For this procedure, higher doses up to 5.0 mg/kg ICG are administered to the patient up to 24 prior to surgery, leading to accumulation in tumor tissue. Assuming that ICG binds to serum albumin, it can pass through a disrupted blood-brain barrier and is retained due to a lack of clearance [55]. Fluorescence is visualized using a near-infrared (NIR) camera (700–850 nm), integrated into the surgical microscope. An advantage of ICG is that it has excitation and emission in the NIR region of the spectrum, enabling visualization of ICG fluorescence even in deeper regions [56]. However, so far, there are no studies showing a benefit of ICG for the improvement of the extent of resection in malignant gliomas.

NIR endoscopy with ICG can support intraoperatively to differentiate between benign and malignant lesions in the examination of mucosal head and neck lesions with a sensitivity and specificity for the detection of malignant lesions of 90.5% and 90.9%, respectively [57], and has shown to be a useful diagnostic tool for estimating the invasivity of gastric tumors [58].

In oncological surgery, in addition to maximal safe tumor resection, an adequate reconstruction plays an important role to maintain quality of life and prevent secondary complications [59, 60]. ICG angiography is helpful for assessing blood flow and tissue perfusion and can be used in general in the pre-, intra-, and postoperative setting [46, 61]. This justifies that ICG angiography has found its routine application in plastic-reconstructive surgery [62], e.g., for breast reconstruction after mastectomy using various types of flaps [63, 64] or for evaluation of the quality of perfusion at the anastomotic site of other surgical flaps after anatomical lung resection [60], or for reconstruction with free flaps after resection of oral cancer [65].

ICG has been extensively used in vascular neurosurgery for direct intraoperative assessment of aneurysms or arteriovenous malformations and the patency of the surrounding vessel structures via microscope-integrated near-infrared ICG videoangiography [13, 66–70] (Fig. 13.1) or as the next step via an endoscope with the integration of videoangiography to gain a wider and angled view of the aneurysm and its associated vessels [71, 72]. Similar roles does ICG angiography play in vascular and cardiac surgery for evaluation of patency of coronary artery bypass grafting [73, 74] and assessment of blood flow in the peripheral arteries in patients with abdominal

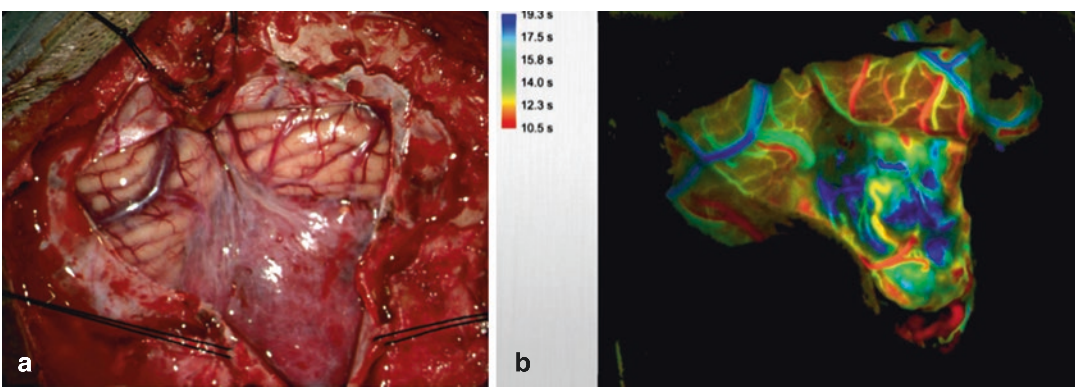

Fig. 13.1 ICG angiography in a patient with a cerebellar hemangioblastoma. (**a**) Tumor under white light. (**b**) Angioarchitecture and surrounding vessels are visualized and color-coded via ICG angiography

aortic aneurysms [75].

Further indications for ICG are cholangiography for determination of biliary anatomy in laparoscopic cholecystectomy [76–78], assessment of perfusion during kidney [79, 80], liver and pancreas transplantation [81], evaluation of intestinal anastomosis after esophagectomy and colorectal resection [82–85], and neurosurgical endoscopic procedures in case of a sellar lesion for anatomical visualization of blood supply of adjacent structures, like the pituitary and the optic nerves [86].

In summary, ICG is extensively used in a huge variety of medical subspecialties for various indications. However, so far, only little randomized controlled prospective trials have been carried out to evaluate the importance of ICG and its benefit for the treatment of different medical disorders. Most of the mentioned results so far rely on case studies and monocentric experience. But the load of new publications and the rising of reports on possible indications for ICG make ICG an attractive and possible relevant tool for FGS. It convinces through its widespread use including angiography, lymphography, tumor imaging, and fluorescence endoscopy depending on the timing and dosage of ICG and the tools used for visualization [87].

5-Aminolevulinic Acid (5-ALA)

5-Aminolevulinic acid (5-ALA) is a natural metabolite in the heme-pathway and is metabolized into protoporphyrin IX (PPIX), a strongly fluorescent precursor of heme. In brain tumor surgery, 5-ALA is considered the most intensely studied fluorescent agent worldwide and approved both by the U.S. Food and Drug Administration (FDA) and the European Medicines Agency (EMA) for intraoperative imaging of high-grade gliomas. 5-ALA is administered orally at a dosage of 20 mg/kg body weight around 3 hours before the induction of anesthesia. It is selectively taken up by glioma cells and converted into PPIX in tumor cells. Tumor cells can be visualized using a surgical microscope with a xenon light source that can be switched between white and violet-blue light (wavelength: 370–440 nm) and is equipped with an emission filter for visualization of red tumor fluorescence at a peak of 635 and 704 nm [15, 88–90]. Fluorescence becomes visible after 3 hours, with a peak after 6–8 hours [89–91]. High-grade gliomas typically show a solid red fluorescence that becomes slightly pink at the tumor margins, representing the tumor infiltrating zone [92] (Fig. 13.2).

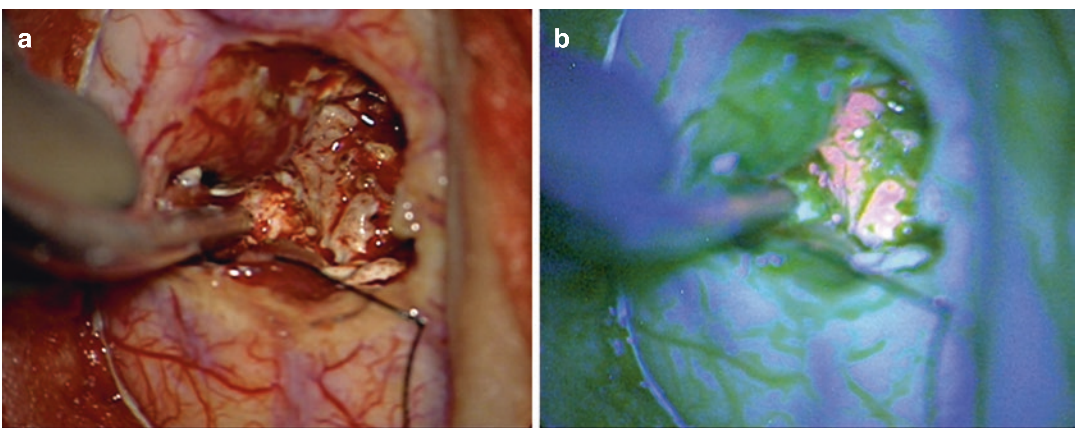

Fig. 13.2 5-ALA-guided resection of glioblastoma. (**a**) Tumor under white light, delineation between tumor and normal tissue is almost impossible. (**b**) Tumor under violet light, showing a clear and solid fluorescence in the tumor

These highly malignant and aggressive tumors are characterized by their infiltrative nature and the lack of a distinct histological border to normal brain tissue. Several studies have supported the benefit of complete resection of contrast-enhancing tumors on overall survival [93–97]. However, identification and delineation of tumor tissue from normal brain only by visual impression and haptic information is often impossible [98]. 5-ALA has a high specificity of 100% and sensitivity of up to 85% for the detection of malignant cells [15].

A randomized controlled multicenter phase III study demonstrated a clinical benefit of 5-ALA regarding the extent of tumor resection (65% in the 5-ALA group and 36% in the white light group, $p < 0.001$) and progression-free survival in malignant gliomas [6]. With the usage of 5-ALA nowadays and due to confidence in the use of the method and intraoperative neuromonitoring, tumor resection rates between 80% and 100% have been reported [99, 100].

Even in recurrent glioblastoma, several small case studies confirm a benefit of 5-ALA-guided resection regarding the amount of tumor removal [101–106].

In addition, 5-ALA has advantages for detecting anaplastic foci in the management of low-grade gliomas [107–110]. Furthermore, 5-ALA bears the potential for resection of other non-glial brain tumors in individual cases, like meningiomas [111–116], cerebral metastases [106, 117, 118], pediatric brain tumors [119–123], intracranial lymphomas [124–127], hemangioblastomas [128, 129], ependymomas [123], subependymomas [130], and germ cell tumors [131]. However, so far, only minor series and case reports are available, limiting drawing any conclusions regarding the usage of 5-ALA for non-glial tumors, and further studies are warranted to explore the full value of 5-ALA for other tumor entities.

Outside the central nervous system, 5-ALA has been evaluated in the usage of visualization of prostate cancer and is feasible in showing the presence of residual tumor at the surgical margins [132–134]. Recently, a multicenter phase III study has been carried out and revealed a high diagnostic efficacy and safety of 5-ALA for transurethral resection of bladder cancer in the identification of tumor tissue [135].

5-ALA has a high toxicological safety; only minor side effects like transient skin phototoxicity or temporarily elevated liver enzymes have been observed [6, 136].

Fluorescein Sodium

Fluorescein sodium is a fluorescent biomarker with characteristic yellow-green fluorescence; it has a peak absorption between 465 and 480 nm and an emission peak at 500–530 nm. Fluorescence can also be visualized under white light, when administered in high concentrations (20 mg/kg body weight) [137]. Fluorescein is widely being used in ophthalmic surgery for retinal angiography and detection of corneal abrasions [138]. Initially introduced by George E. Moore in 1947 for visualization of brain tumors, fluorescein is presently under investigation in the field of neurosurgery [11, 12]. After intravenous application in a dosage of 3–5 mg/kg body weight just after induction of anesthesia, fluorescein is distributed via the bloodstream into all perfused tissues, extravasates through the disrupted blood-brain barrier (BBB), and then highlights areas of BBB disruption related to tumor growth, increased vascular permeability, and neovascularization [11, 138–141]. Visualization is enabled by special fluorescent filters that are incorporated into modern surgical microscopes, e.g., the FL650 System (Leica Microscopes) and YELLOW 560 system (Carl Zeiss) (Fig. 13.3).

Fluorescein is a safe, robust, and inexpensive fluorophore. It can lead to transient discoloration of skin and urine after administration, and single cases of anaphylactic reactions have been described [142].

Several studies, encouraged by the success of 5-ALA, aimed at analyzing the efficacy and applicability of the comparably less expensive fluorescence agent fluorescein for resection of malignant gliomas and suggest promising outcomes regarding the improvement of the extent of resection with gross total resection (GTR)

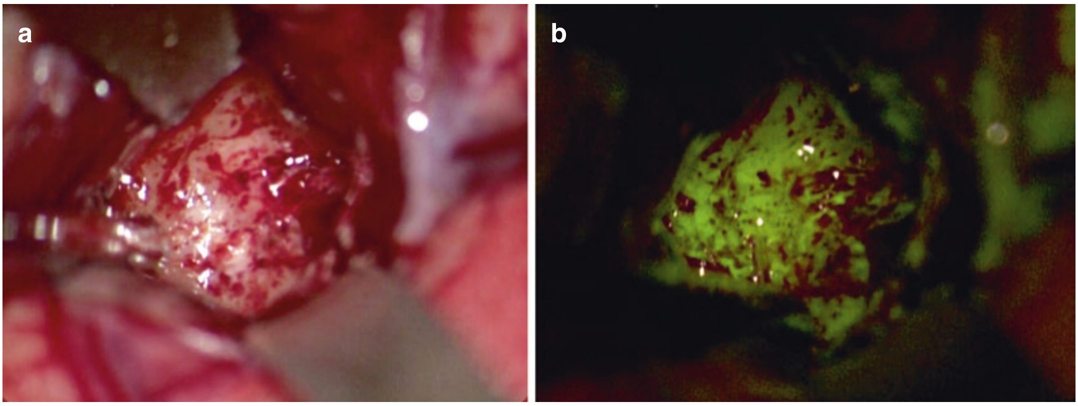

Fig. 13.3 Fluorescein-guided resection of glioblastoma. (**a**) Tumor under white light. (**b**) Tumor after application of fluorescein under YELLOW 560 filter

rates ranging from 53% to 100% [139, 143–149]. So far, the evidence for the usage of fluorescein in malignant gliomas is limited to small cohorts.

A single-arm phase II study (FLUGLIO) revealed that fluorescein-guided glioma surgery is safe and feasible [150], but still, randomized trials are warranted to investigate the possible effect of fluorescein in terms of survival and extent of resection. All studies so far are single-armed, and selection bias in these studies cannot be ruled out.

A major limitation with the usage of fluorescein is the fact that fluorescein mainly marks areas with BBB breakdown that are somewhat but not strictly related to tumor tissue, making it an ideal marker for edema propagation, rather than being tumor-cell-specific, such is the case with 5-ALA [139, 151, 152]. In addition, during surgery, normal perfused tissue will fluoresce due to fluorescein in plasma, and any injury of normal brain tissue will lead to unselective extravasation of fluorescein from the bloodstream along the cut margins. Timing of application is critical, as the distribution of fluorescein in tissue follows a certain time course, possibly leading to unselective extravasation after a half-life of 264 minutes and staining and the subsequent danger of resection of non-tumorous tissue [151].

The simultaneous usage of fluorescein and 5-ALA has been investigated for the resection of malignant gliomas, resulting in highly specific tumor visualization (PPIX) and enhanced background brightness (fluorescein) at the same time [153]. Fluorescence was visualized using a filter that allows visualization of both fluorophores PPIX and fluorescein, referred to as a YB 475 filter [154].

Additional applications of fluorescein are cerebral metastases, where the use of fluorescein has been used for resection, and gross total resection (GTR) rates of 83–100% have been reported [140, 155, 156], meningiomas, either to evaluate surrounding and attached vessels via fluorescence angiography or to help enhance the contrast between normal brain structures and cranial nerves and tumors in skull base surgery [157, 158]. Furthermore, fluorescein can be used to visualize primary CNS lymphomas and obtain diagnostic samples during biopsy [140, 159].

Similar to ICG, fluorescein is used for fluorescence videoangiography, which can be helpful in the management of cerebral aneurysms or arteriovenous malformations [160–162].

Methylene Blue (MB)

Methylene blue (MB), mostly known as a dark blue contrast agent, has a long history in several areas of medicine. It was the first synthetic medication used for the treatment of malaria, pioneered by Paul Ehrlich and Paul Guttmann by the end of the nineteenth century [163]. It is used as a medication for the treatment of methemoglobinemia [164].

When diluted, MB acts as a fluorescent agent that emits light in the near-infrared range with an excitation peak of 670 nm and an emission peak of 690 nm [165]. A common use is sentinel lymph node mapping in a diversity of tumors using MB as a dying agent in combination with a radioisotope [14, 166]. Recently, the near-infrared fluorescence capabilities of MB have been used to develop a new technique, referred to as NIR-sentinel lymph node mapping using MB, in many cases now replaced by ICG [167]. MB has also been used for tumor identification in breast cancer [168], pancreatic and neuroendocrine tumors [169, 170], and parathyroid adenomas [171, 172]. As MB is eliminated renally, it can be well used for ureter mapping during abdominal surgery [173–175]. In low doses (<2 mg/kg), MB is considered safe. However, MB can induce severe adverse effects such as hemolytic anemia, arrhythmias, and coronary vasoconstriction [176].

Novel Techniques and Approaches in Fluorescence-Guided Surgery

Despite the broad use and the advantages of the above-discussed fluorescence imaging techniques, there are still some limitations, mainly addressing the lack of high sensitivity and specificity for the detection of cancer cells. Consequently, research is ongoing. Requirements for an ideal fluorescent imaging probe are a high contrast between malignant and normal tissue [177], low toxicity, and high tumor selectivity [87]. A new generation of FGS aims at the introduction of tumor-target-specific antibodies or peptides, conjugated to fluorescent agents. Most of these technologies are presently in their fledging stage and subject to intensive preclinical and early-stage clinical research.

Folate-Targeted Fluorescence-Guided Surgery

Targeting biomarkers that are specifically overexpressed on tumor cells enable a more selective approach to cancer treatment and imaging. One of these biomarkers is the folate receptor, which is commonly upregulated on a number of cancers of epithelial origin, including breast, lung, renal, and ovarian cancers [178]. For fluorescence-guided surgery, folate is conjugated to fluorescent agents, e.g., fluorescein isothiocyanate (FITC; also known as EC17), an agent with fluorescent properties in the visible light spectrum (500 nm) [179, 180]. In ovarian cancer, small series showed the feasibility of intraoperative imaging of cancer metastases, leading to the detection of 16% additional malignant lesions compared to palpation or inspection with the naked eye [179]. Lung adenocarcinomas can also be detected with folate-FITC, a recent study demonstrated fluorescence in 92% (46/50) of patients. This approach might facilitate minimally invasive surgery, to overcome its limitation of the lack of haptic information [47, 181–183]. Promising results have been shown for breast cancer, as well [179]. Limitations of this technique base on the fluorescence within the visible spectrum, not providing depth penetration, accompanied by a lack of illumination of buried tumor nodules and autofluorescence of nonmalignant lesions, leading to false-positive results [47, 179]. In an attempt to overcome this limitation, a folate analog conjugated to a fluorophore that fluoresces in the NIR spectrum, OTL38, has been introduced [184]. OTL38 has been successfully used for the detection of lung cancer [185, 186] and ovarian cancer, leading to an additional 29% of resection of malignant lesions [187], renal cancer [188], and pituitary adenomas [189, 190].

Tumor-Specific Antibody-Based Fluorescence-Guided Surgery

A further approach for selective tumor-targeting with fluorescence-guided surgery is the use of tumor-specific monoclonal antibodies that are conjugated to fluorescently labeled dyes. There are currently multiple ongoing trials for evaluating the role and benefit of fluorescently labeled antibodies to image cancer, targeting a variety of cancer-specific markers [191, 192]. The most frequently assessed target is the human epidermal growth factor receptor (EGFR), commonly overexpressed in head and neck cancer [193]. A phase I trial investigated the applicability of cetuximab conjugated to the near-infrared fluorescent dye IRDye800 in patients undergoing surgical resection for head and neck cancer and demonstrated high safety and precise identification of tumor tissue [194], with further studies showing that this technique can be used for the identification of additional positive lymph node during neck dissection [195]. Recently, panitumumab-IRDye800CW has also shown to be helpful in intraoperative decision-making in head and neck cancer regarding the detection of unanticipated tumor regions [196]. In patients with breast cancer, the NIR fluorescent tracer bevacizumab-IRDye800CW targeting vascular epithelial growth factor (VEGF) has been used with promising results [197]; further targets, currently under preclinical investigation, are anti-human epidermal growth factor receptor (HER) 2 antibody trastuzumab, labeled with IRDye800CW for breast cancer [198, 199], carcinoembryonic antigen (CEA) [200], anti-CA19-9 for intraoperative imaging of pancreatic tumors [201], and anti-prostate-specific membrane antigen (PSMA) antibody for prostate cancer [202]. For patients with peritoneal carcinomatosis of the colorectal region, bevacizumab-IRDye800CW is currently under investigation [203].

All these conjugates of antibody and fluorescent agent are typically always "on" and emit fluorescence signals. A further step toward higher target/background ratios and advanced sensitivity and specificity is the development of activatable fluorescent probes that only emit signals when bound specifically to tumor cells, whereas unbound probes do not yield a signal [87, 204]. Activation occurs either enzymatically, by endolysosomal processing or due to particular physiological conditions in tumor tissue [87]. Several preclinical studies have been carried out and demonstrated the possible advantages of this method [205–208]. LUM015 was the first protease-activatable fluorescent imaging probe to be tested in a clinical study in patients with breast cancer. A selective distribution of LUM15 to tumor cells and a high target/background fluorescence ratio have been found [209]. These data encouraged further research revealing promising data regarding the translation into clinical use [210]. An additional phase I study using AVB-620, a further protease-activatable fluorescent peptide, was carried out in breast cancer patients, again indicating high safety and the potential of intraoperative real-time detection of tumor and metastatic lymph nodes. Currently, phase II studies have been emerged [211, 212].

In summary, these data suggest that commonly available antibodies conjugated to fluorescent probes provide the opportunity to identify subclinical tumor manifestation and possible improving outcomes in oncological surgery. However, further clinical trials are warranted to prove this promising concept.

Peptide-Based Fluorescence-Guided Surgery

Besides cancer-specific antibodies, tumor-targeting peptides have been used for FGS. Compared to antibodies, peptides have the advantage of rapid distribution and absent immunogenicity [213, 214].

BLZ-100 (tozuleristide), extracted from the venom of scorpions, has been conjugated to the NIR fluorophore ICG [215, 216]. A high affinity of BLZ-100 after administration prior to surgery toward human gliomas has been shown [217], and a phase I study in low- and high-grade gliomas has revealed high safety and the potential use of this approach to selectively visualize glioma cells [218].

Other targets like the cholecystokinin-2 (CCK2)/gastrin receptor or the gastrin-releasing peptide receptor (GRPR) for peptide-based fluorescence visualization of a variety of tumors are currently under preclinical investigation [219–221].

Advances in Fluorescence-Guided Surgery

The substantial number of clinical trials and emerging new techniques in FGS for a variety of medical indications can be attributed to the numerous advantages of this technique. In effect, FGS aids in the delineation of tumor tissue from

Table 13.2 Advantages and disadvantages of fluorescence-guided surgery

Advantages	Disadvantages
Delineation between normal and pathological tissue and enhanced tumor visualization [222] Reduction of operating time [87] Low cost Real-time visualization Precision surgery: Detection of microscopical tumors and residual lesions – optimizing locoregional control [262] Decrease the need for second-look surgeries [87] More complete surgical resection [6] and more efficient adjuvant treatment [222] Preservation of normal and vital tissue, such as nerves, vessels, ureters; maintaining the function of daily living [263] Improved functional outcome, quality of life, decreased morbidity [222] Time-saving No interruption of surgical workflow Absence of ionizing radiation [264] High specificity [264] Complement the tactile-limited field during minimally invasive surgery [222]	Low background illumination and loss of optical information [153] Requires special cameras and instruments to be visualized Time dependency between application and visualization [139, 151] Subjective interpretation of the presence and intensity of fluorescence Lack of tumor specificity in some cases Passive labeling (fluorescein) [139, 151] Numerous regulatory barriers before approval [222]

Summary of major advantages and disadvantages of FGS, not all apply to the various fluorescent agents that are being discussed

healthy tissue, lowering the risk of residual tumor tissue and positive tumor margins while at the same time improving safety by avoiding unnecessary damage to normal tissue [87]. Additionally, it is easy to use with high safety and in most cases high specificity. A major advantage is that FGS provides real-time information and the surgeon's workflow is not interrupted. Low background information and loss of optical information often require the surgeon to switch between fluorescent and white light mode. In addition, FGS and especially the introduction of new methods and the expansion of medial indications face numerous regulatory barriers that prolong or hinder the translation into clinical practice. A major barrier is the need for approval for both the fluorescent agent and imaging device [222]. Further advantages and disadvantages are summarized in Table 13.2.

Future Perspective and Conclusion

FGS aims at better intraoperative visualization of pathological and vital structures to improve surgical outcomes regarding the safety and extent of resection in the case of malignant tumors. It can help overcome the limitation of human eyesight and add optical information to the haptic and tactile features, used by a surgeon. The increasing number of clinical trials investigating various fluorescent agents for a huge variety of indications emphasizes the great potential that FGS bears.

In many medical fields, with neurosurgery currently being in the lead, several of these techniques have been already integrated into daily clinical routine. FGS gives the opportunity to bridge the gap between preoperative tumor imaging and intraoperative real-time tumor-specific visualization. However, current fluorescent imaging methods still have to face individual limitations, and as a consequence, further research is ongoing to overcome these limitations. One issue is the fact that currently, the interpretation of the presence and intensity of fluorescence relies on the subjective impression of the surgeon. Therefore, several attempts have been undertaken to quantify fluorescence, e.g., using spectroscopic techniques when operating on gliomas with the help of handheld devices that allow quantification of fluorescence, even when there is no visible fluorescence under the microscope, a common aspect in low-grade gliomas [223, 224].

A major disadvantage of some broadly used fluorescent agents, like fluorescein or methylene blue, is the fact that these agents do not specifically bind to tumor cells and rather use other indirect mechanisms, like enhanced permeability to target cancer cells, bearing the risk of resection of non-tumorous tissue due to false-positive staining effects [139, 151]. As a consequence, the introduction of targeted fluorescence with more specific tumor labeling is under current investigation, and so far, several preclinical and clinical studies have been carried out using fluorescent agents that bind exclusively to cancer-specific targets as discussed in this chapter. Innovations of imaging devices will improve the view of the surgical field, possibly detecting additional optical features in tumor tissue [56].

The optical properties of the presented fluorescent agents are of importance for successful tumor imaging and determine the amount of autofluorescence and tissue depth penetration. In particular, fluorescent agents that emit in the NIR have the advantage of low autofluorescence, enabling a higher target/background ratio and imaging of targets below the surface [179]. Consequently, the attention has shifted toward developing tumor-targeting antibodies conjugated with fluorophores in the NIR.

In addition to imaging, the use of fluorescence offers the possibility for photodynamic therapy (PDT). This concept has been used for the treatment of malignant gliomas, as 5-ALA-derived PPiX is capable of both, tumor fluorescence and acting as a strong photosensitizer [89, 225]. PDT is based on a photochemical reaction activated by light, and after excitation with laser light, reactive oxygen species and free radicals are released that lead to direct cytotoxic effects on cancer cells and the induction of immune responses [226, 227]. Several small studies have shown promising results for the treatment of malignant gliomas [228–231].

Potential clinical implications can be found in a new method referred to as near-infrared photoimmunotherapy (NIR-PIT), based on tumor-targeting antibodies that are conjugated to photoabsorbing dyes (IRDye700DX) that are capable of fluorescence and have cytotoxic effects to cells to which they are conjugated, offering a dual approach, labeling of cancer cells, and selective elimination [87, 232]. Several authors reported encouraging results in preclinical studies [233–236].

In summary, FGS offers a wide spectrum of surgical imaging and potential therapeutic tools, complementing the tactile feature of surgeons to improve accuracy and move a step forward toward precision surgery and targeted therapy.

References

1. O'Kelly Priddy CM, Forte VA, Lang JE. The importance of surgical margins in breast cancer. J Surg Oncol. 2016;113(3):256–63.
2. Haque R, Contreras R, McNicoll MP, Eckberg EC, Petitti DB. Surgical margins and survival after head and neck cancer surgery. BMC Ear Nose Throat Disord. 2006;6:2.
3. Solaini L, Gardini A, Passardi A, Mirarchi MT, D'Acapito F, La Barba G, et al. Preoperative chemotherapy and resection margin status in colorectal liver metastasis patients: a propensity score-matched analysis. Am Surg. 2019;85(5):488–93.
4. Dotan ZA, Kavanagh K, Yossepowitch O, Kaag M, Olgac S, Donat M, et al. Positive surgical margins in soft tissue following radical cystectomy for bladder cancer and cancer specific survival. J Urol. 2007;178(6):2308–12; discussion 13.
5. Predina JD, Keating J, Patel N, Nims S, Singhal S. Clinical implications of positive margins following non-small cell lung cancer surgery. J Surg Oncol. 2016;113(3):264–9.
6. Stummer W, Pichlmeier U, Meinel T, Wiestler OD, Zanella F, Reulen HJ, et al. Fluorescence-guided surgery with 5-aminolevulinic acid for resection of malignant glioma: a randomised controlled multicentre phase III trial. Lancet Oncol. 2006;7(5):392–401.
7. Jaafar H. Intra-operative frozen section consultation: concepts, applications and limitations. Malays J Med Sci. 2006;13(1):4–12.
8. Orosco RK, Tapia VJ, Califano JA, Clary B, Cohen EEW, Kane C, et al. Positive surgical margins in the 10 most common solid cancers. Sci Rep. 2018;8(1):5686.
9. Schulz C, Waldeck S, Mauer UM. Intraoperative image guidance in neurosurgery: development, current indications, and future trends. Radiol Res Pract. 2012;2012:197364.
10. Senft C, Bink A, Franz K, Vatter H, Gasser T, Seifert V. Intraoperative MRI guidance and extent of resection in glioma surgery: a randomised, controlled trial. Lancet Oncol. 2011;12(11):997–1003.

11. Moore GE. Fluorescein as an agent in the differentiation of normal and malignant tissues. Science. 1947;106(2745):130–1.
12. Moore GE, Peyton WT, et al. The clinical use of fluorescein in neurosurgery; the localization of brain tumors. J Neurosurg. 1948;5(4):392–8.
13. Raabe A, Beck J, Gerlach R, Zimmermann M, Seifert V. Near-infrared indocyanine green video angiography: a new method for intraoperative assessment of vascular flow. Neurosurgery. 2003;52(1):132–9; discussion 9.
14. Peek MC, Charalampoudis P, Anninga B, Baker R, Douek M. Blue dye for identification of sentinel nodes in breast cancer and malignant melanoma: a systematic review and meta-analysis. Future Oncol. 2017;13(5):455–67.
15. Stummer W, Stocker S, Wagner S, Stepp H, Fritsch C, Goetz C, et al. Intraoperative detection of malignant gliomas by 5-aminolevulinic acid-induced porphyrin fluorescence. Neurosurgery. 1998;42(3):518–25; discussion 25–6.
16. Kaplan-Marans E, Fulla J, Tomer N, Bilal K, Palese M. Indocyanine green (ICG) in urologic surgery. Urology. 2019;132:10–7.
17. Nakaseko Y, Ishizawa T, Saiura A. Fluorescence-guided surgery for liver tumors. J Surg Oncol. 2018;118(2):324–31.
18. Olson MT, Ly QP, Mohs AM. Fluorescence guidance in surgical oncology: challenges, opportunities, and translation. Mol Imaging Biol. 2019;21(2):200–18.
19. Cherrick GR, Stein SW, Leevy CM, Davidson CS. Indocyanine green: observations on its physical properties, plasma decay, and hepatic extraction. J Clin Invest. 1960;39:592–600.
20. Pathak RA, Hemal AK. Intraoperative ICG-fluorescence imaging for robotic-assisted urologic surgery: current status and review of literature. Int Urol Nephrol. 2019;51(5):765–71.
21. Reinhart MB, Huntington CR, Blair LJ, Heniford BT, Augenstein VA. Indocyanine green: historical context, current applications, and future considerations. Surg Innov. 2016;23(2):166–75.
22. Shimizu S, Kamiike W, Hatanaka N, Yoshida Y, Tagawa K, Miyata M, et al. New method for measuring ICG Rmax with a clearance meter. World J Surg. 1995;19(1):113–8; discussion 8.
23. Jung SY, Han JH, Park SJ, Lee EG, Kwak J, Kim SH, et al. The sentinel lymph node biopsy using indocyanine green fluorescence plus radioisotope method compared with the radioisotope-only method for breast cancer patients after neoadjuvant chemotherapy: a prospective, randomized, open-label, single-center phase 2 trial. Ann Surg Oncol. 2019;26(8):2409–16.
24. Kitai T, Inomoto T, Miwa M, Shikayama T. Fluorescence navigation with indocyanine green for detecting sentinel lymph nodes in breast cancer. Breast Cancer. 2005;12(3):211–5.
25. Kitai T, Kawashima M. Transcutaneous detection and direct approach to the sentinel node using axillary compression technique in ICG fluorescence-navigated sentinel node biopsy for breast cancer. Breast Cancer. 2012;19(4):343–8.
26. Murawa D, Hirche C, Dresel S, Hunerbein M. Sentinel lymph node biopsy in breast cancer guided by indocyanine green fluorescence. Br J Surg. 2009;96(11):1289–94.
27. Vermersch C, Raia-Barjat T, Chapelle C, Lima S, Chauleur C. Randomized comparison between indocyanine green fluorescence plus (99m)technetium and (99m)technetium alone methods for sentinel lymph node biopsy in breast cancer. Sci Rep. 2019;9(1):6943.
28. KleinJan GH, van Werkhoven E, van den Berg NS, Karakullukcu MB, Zijlmans H, van der Hage JA, et al. The best of both worlds: a hybrid approach for optimal pre- and intraoperative identification of sentinel lymph nodes. Eur J Nucl Med Mol Imaging. 2018;45(11):1915–25.
29. Knackstedt RW, Couto RA, Gastman B. Indocyanine green fluorescence imaging with lymphoscintigraphy for sentinel node biopsy in head and neck melanoma. J Surg Res. 2018;228:77–83.
30. Pameijer CR, Leung A, Neves RI, Zhu J. Indocyanine green and fluorescence lymphangiography for sentinel node identification in patients with melanoma. Am J Surg. 2018;216(3):558–61.
31. Bredell MG. Sentinel lymph node mapping by indocyanin green fluorescence imaging in oropharyngeal cancer – preliminary experience. Head Neck Oncol. 2010;2:31.
32. Nakamura T, Kogashiwa Y, Nagafuji H, Yamauchi K, Kohno N. Validity of sentinel lymph node biopsy by ICG fluorescence for early head and neck cancer. Anticancer Res. 2015;35(3):1669–74.
33. van der Vorst JR, Schaafsma BE, Verbeek FP, Keereweer S, Jansen JC, van der Velden LA, et al. Near-infrared fluorescence sentinel lymph node mapping of the oral cavity in head and neck cancer patients. Oral Oncol. 2013;49(1):15–9.
34. Harke NN, Godes M, Wagner C, Addali M, Fangmeyer B, Urbanova K, et al. Fluorescence-supported lymphography and extended pelvic lymph node dissection in robot-assisted radical prostatectomy: a prospective, randomized trial. World J Urol. 2018;36(11):1817–23.
35. Jeschke S, Lusuardi L, Myatt A, Hruby S, Pirich C, Janetschek G. Visualisation of the lymph node pathway in real time by laparoscopic radioisotope- and fluorescence-guided sentinel lymph node dissection in prostate cancer staging. Urology. 2012;80(5):1080–6.
36. Manny TB, Patel M, Hemal AK. Fluorescence-enhanced robotic radical prostatectomy using real-time lymphangiography and tissue marking with percutaneous injection of unconjugated indocyanine green: the initial clinical experience in 50 patients. Eur Urol. 2014;65(6):1162–8.
37. Yamashita S, Tokuishi K, Miyawaki M, Anami K, Moroga T, Takeno S, et al. Sentinel node navigation surgery by thoracoscopic fluorescence imaging

system and molecular examination in non-small cell lung cancer. Ann Surg Oncol. 2012;19(3):728–33.
38. Kinami S, Kosaka T. Laparoscopic sentinel node navigation surgery for early gastric cancer. Transl Gastroenterol Hepatol. 2017;2:42.
39. Takahashi N, Nimura H, Fujita T, Mitsumori N, Shiraishi N, Kitano S, et al. Laparoscopic sentinel node navigation surgery for early gastric cancer: a prospective multicenter trial. Langenbeck's Arch Surg. 2017;402(1):27–32.
40. Handgraaf HJ, Boogerd LS, Verbeek FP, Tummers QR, Hardwick JC, Baeten CI, et al. Intraoperative fluorescence imaging to localize tumors and sentinel lymph nodes in rectal cancer. Minim Invasive Ther Allied Technol. 2016;25(1):48–53.
41. Liberale G, Galdon MG, Moreau M, Vankerckhove S, El Nakadi I, Larsimont D, et al. Ex vivo detection of tumoral lymph nodes of colorectal origin with fluorescence imaging after intraoperative intravenous injection of indocyanine green. J Surg Oncol. 2016;114(3):348–53.
42. van der Pas MH, Ankersmit M, Stockmann HB, Silvis R, van Grieken NC, Bril H, et al. Laparoscopic sentinel lymph node identification in patients with colon carcinoma using a near-infrared dye: description of a new technique and feasibility study. J Laparoendosc Adv Surg Tech A. 2013;23(4):367–71.
43. Hachey KJ, Gilmore DM, Armstrong KW, Harris SE, Hornick JL, Colson YL, et al. Safety and feasibility of near-infrared image-guided lymphatic mapping of regional lymph nodes in esophageal cancer. J Thorac Cardiovasc Surg. 2016;152(2):546–54.
44. Yuasa Y, Seike J, Yoshida T, Takechi H, Yamai H, Yamamoto Y, et al. Sentinel lymph node biopsy using intraoperative indocyanine green fluorescence imaging navigated with preoperative CT lymphography for superficial esophageal cancer. Ann Surg Oncol. 2012;19(2):486–93.
45. Emile SH, Elfeki H, Shalaby M, Sakr A, Sileri P, Laurberg S, et al. Sensitivity and specificity of indocyanine green near-infrared fluorescence imaging in detection of metastatic lymph nodes in colorectal cancer: systematic review and meta-analysis. J Surg Oncol. 2017;116(6):730–40.
46. Burnier P, Niddam J, Bosc R, Hersant B, Meningaud JP. Indocyanine green applications in plastic surgery: a review of the literature. J Plast Reconstr Aesthet Surg. 2017;70(6):814–27.
47. Newton AD, Predina JD, Nie S, Low PS, Singhal S. Intraoperative fluorescence imaging in thoracic surgery. J Surg Oncol. 2018;118(2):344–55.
48. Zhang C, Lin H, Fu R, Zhang T, Nie Q, Dong S, et al. Application of indocyanine green fluorescence for precision sublobar resection. Thorac Cancer. 2019;10(4):624–30.
49. Liberale G, Vankerckhove S, Caldon MG, Ahmed B, Moreau M, Nakadi IE, et al. Fluorescence imaging after indocyanine green injection for detection of peritoneal metastases in patients undergoing cytoreductive surgery for peritoneal carcinomatosis from colorectal cancer: a pilot study. Ann Surg. 2016;264(6):1110–5.
50. Huang SW, Ou JJ, Wong HP. The use of indocyanine green imaging technique in patient with hepatocellular carcinoma. Transl Gastroenterol Hepatol. 2018;3:95.
51. Ishizawa T, Masuda K, Urano Y, Kawaguchi Y, Satou S, Kaneko J, et al. Mechanistic background and clinical applications of indocyanine green fluorescence imaging of hepatocellular carcinoma. Ann Surg Oncol. 2014;21(2):440–8.
52. Morita Y, Sakaguchi T, Unno N, Shibasaki Y, Suzuki A, Fukumoto K, et al. Detection of hepatocellular carcinomas with near-infrared fluorescence imaging using indocyanine green: its usefulness and limitation. Int J Clin Oncol. 2013;18(2):232–41.
53. Tummers QR, Hoogstins CE, Peters AA, de Kroon CD, Trimbos JB, van de Velde CJ, et al. The value of intraoperative near-infrared fluorescence imaging based on enhanced permeability and retention of indocyanine green: feasibility and false-positives in ovarian cancer. PLoS One. 2015;10(6):e0129766.
54. Veys I, Pop FC, Vankerckhove S, Barbieux R, Chintinne M, Moreau M, et al. ICG-fluorescence imaging for detection of peritoneal metastases and residual tumoral scars in locally advanced ovarian cancer: a pilot study. J Surg Oncol. 2018;117(2):228–35.
55. Lee JY, Thawani JP, Pierce J, Zeh R, Martinez-Lage M, Chanin M, et al. Intraoperative near-infrared optical imaging can localize gadolinium-enhancing gliomas during surgery. Neurosurgery. 2016;79(6):856–71.
56. Valdes PA, Roberts DW, Lu FK, Golby A. Optical technologies for intraoperative neurosurgical guidance. Neurosurg Focus. 2016;40(3):E8.
57. Schmidt F, Dittberner A, Koscielny S, Petersen I, Guntinas-Lichius O. Feasibility of real-time near-infrared indocyanine green fluorescence endoscopy for the evaluation of mucosal head and neck lesions. Head Neck. 2017;39(2):234–40.
58. Kimura T, Muguruma N, Ito S, Okamura S, Imoto Y, Miyamoto H, et al. Infrared fluorescence endoscopy for the diagnosis of superficial gastric tumors. Gastrointest Endosc. 2007;66(1):37–43.
59. Aristokleous I, Saddiq M. Quality of life after oncoplastic breast-conserving surgery: a systematic review. ANZ J Surg. 2019;89(6):639–46.
60. Kawamoto N, Anayama T, Okada H, Hirohashi K, Miyazaki R, Yamamoto M, et al. Indocyanine green fluorescence/thermography evaluation of intercostal muscle flap vascularization. Thorac Cancer. 2018;9(12):1631–7.
61. Griffiths M, Chae MP, Rozen WM. Indocyanine green-based fluorescent angiography in breast reconstruction. Gland Surg. 2016;5(2):133–49.
62. Holm C, Dornseifer U, Sturtz G, Ninkovic M. Sensitivity and specificity of ICG angiography in free flap reexploration. J Reconstr Microsurg. 2010;26(5):311–6.

63. Duggal CS, Madni T, Losken A. An outcome analysis of intraoperative angiography for postmastectomy breast reconstruction. Aesthet Surg J. 2014;34(1):61–5.
64. Murray JD, Jones GE, Elwood ET, Whitty LA, Garcia C. Fluorescent intraoperative tissue angiography with indocyanine green: evaluation of nipple-areola vascularity during breast reduction surgery. Plast Reconstr Surg. 2010;126(1):33e–4e.
65. Eguchi T, Kawaguchi K, Basugi A, Kanai I, Hamada Y. Intraoperative real-time assessment of blood flow using indocyanine green angiography after anastomoses in free-flap reconstructions. Br J Oral Maxillofac Surg. 2017;55(6):628–30.
66. Dashti R, Laakso A, Niemela M, Porras M, Hernesniemi J. Microscope-integrated near-infrared indocyanine green videoangiography during surgery of intracranial aneurysms: the Helsinki experience. Surg Neurol. 2009;71(5):543–50; discussion 50.
67. de Oliveira JG, Beck J, Seifert V, Teixeira MJ, Raabe A. Assessment of flow in perforating arteries during intracranial aneurysm surgery using intraoperative near-infrared indocyanine green videoangiography. Neurosurgery. 2007;61(3 Suppl):63–72; discussion 3.
68. Hanggi D, Etminan N, Steiger HJ. The impact of microscope-integrated intraoperative near-infrared indocyanine green videoangiography on surgery of arteriovenous malformations and dural arteriovenous fistulae. Neurosurgery. 2010;67(4):1094–103; discussion 103–4.
69. Imizu S, Kato Y, Sangli A, Oguri D, Sano H. Assessment of incomplete clipping of aneurysms intraoperatively by a near-infrared indocyanine green-video angiography (Niicg-Va) integrated microscope. Minim Invasive Neurosurg. 2008;51(4):199–203.
70. Raabe A, Nakaji P, Beck J, Kim LJ, Hsu FP, Kamerman JD, et al. Prospective evaluation of surgical microscope-integrated intraoperative near-infrared indocyanine green videoangiography during aneurysm surgery. J Neurosurg. 2005;103(6):982–9.
71. Fischer G, Rediker J, Oertel J. Endoscope- versus microscope-integrated near-infrared indocyanine green videoangiography in aneurysm surgery [published online ahead of print, 2018 Oct 1]. J Neurosurg. 2018;1-10. doi:10.3171/2018.4.JNS172650 Print edition Nov 2019, Volume 131.
72. Nishiyama Y, Kinouchi H, Senbokuya N, Kato T, Kanemaru K, Yoshioka H, et al. Endoscopic indocyanine green video angiography in aneurysm surgery: an innovative method for intraoperative assessment of blood flow in vasculature hidden from microscopic view. J Neurosurg. 2012;117(2):302–8.
73. Desai ND, Miwa S, Kodama D, Cohen G, Christakis GT, Goldman BS, et al. Improving the quality of coronary bypass surgery with intraoperative angiography: validation of a new technique. J Am Coll Cardiol. 2005;46(8):1521–5.
74. Yamamoto M, Orihashi K, Nishimori H, Handa T, Kondo N, Fukutomi T, et al. Efficacy of intraoperative HyperEye Medical System angiography for coronary artery bypass grafting. Surg Today. 2015;45(8):966–72.
75. Yamamoto M, Orihashi K, Nishimori H, Wariishi S, Fukutomi T, Kondo N, et al. Indocyanine green angiography for intra-operative assessment in vascular surgery. Eur J Vasc Endovasc Surg. 2012;43(4):426–32.
76. Boni L, David G, Mangano A, Dionigi G, Rausei S, Spampatti S, et al. Clinical applications of indocyanine green (ICG) enhanced fluorescence in laparoscopic surgery. Surg Endosc. 2015;29(7):2046–55.
77. Hiwatashi K, Okumura H, Setoyama T, Ando K, Ogura Y, Aridome K, et al. Evaluation of laparoscopic cholecystectomy using indocyanine green cholangiography including cholecystitis: a retrospective study. Medicine (Baltimore). 2018;97(30):e11654.
78. Ishizawa T, Bandai Y, Ijichi M, Kaneko J, Hasegawa K, Kokudo N. Fluorescent cholangiography illuminating the biliary tree during laparoscopic cholecystectomy. Br J Surg. 2010;97(9):1369–77.
79. Aslim EJ, Lee FJ, Gan VHL. The utility of intraoperative near infrared fluorescence (NIR) imaging with indocyanine green (ICG) for the assessment of kidney allograft perfusion. J Transplant. 2018;2018:6703056.
80. Vignolini G, Sessa F, Greco I, Cito G, Vanacore D, Cocci A, et al. Intraoperative assessment of ureteral and graft reperfusion during robotic kidney transplantation with indocyanine green fluorescence videography. Minerva Urol Nefrol. 2019;71(1):79–84.
81. Panaro F, Benedetti E, Pineton de Chambrun G, Habibeh H, Leon P, Bouyabrine H, et al. Indocyanine green fluorescence angiography during liver and pancreas transplantation: a tool to integrate perfusion statement's evaluation. Hepatobiliary Surg Nutr. 2018;7(3):161–6.
82. Blanco-Colino R, Espin-Basany E. Intraoperative use of ICG fluorescence imaging to reduce the risk of anastomotic leakage in colorectal surgery: a systematic review and meta-analysis. Tech Coloproctol. 2018;22(1):15–23.
83. Boni L, Fingerhut A, Marzorati A, Rausei S, Dionigi G, Cassinotti E. Indocyanine green fluorescence angiography during laparoscopic low anterior resection: results of a case-matched study. Surg Endosc. 2017;31(4):1836–40.
84. De Nardi P, Elmore U, Maggi G, Maggiore R, Boni L, Cassinotti E, et al. Intraoperative angiography with indocyanine green to assess anastomosis perfusion in patients undergoing laparoscopic colorectal resection: results of a multicenter randomized controlled trial. Surg Endosc. 2019;34(1):53–60.
85. Slooter MD, Eshuis WJ, Cuesta MA, Gisbertz SS, van Berge Henegouwen MI. Fluorescent imaging using indocyanine green during esophagectomy to prevent surgical morbidity: a systematic review and meta-analysis. J Thorac Dis. 2019;11(Suppl 5):S755–S65.

86. Hide T, Yano S, Shinojima N, Kuratsu J. Usefulness of the indocyanine green fluorescence endoscope in endonasal transsphenoidal surgery. J Neurosurg. 2015;122(5):1185–92.
87. Nagaya T, Nakamura YA, Choyke PL, Kobayashi H. Fluorescence-guided surgery. Front Oncol. 2017;7:314.
88. Colditz MJ, Leyen K, Jeffree RL. Aminolevulinic acid (ALA)-protoporphyrin IX fluorescence guided tumour resection. Part 2: theoretical, biochemical and practical aspects. J Clin Neurosci. 2012;19(12):1611–6.
89. Stummer W, Stepp H, Moller G, Ehrhardt A, Leonhard M, Reulen HJ. Technical principles for protoporphyrin-IX-fluorescence guided microsurgical resection of malignant glioma tissue. Acta Neurochir (Wien). 1998;140(10):995–1000.
90. Stummer W, Suero ME. Fluorescence imaging/agents in tumor resection. Neurosurg Clin N Am. 2017;28(4):569–83.
91. Kaneko S, Suero Molina E, Ewelt C, Warneke N, Stummer W. Fluorescence-based measurement of real-time kinetics of protoporphyrin IX after 5-aminolevulinic acid administration in human in situ malignant gliomas. Neurosurgery. 2019;85(4):E739–46.
92. Stummer W, Novotny A, Stepp H, Goetz C, Bise K, Reulen HJ. Fluorescence-guided resection of glioblastoma multiforme by using 5-aminolevulinic acid-induced porphyrins: a prospective study in 52 consecutive patients. J Neurosurg. 2000;93(6):1003–13.
93. Stummer W, Reulen HJ, Meinel T, Pichlmeier U, Schumacher W, Tonn JC, et al. Extent of resection and survival in glioblastoma multiforme: identification of and adjustment for bias. Neurosurgery. 2008;62(3):564–76; discussion 76.
94. Lacroix M, Abi-Said D, Fourney DR, Gokaslan ZL, Shi W, DeMonte F, et al. A multivariate analysis of 416 patients with glioblastoma multiforme: prognosis, extent of resection, and survival. J Neurosurg. 2001;95(2):190–8.
95. Sanai N, Polley MY, McDermott MW, Parsa AT, Berger MS. An extent of resection threshold for newly diagnosed glioblastomas. J Neurosurg. 2011;115(1):3–8.
96. Brown TJ, Brennan MC, Li M, Church EW, Brandmeir NJ, Rakszawski KL, et al. Association of the extent of resection with survival in glioblastoma: a systematic review and meta-analysis. JAMA Oncol. 2016;2(11):1460–9.
97. Marko NF, Weil RJ, Schroeder JL, Lang FF, Suki D, Sawaya RE. Extent of resection of glioblastoma revisited: personalized survival modeling facilitates more accurate survival prediction and supports a maximum-safe-resection approach to surgery. J Clin Oncol. 2014;32(8):774–82.
98. Orringer D, Lau D, Khatri S, Zamora-Berridi GJ, Zhang K, Wu C, et al. Extent of resection in patients with glioblastoma: limiting factors, perception of resectability, and effect on survival. J Neurosurg. 2012;117(5):851–9.
99. Coburger J, Hagel V, Wirtz CR, Konig R. Surgery for glioblastoma: impact of the combined use of 5-aminolevulinic acid and intraoperative MRI on extent of resection and survival. PLoS One. 2015;10(6):e0131872.
100. Della Puppa A, De Pellegrin S, d'Avella E, Gioffre G, Rossetto M, Gerardi A, et al. 5-aminolevulinic acid (5-ALA) fluorescence guided surgery of high-grade gliomas in eloquent areas assisted by functional mapping. Our experience and review of the literature. Acta Neurochir (Wien). 2013;155(6):965–72; discussion 72.
101. Diez Valle R, Tejada Solis S, Idoate Gastearena MA, Garcia de Eulate R, Dominguez Echavarri P, Aristu Mendiroz J. Surgery guided by 5-aminolevulinic fluorescence in glioblastoma: volumetric analysis of extent of resection in single-center experience. J Neuro-Oncol. 2011;102(1):105–13.
102. Lau D, Hervey-Jumper SL, Chang S, Molinaro AM, McDermott MW, Phillips JJ, et al. A prospective Phase II clinical trial of 5-aminolevulinic acid to assess the correlation of intraoperative fluorescence intensity and degree of histologic cellularity during resection of high-grade gliomas. J Neurosurg. 2016;124(5):1300–9.
103. Nabavi A, Thurm H, Zountsas B, Pietsch T, Lanfermann H, Pichlmeier U, et al. Five-aminolevulinic acid for fluorescence-guided resection of recurrent malignant gliomas: a phase ii study. Neurosurgery. 2009;65(6):1070–6; discussion 6–7.
104. Hickmann AK, Nadji-Ohl M, Hopf NJ. Feasibility of fluorescence-guided resection of recurrent gliomas using five-aminolevulinic acid: retrospective analysis of surgical and neurological outcome in 58 patients. J Neuro-Oncol. 2015;122(1):151–60.
105. Kamp MA, Felsberg J, Sadat H, Kuzibaev J, Steiger HJ, Rapp M, et al. 5-ALA-induced fluorescence behavior of reactive tissue changes following glioblastoma treatment with radiation and chemotherapy. Acta Neurochir (Wien). 2015;157(2):207–13; discussion 13–4.
106. Utsuki S, Miyoshi N, Oka H, Miyajima Y, Shimizu S, Suzuki S, et al. Fluorescence-guided resection of metastatic brain tumors using a 5-aminolevulinic acid-induced protoporphyrin IX: pathological study. Brain Tumor Pathol. 2007;24(2):53–5.
107. Hendricks BK, Sanai N, Stummer W. Fluorescence-guided surgery with aminolevulinic acid for low-grade gliomas. J Neuro-Oncol. 2019;141(1):13–8.
108. Jaber M, Ewelt C, Wolfer J, Brokinkel B, Thomas C, Hasselblatt M, et al. Is visible aminolevulinic acid-induced fluorescence an independent biomarker for prognosis in histologically confirmed (World Health Organization 2016) low-grade gliomas? Neurosurgery. 2019;84(6):1214–24.
109. Jaber M, Wolfer J, Ewelt C, Holling M, Hasselblatt M, Niederstadt T, et al. The value of 5-aminolevulinic acid in low-grade gliomas and high-grade gliomas lacking glioblastoma imaging features:

an analysis based on fluorescence, magnetic resonance imaging, 18F-fluoroethyl tyrosine positron emission tomography, and tumor molecular factors. Neurosurgery. 2016;78(3):401–11; discussion 11.

110. Widhalm G, Olson J, Weller J, et al. The value of visible 5-ALA fluorescence and quantitative protoporphyrin IX analysis for improved surgery of suspected low-grade gliomas [published online ahead of print, 2019 May 10]. J Neurosurg. 2019;1–10.
111. Coluccia D, Fandino J, Fujioka M, Cordovi S, Muroi C, Landolt H. Intraoperative 5-aminolevulinic-acid-induced fluorescence in meningiomas. Acta Neurochir (Wien). 2010;152(10):1711–9.
112. Cornelius JF, Slotty PJ, Kamp MA, Schneiderhan TM, Steiger HJ, El-Khatib M. Impact of 5-aminolevulinic acid fluorescence-guided surgery on the extent of resection of meningiomas--with special regard to high-grade tumors. Photodiagn Photodyn Ther. 2014;11(4):481–90.
113. Della Puppa A, Rustemi O, Gioffre G, Troncon I, Lombardi G, Rolma G, et al. Predictive value of intraoperative 5-aminolevulinic acid-induced fluorescence for detecting bone invasion in meningioma surgery. J Neurosurg. 2014;120(4):840–5.
114. Kajimoto Y, Kuroiwa T, Miyatake S, Ichioka T, Miyashita M, Tanaka H, et al. Use of 5-aminolevulinic acid in fluorescence-guided resection of meningioma with high risk of recurrence. Case report. J Neurosurg. 2007;106(6):1070–4.
115. Millesi M, Kiesel B, Mischkulnig M, Martinez-Moreno M, Wohrer A, Wolfsberger S, et al. Analysis of the surgical benefits of 5-ALA-induced fluorescence in intracranial meningiomas: experience in 204 meningiomas. J Neurosurg. 2016;125(6):1408–19.
116. Valdes PA, Bekelis K, Harris BT, Wilson BC, Leblond F, Kim A, et al. 5-Aminolevulinic acid-induced protoporphyrin IX fluorescence in meningioma: qualitative and quantitative measurements in vivo. Neurosurgery. 2014;10(Suppl 1):74–82; discussion 3.
117. Kamp MA, Fischer I, Buhner J, Turowski B, Cornelius JF, Steiger HJ, et al. 5-ALA fluorescence of cerebral metastases and its impact for the local-in-brain progression. Oncotarget. 2016;7(41):66776–89.
118. Kamp MA, Munoz-Bendix C, Mijderwijk HJ, Turowski B, Dibue-Adjei M, von Sass C, et al. Is 5-ALA fluorescence of cerebral metastases a prognostic factor for local recurrence and overall survival? J Neuro-Oncol. 2019;141(3):547–53.
119. Beez T, Sarikaya-Seiwert S, Steiger HJ, Hanggi D. Fluorescence-guided surgery with 5-aminolevulinic acid for resection of brain tumors in children--a technical report. Acta Neurochir (Wien). 2014;156(3):597–604.
120. Kim AV, Khachatryan VA. [Intraoperative fluorescence diagnosis using 5-aminolevulinic acid in surgical treatment of children with recurrent neuroepithelial tumors]. Zh Vopr Neirokhir Im N N Burdenko 2017;81(1):51–7.
121. Schwake M, Schipmann S, Muther M, Kochling M, Brentrup A, Stummer W. 5-ALA fluorescence-guided surgery in pediatric brain tumors-a systematic review. Acta Neurochir (Wien). 2019;161(6):1099–108.
122. Skjoth-Rasmussen J, Bogeskov L, Sehested A, Klausen C, Broholm H, Nysom K. The use of 5-ALA to assist complete removal of residual non-enhancing part of childhood medulloblastoma: a case report. Childs Nerv Syst. 2015;31(11):2173–7.
123. Stummer W, Rodrigues F, Schucht P, Preuss M, Wiewrodt D, Nestler U, et al. Predicting the "usefulness" of 5-ALA-derived tumor fluorescence for fluorescence-guided resections in pediatric brain tumors: a European survey. Acta Neurochir (Wien). 2014;156(12):2315–24.
124. Evers G, Kamp M, Warneke N, Berdel W, Sabel M, Stummer W, et al. 5-Aminolaevulinic acid-induced fluorescence in primary central nervous system lymphoma. World Neurosurg. 2017;98:375–80.
125. Kiesel B, Millesi M, Woehrer A, Furtner J, Bavand A, Roetzer T, et al. 5-ALA-induced fluorescence as a marker for diagnostic tissue in stereotactic biopsies of intracranial lymphomas: experience in 41 patients. Neurosurg Focus. 2018;44(6):E7.
126. Yamamoto T, Ishikawa E, Miki S, Sakamoto N, Zaboronok A, Matsuda M, et al. Photodynamic diagnosis using 5-aminolevulinic acid in 41 biopsies for primary central nervous system lymphoma. Photochem Photobiol. 2015;91(6):1452–7.
127. Yun J, Iwamoto FM, Sonabend AM. Primary central nervous system lymphoma: a critical review of the role of surgery for resection. Arch Cancer Res. 2016;4(2):1.
128. Lyons MK. The application of intraoperative fluorescence utilizing 5-aminolevulinic acid in detection of residual cerebellar hemangioblastoma following visually assessed gross total resection. Neurol India. 2011;59(4):499–500.
129. Utsuki S, Oka H, Kijima C, Miyajima Y, Hagiwara H, Fujii K. Utility of intraoperative fluorescent diagnosis of residual hemangioblastoma using 5-aminolevulinic acid. Neurol India. 2011;59(4):612–5.
130. Bernal Garcia LM, Cabezudo Artero JM, Marcelo Zamorano MB, Gilete TI. Fluorescence-guided resection with 5-aminolevulinic acid of subependymomas of the fourth ventricle: report of 2 cases: technical case report. Neurosurgery. 2015;11(Suppl 2):E364–71.. discussion E71
131. Takeda J, Nonaka M, Li Y, Komori Y, Kamei T, Iwata R, et al. 5-ALA fluorescence-guided endoscopic surgery for mixed germ cell tumors. J Neuro-Oncol. 2017;134(1):119–24.
132. Adam C, Salomon G, Walther S, Zaak D, Khoder W, Becker A, et al. Photodynamic diagnosis using 5-aminolevulinic acid for the detection of positive surgical margins during radical prostatectomy in patients with carcinoma of the prostate: a multicen-

tre, prospective, phase 2 trial of a diagnostic procedure. Eur Urol. 2009;55(6):1281–8.
133. Fukuhara H, Inoue K, Kurabayashi A, Furihata M, Shuin T. Performance of 5-aminolevulinic-acid-based photodynamic diagnosis for radical prostatectomy. BMC Urol. 2015;15:78.
134. Zaak D, Sroka R, Khoder W, Adam C, Tritschler S, Karl A, et al. Photodynamic diagnosis of prostate cancer using 5-aminolevulinic acid--first clinical experiences. Urology. 2008;72(2):345–8.
135. Nakai Y, Inoue K, Tsuzuki T, Shimamoto T, Shuin T, Nagao K, et al. Oral 5-aminolevulinic acid-mediated photodynamic diagnosis using fluorescence cystoscopy for non-muscle-invasive bladder cancer: a multicenter phase III study. Int J Urol. 2018;25(8):723–9.
136. Teixidor P, Arraez MA, Villalba G, Garcia R, Tardaguila M, Gonzalez JJ, et al. Safety and efficacy of 5-aminolevulinic acid for high grade glioma in usual clinical practice: a prospective cohort study. PLoS One. 2016;11(2):e0149244.
137. Shinoda J, Yano H, Yoshimura S, Okumura A, Kaku Y, Iwama T, et al. Fluorescence-guided resection of glioblastoma multiforme by using high-dose fluorescein sodium. Technical note. J Neurosurg. 2003;99(3):597–603.
138. Rabb MF, Burton TC, Schatz H, Yannuzzi LA. Fluorescein angiography of the fundus: a schematic approach to interpretation. Surv Ophthalmol. 1978;22(6):387–403.
139. Diaz RJ, Dios RR, Hattab EM, Burrell K, Rakopoulos P, Sabha N, et al. Study of the biodistribution of fluorescein in glioma-infiltrated mouse brain and histopathological correlation of intraoperative findings in high-grade gliomas resected under fluorescein fluorescence guidance. J Neurosurg. 2015;122(6):1360–9.
140. Hamamcioglu MK, Akcakaya MO, Goker B, Kasimcan MO, Kiris T. The use of the YELLOW 560 nm surgical microscope filter for sodium fluorescein-guided resection of brain tumors: our preliminary results in a series of 28 patients. Clin Neurol Neurosurg. 2016;143:39–45.
141. Schebesch KM, Brawanski A, Hohenberger C, Hohne J. Fluorescein sodium-guided surgery of malignant brain tumors: history, current concepts, and future project. Turk Neurosurg. 2016;26(2):185–94.
142. Dilek O, Ihsan A, Tulay H. Anaphylactic reaction after fluorescein sodium administration during intracranial surgery. J Clin Neurosci. 2011;18(3):430–1.
143. Acerbi F, Broggi M, Eoli M, Anghileri E, Cavallo C, Boffano C, et al. Is fluorescein-guided technique able to help in resection of high-grade gliomas? Neurosurg Focus. 2014;36(2):E5.
144. Chen B, Wang H, Ge P, Zhao J, Li W, Gu H, et al. Gross total resection of glioma with the intraoperative fluorescence-guidance of fluorescein sodium. Int J Med Sci. 2012;9(8):708–14.
145. Francaviglia N, Iacopino DG, Costantino G, Villa A, Impallaria P, Meli F, et al. Fluorescein for resection of high-grade gliomas: a safety study control in a single center and review of the literature. Surg Neurol Int. 2017;8:145.
146. Hohne J, Schebesch KM, de Laurentis C, Akcakaya MO, Pedersen CB, Brawanski A, et al. Fluorescein sodium in the surgical treatment of recurrent glioblastoma multiforme. World Neurosurg. 2019;125:e158–64.
147. Hong J, Chen B, Yao X, Yang Y. Outcome comparisons of high-grade glioma resection with or without fluorescein sodium-guidance. Curr Probl Cancer. 2019;43(3):236–44.
148. Koc K, Anik I, Cabuk B, Ceylan S. Fluorescein sodium-guided surgery in glioblastoma multiforme: a prospective evaluation. Br J Neurosurg. 2008;22(1):99–103.
149. Schebesch KM, Proescholdt M, Hohne J, Hohenberger C, Hansen E, Riemenschneider MJ, et al. Sodium fluorescein-guided resection under the YELLOW 560 nm surgical microscope filter in malignant brain tumor surgery – a feasibility study. Acta Neurochir (Wien). 2013;155(4):693–9.
150. Acerbi F, Broggi M, Schebesch KM, Hohne J, Cavallo C, De Laurentis C, et al. Fluorescein-guided surgery for resection of high-grade gliomas: a multicentric prospective phase II study (FLUOGLIO). Clin Cancer Res. 2018;24(1):52–61.
151. Stummer W. Poor man's fluorescence? Acta Neurochir (Wien). 2015;157(8):1379–81.
152. Stummer W, Gotz C, Hassan A, Heimann A, Kempski O. Kinetics of Photofrin II in perifocal brain edema. Neurosurgery. 1993;33(6):1075–81; discussion 81–2.
153. Suero Molina E, Wölfer J, Ewelt C. Dual-labeling with 5-aminolevulinic acid and fluorescein for fluorescence-guided resection of high-grade gliomas: technical note. J Neurosurg. 2018;128(2):399–405.
154. Suero Molina E, Ewelt C, Warneke N, et al. Dual labeling with 5-aminolevulinic acid and fluorescein in high-grade glioma surgery with a prototype filter system built into a neurosurgical microscope: technical note [published online ahead of print, 2019 Apr 26]. J Neurosurg. 2019;1–7. doi:10.3171/2018.12.JNS18242.
155. Hohne J, Hohenberger C, Proescholdt M, Riemenschneider MJ, Wendl C, Brawanski A, et al. Fluorescein sodium-guided resection of cerebral metastases-an update. Acta Neurochir (Wien). 2017;159(2):363–7.
156. Okuda T, Kataoka K, Yabuuchi T, Yugami H, Kato A. Fluorescence-guided surgery of metastatic brain tumors using fluorescein sodium. J Clin Neurosci. 2010;17(1):118–21.
157. Akcakaya MO, Goker B, Kasimcan MO, Hamamcioglu MK, Kiris T. Use of sodium fluorescein in meningioma surgery performed under the YELLOW-560 nm surgical microscope filter: feasibility and preliminary results. World Neurosurg. 2017;107:966–73.
158. da Silva CE, da Silva VD, da Silva JL. Convexity meningiomas enhanced by sodium fluorescein. Surg Neurol Int. 2014;5:3.

159. Schebesch KM, Hoehne J, Hohenberger C, Acerbi F, Broggi M, Proescholdt M, et al. Fluorescein sodium-guided surgery in cerebral lymphoma. Clin Neurol Neurosurg. 2015;139:125–8.
160. Bretonnier M, Henaux PL, Morandi X, Le Reste PJ. Fluorescein-guided resection of brain arteriovenous malformations: a short series. J Clin Neurosci. 2018;52:37–40.
161. Feng S, Zhang Y, Sun Z, Wu C, Xue Z, Ma Y, et al. Application of multimodal navigation together with fluorescein angiography in microsurgical treatment of cerebral arteriovenous malformations. Sci Rep. 2017;7(1):14822.
162. Hashimoto K, Kinouchi H, Yoshioka H, Kanemaru K, Ogiwara M, Yagi T, et al. Efficacy of endoscopic fluorescein video angiography in aneurysm surgery-novel and innovative assessment of vascular blood flow in the dead angles of the microscope. Oper Neurosurg (Hagerstown). 2017;13(4):471–81.
163. Schirmer RH, Adler H, Pickhardt M, Mandelkow E. Lest we forget you – methylene blue…. Neurobiol Aging. 2011;32(12):2325e7–16.
164. Ponce Rios JD, Yong R, Calner P. Code blue: life-threatening methemoglobinemia. Clin Pract Cases Emerg Med. 2019;3(2):95–9.
165. Polom W, Markuszewski M, Rho YS, Matuszewski M. Usage of invisible near infrared light (NIR) fluorescence with indocyanine green (ICG) and methylene blue (MB) in urological oncology. Part 1. Cent European J Urol. 2014;67(2):142–8.
166. Zakaria S, Hoskin TL, Degnim AC. Safety and technical success of methylene blue dye for lymphatic mapping in breast cancer. Am J Surg. 2008;196(2):228–33.
167. Chu M, Wan Y. Sentinel lymph node mapping using near-infrared fluorescent methylene blue. J Biosci Bioeng. 2009;107(4):455–9.
168. Tummers QR, Verbeek FP, Schaafsma BE, Boonstra MC, van der Vorst JR, Liefers GJ, et al. Real-time intraoperative detection of breast cancer using near-infrared fluorescence imaging and methylene blue. Eur J Surg Oncol. 2014;40(7):850–8.
169. van der Vorst JR, Vahrmeijer AL, Hutteman M, Bosse T, Smit VT, van de Velde CJ, et al. Near-infrared fluorescence imaging of a solitary fibrous tumor of the pancreas using methylene blue. World J Gastrointest Surg. 2012;4(7):180–4.
170. Winer JH, Choi HS, Gibbs-Strauss SL, Ashitate Y, Colson YL, Frangioni JV. Intraoperative localization of insulinoma and normal pancreas using invisible near-infrared fluorescent light. Ann Surg Oncol. 2010;17(4):1094–100.
171. Hillary SL, Guillermet S, Brown NJ, Balasubramanian SP. Use of methylene blue and near-infrared fluorescence in thyroid and parathyroid surgery. Langenbeck's Arch Surg. 2018;403(1):111–8.
172. van der Vorst JR, Schaafsma BE, Verbeek FP, Swijnenburg RJ, Tummers QR, Hutteman M, et al. Intraoperative near-infrared fluorescence imaging of parathyroid adenomas with use of low-dose methylene blue. Head Neck. 2014;36(6):853–8.
173. Al-Taher M, van den Bos J, Schols RM, Bouvy ND, Stassen LP. Fluorescence ureteral visualization in human laparoscopic colorectal surgery using methylene blue. J Laparoendosc Adv Surg Tech A. 2016;26(11):870–5.
174. van Manen L, Handgraaf HJM, Diana M, Dijkstra J, Ishizawa T, Vahrmeijer AL, et al. A practical guide for the use of indocyanine green and methylene blue in fluorescence-guided abdominal surgery. J Surg Oncol. 2018;118(2):283–300.
175. Verbeek FP, van der Vorst JR, Schaafsma BE, Swijnenburg RJ, Gaarenstroom KN, Elzevier HW, et al. Intraoperative near infrared fluorescence guided identification of the ureters using low dose methylene blue: a first in human experience. J Urol. 2013;190(2):574–9.
176. Ginimuge PR, Jyothi SD. Methylene blue: revisited. J Anaesthesiol Clin Pharmacol. 2010;26(4):517–20.
177. Te Velde EA, Veerman T, Subramaniam V, Ruers T. The use of fluorescent dyes and probes in surgical oncology. Eur J Surg Oncol. 2010;36(1):6–15.
178. Fernandez M, Javaid F, Chudasama V. Advances in targeting the folate receptor in the treatment/imaging of cancers. Chem Sci. 2018;9(4):790–810.
179. Tummers QR, Hoogstins CE, Gaarenstroom KN, de Kroon CD, van Poelgeest MI, Vuyk J, et al. Intraoperative imaging of folate receptor alpha positive ovarian and breast cancer using the tumor specific agent EC17. Oncotarget. 2016;7(22):32144–55.
180. van Dam GM, Themelis G, Crane LM, Harlaar NJ, Pleijhuis RG, Kelder W, et al. Intraoperative tumor-specific fluorescence imaging in ovarian cancer by folate receptor-alpha targeting: first in-human results. Nat Med. 2011;17(10):1315–9.
181. Kennedy GT, Okusanya OT, Keating JJ, Heitjan DF, Deshpande C, Litzky LA, et al. The optical biopsy: a novel technique for rapid intraoperative diagnosis of primary pulmonary adenocarcinomas. Ann Surg. 2015;262(4):602–9.
182. Okusanya OT, DeJesus EM, Jiang JX, Judy RP, Venegas OG, Deshpande CG, et al. Intraoperative molecular imaging can identify lung adenocarcinomas during pulmonary resection. J Thorac Cardiovasc Surg. 2015;150(1):28–35e1.
183. Predina JD, Okusanya O, D Newton A, Low P, Singhal S. Standardization and optimization of intraoperative molecular imaging for identifying primary pulmonary adenocarcinomas. Mol Imaging Biol. 2018;20(1):131–8.
184. Mahalingam SM, Kularatne SA, Myers CH, Gagare P, Norshi M, Liu X, et al. Evaluation of novel tumor-targeted near-infrared probe for fluorescence-guided surgery of cancer. J Med Chem. 2018;61(21):9637–46.
185. Predina JD, Newton AD, Keating J, Dunbar A, Connolly C, Baldassari M, et al. A phase I clinical trial of targeted intraoperative molecular imaging

for pulmonary adenocarcinomas. Ann Thorac Surg. 2018;105(3):901–8.
186. Predina JD, Newton AD, Xia L, Corbett C, Connolly C, Shin M, et al. An open label trial of folate receptor-targeted intraoperative molecular imaging to localize pulmonary squamous cell carcinomas. Oncotarget. 2018;9(17):13517–29.
187. Hoogstins CE, Tummers QR, Gaarenstroom KN, de Kroon CD, Trimbos JB, Bosse T, et al. A novel tumor-specific agent for intraoperative near-infrared fluorescence imaging: a translational study in healthy volunteers and patients with ovarian cancer. Clin Cancer Res. 2016;22(12):2929–38.
188. Shum CF, Bahler CD, Low PS, Ratliff TL, Kheyfets SV, Natarajan JP, et al. Novel use of folate-targeted intraoperative fluorescence, OTL38, in robot-assisted laparoscopic partial nephrectomy: report of the first three cases. J Endourol Case Rep. 2016;2(1):189–97.
189. Cho SS, Zeh R, Pierce JT, Jeon J, Nasrallah M, Adappa ND, et al. Folate receptor near-infrared optical imaging provides sensitive and specific intraoperative visualization of nonfunctional pituitary adenomas. Oper Neurosurg (Hagerstown). 2019;16(1):59–70.
190. Lee JYK, Cho SS, Zeh R, Pierce JT, Martinez-Lage M, Adappa ND, et al. Folate receptor overexpression can be visualized in real time during pituitary adenoma endoscopic transsphenoidal surgery with near-infrared imaging. J Neurosurg. 2018;129(2):390–403.
191. Moore LS, Rosenthal EL, de Boer E, Prince AC, Patel N, Richman JM, et al. Effects of an unlabeled loading dose on tumor-specific uptake of a fluorescently labeled antibody for optical surgical navigation. Mol Imaging Biol. 2017;19(4):610–6.
192. Rosenthal EL, Warram JM, de Boer E, Basilion JP, Biel MA, Bogyo M, et al. Successful translation of fluorescence navigation during oncologic surgery: a consensus report. J Nucl Med. 2016;57(1):144–50.
193. Suh Y, Amelio I, Guerrero Urbano T, Tavassoli M. Clinical update on cancer: molecular oncology of head and neck cancer. Cell Death Dis. 2014;5:e1018.
194. Rosenthal EL, Warram JM, de Boer E, Chung TK, Korb ML, Brandwein-Gensler M, et al. Safety and tumor specificity of cetuximab-IRDye800 for surgical navigation in head and neck cancer. Clin Cancer Res. 2015;21(16):3658–66.
195. Rosenthal EL, Moore LS, Tipirneni K, de Boer E, Stevens TM, Hartman YE, et al. Sensitivity and specificity of cetuximab-IRDye800CW to identify regional metastatic disease in head and neck cancer. Clin Cancer Res. 2017;23(16):4744–52.
196. van Keulen S, Nishio N, Fakurnejad S, Birkeland A, Martin BA, Lu G, et al. The clinical application of fluorescence-guided surgery in head and neck cancer. J Nucl Med. 2019;60(6):758–63.
197. Lamberts LE, Koch M, de Jong JS, Adams ALL, Glatz J, Kranendonk MEG, et al. Tumor-specific uptake of fluorescent bevacizumab-IRDye800CW microdosing in patients with primary breast cancer: a phase I feasibility study. Clin Cancer Res. 2017;23(11):2730–41.
198. Terwisscha van Scheltinga AG, van Dam GM, Nagengast WB, Ntziachristos V, Hollema H, Herek JL, et al. Intraoperative near-infrared fluorescence tumor imaging with vascular endothelial growth factor and human epidermal growth factor receptor 2 targeting antibodies. J Nucl Med. 2011;52(11):1778–85.
199. Wu J, Ma R, Cao H, Wang Z, Jing C, Sun Y, et al. Intraoperative imaging of metastatic lymph nodes using a fluorophore-conjugated antibody in a HER2/neu-expressing orthotopic breast cancer mouse model. Anticancer Res. 2013;33(2):419–24.
200. Metildi CA, Kaushal S, Pu M, Messer KA, Luiken GA, Moossa AR, et al. Fluorescence-guided surgery with a fluorophore-conjugated antibody to carcinoembryonic antigen (CEA), that highlights the tumor, improves surgical resection and increases survival in orthotopic mouse models of human pancreatic cancer. Ann Surg Oncol. 2014;21(4):1405–11.
201. McElroy M, Kaushal S, Luiken GA, Talamini MA, Moossa AR, Hoffman RM, et al. Imaging of primary and metastatic pancreatic cancer using a fluorophore-conjugated anti-CA19-9 antibody for surgical navigation. World J Surg. 2008;32(6):1057–66.
202. Nakajima T, Mitsunaga M, Bander NH, Heston WD, Choyke PL, Kobayashi H. Targeted, activatable, in vivo fluorescence imaging of prostate-specific membrane antigen (PSMA) positive tumors using the quenched humanized J591 antibody-indocyanine green (ICG) conjugate. Bioconjug Chem. 2011;22(8):1700–5.
203. Harlaar NJ, Koller M, de Jongh SJ, van Leeuwen BL, Hemmer PH, Kruijff S, et al. Molecular fluorescence-guided surgery of peritoneal carcinomatosis of colorectal origin: a single-centre feasibility study. Lancet Gastroenterol Hepatol. 2016;1(4):283–90.
204. Kobayashi H, Choyke PL. Target-cancer-cell-specific activatable fluorescence imaging probes: rational design and in vivo applications. Acc Chem Res. 2011;44(2):83–90.
205. Hama Y, Urano Y, Koyama Y, Kamiya M, Bernardo M, Paik RS, et al. A target cell-specific activatable fluorescence probe for in vivo molecular imaging of cancer based on a self-quenched avidin-rhodamine conjugate. Cancer Res. 2007;67(6):2791–9.
206. Mieog JS, Hutteman M, van der Vorst JR, Kuppen PJ, Que I, Dijkstra J, et al. Image-guided tumor resection using real-time near-infrared fluorescence in a syngeneic rat model of primary breast cancer. Breast Cancer Res Treat. 2011;128(3):679–89.
207. Sheth RA, Upadhyay R, Stangenberg L, Sheth R, Weissleder R, Mahmood U. Improved detection of ovarian cancer metastases by intraoperative quantitative fluorescence protease imaging in a pre-clinical model. Gynecol Oncol. 2009;112(3):616–22.
208. Urano Y, Asanuma D, Hama Y, Koyama Y, Barrett T, Kamiya M, et al. Selective molecular imaging of

viable cancer cells with pH-activatable fluorescence probes. Nat Med. 2009;15(1):104–9.
209. Whitley MJ, Cardona DM, Lazarides AL, Spasojevic I, Ferrer JM, Cahill J, et al. A mouse-human phase 1 co-clinical trial of a protease-activated fluorescent probe for imaging cancer. Sci Transl Med. 2016;8(320):320ra4.
210. Smith BL, Gadd MA, Lanahan CR, Rai U, Tang R, Rice-Stitt T, et al. Real-time, intraoperative detection of residual breast cancer in lumpectomy cavity walls using a novel cathepsin-activated fluorescent imaging system. Breast Cancer Res Treat. 2018;171(2):413–20.
211. Miampamba M, Liu J, Harootunian A, Gale AJ, Baird S, Chen SL, et al. Sensitive in vivo visualization of breast cancer using ratiometric protease-activatable fluorescent imaging agent, AVB-620. Theranostics. 2017;7(13):3369–86.
212. Unkart JT, Chen SL, Wapnir IL, Gonzalez JE, Harootunian A, Wallace AM. Intraoperative tumor detection using a ratiometric activatable fluorescent peptide: a first-in-human phase 1 study. Ann Surg Oncol. 2017;24(11):3167–73.
213. Reubi JC, Maecke HR. Peptide-based probes for cancer imaging. J Nucl Med. 2008;49(11):1735–8.
214. Staderini M, Megia-Fernandez A, Dhaliwal K, Bradley M. Peptides for optical medical imaging and steps towards therapy. Bioorg Med Chem. 2018;26(10):2816–26.
215. Lyons SA, O'Neal J, Sontheimer H. Chlorotoxin, a scorpion-derived peptide, specifically binds to gliomas and tumors of neuroectodermal origin. Glia. 2002;39(2):162–73.
216. Parrish-Novak J, Byrnes-Blake K, Lalayeva N, Burleson S, Fidel J, Gilmore R, et al. Nonclinical profile of BLZ-100, a tumor-targeting fluorescent imaging agent. Int J Toxicol. 2017;36(2):104–12.
217. Butte PV, Mamelak A, Parrish-Novak J, Drazin D, Shweikeh F, Gangalum PR, et al. Near-infrared imaging of brain tumors using the tumor paint BLZ-100 to achieve near-complete resection of brain tumors. Neurosurg Focus. 2014;36(2):E1.
218. Patil CG, Walker DG, Miller DM, Butte P, Morrison B, Kittle DS, et al. Phase 1 safety, pharmacokinetics, and fluorescence imaging study of tozuleristide (BLZ-100) in adults with newly diagnosed or recurrent gliomas. Neurosurgery. 2019;85(4):E641–9.
219. Cai QY, Yu P, Besch-Williford C, Smith CJ, Sieckman GL, Hoffman TJ, et al. Near-infrared fluorescence imaging of gastrin releasing peptide receptor targeting in prostate cancer lymph node metastases. Prostate. 2013;73(8):842–54.
220. Kossatz S, Behe M, Mansi R, Saur D, Czerney P, Kaiser WA, et al. Multifactorial diagnostic NIR imaging of CCK2R expressing tumors. Biomaterials. 2013;34(21):5172–80.
221. Ma L, Yu P, Veerendra B, Rold TL, Retzloff L, Prasanphanich A, et al. In vitro and in vivo evaluation of Alexa Fluor 680-bombesin[7-14]NH2 peptide conjugate, a high-affinity fluorescent probe with high selectivity for the gastrin-releasing peptide receptor. Mol Imaging. 2007;6(3):171–80.
222. Tipirneni KE, Warram JM, Moore LS, Prince AC, de Boer E, Jani AH, et al. Oncologic procedures amenable to fluorescence-guided surgery. Ann Surg. 2017;266(1):36–47.
223. Valdes PA, Jacobs V, Harris BT, Wilson BC, Leblond F, Paulsen KD, et al. Quantitative fluorescence using 5-aminolevulinic acid-induced protoporphyrin IX biomarker as a surgical adjunct in low-grade glioma surgery. J Neurosurg. 2015;123(3):771–80.
224. Valdes PA, Leblond F, Kim A, Harris BT, Wilson BC, Fan X, et al. Quantitative fluorescence in intracranial tumor: implications for ALA-induced PpIX as an intraoperative biomarker. J Neurosurg. 2011;115(1):11–7.
225. Kennedy JC, Pottier RH, Pross DC. Photodynamic therapy with endogenous protoporphyrin IX: basic principles and present clinical experience. J Photochem Photobiol B. 1990;6(1–2):143–8.
226. Chilakamarthi U, Giribabu L. Photodynamic therapy: past, present and future. Chem Rec. 2017;17(8):775–802.
227. Maeding N, Verwanger T, Krammer B. Boosting tumor-specific immunity using PDT. Cancers (Basel). 2016;8(10):E91.
228. Beck TJ, Kreth FW, Beyer W, Mehrkens JH, Obermeier A, Stepp H, et al. Interstitial photodynamic therapy of nonresectable malignant glioma recurrences using 5-aminolevulinic acid induced protoporphyrin IX. Lasers Surg Med. 2007;39(5):386–93.
229. Johansson A, Faber F, Kniebuhler G, Stepp H, Sroka R, Egensperger R, et al. Protoporphyrin IX fluorescence and photobleaching during interstitial photodynamic therapy of malignant gliomas for early treatment prognosis. Lasers Surg Med. 2013;45(4):225–34.
230. Johansson A, Palte G, Schnell O, Tonn JC, Herms J, Stepp H. 5-Aminolevulinic acid-induced protoporphyrin IX levels in tissue of human malignant brain tumors. Photochem Photobiol. 2010;86(6):1373–8.
231. Stummer W, Beck T, Beyer W, Mehrkens JH, Obermeier A, Etminan N, et al. Long-sustaining response in a patient with non-resectable, distant recurrence of glioblastoma multiforme treated by interstitial photodynamic therapy using 5-ALA: case report. J Neuro-Oncol. 2008;87(1):103–9.
232. Mitsunaga M, Ogawa M, Kosaka N, Rosenblum LT, Choyke PL, Kobayashi H. Cancer cell-selective in vivo near infrared photoimmunotherapy targeting specific membrane molecules. Nat Med. 2011;17(12):1685–91.
233. Aung W, Tsuji AB, Sugyo A, Takashima H, Yasunaga M, Matsumura Y, et al. Near-infrared photoimmunotherapy of pancreatic cancer using an indocyanine green-labeled anti-tissue factor antibody. World J Gastroenterol. 2018;24(48):5491–504.
234. Kiss B, van den Berg NS, Ertsey R, McKenna K, Mach KE, Zhang CA, et al. CD47-targeted near-

infrared photoimmunotherapy for human bladder cancer. Clin Cancer Res. 2019;25(12):3561–71.
235. Nagaya T, Nakamura Y, Sato K, Harada T, Choyke PL, Kobayashi H. Near infrared photoimmunotherapy of B-cell lymphoma. Mol Oncol. 2016;10(9):1404–14.
236. Sato K, Nagaya T, Choyke PL, Kobayashi H. Near infrared photoimmunotherapy in the treatment of pleural disseminated NSCLC: preclinical experience. Theranostics. 2015;5(7):698–709.
237. Keating J, Singhal S. Novel methods of intraoperative localization and margin assessment of pulmonary nodules. Semin Thorac Cardiovasc Surg. 2016;28(1):127–36.
238. Kim HK, Quan YH, Choi BH, Park JH, Han KN, Choi Y, et al. Intraoperative pulmonary neoplasm identification using near-infrared fluorescence imaging. Eur J Cardiothorac Surg. 2016;49(5):1497–502.
239. Mao Y, Chi C, Yang F, Zhou J, He K, Li H, et al. The identification of sub-centimetre nodules by near-infrared fluorescence thoracoscopic systems in pulmonary resection surgeries. Eur J Cardiothorac Surg. 2017;52(6):1190–6.
240. Okusanya OT, Holt D, Heitjan D, Deshpande C, Venegas O, Jiang J, et al. Intraoperative near-infrared imaging can identify pulmonary nodules. Ann Thorac Surg. 2014;98(4):1223–30.
241. Sekine Y, Itoh T, Toyoda T, et al. Precise Anatomical Sublobar Resection Using a 3D Medical Image Analyzer and Fluorescence-Guided Surgery With Transbronchial Instillation of Indocyanine Green. Semin Thorac Cardiovasc Surg. 2019;31(3):595–602. doi:10.1053/j.semtcvs.2019.01.004.
242. Tanaka C, Kanda M, Funasaka K, et al. Detection of indocyanine green fluorescence to determine tumor location during laparoscopic gastrectomy for gastric cancer: Results of a prospective study. Asian J Endosc Surg. 2020;13(2):160–167. doi:10.1111/ases.12710.
243. Hirche C, Dresel S, Krempien R, Hunerbein M. Sentinel node biopsy by indocyanine green retention fluorescence detection for inguinal lymph node staging of anal cancer: preliminary experience. Ann Surg Oncol. 2010;17(9):2357–62.
244. Narushima M, Yamamoto T, Ogata F, Yoshimatsu H, Mihara M, Koshima I. Indocyanine green lymphography findings in limb lymphedema. J Reconstr Microsurg. 2016;32(1):72–9.
245. Ogata F, Narushima M, Mihara M, Azuma R, Morimoto Y, Koshima I. Intraoperative lymphography using indocyanine green dye for near-infrared fluorescence labeling in lymphedema. Ann Plast Surg. 2007;59(2):180–4.
246. Adelsberger R, Fakin R, Mirtschink S, Forster N, Giovanoli P, Lindenblatt N. Bedside monitoring of free flaps using ICG-fluorescence angiography significantly improves detection of postoperative perfusion impairment(#)(). J Plast Surg Hand Surg. 2019;53(3):149–54.
247. Hitier M, Cracowski JL, Hamou C, Righini C, Bettega G. Indocyanine green fluorescence angiography for free flap monitoring: a pilot study. J Craniomaxillofac Surg. 2016;44(11):1833–41.
248. Pestana IA, Coan B, Erdmann D, Marcus J, Levin LS, Zenn MR. Early experience with fluorescent angiography in free-tissue transfer reconstruction. Plast Reconstr Surg. 2009;123(4):1239–44.
249. He P, Huang T, Fang C, Su S, Tian J, Xia X, et al. Identification of extrahepatic metastasis of hepatocellular carcinoma using indocyanine green fluorescence imaging. Photodiagn Photodyn Ther. 2019;25:417–20.
250. Kawakita N, Takizawa H, Sawada T, Matsumoto D, Tsuboi M, Toba H, et al. Indocyanine green fluorescence imaging for resection of pulmonary metastasis of hepatocellular carcinoma. J Thorac Dis. 2019;11(3):944–9.
251. Lee JYK, Pierce JT, Zeh R, Cho SS, Salinas R, Nie S, et al. Intraoperative near-infrared optical contrast can localize brain metastases. World Neurosurg. 2017;106:120–30.
252. Lee JYK, Pierce JT, Thawani JP, Zeh R, Nie S, Martinez-Lage M, et al. Near-infrared fluorescent image-guided surgery for intracranial meningioma. J Neurosurg. 2018;128(2):380–90.
253. Coburger J, Engelke J, Scheuerle A, Thal DR, Hlavac M, Wirtz CR, et al. Tumor detection with 5-aminolevulinic acid fluorescence and Gd-DTPA-enhanced intraoperative MRI at the border of contrast-enhancing lesions: a prospective study based on histopathological assessment. Neurosurg Focus. 2014;36(2):E3.
254. Schucht P, Beck J, Abu-Isa J, Andereggen L, Murek M, Seidel K, et al. Gross total resection rates in contemporary glioblastoma surgery: results of an institutional protocol combining 5-aminolevulinic acid intraoperative fluorescence imaging and brain mapping. Neurosurgery. 2012;71(5):927–35; discussion 35–6.
255. Schucht P, Knittel S, Slotboom J, Seidel K, Murek M, Jilch A, et al. 5-ALA complete resections go beyond MR contrast enhancement: shift corrected volumetric analysis of the extent of resection in surgery for glioblastoma. Acta Neurochir (Wien). 2014;156(2):305–12; discussion 12.
256. Stummer W, Tonn JC, Goetz C, Ullrich W, Stepp H, Bink A, et al. 5-Aminolevulinic acid-derived tumor fluorescence: the diagnostic accuracy of visible fluorescence qualities as corroborated by spectrometry and histology and postoperative imaging. Neurosurgery. 2014;74(3):310–9; discussion 9–20.
257. Wilbers E, Hargus G, Wolfer J, Stummer W. Usefulness of 5-ALA (Gliolan(R))-derived PPX fluorescence for demonstrating the extent of infiltration in atypical meningiomas. Acta Neurochir (Wien). 2014;156(10):1853–4.

258. Inoue K, Matsuyama H, Fujimoto K, Hirao Y, Watanabe H, Ozono S, et al. The clinical trial on the safety and effectiveness of the photodynamic diagnosis of non-muscle-invasive bladder cancer using fluorescent light-guided cystoscopy after oral administration of 5-aminolevulinic acid (5-ALA). Photodiagn Photodyn Ther. 2016;13:91–6.
259. Alkalay R, Alcalay J, Maly A, Ingber A, Fritsch C, Ruzicka T, et al. Fluorescence imaging for the demarcation of basal cell carcinoma tumor borders. J Drugs Dermatol. 2008;7(11):1033–7.
260. Gao RW, Teraphongphom N, de Boer E, van den Berg NS, Divi V, Kaplan MJ, et al. Safety of panitumumab-IRDye800CW and cetuximab-IRDye800CW for fluorescence-guided surgical navigation in head and neck cancers. Theranostics. 2018;8(9):2488–95.
261. Nishio N, van den Berg NS, van Keulen S, et al. Optimal Dosing Strategy for Fluorescence-Guided Surgery with Panitumumab-IRDye800CW in Head and Neck Cancer. Mol Imaging Biol. 2020;22(1):156-164. doi:10.1007/s11307-019-01358-x.
262. Rosenthal EL, Warram JM, Bland KI, Zinn KR. The status of contemporary image-guided modalities in oncologic surgery. Ann Surg. 2015;261(1):46–55.
263. Vahrmeijer AL, Hutteman M, van der Vorst JR, van de Velde CJ, Frangioni JV. Image-guided cancer surgery using near-infrared fluorescence. Nat Rev Clin Oncol. 2013;10(9):507–18.
264. Xi L, Jiang H. Image-guided surgery using multimodality strategy and molecular probes. Wiley Interdiscip Rev Nanomed Nanobiotechnol. 2016;8(1):46–60.

14 A Virtual Reality for the Digital Surgeon

Diana Velazquez-Pimentel, Thomas Hurkxkens, and Jean Nehme

Overview of Virtual Reality in Surgery

Virtual reality (VR) is "an artificial environment experienced through sensory stimuli provided by a computer and in which one's actions partially determine what happens in the environment" [1]. The term was first coined in 1965 by Ivan Sutherland, in a pivotal article that first described VR as an "ultimate display [...] within which the computer can control the existence of matter" [2]. Later, the concept saw widespread commercialization in the production and release of the first consumer VR tool for the gaming industry (Autodesk VR, 1988). The application of VR in healthcare research quickly followed and focused on visualizing complex medical data for the purposes of preoperative planning and endoscopic training (MIST-VR, 1997) [3–6].

Rapid successive breakthroughs in information technology have resulted in the rise of affordable VR headsets, including the Oculus Rift (Facebook), the HTC Vive (HTC), and the Sony PlayStation VR (Sony) [7]. This digital revolution has generated a surge of entrepreneurial (Fig. 14.1) and academic (Fig. 14.2) activities worldwide (Fig. 14.3), in a race to study the processes and effects of VR in the real world and translate them to practical applications [7, 8]. Thanks to the combined efforts of all stakeholders, VR is in a unique position to succeed as a digital platform.

Surgery is among the most influential adopters of VR. According to a recent cluster and network analysis, surgery alone made up 7.7% of all VR-related academia. Other notable clinical applications are outlined in Table 14.1. In surgical care (Fig. 14.4), VR represents more than a series of point solutions. Instead, it acts as an enterprise capability to optimize education, enhance productivity, and consolidate available resources without compromising patient safety. Culturally, VR plays an important and ongoing role in a paradigm shift towards patient-centric delivery of healthcare.

This chapter defines VR and outlines how this technology can be utilized in healthcare. Current use-case of VR in surgery, including barriers to implementation, future avenues in research and real-world applications are discussed.

D. Velazquez-Pimentel
Barts and the London School of Medicine and Dentistry, London, UK

T. Hurkxkens
Digital Learning Hub, Imperial College London, London, UK

J. Nehme (✉)
Digital Surgery, London, UK
e-mail: jean@touchsurgery.com

S. Atallah (ed.), *Digital Surgery*, https://doi.org/10.1007/978-3-030-49100-0_14

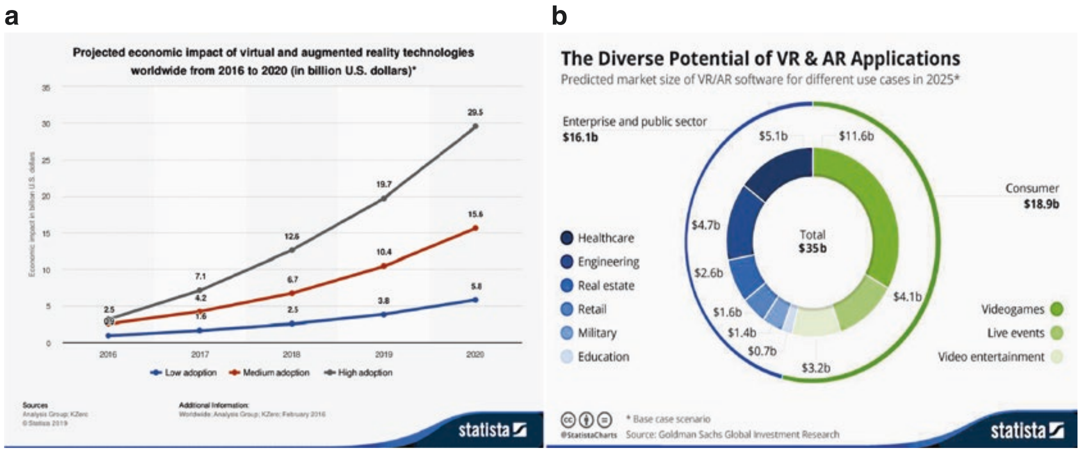

Fig. 14.1 Predicted market size for VR technologies. (**a**) The projected economic impact of VR and augmented reality technologies from 2016 to 2020, depending on adoption. (**b**) The predicted market size of VR and augmented reality software for different use cases by 2025. Data from [9]

Fig. 14.2 Timeline of results for PubMed searches. Graph shows the total number of PubMed indexed articles per year for various related search terms between 1985 and 2018

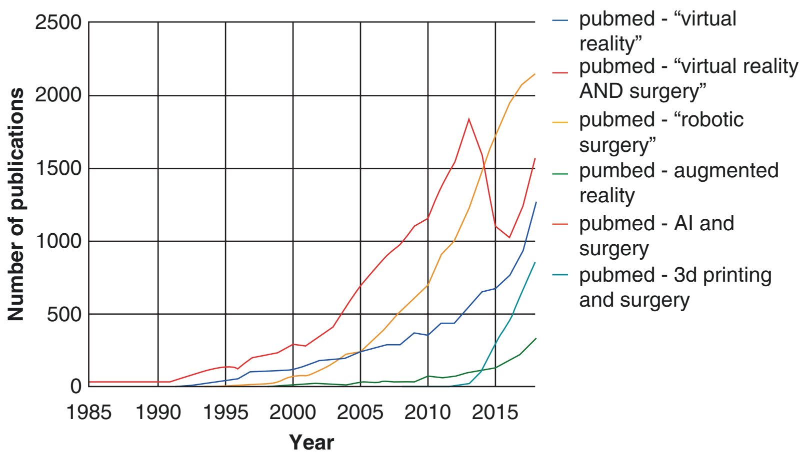

How Is the Technology Delivered?

This section explores the delivery of VR technology. To achieve immersion and presence in a 3D environment, VR technology must successfully create false perceptions of real stimuli – an illusion. Illusions in VR can be classified into place illusions, plausibility illusions, and avatar embodiment illusions. These are achieved using visual and auditory stimuli, with varying levels of haptic feedback and vestibular displays.

Broadly speaking, there are three tiers of VR immersion, outlined in Table 14.2 [10–12]. Despite sharing the same key components, VR systems differ in their degrees of immersion, and each system has its inherent advantages and limitations to the user experience.

VR visual content can be either computer-generated animations or 360-degree-stitched video (recorded or live-streamed) [3, 10]. In computer-generated content, a user can actively participate in a scene that can react to their actions in real time. In video content, current video capture technology limits participation to a single locus, restricting the user to the role of an observer only.

Fig. 14.3 Visual representation of countries involved in VR research. The node dimension represents the centrality of the country involved. (From: Cipresso, Giglioli, Raya, and Riva [3] (© 2018 Open Access))

Table 14.1 Results from network and cluster analysis

%	Frequency	Subject category (for the period)
42.15	9131	Computer Science (1990–2016)
28.66	6210	Engineering (1990–2016)
8.21	1779	Psychology (1990–2016)
7.15	1548	Neurosciences and neurology (1992–2016)
5.85	1418	Surgery (1992–2016)
4.80	1040	Neurosciences (1992–2016)
4.74	1027	Imaging science and photographic technology (1992–2016)
4.30	931	Education and educational research (1992–2016)
3.92	849	Robotics (1992–2016)
%	**Frequency**	**Subject category (2011–2016)**
29.80	2311	Computer science
25.44	1973	Engineering
11.10	861	Neurosciences and neurology
9.32	723	Psychology
7.70	597	Surgery
7.53	584	Neurosciences
6.02	467	Education and educational research
5.54	430	Rehabilitation
4.42	343	Clinical neurology
3.92	304	Material science

Data from [3]

Delivering the VR User Experience

Visual Apparatus

Visual stimuli can be delivered through everyday flat screens, VR headsets, or more complex systems such as the Cave Automatic Virtual Environment (CAVE) (Table 14.3) [13].

Haptic, Tactile, and Vestibular Displays

Displays provide visual material, binaural stimuli, and tactile and/or haptic feedback to create a 3D virtual environment, with which the user can freely interact (Table 14.4) [10]. VR applications in surgery often make use of haptic feedback. Haptic devices offer tactile and force stimuli to the user to emulate cutaneous and kinesthetic sensations that would be caused by objects in the surgical field.

Fig. 14.4 VR in surgery. A summary of the different use cases, including education, public health promotion, preoperative planning, intraoperative support, postoperative management, and healthcare planning

Table 14.2 Degrees of immersion

VR immersion	Description	Advantages	Examples in surgery
Non-immersive systems	Use desktop computers to reproduce 2D images of the world	Cheap and simple	Touch surgery[a], Lapmentor[b], EchoPixel[c]
Semi-immersive systems	Provide a dynamic 3D scene on a monitor, coupled to the head position of the user	Accessible technology	Touch surgery immersive training[a], OssoVR[d], Immersive touch[e], Fundamental VR[f]
Immersive systems	Provide a complete simulation supporting several sensory output devices, e.g., head-mounted displays, audio devices, haptic devices	Enhanced stereoscopic view of the environment, multiple sensory outputs including haptic technology	Lapmentor VR[b], OramaVR[g]

Data from [10–12]
[a]www.touchsurgery.com
[b]www.simbionix.com
[c]www.echopixeltech.com
[d]www.ossovr.com
[e]www.immersivetouch.com
[f]www.fundamentalvr.com
[g]www.oramavr.com

Table 4.3 Types of VR visual feedback

Visual system	Description	Examples
Desktop display	Single screen displays a virtual world with which the user can interact using a joystick or touch technology as their own avatar	iPhone[a], Nintendo DS[b], Virtual Worlds[c], Second Life[d]
Large-scale screens	Large-scale screen delivers VR to the user. Eye-tracking and motion-tracking allow the user to interact	MyRide+[e]
Phone-based HMD	Mobile phone is placed within a head-mounted display for the user to view VR content	Google Cardboard[f]
Tethered HMD	HMD is connected to a high-powered PC to view VR content. Offers the highest quality VR	HTC Vive[g], Oculus Rift[h]
Standalone HMD	Cordless headset displays VR content without requiring a phone or being tethered to a PC. The computer is within the headset	Oculus Go[h]
CAVE Automatic Virtual Environment	Projection-based VR display recreates a scene by projecting and displaying a VR environment on three or six walls	VisCube[i]
EON iDome	Geodesic projection-based VR allows immersion for up to 24 users	EON iDome[j]

Data from [13]
[a]www.apple.com
[b]www.nintendo.com
[c]www.virtualworlds.co.uk
[d]www.secondlife.com
[e]www.fitness-gaming.com
[f]vr.google.com
[g]www.vive.com
[h]www.oculus.com
[i]www.visbox.com
[j]www.eonreality.com
Note: HMD is an abbreviation of head-mounted display

Table 14.4 Haptic, tactile, and vestibular displays

Display	Description	Benefits	Examples
Tactile display	Wearable devices that provide proprioceptive, light touch, and crude touch feedback to the user	Facilitates fine manipulation of virtual objects Can be combined with end-effector displays Cheaper Mobile	Haptx Glove[a], VR Gluv[b], Manus VR[c] Sense Glove[d] Pin actuators Haptic suits
End-effector display	Provides a means to simulate grasping and probing objects	World-grounded or body-grounded systems	Lapmentor VR[e]
Robotic shape display	Uses robotics to present physical objects to user's fingertips	Provides realism and authenticity Can integrate 4D effects	Robotic arms
Passive haptics	Use the physical forms of real objects to portray physical features in a virtual world	Simplistic, inexpensive way to provide haptic feedback	Props
Vestibular display	Motion-based platforms, moving platforms, and other adjunct devices that replicate movement	Provides realism, allows user to interact using locomotion	Omni by Virtux[f]
Other types of displays include olfactory and gustatory			

Data from [10]
[a]https://haptx.com/
[b]https://www.vrgluv.com/
[c]https://manus-vr.com/
[d]https://www.senseglove.com/
[e]https://simbionix.com/simulators/lap-mentor/
[f]https://www.virtuix.com/

Virtual Reality as an Emerging Educational Strategy

Historically, surgical training has relied on Halsted's model of "see one, do one, teach one" [14, 15]. This apprenticeship model is no longer appropriate, as it cannot reliably monitor or predict the output of a training program. The apprenticeship model lacks reliable, objective feedback, which is essential for continuing professional development and is also known to be closely associated with risks to patient safety. Ongoing shifts in surgical culture, specifically the evolution of technically demanding skills and increasingly short-term trainer-trainee relationships, have demanded a change in traditional educational approaches. Time spent out of the operating room (OR) must now be efficiently utilized to bridge conceptual and technical gaps in learning [16–18]. VR presents a unique opportunity to drive change in surgical training and to provide coaching of necessary skills in a risk-free, low-pressure environment [19]. VR inherently requires active learner engagement, which is widely recognized as a cornerstone of effective learning [20–22].

Evidence to support VR simulations in medical education is abundant. In response, institutions have rapidly adopted fully staffed VR simulation centers to improve their training programs. VR simulations present several advantages over physical high-fidelity simulations, including learner engagement, cost, and convenience. Examples range from basic box trainers and simple desktop applications to complex haptic simulators [23–25].

VR technologies are continually changing the way humans interact with their surrounding environments, and this phenomenon has particular applications in experiential learning. It has been long established that a blended approach to learning is more effective than an isolated training modality, so, rather than being a "blue ocean" approach, VR should be used in conjunction with existing educational methods. It is vital that educators recognize the place of VR in the pedagogical landscape for its potential to be fully realized (Fig. 14.5) [26–33].

In surgical training, VR can improve surgical skills using relatively simple assignments, such as 3D exploration of anatomical structures (Box 14.1), or more sophisticated high-fidelity simulations involving a virtual OR (Box 14.2) [34, 35].

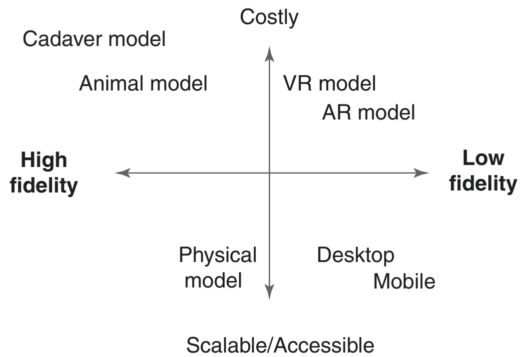

Fig. 14.5 Training models in surgery, demonstrating the different approaches to model-based education according to fidelity and scalability

These applications allow surgeons to rehearse procedures, refine skills, and refresh knowledge to improve both technical and cognitive masteries (Box 14.3) [36, 37]. Given the zero-risk environment, VR enables surgeons to encounter and experience complicated (Box 14.4), risky, or rare (Box 14.5) surgical cases to diversify their training portfolios. Moreover, VR can transform traditional video- or paper-based training courses into engaging, immersive e-learning experiences. Such VR training experiences can include basic mandatory courses i.e. fire safety, or more complicated technical courses on the use of surgical tools using "digital twins" (Box 14.6) [38].

In addition to technical skills, VR can be used to develop cognitive and behavioral competencies such as situational awareness, cue recognition, communication, teamwork, and decision-making, many of which are formally mandated by medical governing bodies like the GMC or ACGME. The development of "soft" skills central to effective surgical care should be integrated into the training of the entire OR team (Boxes 14.7 and 14.8). Furthermore, VR promotes a flexible, interdisciplinary approach to education by facilitating multiuser involvement and removing geographical barriers. Despite the known benefits of a multidisciplinary approach, current educational training sessions are typically conducted in silos, due to geographic, logistic, and scheduling restraints [39]. VR solutions allow training sessions to transcend these limitations such that members of the multidisciplinary team can train together in a computer-generated environment (Box 14.9) [40, 41].

Education Case Examples

Box 14.1 Teaching Medical Anatomy
Although cadavers are considered the gold standard for teaching human anatomy, there are substantial financial, ethical, and logistical constraints to their use, which have led to poor anatomical training practices worldwide [42]. VR allows structural anatomy to be visualized with stereopsis, potentially enabling faithful replication of human anatomy in a purely digital format to reduce the reliance on cadavers [43]. To date, there have been some data favoring VR technologies in anatomical education, although there is no definitive data that VR teaching is superior to non-cadaveric traditional modalities. Regardless, VR is a unique and powerful solution to the current deficits in anatomical training [36, 44, 45]. Educators at Lucile Packard Children's Hospital, Stanford, have used VR to help students and residents understand complex congenital heart defects. This method has since been validated as both viable and effective in a small pilot study [46]. Using a VR headset, students can inspect and manipulate virtual models of common congenital lesions, drawn from a specially built VR library. Each educational program is designed to provide a deeper understanding of the physiological and hemodynamic sequelae of one specific anatomical lesion [47].

Box 14.2 Familiarization with Surgical Workflows
In classic medical education, students and residents act as spectators in a surgical environment. The goal is to familiarize themselves with workflow of a surgical procedure. However, space and time constraints means the learning experience is similarly limited. Enterprises such as Digital Surgery (https://digitalsurgery.com/) have developed educational modules that allow a user to undergo the same observational experience through a VR headset. The experience, is enhanced by VR, by allowing them to participate in the procedure in a risk-free environment (Fig. 14.6). Digital Surgery has also developed a non-immersive VR mobile application, Touch Surgery [48, 49], which was proven effective for cognitive training and transferability of skills in a recent controlled study [50]. Among other advantages, the app enables the provision of high-quality training to surgeons in low- and middle-income countries [51].

Fig. 14.6 VR external fixation demo. A screenshot from Digital Surgery's VR module for open reduction and external fixation. Image shows a fully equipped operating room where the user can interact with the environment and carry out the procedure in real time. (Copyright (2019) Digital Surgery Limited with permission)

Fig. 14.7 OssoVR open knee surgery simulation. An open knee surgery screenshot from a training module where the user can interact in the operating room in real time. (Courtesy of OssoVR, with permission)

Box 14.3 Developing Technical Skills
Luciano et al. used a VR simulator made by ImmersiveTouch (https://www.immersivetouch.com) to simulate percutaneous spinal needle placement. Other companies, including ORamaVR (http://oramavr.com/) and OssoVR (https://ossovr.com/), have developed training modules to rehearse technical skills demanded by orthopedic surgery (Fig. 14.7). Their study recorded a significant improvement in performance accuracy between each placement attempt [52]. Similarly strong evidence exists for the transfer of laparoscopic skills in laboratory environments [53]. However, to date, no studies have evidenced demonstrable translation of technical skills to clinical practice, whether the improvement or retention thereof.

Box 14.4 Managing Crisis Scenarios
VR could allow surgical residents to troubleshoot and manage real-life crises. Abelson et al. described a VR module where there is a loss of laparoscopic visualization during a cholecystectomy, a critical situation that users are required to resolve. The authors envisaged a future tool where users can continue to operate, live through the repercussions of their errors, and ultimately fix their mistakes in a real-time VR environment [54].

Box 14.5 Experiencing Rare Procedures
Kuernov et al. described user acceptance and effectiveness of a VR module for a laparoscopic adrenalectomy procedure. This is a rare and complex procedure that many surgeons may never encounter in their surgical careers. The authors found high user acceptability among residents, fellows, and experienced surgeons. More importantly, their survey results showed that participants preferred the VR module, with expert debriefing and reflection, over one-on-one instruction [55].

Fig. 14.8 A virtual hospital. Clinical modules designed and created on Second Life. In this simulation, users can interact in the 3D hospital to diagnose and manage patients with an acute abdomen at varying levels of difficulty. (From Patel et al. [57]. Reprinted with permission from Elsevier)

Box 14.6 Applications in Medical Device Industry

Digital Surgery (https://digitalsurgery.com/) has deployed VR to provide high-fidelity training for medical device setup. Bespoke VR simulations allow high-quality training and refresher courses to be delivered to healthcare professionals in an engaging manner [56]. Digital twins have great application in research and development, where complex OR systems and interactions can be tested, controlled, and optimized in simulations before commitment to manufacture.

Box 14.7 Realistic Decision-Making in a Virtual Hospital

Patel et al. described a 3D virtual world accessible via desktop browser, where surgical trainees are required to manage a series of nine cases. The VR program, created on Second Life (https://secondlife.com/), requires the assessment and management of the acute abdomen (lower gastrointestinal bleed, acute pancreatitis, small bowel obstruction) at three levels of difficulty. Figure 14.8 shows a virtual patient receiving initial management and the surgeon avatar reviewing blood results. The study was able to confirm face, content, and construct validity for eight of the nine cases and demonstrated assessment of decision-making skills in VR [57].

Box 14.8 Training for Situational and Spatial Awareness

In a recent paper, Izard et al. described the use of a 360-degree camera in an OR, footage from which was stitched together for the purposes of training in-OR situational awareness. They described a spherical virtual environment that immersed the user in the recording of the OR as if they were physically present. A video of the technology is available online (https://www.youtube.com/watch?v=IQCSzc7oACA&feature=youtu.be) [58]. VR has also been deployed to immerse a user in emergency situations in the OR using 3D video recordings (https://www.youtube.com/watch?v=CfZPbw4qoP4). Similar VR methods have been successfully used to train healthcare professionals to respond to mass-casualty incidents [59].

Box 14.9 Team Training
VR allows multiple users to coexist in a virtual environment. Touch Surgery Immersive Training by Digital Surgery (https://digitalsurgery.com/) enables simultaneous team training for all members of the multidisciplinary team, regardless of geographic boundaries (https://www.youtube.com/watch?v=3tpnRFshvsA). Figure 14.9 shows a surgeon and an assistant working together. The participants can interact in real time, and they are required to work together to complete the specified task.

Virtual Reality as a Surgical Support Tool

VR has received increasing attention as a surgical support tool, which has led to the advent of VR solutions to streamline the delivery of surgical care.

Preoperative Planning

Preoperative planning refers to computer-assisted modeling and visualization of anatomy to define, practice, and refine a patient-specific operative workflow.

Today, image data, including computerized tomography (CT) scans and magnetic resonance imaging (MRI), can be processed and projected on VR headsets to allow surgeons to engage in novel and patient-specific surgical planning (Boxes 14.10 and 14.11). This is a unique way to plan for complex procedures, such as those that deal with intricate bony structures (e.g., cranial, maxillary, or pelvic bones).

Equally, VR image data can be deployed to inform the approach of procedures that require special attention. Its use has been documented for maxillofacial, neurological, hepatic, orthopedic, and fetal procedures [60–63]. Some of these studies enhance user immersion using adjunct haptic devices. For example, dynamic mesh models can facilitate tactile feedback during bone

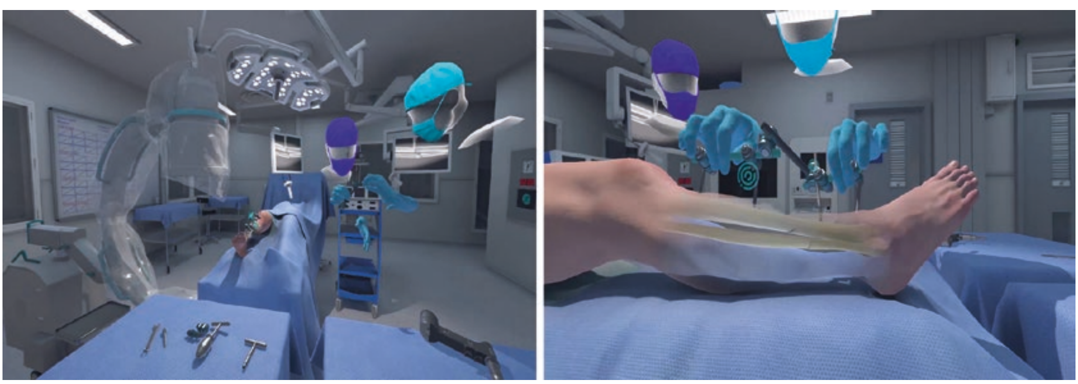

Fig. 14.9 Surgeon and assistant work together in Touch Surgery Immersive Training. This figure demonstrates two users working together in a VR module. Users can interact verbally and physically in the virtual environment. In this image, one user (*purple*) is able to coach and mentor the second user (*blue*) and assist the virtual surgery in real time. (© Digital Surgery Limited, with permission)

drilling, cutting, and burring. However, current limitations in haptic outputs narrow the benefits and scope of this advancement.

Intraoperative Surgical Navigation

Surgical navigation describes systems, software or otherwise, that provide real-time intraoperative support. This can include surgical plans or patient-specific anatomical guides. Similar to GPS navigation systems, software can perform complex calculations to determine the best approach to a particular case when given predetermined constraints, such as the required outcome and/or initial patient characteristics (Box 14.11) [64].

VR can be used by the surgeon to rehearse a surgical workflow and to prepare an OR team for a surgeon- or patient-specific approach [65, 66]. In the OR, workflows can be displayed for non-immersive real-time support (Box 14.12) or enhanced using augmented reality, as discussed elsewhere. Similarly, VR can be used by a nonoperating surgeon for remote proctoring, or even remote surgery, which can be particularly useful to ensure safe access to surgery in rural areas, for instance, during military deployments [67].

Postoperative Reflection

Reflection is a process of seeking an understanding of self or situations to inform future actions. It is accepted that reflection is a valuable learning technique for healthcare professionals, and its importance is highlighted by numerous bodies that govern healthcare education [68, 69]. VR can advance reflection by helping healthcare professionals to relive a situation that they have encountered. Individuals can rewatch themselves or others in a 3D virtual environment to facilitate meaningful discussion centered around improving patient outcomes [70, 71].

Clinical Governance

Space optimization and sustainable design are essential to high-quality, efficient care in hospitals. A recent review suggested that evidence-based design to optimize configurational and environmental issues had positive effects on workflow, workplace culture, and interactions between stakeholders, including surgeons, nurses, patients, caregivers, and next of kin [72]. Changing population needs, increasing demands on healthcare systems, and the growing role of medical devices have led to complex OR space optimization [73].

VR allows OR managers and hospital commissioners to experiment with the layout and space usage of an OR, or indeed a hospital, prior to making infrastructure changes. VR studies of space dynamics can improve the layout of an OR depending on the requirements of specific procedures and equipment (Box 14.13) [74].

Evidence shows that appropriate OR setup enhances ergonomics, team coordination, and surgical productivity and reduces the overall time taken to complete an operation. All of these outcomes have clear benefits for the hospital, the surgeon, and the patient [83]. Moreover, VR modeling can inform risk management strategies, including policies to minimize radiation or define sterility barriers, with the ultimate goal of achieving better patient safety and limiting the impacts of occupational hazards [75, 76].

Surgical Practice Case Examples

Box 14.10 Manipulation of Medical Image Data

Stanford engineers have described a new software system that combines medical image data of the brain from different sources (CT, MRI, angiograms) to create a 3D model of an individual patient's anatomy. A model thus created can be manipulated by physicians in VR. This "window into the brain" ensures anatomical deficits, such as aneurysms, are clearly identified and understood prior to a surgical procedure. The technology has already been successfully applied to allow surgical residents to view angiograms in VR in preparation for surgery [77]. EchoPixel (https://www.echopixeltech.com) has created a non-immersive VR system for 3D visualization, derived from CT scans of the brain, chest, abdomen, and pelvis. EchoPixel technology is already used at over 20 sites in the United States, and they are seeking to build an evidence base to support its wider adoption, with a current focus on real-life cases of congenital heart anomalies [78–80].

Box 14.11 Surgical Planning
Babel VR (https://www.cbrg.ox.ac.uk/cbrg/babelVR.html) is an open source software tool developed by researchers at Oxford University. It renders medical image data using meshes, machine learning, and segmentation to maximize clinical utility and to permit the addition of 3D annotations and real measurements (https://www.youtube.com/watch?time_continue=25&v=xVlCiwK35Cw) [81]. ImmersiveTouch (https://www.immersivetouch.com/) is a pioneering company whose technology makes a digital twin of image data to provide an unobstructed VR view, thus facilitating the reading and analysis of critical scan information. Their technology has received FDA approval and CE marking and is in use in hospitals in Baltimore, Chicago, and Austin.

Box 14.12 Non-immersive in-OR Assistance
Surgeons at Mount Sinai described the use of the CaptiView operating microscope, which features integrated graphics (https://www.leica-microsystems.com/products/surgical-microscopes/p/captiview/) to enhance real-time visualization of anatomy during neurosurgical procedures. CaptiView is a unique one-device solution that delivers enhanced imaging through a surgical microscope. The integration of VR into the microscope can potentially avoid interruption of the surgical flow and minimizes the impact of gross movements from the surgeon. This device is an example of a bridge between VR and augmented reality (Fig. 14.10).

Box 14.13 Space Planning in the OR
Commercial software packages such as Virtual Worlds (https://www.virtualworlds.co.uk/) and Planner 5D (https://planner5d.com/) can facilitate OR planning. Digital Surgery has developed a prototype OR planner, which has demonstrated both feasibility and interest from OR staff (Fig. 14.11) [82].

Future Applications

> Reality is nothing more than experiences interpreted by the brain whether perceived by physical senses in the real word or by electrical impulses in the virtual world – Micheal Abrash

Schmidt and Cohen (2013) postulated that, by 2025, advancements in technology would have made the “physical self” indistinguishable from the “virtual self”. In their provocative discourse, the authors described a world where humans could live simultaneously in both the real world and a computer-generated world [84]. Experts agree that VR brings a new wave of digital technologies with the potential to fundamentally change the nature of human interaction and transform the world as we know it. This section considers current limitations and emerging applications of VR in healthcare.

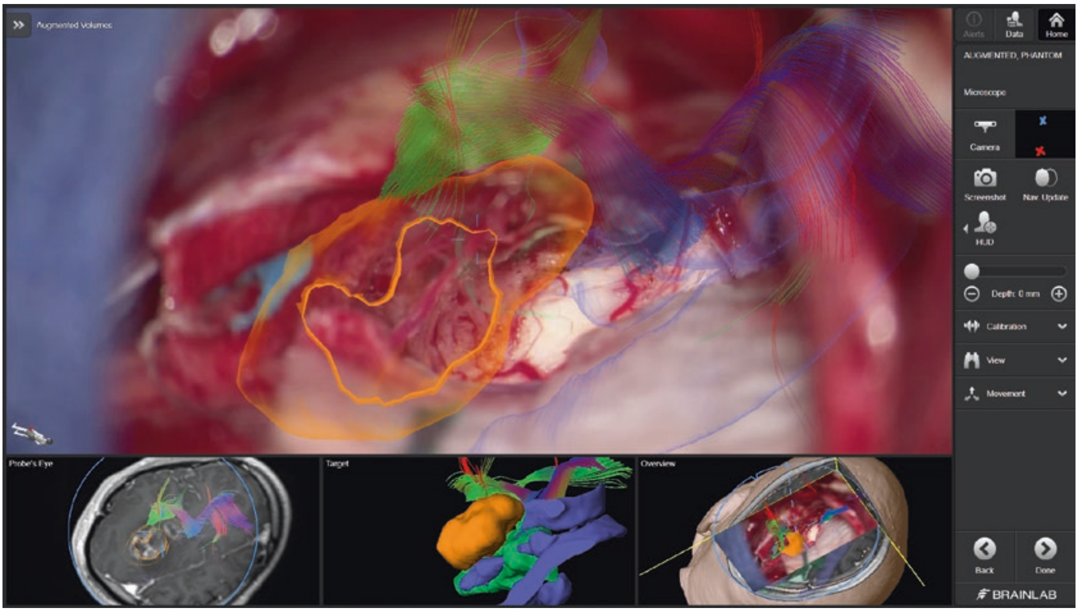

Fig. 14.10 CaptiView microscope. This figure shows the CaptiView microscope being used for brain surgery. The real-time image shows imaging data to minimize intraoperative disruption. (© 2020 Brainlab AG, with permission)

Fig. 14.11 A VR operating room planner. A 3D space planner where users can model and simulate changes in equipment and layout in an OR. (Copyright (2019) Digital Surgery Limited, with permission)

Barriers to Implementation

Surgical Education

A recent systematic review by Kyaw et al. (2019), focusing on VR training for healthcare professionals, found no applicable studies before 2005. This reflects the relatively nascent stage of VR in medical education [37]. Therefore, as one would expect, hard evidence of the efficacy of VR in surgical training remains largely unsubstantiated, especially when compared with VR training in other domains [85]. To date, skill transfer validity has only been demonstrated in cadavers and ex vivo tissue. Currently, no relevant data concerning the clinical effects of VR simulator training have been published. Future research must aim to prove the clinical utility of VR training, i.e. improved patient outcomes, reduced training costs, and/or reduced care costs [19].

It is clear that VR has the potential to transform traditional surgical education curricula, including high-stakes examinations, outcome assessments, accreditation, and revalidation. As a central component of this shift, educators must generate and regularly revise curricula that can guarantee surgical trainees exit their training programs with the necessary range of clinical, technical, and humanistic skills to deliver the best quality surgical care [41]. Parallel to ongoing research in curricula for robotic surgeons, this exercise ensures the standardization and vetting of clear learning objectives. Innovators can ensure VR training technology develops to meet said objectives, and data generated can be used to inform and justify ongoing research efforts to leverage VR technology [86].

Combined, these measures would allow research groups to assure the effectiveness (i.e. ability to meet objectives) and efficiency (i.e. cost and time savings) of VR training simulators where current evidence is lacking.

Surgical Care

The healthcare industry is poised for disruption. However, in current times, real-world clinical applications of VR remain in their nascent stages. Considerable efforts are required to integrate VR into healthcare systems.

"In vitro" endeavors have shown compelling results. Subsequent breakthroughs and widespread clinical adoption are likely to ensue once rigorous, controlled, and randomized studies prove the clinical efficacy of VR [65]. Given the high potential for change, ethics and governance boards must allow acceptable patient risk for clinical validation of VR. Similarly, research groups, academics, and hospitals should prioritize research in this field at all stages of surgical care. Valid, high-quality data will increase the availability of funding for further development of VR, and the adoption of VR technology in clinical environments will follow.

Other barriers to implementation mostly relate to production costs. Unlike other industries, healthcare cannot afford to oversimplify VR simulations, as doing so risks diminishing the core validity outcome measures that are critical for data generation, implementation, and adoption. This issue has been highlighted by Sethia et al. (2015) and Kim et al. (2017). Both reviews agreed that current VR solutions tend to compromise on image processing, which results in the loss of subtle features of human anatomy [65, 87]. Research groups should use the most up-to-date software and hardware available to achieve the acceptable fidelity that can translate to tangible patient outcomes, which in turn would justify the higher expenditure.

Existing VR Technology

According to Slater (2009), achieving a sense of presence in a virtual world is dependent on two primary components: "place illusion" and "plausibility illusion" [88]. While clinicians find ways to prove clinical utility, the engineering community is working towards optimizing the user experience and telepresence to achieve full immersion. In the last 18 months alone, technological developments have had a vast impact on user comfort and ergonomics, with Oculus announcing that their latest technology is able to track hand movements with computer vision, eliminating the need for restrictive controllers. Although "tech-stack" advancements are relentless, key challenges remain, including computer processing power, haptic technologies, and device portability (size, weight). To complicate the challenges further, all interfaces must be intuitive, easy to use, and fully customizable in real time to adjust to the user's needs.

Emerging Applications

The seamless integration and intersection of VR with other technologies, such as wearable biofeedback sensors, improved haptics, artificial intelligence (AI), deep learning, and big data analytics, are likely to make VR even more influential in healthcare and beyond.

Currently, VR modules and applications are produced and experienced in an isolated environment, away from the real world. Future advancements will move towards *interreality*. New technologies, such as wearable biosensors, will bridge the gap between the physical and virtual worlds to produce a closed-loop experience [89–91]. This will not only increase the scope for clinical applications of VR but, critically, will also advance healthcare towards a model of decentralized patient care.

Today, virtual worlds are built and engineered to mimic the real world. The future will allow us to populate these worlds. AI and deep learning show great promise of increasing the interactivity of our virtual worlds. Clinically, AI can improve VR modeling software to inform and promote data-driven decision-making at the patient level, hospital management level, and even population level. The synergy of AI and VR has considerable potential to transform and streamline one-to-one healthcare delivery. Once telepresence is achieved, diagnostics and monitoring can be delivered through VR directly to a patient's home. This will improve the patient experience, integrate and maximize healthcare resources, and reduce healthcare inequality caused by geographical or economic disparities. In education, improvements in deep learning will enable adaptive simulations that challenge users to react and manage situations akin to those on the wards, in clinics, and in the OR.

Looking more broadly, immersive technologies can be classified along a continuum: (1) true VR as discussed in this chapter, (2) mixed reality, and (3) augmented reality. As technology improves, the boundaries between (1), (2), and (3) will begin to blur, and users will be able to switch between the three on demand with a single headset. In healthcare, immersive technologies will allow a surgeon to have greater situational awareness in the real world, greatly improving their use case.

Improvements in hardware, specifically, haptic feedback and interfaces, are required to achieve true telepresence. Future VR systems will have a short latency time and high sensitivity to the movements of the handheld controllers. Currently, delays and long latency periods between user inputs and haptic outputs retract from the sense of realism.

Conclusion

VR technology has provided a means to immerse users in computer-generated worlds. Until recently, such technology in healthcare was restricted to desktop screens, cumbersome simulation mannequins, and static paper-based cases. User appetite for heightened interactivity and authenticity is rapidly emerging. This increase in demand has led to clear use cases for VR in healthcare, each hypothesized to improve patient outcomes.

This review of existing applications of VR in surgical science illustrates key milestones that have been met in recent years. Broadly speaking, applications of VR in surgery include education, surgical support, and data science. The widespread adoption of this technology will be dependent on the generation of valid data to support clinical efficacy. Alongside advancements in technical capabilities, improvements in user comfort and reduction in costs will ensure the longevity of this technology in day-to-day clinical operations. Excitingly, the synergy between

VR and other emerging technologies (big data, AI, haptic interfaces, etc.) only adds further dimensions to the clinical utility of VR for surgeons.

Key Points

- VR is used in healthcare facilities today as an emerging educational strategy and a surgical support tool.
- Recent advancements in software and hardware have reduced consumer costs and allowed better user immersion. The relatively low cost means that VR is now both accessible and affordable, factors that are likely going to drive increased adoption in the future.
- VR is currently in its early days. To progress towards clinical adoption, providers, researchers, and patients should determine acceptable risks in real-world scenarios to create opportunities to prove the clinical efficacy of surgical VR.
- Future integrations of other emerging technologies will realize the vision of *interreality*. This means a coexistence of the virtual world and the real world.

References

1. Webster. The Merriam-Webster Dictionary, International Edition; 2016.
2. [No title]. http://worrydream.com/refs/Sutherland%20-%20The%20Ultimate%20Display.pdf. Accessed 11 Sept 2019.
3. Cipresso P, Giglioli IAC, Raya MA, Riva G. The past, present, and future of virtual and augmented reality research: a network and cluster analysis of the literature. Front Psychol. 2018;9:2086.
4. Chinnock C. Virtual reality in surgery and medicine. Hosp Technol Ser. 1994;13:1–48.
5. Cyberspace: The New Explorers: Autodesk : Free Download, Borrow, and Streaming : Internet Archive.
6. Wilson MS, Middlebrook A, Sutton C, Stone R, McCloy RF. MIST VR: a virtual reality trainer for laparoscopic surgery assesses performance. Ann R Coll Surg Engl. 1997;79:403–4.
7. Castelvecchi D. Low-cost headsets boost virtual reality's lab appeal. Nature. 2016;533:153–4.
8. MEDLINE/ PubMed. SpringerReference. https://doi.org/10.1007/springerreference_65284.
9. Statista - The Statistics Portal [Internet]. Statista. 2019 [cited 17 October 2019]. Available from: https://www.statista.com/.
10. Parisi T. Learning virtual reality: developing immersive experiences and applications for desktop, web, and mobile. Sebastopol, CA;O'Reilly Media, Inc.; 2015.
11. Sugand K, Mawkin M, Gupte C. Validating Touch Surgery™: A cognitive task simulation and rehearsal app for intramedullary femoral nailing. Injury. 2015;46:2212–6.
12. Morone PJ, Bekelis K, Root BK, Singer RJ. Development and validation of a mobile device-based external ventricular drain simulator. Oper Neurosurg (Hagerstown). 2017;13:603–8.
13. Sherman WR, Craig AB. Understanding virtual reality: Interface, application, and design. Berkeley CA; Morgan Kaufmann; 2018.
14. Pellegrini VD Jr, Ferguson PC, Cruess R, Cruess S, Briggs TWR. Sufficient competence to enter the unsupervised practice of orthopaedics: what is it, when does it occur, and do we know it when we see it? AOA critical issues. J Bone Joint Surg Am. 2015;97:1459–64.
15. Kotsis SV, Chung KC. Application of the "see one, do one, teach one" concept in surgical training. Plast Reconstr Surg. 2013;131:1194–201.
16. Moorthy K, Munz Y, Sarker SK, Darzi A. Objective assessment of technical skills in surgery. BMJ. 2003;327:1032–7.
17. Talbot CL, Holt EM, Gooding BWT, Tennent TD, Foden P. The shoulder objective practical assessment tool: evaluation of a new tool assessing residents learning in diagnostic shoulder arthroscopy. Arthroscopy. 2015;31:1441–9.
18. Jakimowicz JJ, Cuschieri A. Time for evidence-based minimal access surgery training--simulate or sink. Surg Endosc. 2005;19:1521–2.
19. Yiannakopoulou E, Nikiteas N, Perrea D, Tsigris C. Virtual reality simulators and training in laparoscopic surgery. Int J Surg. 2015;13:60–4.
20. Zhuang W, Xiao Q. Facilitate active learning: the role of perceived benefits of using technology. J Educ Bus. 2018;93:88–96.
21. Shatto B, Erwin K. Teaching millennials and generation Z: bridging the generational divide. Creat Nurs. 2017;23:24–8.
22. Sonnleitner K. From sage on the stage to guide on the side. Zeitschrift für Didaktik der Rechtswissenschaft. 2016;3:288–302.
23. Paolis LTD, De Paolis LT. Serious game for laparoscopic suturing training. In: 2012 Sixth international

conference on complex, intelligent, and software intensive systems. 2012. https://doi.org/10.1109/cisis.2012.175.
24. Ricciardi F, De Paolis LT. A comprehensive review of serious games in health professions. Int J Comput Games Technol. 2014;2014:1–11.
25. Wang R, DeMaria S Jr, Goldberg A, Katz D. A systematic review of serious games in training health care professionals. Simul Healthc. 2016;11:41–51.
26. Feifer A, Al-Ammari A, Kovac E, Delisle J, Carrier S, Anidjar M. Randomized controlled trial of virtual reality and hybrid simulation for robotic surgical training. BJU Int. 2011;108:1652–6; discussion 1657.
27. Diesen DL, Erhunmwunsee L, Bennett KM, Ben-David K, Yurcisin B, Ceppa EP, Omotosho PA, Perez A, Pryor A. Effectiveness of laparoscopic computer simulator versus usage of box trainer for endoscopic surgery training of novices. J Surg Educ. 2011;68:282–9.
28. Orzech N, Palter VN, Reznick RK, Aggarwal R, Grantcharov TP. A comparison of 2 ex vivo training curricula for advanced laparoscopic skills: a randomized controlled trial. Ann Surg. 2012;255:833–9.
29. Jensen K, Ringsted C, Hansen HJ, Petersen RH, Konge L. Simulation-based training for thoracoscopic lobectomy: a randomized controlled trial. Surg Endosc. 2014;28:1821–9.
30. Khan MW, Lin D, Marlow N, Altree M, Babidge W, Field J, Hewett P, Maddern G. Laparoscopic skills maintenance: a randomized trial of virtual reality and box trainer simulators. J Surg Educ. 2014;71:79–84.
31. Loukas C, Nikiteas N, Schizas D, Lahanas V, Georgiou E. A head-to-head comparison between virtual reality and physical reality simulation training for basic skills acquisition. Surg Endosc. 2012;26:2550–8.
32. Munz Y, Kumar BD, Moorthy K, Bann S, Darzi A. Laparoscopic virtual reality and box trainers: is one superior to the other? Surg Endosc. 2004;18:485–94.
33. Kowalewski K-F, Hendrie JD, Schmidt MW, Proctor T, Paul S, Garrow CR, Kenngott HG, Müller-Stich BP, Nickel F. Validation of the mobile serious game application Touch Surgery™ for cognitive training and assessment of laparoscopic cholecystectomy. Surg Endosc. 2017;31:4058–66.
34. Pfandler M, Lazarovici M, Stefan P, Wucherer P, Weigl M. Virtual reality-based simulators for spine surgery: a systematic review. Spine J. 2017;17:1352–63.
35. Haubruck P, Nickel F, Ober J, et al. Evaluation of app-based serious gaming as a training method in teaching chest tube insertion to medical students: randomized controlled trial. J Med Internet Res. 2018;20:e195.
36. Moro C, Štromberga Z, Raikos A, Stirling A. The effectiveness of virtual and augmented reality in health sciences and medical anatomy. Anat Sci Educ. 2017;10:549–59.
37. Kyaw BM, Saxena N, Posadzki P, et al. Virtual reality for health professions education: systematic review and meta-analysis by the digital health education collaboration. J Med Internet Res. 2019;21:e12959.
38. Li L, Yu F, Shi D, Shi J, Tian Z, Yang J, Wang X, Jiang Q. Application of virtual reality technology in clinical medicine. Am J Transl Res. 2017;9:3867–80.
39. Arriaga AF, Gawande AA, Raemer DB, et al. Pilot testing of a model for insurer-driven, large-scale multicenter simulation training for operating room teams. Ann Surg. 2014;259:403–10.
40. Howe J, Puthumana J, Hoffman D, et al. Development of virtual simulations for medical team training: an evaluation of key features. Proceedings of the International Symposium on Human Factors and Ergonomics in Health Care. 2018;7:261–6.
41. Olasky J, Sankaranarayanan G, Seymour NE, et al. Identifying opportunities for virtual reality simulation in surgical education: a review of the proceedings from the innovation, design, and emerging alliances in surgery (IDEAS) conference: VR surgery. Surg Innov. 2015;22:514–21.
42. Singh K, Bharatha A, Sa B, Adams OP, Majumder MAA. Teaching anatomy using an active and engaging learning strategy. BMC Med Educ. 2019;19:149.
43. Bairamian D, Liu S, Eftekhar B. Virtual reality angiogram vs 3-dimensional printed angiogram as an educational tool-A comparative study. Neurosurgery. 2019;85:E343–9.
44. Yammine K, Violato C. A meta-analysis of the educational effectiveness of three-dimensional visualization technologies in teaching anatomy. Anat Sci Educ. 2015;8:525–38.
45. Izard SG, Méndez JAJ. Virtual reality medical training system. In: Proceedings of the fourth international conference on technological ecosystems for enhancing multiculturality: ACM; 2016. p. 479–85.
46. Maresky HS, Oikonomou A, Ali I, Ditkofsky N, Pakkal M, Ballyk B. Virtual reality and cardiac anatomy: exploring immersive three-dimensional cardiac imaging, a pilot study in undergraduate medical anatomy education. Clin Anat. 2019;32:238–43.
47. Silva JNA, Southworth M, Raptis C, Silva J. Emerging applications of virtual reality in cardiovascular medicine. JACC Basic Transl Sci. 2018;3:420–30.
48. Mandler AG. Touch surgery: a twenty-first century platform for surgical training. J Digit Imaging. 2018;31:585–90.
49. Tulipan J, Miller A, Park AG, Labrum JT 4th, Ilyas AM. Touch surgery: analysis and assessment of validity of a hand surgery simulation "App.". Hand. 2019;14:311–6.
50. Chidambaram S, Erridge S, Leff D, Purkayastha S. A randomized controlled trial of skills transfer: from touch surgery to laparoscopic cholecystectomy. J Surg Res. 2019;234:217–23.
51. Bunogerane GJ, Taylor K, Lin Y, Costas-Chavarri A. Using touch surgery to improve surgical education in low- and middle-income settings: a randomized control trial. J Surg Educ. 2018;75:231–7.
52. Luciano CJ, Banerjee PP, Sorenson JM, Foley KT, Ansari SA, Rizzi S, Germanwala AV, Kranzler L, Chittiboina P, Roitberg BZ. Percutaneous spinal

fixation simulation with virtual reality and haptics. Neurosurgery. 2013;72 Suppl 1:89–96.
53. Purkayastha S, Tilney HS, Georgiou P, Athanasiou T, Tekkis PP, Darzi AW. Laparoscopic cholecystectomy versus mini-laparotomy cholecystectomy: a meta-analysis of randomised control trials. Surg Endosc. 2007;21:1294–300.
54. Abelson JS, Silverman E, Banfelder J, Naides A, Costa R, Dakin G. Virtual operating room for team training in surgery. Am J Surg. 2015;210:585–90.
55. Kurenov S, Cendan J, Dindar S, Attwood K, Hassett J, Nawotniak R, Cherr G, Cance WG, Peters J. Surgeon-authored virtual laparoscopic adrenalectomy module is judged effective and preferred over traditional teaching tools. Surg Innov. 2017;24:72–81.
56. Allcoat D, von Mühlenen A. Learning in virtual reality: effects on performance, emotion and engagement. Res Learn Technol. 2018. https://doi.org/10.25304/rlt.v26.2140.
57. Patel V, Aggarwal R, Cohen D, Taylor D, Darzi A. Implementation of an interactive virtual-world simulation for structured surgeon assessment of clinical scenarios. J Am Coll Surg. 2013;217:270–9.
58. Izard SG, Juanes JA, García Peñalvo FJ, Estella JMG, Ledesma MJS, Ruisoto P. Virtual reality as an educational and training tool for medicine. J Med Syst. 2018;42:50.
59. Wilkerson W, Avstreih D, Gruppen L, Beier K-P, Woolliscroft J. Using immersive simulation for training first responders for mass casualty incidents. Acad Emerg Med. 2008;15:1152–9.
60. Pratt R, Deprest J, Vercauteren T, Ourselin S, David AL. Computer-assisted surgical planning and intraoperative guidance in fetal surgery: a systematic review. Prenat Diagn. 2015;35:1159–66.
61. Stella F, Dolci G, Dell'Amore A, Badiali G, De Matteis M, Asadi N, Marchetti C, Bini A. Three-dimensional surgical simulation-guided navigation in thoracic surgery: a new approach to improve results in chest wall resection and reconstruction for malignant diseases. Interact Cardiovasc Thorac Surg. 2014;18:7–12.
62. Sakamoto T. Roles of universal three-dimensional image analysis devices that assist surgical operations. J Hepatobiliary Pancreat Sci. 2014;21:230–4.
63. Mendez A, Hussain T, Hosseinpour A-R, Valverde I. Virtual reality for preoperative planning in large ventricular septal defects. Eur Heart J. 2019;40:1092.
64. Riener R, Harders M. VR for planning and intraoperative support. In: Riener R, Harders M, editors. Virtual reality in medicine. London: Springer London; 2012. p. 211–23.
65. Sethia R, Wiet GJ. Preoperative preparation for otologic surgery. Curr Opin Otolaryngol Head Neck Surg. 2015;23:355–9.
66. Kockro RA, Killeen T, Ayyad A, Glaser M, Stadie A, Reisch R, Giese A, Schwandt E. Aneurysm surgery with preoperative three-dimensional planning in a virtual reality environment: technique and outcome analysis. World Neurosurg. 2016;96:489–99.
67. Bilgic E, Turkdogan S, Watanabe Y, Madani A, Landry T, Lavigne D, Feldman LS, Vassiliou MC. Effectiveness of telementoring in surgery compared with on-site mentoring: a systematic review. Surg Innov. 2017;24:379–85.
68. Sandars J. The use of reflection in medical education: AMEE Guide No. 44. Med Teach. 2009;31:685–95.
69. General Medical Council (Great Britain). Good medical practice. General Medical Council. 2001.
70. Gibbs G. Learning by doing: a guide to teaching and learning methods. Oxford: Further Education Unit. Oxford Polytechnic; 1988.
71. Hatton N, Smith D. Reflection in teacher education: towards definition and implementation. Teach Teach Educ. 1995;11:33–49.
72. [No title]. https://discovery.ucl.ac.uk/id/eprint/1425894/1/Pachilova_Sailer2013_EBD_PatientCaregiverInterface_D4H13_Vol2_web.pdf. Accessed 21 Oct 2019.
73. Alarcon A, Berguer R. A comparison of operating room crowding between open and laparoscopic operations. Surg Endosc. 1996;10:916–9.
74. Dexter F, Ledolter J, Wachtel RE. Tactical decision making for selective expansion of operating room resources incorporating financial criteria and uncertainty in subspecialties' future workloads. Anesth Analg. 2005;100:1425–32.
75. Barbagallo S, Corradi L, de Ville de Goyet J, Iannucci M, Porro I, Rosso N, Tanfani E, Testi A. Optimization and planning of operating theatre activities: an original definition of pathways and process modeling. BMC Med Inform Decis Mak. 2015;15:38.
76. Joseph A, Khoshkenar A, Taaffe KM, Catchpole K, Machry H, Bayramzadeh S, RIPCHD.OR study group. Minor flow disruptions, traffic-related factors and their effect on major flow disruptions in the operating room. BMJ Qual Saf. 2019;28:276–83.
77. Virtual reality system helps surgeons, reassures patients. In: Medical Center Development. https://medicalgiving.stanford.edu/news/virtual-reality-system-helps-surgeons-reassures-patients.html. Accessed 18 Sept 2019.
78. [No title]. https://www.echopixeltech.com/pdfs/lu_poster1.pdf. Accessed 24 Sept 2019.
79. Mohammed MAA, Khalaf MH, Kesselman A, Wang DS, Kothary N. A role for virtual reality in planning endovascular procedures. J Vasc Interv Radiol. 2018;29:971–4.
80. Ballocca F, Meier LM, Ladha K, Qua Hiansen J, Horlick EM, Meineri M. Validation of quantitative 3-dimensional transesophageal echocardiography mitral valve analysis using stereoscopic display. J Cardiothorac Vasc Anesth. 2019;33:732–41.
81. Babel VR. https://www.cbrg.ox.ac.uk/cbrg/babelVR.html. Accessed 18 Sept 2019.
82. [No title]. https://www.cras-eu.org/past%20events/cras-2018-pages/CRAS_2018_proceedings.pdf. Accessed 3 Oct 2019.

83. Stolk B, Abdoelrahman F, Koning AHJ, Wielinga P, van der Spek P. Mining the human genome using virtual reality. In: Proceedings of the fourth eurographics workshop on parallel graphics and visualization, EGPGV 2002, Blaubeuren, 9–10 Sept 2002. p. 17–21.
84. Schmidt E, Cohen J. The new digital age: reshaping the future of people, nations and business. New York; John Murray; 2013.
85. Alaker M, Wynn GR, Arulampalam T. Virtual reality training in laparoscopic surgery: a systematic review & meta-analysis. Int J Surg. 2016;29:85–94.
86. [No title]. https://pdfs.semanticscholar.org/8720/1ba9d513efaddb72d94b8b3521546366d5a2.pdf. Accessed 4 Oct 2019.
87. Kim Y, Kim H, Kim YO. Virtual reality and augmented reality in plastic surgery: a review. Arch Plast Surg. 2017;44:179–87.
88. Slater M. Place illusion and plausibility can lead to realistic behaviour in immersive virtual environments. Philos Trans R Soc Lond Ser B Biol Sci. 2009;364:3549–57.
89. Riva G, Raspelli S, Algeri D, Pallavicini F, Gorini A, Wiederhold BK, Gaggioli A. Interreality in practice: bridging virtual and real worlds in the treatment of posttraumatic stress disorders. Cyberpsychol Behav Soc Netw. 2010;13:55–65.
90. Riva G, Raspelli S, Pallavicini F, Grassi A, Algeri D, Wiederhold BK, Gaggioli A. Interreality in the management of psychological stress: a clinical scenario. Stud Health Technol Inform. 2010;154:20–5.
91. Gaggioli A, Pallavicini F, Morganti L, et al. Experiential virtual scenarios with real-time monitoring (interreality) for the management of psychological stress: a block randomized controlled trial. J Med Internet Res. 2014;16:e167.

15 Robotic Automation for Surgery

Hossein Dehghani and Peter C. W. Kim

Introduction

Today, it is not surprising that the general public and most surgeons in practice identify the label 'medical robot' with Intuitive's da Vinci System in view of the fact that now more than 5000 units have been in use and after more than one million soft tissue surgical procedures have been performed using this platform [1, 2]. Despite the unfettered monopoly in the soft tissue surgery market for two decades, less than 10% of the overall soft tissue surgery in the USA and less than 0.5% of all surgery globally are currently performed using the Intuitive Surgical System [1–3]. As far as technology diffusion is considered, one would not highlight the Intuitive story as a success, regardless of enabling nature of its technology – particularly in improving minimally invasive dexterity in deep and narrow domains of urologic and gynecologic surgeries [3, 4]. Cost and utilization are usually highlighted as the primary cause for this poor adoption, and today, more than 80 companies are in the marketplace competing to develop the next iterations of the so-called surgical robots hoping to improve mostly on the adoption rate [5, 6]. However, for any actuated tool or for a surgical robot to enjoy better adoption, it requires a crucial disruption in the current robotic surgery paradigm with not just improvements in cost, utilization and dexterity of human-manipulated end effectors but a fundamental shift and emphasis on incorporating better perception and intelligence.

The paradigm shift in surgery towards progressively more minimally invasive approach in the past three decades, whether tools are manual or actuated, represents significantly underappreciated transition from analogue to a digital era in the history of surgery over the last 2500 years (Fig. 15.1). In fact, only with the digital transition, increasingly more image-guided interventional technologies with direct linear trajectories, relatively predictable environment and tissue deformity, and minimal end effector dexterity are starting to demonstrate clinical utility and benefits [7–9]. These intelligent technologies, which can perceive-plan-act-react with real-time monitoring, include MR-guided high-intensity focused ultrasound (HIFU) for tumour ablation, stereotactic radiation therapy, infrared-/ultrasound-guided blood sampling, endoscope holder, hair follicle harvesting robotics and the like [7–10]. Indeed, the incorporation of some decision support for planning, which includes generating options based on real-time sensor inputs and recommending (ultimately) supervised, collaborative and interdependent decisions to act, is not only possible and feasible but also desired and perhaps inevitable in view of non-linearly

H. Dehghani
Activ Surgical, Boston, MA, USA

P. C. W. Kim (✉)
Department of Surgery, Brown University; Active Surgical, Boston, MA, USA
e-mail: PKim@activsurgical.com; Peter.kim@brownphysicians.org

S. Atallah (ed.), *Digital Surgery*, https://doi.org/10.1007/978-3-030-49100-0_15

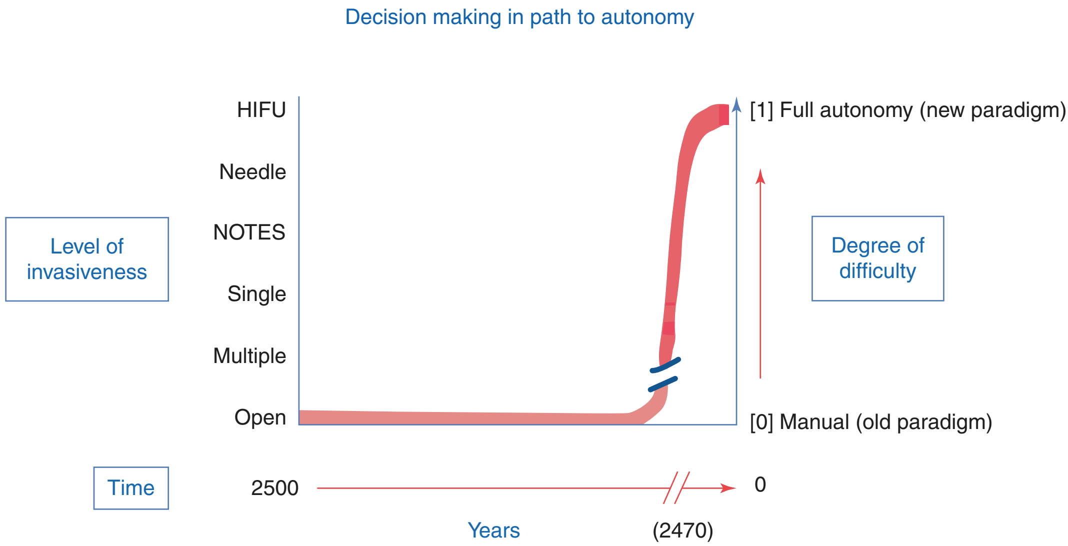

Fig. 15.1 The relative complexity of invasiveness and degrees of dexterity required are scaled from top to bottom on the left *Y*-axis. The autonomy/automation scale from 0 to 1 is shown on the right *Y*-axis. The time is depicted on the *X*-axis, while the sigmoid curve represents the trajectory in decision making in path to autonomy

improving sensors and intelligence processing and algorithms in this digital era [10–14]. Beyond cost and utilization as the major challenge to much broader adoption of 'surgical robots', a new paradigm of surgical intelligence driving some degree of automation and autonomy initially at subtask and then task levels but eventually at systems level promises an enhanced adoption of the technology with measurable metrics on improved outcome, safety and accessibility [11, 12]. The goal of a 'surgical robot' should be viewed not just an ancillary technology as a set of versatile tools that extend the surgeon's ability to an approved level of competency to practice clinically but potentially an enabling technology beyond human dexterity into a digital intelligence that could potentially expand a surgeon's capacity and capability to a level of digitally accessible proficiency [15–18].

Terminology and Definition

For the purpose of this chapter, we will narrow the definition of a surgical robot and the scope of discussion as *a computer-assisted actuated device consisting of dexterity, perception and intelligence functionalities for hard and soft tissue surgery* [18–21]. It should be noted that all actuated devices in the marketplace for clinical use with exception of a handful of devices stated above are simply considered tele-manipulated endoscopic tools and do not fall into a 'robot' in their definition, manufacturing requirements and regulatory approval process [10, 17]. Despite the recent introduction of ISO 15066 standard on 'collaborative robots and devices' to accommodate the safety requirement for personal care service robots cohabiting the same working environment, the current paradigm of surgical robot still falls outside of any standard definition of 'robot' due to the absence of any degree of 'autonomy', particularly in soft tissue space [10].

The basic mechanics of current surgical robots in its three key domains – dexterity, perception and intelligence – remain in an industrial stage predominantly (or exclusively) and are still controlled by human operators with minimal integration of computing capabilities for sensing and cognition. In most instances, current surgical robots only provide some assistance with tele-manipulated dexterity dimensions, such as motion scaling and tremor control [22]. Such initial interests and emphasis on action side (dexterity) of robotic functionalities have yielded limited advances in automated tasks, with real-time monitoring and supervision capabilities to date only in relatively straightforward applications – such as in needle-guided delivery, MR-guided high-intensity focused ultrasound, stereotaxis, radiation therapy and some tasks in orthopaedic robotic functionalities (Fig. 15.1).

However, motivations to consider automated or autonomous functionalities even at this early stage of development in the field, when there is not even clarity nor consensus on definition, potential needs and requirements of the technology and future development, remain real and inevitable. This is driven by an unrecognized and underappreciated transition of surgery (especially in the soft tissue space) into a digital era and increasing capability of transforming big data into deep smart data in perception and cognition that can, initially, decision support in human-machine interdependent collaborative paradigm, to a supervised model and, ultimately, to a fully autonomous paradigm. The transferrable concepts on the benefits of robotic and automated tasks from industrial space into surgery potentially promise enhanced efficiency and effectiveness, improved standardization and optimization, and a much broader adoption and accessibility to the product, which, in this case, would translate into improved patient outcomes, safety and accessibility [22]. Just imagine a future scenario when a surgery for anyone at the point of care is done with the maximal efficiency and effectiveness, without surgeon competence and proficiency variance, optimized through access to collective surgical experience through connectivity and accessibility to anyone at the point of care.

The term *general intelligence* is loosely defined as the ability to learn or understand, to rationalize new or trying situations and to have the capacity to reason and problem solve. The act of *prospection*, the ability of solving problems that have never been encountered, is the essence of general intelligence, meaning *thinking differently and acting better*. Thus, true general intelligence is the ability of an agent to interpret and respond to an unknown environment. For instance, a human is capable to start and continue a conversation without prior knowledge about the listener(s) or the topic of conversation. He/she knows how to use language but does not know what would be used. Similarly, intelligence in surgery can be much narrowly defined as *how to interact with the environment to achieve the best clinical outcome at specific tasks, subtasks and systems level functionalities* [11].

One subset of intelligence is *autonomy*. Autonomy implies a real-time monitoring of the interaction between the agent and environment where sensory input is processed to generate options and selected for action for intended purpose of addressing de novo problems [10, 19, 23]. It also implies that the consequence of the action is recording/remembering – thus guiding future generation and selection of options in the reasoning and problem solving. Since autonomy is a dynamic and scalable concept (not a static binary state), it can be seen as a spectrum ranging from zero autonomy (human driven) to semi-autonomous (shared or supervised autonomy), to full autonomous, wherein the system performs purely on its own without any human intervention for the purpose of reasoning, problem solving and acting.

In contrast, robotic automation assumes some standardization in reasoning, problem solving and action at task, subtask or systems level – where a mechanism or technology can perform a process or procedure with minimal human assistance in the context of finite options. It implies that both the agent and environment are known in which an iterative preprogrammed task or subtask is carried out, or the system functions on its own without or with minimal human intervention. While surgical robot operating in a known universe can adjust its task performance in response to dynamic tracking of tissue (e.g. to compensate for patient motion related to breathing artefact), an advance algorithm programmed in finite probabilities enabling deterministic options for robot would not be considered intelligence nor autonomy. On the other hand, consider how a surgeon ties suturing string. She/he first identified the target tissue and workspace required for manoeuvring. The depth of needle bite or tension in a thread is constantly monitored along with the constant movement compensation [10, 21, 24, 25]. Seemingly automatic steps and movements are based on examples and experiences built over the years, and each step represents unique reasoning, problem solving and action – in terms of age, medical history and intraoperative circumstances (e.g. lighting). Since such variations are not predictable or predetermined, real-time response to mitigate any risk is required. Therefore, *intelligence is the essential part of autonomy*. Safety is part of intelligence.

Classification of Surgical Robots on Levels of Autonomy

Although medical robots can be categorized in many ways from technologic to technical – such as discipline- or anatomic-specific applications and intended operating environment – the fundamental purpose of their existence is to improve caregivers' capacity and capability in healthcare environments [11, 12]. For the purpose of discussion in this chapter, particularly in the context of *robotic automation in surgery*, we will focus the scope of our discussion to surgical robots. Specifically, we will focus on soft and hard tissue surgical robots, in view of the fact that, even in this narrowly defined area, there are upwards of 80 commercial activities to enter this marketplace. The human-machine interface will be most directly impacted with permeating influence of intelligence and autonomy [5, 10, 11].

It should be noted that there are no standards or guidelines regarding the level of autonomy or degrees of automation regarding surgical robots today. Any discussion is inferred from the levels of automation, as defined by the Society of Automotive Engineers (SAE) in the car industry. Under SAE guidelines, there is a categorical scale from 0 → 5, where there is no automation and autonomy in level 0, but there is a full automation in level 5, with progressively increasing levels of control and performing tasks assumed by the vehicle for the purpose of driving [26, 27]. The whole systems level intelligence and autonomy are somewhat simplified or structured in the sense that the tasks at hand (namely, the automated driving from point A to B) is finite and transpires in an inorganic/inanimate environment. Although such a framework is dynamic (having to account for traffic and obstacles), it is not deformable or immobile and thus presents a paradigm that is somewhat predictable and structured [19, 26, 27].

A number of investigators have further adapted, scaled, refined and then categorized the 0 → 5 levels of autonomy scale from the SAE framework and made them applicable to medical robots, with additional levels from 0 → 9 or more depending on autonomous capabilities and involvement of human control [26, 27]. Given that there are only handful of surgical robotic systems in clinical practice with limited 'automated' capabilities today, for the purpose of this chapter and conceptual simplicity, we define the scale or levels of autonomy in surgical robots in a binary scale of 0 → 1, where 0 is fully manual and 1 is a fully autonomous state (Table 15.1).

Whether one defines the basic requirements and components of automation/autonomy in a tripartite perception-planning-action loop or more refined monitoring-generating-selecting-executing feedback loop, any autonomous capability as a part of specific task/subtask intelligence in a surgical robot stipulates a demonstration of *problem solving capability* that is in real-time response to a de novo problem [10, 19]. All surgical robots in clinical practice today are displaying automated capability as a part of intelligence; however, they are not autonomous by design, in part due to regulatory and safety reasons. Thus, they have finite options predicated upon known, supervised learning [12, 18, 19]. For example, in hard tissue application, with relatively non-deformable immobile target tissue

Table 15.1 Automation vs. autonomy

Human-machine interface	0 (100% manual)	➔	1 (100% autonomous)
Requirements *Automation*	0	➔	1 (real-time monitoring)
Autonomy	0	➔	1 (degree of selecting)

of interest, with limited complexity of surgical task/subtask in a structured setting (such as milling in joint replacement or delivery of radiation), real-time monitoring based on high sensory input (such as radiologic and electromagnetic fiducials) provides sufficient precision and accuracy of 'automation' for clinical efficacy for clearly defined task options and performance metrics [10, 13, 18].

Examples of these automated robotic systems include RoboDoc in orthopaedic surgery, Veebot for blood sampling, Artas for hair follicle harvesting, CyberKnife for stereotactic radiotherapy, Artis Zeego for interventional imaging and AutoLap for endoscope holding [10, 18]. In the future, with increasing digital dataset accrued from annotated operative scenes, kinematic data from actuated surgical robotic tools, and application of more flexible forms of machine learning, such as unsupervised reinforcement learning (RL) or neural network, it is anticipated that the surgical robot will display a true autonomous capability. As stated previously, this will proceed in a stepwise fashion, with machine automation initially at subtask level, followed by task level, and ultimately systems level [10, 18].

Overview of Soft and Hard Tissue Robot-Assisted Surgery

With more than 80 robotic systems currently in research and development poised to enter the marketplace, the exercise of capturing and categorizing a complete list according to degrees and levels of automation and/or autonomy would not be practical nor meaningful [10, 17]. However, since there are automated and semiautomated systems already in the 'hard tissue' clinical space (mainly for orthopaedic and spine-based neurosurgical procedures), it would be informative to highlight the general principles and parameters behind clinical and preclinical automated or autonomous systems, such as complexity of subtasks or tasks, environmental variable (static vs. dynamic), degrees of involvement or human control required, relative degree and fidelity of real time sensory monitoring, incorporation of any perioperative sensory data such as preoperative imaging and technology readiness levels [10, 11, 18].

As illustrated in the previous section, what enables automation in the context of acceptable clinical standards and due diligence required for safety is the fidelity of real-time monitoring of sensory inputs, coupled with the relative complexity of subtask or task to be performed at hand [10, 11, 18]. Autonomy for surgical robot in contrast requires a generation of potential options based on real-time monitoring of sensory inputs from the operative field and selection of options in the context of best desired or intended outcome and safety for a problem previously encounter [19]. In the current paradigm and standards of relatively broad range of approved clinical competence for human surgeons and given the tight reproducible requirements needed for the regulatory approval of technology, specific subtask and task automation is feasible and will likely demonstrate non-inferiority to fully manual task. Meanwhile, collaborative to fully autonomous tasks in surgery await not just more voluminous but deeper data, even for a very narrow specific intelligent surgical task in the future.

Hard Tissue Surgical Robots

The hard tissue space (including, but not limited to, the skeletal system) is an obvious and natural place to initial applications for automated or autonomous task. Although there are remaining challenges, these tissues are considered perceptively static and non-deformable as compared to soft tissue, such as the intestine or liver, and can be positioned in an immobile way to be tracked with surface, radiologic or electromagnetic fiducials including co-registration of preoperative imaging for finite scenario simulations. In addition, the surgical field and environment can be predictably structured such that an automated subtask or task can be carried out to the level of clinically acceptable non-inferior outcomes and increasingly superior safer outcomes with lower operative morbidity [10, 11, 17]. The human factor attributed variations such as instrument position accuracy, individual surgeon variance in situational awareness and decision preference can be somewhat mitigated with automated functionalities, especially with higher-level real-time tracking capability [10, 17]. However, imprecision and discordance with preoperative imaging, background noise such as target and surgical field movement, caused by heartbeat and respiration, pose ongoing challenges and limit the applications to a subtask level such as milling or linear trajectory of a hard tissue surgical tasks [10, 17]. Despite these challenges, there are already handfuls of systems in clinical practice that are starting to demonstrate a clear clinical utility in both outcome and safety in orthopaedic and neurosurgical domains [10, 17]. These include Mazor from Medtronics, MAKO surgical robot (MAKO Surgical Corp., Fort Lauderdale, FL), Navio from Smith and Nephew, ExcelsiusGPS® from Globus Medical, RoboDoc (THINK Surgical TSolution-One®), BRIGIT (MEDTECH, FR) and NeuroMate (Integrated Surgical systems) [10, 17]. TSolution highlights the most automated interventional system in the current marketplace with an active automated, image-based robotic milling system that enables the surgeon to attain a consistently accurate implant component positioning [5–10].

Soft Tissue Surgical Robots

In contradistinction to hard tissue surgical robots, the deformability and mobility of soft tissue targets and the unpredictability of unstructured surgical environment pose challenges, which are orders of magnitude greater, even for simple accessory tracking of any subtask, tissue or tools in the surgical field [28, 29]. There are accessory functions for subtasks of 'robotic action' such as tremor reduction, motion scaling, motion filtering and shared control [30–34]. However, other than the recent demonstration of feasibility of execution of clinically relevant autonomous surgical task in a preclinical model by Activ Surgical, known as Smart Tissue Autonomous Robot (STAR), no automated or autonomous surgical subtask or task has been convincingly demonstrated to date, including summarized TRL in Table 15.2 [11]. For any automated or autonomous subtask to be performed in soft tissue space in the future, the key technologies of the three domains in surgical robotic capabilities that require further critical development are the real-time tracking, computer vision and surgical intelligence of generating and selecting potential options for intended task and acceptable outcome.

Future Development and Directions

The critical benefits of robotic and automated tasks transferable from industrial space into surgery include enhanced efficiency and effectiveness, improved standardization and optimization, and much broader adoption and accessibility to the product which in this case would be a better outcome, safety and accessibility [10, 11, 18]. Although there are credible beginnings of these benefits at subtask and task levels in the hard tissue surgical robot, significant amount of work needs to be done to bring automation and autonomy to surgical robots. The objective would be to improve the outcome, safety and accessibility to best practice at the point of care, especially in soft tissue surgery. What is driving this inevitable opportunity is the recognition of potential benefits of unrecognized and underappreciated digital data, which can be organized into meaningful and actionable deep data in surgery. As the transition to a digital realm takes place, efforts are increasing and focused to improve surgical vision from analogue human vision (restricted to Red-Green-Blue (RGB) spectrum) and human perception of anatomy to real-time, multispectral physiologic visualization technology of not just morphologic data but *functional* information as well. This will also include supervised and unsupervised machine learning applications, analysis and decision support to ultimately automated and autonomous generation/selection and execution of better surgical options and increasing awareness and acceptance of collaborative and interdependent paradigms in human-machine interface [10, 11, 18].

Table 15.2 The current state of autonomy in surgical robots

Tissue type	Soft (GI, GU, GYN, thorax)			Hard bone (brain)		
Mode	Passive Master-slave	Semi-active Semi-autonomous	Active Fully autonomous	Passive Master-slave	Semi-active Semi-autonomous	Active Fully autonomous
Products	Intuitive TransEnterix Medrobotics Auris	N	N	OMNIBotics	Stryker (MAKO) S & N (NAVIO) MAZOR Excelsius	Think surgical
DATA						
Preop						
EMR	N	N	N	N	N	N
Imaging	CT, MR	CT, MR	CT, MR	CT, MR	CT, MR	CT, MR
Intraop:						
(Real-time tracking)	N	N	N	Fluoroscopy	Fluoroscopy EM fiducial	Fluoroscopy EM fiducial
Spectral	Y	N	N	N	N	N
Spatial	N	N	N	N	N	N
Planning (Patient-specific simulation)	N	N	N	N	Y	Y
Decision support	N	N	N	N	Y	Y
NASA TRL	9	3	3	9	9	9
SAE (Level of autonomy)	0	1	2	1	1	3
Near future potential application	Planning, decision support, geo-fencing, tissue classification, margin detection Suturing: anastomosis, incision, closure			Planning, decision support, geo-fencing		

Y Yes, *N* No, *EM* electromagnetic, *TRL* technology readiness level, *SAE* Society of Automotive Engineers

Computer Vision

Despite the enabling nature of dexterity in robotic-assisted surgery, *surgeons overwhelmingly rely on vision as their dominant source of sensory feedback during operation.* The critical pivot to minimal-access endoscopic and endoluminal surgery over the past three decades has largely been the result of the availability of compact, high-resolution digital video cameras attached to borescopic optics. Other than benefits from changed surgical approach from open to minimal access, most of critical and equipoised comparisons between laparoscopic MIS and robotic-assisted surgery have yielded very marginal gains due to the fact that the vision remains entirely limited to the RGB range, and all surgical decision and action rely entirely on individual surgeon's interpretation, analysis, abstraction and recall [10, 11, 18]. The future surgical vision enabling automated or autonomous functionalities will include not just anatomical information from high-definition RGB interpreting geometric and colour information of intraoperative scene, but it will also provide additional hidden structural and physiologic information, such as that furnished by multi- and hyperspectral imaging systems, which analyse images with tens or hundreds of colour channels from the ultraviolet to the near, to far-infrared spectra, enhanced optically or chemically using the next generation of chemical signal enhancers beyond indocyanine green (ICG), to quantum dots, to speckles [35–39]. We expect that the initial application of this physiologic imaging will be for geo-surveillance to geo-fencing with the incorporation of spatial coordinates based on 3D imaging to mitigate any unrecognized or unintended injury to critical structures. Ultimately, computer vision can enable target tissue classification – such as for the determination of precise and accurate tumour margins during oncologic surgical dissections [37–40].

Real-time deformable tissue tracking is still a very difficult task. However, more precise quantitative depth perception with clearer tissue target-to-background contrast and optimized surgical task action, based on tissue health and subsurface tissue information, would significantly improve the surgeon's operative decisions and, in turn, the functional outcome of a surgical task. In the current clinical paradigm, a human operator (the surgeon) perceives, plans and executes every facet of a surgical task. However, for a robot to carry out a similar surgical task collaboratively or independently, a computer vision system needs to generate a visual representation of the environment expressed in 3D coordinates that enables real-time tracking of deformable and mobile soft tissues in unstructured surgical environments, with situational awareness of changing surgical anatomy and pathology, in the context of the intended procedure. For computer vision to detect, segment, classify and track in 3D coordinates in real-time, dimensional geometric information, in the form of depth maps or point clouds, can be obtained directly from special 3D cameras or estimated from monocular images using shape-from-shading or structure-from-motion techniques and passive optical technique that only requires images such as stereoscopy, monocular Shape-from-X (SfX) and simultaneous localization and mapping (SLAM), while the most well-known active methods are based on structured light and time-of-flight (ToF) [10, 11, 18, 41–43]. Other approaches include Deformable Shape-from-Motion and Shape-from-Shading technique [44, 45].

Machine Learning

An intelligence algorithm that can plan safe, effective and efficient clinical decisions for the intended tasks in a recognizable clinical context, or previously unexperienced scenario, is the foundation of any automation or true surgical autonomy. Such tasks would have been normally carried out only by the surgeon using a serial mental abstraction of images and memory recall. However, with accrual of deep digital data, one can envision a surgical robot capable of invoking a dexterity algorithm to control the end effectors, executing the plan and the task in a tight feedback loop, possibly invoking the intelligence algorithm to update the overall plan in real time.

We are experiencing a remarkable change in our lives outside of surgery due to the convergence of the growing digitalization of the world – this includes our ever-accelerating computational hardware capacity and increasingly sophisticated machine learning algorithms. Beyond the earlier classification and pattern recognition of static digital datasets, our lives are increasingly powered by machine learning-based technologies from web searches to content filtering on social networks, to medical diagnostic applications in radiology, dermatology and (more recently) pathology [18, 46–48]. In contrast to conventional machine learning techniques with limited abilities to process natural data in their raw form, more recent representation learning techniques allow a machine to be fed with raw data and to automatically discover the representations needed for detection or classification. These deep learning methods are representation learning methods with multiple levels of representation, obtained by composing simple but non-linear modules that each transforms the representation at one level (starting with the raw input) into a representation at a higher, slightly more abstract level. With the composition of enough such transformations, very complex functions can be learned [19, 20, 47, 48].

The key aspect of deep learning is that these layers of features are not designed by humans but are rather learned from data using a general-purpose learning procedure. Reinforcement learning (RL) is a class of machine learning in which an agent learns what action to take at any situation (state) to maximize the future reward (expected return) without a priori knowledge about optimal actions. This differs from learning through trial-and-error exploration [49]. There is a trade-off between exploration and exploitation. Recently, reinforcement learning has been applied in soft tissue manipulation requiring a complex model for tissue dynamics where RL was used to train a robot to indirectly guide tissue target points to desired positions, visual suture planning and collision avoidance [50, 51]. With increasing convergence of lots and beginnings of deep 'intelligent' operative field tissue and scene and kinematic device data, deep machine learning methods can and will be increasingly and inevitably applied to next-generation vision and intelligence algorithms in surgery for perceiving, planning and executing complex surgical tasks enabling autonomy [19, 20, 47, 48, 52, 53].

References

1. Intuitive Surgical Upside If da Vinci Systems Reaches 25% Share In Global Surgical Robots Market? [Internet]. [cited 2019 Oct 26]. Available from: https://www.forbes.com/sites/greatspeculations/2019/03/27/intuitive-surgical-upside-if-da-vinci-systems-reaches-25-share-in-global-surgical-robots-market/#6f29e66c4fac.
2. Simaan N, Yasin RM, Wang L. Medical technologies and challenges of robot-assisted minimally invasive intervention and diagnostics. Annu Rev Control Robot Auton Syst. 2018;1(1):465–90.
3. Fletcher SA, Cole AP, Berg S, Pucheril D, Trinh Q-D. Adoption of robotic surgery: driven by market competition or a desire to improve patient care? Lancet Oncol. 2018;19(2):e66.
4. Smyth JK, Deveney KE, Sade RM. Who should adopt robotic surgery, and when? Ann Thorac Surg. 2013;96(4):1132–7.
5. Patel V. The 10th Society of Robotic Surgery meeting. 2019.
6. Yu H-Y, Friedlander DF, Patel S, Hu JC. The current status of robotic oncologic surgery. CA Cancer J Clin. 2013;63(1):45–56.
7. Moustris GP, Hiridis SC, Deliparaschos KM, Konstantinidis KM. Evolution of autonomous and semi-autonomous robotic surgical systems: a review of the literature. Int J Med Robot Comput Assist Surg MRCAS. 2011;7(4):375–92.
8. Adler JR, Chang SD, Murphy MJ, Doty J, Geis P, Hancock SL. The Cyberknife: a frameless robotic system for radiosurgery. Stereotact Funct Neurosurg. 1997;69(1–4 Pt 2):124–8.
9. Eranki A, Srinivasan P, Ries M, Kim A, Lazarski CA, Rossi CT, et al. High intensity focused ultrasound (HIFU) triggers immune sensitization of refractory murine neuroblastoma to checkpoint inhibitor therapy. Clin Cancer Res Off J Am Assoc Cancer Res. 2020;26(5):1152.
10. Haidegger T. Autonomy for surgical robots: concepts and paradigms. IEEE Trans Med Robot Bionics. 2019;1(2):65–76.
11. Shademan A, Decker RS, Opfermann JD, Leonard S, Krieger A, Kim PCW. Supervised autonomous robotic soft tissue surgery. Sci Transl Med. 2016;8(337):337ra64.
12. Hashimoto DA, Rosman G, Rus D, Meireles OR. Artificial intelligence in surgery: promises and perils. Ann Surg. 2018;268(1):70–6.
13. Maier-Hein L, Vedula SS, Speidel S, Navab N, Kikinis R, Park A, et al. Surgical data science for next-generation interventions. Nat Biomed Eng. 2017;1(9):691–6.
14. Hung AJ, Chen J, Gill IS. Automated performance metrics and machine learning algorithms to measure surgeon performance and anticipate clinical outcomes in robotic surgery. JAMA Surg. 2018;153(8):770–1.
15. Chen J, Cheng N, Cacciamani G, Oh P, Lin-Brande M, Remulla D, et al. Objective assessment of robotic surgical technical skill: a systematic review. J Urol. 2019;201(3):461–9.
16. Birkmeyer JD, Finks JF, O'Reilly A, Oerline M, Carlin AM, Nunn AR, et al. Surgical skill and complication rates after bariatric surgery. N Engl J Med. 2013;369(15):1434–42.
17. Ghasem A, Sharma A, Greif DN, Alam M, Maaieh MA. The arrival of robotics in spine surgery: a review of the literature. Spine. 2018;43(23):1670–7.
18. Yang G-Z, Bellingham J, Dupont PE, Fischer P, Floridi L, Full R, et al. The grand challenges of Science Robotics. Sci Robot. 2018;3(14):eaar7650.
19. LeCun Y, Bengio Y, Hinton G. Deep learning. Nature. 2015;521(7553):436–44.
20. Pakhomov D, Premachandran V, Allan M, Azizian M, Navab N. Deep residual learning for instrument segmentation in robotic surgery. In: Suk H-I, Liu M, Yan P, Lian C, editors. Machine learning in medical imaging. Cham: Springer International Publishing; 2019. p. 566–73. (Lecture Notes in Computer Science).
21. Nguyen TT, Nguyen ND, Bello F, Nahavandi S. A new tensioning method using deep reinforcement learning for surgical pattern cutting. In: 2019 IEEE International Conference on Industrial Technology ICIT. 2019. p. 1339–44.
22. Bohn R. The development of intelligent systems for industrial use: an empirical investigation. In: Research on technological innovation, management, and policy. Greenwich: J.A.I; 1986. p. 169–211.
23. Paxton C, Barnoy Y, Katyal K, Arora R, Hager GD. Visual robot task planning. In: 2019 international conference on robotics and automation (ICRA). 2019. p. 8832–8.
24. Dehghani H, Farritor S, Oleynikov D, Terry B. Automation of suturing path generation for da Vinci-Like surgical robotic systems. In: American Society of Mechanical Engineers Digital Collection;

2018 [cited 2019 Oct 22]. Available from: https://asme-digitalcollection.asme.org/BIOMED/proceedings/DMD2018/40789/V001T07A008/271978.
25. Sen S, Garg A, Gealy DV, McKinley S, Jen Y, Goldberg K. Automating multi-throw multilateral surgical suturing with a mechanical needle guide and sequential convex optimization. In: 2016 IEEE international conference on robotics and automation (ICRA). 2016. p. 4178–85.
26. National Motor Vehicle Crash Causation Survey: Report to Congress. :47.
27. THE ROAD AHEAD National Highway Traffic Safety Administration Strategic Plan 2016–2020.
28. Dehghani Ashkezari H, Mirbagheri A, Farahmand F, Behzadipour S, Firoozbakhsh K. Real time simulation of grasping procedure of large internal organs during laparoscopic surgery. In: 2012 annual international conference of the IEEE engineering in medicine and biology society. 2012. p. 924–7.
29. Dehghani Ashkezari H, Mirbagheri A, Behzadipour S, Farahmand F. A mass-spring-damper model for real time simulation of the frictional grasping interactions between surgical tools and large organs. Sci Iran Int J Sci Technol. 2015;22(5):1833–41.
30. Heredia-Pérez SA, Harada K, Padilla-Castañeda MA, Marques-Marinho M, Márquez-Flores JA, Mitsuishi M. Virtual reality simulation of robotic transsphenoidal brain tumor resection: evaluating dynamic motion scaling in a master-slave system. Int J Med Robot [Internet]. 2019 Feb [cited 2019 Oct 22];15(1). Available from: https://www.ncbi.nlm.nih.gov/pmc/articles/PMC6587960/.
31. Prasad SM, Prasad SM, Maniar HS, Chu C, Schuessler RB, Damiano RJ. Surgical robotics: impact of motion scaling on task performance. J Am Coll Surg. 2004;199(6):863–8.
32. Yuen SG, Kettler DT, Novotny PM, Plowes RD, Howe RD. Robotic motion compensation for beating heart intracardiac surgery. Int J Robot Res. 2009;28(10):1355–72.
33. Lindgren K, Huang K, Hannaford B. Towards real-time surface tracking and motion compensation integration for robotic surgery. In: 2017 IEEE/SICE international symposium on system integration (SII). 2017. p. 450–6.
34. MacLachlan RA, Becker BC, Tabarés JC, Podnar GW, Lobes LA Jr, Riviere CN. Micron: an actively stabilized handheld tool for microsurgery. IEEE Trans Robot. 2012;28(1):195–212.
35. Heeman W, Steenbergen W, van Dam GM, Boerma EC. Clinical applications of laser speckle contrast imaging: a review. J Biomed Opt. 2019;24(8):080901.
36. Son GM, Kwon MS, Kim Y, Kim J, Kim SH, Lee JW. Quantitative analysis of colon perfusion pattern using indocyanine green (ICG) angiography in laparoscopic colorectal surgery. Surg Endosc. 2019;33(5):1640–9.
37. Schwaitzberg SD, Scott DJ, Jones DB, McKinley SK, Castrillion J, Hunter TD, et al. Threefold increased bile duct injury rate is associated with less surgeon experience in an insurance claims database: more rigorous training in biliary surgery may be needed. Surg Endosc. 2014;28(11):3068–73.
38. Zuzak KJ, Naik SC, Alexandrakis G, Hawkins D, Behbehani K, Livingston EH. Characterization of a near-infrared laparoscopic hyperspectral imaging system for minimally invasive surgery. Anal Chem. 2007;79(12):4709–15.
39. Yoon J, Joseph J, Waterhouse DJ, Luthman AS, Gordon GSD, di Pietro M, et al. A clinically translatable hyperspectral endoscopy (HySE) system for imaging the gastrointestinal tract. Nat Commun. 2019;10(1):1–13.
40. Stroh M, Zimmer JP, Duda DG, Levchenko TS, Cohen KS, Brown EB, et al. Quantum dots spectrally distinguish multiple species within the tumor milieu in vivo. Nat Med. 2005;11(6):678–82.
41. Huber-Mörk R, Štolc S, Soukup D, Holländer B. Shape from refocus. In: Bebis G, Boyle R, Parvin B, Koracin D, McMahan R, Jerald J, et al., editors. Advances in visual computing. Cham: Springer International Publishing; 2014. p. 153–62. (Lecture Notes in Computer Science).
42. Mirota DJ, Ishii M, Hager GD. Vision-based navigation in image-guided interventions. Annu Rev Biomed Eng. 2011;13:297–319.
43. Nguyen T-N, Huynh H-H, Meunier J. 3D reconstruction with time-of-flight depth camera and multiple mirrors. IEEE Access. 2018;6:38106–14.
44. Maier-Hein L, Mountney P, Bartoli A, Elhawary H, Elson D, Groch A, et al. Optical techniques for 3D surface reconstruction in computer-assisted laparoscopic surgery. Med Image Anal. 2013;17(8):974–96.
45. Barron JT, Malik J. Shape, illumination, and reflectance from shading. IEEE Trans Pattern Anal Mach Intell. 2015;37(8):1670–87.
46. Esteva A, Kuprel B, Novoa RA, Ko J, Swetter SM, Blau HM, et al. Dermatologist-level classification of skin cancer with deep neural networks. Nature. 2017;542(7639):115–8.
47. Pesapane F, Codari M, Sardanelli F. Artificial intelligence in medical imaging: threat or opportunity? Radiologists again at the forefront of innovation in medicine. Eur Radiol Exp. 2018;2(1):35.
48. Eric Topol on the Future of Medicine. Wall Street Journal [Internet]. 2014 Jul 7 [cited 2019 Oct 26]; Available from: https://www.wsj.com/articles/eric-topol-on-the-future-of-medicine-1404765024.
49. Sutton RS, Barto AG. Reinforcement learning: an introduction. MIT Press; 2018. 549 p.
50. [1902.01459] Autonomous tissue manipulation via surgical robot using learning based model predictive control [Internet]. [cited 2019 Oct 21]. Available from: https://arxiv.org/abs/1902.01459.
51. Sangiovanni B, Rendiniello A, Incremona GP, Ferrara A, Piastra M. Deep reinforcement learning for collision avoidance of robotic manipulators. In: 2018 European Control Conference (ECC). 2018. p. 2063–8.

52. Kassahun Y, Yu B, Tibebu AT, Stoyanov D, Giannarou S, Metzen JH, et al. Surgical robotics beyond enhanced dexterity instrumentation: a survey of machine learning techniques and their role in intelligent and autonomous surgical actions. Int J Comput Assist Radiol Surg. 2016;11(4):553–68.

53. De Momi E, Kranendonk L, Valenti M, Enayati N, Ferrigno G. A neural network-based approach for trajectory planning in robot–human handover tasks. Front Robot AI [Internet]. 2016 [cited 2019 Oct 22];3. Available from: https://www.frontiersin.org/articles/10.3389/frobt.2016.00034/full.

3D Bioprinting

16

Ippokratis Pountos, Nazzar Tellisi, Mohammad Ali Darabi, Ahmet Erdem, Tamer Mohamed, Murat Guvendiren, and Nureddin Ashammakhi

Introduction

The human body has limited capacity to regenerate tissues following injury, and healing is often with the formation of scar tissue [1, 2]. The use of autografts is ideal for replacing lost tissues. However, autologous grafts are limited in their availability, and their retrieval can cause donor site morbidity [3]. These circumstances have triggered a large interest in developing engineered tissues and regenerative therapeutics [4], which aim to find solutions toward this end.

Three-dimensional (3D) bioprinting has been expanding tremendously over the last decade (Fig. 16.1). It aims to develop biomimetic and functional tissues addressing the demand for tissue and organ replacement. Its market share is projected to be about $11 billion in 2021 in comparison with $2.2 billion in 2012 [5]. When compared to other tissue engineering approaches, 3D bioprinting offers several advantages (Table 16.1)

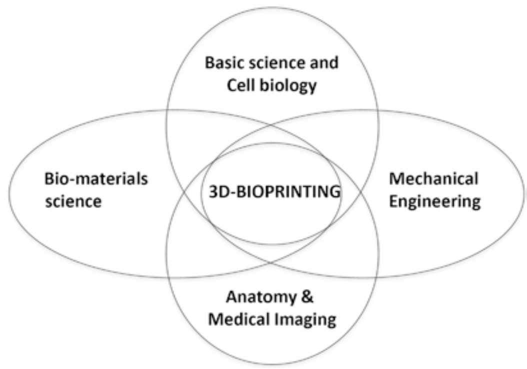

Fig. 16.1 The disciplines contributing to 3D biofabrication of human tissues

I. Pountos (✉) · N. Tellisi
Academic Department of Trauma and Orthopaedics, University of Leeds, Leeds, UK

Chapel Allerton Hospital, Leeds Teaching Hospitals, Leeds, UK
e-mail: pountos@doctors.org.uk

M. A. Darabi
Center for Minimally Invasive Therapeutics (C-MIT), California NanoSystems Institute (CNSI), University of California, Los Angeles, Los Angeles, CA, USA

A. Erdem
Department of Chemistry, Department of Biomedical Engineering, Kocaeli University, Kocaeli, Turkey

T. Mohamed
Aspect Biosystems, Vancouver, BC, Canada

M. Guvendiren
Otto H. York Department of Chemical and Materials Engineering, Department of Biomedical Engineering, New Jersey Institute of Technology, Newark, NJ, USA

N. Ashammakhi
Center for Minimally Invasive Therapeutics (C-MIT), California NanoSystems Institute (CNSI), Department of Radiological Sciences, David Geffen School of Medicine, Department of Biomedical Engineering, Henry Samueli School of Engineering, University of California, Los Angeles, Los Angeles, CA, USA

S. Atallah (ed.), *Digital Surgery*, https://doi.org/10.1007/978-3-030-49100-0_16

Table 16.1 Comparison of different tissue engineering approaches

Methods	Hanging drop method	Microwell-based method	Microfluidics	Magnetic force-based patterning	Bioprinting
Mechanisms	Cellular spheroids are formed by gravitational force	Microwells are fabricated by nonadhesive materials to form cellular spheroids	Micro-flow mediates stacking cells in layers or forming cell spheroids using trapping	Magnetically labeled cells are compacted in spheroids formed under magnetic forces	Cells are deposited in scaffold-based or scaffold-free manner
Size uniformity	++	+++	+++	+++	+++
Microarchitectural controllability	+	++	+++	+++	+++
Scalability	++	+	+	++	+++
Coculture ability	++	++	++	+	+++
High-throughput capability	+	+++	+++	+++	+++
Low risk of cross-contamination	+	+	++	++	+++

From Peng et al. [7]. Reprinted with permission from Elsevier

[6, 7]. More importantly, instead of seeding cells into scaffolds, 3D bioprinting creates a framework for the fabrication of complex cell-laden tissues with specific architectures resembling the target tissue [6, 8]. Provided by a layer-by-layer biofabrication method, cell and growth factor distribution is homogenous, and several biomaterials can be used in the same construct to recapitulate the structure of the target tissue [6, 8, 9]. These advantages have been confirmed by several experimental studies, which show great potential for clinical translation of this technology in the near future [6, 8, 10].

The aim of this chapter is to present the current advances and understanding of 3D bioprinting in the development of viable biomimetic human tissues. The present chapter focuses on the direct bioprinting of such constructs and summarizes the available examples of tissues produced with this technology. The challenges and future perspectives are also discussed.

Three-Dimensional Printing Techniques

Several 3D bioprinting techniques have been developed including extrusion-based bioprinting, light-based bioprinting, and droplet-based bioprinting (Fig. 16.2) [8, 11, 12]. Extrusion-based 3D bioprinting, often referred to as pressure-assisted bioprinting, was developed as a technique for scaffold fabrication. Over the years, the popularity of this technique grew due to its simplicity, diversity, and predictability. Extrusion-based 3D bioprinting can be divided into pneumatic, piston-driven, or screw-driven dispensing [13]. The pneumatic dispensing utilizes air pressure to dispense the biomaterial, while mechanical forces are used for the piston-driven and screw-driven methods [13]. Among the requirements of the bioinks compatible with this technique is a relative viscosity ranging from 30 to 6×10^7 mPa [14]. Factors to consider are the tuning of the viscosity, the state of the bioink prior to bioprinting, and the available biofabrication window [15]. Extrusion-based bioprinting delivers good homogeneity of bioinks, can be performed at room temperature, and can deliver relatively high cell densities. On the other hand, the overall resolution and speed is rather poor compared to other techniques like inkjet bioprinting [14], and some authors have noted deformation of cells and high apoptosis levels [16].

Light-based bioprinting technologies include stereolithography apparatus (SLA), digital light processing or projection (DLP), and laser-induced forward transfer (LIFT). Stereolithography is a

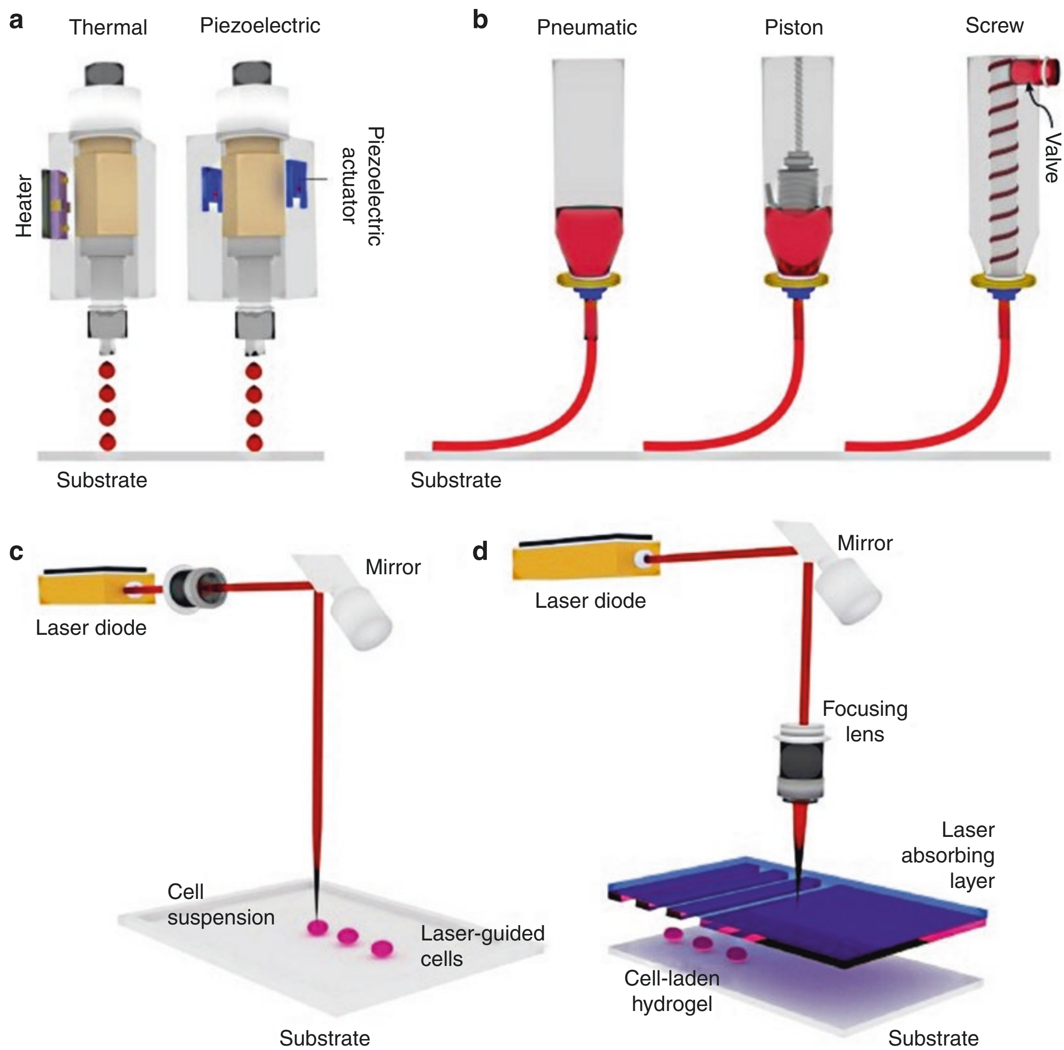

Fig. 16.2 Available 3D bioprinting technologies. (**a**) Thermal and piezoelectric inject printing; (**b**) extrusion bioprinters with pneumatic, piston-, and screw-driven dispensing; (**c**) laser-guided SLA- and DLP-type bioprinter. The difference of SLA and DLP is light sources. While the SLA uses the light source as laser, the DLP uses projector. (**d**) Laser-induced forward transfer (LIFT)-type bioprinter. Laser bioprinter with either driving cells to the substrate or transfer of a vapor bubble containing bioink onto a substrate. (From Knowlton et al. [158]. Reprinted with permission from Elsevier)

light-assisted printing method used to cure light-sensitive bioinks [17, 18]. It involves the curing, i.e., cross-linking, of a cell-laden photo-cross-linkable polymer in a layer-by-layer fashion. Its main advantage is that no printheads are needed, but the printing time is related to the printing resolution and thickness [17, 18]. Gauvin et al. suggested that resolution of 100 μm can be achieved with cell viability higher than 90% [18]. Digital light processing (DLP) utilizes a projector screen to project each print layer [19]. This process is much faster as compared to SLA as it cures the whole layer at once.

Light-based bioprinting technologies also include laser-induced forward transfer (LIFT). Conventional desktop inkjet printing technology led to the development of inkjet-based 3D bioprinting. It involves a noncontact printing process, which can be further subclassified as drop-on-demand inkjet bioprinting, continuous-inkjet bioprinting, and electro-hydrodynamic jet bioprinting [20]. The overall resolution is around 50 μm, but this technology suffers from failure to sustain continuous flow [21]. For this reason, low-viscosity bioinks are required, with viscosities less than 10 mPa [11, 22, 23]. In addition, despite the fact that the inkjet bioprinting technique is fast compared to other methods, printed cell densities and viability are low [14]. The latter could be attributed to shear and thermal stress that are exerted upon the cells from the high temperatures and pressures reached in the thermal actuator element and piezoelectric actuation systems, respectively [11, 22, 23]. LIFT allows the deposition of either solid or liquid materials in high resolution through the effect of pulsed nanosecond laser energy [24]. Although it creates droplets with the aid of laser and although it is commonly regarded as a light-based bioprinting technology, some researchers consider it as one of the droplet-based bioprinting technologies. Following stimulation, a pressure bubble is created that drives the bioink droplet from the donor film to a substrate plate which contains the bioink [21]. The overall resolution achieved is in the region of 10–50 μm. Important parameters that could influence this technique include the laser energy, speed, and the rheological properties of the bioink [22, 24, 25]. Some researchers highlighted low cell survival rates, probably due to the thermal and shearing stress experienced by cells during the process [26].

Bioinks

Bioink is printable formulation for 3D bioprinting, and it is composed of living cells without or with carrier and/or matrix hydrogels. In addition to cells and hydrogels, other additive components such as biomaterials (e.g., bioceramics) and bioactive molecules can be added to the bioink formulation.

Cells

Cells are the main biological component of the bioinks used for 3D bioprinting of functional constructs. Three-dimensional bioprinting should take into account all the different cell types needed to simulate native tissue that needs to be constructed. Accordingly, cells can be of parenchymal type, supportive type, or cells for vascularization. During 3D bioprinting, the cells chosen to be printed will go through a journey that can affect their properties, function, and survival within the newly formed construct [27–29]. This journey begins from their harvesting and extends until their final implantation in vivo, when they are applied for regenerative purposes. Hence, it is essential to minimize the effects from harvesting, handling, culture environment, and media [30]. These cells can be broadly divided into either committed cell types, stem cells [31], and genetically programmed cells [32] to perform specific tasks and functions.

Committed and differentiated human cells could be considered the ideal source for creation of biomimetic tissues. The first issue arising from the use of such cells is the potential host immune reactions in cases of implantation of exogenous cells. Autologous sources are preferred, but donor site morbidity is a potential drawback. In addition, the life span of these cells is limited, and they lose their capacity to proliferate ex vivo. For example, liver cells have been found to have high regeneration capacity in vivo, yet they exhibit poor capacity for expansion in vitro [33]. Except proliferation and survival, the ex vivo manipulation of these cells changes their phenotypic profile. For instance, cardiac valve endothelial cells were shown to express osteogenic markers following isolation [34, 35].

Stem cells can further be subdivided into embryonic stem cells, stem cells from fetal supporting tissues, and adult tissue-derived stem cells. Embryonic stem cells can differentiate in most specialized cell types, and they have an immense capacity to proliferate in an undifferentiated state. There are several drawbacks involved with the use of these cells. Embryos are destroyed during their isolation, which carries ethical issues [36]. In addition, their use has been related to the development of teratomas [37]. An alternative cell source for stem cells is human placenta and amnion. These cells pose less risk for tumorigenesis and pose minimal ethical concerns but require prolonged freezing and thus investment in the infrastructure for their storage [38].

Adult stem cells are the most studied cell type in the last three decades. Adult stem cells are multipotent precursor cells with tremendous cell renewal capacity [39, 40]. They differentiate toward cell types found in their surroundings following cues derived from tissue trauma [39]. They do not trigger an immune reaction. Often, their endogenous production of cytokines and chemokines diminishes unwanted functions like inflammation and cell death [39–41]. Despite their wide use in research, one important drawback is the lack of sufficient knowledge on the underlying physiology and the mechanisms that control their fates [41, 42].

Induced pluripotent stem cells (iPSCs) are somatic cells that have been transformed to an embryonic stem cell-like state following genetic reprogramming [43]. Genetic reprogramming involves the introduction of genes into the cells that force them toward specific properties similar to those seen in pluripotent cells [42]. This forced genetic expression is introduced through viral vectors, and poor yields of iPSCs are reported [44]. Also, the type of the original cell used to create iPSCs can influence the final functions of the derived cells [45–47].

Biomaterials

Hydrogels are the most utilized biomaterials for bioprinting due to their compatibility with living cells [48]. Several other types of biomaterials can be utilized as additives which can range from soft hydrogels to ceramic [49]. There are specific requirements for achieving successful 3D printing that need to be met by the bioinks as was discussed above.

Hydrogels are three-dimensional polymer networks that can hold a significant amount of water and can mimic the elastic modulus of the majority of human tissues except the calcified bodily structures like bone and teeth [50]. Hydrogels can be further subdivided according to their origin into naturally occurring polymers and their derivatives like alginate, collagen, chitosan, gelatin, and hyaluronic acid or synthetic materials like polyethylene glycol, copolymers, and pluronic F127, which can have adaptable structure, composition, and function [13, 51–53]. Naturally occurring polymers are often favored because of the similarities with human extracellular matrix (ECM) such as collagen and its derivatives. Due to their similarities with tissue environment, these biomaterials are ideal for encapsulating cells [13]. On the other hand, they can cause immune reactions, and they also have relatively poor mechanical properties. Natural polymers can be mixed with synthetic polymers such as polyvinyl alcohol, polycaprolactone (PCL), polylactide (PLA), poly(lactide-*co*-glycolide) (PLGA), and poly(3-hydroxybutyrate) to generate hybrid biomaterial, so as to improve the mechanical properties of hydrogels [9, 54–56]. Also some specific nanomaterials can be added for the improving mechanical strength of hydrogel to obtain functional multicomponent bioinks for the preparation of mechanically demanding tissues – such as bone, cartilage, and tendon [57].

In addition to natural and synthetic hydrogels, hydrogels can also be developed from decellularized tissues to create tissue-specific bioinks. For instance, tissues including bone, cartilage, liver, and heart have already been shown to create tissue-specific bioinks [58, 59]. Here, after decellularization of the tissue, it is enzymatically digested and solubilized to form a viscous bioink which, in turn, allows for the encapsulation of cells. Bioinks from decellularized tissue inherently show *thermal gelation*, resulting in gelation (solidification) at body temperature.

Biomolecules

Multifunctionalization of biomaterials [60] is a critical process in tissue engineering. It involves the inclusion of agents that can help in the regulation of cell fates and function through their interactions with cells within the 3D bioprinting construct. These molecules can direct cells in the engineered tissue constructs toward a specific phenotype and guide their migration, proliferation, and differentiation – and they can also influence native cells toward processes such as vascularization of the graft or in situ regeneration [61]. Alternatively, modifications of the biomaterials through the incorporation of bioactive cues, recognition sites, and adhesion molecules have been used [5, 62]. The choice of the biomolecules is dependent on the target tissue that one aims to treat. For bone regeneration, for example, molecules that improve angiogenesis – such as the *vascular endothelial growth factor* (VEGF), *osteogenesis-like growth factors* belonging in the TGF-β superfamily (TGF-β), or the *bone morphogenetic proteins* (BMPs) – have been used [54, 63–65]. Similarly, in nerve regeneration, *neurotrophic factors*, such as the nerve growth factor, *neurotrophin-3*, and *ciliary neurotrophic factor*, have been used [66]. These molecules are the steering forces giving cues to the cells to adopt specific function leading to the healing and incorporation of the graft.

Computer-Aided Design and Manufacturing for Tissue Modeling

The fabrication of biomimetic tissues can be achieved through the use of computer-aided design (CAD) and computer-aided manufacturing (CAM) techniques. CAD is defined as the computer software aiming to design target tissue structure, while CAM is referred as the software used to control the printer during 3D printing. Due to the complexity of tissue anatomical and structural organization, information on the tissue composition at the microscale level is essential. Computed tomography (CT) and magnetic resonance imaging (MRI) can provide information on the geometries and brief structure of calcified and soft tissues [67]. Once this information becomes available, histological 3D sections are designed based on the underlying anatomy of the target tissue. The thickness of these sections depends on the printer's resolution and can range from 100 to 500 μm depending on the machine and material used [67]. CAM technologies are equally important for the creation of the CAD models. CAM takes into account the properties of the underlying tissue and bioinks and aims toward successful creation of target structures. Bioink deformation, stiffness, fusion, nozzle clogging, and viscosity are controlled through CAM [68, 69]. In addition, CAM controls the survival and properties of the cellular components of bioinks [8, 70]. In essence, while CAD is critical for the reproduction of biomimetic tissues, CAM safeguards the quality of the 3D printing process.

Applications

The potential of 3D bioprinting has been shown in a number of applications. The fabrication of biomimetic tissues including bone, cartilage, nerves, cardiovascular tissue, and others has become possible through this technology.

Bone and Cartilage

Bone and cartilage regeneration have been important areas that tissue engineering has addressed over the last decades. Among the challenges mostly faced are the need of recreating the complex organization of these structures, the optimization of the rheological properties, biocompatibility, osteoconductivity, and realizing the potential of implanted grafts to be integrated and remodeled [71, 72].

Evidence from a wide range of 3D bioprinted constructs for bone regeneration has been promising [54]. Some bioinks were found capable of yielding stresses and Young's modulus similar to that of the human bone [57]. It is well recognized that mechanical stability alone is not the only desirable feature of bone constructs; the chosen biomaterials should allow high viability while preserving the osteogenic capacity of osteoprogenitor cells printed within. In fact, some authors highlighted that although materials like PCL and PLGA are mechanically stable, they are not enough to support osteogenesis [73, 74]. On the contrary, other biomaterials, for example, decellularized bone matrix with PCL, were associated with upregulation of osteogenic genes of human adipose-derived stem cells [75]. Similarly, Campos et al. compared the effect of the addition of thermo-responsive agarose in a collagen bioink. This addition improved the mechanical stiffness of the construct [76]. The addition of bioactive glass particles has been shown to improve the mechanical performance while allowing for the construction of a porous construct, mimicking the pores of native human bone [77, 78].

Constructs which allow for the controlled release of molecules that either improves cell viability, angiogenesis, or osteogenesis could be a potential option [79, 80]. Du et al. created a 3D bioprinted gelatin-based bioink encapsulating MSCs and microfibers containing BMP-2. The addition of BMP-2 induced a stronger osteogenic phenotype following culture [80]. In a similar study, incorporating BMP-2 and VEGF to the construct resulted in increased expression of osteoblast-related genes Col1a1, Runx2, and Osx [79].

Cartilage is another important tissue, and its regeneration may benefit from 3D bioprinting. It is a specialized form of elastic connective tissue constituting parts of joints, the outer ear, and the nose. *Articular* cartilage draws most interest as its loss (e.g., in arthritis) is a major cause of morbidity and disability worldwide. Articular cartilage is not vascularized; hence, it is an ideal target for regenerative therapy using 3D bioprinting. However, the ideal cell carrier for chondrocytes is not yet identified, and available suitable materials lack enough mechanical integrity to enable successful function in high-load-bearing sites [81].

Tellisi et al. compared hydrogels, ceramics, and meshes for cartilage tissue engineering [82], and they found that chondrocyte proliferation was more in hydrogels as compared to ceramics and mesh. Daly et al. have also compared a wide range of commonly used hydrogel that included BioINK™, GelMA, alginate, and agarose [81]. The results showed that the choice of bioink can direct the cells to different functions. More specifically, alginate and agarose hydrogels resulted in the formation of tissue rich in type II collagen, i.e., supported the development of hyaline-like chondral tissue. On the other hand, GelMA and BioINK™ led to the development of a more fibrocartilage-like tissue. The combination of nanofibrillated PLGA [83], cellulose, or PLA nanofibers with cell-laden alginate hydrogel was also explored [84, 85]. These approaches were reported to result in improved cell density and better reinforcement of the mechanical strength of the constructs. Another study reported that high-density collagen is an ideal bioink for reconstruction of cartilage due to its capability of maintaining appropriate cell growth and for having mechanical stability [86].

Finally, in situ 3D bioprinting is presenting an attractive option [10]. For example, Di Bella et al. developed a handheld 3D bioprinter in an experimental animal model of critical size cartilage defect [87]. This printer was capable of on-demand filling of these defects with MSCs together with gelatin methacrylamide and HA methacrylate hydrogel. Improved macroscopic and microscopic appearances of the resulting tissue were noted when compared to conventional approaches. A higher amount of newly regenerated cartilage was seen with no signs of subchondral collapse or deformation [87].

Clinical evidence has shown that during the development of arthritis, changes to the underlying bone coexist with loss of cartilage. Therefore, a combined approach might be required. A number of researchers have worked on this principle, aiming for the development of osteochondral constructs rather than bone or cartilage patches [88–92]. In these studies, 3D bioprinted constructs with predesigned mechanical properties were created for potential clinical applications ranging from femoral head to temporomandibular defects [88, 89, 91, 92]. In an experimentally induced proximal humeral defect in rabbits, a customized layer-by-layer 3D bioprinted construct containing transforming growth factor β3 (TGF-β3), HAp powder, and PCL was applied following capture with laser scanning [90]. The authors suggested that the entire articular surface of the synovial joint could regenerate without the addition of cells. It was hypothesized that the regeneration of complex tissues could occur by homing of endogenous cells.

Neural Cells

Nerve injury is the cause of significant disability and represents a clinical challenge due to the poor regenerative capacity of neural tissues. Three-dimensional bioprinting could be applied to nerve regeneration. For example, England et al. created a 3D bioprinted fibrin-based scaffold to guide neurite growth by encapsulating Schwann cells [93]. In cases of nerve loss, hollow nerve conduits composed of either synthetic or natural materials found to promote nerve regeneration [94–96]. Some authors suggested that cells in the bioink enhance the healing potential [97, 98]. In an experimentally created tibial nerve transection with 10 mm gap in rodents, Adams et al. used engineered nerve conduits utilizing fibroblasts and embryonic rat nerve cells [98]. They showed adequate distal motor nerve conduction velocity and large axons within the repaired nerve segment. In a similar study on the sciatic nerve defects in rats, cylindrical layer-by-layer 3D printed grafts were created. The cylinders contained MSCs (90%) and Schwann cells (10%) [97]. In this proof of concept study, the authors showed that this construct performed better than the standard collagen tubes and highlighted the complexities and the numerous adjustments needed to optimize the performance of such grafts.

Blood Vessels

The primary goal of tissue engineering is to create functional structures which could be incorporated into the host after implantation and can withstand the demands of the target tissue. Having complex structures without a vascular network to support the printed cells can lead to failure, because cells can survive on diffusion, only at a farthest distance of 200–400 μm from a feeding blood vessel [99]. In many studies, the lack of vasculature within the graft is surpassed by addition of angiogenic factors to promote angiogenesis. However, there is often a long process before angiogenesis is established; therefore, implanted graft survival is at risk [100].

Although currently the biofabrication of vascularized tissue has not been achieved, several authors evaluated ways to create and incorporate blood vessels into 3D printed grafts [101]. Some authors focused on the creation of large constructs like aortic tissue. One approach involved the use of embryonic fibroblasts and hydrogels printed in a layer-by-layer fashion to form an aortic tissue construct [102]. Another group utilized decellularized ECM with the use of separate layers of human smooth muscle cells, endothelial cells, and fibroblasts to recreate the media, intima, and adventitia layers through perfusion into the corresponding location of the supporting scaffold [103]. The fabrication of smaller blood vessels can be constructed as tubular structures with defined pores of 100–200 μm mimicking the structure of native vasculature [104]. Biomaterial selection is a key aspect. The production of sophisticated human-scale constructs of various sizes and shapes and incorporating microchannels allowing the diffusion of nutrients have been attempted [67, 105].

Muscles and Tendons

Musculoskeletal injuries are common and can result in significant morbidity [106]. Several authors have thus far explored the potential of musculotendinous regeneration through 3D bioprinting. The fabrication of isolated muscle units composed of myotubes and myoblasts resulted in contraction following electrical stimulation like in native muscles [67, 107, 108]. Kang et al. created skeletal muscle units of 15 × 5 × 1 mm which were stretched along the longitudinal axis and responded to stimulation preserving their structural stability [67]. In regard to tendons, only limited groups have developed biomimetic tendon constructs [109]. The main challenge has been defining the ideal bioink, which could achieve structural stability equivalent to that of native tendons. Attempts to develop complex muscle-tendon units mimicking functional human muscle are also available. A two-layer construct composed of thermoplastic polyurethane co-printed with C2C12 cell-containing hydrogel and PCL co-printed with fibroblast-containing hydrogel offered elasticity for muscle development and stiffness for the development of the tendon [110].

Skin

Skin loss can be the outcome of trauma, skin diseases, and burns. Autografts are of limited availability, and substitutes often fail to achieve acceptable outcomes [111, 112]. Tissue engineering with the use of 3D bioprinting could provide an alternative approach, creating multilayered biomimetic structures to serve as skin substitutes (Fig. 16.3). The simplest option is the seeding of cells such as fibroblasts, keratinocytes, and melanocytes in predefined concentrations and layers into biomaterials, mimicking native human skin [113, 114]. The results have shown that these

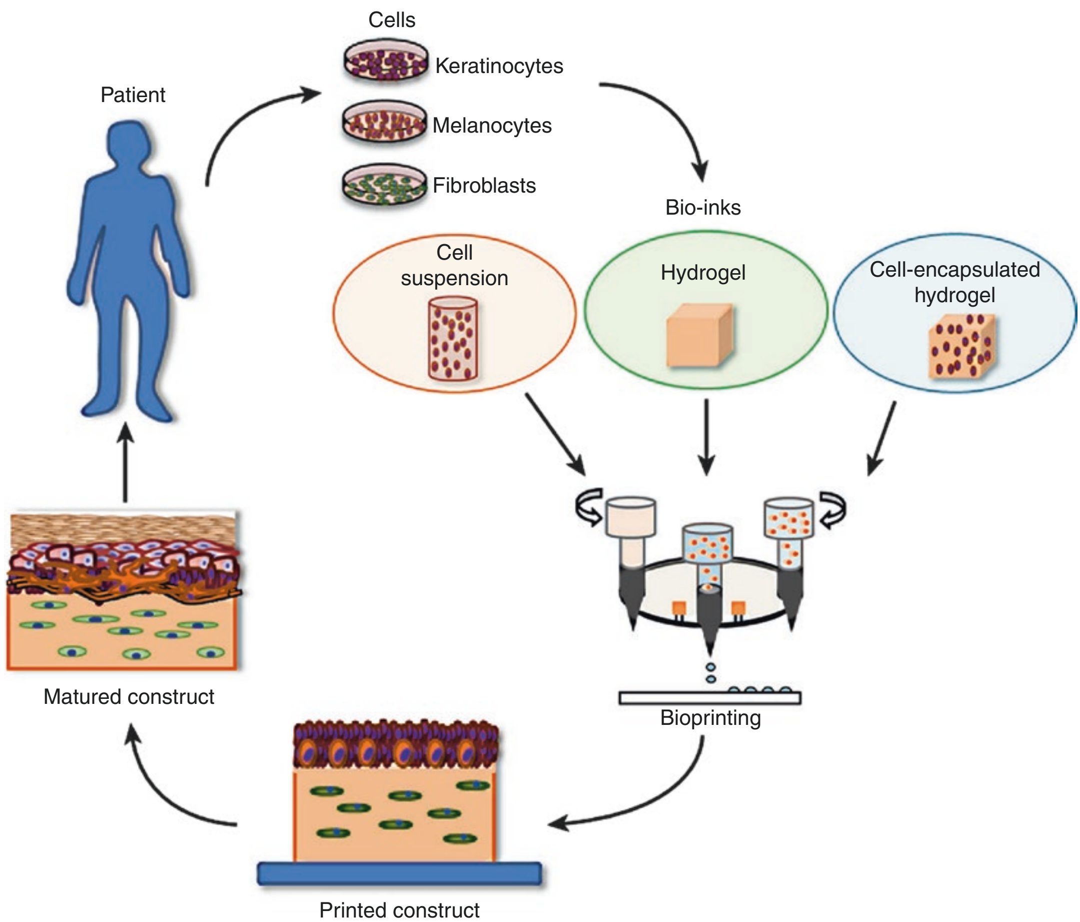

Fig. 16.3 3D bioprinting of skin. Following collection of cells, ex vivo expansion of the cells is commenced. Then 3D bioprinted biomimetic skin is constructed and once matures it is implanted to the patient. (From Ng et al. [159]. Reprinted with permission from Elsevier)

cells survive the printing process, and once implanted in experimental models, they form structures which have histological similarities to normal skin [113, 114].

Min et al. attempted to recreate a multilayer structure of fibroblasts on a collagen hydrogel, which was then covered with layers of melanocytes and keratinocytes [115]. Following histological analysis, the authors reported a distinct skin layer, the presence of pigmentation, and the presence of the outmost layer of normal skin (the stratum corneum). Three-dimensional bioprinting technologies allowing in situ bioprinting have also been developed [10]. In situ 3D bioprinting provides a platform for the creation of fully customized biomimetic structures printed exactly at the site of injury or defect [10]. A number of authors have developed handheld devices capable of ejecting multiple bioinks and demonstrated satisfactory cell survival and fast healing of skin defect [116–118].

Cardiovascular Tissue

Cardiovascular diseases are highly prevailing, and they represent one of the most common causes of death worldwide [119]. Tissue engineering has attempted to identify treatment options to facilitate the prompt repair of the affected tissue, mainly through the implantation of stem cells. Unfortunately, only a small fraction of these cells survive the effects of cytokines, free radicals, and lack of nutrients [120, 121]. Several attempts to create the hierarchical structure of the native myocardium through 3D bioprinting have been described [122, 123]. For example, Zhang et al. developed an endothelialized myocardial tissue by first aligning endothelial cells along the periphery of microfibers [123]. Then endothelial tissue was covered by cardiomyocytes. This construct had features of functional myocardium and expressed rhythmic beating. In a similar study using MSCs, Tijore et al. created microchanneled gelatin hydrogel that promotes human MSC myocardial commitment and supports native cardiomyocyte contractile functionality [122]. The feasibility of creating biomimetic cardiac tissue was also confirmed by Wang et al., who developed cardiac tissues formed with uniformly aligned, dense, and electromechanically coupled cardiac cells expressing the cardiac markers like α-actinin and connexin [124]. Three-dimensionally printed patches for myocardial regenerations were also explored [125, 126]. These patches were composed of human coronary artery-derived endothelial cells, methacrylated collagen, and an alginate matrix. They were found to upregulate cellular proliferation, migration, and differentiation in the damaged myocardium.

In addition to the regeneration of myocardium, the replacement of heart valves can be feasible utilizing 3D bioprinting technology. The construction of aortic valves capable of withstanding the hemodynamic requirements was proposed. Hockaday et al. used photo-cross-linked bioink loaded with porcine interstitial cells to show the feasibility of creating rapidly biomimetic aortic valve tissues with excellent cellular viability and cell engraftment capabilities [127]. Other groups have showed similar results, with some highlighting that the technique used to improve mechanical strength of the construct can adversely affect the viability of the cells [128, 129].

Retina and Cornea

Corneal and retinal diseases are the most important causes of blindness worldwide. At present, there is extensive research exploring the feasibility of engineering structures of the human eye including the cornea, retina, and lens. Isaacson et al. used extrusion 3D printing to fabricate a corneal-like cell-laden structure [130]. In a similar study, Sorkio et al. created a cornea-mimicking tissue using human stem cells and laser-assisted 3D bioprinting [131]. Printed constructs were examined for their microstructural properties, cell viability, and proliferation and for the expression of key proteins (Ki67, p63α, p40, CK3, CK15, collagen type I, VWF) [131]. As far as the retina is concerned, Lorber et al. created a 3D bioprinted construct containing retinal and glial cells [132]. These cells retained their growth-promoting properties and exhibited higher than 70% viability [132]. Other authors highlighted the importance of the ECM as a determinant of cell differentiation [8, 133]. It is crucial the ECM should mimic the characteristics and stiffness of the human retina [8, 133]. In a scaffold-free approach, Masaeli et al. utilized an inkjet 3D bioprinting system to create (with precision) a construct made of photoreceptor cell layer lying on top of a bioprinted retinal pigment epithelial layer [134]. The cells expressed structural markers including opsin B, opsin R/G, MITF, PNA, rhodopsin, and ZO1 and released large amounts of human vascular endothelial growth factor (hVEGF).

Tissue Models

The development of tissue models for studying tissue and organ function, studying disease states, and testing drugs and chemicals represents another important potential application of 3D bioprinting [135]. This can help to overcome the limitations of current in vitro models which rely on the use of two-dimensional (2D) cell cultures. It is argued that 2D models cannot represent appropriately native tissues [136]. In this relation, Maden et al. developed a 3D bioprinted model of human intestinal mucosa mimicking the function and the biochemical and histological characteristic of the native human tissue [137]. Vascularized perfusable liver tissue has been also created. Drug toxicity on 3D printed tissue was also conducted, with the authors suggesting the advantages of this approach for the evaluation of drug-induced liver injury [138]. Commercially available 3D printed liver and kidney tissue is currently available for research purposes [139].

In addition to healthy tissue models, a number of pathologic tissue models based on 3D bioprinting currently exist. For example, such models can be valuable tools for gaining in-depth understanding of tumor progression and invasion – as well as for the study of the interaction between different cell types and treatment of chemotherapeutic drugs [140]. The clinical scenarios are diverse, and models should be designed accordingly. In metastatic bone disease, Zhou et al. developed a biomimetic bone matrix analyzing the interactions between breast cancer cells, fetal osteoblasts, and human bone marrow MSCs [141]. In another study, 3D bioprinted microtissue, recapitulating the in vivo environment of tumor cells in pituitary adenoma, was found to be an excellent model for cancer research [142]. Similarly, uterine cervical tumor models, lung cancer, neuroblastoma, and breast cancer models exist [143–146].

Other Applications

It has to be noted that the potential targets of 3D bioprinting are not limited to the aforementioned applications. At present, numerous other applications based on 3D bioprinting are being explored – especially ones involving the creation of biomimetic soft or solid human tissues. Such structures include the kidney, liver, and trachea. Ali et al. created 3D bioprinted renal constructs exhibiting structural and functional features of the native renal tissue [147]. Lee et al., on the other hand, 3D printed human liver which mimicked the cellular interactions seen within human liver [148]. Hard structures such as the human trachea were printed using PCL, and the constructs were then placed in omentum culture prior to transplantation [149]. This approach facilitated the rapid re-epithelialization and revascularization of the scaffold and prevented postoperative luminal stenosis [149]. Other potential applications of such 3D bioprinting approaches in hard tissue engineering include the creation of knee meniscal tissues, human ear, and auricular cartilage [85, 150–152].

Current Limitations and Future Prospects

Despite the significant advantages seen in 3D bioprinting over the last decades, at present, this technology has several limitations, which prevents its further expansion. These challenges fall into three main categories: *(a)* decoding of human anatomy and physiology, *(b)* manufacturing issues, and *(c)* creation of viable constructs that will integrate and function in vivo.

With regard to decoding human physiology, despite a gross understanding of the structure of human tissues, the underlying interactions at a cellular level are largely obscure. Not infrequently, our understanding of the composition, organization, and interactions occurring within human tissues is based on animal in vivo models and then extrapolated to explain our knowledge gap in humans. Animals are different species, and thus we often see complications and adverse effects to drugs in humans despite the safe results obtained from experimental studies [153].

In terms of manufacturing, several technical difficulties should be overcome. Attempts to improve the resolution of the printed tissues (probably at a cellular level) will open new avenues to 3D bioprinting. This resolution should be maintained throughout the bioprinting process, and drawbacks – like nozzle clogging with highly homogenous bioinks maintaining their viscosity and shear-thinning properties – should be addressed. Further work on developing new biomaterials for 3D bioprinting is required identifying the ideal material for a given tissue and maintaining stability and mechanical rigidity. In cases when hard tissues (such as bone) are to be created, the bioink should maintain mechanical stability to withstand the demands but, at the same time, should allow the migration, proliferation, and differentiation of osteoprogenitor cells to enable the incorporation and remodeling of the newly formed bone.

Another major challenge of 3D bioprinting is the creation of viable and functional constructs. One of the main challenges is to recreate vascularity. It is well known that cells should be in close proximity to the capillaries; otherwise, increased cell death can follow [154]. It can be hypothesized that improving the vascular networks within these structures will facilitate the functionality and integration of these structures to the host. Studying critical size bone defects has shown that the larger the defect is, the longer the *time* is required for healing, and beyond a critical size, healing by regeneration may *not* occur [155]. This time does not purely correspond to the time required for the bony ends to heal, but instead it correlates with time it takes to achieve revascularization of the graft and the incorporation to the host.

Reflecting on the current growth rate of 3D bioprinting and the intensity of research activity, we envision that, in the near future, customized medical applications will be introduced into clinical practice [156, 157]. Complex constructs mimicking native tissues will emerge. This would require extensive knowledge of biomaterials and the capacity to incorporate bioinks of different properties during the same bioprinting session. These materials should be loaded with the exact cell layers and growth factors to develop microenvironments that may closely mimic that of the target native tissue. Further development in the incorporation of a functional vascular tree in printed constructs is an important factor required to achieve success. Despite the fact that all aforementioned challenges are important, decoding and understanding human anatomy and physiology is the most vital element that will unleash the capabilities of 3D bioprinting.

Conclusions

Today, 3D bioprinting is a rapidly evolving technology for tissue engineering. It enables the fabrication of biomimetic tissues in a fast manner and with high precision. Despite the increasing number of studies presenting its potential role in clinical practice, several challenges are still facing the manufacturing process. The selection of bioinks suitable for a given target tissue, the lack of a vascular tree to support the cellular elements, and the final integration of a functional replacement to the host are among the most important challenges. These challenges will ultimately be overcome via coordinated work that involves biologists, bioengineers, and clinicians.

Conflict of Interest No benefits in any form have been received or will be received from a commercial party related directly or indirectly to the subject of this chapter.

References

1. Arealis G, Nikolaou VS. Bone printing: new frontiers in the treatment of bone defects. Injury. 2015;46 Suppl 8:S20–2.
2. Bara JJ, Dresing I, Zeiter S, Anton M, Daculsi G, Eglin D, Nehrbass D, Stadelmann VA, Betts DC, Muller R, Alini M, Stoddart MJ. A doxycycline inducible, adenoviral bone morphogenetic protein-2 gene delivery system to bone. J Tissue Eng Regen Med. 2018;12:e106–18.
3. Carlisle ER, Fischgrund JS. Chapter 27 - Bone graft and fusion enhancement. In: Errico TJ, Lonner BS, Moulton AW, editors. Surgical management of spinal deformities. Philadelphia: W.B. Saunders; 2009. p. 433–48.
4. Vacanti JP, Langer R. Tissue engineering: the design and fabrication of living replacement devices for surgical reconstruction and transplantation. Lancet. 1999;354:S32–4.
5. Benetti EM, Gunnewiek MK, van Blitterswijk CA, Vancso GJ, Moroni L. Mimicking natural cell environments: design, fabrication and application of bio-chemical gradients on polymeric biomaterial substrates. J Mater Chem B. 2016;4:4244–57.
6. Ashammakhi N, Darabi MA, Pountos I. The dynamic cycle of future personalized and regenerative therapy. J Craniofac Surg. 2019;30:623–5.
7. Peng W, Unutmaz D, Ozbolat IT. Bioprinting towards physiologically relevant tissue models for pharmaceutics. Trends Biotechnol. 2016;34:722–32.
8. Catros S, Fricain J-C, Guillotin B, Pippenger B, Bareille R, Remy M, Lebraud E, Desbat B, Amédée J, Guillemot F. Laser-assisted bioprinting for creating on-demand patterns of human osteoprogenitor cells and nano-hydroxyapatite. Biofabrication. 2011;3:025001.
9. Ashammakhi N, Ahadian S, Xu C, Montazerian H, Ko H, Nasiri R, Barros N, Khademhosseini A. Bioinks and bioprinting technologies to make heterogeneous and biomimetic tissue constructs. Materials Today Bio. 2019;1:100008.
10. Ashammakhi N, Ahadian S, Pountos I, Hu S-K, Tellisi N, Bandaru P, Ostrovidov S, Dokmeci MR, Khademhosseini A. In situ three-dimensional printing for reparative and regenerative therapy. Biomed Microdevices. 2019;21:42.
11. Cui X, Dean D, Ruggeri ZM, Boland T. Cell damage evaluation of thermal inkjet printed Chinese hamster ovary cells. Biotechnol Bioeng. 2010;106:963–9.
12. Wang Z, Abdulla R, Parker B, Samanipour R, Ghosh S, Kim K. A simple and high-resolution stereolithography-based 3D bioprinting system using visible light crosslinkable bioinks. Biofabrication. 2015;7:045009.
13. Ozbolat IT, Hospodiuk M. Current advances and future perspectives in extrusion-based bioprinting. Biomaterials. 2016;76:321–43.
14. Hölzl K, Lin S, Tytgat L, Van Vlierberghe S, Gu L, Ovsianikov A. Bioink properties before, during and after 3D bioprinting. Biofabrication. 2016;8:032002.
15. He Y, Yang F, Zhao H, Gao Q, Xia B, Fu J. Research on the printability of hydrogels in 3D bioprinting. Sci Rep. 2016;6:29977.
16. Leberfinger AN, Ravnic DJ, Dhawan A, Ozbolat IT. Concise review: bioprinting of stem cells for transplantable tissue fabrication. Stem Cells Transl Med. 2017;6:1940–8.
17. Chan V, Zorlutuna P, Jeong JH, Kong H, Bashir R. Three-dimensional photopatterning of hydrogels using stereolithography for long-term cell encapsulation. Lab Chip. 2010;10:2062–70.
18. Gauvin R, Chen Y-C, Lee JW, Soman P, Zorlutuna P, Nichol JW, Bae H, Chen S, Khademhosseini A. Microfabrication of complex porous tissue engineering scaffolds using 3D projection stereolithography. Biomaterials. 2012;33:3824–34.
19. Grigoryan B, Paulsen SJ, Corbett DC, Sazer DW, Fortin CL, Zaita AJ, Greenfield PT, Calafat NJ, Gounley JP, Ta AH. Multivascular networks and functional intravascular topologies within biocompatible hydrogels. Science. 2019;364:458–64.
20. Gudapati H, Dey M, Ozbolat I. A comprehensive review on droplet-based bioprinting: past, present and future. Biomaterials. 2016;102:20–42.
21. Mandrycky C, Wang Z, Kim K, Kim D-H. 3D bioprinting for engineering complex tissues. Biotechnol Adv. 2016;34:422–34.
22. Li J, Chen M, Fan X, Zhou H. Recent advances in bioprinting techniques: approaches, applications and future prospects. J Transl Med. 2016;14:271.
23. Ozbolat IT, Yu Y. Bioprinting toward organ fabrication: challenges and future trends. IEEE Trans Biomed Eng. 2013;60:691–9.
24. Guillemot F, Souquet A, Catros S, Guillotin B. Laser-assisted cell printing: principle, physical parameters versus cell fate and perspectives in tissue engineering. Nanomedicine. 2010;5:507–15.
25. Guillemot F, Souquet A, Catros S, Guillotin B, Lopez J, Faucon M, Pippenger B, Bareille R, Rémy M, Bellance S. High-throughput laser printing of cells and biomaterials for tissue engineering. Acta Biomater. 2010;6:2494–500.
26. Hopp B, Smausz T, Szabó G, Kolozsvari L, Nogradi A, Kafetzopoulos D, Fotakis C. Femtosecond laser printing of living cells using absorbing film-assisted laser-induced forward transfer. Opt Eng. 2012;51:014302.
27. Sotiropoulou PA, Perez SA, Salagianni M, Baxevanis CN, Papamichail M. Characterization of the optimal culture conditions for clinical scale production of human mesenchymal stem cells. Stem Cells. 2006;24:462–71.
28. Kelm JM, Fussenegger M. Microscale tissue engineering using gravity-enforced cell assembly. Trends Biotechnol. 2004;22:195–202.

29. Cukierman E, Pankov R, Stevens DR, Yamada KM. Taking cell-matrix adhesions to the third dimension. Science. 2001;294:1708–12.
30. Pountos I, Corscadden D, Emery P, Giannoudis PV. Mesenchymal stem cell tissue engineering: techniques for isolation, expansion and application. Injury. 2007;38 Suppl 4:S23–33.
31. Bajada S, Mazakova I, Richardson JB, Ashammakhi N. Updates on stem cells and their applications in regenerative medicine. J Tissue Eng Regen Med. 2008;2:169–83.
32. Alluri R, Song X, Bougioukli S, Pannell W, Vakhshori V, Sugiyama O, Tang A, Park SH, Chen Y, Lieberman JR. Regional gene therapy with 3D printed scaffolds to heal critical sized bone defects in a rat model. J Biomed Mater Res A. 2019;107(10):2174–82.
33. Atala A. Tissue engineering, stem cells and cloning: current concepts and changing trends. Expert Opin Biol Ther. 2005;5:879–92.
34. Liu W, Zhong Z, Hu N, Zhou Y, Maggio L, Miri AK, Fragasso A, Jin X, Khademhosseini A, Zhang YS. Coaxial extrusion bioprinting of 3D microfibrous constructs with cell-favorable gelatin methacryloyl microenvironments. Biofabrication. 2018;10:024102.
35. Wylie-Sears J, Aikawa E, Levine RA, Yang J-H, Bischoff J. Mitral valve endothelial cells with osteogenic differentiation potential. Arterioscler Thromb Vasc Biol. 2011;31:598–607.
36. Itskovitz-Eldor J, Schuldiner M, Karsenti D, Eden A, Yanuka O, Amit M, Soreq H, Benvenisty N. Differentiation of human embryonic stem cells into embryoid bodies comprising the three embryonic germ layers. Mol Med. 2000;6:88.
37. Wilmut I. The moral imperative for human cloning. New Sci. 2004;181:16.
38. De Coppi P, Bartsch G Jr, Siddiqui MM, Xu T, Santos CC, Perin L, Mostoslavsky G, Serre AC, Snyder EY, Yoo JJ. Isolation of amniotic stem cell lines with potential for therapy. Nat Biotechnol. 2007;25:100.
39. Pountos I, Giannoudis PV. Biology of mesenchymal stem cells. Injury. 2005;36:S8–S12.
40. Pountos I, Georgouli T, Calori GM, Giannoudis PV. Do nonsteroidal anti-inflammatory drugs affect bone healing? A critical analysis. ScientificWorldJournal. 2012;2012:606404.
41. Giannoudis PV, Pountos I. Tissue regeneration: the past, the present and the future. Injury. 2005;36:S2–5.
42. Takahashi K, Yamanaka S. Induction of pluripotent stem cells from mouse embryonic and adult fibroblast cultures by defined factors. Cell. 2006;126:663–76.
43. Kim JS, Choi HW, Choi S, Do JT. Reprogrammed pluripotent stem cells from somatic cells. Int J Stem Cells. 2011;4:1–8.
44. Lewandowski J, Kurpisz M. Techniques of human embryonic stem cell and induced pluripotent stem cell derivation. Arch Immunol Ther Exp. 2016;64:349–70.
45. Maherali N, Ahfeldt T, Rigamonti A, Utikal J, Cowan C, Hochedlinger K. A high-efficiency system for the generation and study of human induced pluripotent stem cells. Cell Stem Cell. 2008;3:340–5.
46. Aasen T, Raya A, Barrero MJ, Garreta E, Consiglio A, Gonzalez F, Vassena R, Bilić J, Pekarik V, Tiscornia G. Efficient and rapid generation of induced pluripotent stem cells from human keratinocytes. Nat Biotechnol. 2008;26:1276.
47. Brambrink T, Foreman R, Welstead GG, Lengner CJ, Wernig M, Suh H, Jaenisch R. Sequential expression of pluripotency markers during direct reprogramming of mouse somatic cells. Cell Stem Cell. 2008;2: 151–9.
48. Highley CB, Rodell CB, Burdick JA. Direct 3D printing of shear-thinning hydrogels into self-healing hydrogels. Adv Mater. 2015;27:5075–9.
49. Chen Z, Li Z, Li J, Liu C, Lao C, Fu Y, Liu C, Li Y, Wang P, He Y. 3D printing of ceramics: a review. J Eur Ceram Soc. 2019;39:661–87.
50. Sharma S, Srivastava D, Grover S, Sharma V. Biomaterials in tooth tissue engineering: a review. J Clin Diagn Res. 2014;8:309.
51. Lei M, Wang X. Biodegradable polymers and stem cells for bioprinting. Molecules. 2016;21:539.
52. Melchels FP, Domingos MA, Klein TJ, Malda J, Bartolo PJ, Hutmacher DW. Additive manufacturing of tissues and organs. Prog Polym Sci. 2012;37:1079–104.
53. Billiet T, Vandenhaute M, Schelfhout J, Van Vlierberghe S, Dubruel P. A review of trends and limitations in hydrogel-rapid prototyping for tissue engineering. Biomaterials. 2012;33:6020–41.
54. Ashammakhi N, Hasan A, Kaarela O, Byambaa B, Sheikhi A, Gaharwar AK, Khademhosseini A. Advancing frontiers in bone bioprinting. Adv Healthc Mater. 2019;8:1801048.
55. Li X, Cui R, Sun L, Aifantis KE, Fan Y, Feng Q, Cui F, Watari F. 3D-printed biopolymers for tissue engineering application. Int J Polymer Sci. 2014;2014.
56. Chia HN, Wu BM. Recent advances in 3D printing of biomaterials. J Biol Eng. 2015;9:4.
57. Sawkins MJ, Mistry P, Brown BN, Shakesheff KM, Bonassar LJ, Yang J. Cell and protein compatible 3D bioprinting of mechanically strong constructs for bone repair. Biofabrication. 2015;7:035004.
58. Pati F, Jang J, Ha D-H, Kim SW, Rhie J-W, Shim J-H, Kim D-H, Cho D-W. Printing three-dimensional tissue analogues with decellularized extracellular matrix bioink. Nat Commun. 2014;5:3935.
59. Ji S, Guvendiren M. Recent advances in bioink design for 3D bioprinting of tissues and organs. Front Bioeng Biotechnol. 2017;5:23.
60. Follmann HDM, Naves AF, Araujo RA, Dubovoy V, Huang X, Asefa T, Silva R, Oliveira ON. Hybrid materials and nanocomposites as multifunctional biomaterials. Curr Pharm Des. 2017;23:3794–813.
61. Ashammakhi N, Clerk-Lamalice O, Baroud G, Darabi MA, Georgy B, Beall D, Wagoner D. Spine intervention—an update on injectable biomaterials. Can Assoc Radiol J. 2019;70:37–43.
62. Mitchell AC, Briquez PS, Hubbell JA, Cochran JR. Engineering growth factors for regenerative medicine applications. Acta Biomater. 2016;30:1–12.

63. Ashammakhi N. Drug release: proper control to help clinical application DISCUSSION. J Craniofac Surg. 2018;29:124–5.
64. Pountos I, Jones E, Tzioupis C, McGonagle D, Giannoudis P. Growing bone and cartilage: the role of mesenchymal stem cells. J Bone Joint Surg Br. 2006;88(4):421–6.
65. Pountos I, Georgouli T, Henshaw K, Bird H, Jones E, Giannoudis PV. The effect of bone morphogenetic protein-2, bone morphogenetic protein-7, parathyroid hormone, and platelet-derived growth factor on the proliferation and osteogenic differentiation of mesenchymal stem cells derived from osteoporotic bone. J Orthop Trauma. 2010;24:552–6.
66. Petcu EB, Midha R, McColl E, Popa-Wagner A, Chirila TV, Dalton PD. 3D printing strategies for peripheral nerve regeneration. Biofabrication. 2018;10:032001.
67. Kang H-W, Lee SJ, Ko IK, Kengla C, Yoo JJ, Atala A. A 3D bioprinting system to produce human-scale tissue constructs with structural integrity. Nat Biotechnol. 2016;34:312.
68. Mézel C, Souquet A, Hallo L, Guillemot F. Bioprinting by laser-induced forward transfer for tissue engineering applications: jet formation modeling. Biofabrication. 2010;2:014103.
69. Gruene M, Pflaum M, Deiwick A, Koch L, Schlie S, Unger C, Wilhelmi M, Haverich A, Chichkov B. Adipogenic differentiation of laser-printed 3D tissue grafts consisting of human adipose-derived stem cells. Biofabrication. 2011;3:015005.
70. McCune M, Shafiee A, Forgacs G, Kosztin I. Predictive modeling of post bioprinting structure formation. Soft Matter. 2014;10:1790–800.
71. Huey DJ, Hu JC, Athanasiou KA. Unlike bone, cartilage regeneration remains elusive. Science. 2012;338:917–21.
72. Carreira A, Lojudice F, Halcsik E, Navarro R, Sogayar M, Granjeiro J. Bone morphogenetic proteins: facts, challenges, and future perspectives. J Dent Res. 2014;93:335–45.
73. Park SH, Park DS, Shin JW, Kang YG, Kim HK, Yoon TR, Shin J-W. Scaffolds for bone tissue engineering fabricated from two different materials by the rapid prototyping technique: PCL versus PLGA. J Mater Sci Mater Med. 2012;23:2671–8.
74. Seyednejad H, Gawlitta D, Kuiper RV, de Bruin A, van Nostrum CF, Vermonden T, Dhert WJ, Hennink WE. In vivo biocompatibility and biodegradation of 3D-printed porous scaffolds based on a hydroxyl-functionalized poly (ε-caprolactone). Biomaterials. 2012;33:4309–18.
75. Rindone, Nyberg E, Grayson WL. 3D-Printing Composite Polycaprolactone-Decellularized Bone Matrix Scaffolds for Bone Tissue Engineering Applications. Methods Mol Biol. 2018;1577:209–226. https://doi:10.1007/7651_2017_37.
76. Duarte Campos DF, Blaeser A, Buellesbach K, Sen KS, Xun W, Tillmann W, Fischer H. Bioprinting organotypic hydrogels with improved mesenchymal stem cell remodeling and mineralization properties for bone tissue engineering. Adv Healthc Mater. 2016;5:1336–45.
77. Luo Y, Wu C, Lode A, Gelinsky M. Hierarchical mesoporous bioactive glass/alginate composite scaffolds fabricated by three-dimensional plotting for bone tissue engineering. Biofabrication. 2012;5:015005.
78. Wang X, Tolba E, Schröder HC, Neufurth M, Feng Q, Diehl-Seifert B, Müller WE. Effect of bioglass on growth and biomineralization of SaOS-2 cells in hydrogel after 3D cell bioprinting. PLoS One. 2014;9:e112497.
79. Echave MC, Pimenta-Lopes C, Pedraz JL, Mehrali M, Dolatshahi-Pirouz A, Ventura F, Orive G. Enzymatic crosslinked gelatin 3D scaffolds for bone tissue engineering. Int J Pharm. 2019;562:151–61.
80. Du M, Chen B, Meng Q, Liu S, Zheng X, Zhang C, Wang H, Li H, Wang N, Dai J. 3D bioprinting of BMSC-laden methacrylamide gelatin scaffolds with CBD-BMP2-collagen microfibers. Biofabrication. 2015;7:044104.
81. Daly AC, Critchley SE, Rencsok EM, Kelly DJ. A comparison of different bioinks for 3D bioprinting of fibrocartilage and hyaline cartilage. Biofabrication. 2016;8:045002.
82. Tellisi N, Ashammakhi N. Comparison of meshes, gels and ceramic for cartilage tissue engineering in vitro. Eur J Plast Surg. 2012;35:159–70.
83. Wimpenny I, Ashammakhi N, Yang Y. Chondrogenic potential of electrospun nanofibres for cartilage tissue engineering. J Tissue Eng Regen Med. 2012;6:536–49.
84. Narayanan LK, Huebner P, Fisher MB, Spang JT, Starly B, Shirwaiker RA. 3D-bioprinting of polylactic acid (PLA) nanofiber–alginate hydrogel bioink containing human adipose-derived stem cells. ACS Biomater Sci Eng. 2016;2:1732–42.
85. Ávila HM, Schwarz S, Rotter N, Gatenholm P. 3D bioprinting of human chondrocyte-laden nanocellulose hydrogels for patient-specific auricular cartilage regeneration. Bioprinting. 2016;1:22–35.
86. Rhee S, Puetzer JL, Mason BN, Reinhart-King CA, Bonassar LJ. 3D bioprinting of spatially heterogeneous collagen constructs for cartilage tissue engineering. ACS Biomater Sci Eng. 2016;2:1800–5.
87. Di Bella C, Duchi S, O'Connell CD, Blanchard R, Augustine C, Yue Z, Thompson F, Richards C, Beirne S, Onofrillo C. In situ handheld three-dimensional bioprinting for cartilage regeneration. J Tissue Eng Regen Med. 2018;12:611–21.
88. Ding C, Qiao Z, Jiang W, Li H, Wei J, Zhou G, Dai K. Regeneration of a goat femoral head using a tissue-specific, biphasic scaffold fabricated with CAD/CAM technology. Biomaterials. 2013;34:6706–16.
89. Tarafder S, Koch A, Jun Y, Chou C, Awadallah MR, Lee CH. Micro-precise spatiotemporal delivery system embedded in 3D printing for complex tissue regeneration. Biofabrication. 2016;8:025003.
90. Lee CH, Cook JL, Mendelson A, Moioli EK, Yao H, Mao JJ. Regeneration of the articular surface of the rabbit synovial joint by cell homing: a proof of concept study. Lancet. 2010;376:440–8.

91. Woodfield T, Guggenheim M, Von Rechenberg B, Riesle J, Van Blitterswijk C, Wedler V. Rapid prototyping of anatomically shaped, tissue-engineered implants for restoring congruent articulating surfaces in small joints. Cell Prolif. 2009;42:485–97.
92. Shim J-H, Jang K-M, Hahn SK, Park JY, Jung H, Oh K, Park KM, Yeom J, Park SH, Kim SW. Three-dimensional bioprinting of multilayered constructs containing human mesenchymal stromal cells for osteochondral tissue regeneration in the rabbit knee joint. Biofabrication. 2016;8:014102.
93. England S, Rajaram A, Schreyer DJ, Chen X. Bioprinted fibrin-factor XIII-hyaluronate hydrogel scaffolds with encapsulated Schwann cells and their in vitro characterization for use in nerve regeneration. Bioprinting. 2017;5:1–9.
94. Lee S-J, Zhu W, Heyburn L, Nowicki M, Harris B, Zhang LG. Development of novel 3-D printed scaffolds with core-shell nanoparticles for nerve regeneration. IEEE Trans Biomed Eng. 2016;64:408–18.
95. Radulescu D, Dhar S, Young CM, Taylor DW, Trost H-J, Hayes DJ, Evans GR. Tissue engineering scaffolds for nerve regeneration manufactured by ink-jet technology. Mater Sci Eng C. 2007;27:534–9.
96. Evans G, Brandt K, Widmer M, Lu L, Meszlenyi R, Gupta P, Mikos A, Hodges J, Williams J, Gürlek A. In vivo evaluation of poly (L-lactic acid) porous conduits for peripheral nerve regeneration. Biomaterials. 1999;20:1109–15.
97. Owens CM, Marga F, Forgacs G, Heesch CM. Biofabrication and testing of a fully cellular nerve graft. Biofabrication. 2013;5:045007.
98. Adams AM, Van Dusen KW, Kostrominova TY, Mertens JP, Larkin LM. Scaffoldless tissue-engineered nerve conduit promotes peripheral nerve regeneration and functional recovery after tibial nerve injury in rats. Neural Regen Res. 2017;12:1529.
99. Atala A, Kasper F, Mikos A. Engineering complex tissues. Sci Transl Med. 2012;4(160):160rv112.
100. Pountos I, Panteli M, Panagiotopoulos E, Jones E, Giannoudis PV. Can we enhance fracture vascularity: what is the evidence? Injury. 2014;45:S49–57.
101. Shahabipour F, Ashammakhi N, Oskuee RK, Bonakdar S, Hoffman T, Shokrgozar MA, Khademhosseini A. Key components of engineering vascularized three-dimensional bioprinted bone constructs. Transl Res. 2020;216:57–76.
102. Kucukgul C, Ozler SB, Inci I, Karakas E, Irmak S, Gozuacik D, Taralp A, Koc B. 3D bioprinting of biomimetic aortic vascular constructs with self-supporting cells. Biotechnol Bioeng. 2015;112:811–21.
103. Xu Y, Hu Y, Liu C, Yao H, Liu B, Mi S. A novel strategy for creating tissue-engineered biomimetic blood vessels using 3D bioprinting technology. Materials. 2018;11:1581.
104. Huber B, Engelhardt S, Meyer W, Krüger H, Wenz A, Schönhaar V, Tovar G, Kluger P, Borchers K. Blood-vessel mimicking structures by stereolithographic fabrication of small porous tubes using cytocompatible polyacrylate elastomers, biofunctionalization and endothelialization. J Funct Biomater. 2016;7:11.
105. Zhao L, Lee VK, Yoo S-S, Dai G, Intes X. The integration of 3-D cell printing and mesoscopic fluorescence molecular tomography of vascular constructs within thick hydrogel scaffolds. Biomaterials. 2012;33:5325–32.
106. Gheno R, Cepparo JM, Rosca CE, Cotten A. Musculoskeletal disorders in the elderly. J Clin Imaging Sci. 2012;2:39.
107. Peele BN, Wallin TJ, Zhao H, Shepherd RF. 3D printing antagonistic systems of artificial muscle using projection stereolithography. Bioinspir Biomim. 2015;10:055003.
108. Altomare L, Riehle M, Gadegaard N, Tanzi M, Farè S. Microcontact printing of fibronectin on a biodegradable polymeric surface for skeletal muscle cell orientation. Int J Artif Organs. 2010;33:535–43.
109. Toprakhisar B, Nadernezhad A, Bakirci E, Khani N, Skvortsov GA, Koc B. Development of bioink from decellularized tendon extracellular matrix for 3D bioprinting. Macromol Biosci. 2018;18:1800024.
110. Merceron TK, Burt M, Seol Y-J, Kang H-W, Lee SJ, Yoo JJ, Atala A. A 3D bioprinted complex structure for engineering the muscle–tendon unit. Biofabrication. 2015;7:035003.
111. J.K. Robinson, C.W. Hanke, D.M. Siegel, A. Fratila, A.C. Bhatia, T.E. Rohrer, Surgery of the skin E-book: procedural dermatology, Elsevier health sciences 2014.
112. Campana V, Milano G, Pagano E, Barba M, Cicione C, Salonna G, Lattanzi W, Logroscino G. Bone substitutes in orthopaedic surgery: from basic science to clinical practice. J Mater Sci Mater Med. 2014;25:2445–61.
113. Lee V, Singh G, Trasatti JP, Bjornsson C, Xu X, Tran TN, Yoo S-S, Dai G, Karande P. Design and fabrication of human skin by three-dimensional bioprinting. Tissue Eng Part C Methods. 2013;20:473–84.
114. Koch L, Deiwick A, Schlie S, Michael S, Gruene M, Coger V, Zychlinski D, Schambach A, Reimers K, Vogt PM. Skin tissue generation by laser cell printing. Biotechnol Bioeng. 2012;109:1855–63.
115. Min D, Lee W, Bae IH, Lee TR, Croce P, Yoo SS. Bioprinting of biomimetic skin containing melanocytes. Exp Dermatol. 2018;27:453–9.
116. Skardal A, Mack D, Kapetanovic E, Atala A, Jackson JD, Yoo J, Soker S. Bioprinted amniotic fluid-derived stem cells accelerate healing of large skin wounds. Stem Cells Transl Med. 2012;1:792–802.
117. Albanna M, Binder KW, Murphy SV, Kim J, Qasem SA, Zhao W, Tan J, El-Amin IB, Dice DD, Marco J, Green J, Xu T, Skardal A, Holmes JH, Jackson JD, Atala A, YooIn JJ. Situ bioprinting of autologous skin cells accelerates wound healing of extensive excisional full-thickness wounds. Sci Rep. 2019;9:856. Published online 2019 Feb 12. doi:10.1038/s41598-018-38366-w.

118. Binder KW, Zhao W, Aboushwareb T, Dice D, Atala A, Yoo JJ. In situ bioprinting of the skin for burns. J Am Coll Surg. 2010;211:S76.
119. Gaziano T, Reddy K, Paccaud F, Horton S. Chapter 33: Cardiovascular disease. In: Disease control priorities in developing countries. Washington (DC): World Bank; 2006.
120. Wang QL, Wang HJ, Li ZH, Wang YL, Wu XP, Tan YZ. Mesenchymal stem cell-loaded cardiac patch promotes epicardial activation and repair of the infarcted myocardium. J Cell Mol Med. 2017;21:1751–66.
121. Domenech M, Polo-Corrales L, Ramirez-Vick JE, Freytes DO. Tissue engineering strategies for myocardial regeneration: a cellular versus cellular scaffolds? Tissue Eng Part B Rev. 2016;22:438–58.
122. Tijore A, Irvine SA, Sarig U, Mhaisalkar P, Baisane V, Venkatraman S. Contact guidance for cardiac tissue engineering using 3D bioprinted gelatin patterned hydrogel. Biofabrication. 2018;10:025003.
123. Zhang YS, Arneri A, Bersini S, Shin S-R, Zhu K, Goli-Malekabadi Z, Aleman J, Colosi C, Busignani F, Dell'Erba V. Bioprinting 3D microfibrous scaffolds for engineering endothelialized myocardium and heart-on-a-chip. Biomaterials. 2016;110:45–59.
124. Wang Z, Lee SJ, Cheng H-J, Yoo JJ, Atala A. 3D bioprinted functional and contractile cardiac tissue constructs. Acta Biomater. 2018;70:48–56.
125. Gaetani R, Feyen DA, Verhage V, Slaats R, Messina E, Christman KL, Giacomello A, Doevendans PA, Sluijter JP. Epicardial application of cardiac progenitor cells in a 3D-printed gelatin/hyaluronic acid patch preserves cardiac function after myocardial infarction. Biomaterials. 2015;61:339–48.
126. Izadifar M, Chapman D, Babyn P, Chen X, Kelly ME. UV-assisted 3D bioprinting of nanoreinforced hybrid cardiac patch for myocardial tissue engineering. Tissue Eng Part C Methods. 2018;24:74–88.
127. Hockaday L, Kang K, Colangelo N, Cheung P, Duan B, Malone E, Wu J, Girardi L, Bonassar L, Lipson H. Rapid 3D printing of anatomically accurate and mechanically heterogeneous aortic valve hydrogel scaffolds. Biofabrication. 2012;4:035005.
128. Kang LH, Armstrong PA, Lee LJ, Duan B, Kang KH, Butcher JT. Optimizing photo-encapsulation viability of heart valve cell types in 3D printable composite hydrogels. Ann Biomed Eng. 2017;45:360–77.
129. Duan B, Hockaday LA, Kang KH, Butcher JT. 3D bioprinting of heterogeneous aortic valve conduits with alginate/gelatin hydrogels. J Biomed Mater Res A. 2013;101:1255–64.
130. Isaacson A, Swioklo S, Connon CJ. 3D bioprinting of a corneal stroma equivalent. Exp Eye Res. 2018;173:188–93.
131. Lorber B, Hsiao W-K, Hutchings IM, Martin KR. Adult rat retinal ganglion cells and glia can be printed by piezoelectric inkjet printing. Biofabrication. 2013;6:015001.
132. Wang P, Li X, Zhu W, Zhong Z, Moran A, Wang W, Zhang K, Chen S. 3D bioprinting of hydrogels for retina cell culturing. Bioprinting. 2018;12. Bioprinting 2018;11:e00029. https://doi:10.1016/j.bprint.2018.e00029.
133. Mitrousis N, Tam RY, Baker AE, van der Kooy D, Shoichet MS. Hyaluronic acid-based hydrogels enable rod photoreceptor survival and maturation in vitro through activation of the mTOR pathway. Adv Funct Mater. 2016;26:1975–85.
134. Masaeli E, Forster V, Picaud S, Karamali F, Nasr-Esfahani M-H, Marquette CA. Tissue engineering of retina through high resolution 3-dimentional inkjet bioprinting. Biofabrication. 2020;12(2):025006.
135. Heinrich MA, Bansal R, Lammers T, Zhang YS, Michel Schiffelers R, Prakash J. 3D-bioprinted mini-brain: a glioblastoma model to study cellular interactions and therapeutics. Adv Mater. 2019;31:1806590.
136. Fetah KL, DiPardo BJ, Kongadzem EM, Tomlinson JS, Elzagheid A, Elmusrati M, Khademhosseini A, Ashammakhi N. Cancer modeling-on-a-chip with future artificial intelligence integration. Small. 2019;15(50):1901985.
137. Massa S, Sakr MA, Seo J, Bandaru P, Arneri A, Bersini S, Zare-Eelanjegh E, Jalilian E, Cha B-H, Antona S. Bioprinted 3D vascularized tissue model for drug toxicity analysis. Biomicrofluidics. 2017;11:044109.
138. Nguyen DG, Funk J, Robbins JB, Crogan-Grundy C, Presnell SC, Singer T, Roth AB. Bioprinted 3D primary liver tissues allow assessment of organ-level response to clinical drug induced toxicity in vitro. PLoS One. 2016;11:e0158674.
139. Gilbert F, O'Connell CD, Mladenovska T, Dodds S. Print me an organ? Ethical and regulatory issues emerging from 3D bioprinting in medicine. Sci Eng Ethics. 2018;24:73–91.
140. Ma X, Liu J, Zhu W, Tang M, Lawrence N, Yu C, Gou M, Chen S. 3D bioprinting of functional tissue models for personalized drug screening and in vitro disease modeling. Adv Drug Deliv Rev. 2018;132:235–51.
141. Zhou X, Zhu W, Nowicki M, Miao S, Cui H, Holmes B, Glazer RI, Zhang LG. 3D bioprinting a cell-laden bone matrix for breast cancer metastasis study. ACS Appl Mater Interfaces. 2016;8:30017–26.
142. Diao J, Zhang C, Zhang D, Wang X, Zhang J, Ma C, Deng K, Jiang T, Jia W, Xu T. Role and mechanisms of a three-dimensional bioprinted microtissuemodel in promoting proliferation and invasion of growth-hormone-secreting pituitary adenoma cells. Biofabrication. 2019;11:025006. doi:10.1088/1758-5090/aaf7ea.
143. Wang X, Zhang X, Dai X, Wang X, Li X, Diao J, Xu T. Tumor-like lung cancer model based on 3D bioprinting. 3 Biotech. 2018;8:501.
144. Cleversey C, Robinson M, Willerth SM. 3D printing breast tissue models: a review of past work and directions for future work. Micromachines. 2019;10:501.
145. Duarte Campos DF, Bonnin Marquez A, O'Seanain C, Fischer H, Blaeser A, Vogt M, Corallo D, Aveic S. Exploring cancer cell behavior in vitro in three-

dimensional multicellular bioprintable collagen-based hydrogels. Cancers (Basel). 2019;11:180.
146. Zhao Y, Yao R, Ouyang L, Ding H, Zhang T, Zhang K, Cheng S, Sun W. Three-dimensional printing of Hela cells for cervical tumor model in vitro. Biofabrication. 2014;6:035001.
147. Ali M, Yoo JJ, Zahran F, Atala A, Lee SJ. A photo-crosslinkable kidney ECM-derived bioink accelerates renal tissue formation. Adv Healthc Mater. 2019;8:1800992.
148. Lee JW, Choi Y-J, Yong W-J, Pati F, Shim J-H, Kang KS, Kang I-H, Park J, Cho D-W. Development of a 3D cell printed construct considering angiogenesis for liver tissue engineering. Biofabrication. 2016;8:015007.
149. Park HS, Lee JS, Jung H, Kim DY, Kim SW, Sultan MT, Park CH. An omentum-cultured 3D-printed artificial trachea: in vivo bioreactor. Artif Cells Nanomed Biotechnol. 2018;46:S1131–40.
150. Mannoor MS, Jiang Z, James T, Kong YL, Malatesta KA, Soboyejo WO, Verma N, Gracias DH, McAlpine MC. 3D printed bionic ears. Nano Lett. 2013;13:2634–9.
151. Reiffel AJ, Kafka C, Hernandez KA, Popa S, Perez JL, Zhou S, Pramanik S, Brown BN, Ryu WS, Bonassar LJ. High-fidelity tissue engineering of patient-specific auricles for reconstruction of pediatric microtia and other auricular deformities. PLoS One. 2013;8:e56506.
152. Markstedt K, Mantas A, Tournier I, Martínez Ávila H, Hägg D, Gatenholm P. 3D bioprinting human chondrocytes with nanocellulose–alginate bioink for cartilage tissue engineering applications. Biomacromolecules. 2015;16:1489–96.
153. Naughton CA. Drug-induced nephrotoxicity. Am Fam Physician. 2008;78:743–50.
154. Kaully T, Kaufman-Francis K, Lesman A, Levenberg S. Vascularization—the conduit to viable engineered tissues. Tissue Eng Part B Rev. 2009;15:159–69.
155. Kheirallah M, Almeshaly H. Oral health case reports. OMICS. 2016;2:3.
156. Pountos I, Tellisi N, Ashammakhi N. Potential clinical applications of three-dimensional bioprinting. 3D bioprinting in medicine. Springer. 2019;101–25.
157. Tellisi N, Ashammakhi NA, Billi F, Kaarela O. Three dimensional printed bone implants in the clinic. J Craniofac Surg. 2018;29:2363–7.
158. Knowlton S, Onal S, Yu CH, Zhao JJ, Tasoglu S. Bioprinting for cancer research. Trends Biotechnol. 2015;33:504–13.
159. Ng WL, Wang S, Yeong WY, Naing MW. Skin bioprinting: impending reality or fantasy? Trends Biotechnol. 2016;34:689–99.

17 Augmented Reality for Interventional Procedures

Atul Gupta, Daniel Ruijters, and Molly L. Flexman

Introduction

The progression from open surgery to minimally invasive, image-guided therapy (IGT) has dramatically accelerated over the past three decades. No longer does a physician need to surgically open the patient in order to physically see and touch the part of the body where repair is required. Today, imaging technologies like X-ray and ultrasound allow real-time, in-body visualization of instruments and anatomy without the need for surgical incisions. These advancements – coupled with the ongoing miniaturization of endovascular and percutaneous devices such as balloons, catheters, and stents – have allowed interventional radiologists, cardiologists, and endovascular surgeons to perform procedures within nearly every organ system. The ability to perform procedures as diverse as cardiac valve replacement, aneurysm treatment, coronary artery angioplasty, tumor embolization, and spine fracture repair – all without general anesthesia via incisions often no larger than a pencil point – has resulted in patient recoveries measured in hours to days, rather than weeks as seen with traditional open surgical repairs. Faster recoveries, shorter procedure times, improved outcomes, and reduced costs have resulted in widespread clinical acceptance of minimally invasive image-guided procedures.

During modern interventional procedures, teams made up of physicians, technologists, and nurses increasingly rely upon diverse sources of data, including physiologic monitoring, live X-ray, historic radiologic studies, live 2D and 3D navigation roadmaps, ultrasound and echocardiography, device data, and electronic health record data. As IGT procedures have increased in complexity over the last several decades, interventional physicians are no longer able to rely on the historic two-display 15″ monochromatic monitor setup. With input from interventionalists, advanced procedure suites are being retooled and remodeled to include several monitors and windows to display this plethora of data. We now rely on large 58″ LED color displays subdivided into as many as 16 smaller windows each containing a different source of medical information. Not surprisingly, this solution is suboptimal.

The bulky display is rarely in an ergonomically perfect position or layout for every member of the team. Also, different individuals rely on different windows of information. 3D medical imagery can only be displayed in 2D, changes in window size or input necessitate distracting manual button presses, and as teams move around the

A. Gupta (✉)
Philips, Cambridge, MA, USA
e-mail: atul.gupta@philips.com

D. Ruijters
Philips Image Guided Therapy, Best, The Netherlands

M. L. Flexman
Philips Research, Cambridge, MA, USA

S. Atallah (ed.), *Digital Surgery*, https://doi.org/10.1007/978-3-030-49100-0_17

patient, the large physical screen also needs to be adjusted. This is quite difficult and time-consuming in a crowded and sterile operative environment.

Augmented reality (AR) now allows us to see the real world superimposed with live data and 3D medical imagery needed to guide precision therapy. Ideally, an interventionalist should be able to keep their hands on the instruments and their eyes on the patient and to see the contextually relevant digital information at any given point in time. Data should be displayed as a 3D hologram when required and in an ergonomically optimal size and position. Perhaps even more importantly, rather than having to shift focus away from the patient to press physical buttons (required to operate interventional equipment), an AR-powered interventional suite can allow control of the entire interventional system and environment with voice recognition, eye tracking, and advanced intuitive gestures.

Preoperative Image Fusion for Intraoperative Guidance

Augmented reality applications during interventional application can intuitively integrate preprocedural information during the course of the procedure. In this section, we will describe several examples of such augmented reality applications and discuss their properties, benefits, and challenges.

Overlay of 3D Preoperative Vasculature on Live X-Ray Fluoroscopy

X-ray fluoroscopy can be used to navigate a guidewire or catheter through blood vessels and to monitor the deployment of intravascular devices. While iodine contrast medium can be injected to visualize the vessel lumen, there are several associated limitations. First, every movement of the C-arm gantry or patient table will invalidate any earlier acquired vessel map for overlay and would therefore require another contrast injection, which is undesirable due to the toxic nature of iodine contrast. Furthermore, the 2D nature of the X-ray fluoroscopy images misses the 3D morphology information and hampers the interpretation of overlapping vessels and bifurcations. By augmenting the live X-ray fluoroscopy images to also show the intravascular devices together with pre- or periprocedural 3D vascular information obtained by various imaging modalities (e.g., magnetic resonance angiography (MRA), computed tomography angiography (CTA), or 3D rotational angiography (3D-RA)), these limitations can be overcome.

The technology of combining an earlier recorded vascular image with the live image stream of intravascular devices (guidewires, catheters, stents, etc.) is known as *roadmapping*. When the vascular image is a 3D image, this technique is known as *3D roadmapping*, and when it originates from a CT or MR, this is known as a *CT roadmap* (Figs. 17.1 and 17.2) or *MR roadmap* (Fig. 17.3), respectively. The augmentation of the live data stream requires that a mapping (co-registration) between the frames of reference of each data source is obtained. This is sufficient for many applications, with limited deformations, via a rigid registration (i.e., consisting of translation and rotation only). The registration can be based on *knowledge of the geometry state* (viewing incidence, table position, etc.) or *on the image content.* For multimodality registration (CT or MR roadmap), either an intermediate cone-beam CT (CBCT) can be acquired or two (or more) X-ray fluoroscopy images from different angles (Fig. 17.1). Since the CBCT is acquired with the same equipment as the X-ray fluoroscopy images, their registration can be geometry based, which can be calculated instantly. The CBCT can then be registered with the CT or MR using an image-based algorithm, which can be conducted more accurately and robustly than directly registering the CT or MR to the fluoroscopy data, due to the richer morphological content of the CBCT data.

Since the image-based registration can rely on anatomical landmarks and does not require contrast injection, it is possible to deploy the

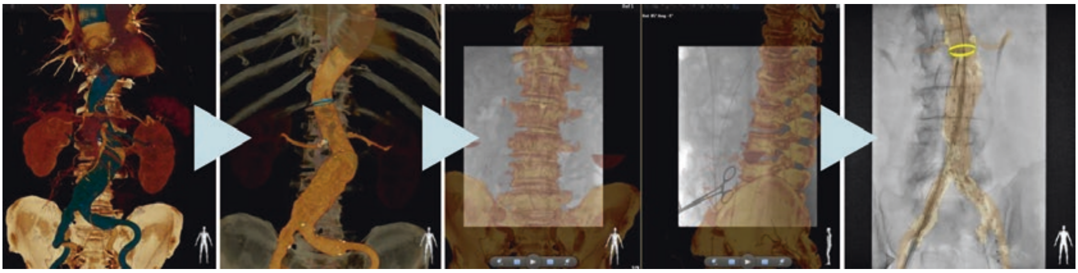

Fig. 17.1 To overlay vessels segmented from CT, four steps are followed: (1) segmentation of the vessels; (2) optionally, placing landmarks for navigation; (3) registering the CT in two angulated views with fluoroscopy X-ray; and (4) fused overlay of CT, showing the vessel tree, and live fluoroscopy showing the intravascular devices, such as the guidewire, catheter, and stents

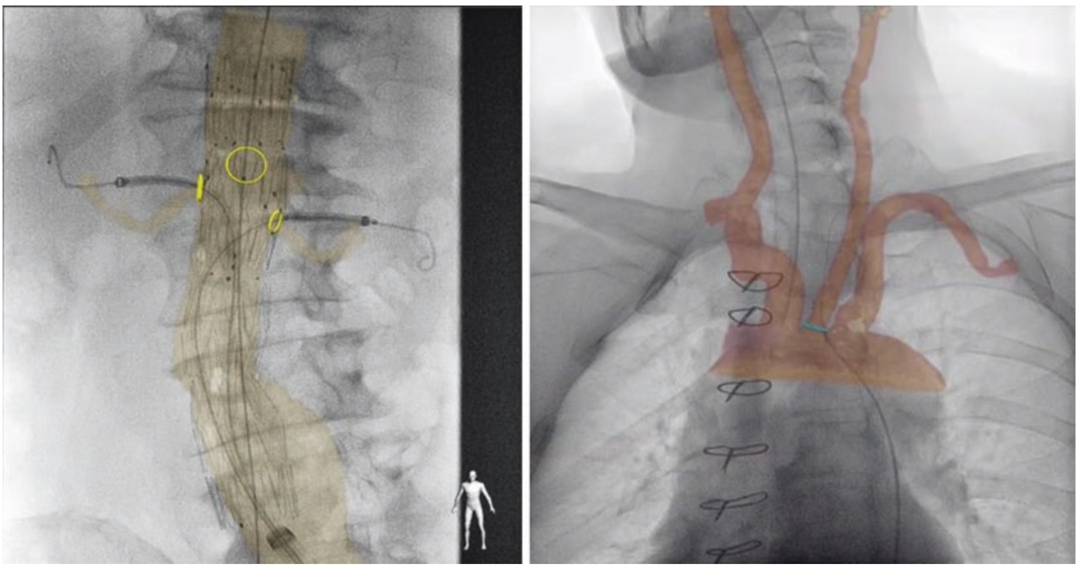

Fig. 17.2 Left: Endovascular repair of juxtarenal abdominal aortic aneurysm (*Courtesy of Prof. Dr. Mark Schermerhorn, BIDMC, Boston, USA*). Right: Left common carotid stenting. (*Courtesy of Prof. Dr. Frank Vermassen, University of Ghent, Belgium*)

intravascular devices using such multi-modality roadmapping guidance with minimal or no iodine contrast agent during the intervention [1]. Clinical applications cover the entire vascular system and comprise neurovascular, such as aneurysm embolization, arteriovenous malformations [2, 3] (Fig. 17.4), aortic stenting (Figs. 17.1 and 17.2), cardiac procedures such as coronary chronic total occlusions [4] (Fig. 17.5) and structural heart disease treatment [5, 6], liver trans-arterial chemo embolization, uterine artery embolization [7] (Fig. 17.3), and many others.

Pre-procedural Needle Path Planning Overlaid on Live Imaging

Pre- and perioperative morphological imaging allows for the precise planning of needle puncture paths for a multitude of applications – such as trans-apical access for intracardiac procedures,

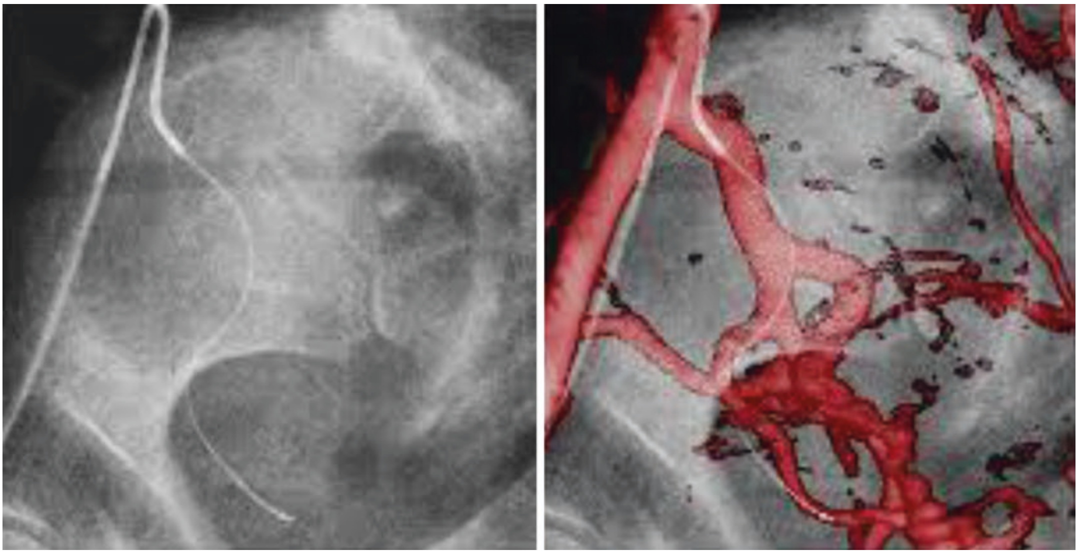

Fig. 17.3 MR angiography overlay on live fluoroscopy for uterine artery embolization. (*Courtesy Dr. Atul Gupta, Philadelphia, PA, USA*)

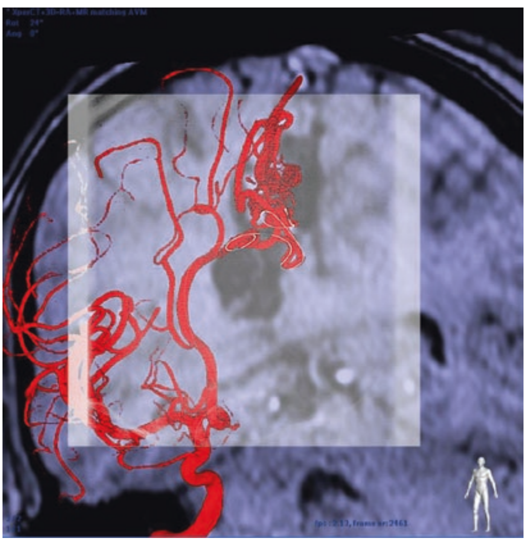

Fig. 17.4 Three image sources visualized in a combined augmented image. The live X-ray fluoroscopy image, the peri-interventional 3DRA vasculature, and a slab from the pre-interventional MR data. The fluoroscopy image shows the real-time position of the guidewire, the 3DRA shows the vessel lumen, and the MR contains the arteriovenous malformation nidus and soft-tissue information. The MR slab is positioned parallel to the view port at the guidewire tip. (*Courtesy of Prof. Dr. Jacques Moret and Prof. Dr. Laurent Spelle, Hôpital Bicêtre, Paris, France*)

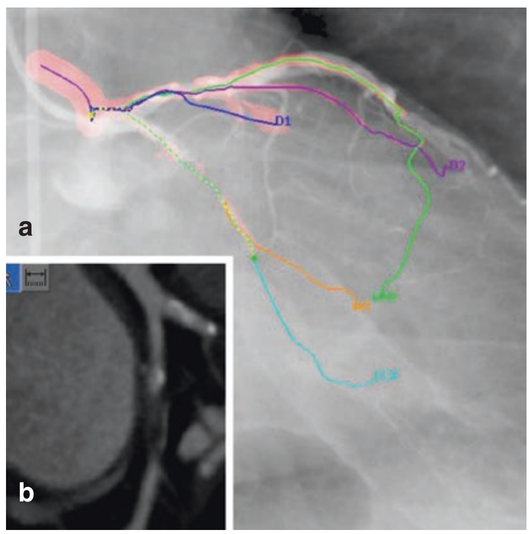

Fig. 17.5 Fusion of CT and X-ray images (roadmapping) (**a**) and the corresponding MPR (**b**) for a coronary artery with a chronic total occlusion. On the live X-ray angiography images, the vessel distal from the occlusion remains invisible, but the augmentation of the images with the vessels from the CTA, which benefits from retrograde filling of contrast injected intravenously, unveils the distal part of the coronary artery. (*Courtesy of Dr. Harvey S. Hecht, Lenox Hill Hospital, New York, NY, USA*)

biopsies, intra-tumoral injections, and vertebral applications. For many of these applications, it is important to accurately reach the foreseen target position while avoiding critical structures, such as major vessels and nerve structures. In order to safely, reliably, and accurately execute on a needle puncture plan, it is beneficial to augment live imaging with pre-procedurally planned needle path. The live imaging may be ultrasound, X-ray, or optical cameras, depending on the exact clinical application and targeted structures and tissues.

Commercial solutions to augment live fluoroscopy-guided needle puncture with pre-interventional planning include, but are not limited to, XperGuide (Philips, the Netherlands), Syngo Needle Guidance (Siemens Healthineers, Germany), and Innova TrackVision (GE Healthcare, USA). Prior to patient puncturing, the optimal needle paths are planned on a pre-operative computed tomography (CT) dataset. Determination of the most optimal needle trajectory is initiated by marking the ultimate needle point, located in the lesion center. A line is drawn toward the skin boundary, continuously checking whether it traverses any critical anatomical structures or impenetrable bones [8]. The pre-planned path is then used intraoperatively to align the needle in the fluoroscopy image with the target (Fig. 17.6). After the needle has been inserted, the fluoroscopy C-arm is rotated to an appropriate view to monitor the needle progression and observe any deviations from the pre-planned path.

Needle manipulation poses different challenges compared to catheter manipulation, as the needle shaft and handle are typically within the X-ray field of view. Also, ultrasound guidance has its limitations, as the needle produces a shadow in the ultrasound image, and it is not always easy to keep the needle within the field of view. These limitations can be overcome by using tracking technologies to determine the current position of the needle in real time. When the tracking is performed by optical cameras, the optical images can be augmented with the needle position and pre-interventional planning and image data (Fig. 17.7) [9, 10].

Intraoperative Fusion and Guidance

Next to the augmentation of a live data stream with pre-interventional data, it can also be beneficial to integrate multiple live data sources into a single combined representation. Such a combined augmented view can reduce the information overload for the interventional staff, creating greater insights into the interfaces and interactions between the different data sources.

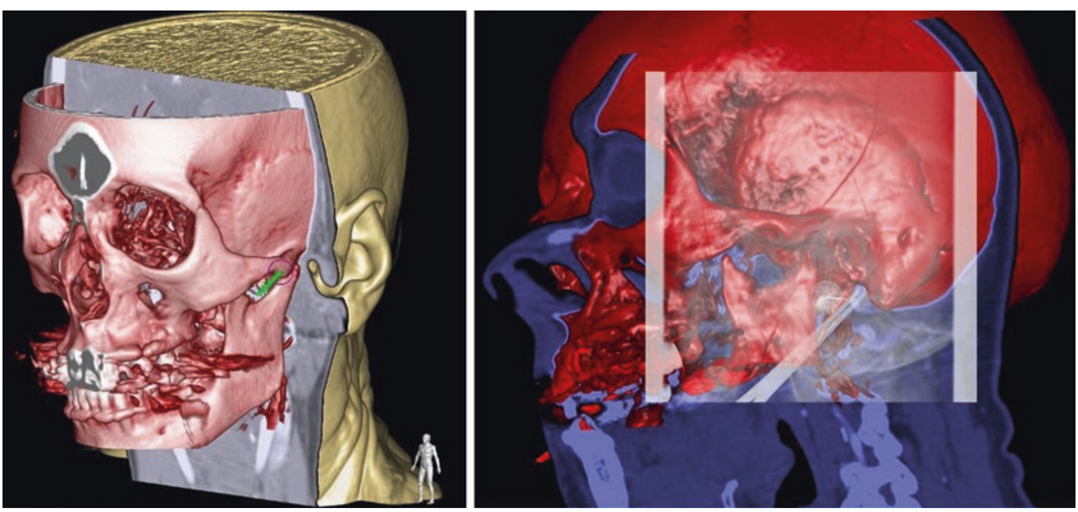

Fig. 17.6 A pre-planned path (left) and live augmentation of the fluoroscopy image with the pre-planned entry point and pre-op CT data. (*Courtesy of Prof. Dr. Jacques Moret and Prof. Dr. Laurent Spelle, Hôpital Bicêtre, Paris, France*)

One example of the combination of multiple real-time image sources concerns the integration of live transesophageal echo (TEE) and live X-ray fluoroscopy for structural heart disease procedures. TEE provides soft-tissue visualization, which is indispensable when assessing valvular leaflet motion and morphology, as well as dynamic blood flow and regurgitation with color Doppler. X-ray fluoroscopy shows the intracardiac devices and iodinated contrast and has a larger field of view.

Fig. 17.7 Real-time augmented image, combining live optical images, needle planning, and pre-interventional cone-beam CT in a single easy to interpret visualization

Traditionally, the X-ray and the TEE are visualized on separate displays or windows and require "3D mental mapping", often making it challenging for physicians to relate orientation, scale, and positioning of the device relative to the native soft-tissue anatomy. This can be overcome by real-time co-registration of the TEE to the live fluoroscopy images. When such co-registration is established, landmark features and segmentations extracted from one image source can be displayed on the other image source. Also, both images can be combined in a single fused image (Fig. 17.8). With EchoNavigator (Philips, the Netherlands), the live co-registration is achieved by fitting a model of the TEE probe to the fluoroscopy, where it is clearly visible. This type of augmentation has been used in left atrial appendage, atrial septal defect and

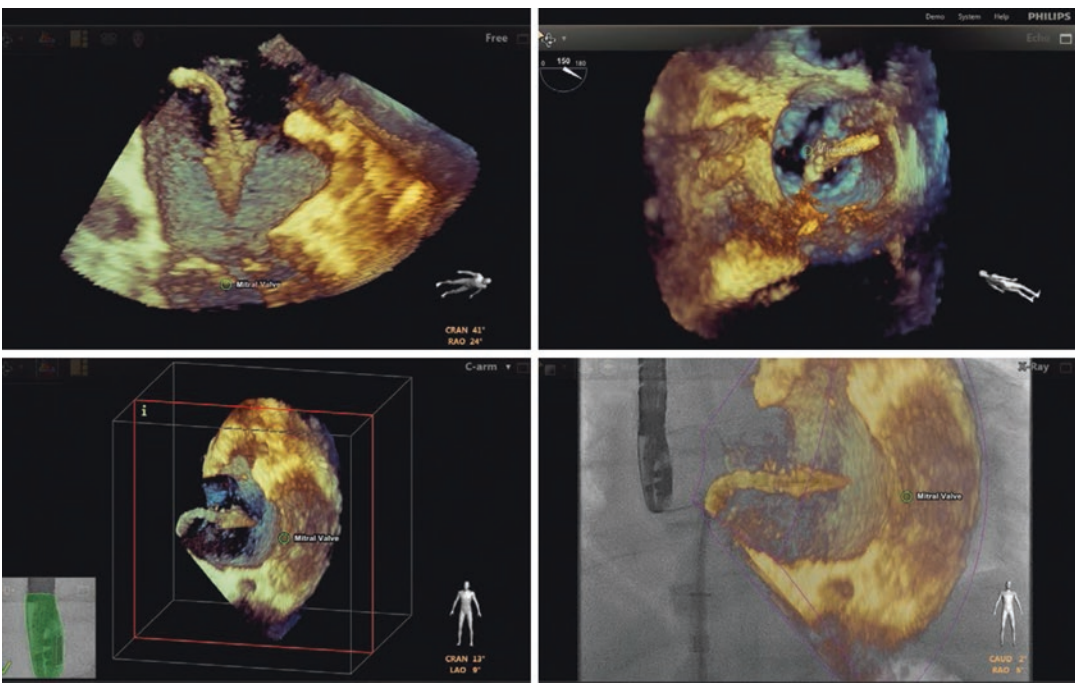

Fig. 17.8 The fusion of live fluoroscopic and live echo images helps in understanding the relationship between soft-tissue anatomy and devices for fast and accurate interventions in structural heart disease. (*Courtesy of Prof. John Carroll, MD, Interventional Cardiologist, University of Colorado, Denver*)

paravalvular leak closure, transaortic valve repair, and MitraClip® procedures [11–13].

Intravascular ultrasound (IVUS) is a very suitable tool to assess the vessel lumen, atheromatous and vulnerable plaque, exact cross-sectional appraisal of stenosis, and other vessel characteristics crucial for treatment planning via percutaneous coronary interventions (PCI). A limitation, however, is the difficulty to correlate the findings with the location on the angiogram, which is used as a roadmap during stent deployment. By acquiring an X-ray fluoroscopy sequence during the pullback of the IVUS probe and co-registering both image sources, the information can be appreciated in combination [14] (Fig. 17.9). The co-location of all relevant information is particularly facilitated when the X-ray fluoroscopy of the catheter with the IVUS probe is additionally co-registered to a pre-acquired angiogram, the cross-sectional IVUS images and the projective angiographic overview image of the coronary vessel tree [15, 16]. This so-called dynamic coronary roadmap (Fig. 17.10) can also lead to reduced iodine contrast medium usage and fluoroscopy time when used during the entire procedure [16].

Head-Mounted Displays in the Interventional Room

Head-mounted displays (HMDs) have reached a critical point in recent years, with the specifi-

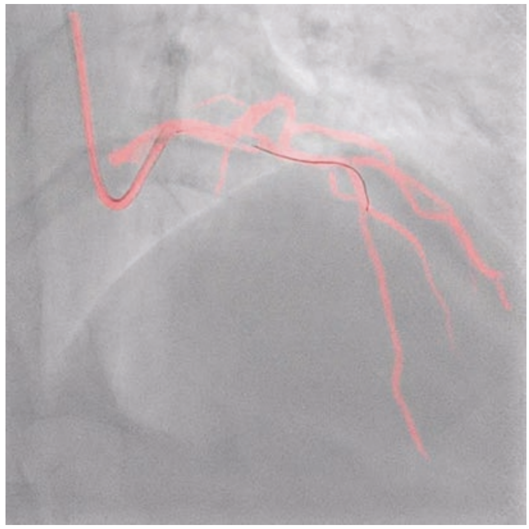

Fig. 17.10 In a dynamic coronary roadmap, the live fluoroscopy image containing the guidewire is fused with the pre-acquired angiogram (red), matched in cardiac phase and location

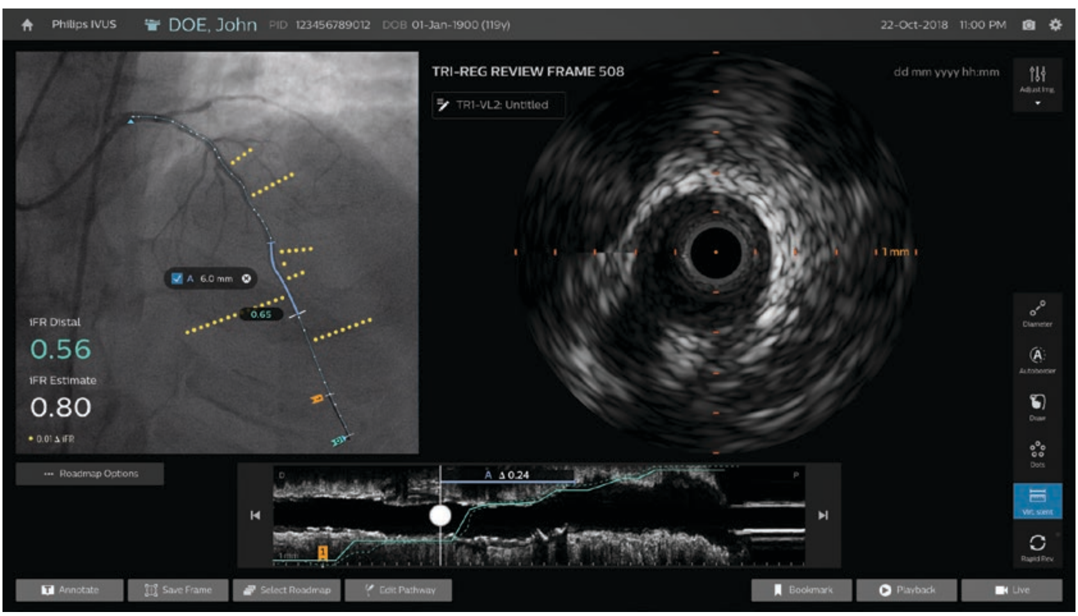

Fig. 17.9 The location of the IVUS cross section and the IVUS pullback stack is matched with the angiographic overview image, based on time stamping and catheter tip detection

cations entering a range that makes them suitable for a variety of applications [17]. Applying head-mounted displays to interventional procedures comes with unique requirements that differ from those encountered in other arenas, such as automotive, education, or architecture. Some considerations for HMDs that are of importance for interventional use are described below.

Sterility and Cleanability

The clinical practice guideline for interventional procedures describes appropriate surgical attire for interventional radiologists designed to minimize passage of microorganisms between personnel and the patient [18]. This recommended attire includes a surgical cap, face mask, scrubs, and sterile gown. Head-mounted displays should be compatible with existing attire recommendations, with special attention to slipping, due to surgical caps, and fogging, due to face masks.

Personal eyeglasses are non-sterile and can cause contamination if they interact with the sterile field – for example, by touching of eyeglasses by the surgeons during the operation or by them falling off the surgeon and onto the sterile area. Eyeglasses are a source of surgical infection and should be disinfected [19]. Thus, a head-mounted display introduced into the interventional room does not need to be sterile, but does need to be suitable for disinfection. HMDs for interventional use can be designed with materials or draped in order to make them more conducive to cleaning and disinfecting.

Radiation Safety

Interventional procedures that make use of fluoroscopy also require personal protective devices for the staff including aprons, thyroid shields, gloves, and eyeglasses. Leaded eyeglasses with large lenses and protective side shields provide more protection than eyeglasses without these features [20]. Head-mounted displays for interventional procedures should include appropriate lead lenses and side shields or should be compatible with existing leaded eyeglasses.

Comfort

As interventional staff are already wearing personal protective equipment including lead aprons weighing up to 8 Kg and lead goggles weighing up to 100 g, it is important to consider the impact of any additional wearables to their comfort. Key considerations include the weight, heat dissipation, and ease of adjustment. A sterile operator will not be able to touch the HMD, so the device should be comfortable without frequent readjustment or adjustable by a non-sterile additional person [21].

Distraction

Some HMD lenses make use of tinting to reduce the ambient light to the wearer. During interventional procedures, it is important to consider if a tint to the display is clinically acceptable. The ability to easily flip up or remove the HMD is helpful if there are specific moments in the procedure where the operator desires a real-world view. In addition, minimal obstruction to the peripheral vision of the operator helps to maintain awareness of the surroundings. Studies reveal that nonverbal communication including eye gaze that occurs between staff during procedures is important [22]. User interfaces should be designed to minimize distraction to the wearer and to minimize unintended interactions with the HMD.

Quality of Display

The quality of the image display has many factors that contribute to the clinical utility. Some of them are known from 2D displays [23], such as the following:

- Resolution (e.g., pixel density)
- Pixel size
- Brightness (luminance)
- Contrast ratio
- Refresh rate

Other factors are more specific to HMDs and include the following:

- Field of view of the display
- Number and location of focal planes
- Distortions and aberrations

Fig. 17.11 Augmented reality HMDs virtualize the physical screens into a personalized, flexible display for each user

Virtual Screens and Controls

Minimally invasive procedures rely on multiple sources of information during the procedures. These sources include intraoperative imaging (e.g., fluoroscopy, digital subtraction angiography, cone-beam computed tomography, ultrasound, optical coherence tomography), hemodynamic monitoring, preoperative information (e.g., imaging, patient records, planning), advanced applications, and procedure-specific device feedback (e.g., electrophysiology impedance mapping). Typically, one or more physical displays are used to share this information with multiple staff members in the procedure room. The positions of the physical displays are constrained by many factors including sterility, position of staff in the room, and equipment. In some cases, the displays are flexibly mounted and the content is dynamically configurable. However, it is still challenging to optimally position physical screens for all members of the interventional team while avoiding other equipment and preserving sterility. This leads to poor ergonomics, reduced access to information, and impeded communication within the team.

Virtualizing the screens via a wearable head-mounted display, as shown in Fig. 17.11, allows for a flexible display whose content can be configured on the fly, repositioned, and shared with others when needed. The virtual screen is not limited in its size, position, and orientation. If desired, it can also be automatically positioned with respect to the user (e.g., always following the user as the user changes her/his position). Virtual screens are not subject to some of the common issues with physical screens – such as glare, dirt, and/or view obstruction resultant from a team member standing in front of the screen.

The following parameters are important for holographic displays that show virtual screens in an interventional procedure:

- Access to relevant information sources
- Latency
- Resolution
- Contrast

To bring ergonomic benefits, the user should be able to configure the virtual screens in a flexible and personal way, bringing optimal access to meaningful information at each phase of the procedure. The screens should have the following functionality:

- Select sources
- Resize
- Position in a static location or follow the user gaze (configurable)
- Zoom in/out
- Control brightness

Users should also be able to extend their virtual environment to have control of interfaces. Studies have explored the use of touchless control of interfaces in the interventional setting including voice control, touchless gesture, and eye gaze [24, 25]. The main challenges identified are related to the usability and intuitiveness, as well as the integration into systems. Some of the benefits included avoiding workflow disturbances such as leaving the sterile field or asking non-sterile assistants to help with the image navigation process.

Wearable devices enable these same interfaces within one headset, which allows the various interfaces to be used together and with potentially improved usability due to the additional potential for enhanced audio and visual feedback via the holographic display. For example, using eye gaze together with a voice command "zoom in" can allow for zooming in of fluoroscopy images at the position of the gaze.

Each interaction method brings unique advantages and disadvantages to the interventional procedure, as outlined in Table 17.1.

Table 17.1 Overview of interaction modes supported by most head-mounted displays

Interaction mode	Advantages	Disadvantages
Voice	Hands-free Natural	Robustness to OR environment [21] Performance across languages, accents Command recall by operator
Gesture	Complex 3D manipulations Direct-touch interaction with virtual buttons	Requires use of one or more hands Learning curve
Head gaze	Silent Hands-free	Unnatural head movement
Eye gaze	Silent Hands-free Conveys intent	Could contribute to eye strain and distraction
Controllers	Fine control Robust	Not hands-free Additional object introduced to OR Must be draped or sterile

Virtualization of system control may have some commands where mechanisms to prevent inadvertent activation are necessary. There are multiple mechanisms available:

- A wake-up command to enable voice control
- "Accepting" of commands through a physical button or switch
- Multiple input activators required simultaneously (e.g., gaze plus voice)

Holographic Guidance

There are increasing sources of 3D information available in interventional procedures today. This includes both preoperative imaging data such as MRI and CT, intraoperative imaging data such as 3D transesophageal echocardiography (TEE), and intraoperative device shape and position via device tracking technologies such as optical tracking, electromagnetic sensing, and fiber-optic sensing. This 3D information is typically displayed on a 2D screen with a mouse, keyboard, or touch screen for interaction.

3D Holographic Models

3D holographic models based on preoperative imaging can be used both preoperatively for planning and simulation and intraoperatively as a reference. Both Medivis and Novarad have FDA 510(k) clearance for the display of 3D holograms based on a DICOM dataset from MRI or CT. Typically, the imaging data is segmented into a model that is then represented as a hologram. Studies investigating the use of 3D holographic models for intraoperative guidance in phantom, animal models, and clinical use [26–30] report improved anatomical understanding, better 3D perception, and the ability to more easily plan trajectories and make measurements. Figure 17.12 shows a holographic model of an abdominal aortic aneurysm shared between the interventional team.

Intraoperative Device Visualization

A natural extension of the 3D anatomical hologram in interventional procedures is to augment it with a 3D hologram of the navigational device (e.g., catheter, guidewire). Studies have shown that this provides improved depth understanding, faster navigation, and less catheter manipulations [31–33]. Figure 17.13 shows the SentiAR holographic visualization of the cardiac geometry, electroanatomic maps, and the therapy device for use in electrophysiology (EP) [31].

Fig. 17.12 Hologram of an abdominal aortic aneurysm shared between multiple users using Philips Azurion with HoloLens 2 (work in progress)

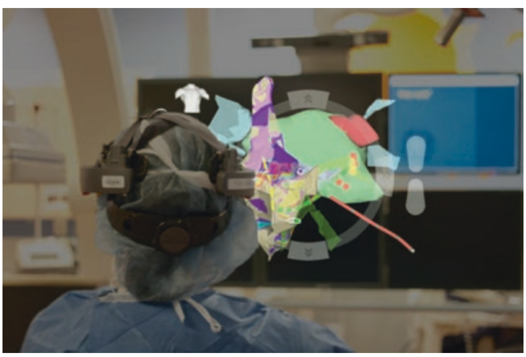

Fig. 17.13 This image demonstrates the intraprocedural use of the SentEP engine (SentiAR) deployed on the Microsoft HoloLens mixed reality headset. The cardiac geometry and electroanatomic maps displayed are created using the EnSite Velocity mapping system (St Jude Medical). The electrophysiologist (EP) is looking at two cardiac chambers. The right atrium has an overlaid voltage map (to assess the electrical health of the atrium), while the left atrium displays the anatomy. We can see real-time catheter locations within the geometry, as well as markers at ablation sites

Patient Overlay

A further extension of the utility of 3D holographic models is to overlay them on the patient intraoperatively. This allows for improved spatial perception of the internal anatomical structures with regard to the patient and can also facilitate tool guidance. In a study of six patients, Pratt et al. demonstrated that they could use AR intraoperatively to identify, dissect, and execute vascular pedunculated flaps during reconstructive surgery [34] (Fig. 17.14).

Registration between the patient and the hologram is a key step for overlay. It can be done in multiple ways including manually (visually) [34–36], using a marker that is visible in both the hologram and in the real world such as a CT grid [37], fiducial markers [38], or surface digitization [39]. Once the hologram is registered, it must then maintain its position reliably. Studies have implemented multiple methods, including the native HoloLens SLAM localization [34, 40], optical markers [41], or an optical tracking system [33].

Future Vision

The use of augmented reality in interventional procedures has rapidly expanded in recent years, as head-mounted displays have become more suitable for clinical use. Early studies have shown the benefit of these displays in simulation, understanding complex 3D anatomy, communication, ergonomics, and tool manipulation. However, some limitations still need to be overcome before these devices can be standard tools in the interventional procedure. Just as was seen with mobile phones and PCs, it appears that an AR "arms race" between vendors has begun. This will result in rapid improvements in image quality, increasing field of view, and more accurate and sophisticated gesture controls, voice recognition, and eye tracking. Devices will become smaller and lighter, with longer battery lives. Image-guided therapy companies will continue to refine what the proper user interaction should be, develop more sophisticated navigation software tailored

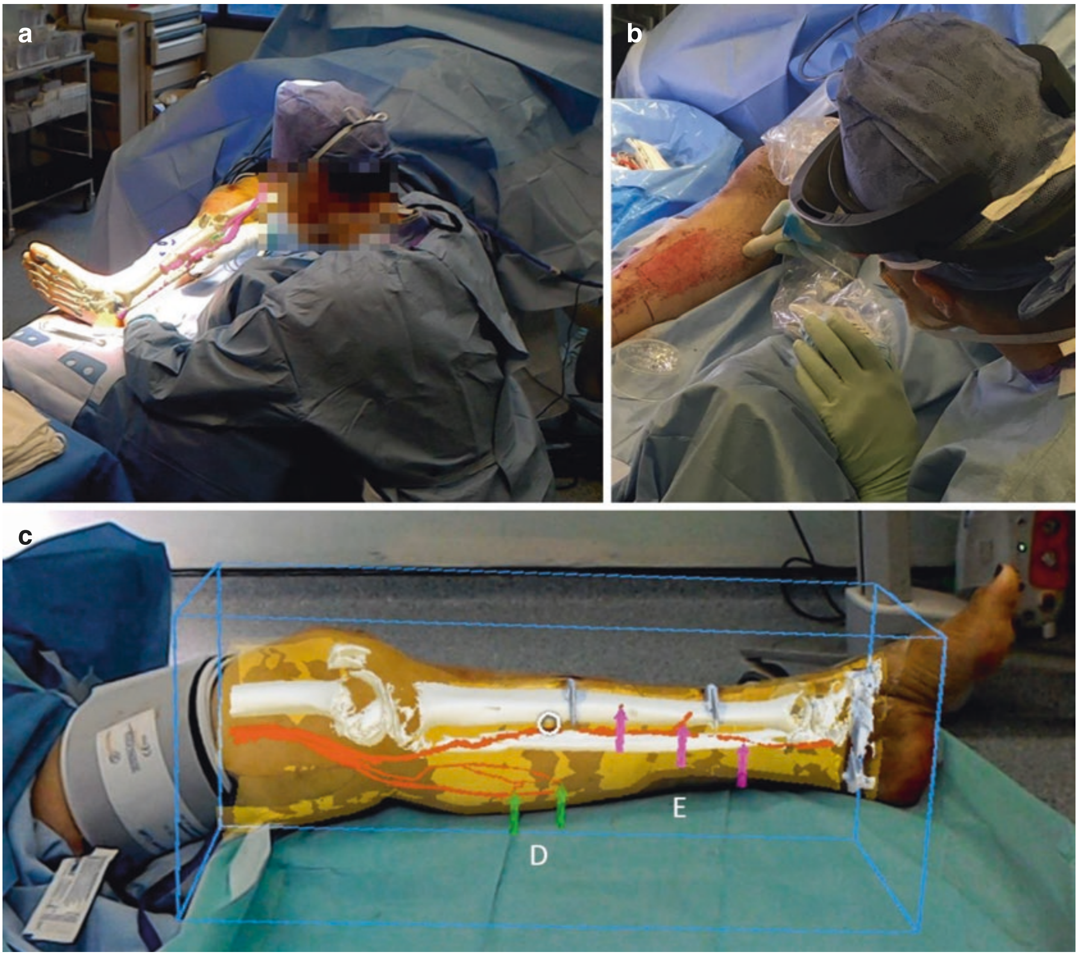

Fig. 17.14 (**a**) Intraoperative mixed reality capture showing a patient undergoing vascular free flap surgery with a render of osseous and vascular perforator anatomy registered to the surgeon's field of view. (**b**) Perioperative perforator localization using traditional handheld Doppler. (**c**) Perioperative mixed reality capture showing blood vessels are portrayed in red and bones in white, with (**d**) medial sural artery perforators and (**e**) tibialis perforators indicated with arrows. The operating surgeon is able to appreciate the vascular perforator anatomy beneath the skin while operating and thus is able to understand the information from the CT scan directly in the operating theatre. From Pratt P et al. [34]. Open access. This article is distributed under the terms of the Creative Commons Attribution 4.0 International License (http://creativecommons.org/licenses/by/4.0/)

for AR, and help users better navigate smart devices in the holographic world. And AR display vendors are even exploring how brain-computer interfaces could one day turn thoughts and intent into commands.

This rapid innovation in digital health technologies (like AR) has resulted in regulatory bodies like the FDA to begin convening panels composed of physicians, scientists, industry, and patients, to better understand how to more rapidly accelerate AR in healthcare but in the *safest manner possible.* The advancement of today's prototype devices into approved medical devices is inevitable, and this will enable use by the broader interventional and surgical community.

References

1. Kobeiter H, Nahum J, Becquemin J-P. Zero-contrast thoracic endovascular aortic repair using image fusion. Circulation. 2011;124:e280–2.

2. Ruijters D, Homan R, Mielekamp P, van de Haar P, Babic D. Validation of 3D multimodality roadmapping in interventional neuroradiology. Phys Med Biol. 2011;56(16):5335–54. https://doi.org/10.1088/0031-9155/56/16/017.
3. Blanc R, Seiler A, Robert T, et al. Multimodal angiographic assessment of cerebral arteriovenous malformations: a pilot study. J Neurointerv Surg. 2015;7:841–7. https://doi.org/10.1136/neurintsurg-2014-011402.
4. Wink O, Hecht HS, Ruijters D. Coronary computed tomographic angiography in the cardiac catheterization laboratory: current applications and future developments, cardiology clinics, Advances in coronary angiography, S. J Chen and J D Carroll, 2009;27(3):513–29. https://doi.org/10.1016/j.ccl.2009.04.002.
5. Goreczny S, Dryzek P, Moszura T. Novel 3-dimensional image fusion software for live guidance of percutaneous pulmonary valve implantation. Circ Cardiovasc Interv. 2016;9(7). https://doi.org/10.1161/CIRCINTERVENTIONS.116.003711.
6. Kliger C, Jelnin V, Sharma S, Panagopoulos G, Einhorn BN, Kumar R, Cuesta F, Maranan L, Kronzon I, Carelsen B, Cohen H, Perk G, van den Boomen R, Sahyoun C, Ruiz CE. CT angiography-fluoroscopy fusion imaging for percutaneous transapical access. JACC Cardiovasc Imaging. 2014;7:169–77. https://doi.org/10.1016/j.jcmg.2013.10.009.
7. Gupta A, Grunhagen T. Live MR angiographic roadmapping for uterine artery embolization: a feasibility study. J Vasc Interv Radiol. 2013;24(11):1690–7. https://doi.org/10.1016/j.jvir.2013.07.013.
8. Spelle L, Ruijters D, Babic D, Homan R, Mielekamp P, Guillermic J, Moret J. First clinical experience in applying XperGuide in embolization of jugular paragangliomas by direct intratumoral puncture. Int J Comput Assist Radiol Surg. 2009;4(6):527–33. https://doi.org/10.1007/s11548-009-0370-6.
9. Elmi-Terander A, Skulason H, Söderman M, Racadio J, Homan R, Babic D, van der Vaart N, Nachabe R. Surgical navigation technology based on augmented reality and integrated 3D intraoperative imaging: a spine cadaveric feasibility and accuracy study. Spine (Phila Pa 1976). 2016;41(21):E1303–11.
10. Racadio JM, Nachabe R, Homan R, Schierling R, Racadio JM, Babić D. Augmented reality on a C-Arm system: a preclinical assessment for percutaneous needle localization. Radiology. 281(1):249–55. https://doi.org/10.1148/radiol.2016151040.
11. Gafoor S, Schulz P, Heuer L, Matic P, Franke J, Bertog S, Reinartz M, Vaskelyte L, Hofmann I, Sievert H. Use of EchoNavigator, a novel echocardiography-fluoroscopy overlay system, for transseptal puncture and left atrial appendage occlusion. J Interv Cardiol. 2015;28:215–7. https://doi.org/10.1111/joic.12170.
12. Balzer J, Zeus T, Hellhammer K, Veulemans V, Eschenhagen S, Kehmeier E, Meyer C, Rassaf T, Kelm M. Initial clinical experience using the EchoNavigator(®)-system during structural heart disease interventions. World J Cardiol. 2015;7(9):562–70. https://doi.org/10.4330/wjc.v7.i9.562.
13. Kim BH, Koh Y-S, Lee K-Y, Chung W-B. Three-dimensional EchoNavigator system guided transcatheter closure of paravalvular leakage. J Cardiovasc Imaging. 2019;27(3):227–9. https://doi.org/10.4250/jcvi.2019.27.e30.
14. Frimerman A, Abergel E, Blondheim DS, Shotan A, Meisel S, Shochat M, Punjabi P, Roguin A. Novel method for real time co-registration of IVUS and coronary angiography. J Interv Cardiol. 2016;29(2) https://doi.org/10.1111/joic.12279.
15. Piayda K, Kleinebrecht L, Afzal S, Bullens R, ter Horst I, Polzin A, Veulemans V, Dannenberg L, Wimmer AC, Jung C, Bönner F, Kelm M, Hellhammer K, Zeus T. Dynamic coronary roadmapping during percutaneous coronary intervention: a feasibility study. Eur J Med Res. 2018;23:36.
16. Yabe T, Muramatsu T, Tsukahara R, et al. The impact of percutaneous coronary intervention using the novel dynamic coronary roadmap system. Heart Vessel. 2019. https://doi.org/10.1007/s00380-019-01502-1.
17. Chen L, Day TW, Tang W, John NW. Recent developments and future challenges in medical mixed reality. In: 2017 IEEE international symposium on mixed and augmented reality (ISMAR). 2017.
18. Chan D, et al. Joint practice guideline for sterile technique during vascular and interventional radiology procedures: from the Society of Interventional Radiology, Association of perioperative Registered Nurses, and Association of Radiologic and Imaging Nursing, for the Society of Interventional Radiology (Wael Saad, MD, Chair), Standards of Practice Committee, and Endorsed by the Cardiovascular Interventional Radiological Society of Europe and the Canadian Interventional Radiology Association. J Vasc Interv Radiol. 2012;23:1603–12.
19. Butt U, Saleem U, Yousuf K, El-Bouni T, Chambler A, Eid AS. Infection risk from surgeons' eyeglasses. J Orthop Surg. 2012;20(1):75–7. https://doi.org/10.1177/230949901202000115.
20. Miller DL, Vañó E, Bartal G, et al. Occupational radiation protection in interventional radiology: a joint guideline of the Cardiovascular and Interventional Radiology Society of Europe and the Society of Interventional Radiology. Cardiovasc Intervent Radiol. 2010;33(2):230–9. https://doi.org/10.1007/s00270-009-9756-7.
21. Mewes A, Hensen B, Wacker F, et al. Touchless interaction with software in interventional radiology and surgery: a systematic literature review. Int J Comput Assist Radiol Surg. 2017;12(2):291–305. https://doi.org/10.1007/s11548-016-1480-6.
22. Weldon SM, et al. Communication in the operating theatre. Br J Surg. 2013;100(13):1677–88.
23. Kagadis GC, et al. Medical imaging displays and their use in image interpretation. Radiographics. 2013;33(1):275–90.
24. Mewes A, Hensen B, Wacker F, Hansen C. Touchless interaction with software in interventional radiology

and surgery: a systematic literature review. Int J Comput Assist Radiol Surg. 2017;12(2):291–305.
25. Homayoon B, Chung J, Gandhi RT, Liu DM. Early clinical experience with a touchless image navigation interface for the endovascular suite. Minim Invasive Ther Allied Technol. 2019;8:1–8.
26. Jang J, Tschabrunn CM, Barkagan M, Anter E, Menze B, Nezafat R. Three-dimensional holographic visualization of high-resolution myocardial scar on HoloLens. PLos One. 2018;13(10):e0205188.
27. Brun H, et al. Mixed reality holograms for heart surgery planning: first user experience in congenital heart disease. Eur Heart J Cardiovasc Imaging. 2019;20(8):883–8.
28. Rynio P, et al. Holographically-guided endovascular aneurysm repair. J Endovasc Ther. 2019;26(4):544–7.
29. Bruckheimer E, et al. Computer-generated real-time digital holography: first time use in clinical medical imaging. Eur Heart J Cardiovasc Imaging. 2016;17:845–9.
30. Ballocca F, et al. Validation of quantitative 3-dimensional transesophageal echocardiography mitral valve analysis using stereoscopic display. J Cardiothorac Vasc Anesth. 2019;33(3):732–41.
31. Silva JNA, Southworth M, Raptis C, Silva J. Emerging applications of virtual reality in cardiovascular medicine. JACC Basic Transl Sci. 2018;3(3):420–30.
32. Kuhlemann I, Kleemann M, Jauer P, Schweikard A, Ernst F. Towards X-ray free endovascular interventions – using HoloLens for on-line holographic visualization. Healthc Technol Lett. 2017;4(5):184–7.
33. Meulstee JW, et al. Toward holographic-guided surgery. Surg Innov. 2019;26(1):86–94.
34. Pratt P, Ives M, Lawton G, Simmons J, Radev N, Spyropoulou L, Amiras D. Through the HoloLens™ looking glass: augmented reality for extremity reconstruction surgery using 3D vascular models with perforating vessels. Eur Radiol Exp. 2018;2:2.
35. Mitsuno D, Ueda K, Hirota Y, Ogino M. Effective application of mixed reality device HoloLens: simple manual alignment of surgical field and holograms. Plast Reconstr Surg. 2019;143(2):647–51.
36. Incekara F, et al. Clinical feasibility of a wearable mixed-reality device in neurosurgery. World Neurosurg. 2018;118:e422–7.
37. Park B, et al. Registration of 3D holographic models of patient imaging onto a CT grid: assessment of manual and automatic techniques using HoloLens. JVIR. 2019. Abstract No. 289.
38. Li Y, et al. A wearable mixed-reality holographic computer for guiding external ventricular drain insertion at the bedside. J Neurosurg. 2018;131(5):1–8.
39. Liebmann F, et al. Pedicle screw navigation using surface digitization on the Microsoft HoloLens. Int J Comput Assist Radiol Surg. 2019;14(7):1157–65.
40. Hajek J, et al. Closing the calibration loop: an inside-out-tracking paradigm for augmented reality in orthopedic surgery. In: Proceedings of the conference on medical image computing and computer assisted intervention, 2018. p. 1–8.
41. Frantz T, Jansen B, Duerinck J, Vandemeulebroucke J. Augmenting Microsoft's HoloLens with vuforia tracking for neuronavigation. Healthc Technol Lett. 2018;5(5):221–5.

18

The Visible Patient: Augmented Reality in the Operating Theater

Luc Soler, Alexandre Hostettler, Toby Collins, Patrick Pessaux, Didier Mutter, and Jacques Marescaux

Introduction

The introduction of an optical device into the abdomen of a patient in order to carry out a surgical procedure via a miniaturized camera represented a major evolution in the surgical world of the twentieth century: the "minimally invasive" surgery era was born. Although the benefits for patients of laparoscopic surgery have been clearly demonstrated, it brings up new difficulties for surgeons by greatly reducing maneuvering capabilities. The first difficulty is the loss of several senses, such as the sense of touch, along with a modification in the force feedback. This lack of force feedback is also exemplified by current robotic systems, such as the da Vinci surgical system (Intuitive Surgical, Inc. Sunnyvale, CA, USA), currently the most used surgical robot worldwide. However, the use of stereoscopic vision allowed surgeons to lessen that perception limit by providing a 3D view of the operative field, filmed via dual cameras. Another solution applicable to both monoscopic and stereoscopic systems consists in using virtual reality (VR) and augmented reality (AR).

Indeed, from a patient's medical image (CT scan or MRI), VR software provides a 3D visualization of the patient. This visualization can be performed directly from the medical image (with direct volume rendering) or after image processing by 3D surface rendering. Although direct volume rendering is visually appealing, it can

L. Soler (✉)
Visible Patient, Strasbourg, Grand Est, France

University of Medicine of Strasbourg, Strasbourg, France
e-mail: luc.soler@visiblepatient.com

A. Hostettler · T. Collins
Research & Development, Research Institute Against Digestive Cancers (IRCAD), Strasbourg, France

P. Pessaux
Hepato-Biliary and Pancreatic Surgical Unit, Department of Digestive and Endocrine Surgery, Institute of Image-Guided Surgery, University Hospital of Strasbourg, Strasbourg, France

University of Medicine of Strasbourg, Strasbourg, France

Research Institute Against Digestive Cancers (IRCAD), Strasbourg, France

D. Mutter
University of Medicine of Strasbourg, Strasbourg, France

Research Institute Against Digestive Cancers (IRCAD), Strasbourg, France

Department of Digestive and Endocrine Surgery, Institute of Image-Guided Surgery, University Hospital of Strasbourg, Strasbourg, France

J. Marescaux
Research Institute Against Digestive Cancers (IRCAD), Strasbourg, France

Institute of Image-Guided Surgery (IHU Strasbourg), Strasbourg, France

S. Atallah (ed.), *Digital Surgery*, https://doi.org/10.1007/978-3-030-49100-0_18

provide very limited benefit in comparison with the 3D surface rendering that starts with computer-based 3D modeling of organs and pathology extracted from the medical image. In fact, due to an improved preoperative knowledge of patient-specific anatomy, practitioners can establish an improved diagnosis and plan a best-suited therapy for any given operation. As we will illustrate, this represents the first major progress of surgery.

Augmented reality is an extension of VR that consists of fusing the VR view with the real view of the patient in the same position and shape: in this way, the patient becomes virtually transparent. To be efficient, the VR view must be perfectly registered onto the real view. The registration process consists first of computing and tracking the position and orientation of the real camera or of the surgeon's eyes. Then, this position and orientation of the camera, or of the human eye field of vision, will be reproduced on the virtual camera view of the anatomical or pathological structures. In case of the camera, registration will finally allow for a fusion between the *video view* and the *virtual video view* providing a kind of virtual transparency from a simple display. In case of surgeon eyes, registration will allow for a same virtual video view on an AR see-through display – such as AR glasses.

Registration can be performed interactively or automatically. It can be rigid (only position of camera or eyes is computed) or nonrigid (real organ movements and deformation are detected and reproduced on the virtual model of the patient). Several interactive systems have been developed and applied to humans, demonstrating the benefit of AR in surgical oncology, but limitations related to organ deformation are also underscored. Automatic nonrigid registration is today the main research goal of most teams trying to provide efficient computer-based intraoperative assistance.

By combining this preoperative 3D modeling with intraoperative information, two major computer-assisted surgical procedures have been developed: *computer-assisted guiding systems*, using real information to control the virtual environment, and *augmented reality (AR) systems* that superimpose virtual information onto real images [1]. These make up for the lack of touch by improving surgical images augmented by virtual information. Computer assistance will therefore avoid having to locate tumors or vessels using the sense of touch, providing visualization through virtual transparency instead. As we will illustrate, by combining these systems with robotic devices, these innovations will lead to the optimization of the surgical procedure. In this chapter, we will present the various elements of computer-aided surgery, providing the reader with an understanding of these major innovations. How computer-aided surgery can be used in combination with minimal access surgery will be also be discussed.

Virtual Reality: First Example of Computer-Assisted Surgery

The first expected benefit of a computer-assisted system applied to patient-specific anatomy is to provide a fast, efficient, and easy way to implement a view of the patient's anatomy. Any software meeting these needs should allow for the reading of images recorded during clinical encounter in Digital Imaging and Communications in Medicine (DICOM), the international standard format. Moreover, such software should provide at least two types of immediate rendering: a 2D view of image slices and a composite 3D view. Currently, many of the available software applications for the visualization consoles of radiology departments must either be paid for or can be freely downloaded from the Internet. Osirix™ (www.osirix-viewer.com) is the most ubiquitous and most used software by radiologists today. Although it is very complete, it presents two drawbacks: (a) it only works on Mac OS, and (b) its user interface is not particularly intuitive for surgeons, as it shares similarities to complex post-processing software employed by radiology systems. Whether it is free (research version) or must be paid for (CE-marked version), we have noticed that these software applications are scarcely used by surgeons due to their complexity – that is, the user interface is submerged with complicated options, and lengthy training is sometimes required to use the software.

To overcome this recurring drawback, we have developed a software, Visible Patient Planning™ (©Visible Patient 2014, https://www.visiblepatient.com/en/products/software), that is CE marked and FDA approved and free of charge. Moreover, Visible Patient Planning works on both Mac OS and Windows operating systems. Whichever workstation you use – Osirix or Visible Patient Planning – the first advantage for surgeons is direct volume rendering which is automatically computed by the software from the CT or MRI slices of the DICOM image (Fig. 18.1). This no-cost technique can be sufficient for a good 3D visualization of anatomical and pathological structures and can thus be a useful tool for preoperative planning [2–4]. In order to see internal structures, the initial voxel gray level is replaced by an associated voxel color and transparency. This transparency allows one to distinguish more contrasted anatomical or pathological structures, even when they are not delineated in reality. That volume can also be cut along the three main axes (axial, coronal, or sagittal) or with an oblique mouse-controlled plane. In clinical practice, direct volume rendering can be of great preoperative interest. This is the case for all malformation pathologies – in particular vascular or bone malformations – but also for thoracic and digestive pathologies.

Direct volume rendering is thus a very useful tool as it is freely accessible without any preprocessing; however, it does have some limitations. It cannot provide the volume of organs nor their dimensions since these organs are not delineated. For the same reason, it is not possible to provide volume after resection or to subtract a section of these structures without subtracting neighboring structures. To overcome this limit, each anatomical and pathological structure in the medical image has to be delineated. Such a delineation, called "segmentation," can be performed with a specific workstation available from various vendors (Myrian™ from Intrasense, Synapse™ from Fuji) or through a distant online service that can be compared to a medical analysis laboratory (Visible Patient Service). In the first solution, hospitals pay for a workstation, and then physicians can use it by themselves to perform 3D modeling. In the second solution, hospitals pay the image analysis for each patient just like they

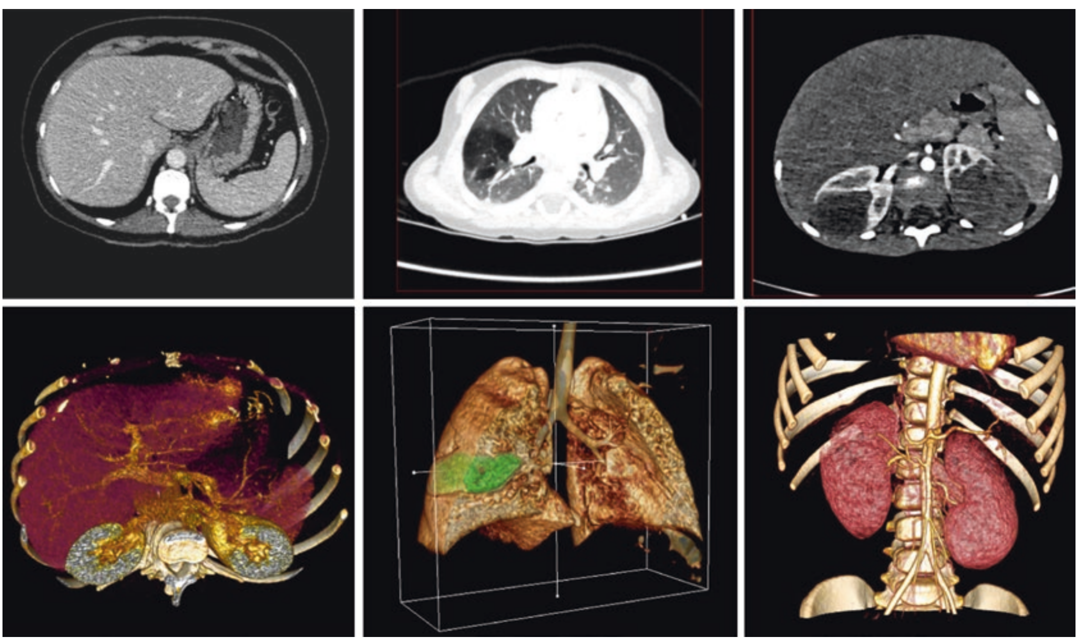

Fig. 18.1 Direct volume rendering (second line) of three different clinical cases from their DICOM image (first line), here from CT scan of liver (left), lung (middle), and kidney (right) using Visible Patient Planning™ software

would pay for other third-party services, such as histology and surgical pathology analysis. Moreover, this latter fee-for-service model is currently covered by some private insurance companies in France (more than 17% of French citizen are thus covered in France in 2019), making it more easily accessible. Each solution (onsite or online) allows for 3D surface rendering of organs, as well as for volume computation of delineated structures. In this set of solutions, Visible Patient Service is today the only service available for any part of the body and for any pathology or organ ranging from infant to adult. The result of the 3D modeling process can be visualized from the free Visible Patient Planning software through surface rendering but can also be fused with volume rendering (Fig. 18.2).

This surface rendering of delineated structures provides a more advanced anatomical view of the patient, but it remains insufficient for several types of surgery – such as partial resection, which requires preoperative evaluation of future volumes remaining after resection. More advanced solutions provide the opportunity to simulate virtual resection and to (preoperatively) obtain the resulting volume. Some software, such as Myrian™, provides this possibility from virtual cutting planes. Some other software systems, such as Synapse™ or Visible Patient Planning™, have a more anatomy-oriented approach based on vascular territory simulation, with the option, for example, to apply a virtual vascular clip which the user is able to manipulate and position in an interactive fashion (Fig. 18.3).

By defining the vascular territories (i.e., distributions), the resulting patient-specific anatomy is then not only a geometrical, patient-specific anatomy but is also a *functional* anatomy that can be

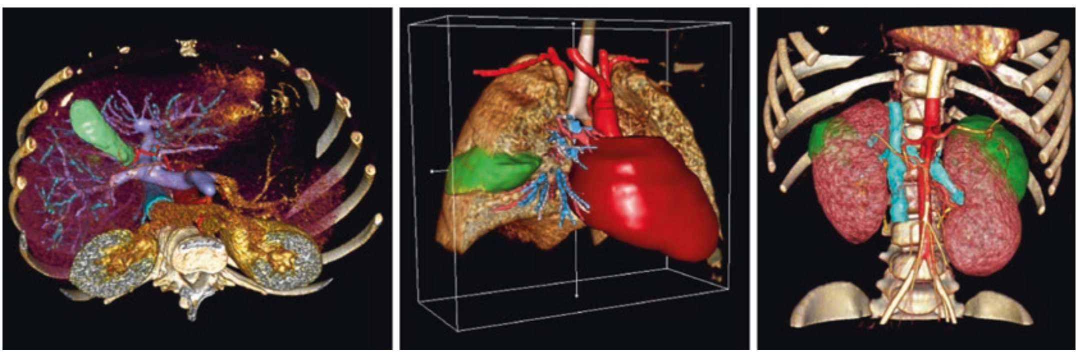

Fig. 18.2 Visible Patient Planning™ fusion between direct volume rendering and surface rendering of organs provided by the Visible Patient online service of the same patients as Fig. 18.1

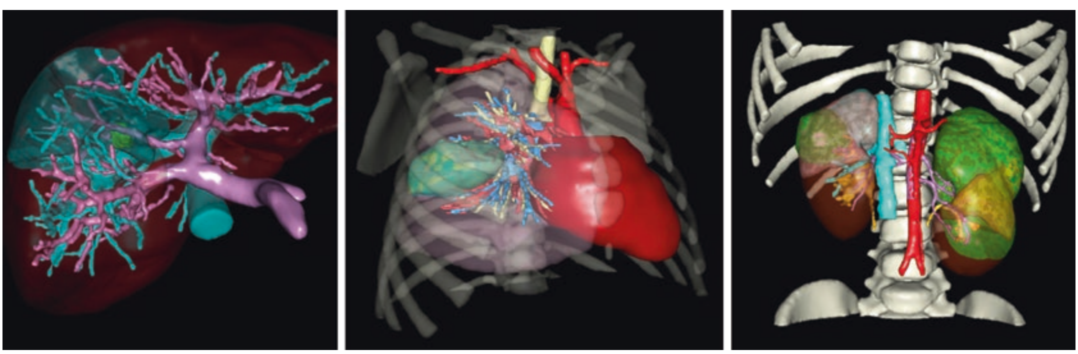

Fig. 18.3 Virtual clip applying and resulting devascularized territories simulated by Visible Patient Planning™ for the same patients as Fig. 18.1

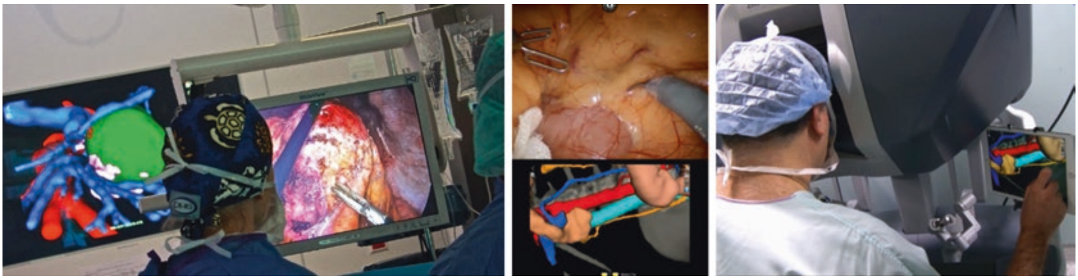

Fig. 18.4 Intraoperative use of Visible Patient Planning™ plugged on Operative Display (left) or on robotic display (right)

used preoperatively to define a surgical procedure more accurately. It can also be used intraoperatively to guide the surgeons, owing to the development of intraoperative VR tools. For instance, the Visible Patient Planning™ software can be brought inside the operating room to directly visualize the result on a laptop or smartphone or indirectly by plugging into an OR ready display; it can even be adapted to existing surgical robotic systems, such as the da Vinci surgical system (Intuitive Surgical, Inc.) (Fig. 18.4).

Benefits of Virtual Reality in Minimal Access Surgery

To illustrate clinical benefits of such patient-specific, computer-assisted anatomy and surgical planning system, for several years, we have applied it using the Visible Patient Service (www.visiblepatient.com) to a wide range of surgical procedures in digestive, thoracic, urological, endocrine, and pediatric procedures [5, 6]. We will here limit our description of clinical benefits to the same three patients illustrated on previous illustrations (Figs. 18.1, 18.2, and 18.3). Then, we will discuss published clinical data highlighting the clinical benefits of such computer-assisted, patient-specific anatomic modeling.

The first patient was a 55-year-old patient diagnosed with a hepatocarcinoma. From the CT image only, a single lesion was detected on the back of the right hepatic vein, i.e., the most right-hand part of the liver (refer to Fig. 18.5, *yellow circle on left*). The Online Visible Patient 3D modeling provided a 3D modeling of an additional nodule (refer to Figs. 18.5 and 18.6, *red circle*). This was subsequently validated by a qualified radiologist (after the medical images were re-examined) as a potential hepatic tumor. This second tumor was located between the median hepatic vein and the right hepatic vein, that is, again in the right liver. Additional information obtained from the radiological department was that the right liver volume measured approximately 60% of the total liver volume; this volume was computed without the Visible Patient Planning software. By analyzing this radiological volume estimate of the right lobe of the liver and by using standard anatomical landmarks, the surgical team obtained a much clearer clinical picture. In this example, it became evident that a formal right liver resection, due to the position of the second tumor (Fig. 18.5, *red circle*) being in too close of proximity with large neighboring vessels, would make resection hazardous. The surgeons were now also able to appreciate that even ablation of the secondary tumor would be problematic, due to the juxtaposition to large vessels which would create a heat sink.

But by using the Visible Patient Planning software, surgeons simulated this particular right liver resection by virtually clipping the right branch. The *orange territory* on Fig. 18.6 represents this right hepatic lobe, but neither tumor was located in this real portal vein territory (representing only 45% of the liver volume). By virtually clipping the left portal branch (Fig. 18.6, *blue territory*), both tumors were localized to this devascularized left liver segment, representing 55% of the liver volume. Finally, by analyzing more accurately the reason of this error, it was

Fig. 18.5 Three axial slices of the first patient with two small hepatic tumors (circles)

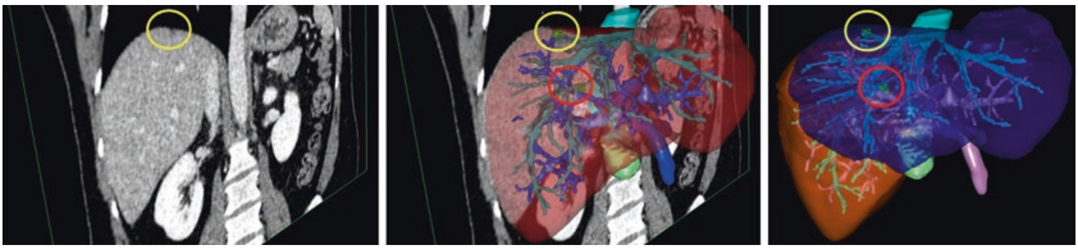

Fig. 18.6 3D modeling provided online by Visible Patient Service and allowing to visualize two hepatic tumors (circles). From virtual clip applying performed with Visible Patient Planning software, the 3D view of the left liver (blue) and the right liver (orange) shows the location of both tumors in the left liver and not in the right liver

apparent in 3D reconstruction that this patient had absent right paramedian branches providing blood flow to liver segments V and VIII. An anomalous branch, arising from the left portal vein, provided blood supply to a territory located in the vicinity of segment VIII but vascularized from the left portal branch. Virtual clip application on this branch thus provided the smallest territory to resect (13,3% of the liver volume; corresponding to the *teal area in left most image,* Fig. 18.3). *In sum, this simulation allowed the surgical team to plan the operation such that an R0 resection could be performed while preserving the maximum amount of unaffected liver parenchyma.*

This example illustrates the well-known problem of hepatic anatomical variation already described by Couinaud [7]. In fact, studies demonstrate that in more than one-third of hepatic surgical interventions, 3D modeling and preoperative simulation allow surgeons to correct errors of the initial surgical planning [3, 8]. Another study suggests that, for certain interventions, operating time can be reduced by 25%; furthermore, operative morbidity can be decreased by more than one-third [9]. These impressive results illustrate the importance of analyzing properly the anatomical variation of the liver. Moreover, this illustrates the quite real benefit to patients achieved by using computer-assisted patient-specific 3D modeling preoperatively to best plan the surgical approach, to enhance the understanding of anatomic variation and aberrant vasculature, and to avoid medical image interpretation errors in liver surgery so that patient outcomes are optimized.

But it is valid to apply such models to alternative organs – such as the lung? Lung cancer resections are today approached in a fashion similar to hepatectomy, by resecting the afflicted portion of the bronchial tree – metaphorically analogous to trimming a diseased branch from a living tree to preserve the healthy part. Like hepatic surgery, the operative challenge lies in *appropriately defining of the territories of that bronchial tree,* which are difficult to discern from a simple computed tomography image. Adding to the level of complexity is the fact that the pathology in question, whether malignant or benign, can locally modify the anatomy or mask landmarks that *are* however present in the image. The second example, illustrated in Fig. 18.7, is of a 6-month-old infant presenting with a lung cyst due to cystic adenomatoid lung disease. This is a pathologic abnormality of the pulmonary system that requires the diseased segment of the bronchial tree to be surgically resected with an approach analogous to that used for the resection of cancer pathology. From the computed tomography image of this child, the cyst created by this disease (Fig. 18.7, *black portion in the center of the left image*) seemed located in the upper lobe of the right lung. This was the diagnosis realized by the radiological team and validated by the surgical team. But after 3D modeling (utilizing the Visible Patient Service), virtual clip applying performed by the surgeon showed that the cyst (Fig. 18.7, *shaded green in the right-most image*) was *not* in the upper right lobe (Fig. 18.7, *right-most image, anatomic right lobe highlighted in yellow*). Consequent to 3D modeling, the surgery was modified and realized perfectly, thus validating the efficiency of the preoperative simulation. This approach underscores the advantage of using 3D modeling for complex operative cases, a crucial aspect of digital surgery.

We can now appreciate how 3D modeling provides benefits in the preoperative planning phase of both pulmonary and hepatic surgeries. As demonstrated by these examples, preoperative virtual clip applying provides surgeons with the ability to simulate bronchial territories as well as to simulate portal vein territories of the liver. Moreover, the 3D modeling of internal lung structures is not limited to the bronchial system but also includes pulmonary arteries and veins. This allows one to avoid errors in territory definition and to improve the surgical therapy planning as validated in several recent articles and clinical studies [10–13]. These first two clinical applications exemplify the benefits of computer-assisted, patient-specific 3D anatomy in surgical procedures using the functional anatomy definition and framework. Liver and lung have anatomically defined vascular territories that anatomical variations can distort the true clinical picture, thereby creating errors in choice of treatment.

In the last example, 3D modeling is applied to the renal system, which differs from the hepatic and pulmonary architecture in that kidneys do *not* have functional anatomical segmentation. However, kidneys do present other challenges, at times, due to critical variations in vascular anatomy. In this example (refer to Figs. 18.1, 18.2, and 18.3), a 5-year-old child was diagnosed with double nephroblastoma. Even though this cancer is relatively frequent in adults, very few children are diagnosed with this condition (in France, 130

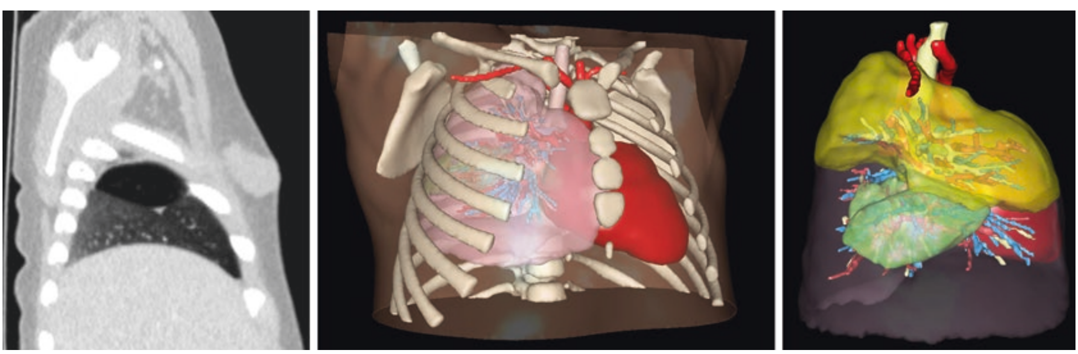

Fig. 18.7 Cystic adenomatoid lung disease detected in the right upper lobe from a CT scan (left) of a 6-month-old patient. 3D modeling (center) provided by Visible Patient online service and the clip applying simulation of the right upper lobe (yellow) showed that the cyst was not in this territory and avoided the error preoperatively

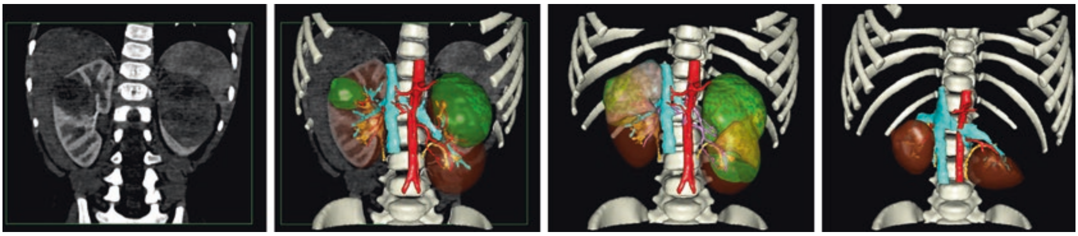

Fig. 18.8 Double nephroblastoma detected on both kidneys of a 5-year-old child. Thanks to 3D modeling and preoperative simulation of clip applying using Visible Patient Service and Planning software, a partial resection of each kidney was validated and realized. As illustrated on the right, 1 year later the patient seems to be cured

new pediatric patients versus 13,000 new adult patients are diagnosed each year). From the CT scan image (Fig. 18.8, *left-most image*), the expert surgical team for this kind of surgery planned to resect *half of the right kidney* and a *full resection of the left kidney*, where, according to the standard CT image, tumor invasion would not permit a lesser approach. This aggressive surgery would necessarily induce renal insufficiency, which would likely translate into ≤6 months of dialysis dependency. These 6 months will allow for oncologic surveillance, especially regarding local regrowth in the lower part of the remaining right kidney. After these 6 months, and if no tumor has appeared, left renal transplant could be undertaken. Transplant will increase the child's life expectancy by more than 50 years but will also induce lifelong antirejection treatment. This therapeutic proposition is submitted to a second team, also expert in that kind of pathology, for a second medical opinion. The second team validates this choice of treatment and agreed with the plan of care proposed.

With two highly experienced teams concurring on the planned surgical approach, could 3D modeling provide new insights that alter the surgeon's decision? From 3D modeling and by using the *Visible Patient Planning*™ software, the surgeon simulated surgical clip applying (i.e., analyzing what effect would result by the ligation or clipping of specific vessels during resection). This validated the possibility of resecting only half of the right kidney (as proposed). Specifically, this modeling confirmed that 50.9% of the right kidney would remain functional after surgery. But the surprise came from analysis of the left kidney – when simulating surgery, the surgeon observed that *it was technically possible to preserve one-third of the left kidney function.* Volume computation provided by the software demonstrated that the remaining renal parenchyma (on the left and on the right) after surgery would have a slightly greater volume than the volume of one kidney in a child of that age and size. Based on this information, the surgeon chose to modify the surgical plan. Now, preservation of the left kidney was reconsidered by the primary team, and it was subsequently validated by a second team. The operation was performed in two stages. No renal insufficiency was observed after resection of the diseased segments from both of the child's kidneys. The child went back to school 2 months after staged resection. One year later, the control image shows no tumor regrowth, and the child is in perfect health condition (Fig. 18.8, *right-most image*).

As illustrated by this example, the same benefits observed in the preoperative planning for liver and lung resection can be appreciated for the renal system – by using virtual clips and analyzing various outcomes through computer-assisted 3D modeling of specific patients. Such 3D modeling can be used for alternative urological operations and a variety of pathology, such as renal pelvis dilatation (Fig. 18.9, *left image*), crossed or crossed fused renal ectopia (Fig. 18.9, *middle image*), or kidney transplant (Fig. 18.9, *right image*). In any case, the precise 3D visualization of vascular structures, ureters, and surrounding organs provides a major benefit in surgical procedure planning [14–16].

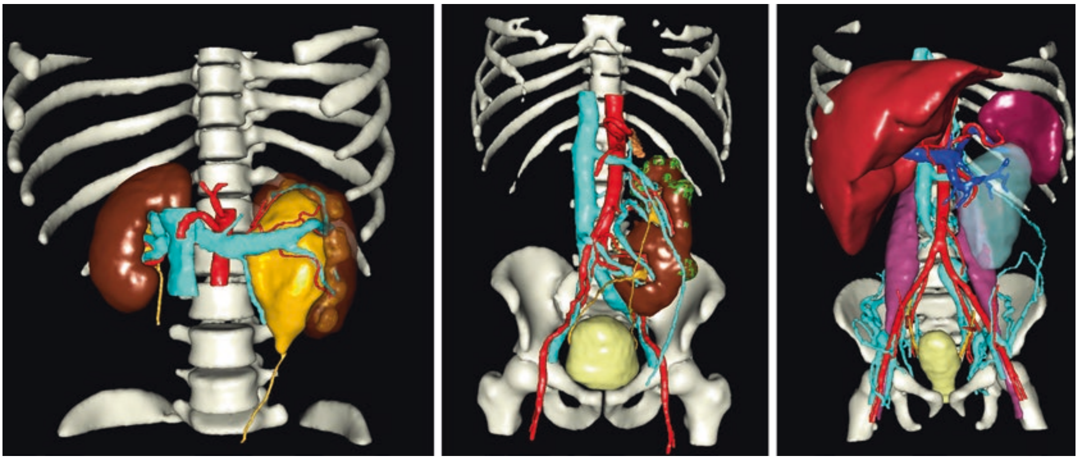

Fig. 18.9 Left renal pelvis dilatation (left), left crossed fused renal ectopia (middle), and simulation of kidney transplant (in blue on the right)

Augmented Reality as a Framework for Computer-Assisted Surgery

Preoperative surgical planning and simulation can significantly improve the efficiency of a surgical procedure secondary to better preoperative knowledge of the patient's anatomy. However, the preoperative use of such systems is not sufficient to ensure safety *during* the surgical procedure. Such refinement can be provided by an intraoperative use of virtual reality, utilizing the concept of augmented reality (AR). In this context, AR *consists of superimposing the preoperative 3D patient modeling onto the live intraoperative view of the patient.* An efficient AR means thus an efficient registration of the virtual view on the real view. AR will then provide a transparency view of patients through an image overlay of the patient's model superimposed onto the patient's view. There are several ways to define it from the rendering techniques, the visualization system, the see-through area, and, more frequently, the registration techniques [17]. The AR view can be *external* (as in open surgery) to "see through" the patient's skin, or it can be *internal* (e.g., as in laparoscopic surgery) to see through an organ. These two AR views can then be *direct* (without camera) or *indirect* (with a camera) (Fig. 18.10). Four main image overlay techniques are thus available [18]: *(a)* direct projection of the patient model onto the patient through a video projector [19–21], *(b)* direct visualization through a transparent screen placed between the surgeon and the patient [22] or, more frequently, via AR glasses [23, 24], *(c)* indirect visualization using a camera to provide a patient view visualized on a screen that can overlay the virtual patient model [25, 26], and *(d)* the use of a specific display, such as the robotic 3D view display of the da Vinci robotic system [27, 28]. In the recent past, most solutions were using *indirect visualization* using a laparoscopic or a robotic camera, but the development of the HoloLens AR glasses has currently increased the use of *direct* AR vision. The indirect visualization using a camera is today probably the best available solution, because it provides the camera's point of view regardless of surgeon position or movement. In turn, this avoids classical errors linked to the detection of several points of view.

Whatever the AR view (direct or indirect; internal or external), the main problem is efficient registration between the virtual and the real patient location and shape. Today, registration techniques remain one of the most complex problems to solve and represent an important challenge for AR in the operating theater. Registration can be manual, interactive, semiautomatic, or

Fig. 18.10 Two types of augmented reality (AR) views: Direct AR through AR glasses worn by surgeons provides direct see-through vision of the patient (right image); indirect AR through laparoscopic camera fuses the virtual image of the patient with the video view of the patient (two images on the left display) to provide a new laparoscopic AR view (display in the middle)

automatic. In the case of manual registration [17, 29, 30], the virtual patient is displayed on the AR system (transparent screen, AR glasses, or surgical monitor) and manually oriented and/or resized to fit the same position of the patient. The interactive registration [19] allows for manual definition and selection of a set of landmarks on the virtual and real view of the patient; the software is then able to register automatically both views from these landmarks. In these approaches, once initial registration has been completed, *the movement of the patient or displacement of the user or of the camera will have to be tracked manually by the user and thus corrected manually or interactively.* In a semiautomatic AR method, the registration remains manual or interactive, *but tracking is automated.* It is typically the case of HoloLens-based methods [24], whereby the HoloLens is able to automatically compute surgeon movements in relation to the patient. Finally, the automatic AR is currently the most developed but also the most complex method [18, 20, 31, 32] to succeed. Registration as well as tracking is here realized automatically via *landmark detection and tracking* on organs. This is achievable due to the ability to reconstruct organ surfaces automatically and in real time.

Fully automatic registration remains a major challenge today and is subject to ongoing research. These challenges are due to the difficulty of obtaining accurate registration in soft tissue surgery. There are three kinds of movements that have to be tracked in real time and compensated for to maintain accurate registration. They are as follows: *(a)* gross patient movement (e.g., the patient sliding laterally off of the operating table), *(b)* local organ movement, due to surgeon interaction, and *(c)* deformation caused by physiological movements (breathing and heartbeat). This leads to inaccuracies of registration and subsequent imprecise overlap of 3D virtual images and real-life images. To overcome such limits, registration must be both rigid and adaptable. Usually, registration is done at the beginning of surgery without taking movement into account (rigid registration). If a single body-wide movement can be solved through new intraoperative registration processes, other movements would require complex algorithms, based on nonrigid (i.e., adaptive) registration.

To solve such a problem, several approaches have been proposed [1, 17]. One of the most developed approaches consists in using intraoperative medical images (US, MRI, or CT), capa-

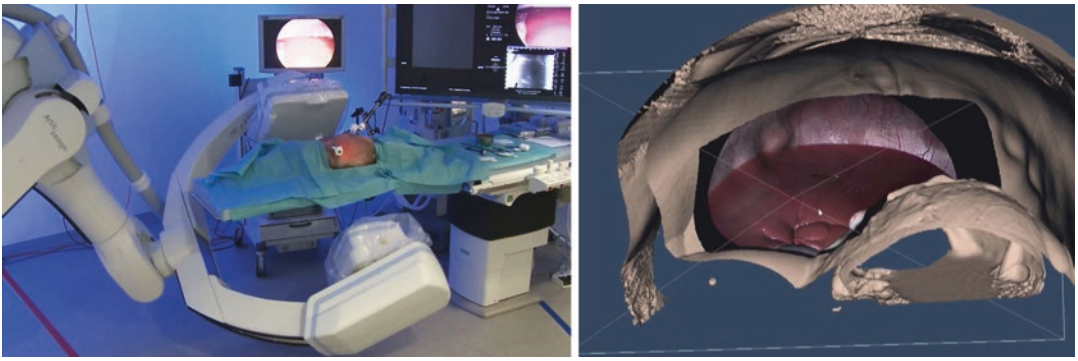

Fig. 18.11 The Dyna-CT images provided by the Artis Zeego (left) allow to detect the laparoscope position in the image and then to register video and medical image (right)

ble of providing the true shape of organs during the surgical procedure. The purpose of using an extra imaging system intraoperatively is *to determine the complete deformation of the region of interest (ROI) between the time of the preoperative acquisition and the intraoperative state of that same area.* This then allows for *nonrigid registration* of the preoperative 3D data onto acquisitions performed intraoperatively [33]. In surgical practice, most of the work is based on intraoperative ultrasonography and MRI [34]. However, one approach seems promising due to the popularization of intraoperative scanners (e.g., CBCT) in so-called "hybrid" operating rooms. Image acquisition from such a system can serve as an intermediary in the registration process between the preoperative scan and the laparoscopic images and can help compensate for the deformation between the preoperative and intraoperative states.

A new paradigm to automatically register the referential frame of the intraoperative model with that of the endoscopic camera, without any external tracking system, has been proposed [35]. *By including the distal part of the endoscope within the intraoperative acquisition field and holding it with an articulated arm, it is possible to estimate the direction of the optical axis and the position of the optical center in the reconstructed volume.* This approach allows one to determine directly the correspondence between the endoscopic camera and the intraoperative scanner (in our experience, the Artis Zeego by Siemens was used) and thus to register data fully automatically (Fig. 18.11).

With intraoperative medical image acquisition and registration (with the intraoperative video view), it remains mandatory to *nonrigidly register* the preoperative 3D modeling of the patient with the intraoperative image in order account for organ deformation. Our previous work [36] proposed an approach that computes nonrigid registration of a preoperative patient model (including abdominal wall, viscera organs, and the liver) using information analysis of an intraoperative image of the patient. The adaptation of this method based on CT scan imaging to Dyna-CT imaging allowed a fully automatic nonrigid registration of preoperative modeling onto the video view of the patient to be obtained [37, 38].

After solving this automatic initial nonrigid registration, the remaining problem consists of correcting in real time this nonrigid registration in order to account for organ deformation – resultant form breathing movement and surgeon interaction. To solve such a problem, our solution consists of a predictive real-time simulation of organ deformation, by tracking tool movement and organ deformation in video images. As we showed for physiological breathing movements [39], *such an approach is feasible by preoperatively modeling the patient, along with his/her physiological movements, and by simulating these movements intraoperatively.* The simulation is controlled by real patient information (skin surface features) tracked and extracted in

Fig. 18.12 Sample of temporal registration from Mountney et al. research work [35] allowing to correct in real-time deformation of the liver due to breathing movement

real time, based on an analysis of video images. At our center, results showed that this solution provides a high level of accuracy. Specifically, ±2 mm accuracy for real-time registration of deformable organs was achieved.

A similar idea can be applied to laparoscopic surgery. Analysis of stereo-laparoscopic video images, replacing the external video image analysis, can be performed. During abdominal surgery, tissue and organs are continuously deforming, and the surgeon is free to move the laparoscopic camera. *The objective of the temporal registration is then to modify the model shape and location of an organ in the same way as the real organ by tracking its deformation and movement in real time* (Fig. 18.12). Several methods have been developed based on real-time virtual surface reconstruction of the organ [40, 41], mechanical modeling of the organ [42, 43], and feature tracking using simultaneous localization and mapping (SLAM) [44]. The resulting precision is currently limited to ± 5 mm, but it will be improved progressively through the addition of patient-specific elasticity and viscosity modeling of organs, owing to advancements in the field of elastography [45].

Benefits of Augmented Reality in Minimal Access Surgery

As delineated in a recent publication that describes the state of the art for AR in laparoscopy [17], it is difficult to compare the outcomes of various AR techniques in the literature for several important reasons. This is a developing field, and therefore standardized algorithms are still under development. There is substantial discrepancy in the algorithms used and discrepancy in the reported registration accuracy (mean value 5.38 mm, range 0.93–10.59 mm). Furthermore, each AR system uses different amounts of user interaction (manual, semiautomatic, or automatic), requiring different levels of human input and skills. There is also inconsistency in the method for measuring accuracy. Some use the registration error on anatomic landmarks (measured in pixels or in 3D space), while others measure AR-guided resection margins. However, all authors indicated that augmented reality provides temporary, precise enough virtual transparency of the patient that can be helpful in determining where the anatomical and pathological structures are located inside the patient. Unlike VR, this AR assistance is today complex and difficult to measure. Notwithstanding, AR has raised high expectations for surgeons. In fact, combined with robot, such an AR system will allow for the automation of complex or repetitive gestures. Major surgical robotic companies are thus currently working on such improvements of their robotic system in order to propose a new generation of surgical robots. But this automation will have to be linked with artificial intelligence in order to provide a real-time retro-control of the robot from the image analysis. It should be the next step of computer-assisted surgery.

Conclusions

We have presented work on computer-assisted minimally invasive surgery based on VR and AR modeling, with real-world case examples. Today, VR techniques are increasingly becoming available and, in select cases, can provide major improvement in the preoperative planning of surgical procedures. AR techniques, although still at an experimental stage, are progressively being tested clinically for minimally invasive surgery, with the objective of using them in routine clinical practice. Initial results show that the system works efficiently but remains limited due to soft tissue deformation which is complex to track. Future solutions will therefore combine predictive simulation and real-time medical image analysis in order to solve these current limitations. To be efficient, patient-specific modeling will have to integrate more information than the geometric model alone. Mechanical properties, functional anatomy, and biological modeling will gradually improve the quality of simulation and prediction which, combined with intraoperative image analysis, will provide the awaited accuracy.

This represents an essential phase for surgical gesture automation, which will allow physicians to reduce surgical errors. Indeed, procedure simulation will allow surgeons to identify the unnecessary or imperfect surgical maneuvers, using it as the blueprint for the actual operation. These maneuvers will then be transmitted to an AI-equipped surgical robotic platform which will be able to precisely reproduce the surgeon's optimized maneuvers. This optimization will be based on AI, the next step of computer-aided surgery.

References

1. Sielhorst T, Feuerstein M, Navab N. Advanced medical displays: a literature review of augmented reality. J Disp Technol. 2008;4(4):451–67.
2. Lima M, Reinberg O, Ruggeri G, de Buys RA, Gargano T, Soler L, Mogiatti M, Cantone N. 3D virtual rendering before laparoscopic partial splenectomy in children. J Pediatr Surg. 2013;48(8):1784–8.
3. Destro F, Maffi M, Gargano T, Ruggeri G, Soler L. Thoracoscopic treatment of congenital malformation of the lung: preliminary experience with preoperative 3D virtual rendering. Lima M, JEMIS. 2013;(1):1–4.
4. Zhu C, Kong S-H, Kim T-H, Park S-H, Ang R, Diana M, Soler L, Suh Y-S, Lee Y-J, Marescaux J, Cao H, Yang H-K. The anatomical configuration of the splenic artery influences suprapancreatic lymph node dissection in laparoscopic gastrectomy: analysis using a 3D volume rendering program. Surg Endosc. 2018;32:3697–705.
5. Soler L, Nicolau S, Pessaux P, Mutter D, Marescaux J. Augmented reality in minimally invasive digestive surgery. In: Lima M, editor. Pediatric digestive surgery. Springer International Publishing Switzerland; 2017. p. 421–32.
6. Soler L, Nicolau S, Pessaux P, Mutter D, Marescaux J. Real-time 3D image reconstruction guidance in liver resection surgery. Hepatobiliary Surg Nutr. 2014;3(2):73–81.
7. Soler L, Mutter D, Pessaux P, Marescaux J. Patient-specific anatomy: the new area of anatomy based on computer science illustrated on liver. J Vis Surg. 2015;1:21.
8. Wang XD, Wang HG, Shi J, Duan WD, Luo Y, Ji WB, Zhang N, Dong JH. Traditional surgical planning of liver surgery is modified by 3D interactive quantitative surgical planning approach: a single-center experience with 305 patients. Hepatobiliary Pancreat Dis Int. 2017;16(3):271–8.
9. He YB, Bai L, Aji T, Jiang Y, Zhao JM, Zhang JH, Shao YM, Liu WY, Wen H. Application of 3D reconstruction for surgical treatment of hepatic alveolar echinococcosis. World J Gastroenterol. 2015;21(35):10200–7.
10. Gossot D, Lutz J, Grigoroiu M, Brian E, Seguin-Givelet A. Thoracoscopic anatomic segmentectomies for lung cancer: technical aspects. J Viz Surg. 2016;2(171):1–8.
11. Le Moal J, Peillon C, Dacher JN, Baste JM. Three-dimensional computed tomography reconstruction for operative planning in robotic segmentectomy: a pilot study. J Thorac Dis. 2018;10(1):196–201.
12. Gossot D, Seguin-Givelet A. Thoracoscopic right S9+10 segmentectomy. J Vis Surg. 2018;4:181.
13. Gossot D, Seguin-Givelet A. Anatomical variations and pitfalls to know during thoracoscopic segmentectomies. J Thorac Dis. 2018;10(Suppl 10):S1134–44.
14. Lachkar AA, Soler L, Diana M, Becmeur F, Marescaux J. Imagen 3D y Urología: Por qué la reconstrucción 3D será obligatoria antes de realizar la cirugía. Arch Esp Urol. 2019;72(3):347–52.
15. Tricard T, Lacreuse I, Louis V, Schneider A, Chaussy Y, Soler L, Moog R, Lang H, Jacqmin D, Becmeur F. Is nephron-sparing surgery relevant for unilateral Wilms tumors? Arch Pediatr. 2017;24(7):650–8.
16. Van Cleynenbreugel B, De Bruyn H, Vos G, Everaerts W, Albersen M, Srirangam SJ. Reduction of warm ischaemia time by preoperative three-dimensional visualisation in robot-assisted partial nephrectomy. Urology: Research and Therapeutics Journal. 2019;2(1):123–33.
17. Bernhardt S, Nicolau SA, Agnus V, Soler L, Doignon C, Marescaux J. The status of augmented reality in laparoscopic surgery as of 2016. Med Image Anal. 2017;37:66–90.
18. Quero G, Lapergola A, Soler L, Shabaz M, Hostettler A, Collins T, Marescaux J, Mutter D, Diana M, Pessaux P. Virtual and augmented reality in oncologic liver surgery. Surg Oncol Clin N Am. 2019;28(1):31–44.

19. Mahvash M, Besharati TL. A novel augmented reality system of image projection for image-guided neurosurgery. Acta Neurochir. 2013;155(5):943–7.
20. Sugimoto M, Yasuda H, Koda K, Suzuki M, Yamazaki M, Tezuka T, Kosugi C, Higuchi R, Watayo Y, Yagawa Y, Uemura S, Tsuchiya H, Azuma T. Image overlay navigation by markerless surface registration in gastrointestinal, hepatobiliary and pancreatic surgery. J Hepatobiliary Pancreat Sci. 2010;17(5):629–36.
21. Watts I, Boulanger P, Kawchuk G. ProjectDR: augmented reality system for displaying medical images directly onto a patient. VRST '17 Proceedings of the 23rd ACM Symposium on Virtual Reality Software and Technology, Gothenburg, Sweden — 8–10 November 2017, N°70.
22. Masamune K, Fichtinger G, Deguet A, Matsuka D, Taylor R. An image overlay system with enhanced reality for percutaneous therapy performed inside CT scanner. 2002, MICCAI 2002, LNCS 2489: 77–84.
23. Rose AS, Kim H, Fuchs H, Frahm JM. Development of augmented-reality applications in otolaryngology-head and neck surgery. Laryngoscope. 2019;129 Suppl 3:S1–S11.
24. Shi L, Luo T, Zhang L, Kang Z, Chen J, Wu F, Luo J. Preliminary use of HoloLens glasses in surgery of liver cancer. Zhong Nan Da Xue Xue Bao Yi Xue Ban. 2018;43(5):500–4.
25. Pessaux P, Diana M, Soler L, Piardi T, Mutter D, Marescaux J. Robotic duodenopancreatectomy assisted with augmented reality and real-time fluorescence guidance. Surg Endosc. 2014;28(8):2493–8.
26. Marescaux J, Diana M, Soler L. Augmented reality and minimally invasive surgery. J GHR. 2013;2(5):555–60.
27. Pessaux P, Soler L, Marzano E, Diana M, Piardi T, Mutter D, Marescaux J. Towards cybernetic surgery: robotic and augmented reality-assisted liver segmentectomy. Langenbeck's Arch Surg. 2015;400(3):381–5.
28. Baste JM, Soldea V, Lachkar S, Rinieri P, Sarsam M, Bottet B, Peillon C. Development of a precision multimodal surgical navigation system for lung robotic segmentectomy. J Thorac Dis. 2018;10(Suppl 10):S1195–204.
29. Hallet J, Soler L, Diana M, Mutter D, Baumert TF, Habersetzer F, Marescaux J, Pessaux P. Trans-thoracic minimally invasive liver resection guided by augmented reality. J Am Coll Surg. 2015;220(5):e55–60.
30. Marescaux J, Rubino F, Arena M, Soler L. Augmented reality assisted laparoscopic adrenalectomy. JAMA. 2004;292(18):2214–5.
31. Bourdel N, Collins T, Pizarro D, Bartoli A, Da Ines D, Perreira B, Canis M. Augmented reality in gynecologic surgery: evaluation of potential benefits for myomectomy in an experimental uterine model. Surg Endosc. 2017;31(1):456–61.
32. Bernhardt S, Nicolau SA, Agnus V, Soler L, Doignon C, Marescaux J. Automatic detection of endoscope in intraoperative CT image: application to AR guidance in laparoscopic surgery. In: IEEE international symposium on biomedical imaging (ISBI 2014). pp. 563–7.
33. Collins T, Pizarro D, Bartoli A, Canis M, Bourdel N. Computer-assisted laparoscopic myomectomy by augmenting the uterus with pre-operative MRI data. In: Mixed and Augmented Reality (ISMAR), 2014 IEEE International Symposium on. IEEE. p. 243–8.
34. Simpson AL, Dumpuri P, Jarnagin WR, Miga MI. Model-assisted image-guided liver surgery using sparse intraoperative data. In: Soft tissue biomechanical modeling for computer assisted surgery. Springer. p. 7–40.
35. Mountney P, Fallert J, Nicolau SA, Soler L, Mewes PW. An augmented reality framework for soft tissue surgery. LNCS. 8673:423–31.
36. Bano J, Hostettler A, Nicolau S, Cotin S, Doignon C, Wu HS, Huang MH, Soler L, Marescaux J. Simulation of pneumoperitoneum for laparoscopic surgery planning. In: Proceedings of MICCAI. 2012. p. 91–8.
37. Bano J, Nicolau SA, Hostettler A, Doignon C, Marescaux J, Soler L. Registration of preoperative liver model for laparoscopic surgery from intraoperative 3d acquisition. In: Augmented reality environments for medical imaging and computer-assisted interventions. Springer Verlag 2014, LNCS 8198. p. 201–10.
38. Bernhardt S, Nicolau SA, Agnus V, Soler L, Doignon C, Marescaux J. Automatic localization of endoscope in intraoperative CT image: a simple approach to augmented reality guidance in laparoscopic surgery. Med Image Anal. 2016;30:130–43.
39. Hostettler A, Nicolau SA, Marescaux J, Soler L. A real-time predictive simulation of abdominal viscera position during quiet free breathing. Prog Biophys Mol Biol. 2010;103(2–3):169–84.
40. Mountney P, Yang GZ. Motion compensated slam for image guided surgery. In: Jiang T, Navab N, Pluim JPW, Viergever MA, editors. MICCAI 2010, Part II. LNCS, vol. 6362. Heidelberg: Springer; 2010. p. 496–504.
41. Mountney P, Fallert J, Nicolau S, Soler L, Mewes PW. An augmented reality framework for soft tissue surgery. Med Image Comput Comput Assist Interv. 2014;17(1):423–31.
42. Haouchine N, Dequidt J, Peterlik I, Kerrien E, Berger MO, Cotin S. Image-guided simulation of heterogeneous tissue deformation for augmented reality during hepatic surgery. In: ISMAR; 2013. p. 199–208.
43. Plantefeve R, Peterlik I, Haouchine N, Cotin S. Patient-specific biomechanical modeling for guidance during minimally-invasive hepatic surgery. Ann Biomed Eng. 2016;44(1):139–53.
44. Mahmoud N, Grasa ÓG, Nicolau SA, Doignon C, Soler L, Marescaux J, Montiel J. On-patient see-through augmented reality based on visual slam. Int J Comput Assist Radiol Surg. 2017;12(1):1–11.
45. Vappou J, Hou G, Marquet F, Shahmirzadi D, Grondin J, Konofagou E. Non-contact, ultrasound-based indentation method for measuring elastic properties of biological tissues using Harmonic Motion Imaging (HMI). Phys Med Biol. 2015;60(7):2853–68.

19 Augmented Cognition in the Operating Room

Roger Daglius Dias, Steven J. Yule, and Marco A. Zenati

Introduction

Recent estimates rank medical errors as the third leading cause of death in the USA, and the majority of the adverse events and errors experienced by hospitalized patients are attributed to surgical care [1]. More importantly, more than half of the adverse events occurring in the operating room (OR) are preventable [2]. Understanding and managing conditions leading to errors is critical to reduce preventable harm to surgical patients [3].

The OR is a complex and dynamic high-risk environment where demands on attention, working memory, and cognitive processing have greatly increased in the last decades, as individuals engage with more data, perform more complex tasks, and exchange a large amount of information. The contribution of human cognition to errors in complex healthcare environments is increasingly being recognized [4]. Many studies have demonstrated a direct relationship between cognitive performance metrics and patient outcomes [5]. Furthermore, suboptimal nontechnical skills, such as teamwork, situational awareness, leadership, and communication, have been implicated in the majority of the adverse events occurring intraoperatively [6].

The practice of surgery entails the use of several elementary and complex cognitive functions, with the ultimate goal of providing high-quality and safe care for patients in the OR. Although cognition underpins virtually all surgical tasks in the OR and is intrinsically associated with surgical outcomes, the efficiency and effectiveness of these processes are not solely a product of the human cognition. In this chapter, we use the conceptual frameworks of *situated cognition* [7], *socio-technical systems* [8], and *distributed cognition* [8, 9], which explain cognition as inherently tied to contexts, transcending the idea of the individual human mind as the sole locus where cognitive functions can take place. In the OR context, cognition is extended outside individual team members' minds toward the entire surgical team, and even further, throughout all human and nonhuman systems involved during surgery. Built upon this paradigm, from individual human cognition to cognitive systems, we discuss the foundations that underlie augmented cognition in the OR, as well as the existing evidence in this realm. Lastly, we

R. D. Dias (✉)
Human Factors & Cognitive Engineering Lab, STRATUS Center for Medical Simulation, Department of Emergency Medicine, Brigham and Women's Hospital, Harvard Medical School, Boston, MA, USA
e-mail: rdias@bwh.harvard.edu

S. J. Yule
STRATUS Center for Medical Simulation, Department of Surgery, Center for Surgery and Public Health, Department of Surgery, Brigham and Women's Hospital, Harvard Medical School, Boston, MA, USA

M. A. Zenati
Department of Surgery, U.S. Department of Veterans Affairs, Brigham and Women's Hospital, Harvard Medical School, Boston, MA, USA

S. Atallah (ed.), *Digital Surgery*, https://doi.org/10.1007/978-3-030-49100-0_19

discuss future implications and applications of cognitive augmentation in the surgical setting.

Cognition and Socio-technical Systems

As with many other complex constructs, in order to comprehend cognition, we need first to define its unit of analysis. Traditionally, the boundaries of cognition are set as the same as individual human minds, in a way that one's cognition finishes at the point where other's cognition starts. Based on this view, cognition is spatially and functionally limited to individual human brains, providing the foundations that explain most of the cognitive processes entailed during individual human tasks [10]. Nevertheless, this framework is not sufficient to explain team-based activities, such as surgery, in which a group of two or more professionals work together and coordinate their tasks to accomplish a common goal. Team cognition is an emergent field that uses systems theory to understand how dynamic configurations and interactions between individuals, subsystems, and the entire system are coordinated to execute various functions. According to this conceptual model, cognition is an emergent team property, delimited by the functional relationships between its elements and not limited to individual team members [11].

In surgery, as in several other high-risk, high-stakes industries (e.g., aviation, oil and gas, space exploration), activities, tasks, and their products are not solely constrained by technical requirements. In fact, under the lens of the socio-technical systems model, surgical teams are inserted into a complex work environment where, in addition to technical performance, social structures, roles, responsibilities, and nontechnical skills (e.g., situational awareness, communication, leadership, teamwork) play a critical role on how well teams will perform and, ultimately, the quality of surgical care rendered [6, 12].

Complex systems, such as cardiac surgery, require teams to perform fast-paced and time-critical tasks. The surgical operative domain is uncertain, complex, and ambiguous and places great demands on the team's cognitive capabilities. Regardless of how competent and expert surgical team members may be, they are still subject to the common cognitive limitations, frailties, and fallibilities that characterize the human brain. In certain situations, high demands imposed by surgical tasks and other factors may exceed the team cognitive capacity, leading to a potentially risky cognitive overload [13].

Built upon the holistic models of team cognition and socio-technical systems, the *distributed cognition* framework [14] extends the cognitive processes entailed in surgery throughout the entire OR, including both human and nonhuman elements in which cognition may take place. Furthermore, this framework conceptualizes cognitive workload and its associated demands and available resources as dynamically distributed among all the cognition elements over the course of surgery [15].

A relevant aspect introduced by the conceptual models discussed above is the fact the ability to carry cognitive processes is not limited to humans. This framework provides the basis for cognition augmentation and can be better comprehended by integrating the fields of knowledge management and information science. According to these fields, data, information, knowledge, and wisdom (DIKW), in this sequence, form a hierarchical model with increased level of processing and understanding from data to wisdom. Basically, *information is processed data, knowledge is processed information, and wisdom is processed knowledge* [10]. Since cognition can be defined as the ability to generate meaning from data, we can now state that not only humans but also machines and computers are entitled to cognition.

Human-Computer Interaction

As computer-based activities become ubiquitous, and our workplace is replete with technology-enabled devices and networks, new types of interaction, communication, and coordination have emerged [9]. Although most of the technological advances achieved in the last decades did improve patient care, they also created new challenges concerning the way in which clinicians interact with computational systems and how these systems are designed and operated.

In fact, the improvement on performance and safety in the OR through technology incorporation comes with the cost of increased complexity. Surgical tasks that once involved only humans now require complex interaction, communication, and coordination between humans and computers. From simple psychomotor tasks to intricate decision-making, computing systems are now embedded into the surgical theater, assisting, supporting, and even acting autonomously [16]. In the same way that a microscope became an essential tool for microsurgical procedures, "magnifying" a surgeon's visual perception with operative devices, such as surgical robots, extends the cognitive capabilities of the surgical team and should be seen as an important element of the OR cognitive system.

Relevant aspects of high-performing teams, such as anticipation, situational awareness, information exchange, and workload allocation, are now investigated in the context of human-machine teaming [17]. There are a growing number of studies investigating the role of robots as active team members in several settings, including healthcare [18].

Nontechnical Skills in Surgery

Nontechnical skills are defined as the cognitive and social skills fundamental to knowledge and expertise in high-demand workplaces. They enable team members to exchange information about their perceptions of ongoing situations (mental models) in order to generate a team-level, shared mental model of understanding, to support error detection, and to share critical information.

Specific frameworks of nontechnical skills exist and have been described in the literature for many professionals. These are commonly centered around a skills taxonomy that is developed specifically for the context and profession being studied. In this sense, "taxonomy" refers to a form of hierarchical grouping of concepts or items that identify, name, and classify items based on shared characteristics. They are used predominantly in the natural sciences, for example, the classifications of organisms and for the periodic table. Nontechnical skills taxonomies arrange groupings of behaviors into ordered categories, often with higher-order categories (e.g., cognitive skills, social skills) explained by lower-level elements of behavior (e.g., gathering information, understanding information).

One example of a widely implemented skills taxonomy is the Nontechnical Skills for Surgeons (NOTSS) system [19], which is used to observe and rate surgeons' behavior in the operating room during both simulated and real procedures. NOTSS is a hierarchical system, comprising categories and elements of nontechnical skills. This is akin to surface and deep features. Refer to Table 19.1 for the NOTSS skills taxonomy, showing the difference between categories and elements.

These behavior marker systems are context-specific, and if high levels of validity are desired, they must be developed for the profession in which they are to be used [20]. For example, the NOTSS system was developed by psychologists, surgeons, and other OR team members and evaluated by panels of consultant surgeons in Scotland and then adapted for implementation in Europe, Australia, North America, Africa, and

Table 19.1 NOTSS taxonomy

	Category	Elements
Cognitive skills	Situation awareness	Gathering information
		Understanding information
		Projecting and anticipating future state
	Decision-making	Considering options
		Selecting and communicating option
		Implementing and reviewing decisions
Social skills	Communication and teamwork	Exchanging information
		Establishing a shared understanding
		Coordinating team activities
	Leadership	Setting and maintaining standards
		Supporting others
		Coping with pressure

Asia. Explicit focus on the skills thought to be relevant for the surgeons from a "bottom-up" perspective is likely more sustainable with greater chance of adoption and buy-in from end users.

A computer-based artificial intelligence (AI) system collaborating as a team member with other humans may alter the nontechnical skill requirements for effective surgical performance. Despite the rise of robotic-assisted surgical systems (e.g., da Vinci surgical systems, intuitive surgical, and other emerging robotic systems such as verb surgical and CMR surgical), the impact on team dynamics and outcomes of these combined human-AI systems are not fully understood. By definition, the human and AI system would perform tasks that are unique and interdependent, with goal attainment only possible by combined efforts (i.e., neither the human nor AI system could achieve tasks alone).

We can speculate that important nontechnical skills for success of these systems could be standard communication protocols, synchronized activities, trust, and cohesion. We know that humans by nature are not entirely predictable and that high functioning team members have high levels of situational awareness and emotional intelligence. The degree to which these human-AI systems will be successful may depend on these variables. Additionally, the adaptive learning nature of the AI team members means that their behavior may not be entirely predictable to the human members. In this context, transparency is another feature that emerges from human-machine cooperativity; studies in communication decision-making in human-robot teams have proposed improvement in team fluency, task performance, and transparency of robot behavior as the pillars and precursors of explainable AI.

Cognitive Workload Monitoring

In order to enable cognitive augmentation, an important aspect to be considered is how we measure different cognitive states overtime. Cognitive workload metrics are widely used for this matter, including during surgical tasks in the OR. Among the several available tools for measurement of cognitive workload in the surgical setting, including self-report questionnaires (e.g., NASA-TLX, SURG-TLX), electroencephalography (EEG), electrodermal conductance, eye-tracking, and near-infrared spectroscopy (fNIRS), *heart rate variability* (HRV) is the most studied method [13]. HRV is established as a sensitive and reliable physiological index of work stress and mental effort [21].

Tools using HRV can be applied in a real time an unobtrusive manner with inexpensive, wearable devices. HRV metrics are based on the analysis of inter-beat intervals (R-R intervals) allowing the quantification of sinoatrial rhythm variability [22]. These HRV variability measures are divided in two broad categories: HRV *frequency*-domain and HRV *time*-domain parameters. Two frequency-domain parameters, *low*-frequency (LF) band and *high*-frequency (HF) band, have been shown to reflect the balance between the sympathetic and parasympathetic autonomic nervous systems. In situations imposing a high cognitive demand, there is a sympathetic predominance, increasing the LF/HF ratio. Other well-established HRV parameters, such as the root mean square of successive differences (RMSSD) and the standard deviation of normal-to-normal (SDNN) inter-beat interval duration, are reflective of parasympathetic control, such that higher cognitive demands decrease these time-domain values. LF/HF ratio, RMSSD, and SDNN have all been used as objective and real-time measures of cognitive workload [23, 24].

Eye movements and changes in pupil dilation provide important information about how users interact with complex visual displays. Both types of data can be obtained by using eye-tracking apparatus that captures eye data in a nearly continuous signal, providing precise information about what the user looks at, how long she/he looks at it, and how much his/her pupils dilate while gaze is maintained. Marshall introduced the Index of Cognitive Activity that allows reliable and rapid estimation of cognitive workload from changes in pupil dilation [25]. Although this approach has been useful in military simulations associated with screen-based tasks under the augmented cognition program funded by the US Department of Defense through DARPA [26], unfortunately it is currently not suitable for intraoperative use in surgery due to its invasiveness and need for continuous screen monitoring and tracking.

The temporal sensitivity and high accuracy of noninvasive brain imaging techniques such as EEG and fNIRS also enable insights into cognitive workload [27]. Both technologies have been used in medical simulation and have demonstrated their utility in this domain but cannot at present be utilized during live surgeries due to their obtrusiveness and physical constraints. While galvanic skin response (GSR) continues to be employed to approximate autonomic nervous system activity by measuring the activity of sweat glands [28], there are practical limitations in collecting GSR data: sensor placements on the fingers and palms, warranting the highest quality signal with a high density of eccrine sweat glands, are unattainable in simulated and live surgeries involving sterile fields.

Automated Assessment of Intraoperative Performance

Currently, the gold standard assessment tools for both technical and nontechnical intraoperative surgical performances are based on observation-based ratings by experts [29, 30]. Although these methods are common practice, several limitations related to post hoc results (i.e., no real-time measures), suboptimal inter-rater reliability, and difficult reproducibility limit these techniques for scalable, real-time cognitive augmentation in the OR.

Computer vision is a branch of artificial intelligence that uses machine learning techniques to gain high-level understanding from digital images or videos. Computer vision applications have been used to recognize and track human activity and even for contextual comprehension. This field may offer unparalleled capabilities for conducting objective and real-time assessments by automatically identifying and tracking clinician activity in the OR [31]. For surgical technical skills, video understanding algorithms have been applied in a number of fields, including industrial robotics, autonomous vehicles, security surveillance, and, more recently, healthcare (e.g., virtual colonoscopies, image acquisition, surgical decision-making). Video understanding may address some of the limitations in traditional mentored or simulation-based approaches for assessing a surgeon's technical skills, including human rater bias and poor scalability. While there has been limited application within the surgical setting, a recent report documented 92.8% accuracy in computer vision's correct identification of steps utilized for sleeve gastrectomy [32]. Prior investigations have documented the reliability of video-based surgical motion analyses for assessing laparoscopic performance in the operating room as compared to the traditional time-intensive, human rater approach [33]. Azari et al. compared expert surgeon's rating assessments to computer-based assessments of technical skills (e.g., suturing, knot tying) including fluidity of motion, tissue handling, and motion economy [34].

For assessment of nontechnical skills, computer vision may be used to assess position, motion, and gestures of surgical team members, providing objective metrics of team dynamics in the OR (e.g., team proximity, team centrality) [35]. These applications may also be used for human factors and ergonomic studies aiming to provide insightful information of surgical team activity for OR space and equipment design. In terms of human-computer interaction in the OR, computer vision applications have been used to create a touchless interface for surgeons, facilitating intangible control of image displays [36].

Surgical Data Science

Surgical data science (SDS) is a new scientific discipline with the objective of improving the quality of interventional healthcare and its value through capturing, organization, analysis, and modeling of data. The goal of SDS is ultimately to improve the value (quality and efficiency) of interventional healthcare [16].

A key element for the SDS field is to establish community metrics and to define what level of reproducibility the field expects for these measures. One way to make such measures and methodologies concrete is to create standardized tools and practices associated with the data (e.g., the JIGSAWS data set). Systematic procedural data collection is currently in its infancy, and large amounts of data, especially in surgery, remain uncaptured. The aviation industry faced a similar crossroads in the 1960s, when the introduction of cockpit voice recorders depended on “the bold support of the airline pilots and the wisdom of the aviation community”; similar buy-in for SDS must occur in the surgical community [37].

Sensor-based data collection and measurement can contribute to initiatives for improving individual, team, unit, and organizational learning in healthcare. For providers, SDS can provide real-time support for clinicians to manage their individual workload efforts and provide feedback on the quantity and quality of interactions with other clinicians. For teams, sensor-based measurement can serve to supplement traditional methods of team improvement, such as clinical team training by providing information on performance patterns and workflow. SDS can automate process mapping to identify bottlenecks in flow or other inefficiencies. Widespread adoption of SDS can provide an analog to aviation’s flight data recorder, allowing playback of real events in simulated environments and sharing generated knowledge [16, 38].

In the context of augmented cognition approaches in the OR, systematic integration of multiple sources of data from both human and machines will be critical. Pertaining to teamwork, SDS can be applied to at least three categories of team outputs: task efficiency, team learning, and effective outcomes. Task efficiency is the most straightforward where sensor-based measurements of teamwork capture reaction times to alerts and alarms. Assessing team learning through sensor-based measurements can include evaluating variability in patterns of effective and ineffective teamwork or changes in more descriptive measures of communication structures. Effective team outcomes, such as staff satisfaction, can be inferred through analyzing patterns of team interaction.

Cognition-Guided Surgery

A consistent body of literature from various fields (e.g., aviation, space, and medicine) has demonstrated that cognitive overload, especially when it arises in the execution of complex processes, leads to deterioration of human performance, increasing the chance of errors [39]. Procedural checklists to guide simulated surgeries proved to be an intervention leading to significantly higher performance outcomes and simultaneously a reduction in errors, when compared to standard practice of completing the procedure by memory. Though notably effective, these checklists were static and agnostic to the context and clinician workload [40].

With the tremendous advances in hardware and software technology that occurred in the last two decades, alongside the scalability of AI and machine learning applications in healthcare, a new interdisciplinary field called *cognition-guided surgery* has emerged [41]. The most important novelty in this field is the ability of developing context-aware systems that not only deliver passive data and information to clinicians but also provide knowledge-based interpretation and prediction of future states. The assistance provided by these cognition-guided systems goes beyond technical and knowledge-based support toward more complex and coordinated human-computer interface, enabling the decrease of human cognitive workload during surgery by alleviating the mental demands imposed by surgical tasks and allocating some cognitive workload to AI agents. These systems fit perfectly into the *distributed cognition* and *situated cognition* models explained earlier in this chapter.

Smart checklists are another example of cognition-guided application in surgery. Previous studies have used detailed process modeling and fault tree analysis to map tasks, subtasks, and process involved during surgery. Based on these models, smart checklists have been developed to guide the surgical team during both routine and unexpected situations (e.g., emergency crisis) in the OR [42].

Conclusions

With the tremendous advances in technology and computational systems that occurred in the last three decades, we have integrated novel technologies in virtually all human activities, with the ultimate goal of improving performance and enhancing safety in the workplace. As a high-stakes, high-risk human activity, with increasing level of complexity, surgery has begun to incorporate computational systems to the clinical workflow in the OR in order to optimize processes and support the surgical team. With the current capabilities of AI, virtual/augmented reality, and wearable sensors, a new era of augmented cognition is gradually being adopted, creating new possibilities and challenges to the OR of the future.

References

1. Makary MA, Daniel M. Medical error—the third leading cause of death in the US. BMJ. 2016;353:i2139.
2. Stefl ME. To err is human: building a safer health system in 1999. Front Health Serv Manag. 2001 Autumn;18(1):1–2.
3. Gawande AA, Zinner MJ, Studdert DM, Brennan TA. Analysis of errors reported by surgeons at three teaching hospitals. Surgery. 2003;133(6):614–21.
4. Zenati MA, Kennedy-Metz L, Dias RD. Cognitive engineering to improve patient safety and outcomes in cardiothoracic surgery. Semin Thorac Cardiovasc Surg [Internet]. 2019. Available from: https://doi.org/10.1053/j.semtcvs.2019.10.011.
5. Patel VL, Kannampallil TG, Shortliffe EH. Role of cognition in generating and mitigating clinical errors. BMJ Qual Saf. 2015;24(7):468–74.
6. Flin R, Youngson GG, Yule S. Enhancing surgical performance: a primer in non-technical skills: CRC Press; Boca Raton, FL. 2015. 223 p.
7. Hutchins E, Palen L. Constructing meaning from space, gesture, and speech [Internet]. In: Discourse, tools and reasoning; 1997. p. 23–40. Available from: https://doi.org/10.1007/978-3-662-03362-3_2.
8. David S, Endicott-Popovsky B. Augmented cognition for socio-technical systems [Internet]. In: Augmented cognition; 2019. p. 133–42. Available from: https://doi.org/10.1007/978-3-030-22419-6_10.
9. Hollan J, Hutchins E, Kirsh D. Distributed cognition: toward a new foundation for human-computer interaction research [Internet]. In: Vol. 7, ACM transactions on computer-human interaction; 2000. p. 174–96. Available from: https://doi.org/10.1145/353485.353487.
10. Fulbright R. Cognitive augmentation metrics using representational information theory [Internet]. In: Augmented cognition. Enhancing cognition and behavior in complex human environments; 2017. p. 36–55. Available from: https://doi.org/10.1007/978-3-319-58625-0_3.
11. Team cognition: Understanding the factors that drive process and performance [Internet]. 2004. Available from: https://doi.org/10.1037/10690-000.
12. Wahr JA, Prager RL, Abernathy JH, Martinez EA, Salas E, Seifert PC, et al. Patient safety in the cardiac operating room: human factors and teamwork [Internet]. Circulation. 2013;128:1139–69. Available from: https://doi.org/10.1161/cir.0b013e3182a38efa.
13. Dias RD, Ngo-Howard MC, Boskovski MT, Zenati MA, Yule SJ. Systematic review of measurement tools to assess surgeons' intraoperative cognitive workload. Br J Surg. 2018;105(5):491–501.
14. Hazlehurst B, Gorman PN, McMullen CK. Distributed cognition: an alternative model of cognition for medical informatics. Int J Med Inform. 2008;77(4):226–34.
15. Hazlehurst B, McMullen CK, Gorman PN. Distributed cognition in the heart room: how situation awareness arises from coordinated communications during cardiac surgery. J Biomed Inform. 2007;40(5):539–51.
16. Maier-Hein L, Vedula SS, Speidel S, Navab N, Kikinis R, Park A, et al. Surgical data science for next-generation interventions. Nat Biomed Eng. 2017;1(9):691–6.
17. Gombolay M, Bair A, Huang C, Shah J. Computational design of mixed-initiative human–robot teaming that considers human factors: situational awareness, workload, and workflow preferences [Internet]. Int J Rob Res. 2017;36:597–617. Available from: https://doi.org/10.1177/0278364916688255.
18. Gombolay M, Yang XJ, Hayes B, Seo N, Liu Z, Wadhwania S, et al. Robotic assistance in the coordination of patient care [Internet]. Int J Rob Res. 2018;37:1300–16. Available from: https://doi.org/10.1177/0278364918778344.
19. Yule S, Flin R, Paterson-Brown S, Maran N, Rowley D. Development of a rating system for surgeons' non-technical skills [Internet]. Med Educ. 2006;40:1098–104. Available from: https://doi.org/10.1111/j.1365-2929.2006.02610.x.
20. Dietz AS, Pronovost PJ, Benson KN, Mendez-Tellez PA, Dwyer C, Wyskiel R, et al. A systematic review of behavioural marker systems in healthcare: what do we know about their attributes, validity and application? [Internet]. BMJ Qual Saf. 2014;23:1031–9. Available from: https://doi.org/10.1136/bmjqs-2013-002457.
21. van Heerden J. A prospective randomized trial on heart rate variability of the surgical team during laparoscopic and conventional sigmoid resection—invited

critique [Internet]. Arch Surg. 2001;136:310. Available from: https://doi.org/10.1001/archsurg.136.3.310.
22. Dias RD, Conboy HM, Gabany JM, Clarke LA, Osterweil LJ, Avrunin GS, et al. Development of an interactive dashboard to analyze cognitive workload of surgical teams during complex procedural care. IEEE Int Interdiscip Conf Cogn Methods Situat Aware Decis Support. 2018;2018:77–82.
23. Avrunin GS, Clarke LA, Conboy HM, Osterweil LJ, Dias RD, Yule SJ, et al. Toward improving surgical outcomes by incorporating cognitive load measurement into process-driven guidance. Softw Eng Healthc Syst SEHS IEEE ACM Int Workshop. 2018;2018:2–9.
24. Kennedy-Metz LR. Evaluation of biofeedback components for the management of acute stress in healthcare [Internet]. Virginia Tech; 2018. Available from: https://vtechworks.lib.vt.edu/handle/10919/86166.
25. Marshall SP. The index of cognitive activity: measuring cognitive workload. In: Proceedings of the IEEE 7th conference on human factors and power plants. 2002. p. 7.
26. St. John M, Kobus DA, Morrison JG, Schmorrow D. Overview of the DARPA augmented cognition technical integration experiment. Int J Hum Comput Interact. 2004;17(2):131–49.
27. Hirshfield LM, Solovey ET, Girouard A, Kebinger J, RJK J, Sassaroli A, et al. Brain measurement for usability testing and adaptive interfaces: an example of uncovering syntactic workload with functional near infrared spectroscopy. In: Proceedings of the SIGCHI conference on human factors in computing systems. New York: ACM; 2009. p. 2185–94. (CHI '09).
28. Das P, Das A, Tibarewala DN, Khasnobish A. Design and development of portable galvanic skin response acquisition and analysis system. In: 2016 international conference on intelligent control power and instrumentation (ICICPI). 2016. p. 127–31.
29. Yule S, Smink DS. Non-technical skills for surgeons: the NOTSS behaviour marker system [Internet]. In: Enhancing surgical performance; 2015. p. 37–60. Available from: https://doi.org/10.1201/b18702-3.
30. Faulkner H, Regehr G, Martin J, Reznick R. Validation of an objective structured assessment of technical skill for surgical residents. Acad Med. 1996;71(12):1363–5.
31. Kadkhodamohammadi A, Gangi A, de Mathelin M, Padoy N. A multi-view RGB-D approach for human pose estimation in operating rooms [Internet]. In: 2017 IEEE winter conference on applications of computer vision (WACV). 2017. Available from: https://doi.org/10.1109/wacv.2017.47.
32. Volkov M, Hashimoto DA, Rosman G, Meireles OR, Rus D. Machine learning and coresets for automated real-time video segmentation of laparoscopic and robot-assisted surgery. In: 2017 IEEE international conference on robotics and automation (ICRA). 2017. p. 754–9.
33. Dosis A, Aggarwal R, Bello F, Moorthy K, Munz Y, Gillies D, et al. Synchronized video and motion analysis for the assessment of procedures in the operating theater. Arch Surg. 2005;140(3):293–9.
34. Azari DP, Frasier LL, Quamme SRP, Greenberg CC, Pugh CM, Greenberg JA, et al. Modeling surgical technical skill using expert assessment for automated computer rating. Ann Surg. 2019;269(3):574–81.
35. Dias RD, Yule SJ, Kennedy-Metz L, Zenati MA. Psychophysiological data and computer vision to assess cognitive load and team dynamics in cardiac surgery. Available from: http://www.ipcai2019.org/pdf/Long_Abstracts/Diaz_etal_IPCAI_2019_Long_Abstract.pdf.
36. Thierfelder N, Wintermantel E, Hagl C, König F. Development of a fully automated testing device for biological, minimal invasive and tissue engineered heart valve prostheses [Internet]. Thorac Cardiovasc Surg. 2015;63. Available from: https://doi.org/10.1055/s-0035-1544364.
37. Goldenberg MG, Jung J, Grantcharov TP. Using data to enhance performance and improve quality and safety in surgery [Internet]. JAMA Surg. 2017;152:972. Available from: https://doi.org/10.1001/jamasurg.2017.2888.
38. Jung JJ, Jüni P, Lebovic G, Grantcharov T. First-year analysis of the operating room black box study. Ann Surg [Internet]. 2018. Available from: https://doi.org/10.1097/SLA.0000000000002863.
39. Ham D-H. Research trends of cognitive systems engineering approaches to human error and accident modelling in complex systems. J Ergon Soc Korea. 2011;30(1):41–53.
40. Arriaga AF, Bader AM, Wong JM, Lipsitz SR, Berry WR, Ziewacz JE, et al. Simulation-based trial of surgical-crisis checklists. N Engl J Med. 2013;368(3):246–53.
41. Kenngott HG, Apitz M, Wagner M, Preukschas AA, Speidel S, Müller-Stich BP. Paradigm shift: cognitive surgery. Innov Surg Sci. 2017;2(3):139–43.
42. Christov SC, Conboy HM, Famigletti N, Avrunin GS, Clarke LA, Osterweil LJ. Smart checklists to improve healthcare outcomes [Internet]. In: Proceedings of the International Workshop on Software Engineering in Healthcare Systems - SEHS '16. 2016. Available from: https://doi.org/10.1145/2897683.2897691

20 Cooperative and Miniature Robotics: Potential Applications in Surgery

Joseph J. Eid and Dmitry Oleynikov

Introduction

Since the 1990s, minimally invasive surgery has seen a rapid progression in development of surgical technologies on both the laparoscopic and robotic platforms. Initially, rigid instruments were inserted into the abdominal cavity to manipulate tissue via small incisions. Currently, minimally invasive surgery includes traditional laparoscopy, robotically assisted laparoscopic surgery, laparoendoscopic single-site (LESS) surgery, and natural orifice transluminal endoscopic surgery (NOTES). These techniques have been associated with less tissue trauma, minimal blood loss, diminished postoperative pain, and faster patient recovery.

The concept of cooperative robotics is currently applied for the observation of multiple stationary and moving targets. This technology has been integrated into surveillance, wildlife research, sports coverage, and search operations before its widespread use in surgical platforms. The simultaneous deployment of such robots helps accomplish a common goal by improving their efficiency and performance. In nonsurgical systems, goal execution is dependent on coordination between the multiple robots themselves and a joint coordination with human operators. In the medical field, various miniature robots have been designed by several bioengineering laboratories to execute specific surgical skills and tasks. At this time, execution is nonautonomous and requires a surgeon-driven collaboration within endoscopic, laparoscopic, or robotic procedures.

The need for cooperation behavior in surgical systems is to enhance human-machine and machine-machine interactions during task delivery while compensating for environmental limitations and interferences. The ultimate goal is to utilize smaller and smaller robots to accomplish complex tasks that could have only been accomplished with large conventional techniques in the past. This may include scenarios in which robots are ingested and are self-assembled to perform specific tasks inside the gastrointestinal tract. We will explore the potential application of such technology in the surgical arena in this chapter.

Cooperative Miniature Robots

Sensing, processing, communication, mobility, and surgical task execution are five main properties essential for cooperative robotic systems. While robots may possess one or more of these functions, in the overall system, some may have a combination of varying functions. For example,

J. J. Eid
Department of Surgery, University of Nebraska Medical Center, Omaha, NE, USA

D. Oleynikov (✉)
Department of Surgery, University of Nebraska Medical Center, Omaha, NE, USA

Virtual Incision Corp, Omaha, NE, USA
e-mail: Dmitry@vitrualincision.com

S. Atallah (ed.), *Digital Surgery*, https://doi.org/10.1007/978-3-030-49100-0_20

while one robot may be responsible for sensing and processing of visual stimuli from the surgical environment, other robots may be responsible for task execution. Currently, cooperation and collaboration of multiple robots is heavily reliant on human operators.

In natural orifice surgery, the utilization of multiple instruments is limited due to the size and complexity of the natural lumen. In vivo porcine models have demonstrated feasibility of multiple miniature robots that would collaboratively participate in improving spatial orientation and providing task assistance. Robots can also be equipped with stereoscopic imaging that would improve depth perception and triangulation between the image plane and the motion of the instruments.

Several miniature robots have been developed for cooperative surgery with various skills. These skills include image acquisition, mobility, luminescence, retraction, and suturing.

Peritoneum-Mounted Imaging Robot Design (Lincoln, Nebraska, USA, Fig. 20.1)

These robots are described peritoneum-mounted devices as part of a cooperative surgical environment. Magnets within the robot and the handles allow for appropriate positioning and panning. A video feedback from surgical targets is provided by the robot's ability to pan and tilt as needed. Designed to meet the needs of the cooperative surgical environment, newer generation robots have integrated LED lighting within their design along with a reduction in their overall diameter.

Mobile Camera Robot Design (Lincoln, Nebraska, USA, Fig. 20.2)

These miniature robots are able to traverse the abdominal cavity using wheels and a steering tail. Adjustable-focus imaging sensors are also integrated within them to provide video feedback to the surgeon. Given their size, they can be inserted into the abdomen using a regular trocar and steered by the surgeon from within.

Lighting Robot Design (Lincoln, Nebraska, USA, Fig. 20.3)

These robots consist of clear outer tubing with multiple LED lights and internal magnets. The magnets are utilized to attach the lighting robot to the outer abdominal wall with the help of an external magnetic handle. Their design also allows them to be inserted intraluminally via a transgastric gastrotomy or intraperitoneally via a regular laparoscopic trocar.

Retraction Robot Design (Lincoln, Nebraska, USA, Fig. 20.4)

These miniature robots are designed for gross tissue manipulation and retraction. They can be

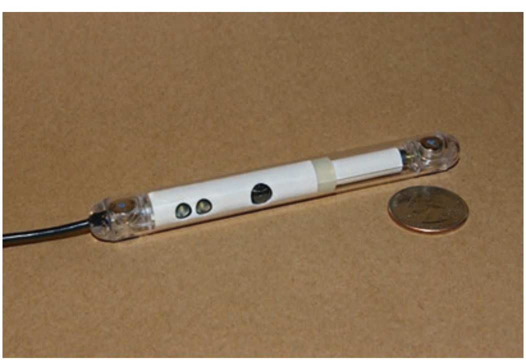

Fig. 20.1 Peritoneum-mounted imaging robot

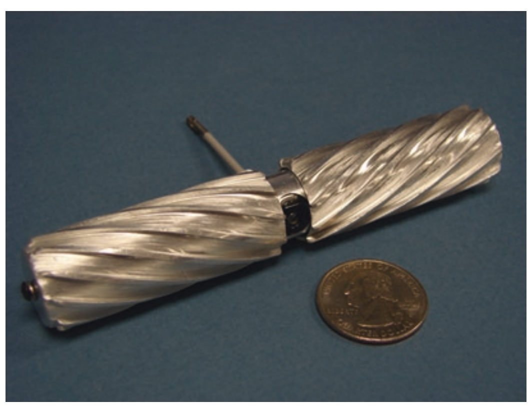

Fig. 20.2 Mobile camera robot

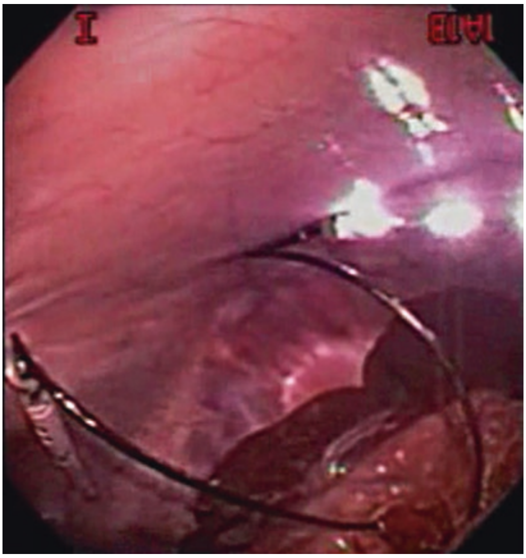

Fig. 20.3 Imaging and lighting miniature robots working cooperatively to provide video feedback of the surgical field to the operator

Fig. 20.4 Mobile retraction robot design

inserted into the human body via a standard laparoscopic trocar or a natural orifice. They may be stationary or mobile. The grasping device is controlled by a drum that winds or unwinds depending on the direction of the rotation. Currently, a laparoscopic or endoscopic device is utilized to direct the gasping device.

In Vivo Dexterous Robot (Lincoln, Nebraska, USA, Fig. 20.5)

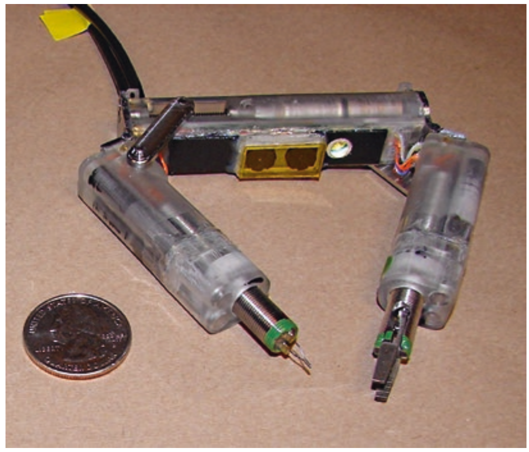

Fig. 20.5 In vivo dexterous robot

The miniature dexterous robot has multiple functions and can be delivered endoscopically into the peritoneal cavity via a gastrostomy. It has the ability to grasp, retract, manipulate, and cauterize tissue. The robot has two arms connected to a central body. The arms are able to rotate in all three dimensions to maximize tissue manipulation and retraction. Each arm is attached to a grasper or a cauterization instrument. All four quadrants of the abdomen can be accessed with this miniature robot. Visual feedback is provided to the surgeon via a standard laparoscope. The robot is controlled remotely from the surgeon's console that includes two controllers, a foot pedal for cautery, and a video feedback display. In a porcine model, this robotic device was able to perform a small bowel dissection and a cholecystectomy. Given the triangulation achieved with this miniature robot, the dynamic grasping arm is able to apply appropriate traction/countertraction to optimize tissue dissection with the cauterizing arm.

Surgical Integration of Multiple Miniature Robotic Devices

Peritoneal-mounted robots have been used to perform a cholecystectomy in a porcine model with the imaging robot being the primary visual feedback provider as opposed to the da Vinci laparoscope. The multiple viewpoints provided by the cooperative robot allowed the surgeon to have a better understanding of the surgical anatomy and environment. In another operation, the peritoneum-mounted robot cooperated with a mobile camera robot and a standard laparoscope. The laparoscope was only used for the initial placement of the peritoneum-mounted and mobile camera robots. The video feedback provided to the surgeon was from both aforementioned cameras. The combined integration of the stationary peritoneal camera and the mobile camera provided a full view of the abdominal cavity and surgical environment. The surgeon was able to drive the mobile camera over bowel and liver without injury to the underlying organs. The overall impact of a combined camera robot approach provided the surgeon with multiple perspectives of the entire peritoneal cavity via a total of three trocar incisions.

In another non-survival porcine model, three miniature robots cooperated in the performance of a NOTES procedure. An endoscope was used to perform a gastrotomy and deliver the robots into the peritoneal cavity. The imaging robots were anchored to the abdominal wall using external magnetic handles. Additional video feedback was provided from a mobile imaging robot. A third robot, the retraction robot, was integral for gross tissue manipulation such as the gallbladder and the small bowel. This procedure demonstrates the ability to integrate multiple miniature robots with traditional laparoscopy to perform procedures.

Limitations and Future Considerations

The increasing integration of cooperative behavior between surgical robots and surgeons can lead to potential risks. This is mainly due to system failures, incorrect analysis of environmental cues, and breaks in communication between robots themselves or between the robots and the operator. Guidelines have been proposed to safeguard human-robot collaboration:

1. Operating surgeons should be in control of all tasks delivered while allowing for transitions in automated functions between robots.
2. Real-time feedback from the surgical field and the robots should be provided to the operating surgeon to allow for evaluation of limitations and functionalities.
3. Continuous interaction with the autonomous robot should be present.
4. Benefits should arise from these interactions to provide efficiency in task execution and work delivered.

Conclusion

The development of well-coordinated and task-specific in vivo robotic devices offers advantages over more traditional transluminal and transabdominal intracavitary surgical environments. *Robots that can cooperate will be able to perform far more complex tasks than a single system.* Swarm robotics is a likely solution for hard-to-reach places such as the intravascular and gastrointestinal environment where route of entry is small and limited. A degree of self-assembly is expected once the robotic systems are deployed. Autonomous and independent task execution has become a reality with the integration and utilization of artificial intelligence algorithms in multiple heterogeneous nonsurgical robotic systems. Further research is being conducted on surgical systems to allow a level of autonomy in surgical task execution and increasing inter-robotic cooperation while maintaining patient safety and good surgical outcomes.

Suggested Reading

1. Khan A, Rinner B, Cavallaro A. Cooperative robots to observe moving targets: review. IEEE Trans Cybern. 2018;48(1):187–98.
2. Lehman AC, Berg KA, Dumpert J, Wood NA, Visty AQ, Rentschler ME, Platt SR, Farritor SM, Oleynikov D. Surgery with cooperative robots. Comput Aided Surg. 2008;13(2):95–105.

3. Tiwari MM, Reynoso JF, Lehman AC, Tsang AW, Farritor SM, Oleynikov D. In vivo miniature robots for natural orifice surgery: state of the art and future perspectives. World J Gastrointest Surg. 2010;2(6):217–23.
4. Zygomalas A, Giokas K, Koutsouris D. In silico investigation of a surgical interface for remote control of modular miniature robots in minimally invasive surgery. Minim Invasive Surg. 2014;2014:307641.
5. Schleer P, Drobinsky S, de la Fuente M, Radermacher K. Toward versatile cooperative surgical robotics: a review and future challenges. Int J Comput Assist Radiol Surg. 2019;14(10):1673–86.

21

Human-Machine Integration and the Evolution of Neuroprostheses

William Kethman and Richard F. ff. Weir

Introduction

It is important to conceptualize this basic fact: The brain acts as the focal point in processing and controlling the sensory and motor functions that allow us to interact with the world. For example, our eyes, ears, and extremities are all "brain-controlled." Through disease and injury, the pathways by which our brain exerts this control are disrupted. The pursuit of restoring function after injury or disease is not new – this is a cornerstone tenet and a fundamental focus of medicine and biomedical engineering sciences. The pursuit of restoring these pathways through brain-machine or peripheral nerve interfaces and allowing individuals to interact with the physical world is in relative infancy. This is the field of *advanced neuroprostheses*.

It is estimated that 1.6 million Americans were living with the loss of a limb in 2005, and it is projected that this number will increase to 3.6 million by 2050 [1]. Of these, more than 500,000 are attributed to upper-limb loss, predominantly caused by trauma. The World Health Organization estimates a far larger burden of disease in the developing world – it is estimated that up to 30 million individuals worldwide are in need of prosthetic or orthotic devices [2]. More broadly, if one considers the potential impact of advanced neuroprosthetic technology in reducing the burden of disease from hearing or vision impairment, over 52 million Americans and vastly more worldwide could potentially benefit from advances in this field [3, 4].

History of Neuroprostheses

The first known prosthetic, dating back to ninth- to sixth-century BC, was discovered in the burial chamber of Sheikh 'Abd el-Qurna in Luxor, Egypt; the great toe of an Egyptian woman was thought to be both cosmetic and functional [5, 6] (Fig. 21.1). From this first prosthetic to the early 1500s, passive prosthetics were demonstrated in use uncommonly – reserved for those who survived the morbidities and mortalities of war-time amputations. It was then that a French army barber-surgeon and early innovator, Ambroise Paré, revolutionized war surgery and care of wounds while developing several artificial upper and lower limbs [7]. These advances in amputation technique and postoperative care led to improved survival and need for prosthetics. These early prosthetics featured locking knee hinges and hand-finger actuation using catches and

W. Kethman (✉)
Department of Surgery, Case Western Reserve University, University Hospitals - Cleveland Medical Center, Cleveland, OH, USA
e-mail: william@kethman.com

R. F. ff. Weir
Biomechatronics Development Laboratory, Department of Bioengineering, College of Engineering, Design, and Computing, University of Colorado - Denver/Anschutz Medical Campus, Aurora, CO, USA

S. Atallah (ed.), *Digital Surgery*, https://doi.org/10.1007/978-3-030-49100-0_21

springs. Some of his early work is, impressively, still in use today in modern prosthetics. These initial prostheses were "body-powered" – advances in design culminated in the development of split-hook upper-extremity body-powered prosthesis in use after World War II [8]. This work and initial designs of traditional cable-lock body-powered prostheses were utilized in conjunction with a surgical technique called *tunnel cineplasty* [9, 10] (Fig. 21.2). Tunnel cineplasty is a surgical procedure where a skin-lined tunnel is formed within the belly of a muscle and a cineplasty pin and control cable are used to manipulate a prosthesis. Mr. Paré's work and those after him are illustrative of the important interplay and reliance that advances in surgical technique have had on this field – a theme especially important in the modern era of neuroprostheses.

Fig. 21.1 Prosthetic toe discovered in Luxor, Egypt, dating to ninth- to sixth-century BC. (©University of Basel, Life Histories of Theban Tombs Project, photographed by Matjaž Kačičnik. Reproduced with permission)

Although debated, Emil du Bois-Reymond is credited with performing the first recording of electrical activity generated by muscles, or electromyography (EMG), in 1849 [11]. It wasn't until 1948, 30 years after the first externally powered prosthesis was developed, that the first myoelectric-controlled prosthesis was demonstrated by Reinhold Reiter in Munich [12, 13]. Despite these accomplishments, myoelectric control was rediscovered in 1962 by Mortensen et al. whom demonstrated voluntary control of a single motor unit in human subjects [14]. This

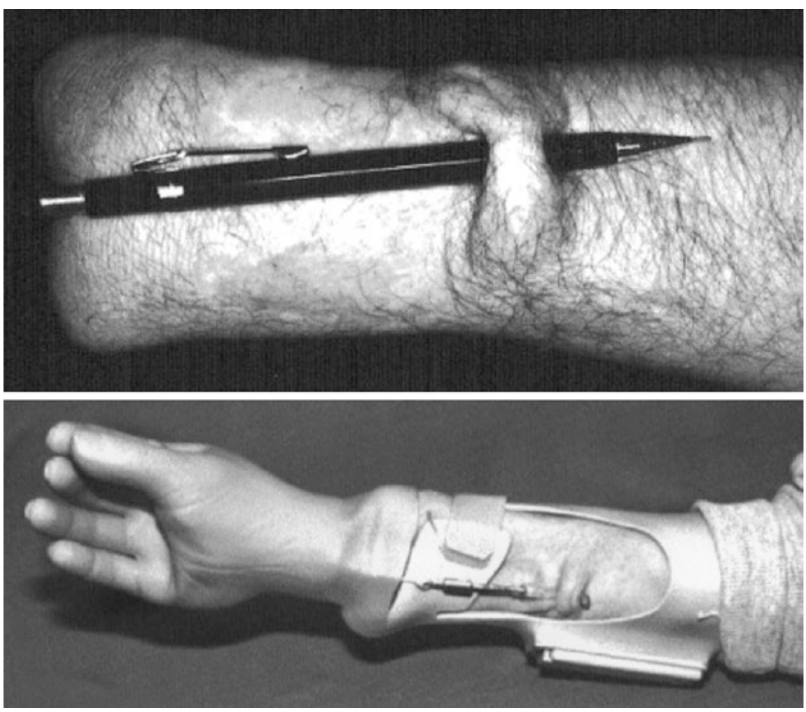

Fig. 21.2 Example of tunnel cineplasty procedure and prosthesis. (Reproduced with permission by Dr. Weir)

Fig. 21.3 Balance between sensor invasiveness and signal specificity for intended use cases

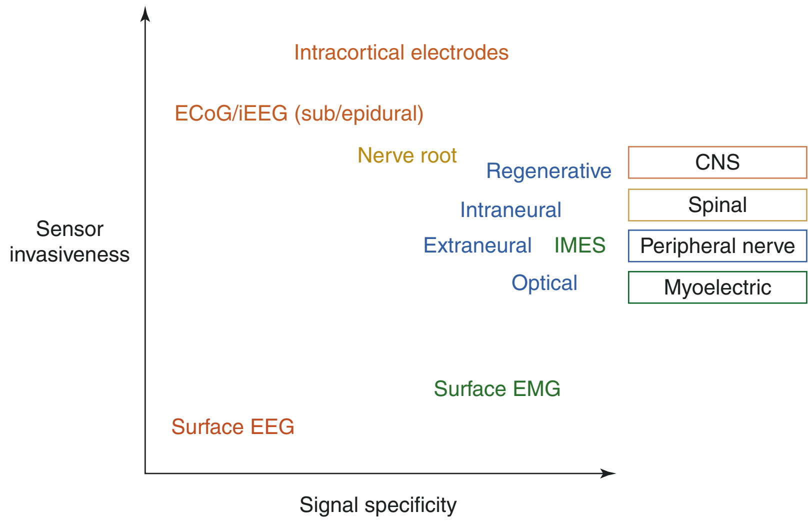

work was advanced by Fetz et al. in 1969 for use in the central nervous system of nonhuman primates. They demonstrated that through conditioning, meaningful cortical-level activity could be recorded and amplified during reinforcement [15]. In 1999, Chapin et al. demonstrated that simultaneous motor cortical recordings in rats could be used to control a robotic arm – this was one of the earliest practical demonstrations of a comprehensive central neural control system – as prior work was largely focused on the development of generic control interfaces [16]. One of the first widespread uses for these technologies to date is in cochlear implants – the first of now over 300,000 implantations worldwide was performed by Djourno and Eyriés in 1957 [17, 18]. These pioneers, among many others, developed the fundamental building blocks of modern neuroprostheses and neural interfaces [19].

Neural Interfaces

A *neural interface* provides a means for transferring data from the nervous system – whether efferent or afferent – to an electromechanical system, such as a prosthetic device or computer system [19]. One of the most humbling and challenging aspects of this field is reliably acquiring and analyzing neural signals over extended period of times due to inherent difficulties in biomechanical coupling. For instance, a transmetacarpal amputee is unlikely to accept the risk of an intracortical neural interface, whereas a surface EMG may lack the specificity necessary for the multi-degree of freedom (DoF) control the patient desires. In order to balance these considerations, numerous efforts are underway targeting a multitude of access points to the central and peripheral nervous system. These efforts exist due to varying levels of neural injury, specificity required for individual applications, and invasiveness by which they are accessed (Fig. 21.3).

Central Nervous System

Injury of the most proximal aspect of the neuronal axis necessitates research and discovery in central nervous system sensing. As with all access points, invasiveness and specificity of approach must be considered. For the purpose of this chapter, we will not review magnetoencephalography, near-infrared spectroscopy, functional magnetic resonance imaging, or other more novel methods and instead focus on those most widely in use currently.

Surface electroencephalography (EEG) is noninvasive, relatively low cost, and generally regarded as a safe method for monitoring and sensing cortical neural activity [20]. Despite these advantages, this method suffers from challenges in longitudinal use, signal integrity, and lack of specificity requiring computationally intensive processing. Efforts by the Defense Advanced Research Projects Agency (DARPA) to encourage development of low-cost, high-quality EEG systems have led to open-source efforts to democratize research and advances in this important field [21, 22].

Intracortical electrodes are regarded as the most invasive means for obtaining neural signals. Kennedy et al. describe a neurotrophic electrode that consists of a glass cone coated with growth factors designed to extend the quality and stability of the electrode over time [23]. This intracortical electrode system, including inductance receiver and radiofrequency transmitters, is implanted subcutaneously and is designed for long-term use. The utility of these intracortical measurements has been demonstrated in patients with brainstem strokes, amyotrophic lateral sclerosis, mitochondrial myopathies, and spinocerebellar degeneration. Wodlinger et al. utilized two 96-electrode microarrays manufactured by Blackrock Microsystems, and advanced signal processing methods have been used to control multi-DOF prosthetics limbs [24]. For some patients, when considering their level of injury or disease characteristics, the risks of intracortical sensor implantation are justified, given the specificity of control that can be achieved.

Peripheral Nervous System

Surface electromyography (sEMG) is a measure of muscle activity from the skin surface generated from propagation of an action potential from peripheral nerves. sEMG is most widely used as a neural interface due to relative signal specificity and lack of invasiveness. Despite these advantages, relatively simplistic signal processing algorithms are currently utilized, and efforts are underway to utilize more complex algorithms to expand the utility of this signal for multi-DoF prosthetics [25–27]. The simplistic signal processing algorithms are utilized because complexity in feature extraction or pattern recognition creates control delay that is often perceived as lack of responsiveness, therefore inhibiting real-time usability [28, 29]. Challenges with the inherent variability of placement of surface electrodes and the computational complexity required of sEMG for multi-DoF applications has led to the development of implantable myoelectric sensors (IMES) and other surgical techniques that enable multi-site sEMG [30] (Fig. 21.4). Different methods employing IMES exist; however, Merrill et al. have demonstrated stability of EMG signals from implanted sensors in both animal and human experiments [31–33]. Long-term animal studies of this method have shown promising signal stability and reproducibility.

Other implantable methods of more directly intercepting neural signals have also been utilized – extraneural, intraneural, and regenerative [34, 35]. Extraneural electrodes surround or apply a small pressure to the peripheral nerve without penetrating or causing injury. Penetrating electrodes, although more sensitive, are plagued by relative rigidity of current electrodes in relation to nerve tissue. This leads to irritation and degeneration of the nerve which limits their long-term application. The most selective direct neural interface is the regenerative electrode designed to allow a transected nerve to grow through a sieve electrode array. The selectivity of this method is attractive, but regenerative electrodes are still under investigation with limited practical use currently.

Challenges experienced in measurement and processing of peripheral neural signals have spawned efforts by surgeons to optimize these biologic signals. These techniques are designed to provide a more reliable, stable, and robust neural input signal. While increasing the number of output signals to enable more complex multi-DoF control. Kuiken et al. developed a technique, targeted muscle reinnervation (TMR), requiring reimplantation and transfer of available peripheral nerves into superficial muscles [36]. This has been demonstrated in individuals who had undergone transhumeral and shoulder disarticulations to control advanced prosthetics developed under the DARPA Revolutionizing Prosthetics program. Gaston et al. employed a

Fig. 21.4 X-ray demonstrating implanted IMES sensors with coil for induction power and wireless data transmission. (Courtesy of Stefan Salminger)

muscle transfer technique in partial hand amputees where the interossei muscles of digits were relocated to the anterior aspect of the metacarpals [37]. This technique enabled more reliable sEMG signals for control of a partial hand prosthetic (Fig. 21.5). Interestingly, these techniques have also been shown to reduce the likelihood of postamputation pain [38]. This mechanism is only partially understood, but it is likely that pain is reduced because residual nerves are engaged actively and have a defined endpoint. This highlights the importance of attention to future rehabilitative options when performing amputations. Partnerships between surgeons, engineers, and researchers are paramount – the combination of advanced electromechanical systems with novel surgical procedures is required for the development of next-generation neuroprostheses.

Integration into the Physical World

Assuming that a reliable and stable interface has been achieved, these signals are then used to control the physical world. Despite advances in prosthetic technology, nearly 23% of such devices are rejected by individuals due to lack of function, durability, and comfort [39]. While durability and comfort are largely dependent on the physical prosthetic design, choice of materials and method for integrating the prosthesis are user-specific. Function is influenced not only by prosthetic design and electromechanical features but also significantly by the number of input commands necessary for use. The increased dexterity of modern prostheses presents unique control challenges that are being solved through innovations in mechanical design, signal analysis, and neural interfaces as previously discussed.

Fig. 21.5 Demonstration of interosseus transfer and use of a myoelectric sEMG partial prosthesis. (Courtesy of OrthoCarolina)

Current prosthesis integration relies on sockets or physical attachments of the prosthesis to the individual's skin and soft tissue. The socket transmits pressure or force from the prosthesis to the individual, representing a key source of discomfort. Adaptive sockets have been developed to intelligently transmit variable forces across the socket during activities as such force is required [40]. These systems improve comfort while delivering a robust practical biomechanical integration.

Osseointegration, or direct coupling of the prosthetic device and user's skeletal system, represents yet another hybrid innovation where novel surgical techniques are paired with technologic advancements. Brånemark et al. have described long-term in-human results of a titanium-implanted two-stage surgical osseointegration, eliminating the need for a prosthetic socket [41]. These methods overcome common challenges with sockets and are thought to increase sensation and prosthetic awareness; nonetheless, additional work is ongoing to reduce infectious complications and improve skeletal remodeling.

Advances in neural interfaces and control systems are fundamentally necessary to achieve complete integration of these systems. However, advances in the design and functionality of prostheses are synergistic and ultimately enable these systems to interact with the physical world. The bebionic® hand (Ottobock, Duderstadt, Germany) is a commercially available, multi-articulating hand with selectable grip patterns to achieve precision control in fine motor tasks [42] (Fig. 21.6). Use of the bebionic® hand has been demonstrated with the use of mechanomyography as a neural control interface [43]. In addition, Mastinu et al. have demonstrated use of Ottobock advanced prostheses with osseo-implantation and epimysial electrode input signals [44]. The SoftHand Pro, inspired by the 19-degree of freedom Pisa/IIT SoftHand, utilizes an adaptive synergy design approach [45, 46]. This multi-DoF hand requires only a single actuator while maximizing function and grasping versatility, inherently simplifying the neural interface required for use. The i-Limb® Quantum (Össur, Reykjavík, Iceland) is a commercially available, multi-articulating prosthetic hand with five individually driven digits [47] (Fig. 21.7). i-Limb® Quantum includes 36 automated grip and grasping functions and anti-drop safety features. It can be controlled with mobile application, muscle, proximity, and gesture inputs to provide freedom of use for individuals. The TASKA (TASKA™ Prosthetics, New Zealand) is a waterproof, commercially available, prosthetic hand with multi-grip functionality and flexible wrist and finger joints [48]. This feature set provides users with a robust system for everyday use.

Under the Revolutionizing Prosthetics program initiated in 2006, DARPA funded The Johns Hopkins University Applied Physics Laboratory (APL) and DEKA Research & Development Corporation [21]. This effort resulted in the development of the APL Modular Prosthetic Limb (MPL) and the DEKA/Life Under Kinetic Evolution (LUKE) arm. The MPL is a modular multilevel upper-extremity prosthesis with up to 26 articulating DoF from the shoulder to the hand [49]. It provides haptic feedback to the user and is controlled with myoelectric inputs utilizing pattern recognition algorithms. The DEKA/LUKE arm is similarly available in transradial, transhumeral, and complete shoulder modular configurations, utilizing ten powered joints with endpoint control for simultaneous joint movements [50, 51]. This system can be uniquely controlled through the multitude of input sensors – EMG, foot movement, mechanical and pressure switches, and linear transducers. The LUKE arm is US Food and Drug Administration (FDA) approved and is commercially available in partnership with Mobius Bionics (Fig. 21.8).

One of the challenges in developing advanced prostheses is defining necessary control inputs and developing algorithms to decode these signals for use in specific applications. Krausz et al. developed a six DoF open-source hand designed as a low-cost research platform as a way to develop and standardize approaches to control algorithms in myoelectric prostheses [45]. The design for this platform is provided open source with a total fabrication and material cost of approximately $3000 – substantially less than commercially available platforms.

Fig. 21.6 ©Ottobock bebionic® multi-articulating modular prosthetic hand. (Courtesy of Ottobock)

Fig. 21.7 i-Limb® Quantum by Össur. (Courtesy of Össur Americas)

Fig. 21.8 LUKE modular prosthetic hand. (Courtesy of Mobius Bionics, LLC)

Opportunities for Discovery

As the applications and uses for neuroprosthetic technology expand, close collaborations between surgeons, researchers, engineers, regulatory and government agencies, and industry are paramount to making them available to those in need. Advances in mechanical, electrical, and computational engineering approaches are aided by combining expertise in biologic systems and surgical techniques to better integrate these systems – expanding their practical use by patients.

References

1. Ziegler-Graham K, MacKenzie EJ, Ephraim PL, Travison TG, Brookmeyer R. Estimating the prevalence of limb loss in the United States: 2005 to 2050. Arch Phys Med Rehabil [Internet]. 2008 Mar [cited 2019 Sep 19];89(3):422–9. Available from: http://www.ncbi.nlm.nih.gov/pubmed/18295618.
2. WHO | Guidelines for Training Personnel in Developing Countries for Prosthetics and Orthotics Services. WHO. 2016.
3. Lin FR, Niparko JK, Ferrucci L. Hearing loss prevalence in the United States. Arch Intern Med. 2011;171(20):1851–2.
4. Vision problems in the U.S. - prevalence of age-related eye disease in America [Internet]. [cited 2019 Sep 22]. Available from: http://www.visionproblemsus.org/index.html.
5. Hernigou P. Ambroise Paré IV: The early history of artificial limbs (from robotic to prostheses). Int Orthop. 2013;37:1195–7.
6. LHTT | Life Histories of Theban Tombs | University of Basel [Internet]. [cited 2019 Sep 22]. Available from: https://lhtt.philhist.unibas.ch/research/toe-prosthesis-from-tt95/.
7. Thurston AJ. Paré and prosthetics: the early history of artificial limbs. ANZ J Surg [Internet]. 2007 Dec [cited 2019 Sep 22];77(12):1114–9. Available from: http://www.ncbi.nlm.nih.gov/pubmed/17973673.
8. Council NR. Terminal research reports on artificial limbs: report of the Committee on Artificial Limbs. 1947. p. 1–100.
9. W SA, Fletcher MJ. Technique of tunnel cineplastic surgery and prosthetic appliances for cineplasty. In: American Academy of Orthopaedic Surgeons instructional course lectures. Ann Arbor: J.W. Edwards; 1953. p. 376–94.
10. Weir RF, Heckathorne CW, Childress DS. Cineplasty as a control input for externally powered prosthetic components. J Rehabil Res Dev [Internet]. [cited 2019 Oct 13];38(4):357–63. Available from: http://www.ncbi.nlm.nih.gov/pubmed/11563487.
11. Du Bois-Reymond E. Untersuchungen über thierische elektricität. Berlin: G. Reimer; 1848. p. 1–743.
12. Ersatzglieder und Arbeitshilfen: Für Kriegsbeschädigte und Unfallverletzte - Moritz Borchardt, Konrad Hartmann, Radike Leymann, Schwiening Schlesinger - Google Books [Internet]. [cited 2019 Oct 13]. Available from: https://books.google.com/books?hl=en&lr=&id=dt3vBgAAQBAJ&oi=fnd&pg=PA822&dq=Ersatzglieder+und+Arbeitshilfen&ots=2Zv-Ekvo-h&sig=Jyg3g8DVGSmu3D73B7eR43BPPmU#v=onepage&q=ErsatzgliederundArbeitshilfen&f=false.
13. Reiter R. Eine Neue Electrokunsthand. 4th ed: Grenzgebite der Medizin; 1948. 133 p.
14. Harrison VF, Mortensen OA. Identification and voluntary control of single motor unit activity in the tibialis anterior muscle. Anat Rec. 1962;144(2):109–16.
15. Fetz EE. Operant conditioning of cortical unit activity. Science (80-). 1969;163(3870):955–8.
16. Chapin JK, Moxon KA, Markowitz RS, Nicolelis MA. Real-time control of a robot arm using simultaneously recorded neurons in the motor cortex. Nat Neurosci [Internet]. 1999 Jul [cited 2019 Sep 22];2(7):664–70. Available from: http://www.ncbi.nlm.nih.gov/pubmed/10404201.
17. Cochlear Implants | NIDCD [Internet]. [cited 2019 Sep 24]. Available from: https://www.nidcd.nih.gov/health/cochlear-implants.
18. Mudry A, Mills M. The early history of the cochlear implant: a retrospective. JAMA Otolaryngol Head Neck Surg [Internet]. 2013 May [cited 2019 Sep 22];139(5):446–53. Available from: http://www.ncbi.nlm.nih.gov/pubmed/23681026.
19. Adewole DO, Serruya MD, Harris JP, Burrell JC, Petrov D, Chen HI, et al. The evolution of neuroprosthetic interfaces. Crit Rev Biomed Eng. 2016;44(1–2):123–52.
20. Mao X, Li M, Li W, Niu L, Xian B, Zeng M, et al. Progress in EEG-based brain robot interaction systems. Comput Intell Neurosci [Internet]. 2017 [cited 2019 Oct 6];2017:1742862. Available from: http://www.ncbi.nlm.nih.gov/pubmed/28484488.
21. Miranda RA, Casebeer WD, Hein AM, Judy JW, Krotkov EP, Laabs TL, et al. DARPA-funded efforts in the development of novel brain-computer interface technologies. J Neurosci Methods [Internet]. 2015 Apr 15 [cited 2019 Sep 19];244:52–67. Available from: http://www.ncbi.nlm.nih.gov/pubmed/25107852.
22. OpenBCI - Open Source Biosensing Tools (EEG, EMG, EKG, and more) [Internet]. [cited 2019 Oct 6]. Available from: https://openbci.com/.
23. Kennedy P, Andreasen D, Bartels J, Ehirim P, Mao H, Velliste M, et al. Making the lifetime connection between brain and machine for restoring and enhancing function. Prog Brain Res [Internet]. 2011 [cited 2019 Sep 19];194:1–25. Available from: http://www.ncbi.nlm.nih.gov/pubmed/21867791.
24. Wodlinger B, Downey JE, Tyler-Kabara EC, Schwartz AB, Boninger ML, Collinger JL. Ten-dimensional anthropomorphic arm control in a human brain-

machine interface: difficulties, solutions, and limitations. J Neural Eng. 2015;12(1):016011.
25. Farina D, Jiang N, Rehbaum H, Holobar A, Graimann B, Dietl H, et al. The extraction of neural information from the surface EMG for the control of upper-limb prostheses: emerging avenues and challenges. IEEE Trans Neural Syst Rehabil Eng [Internet]. 2014 Jul [cited 2019 Sep 19];22(4):797–809. Available from: http://www.ncbi.nlm.nih.gov/pubmed/24760934.
26. Yatsenko D, McDonnall D, Guillory KS. Simultaneous, proportional, multi-axis prosthesis control using multichannel surface EMG. In: Conf Proc. Annu Int Conf IEEE Eng Med Biol Soc IEEE Eng Med Biol Soc Annu Conf [Internet]. 2007 [cited 2019 Sep 19];2007:6134–7. Available from: http://www.ncbi.nlm.nih.gov/pubmed/18003415.
27. Hofmann D, Jiang N, Vujaklija I, Farina D. Bayesian filtering of surface EMG for accurate simultaneous and proportional prosthetic control. IEEE Trans Neural Syst Rehabil Eng [Internet]. 2016 Dec [cited 2019 Aug 4];24(12):1333–41. Available from: http://www.ncbi.nlm.nih.gov/pubmed/26600161.
28. Farrell TR, Weir RF. The optimal controller delay for myoelectric prostheses. IEEE Trans Neural Syst Rehabil Eng. 2007;15(1):111–8.
29. Simon AM, Lock BA, Stubblefield KA. Patient training for functional use of pattern recognition-controlled prostheses. J Prosthetics Orthot. 2012;24(2):56–64.
30. Weir RF ff, Troyk PR, DeMichele GA, Kerns DA, Schorsch JF, Maas H. Implantable myoelectric sensors (IMESs) for intramuscular electromyogram recording. IEEE Trans Biomed Eng [Internet]. 2009 Jan [cited 2019 Oct 15];56(1):159–71. Available from: http://www.ncbi.nlm.nih.gov/pubmed/19224729.
31. Merrill DR, Lockhart J, Troyk PR, Weir RF, Hankin DL. Development of an Implantable Myoelectric Sensor for Advanced Prosthesis Control. Artif Organs [Internet]. 2011 Mar [cited 2019 Aug 4];35(3):249–52. Available from: http://www.ncbi.nlm.nih.gov/pubmed/21371058.
32. McDonnall D, Hiatt S, Smith C, Guillory KS. Implantable multichannel wireless electromyography for prosthesis control. Conf Proc. Annu Int Conf IEEE Eng Med Biol Soc IEEE Eng Med Biol Soc Annu Conf [Internet]. 2012 [cited 2019 Sep 19];2012:1350–3. Available from: http://www.ncbi.nlm.nih.gov/pubmed/23366149.
33. Pasquina PF, Evangelista M, Carvalho AJ, Lockhart J, Griffin S, Nanos G, et al. First-in-man demonstration of a fully implanted myoelectric sensors system to control an advanced electromechanical prosthetic hand. J Neurosci Methods [Internet]. 2015 Apr 15 [cited 2019 Aug 4];244:85–93. Available from: http://www.ncbi.nlm.nih.gov/pubmed/25102286.
34. Schultz AE, Kuiken TA. Neural interfaces for control of upper limb prostheses: the state of the art and future possibilities. PM R. 2011;3(1):55–67.
35. del Valle J, Navarro X. Interfaces with the peripheral nerve for the control of neuroprostheses. Int Rev Neurobiol [Internet]. 2013 [cited 2019 Sep 19];109:63–83. Available from: http://www.ncbi.nlm.nih.gov/pubmed/24093606.
36. Kuiken T. Targeted reinnervation for improved prosthetic function. Phys Med Rehabil Clin N Am [Internet]. 2006 Feb 1 [cited 2019 Aug 4];17(1):1–13. Available from: http://www.ncbi.nlm.nih.gov/pubmed/16517341.
37. Gaston RG, Bracey JW, Tait MA, Loeffler BJ. A novel muscle transfer for independent digital control of a myoelectric Prosthesis: the starfish procedure. J Hand Surg Am [Internet]. 2019 Feb [cited 2019 Sep 19];44(2):163.e1–163.e5. Available from: http://www.ncbi.nlm.nih.gov/pubmed/29908928.
38. Dumanian GA, Potter BK, Mioton LM, Ko JH, Cheesborough JE, Souza JM, et al. Targeted muscle reinnervation treats neuroma and phantom pain in major limb amputees: a randomized clinical trial. Ann Surg [Internet]. 2019 Aug [cited 2019 Oct 24];270(2):238–46. Available from: http://www.ncbi.nlm.nih.gov/pubmed/30371518.
39. Biddiss EA, Chau TT. Upper limb prosthesis use and abandonment: a survey of the last 25 years. Prosthet Orthot Int [Internet]. 2007 Sep 23 [cited 2019 Aug 4];31(3):236–57. Available from: http://www.ncbi.nlm.nih.gov/pubmed/17979010.
40. Shallal C, Li L, Nguyen H, Aronshtein F, Lee SH, Zhu J, et al. An adaptive socket attaches onto residual limb using smart polymers for upper limb prosthesis. IEEE Int Conf Rehabil Robot [Internet]. 2019 [cited 2019 Oct 15];2019:803–8. Available from: http://www.ncbi.nlm.nih.gov/pubmed/31374729.
41. Tsikandylakis G, Berlin Ö, Brånemark R. Implant survival, adverse events, and bone remodeling of osseointegrated percutaneous implants for transhumeral amputees. Clin Orthop Relat Res [Internet]. 2014 Oct [cited 2019 Oct 15];472(10):2947–56. Available from: http://www.ncbi.nlm.nih.gov/pubmed/24879569.
42. Ottobock. bebionic ® Intelligent and precise [Internet]. [cited 2019 Sep 28]. Available from: https://shop.ottobock.us/media/pdf/16297bebionicBrochure.pdf.
43. Wilson S, Vaidyanathan R. Upper-limb prosthetic control using wearable multichannel mechanomyography. In: IEEE international conference on rehabilitation robotics. IEEE Computer Society; 2017. p. 1293–8.
44. Mastinu E, Clemente F, Sassu P, Aszmann O, Brånemark R, Håkansson B, et al. Grip control and motor coordination with implanted and surface electrodes while grasping with an osseointegrated prosthetic hand. [cited 2019 Sep 30]; Available from: https://doi.org/10.1186/s12984-019-0511-2.
45. Godfrey SB, Zhao KD, Theuer A, Catalano MG, Bianchi M, Breighner R, et al. The SoftHand Pro: functional evaluation of a novel, flexible, and robust myoelectric prosthesis. Jan Y-K, editor. PLoS One [Internet]. 2018 Oct 15 [cited 2019 Aug 4];13(10):e0205653. Available from: http://www.ncbi.nlm.nih.gov/pubmed/30321204.
46. Catalano MG, Grioli G, Farnioli E, Serio A, Piazza C, Bicchi A. Adaptive synergies for the design and

control of the Pisa/IIT SoftHand. Int J Robot Res. 2014;33(5):768–82.
47. i-Limb Quantum [Internet]. [cited 2019 Oct 9]. Available from: https://www.ossur.com/prosthetic-solutions/products/touch-solutions/i-limb-quantum.
48. TASKA Prosthetics | Doing More Builds Confidence [Internet]. [cited 2019 Sep 28]. Available from: http://www.taskaprosthetics.com/
49. Perry BN, Moran CW, Armiger RS, Pasquina PF, Vandersea JW, Tsao JW. Initial clinical evaluation of the modular prosthetic limb. Front Neurol [Internet]. 2018 Mar 19 [cited 2019 Sep 30];9:153. Available from: http://www.ncbi.nlm.nih.gov/pubmed/29615956.
50. Cowley J, Resnik L, Wilken J, Smurr Walters L, Gates D. Movement quality of conventional prostheses and the DEKA Arm during everyday tasks. Prosthetics Orthot Int. 2017;41(1):33–40.
51. Resnik L, Klinger SL, Etter K. The DEKA Arm: its features, functionality, and evolution during the Veterans Affairs Study to optimize the DEKA Arm. Prosthet Orthot Int [Internet]. 2014 Dec [cited 2019 Sep 28];38(6):492–504. Available from: http://www.ncbi.nlm.nih.gov/pubmed/24150930.

22 Nonlinear Robotics in Surgery

Deborah Keller, Sam Atallah, Rithvik Seela, Barbara Seeliger, and Eduardo Parra-Davila

Introduction

The purpose for robotics in surgery has evolved over time (Fig. 22.1). It was once a project focused on achieving tele-manipulation using master-slave design (i.e., telesurgery). The most important potential application was providing a surgeon the ability to operate on patients in isolated or hostile regions. The archetypal example being a wounded soldier requiring surgical intervention at a remote battlefield. After telesurgery was achieved in 2001 [1, 2], robotics in surgery and the advancements thereof were continued and became highly refined. For 20 years, only one kind of surgical robotic system was able to penetrate the surgical market and civilian operating theaters. This was the da Vinci Surgical System (Intuitive Surgical, Inc., Sunnyvale, CA, USA), for which surgeons have employed to carry out more than six million procedures worldwide [3].

The da Vinci family of straight-arm robots (*S*, *Si*, *Xi*) was found to be quite suitable for specific types of operations. Perhaps the best application has been the radical prostatectomy. The reason for this is that the gland is difficult to access with conventional laparoscopy, and some aspects, such as suturing of the bladder-urethral anastomosis, are greatly facilitated by the stable da Vinci platform through tremor cancelation, 3D magnification, and gravity-compensating, true wrist effector arms [4–7]. Additionally, the organ lies in a fixed anatomic field, so that once the robotic cart is docked, a surgeon can complete the operation without time-consuming repositioning and re-docking. Likely for the same reasons, gynecologists have been drawn toward robotics as a platform suitable for minimally invasive hysterectomy [8, 9]; many in training have exhibited the phenomena of "leapfrogging" over laparoscopy and adopting robotics without a laparoscopic foundation, leaving some physicians to conclude that perhaps robotics has enabled patients to ultimately have greater access to minimally invasive surgery.

By 2020, nearly every surgical specialist, from cardiothoracic, to colorectal, to foregut

D. Keller
Department of Surgery, Columbia University Medical Center, New York, NY, USA

S. Atallah (✉)
College of Medicine, University of Central Florida, Orlando, FL, USA
e-mail: atallah@post.harvard.edu

R. Seela
Department of Economics, Stanford University, Palo Alto, CA, USA

B. Seeliger
Institute of Image-Guided Surgery, IHU Strasbourg; Research Institute Against Digestive Cancer, IRCAD, Strasbourg, Alsace, France

E. Parra-Davila
Colorectal and General Surgery, Good Samaritan Medical Center, West Palm Beach, FL, USA

S. Atallah (ed.), *Digital Surgery*, https://doi.org/10.1007/978-3-030-49100-0_22

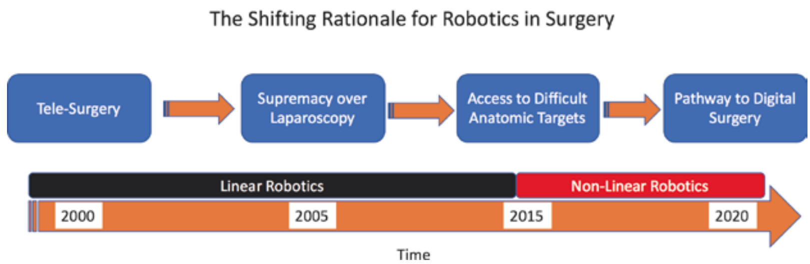

Fig. 22.1 An evolution of *purpose*. As robotic platforms evolve, so too has the rationale for their use in surgical disciplines. The idea of telesurgery was the original foundation for master-slave instrumentation. As surgical robots became commercialized, advocates of the systems focused (for the most part, unsuccessfully) on trying to demonstrate supremacy over its rival minimally invasive approach, laparoscopy. But a newfound focus for robotics in surgery has shifted attention toward accessing difficult anatomic targets and efforts made to design systems for specific routes of access. Ultimately, the future of robotics in surgery will meld advancements in artificial intelligence and machine learning to provide a pathway to digital surgery

surgeon, has gained substantial experience with the da Vinci linear-armed family of robotic platforms to carry out a variety of operations, including some which are considered highly complex, such as the Whipple operation [10–12]. To justify the platform's higher cost, users argue that the improved visualization and instrumentation, even in the absence of haptic feedback, delivers superior quality, although this has not been consistently supported by clinical trials [13]. Nowadays, most comparisons of robotic surgery are directly against laparoscopic surgery. While laparoscopists and robotic surgeons are eager to demonstrate that the MIS technique they use is the better option, both groups of surgeons have been largely unsuccessful. Nevertheless, market pressures have created a fierce and competitive environment whereby patients, surgeons, and referring physicians may seek surgical care with robotic assistance because of a perception that higher technology equates to better surgery.

Focused on the competitive nature of laparoscopy versus robotics, it has been common to hear the expression "anything that can be done with a laparoscope can also be done with a robot." While this generalization is essentially valid, the importance of this comparison is becoming passé as the next frontier in robotics will draw aim in a new direction. There are important differences between laparoscopy and robotics (Table 22.1) that will likely lead to the progression of robotics and the stagnation of laparoscopy.

One important aspect is the evolution of nonlinear mesoscale robotic instrumentation, which is being designed with the objective of reaching difficult anatomic targets. These targets include the oropharynx, the respiratory tree, the vascular tree, and the alimentary tract. In this chapter, we will explore the expanding role of nonlinear robotic systems. Through a flexible design, robotics can provide a pathway to access difficult anatomic targets. Furthermore, as specialization continues, robots are not only being designed with "general-purpose" flexible effector arms, but as we shall see, they are being designed *for specific organ systems* that have posed a formidable challenge for minimally invasive surgeons to date.

Current and Prospective Anatomic Targets for Nonlinear Robots

Current targets
- Digestive tract (hindgut)
- Oropharynx
- Cardiovascular system
- Pulmonary system
- Urinary system (including ureter)

Prospective and future targets
- Biliary tree
- Digestive tract (foregut and midgut)
- Central nervous system
- Female reproductive system (uterus, fallopian tube, and ovary)

Table 22.1 General differences between robotics and laparoscopy

Laparoscopic surgery	Robotic surgery
Basic handheld instruments	Tele-manipulated instruments
2D vision is the standard	3D vision is the standard
Good haptic feedback	Poor haptic feedback
Surgeon physical "work" is uncompensated	Gravity-compensating instrumentation reduces surgeon physical workload
Surgeon at bedside	Surgeon at console (most)
Less suited for digital surgery	Well suited for digital surgery
Limited flexible instruments, manually controlled	High dexterity of straight instruments, wristed motion; nonlinear instruments evolving
Poor access to hard to reach anatomic targets	Good access to hard to reach anatomic targets
Endoluminal surgery possible but limited range (TAMIS)	Endoluminal surgery possible with expanding role of nonlinear robots
Must maintain "straight" line of sight for effector arm entry point to target	With nonlinear systems, there is no line of sight requirement
The bronchus, oropharynx, esophagus, and colon are not accessible	With nonlinear systems, the bronchus, oropharynx, and colon can be accessed
Designed for abdominal and thoracic access	Emerging systems designed specifically for an organ or difficult to reach body cavity
	Example: Monarch™ (Auris Health) pulmonary surgery; Flex® robot (Medrobotics Inc.) for TORS/TARS

Robotics for the Oropharynx

Robotic Transoral Surgery with Linear Systems

While classical robotics with multi-arm linear instruments have been used for transoral surgery [14–20], the approach is limited by reach and specifically the inability to follow the circuitous path of the deep oral cavity and oropharynx. Despite limitations, transoral robotic surgery (TORS) has progressed substantially over the last decade. The first preclinical demonstration of feasibility was performed in 2005 in a canine model [14]. Although shown to be feasible and safe for head and neck surgery [19], questions have been raised about its "teachability" [21]. With advanced skill and appropriate setup, conventional TORS surgeons have suggested that "almost any" oropharynx lesion and many supraglottic and hypoglossal lesions can be resected so long as proper instrument triangulation is assured. Weinstein et al. [17] have been successful at achieving resection with negative margins on a series of 27 patients with T1–T3 cancer of the tonsil with the aid of specialized retractors used to gain access to the oral cavity. Despite the relative success and uptake of classical TORS utilizing the multi-arm da Vinci Surgical System (FDA approved for TORS in 2009), this system was never designed for small body cavity surgery, especially for cavities which require nonlinear points of access for effector arms.

Recognizing the need to have specific robotic systems to address curve-linear anatomic targets such as the oropharynx, two newer nonlinear surgical robots have been successfully utilized for TORS, namely, the (a) da Vinci Single Port (SP) and the (b) Flex® Robotic System.

da Vinci SP Surgical Robotic System for Oropharyngeal Surgery

While, as discussed, the classical da Vinci Surgical System had been successfully used for TORS, head and neck robotic surgeons recognized that there were inherent limitations to this approach. Notably, the linear (rigid) instrument design restricted line-of-sight access, and only two working arms could be used. Furthermore, it is difficult to "cram" three working arms into such a confined workspace. In 2010, the da Vinci *Single Port* (*SP*) Robotic System was introduced into clinical practice on trial, and soon the nonlinear robotic device was explored for TORS initially in a preclinical setting [22–24]. Tateya et al. compared the da Vinci *Si* to the da Vinci *SP* in a cadaveric model and concluded that access was improved with the *SP* variant, in particular for access along the esophageal inlet and the piriform sinus, as well as for facilitating dissection during hypopharyngectomy [25]. Using a single-boom design, three nonlinear 6 mm robotic instruments (each with seven degrees of freedom), as well as a flexible 3D camera head, can be deployed via a 2.5 cm cannula, creating an ultra-low-profile surgical system capable of improved reach in the oropharyngeal cavity (Fig. 22.2). The flexible design is meant to mirror the wrist and elbow joints of human extremities. It allows access to the oral cavity, nasopharynx, hypopharynx, and larynx.

In 2019, Chan et al. reported clinical outcomes on the use of the da Vinci *SP* system for 21 patients undergoing TORS for both benign and malignant neoplasia [26]. Targets included the tonsil and base of the tongue, the nasopharynx, the hypopharynx, and the larynx. In patients undergoing excision for malignancy (principally squamous cell carcinoma), the margins were all negative. In this prospective phase II clinical trial conducted in Hong Kong, the authors concluded that the da Vinci *SP* was both safe and feasible for TORS for the targets mentioned [26].

Flex® Robotic System for Oropharyngeal Surgery

The Flex® Robotic System (Medrobotics Corp., Raynham, MA, USA) is a semi-robotic nonlinear apparatus (Fig. 22.3) which has been designed specifically for two anatomic areas. Namely, the system has been designed to target the oropharynx and, subsequently, the distal colon and rectum. The device was first introduced in Europe, where it has had reasonably good uptake for specific ENT applications [23, 27–31]. The Flex® Robotic System was designed to overcome the challenge of access to target anatomy [29]. Matheis et al. examined clinical outcomes of the first 40 ENT patients treated using the Flex® robot for TORS [29]. Anatomic regions accessed included the oropharynx (35%), hypopharynx (25%), and supraglottic larynx (40%). With an average setup time of 12.4 min (decreasing to a mean of 9 min after the first 20 cases), the majority of anatomic targets were successfully

Fig. 22.2 The da Vinci *SP* Surgical Robotic System is shown. The system deploys three working arms (6 mm dia. each) as well as a stereoscopic 0° camera head via a 2.5 cm cannula. The camera and instrument effector arms have both elbow and wrist flexibility; the system is prototypical for nonlinear robotics in surgery. Such a framework is suited for access to difficult anatomic targets that demand systems which can follow a curved pathway

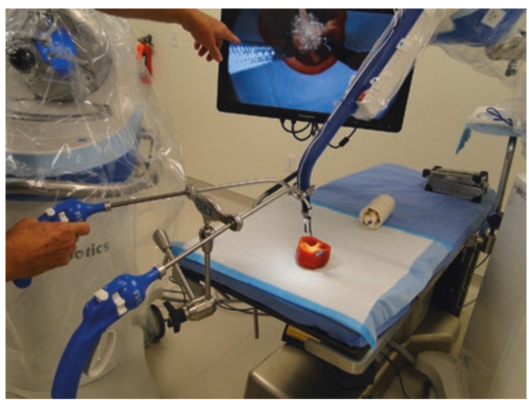

Fig. 22.3 The Flex® Robotic Surgical System is illustrated in a dry laboratory setting. The system (here with the configuration used for oropharyngeal surgery) is designed *specifically* for transanal and transoral access. The two 3.5 mm curve-linear instruments are delivered by laparoscopic-type flexible tip effectors, which are stabilized by a bedrail mounted arm, and are operated by the surgeon, not at a console, but rather at the patient's bedside. The only part of the platform with robotization is the camera head, which is driven with a steering knob (photo, upper left) to the target with a maximum of 17 cm range. The flexible design is intended to improve reach and provide a stable surgical platform for TORS and TARS

reached – but not all of them. Specifically, the Flex® Robotic System was not successful at biopsy for 2 out of 11 intended oropharyngeal targets. For 29 patients undergoing resection, conversion to other means was required in two cases. After the first 40 clinical cases, the authors concluded that the curve-linear robotic platform was safe and feasible for TORS citing excellent "visualization, maneuverability, and tactile feedback" (the latter an advantage which is lacking with da Vinci) [29].

Lang et al. [27] reported outcomes of a European multicenter single-arm study to assess the Flex Robotic System for TORS. Upon evaluating 80 clinical cases (79 of whom were treated in the study protocol), adequate visualization of 94% of anatomic targets was achieved. Of the 75 targets visualized, surgical treatment was completed in 72 (96%) with a mean operative time of 41 min. The most frequently reached target was the base of the tongue, followed by the epiglottis and piriform sinus. In addition to the ease of use and enhanced visualization, the authors believed that there was value in the system's portability relative to the da Vinci Surgical System [27]. Nevertheless, there are limitations of the Flex® robot, including some effector arm lag time and jitter. With only two effector arms (neither of which are robotic) and a cumbersome, slow-driving camera head, the true advantage of the system for ENT applications is the curve-linear platform which allows access to deeper oropharyngeal targets.

Transanal Robotics for the Colon and Rectum

Next-generation robots with flexible design have been explored for their potential application toward (a) oropharyngeal surgery and (b) transanal surgery essentially in tandem. The two body space cavities pose special challenges of access for surgeons which can be ameliorated by the use of properly designed robots. An important similarity between the two disciplines is that targets must be accessed via a natural orifice. Thus, nonlinear systems, with proven feasibility for TORS, have also been shown to be effective for transanal robotic surgery (TARS), albeit with some modification to allow for CO_2 insufflation (not required for TORS) so as to distend the rectal lumen or, in the case of transanal total mesorectal excision (taTME), distend the actualized space within the pelvic outlet. Nevertheless, nonlinear systems for TARS were predicated upon a decade of progress forged with conventional robotic- and laparoscopic-based transanal techniques. This is briefly reviewed in the next section.

Robotic Transanal Surgery with Linear Systems

The prequel to nonlinear robotics for transanal surgery began with a series of developments which occurred in relative rapid succession. First, in 2009, transanal minimally invasive surgery (TAMIS) was introduced [32] as a method of operating within the rectal lumen that carried forward the concept and technique of transanal endoscopic microsurgery (TEM) introduced by Gerhard Buess in 1984 [33]. As the TAMIS platform evolved, it became clear that it could be used as an interface for linear robotic systems. Namely, robotic TAMIS was shown to be successful at first utilizing the da Vinci *S* system in a cadaveric model in 2011 [34] and subsequently for use with the *Si* clinically for local excision of rectal neoplasia [35], followed by more advanced applications, such as robotic taTME [36, 37]. Global experience continues to grow [38–40], especially with the evolution of the da Vinci *Xi* system, since it possesses low-profile arms which are able to more easily negotiate the narrow space. Investigators have also used various patient positions including lateral decubitus, prone jackknife, and dorsal lithotomy to improve point of access and to facilitate docking. Despite advancements in the linear family of da Vinci robotic platforms, these master-slave systems were not designed specifically for transanal access. Even for surgeons experienced with TARS (i.e., robotic TAMIS), docking remains arduous, and the ability to maneuver within the confined rectal lumen can be extremely limited.

While it can be possible to reach targets to the level of the peritoneal reflection, working beyond this point is cumbersome and often requires exchanges of the left and right working arms. Furthermore, while the more advanced *Xi* has slim arms, at the time of this writing, it lacks 5 mm instrument capabilities (as available on *Si*) making it more difficult to maneuver within the rectal lumen or actualized pelvic space, since instrument clashing is increased. TARS surgeons have noted that the larger the effector arm diameter (8 mm for *Xi*), the greater the operative view becomes restricted. For these reasons, robotic colorectal surgeons with expertise in this application agree that in order for TARS to evolve, further advancement in the robotic platform would be required. While laparoscopic-based techniques including taTME and TAMIS remain highly useful, robotic, console-control surgery is probably the best paradigm for the evolution toward information-centric digital surgery, including navigation [41, 42].

Flex® Robotic System for Transanal Surgery

With the success observed with TORS, the Flex® Robotic System was retooled for transanal access for TARS, specifically with the aim of providing colorectal surgeons with higher reach to conduct more advanced procedures. Retooling required (a) a special disposable, single-use gasket and seal; (b) a bedrail-mounted metal, reusable access channel; and (c) insufflation adaptable to AirSeal (ConMed Inc.). In May 2017, the Flex® robot was granted FDA approval for transanal use, and the feasibility of the system as a semi-robotic platform for local excision of rectal neoplasia (Fig. 22.4) as well as transanal total mesorectal excision (taTME) has since been assessed in cadaveric models and in clinical cases, on trial [43–45]. Thus, the Flex® robot (with its specialized colorectal drive) was the first robotic platform to be *specifically* designed for transanal surgery.

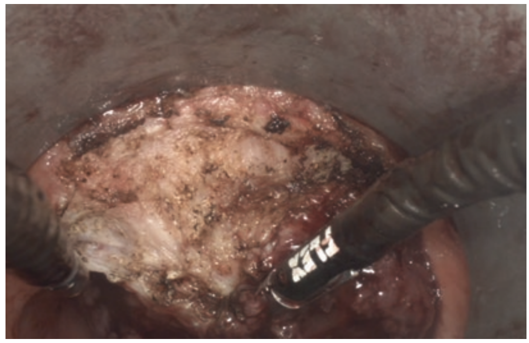

Fig. 22.4 The Flex® Robotic Surgical System, here being used for the excision of a pT1 anterior rectal cancer in a female patient (on trial). The device has also been utilized clinically as a platform for transanal total mesorectal excision. The bedside-operated flexible effector arms allow for potentially improved triangulation. The modification to the Flex® system utilizes a special colorectal drive which includes a single-use seal adaptable to a (reusable) metal, bedrail-mounted rigid access channel. An additional modification provides for the pneumatic delivery of CO_2 necessary for transanal – but not transoral – surgery

In 2017, initial cadaveric experience with the system showing feasibility for both local excision and taTME was reported [43]. It was noted that the Flex® Robotic System's greatest advantage when compared to TEM and TAMIS was that it provided the potential for higher reach along a curve-linear route, thus providing a pathway for "newfound access via the transanal route" [43]. Ultimately, the objective of this curve-linear robotic platform would be to obtain operative access beyond the ~15 cm limit of TEM and TAMIS. It was further proposed that such a nonlinear robotic system could be considered for other so-called "direct target" natural orifice transluminal endoscopic surgery (NOTES) operations (i.e., those in which the viscerotomy is part of the planned procedure and *not* created in a bystander organ) [46]. This included applications for transvaginal hysterectomy, salpingo-oophorectomy using the technique of vaginal access minimally invasive surgery (VAMIS) [44, 47–49], and – in theory – transcecal appendectomy [44].

In 2019, Carmichael et al. [45] reported on their experience with taTME in a series of six male and female cadaveric models (with and, in some cases, without abdominal laparoscopic assistance). The investigators simulated mid and low rectal lesions. Interestingly, in experiments in which distal rectal lesions were simulated ($n = 2$), maneuverability was limited – since the effector arms were in close proximity to the access channel and thus the taTME dissection was not possible in these cases. This was true, despite the high flexibility of the two effector arms (i.e., 85° of motion in any direction). The authors concluded that while the platform was safe and allowed access up to 17 cm, it was not suitable, in its current design, for the surgical treatment of distal rectal pathology [45]. With some potential redesigning, the Flex® Robot System could add significant value for advanced transanal procedures. This would require robotization of the effector arms, achieving a reach that is twice as far as the current system, and solving other technical challenges of the Flex® robot, such as suturing. The latter is an aspect of the system which is much less important for ENT applications, because most ENT procedures are ablations, biopsies, and tumor excisions which do not require suture closure of defects as is sometimes required for colorectal excision of neoplasia – in particular, those proximal to the peritoneal reflection.

da Vinci SP Surgical Robotic System for Transanal Surgery

While the concept of using the da Vinci *SP* for transanal access has been explored for at least 5 years, this specific application is still awaiting FDA approval for clinical use for colorectal surgery. There are important differences and similarities between the da Vinci *SP* and the Flex® Robotic System (Table 22.2). The system requires an interface for transanal access, and a TAMIS-based platform is typically utilized (e.g., GelPOINT Path Transanal Access Platform, Applied Medical Inc., Rancho Santa Margarita, CA). In a cadaveric model, John Marks (Pennsylvania) has reported preliminary out-

Table 22.2 A comparison of the Flex® robot versus the da Vinci Surgical System for TORS and for TARS

Characteristic	da Vinci *Si*/*Xi*	Flex® Robotic	da Vinci *SP*
Platform	Multi-arm robotic system commonly with TAMIS access channel *or* glove port using *Options: Si* or *Xi* da Vinci Surgical System	Flex® Robotic System with colorectal (CR) drive; 28 mm dia., used in conjunction with specialized reusable access channel	Single port; 25 mm dia. system, commonly used with TAMIS access channel
Access channel	Disposable, TAMIS channel, most commonly GelPOINT path transanal access platform Alternatives: *Glove port*, *custom port* bedrail mounted, reusable with hybrid 80 mm GelPOINT faceplate, developed by Marcos Gomez, MD	Flex® Robotic access channel; metal, reusable bedrail mounted diameter 40 mm, length 45 mm or 100 mm	Disposable, TAMIS channel, most commonly GelPOINT path transanal access platform dia. 34 mm, length 44 mm
Effectors and configuration	*Si:* 2 × 5 mm rigid effector arms with 8 mm 30° (up/down lens), Maryland Grasper, hook cautery *Xi:* 2 × 8 mm rigid effector arms, 8 mm 30° (up/down lens), Maryland Grasper, hook cautery of scissors	2 × flexible 3.5 mm instruments; 0° HD lens. Platform disposable, flexible instruments, and access channel reusable	3 × flexible (elbow and wrist) 6 mm instruments, 0° “cobra” (two-joint, flexible) camera – with instrument navigation

(continued)

Table 22.2 (continued)

Characteristic	da Vinci *Si/Xi*	Flex® Robotic	da Vinci *SP*
Optics	3D 30° or 0° HD	2D or 3D 0° HD	3D 0° HD
Effector arm navigation	No	No	Yes
Pneumatics	AirSeal® iFS, PneumoClear, or other commercial systems	AirSeal® iFS, PneumoClear, or other commercial systems	AirSeal® iFS, PneumoClear, or other commercial systems
Patient position for transanal access	Dorsal lithotomy/ Lloyd-Davies	Dorsal lithotomy/ Lloyd-Davies	Dorsal lithotomy/ Lloyd-Davies
Surgeon	At console (assistant for suction, bedside)	At bedside (no assistant)	At console (assistant for suction, beside)
Designed specifically for TORS	No	Yes	No
Design specifically for transanal access	No	Yes	No
FDA status for transanal access	Approved (transanal access is off-label use of device)	Approved	Not yet approved for colorectal use
FDA status for TORS	Approved in 2009	Approved	Approved (for some types of procedures)
Potential advantages	3D vision; tremor cancelation; magnified view; surgeon controls camera at console; semi- (5 mm) or fully (8 mm) wristed instruments; most experience with TORS and transanal procedures	Flexibility allows transmission of platform along circuitous anatomic pathways; single surgeon; robotic camera drive; all effector arm flexion in view of camera lens; 85° of flexion; instruments are never outside of camera view	Three flexible effector arms instead of two; 3D vision; tremor cancelation; magnified view; surgeon controls camera at console; unique "cobra camera"; instrument flexion allows higher reach potentially
Potential disadvantages	Platform cost, difficulty dissecting beyond 7–8 cm from verge due to sacral angulation and instrument torque; 8 mm instruments add bulk and subtract from field view; 5 mm effectors not avail. on *Xi* platform; relies on TAMIS port for transanal access which adds to cost; instrument arm collision	Redefining operative field of view is time intensive; robotic camera and platform movement system use separate module; occasional effector arm jitter and lag time; non-robotic instruments; surgeon at bedside; only two working arms; no easy way to suture; suction irrigation difficult	Platform cost; flexion can occur "behind camera lens" making it more difficult to understand the position of the effector arms; relatively large workspace needed (volume of tennis ball, ~ 150cm^3); no robotic vessel sealer available; relies on TAMIS port for transanal access which adds to cost

TORS transoral robotic surgery, *TARS* transanal robotic surgery, *TAMIS* transanal minimally invasive surgery; PneumoClear: smoke evacuation and TAMIS mode insufflation (Stryker, Inc.); AirSeal® iFS: valveless trocar system and smoke evacuation system (ConMed Inc.); ISB: insufflation stabilization bag (Applied Medical Inc.); SILS™ Port: single-incision laparoscopic surgery (TAMIS port, Covidien-Medtronic)

comes of the da Vinci *SP* for local excision of simulated rectal neoplasia, as well as for segmental "sleeve" excision with robotic sutured anastomosis, demonstrating clear feasibility of complex endoluminal tasks [50]. On trial, Simon Ng (Hong Kong) has explored the use of the da Vinci *SP* for both transabdominal and transanal applications (Fig. 22.5), including the successful performance of the first human taTME (unpublished report). Recently, select clinical test centers in the USA have utilized the *SP* for various colorectal applications in humans (on trial, with IRB

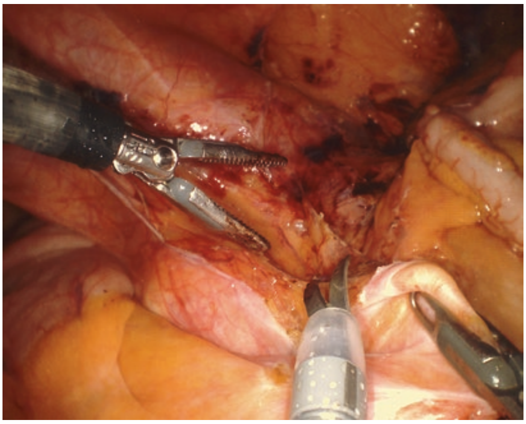

Fig. 22.5 The ability to use the da Vinci *SP* Surgical System for colorectal surgery, including natural orifice and transanal access, is being explored clinically. In this still-frame photograph courtesy of Simon Ng, MD, the *SP* robot is being used to perform a partial colectomy. The three curve-linear instruments and "cobra" 0° stereoscopic camera are delivered through a single incision, allowing a surgeon to operate while minimizing abdominal wall access trauma and, at the same time, preserving the ability to triangulate instruments

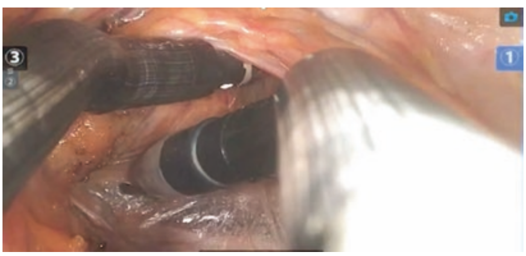

Fig. 22.6 The da Vinci *SP* surgical platform being used to perform transanal total mesorectal excision in a cadaveric model. The posterior dissection is being performed. Unlike with standard TAMIS and TEM, the surgeon has the ability to control a third arm (not shown) to retract and to help actualize the limited workspace beneath the pelvic inlet. The nonlinear effector arms may provide higher reach, allowing surgeons to achieve more dissection from below, with a longer rendezvous period that can improve abdominal-transanal surgeon cooperativity

approval), including transanal operations (Fig. 22.6). While clinical outcomes and initial results for transanal use remain to be reported, it is believed that the nonlinear access could improve transanal reach, mirroring the improved access of the *SP* observed by ENT surgeons with TORS [38].

Further Directions and Innovations

Recently, the idea of operating robotically in two body space cavities simultaneously, with cooperative synchronicity, has been explored utilizing a singular (but modular) robotic system in combination with two surgeons operating from separate workstations. Specifically, this has been investigated for the taTME operation which requires both abdominal and pelvic access. While there are limitations with using the da Vinci Surgical System for this dual-field application [51], it has been shown to be successful in a cadaveric model utilizing the Versius surgical robotic system (CMR Surgical, Cambridge, United Kingdom) [52]. The idea of robotic operation in two fields simultaneously for specific, complex operations carries potential advantages. Specifically, while conserving robotic-grade vision, precision, and motion, it is possible to (a) reduce surgeon workload, (b) decrease overall operative time, and (c) improve operative efficiency. In this way, the patient benefits because quality of surgery improves, and healthcare systems benefit as the capital and maintenance costs are partially absorbed by reducing costly theater time [53].

The next steps for two-field robotic surgery for complex cases may require further advancement of surgical systems with a focus on computerization of robotic platforms (Fig. 22.7). Future advancements may include hybrid modifications, including the combined use of linear and nonlinear systems, which is an area of ongoing research. It is not difficult to envision systems that involve, in the example of taTME, operation utilizing a nonlinear robotic component from below while, from above, using linear robotic components under separate control. Future advances may one day include centralization of the human resources. For example, the surgeons may be in one or more centralized regions allowing for combined surgery to patients in remote locations. Thus, surgeons in different geographic areas could ultimately perform complex two-field surgery cooperatively on a patient residing in a remote geographic region, expanding the reach of global surgery and crossing the fundamental divide of distance (Fig. 22.8). As artificial intelligence

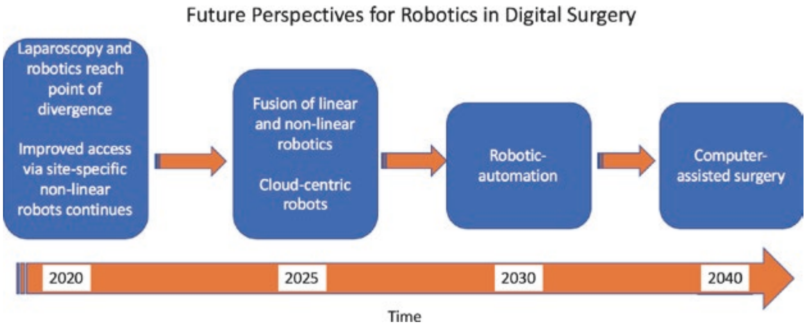

Fig. 22.7 How robotics in surgery are poised to evolve over the coming decades. Robotics and laparoscopy are becoming increasingly divergent, and by 2020, it will become clear that robotic-based surgical platforms, including nonlinear- and continuum-based systems, will be able to provide access to anatomic targets which straight laparoscopic systems will be unable to reach. As the power of nonlinear systems is realized, for some applications, a combined linear and nonlinear robotic system could emerge. At the same time, cloud robotics will become more prevalent, allowing for a stable artificial intelligence platform and for more rapid machine learning. This, in turn, will lead to automated systems and will eventually give rise to computer-assisted surgery

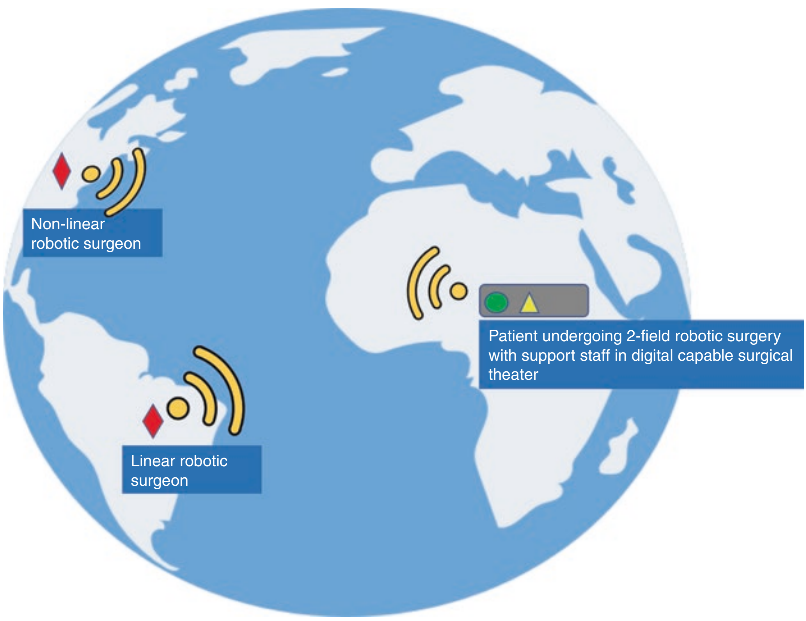

Fig. 22.8 The globalization of surgery requires a democratization of patient access to surgical specialists and the creation of a technological bridge that spans a geographic divide. In the future, consider as an example a framework in which a patient and appropriately equipped robotic operating theater (with surgical support staff) are placed in an underserved location. Suppose the patient requires expertise that is available only in South America and North America. In this construct, two surgeons, working at separate centralized centers, would be able to perform surgery on a patient who requires complex, two-field surgery – such as transanal total mesorectal excision. Hypothetically, the transanal robotic surgeon could use a nonlinear robotic telesurgery in conjunction with the abdominal robotic tele-surgeon using a linear system

becomes integrated into next-generation vision and sensor steering robots, the reliability and reproducibility will improve, allowing a global access to otherwise highly specialized procedures [3]. For operations such as taTME, where *extreme* expertise is required for the transanal portion of the operation [54–56], it would benefit patients to have an expert high-volume surgeon perform this portion of the operation. In the future, such a framework would democratize patient access to surgery.

Robotic Bronchoscopy and Pulmonary Navigation

Based on 2012 data, lung cancer accounts for 19.4% of total cancer deaths worldwide, making it an important global healthcare challenge [57] – even affecting never smokers at age-adjusted rates similar to the incidence of myeloma in men and cervical or thyroid cancer in women aged 40–79 [58]. Early detection, especially by obtaining confirmatory histopathology, can improve clinical outcomes [59]. Due to the curve-linear, branching architecture of the bronchial tree and due the often subcentimetric size of potentially significant pulmonary nodules – especially those in the periphery – access to lesions can be particularly arduous for clinicians. Bronchoscopy for biopsy of mass lesions of the lung parenchyma and respiratory tree can be achieved in a variety of methods. This includes CT-guided biopsy and thoracoscopic approaches; but when these methods are used, there is increased morbidity when compared to the bronchoscopic approach (22.5% vs 2.2%) [60, 61].

Navigated bronchoscopy [62–66] equips the tip of the flexible scope with an electromagnetic tracker. Because the electromagnetic tracker is registered to a patient's pre-procedure CT scan, the tip's position can be determined on imaging in real time during the procedure. One such device – the superDimension™ Navigation System (formally superDimension Ltd., Herzliya, Israel, now Medtronic Inc.) – was shown in 2003 to be feasible in a swine model by Schwarz et al. [64]. However, in clinical practice, the system has had variable diagnostic yield [67].

There are different ways to digitally track a nonlinear device as it is navigated through the bronchi toward a target, including bronchial bifurcation recognition, lumen center localization, centerline pathway tracking, or image correlations [68–71]. However, according to Sganga et al., these techniques are imperfect because they make assumptions about airway geometry and because there are image artifacts that make interpretation challenging as well [72]. The authors instead developed "OffsetNet" – which is the first-of-its-kind deep learning for localization of lung using rendered images. For conserved regions of lung parenchyma, OffsetNet is able to track the bronchoscopic motion with an average position error of 1.4 mm [72]. The deep learning for localization does require training on recorded camera images as well as simulated images to improve performance and bronchoscope tracking. The tracking of the bronchoscope could be coupled with a so-called autonomous agent (i.e., robotic instrumentation) which can use and interpret the information to self-drive the scope toward an anatomic target of interest without reliance on human manipulation.

Today, a number of flexible systems have been developed for lung nodule biopsy with navigation, including the superDimension system (previously described), the bronchoscopic transparenchymal nodule access (BTPNA) using the Archimedes System (Broncus Medical) [73], CrossCountry™ transbronchial access tool (Medtronic) [74, 75], thin convex probe endobronchial ultrasound [76], and electromagnetic-guided transthoracic needle aspiration (EMTTNA) [77, 78].

More recently, in March 2018, the Monarch™ System (Auris Health, Redwood City, CA, USA) received FDA clearance as a robotic, navigated bronchoscopic platform (Fig. 22.9) [79–81]. It is based on a robotically propelled outer sheath with <6 mm dia. as well as an inner telescoping endoscope with dia. measuring 4.4. mm [78], both of which are steerable in four directions, thus allowing for instrument tip pitch and yaw to allow maneuverability at almost any angle (Fig. 22.10) [79]. The system is somewhat complex, and in addition to two robotic arms, the Monarch System uses two interconnected computer systems, a non-real-time computer *and* a real-time computer. Other components include fluidics control, an electromagnetic field generator, and reference electromagnetic sensors [79].

Fig. 22.9 The Monarch™ System (Auris Health) is illustrated. It utilizes two robotic arms and gains bronchial access via the oral route. An interventionalist uses a handheld control box that resembles a gaming console. The device is used to navigate the continuum robotic tip toward its target (photo courtesy of Auris Health, with permission)

Fig. 22.10 The Monarch™ System (Auris Health) is shown in a dry lab model, demonstrating how it is able to navigate narrow passages, even when the angles approach 90°. It is based on a robotically propelled outer sheath with <6 mm dia. as well as an inner telescoping endoscope with dia. measuring 4.4. mm, both of which are steerable in four directions, thus allowing for instrument tip pitch and yaw to be remotely controlled (photo courtesy of Auris Health, with permission)

The bronchoscope is driven robotically by rotary pulleys. Pathways to the target can be planned and computed, providing the clinician with a safe route to arrive at the target lesion (Fig. 22.11). An external electromagnetic field generator is used for navigation and tracking. The potential advantage of robotic systems includes improved control, stability, and access to the periphery, with improved diagnostic yield of target pathology.

There are emerging nonlinear soft robotic systems that have not yet been introduced into clinical practice (pending 510(k) approval), including the Ion™ platform[1] developed by Intuitive Surgical Inc. [78]. The new systems will all combine the advantages of robotics with navigation, creating a fusion of technology that is useful to clinicians and surgeons. This ultimately allows for improved diagnostic yield for otherwise difficult parenchymal targets while maintaining a low morbidity profile. Next steps for navigated robotic bronchoscopy may include translation of this technology to other difficult to access targets beyond the respiratory tree, for example, the alimentary tract. One could envision a system that utilizes navigated robotic colonoscopy to localize colonic targets for biopsy, excision, and ablation.

[1] FDA clearance for Ion in February 2019: https://isrg.intuitive.com/news-releases/news-release-details/u-s-fda-grants-clearance-ion-intuitive/

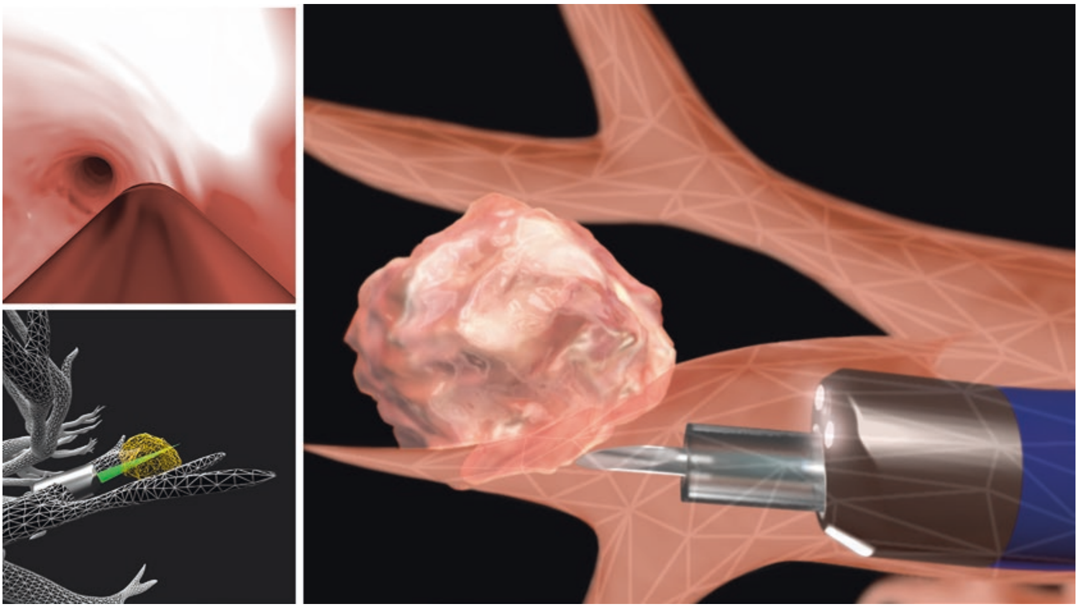

Fig. 22.11 The Monarch™ System (Auris Health) is a fusion of soft robotic technology and navigation technology. The system uses electromagnetic navigation and a robotic steerable robotic system to arrive at the anatomic target. The bronchoscope is driven robotically by rotary pulleys. Pathways to the target can be planned and computed, providing the clinician with a safe route to arrive at the target lesion. Such a design allows it to be used for biopsy of peripheral lesions, obviating the need for invasive procedures, including thoracoscopic surgery (photo courtesy of Auris Health, with permission)

Nonlinear Robotics in Vascular Surgery

The cardiovascular system poses a number of challenges which make access by surgical instruments using conventional minimally invasive techniques nearly impossible. The constant flow of blood and millimetric vessel diameter make endovascular visualization via conventional fiber-optic scopes impractical and frankly unimaginable. Nevertheless, with the aid of live intraoperative roentgenography, wire-guided therapy has found important applications in medicine, especially for stenting and transluminal thrombectomy [82–84]. Such surgical interventions could be integrated with robotics – which could improve wire steering and overall precision and control.

Beyar et al. originally described the technique of performing percutaneous coronary interventions utilizing a remote controlled robotic platform for precision [85]. In the Percutaneous Robotically Enhanced Coronary Intervention (PRECISE) study reported in 2013 by Weisz et al., the safety and feasibility of a robotic-assisted nonlinear platform were validated [86]. In the same year that the PRECISE study was published, the ability to apply flexible robotics to navigate iliofemoral arteries was assessed [87], and this device, developed by Hansen Medical, would serve as a springboard for the launch of Auris Health's Monarch™ System used for flexible endobronchial applications (refer to previous section).

Recently, using "haptic vision" and a millimeter-scale camera and LED, feasibility of camera access within the cardiovascular tree was demonstrated [88]. "Haptic vision" is based on the concept of thigmotaxis, used by insects and some animals to "navigate." Most classically, this is by "wall following" – whereby insects perform thigmotactic navigation by crawling along the edge of a wall to create awareness of the environment. Contacting an object (such as a wall) in the environment is termed *positive* thigmotaxis [89–93]. This is similar to finding your way in pitch-black darkness by feeling (contacting) a wall and following it. Just as your mind can create a “map” and a perception of space within a given surrounding based on feel, so can a robot. Thus, haptic vision, a term coined by Fagogenis et al., allows a robot to construct a map of the environment based on its surroundings and, for example, the cardiac wall it is in contact with to determine the position of target anatomy [88].

Nonlinear Robotics in Urology

da Vinci SP for Urologic Applications

Interest in minimizing the morbidity associated with multiple incisions led to descriptions of single-site laparoscopic procedures for urology. However, technical challenges secondary to restricted linear instrument triangulation, poor ergonomics, and a need for specialized, curvelinear instruments limited the wider adoption of single-incision laparoscopic technology for urology – and for other fields. In May of 2018, the da Vinci Single Port (*SP*) system was approved by the FDA for use in urologic surgery. The *SP* platform achieves a single point of access through one skin/fascial incision. Through this, a port and expanded palette of nonlinear surgical implements are deployed and maneuvered with 360° capability. This improves upon the known benefits of conventional robotic platforms (i.e., precise maneuverability, tremor cancellation, and 3DHD magnified visualization) by adding curvelinear instruments that theoretically enhance access to out-of-reach anatomic targets (all via a minimal abdominal wall incision). Hence, the da Vinci *SP* specifically addresses the limitation of surgeon access to the confined working space in the pelvis. It maintains intracorporeal triangulation while eliminating instrument clashing. In retroperitoneal procedures, the *SP* platform has the ability to access both anterior and posterior tumors with its unique configuration. The transperineal access could be advantageous for both cystectomy and prostatectomy in patients with prior surgery or pelvic radiation. The transvesical access for prostatectomy could avoid risks inherent to intraperitoneal access, pneumoperitoneum induction, and extreme positioning.

The *SP* platform was trialed in cadaveric models, where it proved the ability to operate within a small operative radius, and such trials deemed the platform most appropriate for robotic radical prostatectomy, robotic cystectomy, and intracorporeal ileal conduit construction with pelvic lymph node dissection [94–96]. After the feasibility studies in cadavers and following FDA approval, select trial centers have created an initial body of clinical evidence supporting the use of the da Vinci *SP* for urologic applications. The *SP* has since expanded the scope of procedures for urology, demonstrating feasibility for performing ureteroneocystostomy, radical prostatectomy, partial and radical nephrectomy, radical cystectomy, pyeloplasty, radical prostatectomy, and ureteral reimplantation – as well as other urologic reconstructive surgeries for the ureters, bladder, and kidneys [97–101]. Results to date show similar intraoperative complication rates, operative times, and postoperative outcomes, comparable to multi-port robotic urologic operations. However, these studies should be interpreted with caution. The results represent a small number of series encompassing a heterogenous range of operations from experienced, high-volume robotic surgeons with small sample sizes. Long-term oncological results and larger series are required, as well as additional follow-up, before determining the true benefit of the *SP* platform for general urologic applications.

Robotic Ureteroscopy

Robotic ureteroscopy is an emerging technology that seeks to facilitate procedures within the urinary tract using a nonlinear scope. Relevant studies have primarily tested the Avicenna Roboflex (Fig. 22.12), a flexible robotic ureteroscopic (fURS) device, for ease of use and ergonomic benefits. Rassweiler et al. [102] and Saglam et al. [103] found that this robotic system resulted in

Fig. 22.12 Avicenna Roboflex (ELMED™ Medical Systems Company, Orlando, FL, USA) is a flexible robotic ureteroscope. The master-slave device allows precise scope control and can perform all tasks performed with conventional ureteroscopy. It is operated by a urologist seated at a workstation (shown) that includes dual joysticks with scope drive controls. Proponents of the devices believe it is useful for lithotripsy, enhancing stone fragmentation and dusting. It may also reduce operator fatigue due to improved ergonomics, and at the same time, physician exposure to ionizing radiation is minimized. (Photo provided with permission and courtesy of ELMED™ Medical Systems Company)

significant increases in physician efficiency. Geavlete et al. concluded that treatment of kidney stones could be achieved successfully with robotic tools [104]. Proietti et al. evaluated the physician training process, discovering that individuals without prior surgical experience could swiftly acquire necessary operating skills [105]. Although further development and evaluation of these robotic systems might be necessary, these studies indicate a hopeful future for robotic ureteroscopy.

Robotic Neurosurgery

Linear Systems

The first known use of robotics in neurosurgery surprisingly predated the modern era of robotics in minimally invasive surgery and was reported in the mid-1980s [106]. Today, a multitude of systems have been trialed, some more successful than others [107–118] (Table 22.3). While each of these robots is somewhat unique, they share important similarities, including a rigid, linear effector arm design. In addition, most neurologic robotic surgical systems have been loosely modeled after the master-slave designs or robots used for minimally invasive, keyhole surgery.

However, there are important differences in abdominal versus cranial anatomy that prevent the translation of techniques and instrumentation successfully into the field of neurosurgery. For example, with abdominal robotic surgery, the surgical field is created (i.e., is actualized) by gas insufflation and is relatively large allowing for the working space and triangulation necessary for operation of modern robotic instruments. In contradistinction, the central nervous system lies within a confined bony space that, even upon craniotomy, does not permit access to critical structures and operative targets. Another difference is that for abdominal surgery, exposure to organs can more easily be performed by forcible retraction of other organs (e.g., the liver can be retracted cephalad to gain exposure to the gallbladder or common bile duct), but with neurologic surgery, brain parenchyma cannot tolerate such forcible retraction, and the density of critical neurovascular structures makes organ manipulation as a means to gain operative exposure highly restricted – especially with linear effector arms which are not designed to navigate the curvelinear pathways to arrive at deep, intracranial operative targets.

Nonlinear Systems

Continuum robots are special tele-manipulators that are hyper-redundant [119, 120]. Because of their serpiginous motion, they are often called *snake-arm robots*. This design is particularly well suited to access difficult targets within a confined anatomic space. The Monarch™ and Ion™ robotic bronchoscopes (discussed previously) are examples of continuum robots. Just as access to difficult targets in the lung can be facilitated by continuum robotics, so too can access to the brain parenchyma and intracranial targets.

In 2006, Engh et al. reported their experience in a functional steerable needle which could be

Table 22.3 Robotics in neurologic surgery

System	Manufacturer/developer	Remarks
Programmable Universal Machine for Assembly (PUMA)	Unimation (original)	First robotic stereotactic brain biopsy (1985)
Neuromate® robotic system	Renishaw	Applications include stereotactic electrode implantation for deep brain stimulation and stereoelectroencephalography
NeuroArm	IMRIS Inc. (acquired 2010)	First image-guided, MRI-compatible surgical robot
Neurosurgical robot Minerva	Developed at the University of Lausanne, Switzerland	Pioneered in the mid-1990s; functional for brain biopsy. Precise but project discontinued due to safety concerns
PathFinder	Prosurgics, United Kingdom	Image-guided neurosurgery; near absolute geometric accuracy
NeuRobot	Department of Neurosurgery, Shinshu University School of Medicine, Matsumoto, Japan	Experimental; cadaveric studies only
Robot-Assisted Microsurgery System (RAMS)	NASA JPL in collaboration with MicroDexterity Systems, Inc.	Designed for the brain, eye, ears, nose, throat, and face; provides scale-down human input motions and tremor cancellation
AURORA® Surgiscope System	Rebound therapeutics	Single-use neurologic endoscope; image guidance; applications include evacuation of intracerebral hemorrhage; recent FDA 510(k) clearance in the USA
SpineAssist (Mazor X)	Mazor Robotics (Haifa, Israel; US headquarters – Orlando, FL); originally M.A.S.O.R. Surgical Technologies	Can be integrated with navigation (Stealth Station, Medtronic); 4000 cases worldwide; principle application is spine surgery, especially deformity repair

navigated within brain tissue to arrive at an anatomic target while avoiding critical structures [119]. The authors were able to demonstrate precise trajectory control of a brain biopsy needle in a two-dimensional ex vivo model. The results were best with the use of nitinol wires as opposed to hallow stainless steel needles [119]. In their experimentation, it was possible to control the wire bend to achieve proportional curvature by varying the *duty cycle* (i.e., electric pulse duration) of the needle's spin [119]. Duty cycle is defined as follows:

$$D = \frac{\mathrm{PW}}{T}$$

where D is the duty cycle (expressed as a ratio), PW is the pulse width (i.e., the time when the pulse is active), and T represents the total time. Steering and wire control are thus obtained by varying the duration of PW, which, in turn, controls the degree and direction of bend of a neurosurgical wire as it is navigated through the brain to arrive at a target of interest.

The ability to guide a wire safely into brain parenchyma is one challenge, but creating a micro-wire able to transmit mechanical motion and master-slave manipulation is orders of magnitude more complex. According to Ikuta et al. [120], part of the engineering difficulty in achieving a minimum of five degrees of freedom (DoF) (torsion, grasp, translation, base of joint motion, tip of joint motion) is related to the problem of redundant movement, as well as the management of slack in the wire itself. Despite these and other challenges, progress has been forged toward the development of nonlinear mesoscale (0.1–5 mm) continuum robots suitable for neurologic surgery [121–127].

Kim et al., for example, have developed a prototype flexible, spring-based intracranial robot for neurologic surgery. The system uses three interconnected segments, each with two degrees of freedom (2 DoF), and each can be independently controlled. The device, which is MRI compatible, is controlled by spring actuators via a tendon-driven mechanism [121].

Currently, continuum robots have not been applied clinically. As research scientists and engineers continue to solve the many challenges of mesoscale nonlinear robotics, neurosurgeons may someday be able to use integrated soft robots to navigate the central nervous system, where targets can be localized for biopsy, aneurysm clipping, or even resection of neoplasia.

Other Nonlinear Robotic Systems

Endoluminal Surgical Platforms

Advanced endoscopic procedures including endoluminal and transluminal surgery such as natural orifice transluminal endoscopic surgery (NOTES) are challenging to perform with standard flexible endoscopes. Hence, their adoption has been limited. Even with accessory devices, conventional flexible endoscopes do not provide the desired dexterity for such complex interventions [128, 129]. In particular, interventions like endoscopic submucosal dissection (ESD) – an approach to treat benign and superficial malignant gastrointestinal lesions – are technically challenging. Specialized training is required to achieve competency in the surgical skills and expertise needed to establish proficiency [128, 129]. By enhancing tissue manipulation, exposure, and visualization, robotic-assisted endoscopic surgery addresses the need for improved precision, safety, reliability, and effectiveness [128, 130].

To facilitate triangulation, retraction, and performance of complex tasks such as suturing or knot tying, endoscopic systems with articulated arms have been proposed [131, 132]. The surgical endoscopic platform Anubiscope® was conceived for NOTES [133, 134], while IsisScope® for laparoendoscopic single-site procedures [135] was designed to provide instrument triangulation in flexible endoscopy. The devices were developed in an IRCAD collaboration with KARL STORZ. However, there was a need for two fully trained surgeons to operate these systems. Consequently, the Single-Access Transluminal Robotic Assistant for Surgeons (STRAS) robot was developed in collaboration with the iCube laboratory in Strasbourg, France [132, 136]. This master-slave robotically assisted system enables tele-operated endoscope handling by a single surgeon, to facilitate ESD [132]. The endoscope is inserted manually and connected to the slave system. It houses three working channels for instruments, of which one can accommodate standard endoscopic tools. After insertion of the two tele-operated bendable instruments with 3–4 DoF each, the system has 10+1 DoF controlled by the surgeon [132, 136] (Fig. 22.13). In a series of 18 attempted ESD procedures up to 25 cm from the anal verge, 12 were successfully completed. Technical and surgical difficulties were mainly encountered in the first cases, whereas the last six were completed without system failure or perforations [132]. The system has been reengineered for clinical translation and commercialization. In its current version, Endoluminal Assistant for Surgical Endoscopy (EASE), comprising a 53.5 cm long and 16 mm

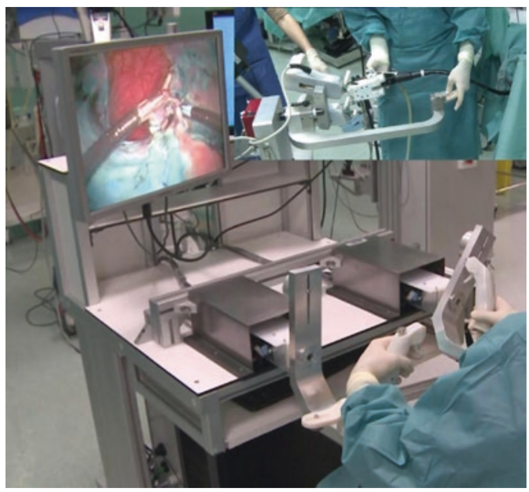

Fig. 22.13 The Single-Access Transluminal Robotic Assistant for Surgeons (STRAS) robot is shown. This master-slave, robotically assisted system enables tele-operated endoscope handling by a single surgeon and allows for colonic submucosal dissection. The endoscope is inserted manually and connected to the slave system (inset). It houses three working channels for instruments, of which one can accommodate standard endoscopic tools. After insertion, the two tele-operated instruments are controlled by the surgeon seated at a workstation, as shown. (Photo courtesy of IRCAD France, iCube Laboratory Strasbourg, and KARL STORZ, reproduced with permission)

maximum shaft diameter detachable flexible endoscope, the system was trialed in a prospective nonrandomized comparative preclinical study. An expert laparoscopic surgeon without robotic or conventional ESD experience performed the robot-assisted ESD procedures, while an experienced endoscopist performed the conventional ESD procedures, resecting a total of 30 "pseudo" tumors within 15–35 cm from the anal verge. The ESD novice using the robotic system had a significantly faster dissection speed, shorter procedural time, and lower perforation rate than the expert endoscopist using the conventional endoscopic technique (based on an experience of >1000 ESD cases). This study demonstrates the potential of this first fully robotic, single-operator, master-slave flexible endoscopic tele-manipulator to enhance the performance of complex endoluminal dissection [137]. Merging the fields of advanced endoscopy and surgery, robotic assistance can promote proficiency and adoption of complex endoscopic approaches, thereby advancing the field of endosurgical interventions, for applications including ESD and NOTES.

Innovations in robotic technology for endoscopy address both diagnostic and therapeutic procedures. Various devices are currently being developed and trialed. Robotic assistance is focused on endoscope locomotion and instrumentation [129, 130]. A tele-operated, magnetic-driven robotic guidance for a soft-tethered stereoscopic capsule system has been proposed as a potential alternative to conventional colonoscopy, with the aim of promoting colorectal cancer screening by reducing patient discomfort and need for sedation [138]. Robotics research further focuses on autonomous operation of such flexible endoscopes [139], including endoscopic ultrasound [140]. When coupled with robotic technologies such as active locomotion and embedded therapeutic modules, tethered and wireless capsule endoscopy devices have additional screening, diagnostic, and therapeutic potential [141, 142]. By 2025, several robotic endoluminal devices currently in development are expected to emerge, and some are currently being evaluated with clinical validation trials, including the endoluminal surgery (ELS) system (ColubrisMX Inc., Houston, TX) (Fig. 22.14).

Titan SPORT™ Surgical System

The Single Port Orifice Robotic Technology (SPORT™) Surgical System (Titan Medical Inc.) is a flexible, nonlinear robotic system designed for single-incision surgery, although other applications are also under investigation. It utilizes an open console/workstation design, and the robotic effector arm is attached to a large, single-boom central unit (Fig. 22.15).

The first reported preclinical series examined the feasibility of single-port procedures utilizing the SPORT™ system on both living porcine and human cadaveric models [143]. The SPORT™ advanced prototype trialed had a 25 mm camera insertion tube including a 3DHD camera head and two (8 mm dia.) robotic, articulating effector arms. The authors performed 12 procedures on six porcine models and one human cadaver utilizing a disposable single-incision gel access port (plus, in some cases, an additional trocar for bedside laparoscopic assistance). These procedures included six cholecystectomies, four Nissen fundoplications (Fig. 22.16), one splenectomy, and one hepatic pedicle dissection. The Objective Structured Assessment of Technical Skills (OSATS) score was used to assess the four experienced laparoscopic surgeons' performance on the surgical system. The OSATS score indicated a short learning curve for the device-related aspects, corresponding to gaining familiarity with the system. Their results demonstrated that the Titan SPORT™ was suitable for the aforementioned procedures and specifically for the critical surgical tasks including grasping, retracting, dissecting, and suturing. Nevertheless, there were some shortcomings, such as a lack of video image brightness with zoom, suboptimal camera control, and limited camera motion range.

Fig. 22.14 An emerging surgical system, the endoluminal surgery (ELS) system, by ColubrisMX Inc. (Houston, TX) is an advanced, robotic endoluminal system currently undergoing clinical validation. (**a**) The console workstation and ELS apparatus are shown, as is the (**b**) robotized effector arms at the tip of the scope. (Photograph provided with permission, ColubrisMX Inc.)

In collaboration with urologists, further procedures were performed in the preclinical setting at IHU Strasbourg, France (unpublished data). They include a single-port prostatectomy and urethral anastomosis on a human cadaver, as well as a series of ten partial and heminephrectomies in the live animal model. Similar to the experience with digestive tract procedures, the SPORT™ system was suitable to perform the critical surgical tasks such as deep pelvic dissection, renal hilum dissection and clamping, renal parenchyma division, and suturing.

Incorporating these preclinical experiences, the flexible endoscopic 3D camera system has been redesigned and an additional 2D camera integrated into the camera insertion tube, to increase the visual field and camera motion range. Further product development as well as 510(k) approval from the FDA is currently pending.

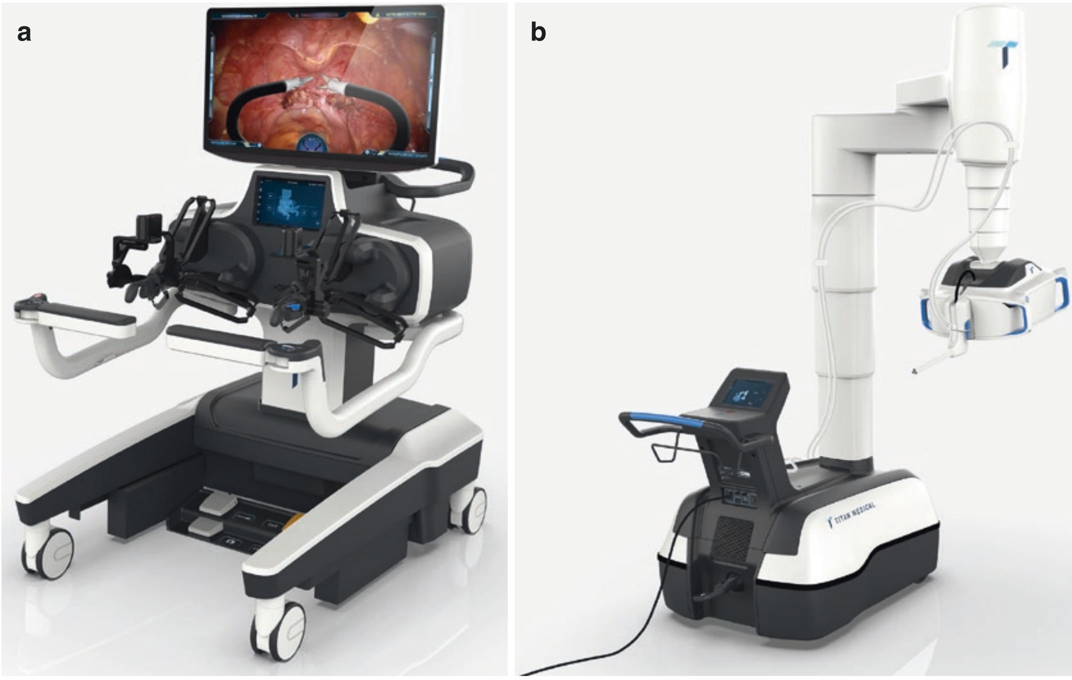

Fig. 22.15 (**a**) The Single Port Orifice Robotic Technology (SPORT™) Surgical System surgical device (Titan Medical Inc.) console provides a workstation for the surgeon, and (**b**) a single-boom system can be delivered into a body space cavity where nonlinear robotic effectors are deployed

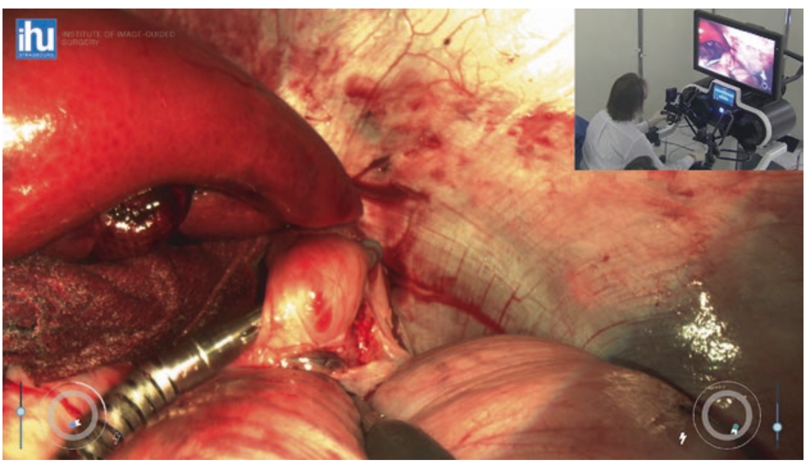

Fig. 22.16 A surgeon at the SPORT™ workstation (inset) performs a Nissen fundoplication in preclinical testing and evaluation in Strasbourg, France. The curvelinear instrumentation provides improved triangulation via a single-incision laparoscopic access port, while the robotic nonlinear instrumentation allows reach to a relatively difficult anatomic target. (Photo provided with permission, IHU Strasbourg, France)

References

1. Marescaux J, Leroy J, Gagner M, Rubino F, Mutter D, Vix M, Butner SE, Smith MK. Transatlantic robot-assisted telesurgery. Nature. 2001;413(6854):379–80.
2. Marescaux J, Leroy J, Rubino F, Smith M, Vix M, Simone M, Mutter D. Transcontinental robot-assisted remote telesurgery: feasibility and potential applications. Ann Surg. 2002;235(4):487–92.
3. Svoboda E. Your robot surgeon will see you now. Nature. 2019;573(7775):S110–1. https://doi.org/10.1038/d41586-019-02874-0.
4. Ficarra V, Novara G, Artibani W, Cestari A, Galfano A, Graefen M, Guazzoni G, Guillonneau B, Menon M, Montorsi F, Patel V. Retropubic, laparoscopic, and robot-assisted radical prostatectomy: a systematic review and cumulative analysis of comparative studies. Eur Urol. 2009;55(5):1037–63.
5. Patel VR, Palmer KJ, Coughlin G, Samavedi S. Robot-assisted laparoscopic radical prostatectomy: perioperative outcomes of 1500 cases. J Endourol. 2008;22(10):2299–306.
6. Berryhill R Jr, Jhaveri J, Yadav R, Leung R, Rao S, El-Hakim A, Tewari A. Robotic prostatectomy: a review of outcomes compared with laparoscopic and open approaches. Urology. 2008;72(1):15–23.
7. Koch MO. Robotic versus open prostatectomy: end of the controversy. J Urol. 2016;196(1):9–10. https://doi.org/10.1016/j.juro.2016.04.047. Epub 2016 Apr 13.
8. Payne TN, Dauterive FR. A comparison of total laparoscopic hysterectomy to robotically assisted hysterectomy: surgical outcomes in a community practice. J Minim Invasive Gynecol. 2008;15(3):286–91.
9. Kho RM, Hilger WS, Hentz JG, Magtibay PM, Magrina JF. Robotic hysterectomy: technique and initial outcomes. Am J Obstet Gynecol. 2007;197(1):113–e1.
10. Cirocchi R, Partelli S, Trastulli S, Coratti A, Parisi A, Falconi M. A systematic review on robotic pancreaticoduodenectomy. Surg Oncol. 2013;22(4):238–46.
11. Orti-Rodríguez RJ, Rahman SH. A comparative review between laparoscopic and robotic pancreaticoduodenectomies. Surg Laparosc Endosc Percutan Tech. 2014;24(2):103–8.
12. Baker EH, Ross SW, Seshadri R, Swan RZ, Iannitti DA, Vrochides D, Martinie JB. Robotic pancreaticoduodenectomy for pancreatic adenocarcinoma: role in 2014 and beyond. J Gastrointest Oncol. 2015;6(4):396.
13. Pigazzi A, Garcia-Aguilar J. Robotic colorectal surgery: for whom and for what? Dis Colon Rectum. 2010;53(7):969–70. https://doi.org/10.1007/DCR.0b013e3181db8055.
14. Weinstein GS, O'Malley BW Jr, Hockstein NG. Transoral robotic surgery: supraglottic laryngectomy in a canine model. Laryngoscope. 2005;115(7):1315–9.
15. Alon EE, Kasperbauer JL, Olsen KD, Moore EJ. Feasibility of transoral robotic-assisted supraglottic laryngectomy. Head Neck. 2012;34(2):225–9.
16. Ansarin M, Zorzi S, Massaro MA, et al. Transoral robotic surgery vs transoral laser microsurgery for resection of supraglottic cancer: a pilot surgery. Int J Med Robot. 2014;10(1):107–12.
17. Weinstein GS, O'Malley BW, Snyder W, Sherman E, Quon H. Transoral robotic surgery: radical tonsillectomy. Arch Otolaryngol Head Neck Surg. 2007;133(12):1220–6.
18. O'Malley BW Jr, Weinstein GS, Snyder W, Hockstein NG. Transoral robotic surgery (TORS) for base of tongue neoplasms. Laryngoscope. 2006;116(8):1465–72.
19. Weinstein GS, O'Malley BW Jr, Magnuson JS, Carroll WR, Olsen KD, Daio L, Moore EJ, Holsinger FC. Transoral robotic surgery: a multicenter study to assess feasibility, safety, and surgical margins. Laryngoscope. 2012;122(8):1701–7.
20. Moore EJ, Olsen KD, Kasperbauer JL. Transoral robotic surgery for oropharyngeal squamous cell carcinoma: a prospective study of feasibility and functional outcomes. Laryngoscope. 2009;119(11):2156–64.
21. Weinstein GS, O'Malley BW Jr, Desai SC, Quon H. Transoral robotic surgery: does the ends justify the means? Curr Opin Otolaryngol Head Neck Surg. 2009;17(2):126–31.
22. Holsinger FC. A flexible, single-arm robotic surgical system for transoral resection of the tonsil and lateral pharyngeal wall: next-generation robotic head and neck surgery. Laryngoscope. 2016;126(4):864–9.
23. Tsang RK, Holsinger FC. Transoral endoscopic nasopharyngectomy with a flexible next-generation robotic surgical system. Laryngoscope. 2016;126(10):2257–62.
24. Chen MM, Orosco RK, Lim GC, Holsinger FC. Improved transoral dissection of the tongue base with a next-generation robotic surgical system. Laryngoscope. 2018;128(1):78–83.
25. Tateya I, Koh YW, Tsang RK, Hong SS, Uozumi R, Kishimoto Y, Sugimoto T, Holsinger FC. Flexible next-generation robotic surgical system for transoral endoscopic hypopharyngectomy: a comparative preclinical study. Head Neck. 2018;40(1):16–23.
26. Chan JY, Tsang RK, Holsinger FC, Tong MC, Ng CW, Chiu PW, Ng SS, Wong EW. Prospective clinical trial to evaluate safety and feasibility of using a single port flexible robotic system for transoral head and neck surgery. Oral Oncol. 2019;94:101–5.
27. Lang S, Mattheis S, Hasskamp P, Lawson G, Güldner C, Mandapathil M, Schuler P, Hoffmann T, Scheithauer M, Remacle M. A European multicenter study evaluating the flex robotic system in transoral robotic surgery. Laryngoscope. 2017;127(2):391–5. https://doi.org/10.1002/lary.26358.
28. Newsome H, Mandapathil M, Koh YW, Duvvuri U. Utility of the highly articulated flex robotic system for head and neck procedures: a cadaveric study.

Ann Otol Rhinol Laryngol. 2016;125(9):758–63. https://doi.org/10.1177/0003489416653409.
29. Mattheis S, Hasskamp P, Holtmann L, Schäfer C, Geisthoff U, Dominas N, Lang S. Flex robotic system in transoral robotic surgery: the first 40 patients. Head Neck. 2017;39(3):471–5. https://doi.org/10.1002/hed.24611.
30. Tateya I, Koh YW, Tsang RK, et al. Flexible next-generation robotic surgical system for transoral endoscopic hypopharyngectomy: a comparative preclinical study. Head Neck. 2018;40(1):16–23. https://doi.org/10.1002/hed.24868.
31. Funk E, Goldenberg D, Goyal N. Demonstration of a transoral robotic supraglottic laryngectomy and total laryngectomy in cadaveric specimens using the medrobotics flex system. Head Neck. 2017;39(6):1218–25.
32. Atallah S, Albert M, Larach S. Transanal minimally invasive surgery: a giant leap forward. Surg Endosc. 2010;24(9):2200–5. https://doi.org/10.1007/s00464-010-0927-z. Epub 2010 Feb 21.
33. Buess G, Hutterer F, Theiss J, Böbel M, Isselhard W, Pichlmaier H. A system for a transanal endoscopic rectum operation. Chirurg. 1984;55(10):677–80.
34. Atallah SB, Albert MR, de Beche-Adams TH, Larach SW. Robotic trans anal minimally invasive surgery in a cadaveric model. Tech Coloproctol. 2011;15(4):461–4. https://doi.org/10.1007/s10151-011-0762-9. Epub 2011 Sep 28.
35. Atallah S, Parra-Davila E, DeBeche-Adams T, Albert M, Larach S. Excision of a rectal neoplasm using robotic transanal surgery (RTS): a description of the technique. Tech Coloproctol. 2012;16(5):389–92. https://doi.org/10.1007/s10151-012-0833-6. Epub 2012 May 15.
36. Atallah S, Nassif G, Polavarapu H, de Beche-Adams T, Ouyang J, Albert M, Larach S. Robotic-assisted transanal surgery for total mesorectal excision (RATS-TME): a description of a novel surgical approach with video demonstration. Tech Coloproctol. 2013;17(4):441–7. https://doi.org/10.1007/s10151-013-1039-2. Epub 2013 Jun 26.
37. Atallah S, Martin-Perez B, Pinan J, Quinteros F, Schoonyoung H, Albert M, Larach S. Robotic transanal total mesorectal excision: a pilot study. Tech Coloproctol. 2014;18(11):1047–53. https://doi.org/10.1007/s10151-014-1181-5. Epub 2014 Jun 24.
38. Medina MG, Tsoraides SS, Dwyer AM. Review and update: robotic transanal surgery (RTAS). Updat Surg. 2018;70(3):369–74. https://doi.org/10.1007/s13304-018-0580-y. Epub 2018 Aug 17.
39. Tomassi MJ, Taller J, Yuhan R, Ruan JH, Klaristenfeld DD. Robotic transanal minimally invasive surgery for the excision of rectal neoplasia: clinical experience with 58 consecutive patients. Dis Colon Rectum. 2019;62(3):279–85. https://doi.org/10.1097/DCR.0000000000001223.
40. Atallah S, Buchs NC, Kim SH. The evolution of robotic TAMIS. In: Transanal minimally invasive surgery (TAMIS) and transanal total mesorectal excision (taTME). Cham: Springer; 2019. p. 153–64.
41. Atallah S, Zenoni S, Kelly J, Tilahun Y, Monson JR. A blueprint for robotic navigation: pre-clinical simulation for transanal total mesorectal excision (taTME). Tech Coloproctol. 2016;20(9):653–4. https://doi.org/10.1007/s10151-016-1511-x. Epub 2016 Aug 10.
42. Atallah S, Parra-Davila E, Melani AG, Romagnolo LG, Larach SW, Marescaux J. Robotic-assisted stereotactic real-time navigation: initial clinical experience and feasibility for rectal cancer surgery. Tech Coloproctol. 2019;23(1):53–63. https://doi.org/10.1007/s10151-018-1914-y. Epub 2019 Jan 17.
43. Atallah S. Assessment of a flexible robotic system for endoluminal applications and transanal total mesorectal excision (taTME): could this be the solution we have been searching for? Tech Coloproctol. 2017;21(10):809–14. https://doi.org/10.1007/s10151-017-1697-6. Epub 2017 Oct 24.
44. Atallah S, Hodges A, Larach SW. Direct target NOTES: prospective applications for next generation robotic platforms. Tech Coloproctol. 2018;22(5):363–71. https://doi.org/10.1007/s10151-018-1788-z. Epub 2018 May 31.
45. Carmichael H, D'Andrea AP, Skancke M, Obias V, Sylla P. Feasibility of transanal total mesorectal excision (taTME) using the Medrobotics Flex® System. Surg Endosc. 2019. https://doi.org/10.1007/s00464-019-07019-y. [Epub ahead of print].
46. Atallah S, Martin-Perez B, Keller D, Burke J, Hunter L. Natural-orifice transluminal endoscopic surgery. Br J Surg. 2015;102(2):e73–92. https://doi.org/10.1002/bjs.9710.
47. Atallah S, Martin-Perez B, Albert M, Schoonyoung H, Quinteros F, Hunter L, Larach S. Vaginal access minimally invasive surgery (VAMIS): a new approach to hysterectomy. Surg Innov. 2015;22(4):344–7. https://doi.org/10.1177/1553350614560273. Epub 2014 Nov 27.
48. Karkia R, Giacchino T, Taylor J, Ghaffar A, Gupta A, Kovoor E. Hysterectomy and Adenextomy via transvaginal natural orifice transluminal endoscopic surgery (vNOTES): a UK perspective with a case series of 33 patients. Eur J Obstet Gynecol Reprod Biol. 2019;242:29–32. https://doi.org/10.1016/j.ejogrb.2019.08.023. Epub 2019 Aug 31.
49. Baekelandt JF, De Mulder PA, Le Roy I, Mathieu C, Laenen A, Enzlin P, Weyers S, Mol BWJ, Bosteels JJA. Transvaginal natural orifice transluminal endoscopic surgery (vNOTES) adnexectomy for benign pathology compared with laparoscopic excision (NOTABLE): a protocol for a randomised controlled trial. BMJ Open. 2018;8(1):e018059. https://doi.org/10.1136/bmjopen-2017-018059.
50. Marks J, Ng S, Mak T. Robotic transanal surgery (RTAS) with utilization of a next-generation single-port system: a cadaveric feasibility study. Tech Coloproctol. 2017;21(7):541–5. https://doi.org/10.1007/s10151-017-1655-3. Epub 2017 Jul 14.

51. Atallah S, DuBose A, Larach SW. Towards the development of simultaneous two-field robotic surgery. Tech Coloproctol. 2016;20(1):71–3. https://doi.org/10.1007/s10151-015-1403-5. Epub 2015 Nov 19.
52. Atallah S, Parra-Davila E, Melani AGF. Assessment of the Versius surgical robotic system for dual-field synchronous transanal total mesorectal excision (taTME) in a preclinical model: will tomorrow's surgical robots promise newfound options? Tech Coloproctol. 2019;23(5):471–7. https://doi.org/10.1007/s10151-019-01992-1. Epub 2019 May 8.
53. Childers CP, Maggard-Gibbons M. Estimation of the acquisition and operating costs for robotic surgery. JAMA. 2018;320(8):835–6. https://doi.org/10.1001/jama.2018.9219.
54. Adamina M, Buchs NC, Penna M, Hompes R, and on behalf of the St. Gallen Colorectal Consensus Expert Group. St. Gallen consensus on safe implementation of transanal total mesorectal excision. Surg Endosc. 2018;32(3):1091–103.
55. Buchs NC, Nicholson GA, Ris F, Mortensen NJ, Hompes R. Transanal total mesorectal excision: a valid option for rectal cancer? World J Gastroenterol. 2015;21(41):11700–8.
56. Wolthuis AM, Bislenghi G, van Overstraeten A, D'Hoore A. Transanal total mesorectal excision: towards standardization of technique. World J Gastroenterol. 2015;21(44):12686–95.
57. Mao Y, Yang D, He J, Krasna MJ. Epidemiology of lung cancer. Surg Oncol Clin. 2016;25(3):439–45.
58. Wakelee HA, Chang ET, Gomez SL, Keegan TH, Feskanich D, Clarke CA, Holmberg L, Yong LC, Kolonel LN, Gould MK, West DW. Lung cancer incidence in never-smokers. J Clin Oncol Off J Am Soc Clin Oncol. 2007;25(5):472.
59. Cruz CS, Tanoue LT, Matthay RA. Lung cancer: epidemiology, etiology, and prevention. Clin Chest Med. 2011;32(4):605–44.
60. Ost DE, Ernst A, Lei X, Kovitz KL, Benzaquen S, Diaz-Mendoza J, Greenhill S, Toth J, Feller-Kopman D, Puchalski J, Baram D. Diagnostic yield and complications of bronchoscopy for peripheral lung lesions. Results of the AQuIRE registry. Am J Respir Crit Care Med. 2016;193(1):68–77.
61. DiBardino DM, Yarmus LB, Semaan RW. Transthoracic needle biopsy of the lung. J Thorac Dis. 2015;7(Suppl 4):S304.
62. Gildea TR, Mazzone PJ, Karnak D, Meziane M, Mehta AC. Electromagnetic navigation diagnostic bronchoscopy: a prospective study. Am J Respir Crit Care Med. 2006;174(9):982–9.
63. Eberhardt R, Anantham D, Herth F, Feller-Kopman D, Ernst A. Electromagnetic navigation diagnostic bronchoscopy in peripheral lung lesions. Chest. 2007;131(6):1800–5.
64. Schwarz Y, Mehta AC, Ernst A, Herth F, Engel A, Besser D, Becker HD. Electromagnetic navigation during flexible bronchoscopy. Respiration. 2003;70(5):516–22.
65. Makris D, Scherpereel A, Leroy S, Bouchindhomme B, Faivre JB, Remy J, Ramon P, Marquette CH. Electromagnetic navigation diagnostic bronchoscopy for small peripheral lung lesions. Eur Respir J. 2007;29(6):1187–92.
66. Schwarz Y, Greif J, Becker HD, Ernst A, Mehta A. Real-time electromagnetic navigation bronchoscopy to peripheral lung lesions using overlaid CT images: the first human study. Chest. 2006;129(4):988–94.
67. Khan I, Chin R, Adair N, Chatterjee A, Haponik E, Conforti J. Electromagnetic navigation bronchoscopy in the diagnosis of peripheral lung lesions. Clin Pulm Med. 2011;18(1):42–5.
68. Visentini-Scarzanella M, Sugiura T, Kaneko T, Koto S. Deep monocular 3D reconstruction for assisted navigation in bronchoscopy. Int J Comput Assist Radiol Surg. 2017;12(7):1089–99.
69. Shen M, Giannarou S, Shah PL, Yang GZ. Branch: bifurcation recognition for airway navigation based on structural characteristics. In: International conference on medical image computing and computer-assisted intervention. Cham: Springer; 10 Sept 2017. p. 182–9.
70. Sánchez C, Esteban-Lansaque A, Borrás A, Diez-Ferrer M, Rosell A, Gil D. Towards a Videobronchoscopy localization system from airway centre tracking. In: VISIGRAPP (4: VISAPP); 2017. p. 352–9.
71. Hofstad EF, Sorger H, Leira HO, Amundsen T, Langø T. Automatic registration of CT images to patient during the initial phase of bronchoscopy: a clinical pilot study. Med Phys. 2014;41(4):041903.
72. Sganga J, Eng D, Graetzel C, Camarillo D. Offsetnet: deep learning for localization in the lung using rendered images. In: 2019 International Conference on Robotics and Automation (ICRA). IEEE; 20 May 2019. p. 5046–52.
73. Herth FJ, Eberhardt R, Sterman D, Silvestri GA, Hoffmann H, Shah PL. Bronchoscopic transparenchymal nodule access (BTPNA): first in human trial of a novel procedure for sampling solitary pulmonary nodules. Thorax. 2015;70(4):326–32.
74. Anciano C, Brown C, Bowling M. Going off road: the first case reports of the use of the transbronchial access tool with electromagnetic navigational bronchoscopy. J Bronchology Interv Pulmonol. 2017;24(3):253–6.
75. Bowling MR, Brown C, Anciano CJ. Feasibility and safety of the transbronchial access tool for peripheral pulmonary nodule and mass. Ann Thorac Surg. 2017;104(2):443–9.
76. Callahan S, Tanner N, Chen A, Bacro T, Silvestri G, Pastis N. Comparison of the thin convex probe endobronchial ultrasound bronchoscope to standard EBUS and flexible bronchoscope: a cadaveric study. Chest. 2016;150(4):979A.

77. Yarmus LB, Arias S, Feller-Kopman D, Semaan R, Wang KP, Frimpong B, Burgess KO, Thompson R, Chen A, Ortiz R, Lee HJ. Electromagnetic navigation transthoracic needle aspiration for the diagnosis of pulmonary nodules: a safety and feasibility pilot study. J Thorac Dis. 2016;8(1):186.
78. Krimsky WS, Pritchett MA, Lau KK. Towards an optimization of bronchoscopic approaches to the diagnosis and treatment of the pulmonary nodules: a review. J Thorac Dis. 2018;10(Suppl 14): S1637.
79. Murgu SD. Robotic assisted-bronchoscopy: technical tips and lessons learned from the initial experience with sampling peripheral lung lesions. BMC Pulm Med. 2019;19(1):89.
80. Graetzel CF, Sheehy A, Noonan DP. Robotic bronchoscopy drive mode of the Auris Monarch platform. In: 2019 International Conference on Robotics and Automation (ICRA). IEEE; 20 May 2019. p. 3895–901.
81. Herron DM, Dong M. Upcoming robotic systems. In: Robotic-assisted minimally invasive surgery. Cham: Springer; 2019. p. 319–21.
82. Sigwart U, Puel J, Mirkovitch V, Joffre F, Kappenberger L. Intravascular stents to prevent occlusion and re-stenosis after transluminal angioplasty. N Engl J Med. 1987;316(12):701–6.
83. Simpson JB, Selmon MR, Robertson GC, Cipriano PR, Hayden WG, Johnson DE, Fogarty TJ. Transluminal atherectomy for occlusive peripheral vascular disease. Am J Cardiol. 1988;61(14):96G–101G.
84. Fogarty TJ, inventor; EDWARDS LAB Inc, assignee. Embolectomy catheter. United States patent US 3,435,826. 1969 Apr 1.
85. Beyar R, Gruberg L, Deleanu D, et al. Remote control percutaneous coronary interventions: concept, validation, and first-in-humans pilot clinical trial. J Am Coll Cardiol. 2006;47:296–300.
86. Weisz G, Metzger DC, Caputo RP, et al. Safety and feasibility of robotic percutaneous coronary intervention: PRECISE (Percutaneous robotically enhanced coronary intervention) Study. J Am Coll Cardiol. 2013;61:1596–600.
87. Bismuth J, Duran C, Stankovic M, et al. A first-in-man study of the role of flexible robotics in overcoming navigation challenges in the ileofemoral arteries. J Vasc Surg. 2013;57:14S–9S.
88. Fagogenis G, Mencattelli M, Machaidze Z, Rosa B, Price K, Wu F, Weixler V, Saeed M, Mayer JE, Dupont PE. Autonomous robotic intracardiac catheter navigation using haptic vision. Sci Robot. 2019;4(29). pii: eaaw1977. https://doi.org/10.1126/scirobotics.aaw1977.
89. Avni R, Tzvaigrach Y, Eilam D. Exploration and navigation in the blind mole rat (Spalax ehrenbergi): global calibration as a primer of spatial representation. J Exp Biol. 2008;211:2817–26.
90. Sharma S, Coombs S, Patton P, de Perera TB. The function of wall-following behaviors in the Mexican blind cavefish and a sighted relative, the Mexican tetra (Astyanax). J Comp Physiol A. 2009;195:225–40.
91. Mitchinson C, Martin J, Grant RA, Prescott TJ. Feedback control in active sensing: rat exploratory whisking is modulated by environmental contact. Proc R Soc B. 2007;274:1035–41.
92. Creed RP, Miller JR. Interpreting animal wall-following behavior. Experientia. 1990;46:758–61.
93. Patullo W, Macmillan DL. Corners and bubble wrap: the structure and texture of surfaces influence crayfish exploratory behavior. J Exp Biol. 2006;209:567–75.
94. Kaouk JH, Sagalovich D, Garisto J. Robot-assisted transvesical partial prostatectomy using a purpose-built single-port robotic system. BJU Int. 2018;122(3):520–4. https://doi.org/10.1111/bju.14194.
95. Ramirez D, Maurice MJ, Kaouk JH. Robotic perineal radical prostatectomy and pelvic lymph node dissection using a purpose built single-port robotic platform. BJU Int. 2016;118(5):829–33.
96. Maurice MJ, Kaouk JH. Robotic radical perineal cystectomy and extended pelvic lymphadenectomy: initial investigation using a purpose-built single-port robotic system. BJU Int. 2017;120(6):881–4. https://doi.org/10.1111/bju.13947.
97. Hebert KJ, Joseph J, Gettman M, Tollefson M, Frank I, Viers BR. Technical considerations of single port ureteroneocystostomy utilizing da Vinci SP platform. Urology. 2019. https://doi.org/10.1016/j.urology.2019.03.020.
98. Agarwal DK, Sharma V, Toussi A, Viers BR, Tollefson MK, Gettman MT, Frank I. Initial experience with da Vinci single-port robot-assisted radical prostatectomies. Eur Urol. 2019. https://doi.org/10.1016/j.eururo.2019.04.001.
99. Kaouk J, Garisto J, Eltemamy M, Bertolo R. Single-port robotic intracorporeal ileal conduit urinary diversion during radical cystectomy using the SP((R)) surgical system: step-by-step technique. Urology. 2019. https://doi.org/10.1016/j.urology.2019.03.023.
100. Dobbs RW, Halgrimson WR, Madueke I, Vigneswaran HT, Wilson JO, Crivellaro S. Single port robot-assisted laparoscopic radical prostatectomy: initial experience and technique with the da Vinci SP platform. BJU Int. 2019. https://doi.org/10.1111/bju.14864.
101. Kaouk J, Garisto J, Eltemamy M, Bertolo R. Step-by-step technique for single-port robot-assisted radical cystectomy and pelvic lymph nodes dissection using the da Vinci((R)) SP surgical system. BJU Int. 2019. https://doi.org/10.1111/bju.14744.
102. Rassweiler J, Fiedler M, Charalampogiannis N, Kabakci AS, Saglam R, Klein JT. Robot-assisted flexible ureteroscopy: an update. Urolithiasis. 2018;46(1):69–77. https://doi.org/10.1007/s00240-017-1024-8. Epub 2017 Nov 23.
103. Saglam R, Muslumanoglu AY, Tokatlı Z, Caşkurlu T, Sarica K, Taşçi Aİ, Erkurt B, Süer E, Kabakci

AS, Preminger G, Traxer O, Rassweiler JJ. A new robot for flexible ureteroscopy: development and early clinical results (IDEAL stage 1-2b). Eur Urol. 2014;66(6):1092–100. https://doi.org/10.1016/j.eururo.2014.06.047. Epub 2014 Jul 21.
104. Geavlete P, Saglam R, Georgescu D, Mulţescu R, Iordache V, Kabakci AS, Ene C, Geavlete B. Robotic flexible ureteroscopy versus classic flexible ureteroscopy in renal stones: the initial Romanian experience. Chirurgia (Bucur). 2016;111(4):326–9.
105. Proietti S, Dragos L, Emiliani E, Butticè S, Talso M, Baghdadi M, Villa L, Doizi S, Giusti G, Traxer O. Ureteroscopic skills with and without Roboflex Avicenna in the K-box® simulator. Cent European J Urol. 2017;70(1):76–80. Published online 2017 Mar 14. https://doi.org/10.5173/ceju.2017.1180.
106. Kwoh YS, Hou J, Jonckheere EA, Hayati S. A robot with improved absolute positioning accuracy for CT-guided stereotactic brain surgery. IEEE Trans Biomed Eng. 1988;35:153–60.
107. Hongo K, Kobayashi S, Kakizawa Y, Koyama J, Goto T, Okudera H, Kan K, Fujie MG, Iseki H, Takakura K. NeuRobot: telecontrolled micromanipulator system for minimally invasive microneurosurgery-preliminary results. Neurosurgery. 2002;51(4):985–8; discussion 988.
108. Sutherland GR, Wolfsberger S, Lama S, Zareinia K. The evolution of neuroArm. Neurosurgery. 2013;72(suppl_1):A27–32.
109. McBeth PB, Louw DF, Rizun PR, Sutherland GR. Robotics in neurosurgery. Am J Surg. 2004;188(4):68–75.
110. Sutherland GR, Latour I, Greer AD. Integrating an image-guided robot with intraoperative MRI. IEEE Eng Med Biol Mag. 2008;27(3):59–65.
111. Sutherland GR, Lama S, Gan LS, Wolfsberger S, Zareinia K. Merging machines with microsurgery: clinical experience with neuroArm. J Neurosurg. 2013;118(3):521–9.
112. Mattei TA, Rodriguez AH, Sambhara D, Mendel E. Current state-of-the-art and future perspectives of robotic technology in neurosurgery. Neurosurg Rev. 2014;37(3):357–66.
113. Eljamel MS. Validation of the PathFinder neurosurgical robot using a phantom. Int J Med Robot. 2007;3(4):372–7.
114. Glauser D, Fankhauser H, Epitaux M, Hefti JL, Jaccottet A. Neurosurgical robot Minerva: first results and current developments. J Image Guid Surg. 1995;1(5):266–72.
115. Le Roux PD, Das H, Esquenazi S, Kelly PJ. Robot-assisted microsurgery: a feasibility study in the rat. Neurosurgery. 2001;48(3):584–9.
116. Bekelis K, Radwan TA, Desai A, Roberts DW. Frameless robotically targeted stereotactic brain biopsy: feasibility, diagnostic yield, and safety. J Neurosurg. 2012;116(5):1002–6. https://doi.org/10.3171/2012.1.JNS111746. Epub 2012 Mar 9.
117. Dreval O, Rynkov I, Kasparova KA, Bruskin A, Aleksandrovskii V, Zil'bernstein V. Results of using Spine Assist Mazor in surgical treatment of spine disorders. interventions (transpedicular fixations). 2014;5(6):9–22.
118. Ghasem A, Sharma A, Greif DN, Alam M, Al Maaieh M. The arrival of robotics in spine surgery: a review of the literature. Spine. 2018;43(23):1670–7.
119. Engh JA, Podnar G, Kondziolka D, Riviere CN. Toward effective needle steering in brain tissue. In: Proceedings of 28th international conference of the IEEE engineering in medicine and biology society, 2006, p. 559–62.
120. Ikuta K, Yamamoto K, Sasaki K. Development of remote microsurgery robot and new surgical procedure for deep and narrow space. Proc IEEE Int Conf Robot Autom. 2003;1:1103–8.
121. Kim Y, Cheng SS, Diakite M, Gullapalli RP, Simard JM, Desai JP. Toward the development of a flexible mesoscale MRI-compatible neurosurgical continuum robot. IEEE Trans Robot. 2017;33(6):1386–97.
122. Su H, Li G, Rucker DC, Webster RJ III, Fischer GS. A concentric tube continuum robot with piezoelectric actuation for MRI-guided closed-loop targeting. Ann Biomed Eng. 2016;44(10):2863–73.
123. Sears P, Dupont P. A steerable needle technology using curved concentric tubes. In: Proceedings 2003 IEEE/RSJ international conference on intelligent robots and systems, 2006, p. 2850–6.
124. Ho M, Kim Y, Cheng SS, Gullapalli R, Desai JP. Design, development, and evaluation of an MRI-guided SMA spring-actuated neurosurgical robot. Int J Robot Res. 2015;34(8):1147–63.
125. Sheng J, Desai JP. Towards a SMA-actuated neurosurgical intracerebral hemorrhage evacuation (niche) robot. In: Proceedings of IEEE/RSJ international conference on intelligent robots and systems, 2015, p. 3805–10.
126. Butler EJ, Hammond-Oakley R, Chawarski S, Gosline AH, Codd P, Anor T, Madsen JR, Dupont PE, Lock J. Robotic neuro-endoscope with concentric tube augmentation. In: 2012 IEEE/RSJ international conference on intelligent robots and systems: IEEE; 2012. p. 2941–6.
127. Benabid AL, Lavallee S, Hoffmann D, Cinquin P, Demongeot J, Danel F. Potential use of robots in endoscopic neurosurgery. In: Minimally invasive neurosurgery I. Vienna: Springer; 1992. p. 93–7.
128. Moura DT, Aihara H, Thompson CC. Robotic-assisted surgical endoscopy: a new era for endoluminal therapies. VideoGIE. 2019;4(9):399–402.
129. Wong JYY, Ho KY. Robotics for advanced therapeutic colonoscopy. Clin Endosc. 2018;51(6):552–7. https://doi.org/10.5946/ce.2018.089. Epub 2018 Aug 21. PMID: 30130838.
130. Boškoski I, Costamagna G. Endoscopy robotics: current and future applications. Dig Endosc.

2019;31(2):119–24. https://doi.org/10.1111/den.13270. Epub 2018 Oct 24. Review.
131. Bardou B, Nageotte F, Zanne P, de Mathelin M. Design of a telemanipulated system for transluminal surgery. Conf Proc IEEE Eng Med Biol Soc. 2009;2009:5577–82. https://doi.org/10.1109/IEMBS.2009.5333486.
132. Légner A, Diana M, Halvax P, Liu YY, Zorn L, Zanne P, Nageotte F, De Mathelin M, Dallemagne B, Marescaux J. Endoluminal surgical triangulation 2.0: a new flexible surgical robot. Preliminary pre-clinical results with colonic submucosal dissection. Int J Med Robot. 2017;13(3). https://doi.org/10.1002/rcs.1819. Epub 2017 May 3. PMID: 28467024.
133. Diana M, Chung H, Liu KH, Dallemagne B, Demartines N, Mutter D, Marescaux J. Endoluminal surgical triangulation: overcoming challenges of colonic endoscopic submucosal dissections using a novel flexible endoscopic surgical platform: feasibility study in a porcine model. Surg Endosc. 2013;27(11):4130–5. https://doi.org/10.1007/s00464-013-3049-6. Epub 2013 Jun 21.
134. Perretta S, Dallemagne B, Barry B, Marescaux J. The ANUBISCOPE® flexible platform ready for prime time: description of the first clinical case. Surg Endosc. 2013;27(7):2630. https://doi.org/10.1007/s00464-013-2818-6. Epub 2013 Feb 23.
135. Leroy J, Diana M, Barry B, Mutter D, Melani AG, Wu HS, Marescaux J. Perirectal oncologic gateway to retroperitoneal endoscopic single-site surgery (PROGRESSS): a feasibility study for a new NOTES approach in a swine model. Surg Innov. 2012;19(4):345–52. https://doi.org/10.1177/1553350612452346. Epub 2012 Jul 1. PMID: 22751618.
136. Zorn L, Nageotte F, Zanne P, Legner A, Dallemagne B, Marescaux J, de Mathelin M. A novel telemanipulated robotic assistant for surgical endoscopy: preclinical application to ESD. IEEE Trans Biomed Eng. 2018;65(4):797–808. https://doi.org/10.1109/TBME.2017.2720739.
137. Mascagni P, Lim SG, Fiorillo C, Zanne P, Nageotte F, Zorn L, Perretta S, de Mathelin M, Marescaux J, Dallemagne B. Democratizing endoscopic submucosal dissection: single-operator fully robotic colorectal endoscopic submucosal dissection in a pig model. Gastroenterology. 2019;156(6):1569–1571.e2. https://doi.org/10.1053/j.gastro.2018.12.046.
138. Bianchi F, Ciuti G, Koulaouzidis A, Arezzo A, Stoyanov D, Schostek S, Oddo CM, Menciassi A, Dario P. An innovative robotic platform for magnetically-driven painless colonoscopy. Ann Transl Med. 2017;5(21):421. https://doi.org/10.21037/atm.2017.09.15.
139. Slawinski PR, Taddese AZ, Musto KB, Sarker S, Valdastri P, Obstein KL. Autonomously controlled magnetic flexible endoscope for colon exploration. Gastroenterology. 2018;154(6):1577–1579.e1. https://doi.org/10.1053/j.gastro.2018.02.037.
140. Norton JC, Slawinski PR, Lay HS, Martin JW, Cox BF, Cummins G, Desmulliez MPY, Clutton RE, Obstein KL, Cochran S, Valdastri P. Intelligent magnetic manipulation for gastrointestinal ultrasound. Sci Robot. 2019;4(31). pii: eaav7725. https://doi.org/10.1126/scirobotics.aav7725.
141. Ciuti G, Caliò R, Camboni D, Neri L, Bianchi F, Arezzo A, Koulaouzidis A, Schostek S, Stoyanov D, Oddo CM, Magnani B, Menciassi A, Morino M, Schurr MO, Dario P. Frontiers of robotic endoscopic capsules: a review. J Microbio Robot. 2016;11(1):1–18. https://doi.org/10.1007/s12213-016-0087-x. Epub 2016 May 2. Review. PMID: 29082124.
142. Slawinski PR, Obstein KL, Valdastri P. Capsule endoscopy of the future: what's on the horizon? World J Gastroenterol. 2015;21(37):10528–41. https://doi.org/10.3748/wjg.v21.i37.10528. Review. PMID: 26457013.
143. Seeliger B, Diana M, Ruurda JP, Konstantinidis KM, Marescaux J, Swanström LL. Enabling single-site laparoscopy: the SPORT platform. Surg Endosc.

23 Artificial Intelligence and Machine Learning: Implications for Surgery

David Hindin

A Brief History of Artificial Intelligence

At its most basic level, artificial intelligence (AI) is a broad field that seeks to create software capable of gathering information and responding in a goal-directed manner, behaving as if it were an intelligent organism [1]. Though often referred to as a single type of technology by the lay media, the study of artificial intelligence itself is incredibly broad, encompassing research across a vast spectrum of disciplines, including philosophy, logic, computer science, biology, neuroscience, mathematics, and more.

The actual term *artificial intelligence* was coined in 1955 by computer and cognitive scientist John McCarthy, assistant professor (at the time) at Dartmouth College. During the following summer of 1956, McCarthy convened a two-month workshop at Dartmouth, an event widely recognized today as formally launching AI as a field [2]. Attendees at the workshop included notable scientists Herbert A. Simon, Allen Newell, and Ray Solomonoff. The conference's stated goals are often used today to demonstrate the optimism (and even naiveté) that has often ushered in new research in AI. The field has captivated the world's imagination from its very outset:

> The study is to proceed on the basis of the conjecture that every aspect of learning or any other feature of intelligence can in principle be so precisely described that a machine can be made to simulate it. An attempt will be made to find how to make machines use language, form abstractions and concepts, solve kinds of problems now reserved for humans, and improve themselves. [3]

Over the six decades since the Dartmouth College Workshop, research in artificial intelligence has experienced alternating cycles of growth, followed by periods of delay. The latter are formally referred to as "AI winters" [4], denoting periods of delayed growth triggered by decreased funding and support from both the US and British governments. Often, these AI winters highlighted a disconnect between the potential promise of AI and the disappointing reality of progress that was much slower than originally anticipated. At the 1956 summit, for example, AI's founders proudly predicted, "machines will be capable, within twenty years, of doing any work a man can do" [5]. At the time of this writing, more than 60 years later, AI is only able to replicate a small proportion of work done by humans (although, as we will see with the utilization of deep neural networks, AI is exponentially more powerful than human brainpower in some areas already).

Beginning in the late 1990s, however, exponential improvements in computational power, combined with decades of research into new software algorithms, catalyzed increasingly powerful advances in AI technology. Other enabling

D. Hindin (✉)
Stanford Byers Center for Biodesign,
Stanford, CA, USA

S. Atallah (ed.), *Digital Surgery*, https://doi.org/10.1007/978-3-030-49100-0_23

technologies leveraged towards advancing AI included faster processors, increased storage, cloud computing, and more [6]. Today, a vast number of our daily interactions with technology are impacted in some form by AI. A 2017 report in MIT's Sloan Management Review, for instance, quoted one in five companies as, "incorporating AI in some offerings or processes" [7]. As of the time of this printing, that number is anticipated to be much larger.

Alongside the growth of artificial intelligence as a field, a variety of subfields have begun to develop as well. These include computer vision, speech recognition, natural language processing, robotics, and more. Many of these subfields leverage a particular form of technology, known as machine learning (ML).

Considered broadly, ML refers to the use of algorithms and statistical models that allow computers to carry out goal-oriented tasks, gradually iterating and improving themselves without additional instructions from humans. While some consider ML to be a subset of AI [8], other researchers now consider ML to be its own distinct field.

One of the primary modalities that drives ML are various forms of software models known as artificial neural networks. These neural networks enable a form of ML known as deep learning (DL). Below, we will further explore the ways that ML (and DL, in particular) is having one of the most radical impacts on surgery and medicine as a whole. First, however, we turn our attention to the primary basis of AI and ML.

Basics of AI and ML

In order to fully understand the potential benefits and risks offered by AI and ML in surgery, a working knowledge of the fundamentals underlying these technologies is critical. A brief overview follows for three of the most broadly recognized pillars of AI and ML: (a) search and optimization, (b) probability and Bayesian networks, and (c) artificial neural networks (ANN).

Search and Optimization

One of the oldest applications of AI, so-called search and optimization programs refer to a variety of algorithms designed to choose the optimum solution from a series of potential options [9]. This early form of AI itself encompasses a broad range of subcategories. The simplest of these are known as "brute force" methods – programs in which a series of options are attempted in blind succession until the correct goal is achieved. For instance, a machine attempting multiple passwords at random until the correct combination is found. Other, more nuanced forms of search and optimization algorithms, such as the Hill Climbing Search, seek to choose solutions which yield the best possible outcome for multiple simultaneous scenarios.

Probability and Bayesian Networks

In probability and Bayesian networks, we see some of the earliest examples of AI and its use in medicine. These algorithms examine a group of potentially related pieces of information and calculate the probability of a given outcome. This lends itself to a variety of applications within medicine, such as predicting diagnoses based on provided symptoms or potentially predicting a given outcome or complication based on various risk factors [10, 11].

Artificial Neural Networks (ANN)

Of all the building blocks of artificial intelligence, the elements that have unlocked perhaps the most explosive growth of AI (especially within medicine) are artificial neural networks (ANN). These networks are software algorithms that were created in an attempt to somewhat mimic the billions of actual neurons that comprise the human brain. In place of physical neurons, however, these artificial neural networks leverage vast networks of interconnected, software-derived nodes (Fig. 23.1).

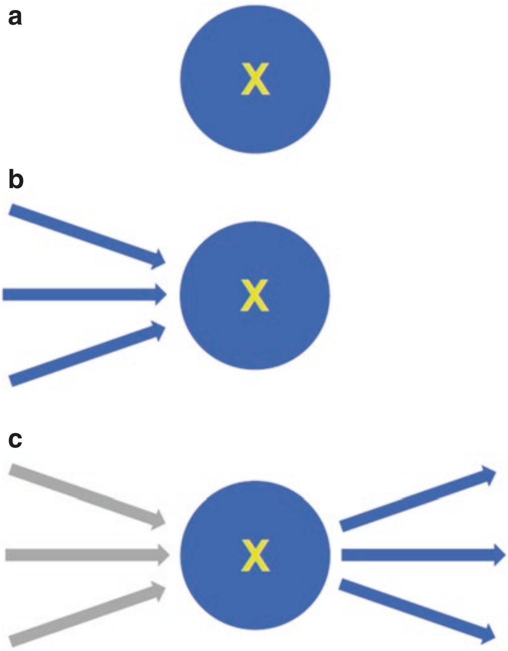

Fig. 23.1 A single node in a neural network (**a**), receiving input from multiple other nodes (**b**), and sending this information out to other nodes in the network (**c**)

In a neural network, the interconnected nodes are themselves arranged in a layered-like structure. At one end of the network is the input layer, which receives information, and at the other end is the network's output layer. In between these two layers are a series of *hidden layers,* as we will discuss below. Each node in a neural network receives some form of data as input, processes that data according to its own unique function (in other words, a specific formula assigned to that particular node), and then sends the resulting data as output through the system to other nodes (Fig. 23.2).

While the *input* and *output layers* may be designed by humans – for instance, an *input layer* created to receive raw image data from a head CT and an *output layer* designed to give a determination of whether there is a presence of intracranial bleeding on the head CT – the *hidden layers* within a neural network are not programmed by humans directly. Instead, the behavior of these inner layers is determined and adjusted entirely by the network itself, through a variety of algorithms, such as *backpropagation* [12].

Fig. 23.2 A simple neural network

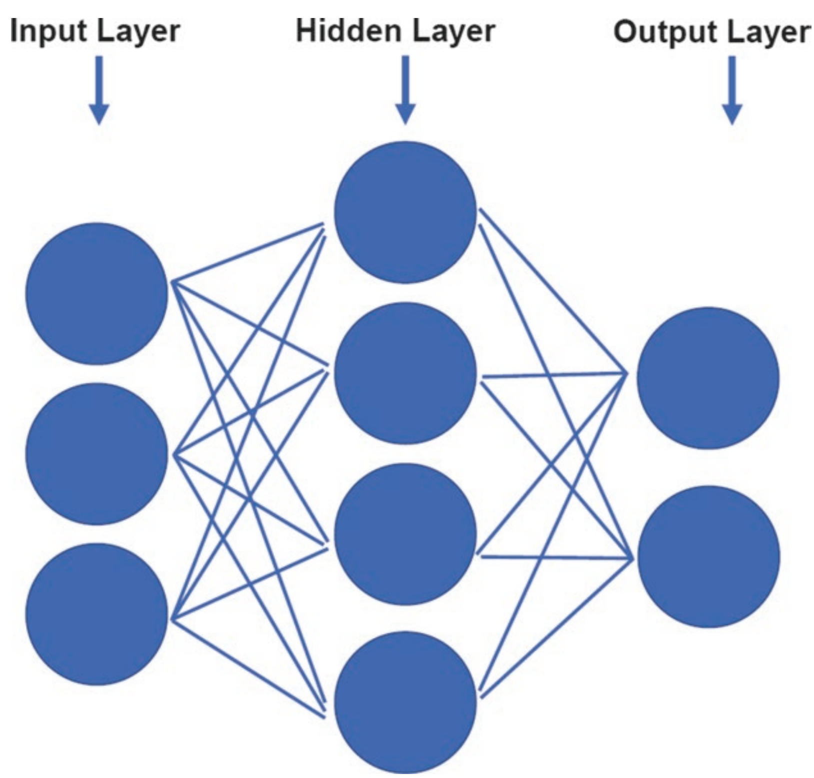

Although the mathematical models of simple, three layer (*input layer, hidden layer, and output layer*) neural networks themselves have been in use since the 1940s [13]. However, a combination of technological advancements in our modern era has enabled the development of much larger neural networks containing *multiple* hidden layers. These contemporary advancements include the availability of massive data sets, the creation of powerful computer processors, the development of cloud computing to store vast amounts of data, and the accessibility of open-source neural network platforms, such as Google's TensorFlow [12]. These much larger neural networks, known as deep neural networks (DNN), have incredibly powerful capabilities. If AI is like the industrial revolution, then its "steam engines" are DNNs.

In order to use a neural network, these algorithms must first undergo a learning phase known as *training*. During the training process, vast amounts of data are fed into the algorithm: a neural network for reading chest X-rays, for instance, was trained on over 100,000 roentgenographs. In so-called supervised learning, a neural network may receive data that has already been partially *labeled*, teaching a machine to learn how to identify a given characteristic (for example, learning to recognize an X-ray containing pneumonia and distinguish this from an X-ray without pneumonia). In *unsupervised learning*, neural networks are allowed to classify data (often, in order to make predictions), without explicit labeling imposed by the human programmer. As will be discussed later, it is critical that care be taken when selecting which data is used to train a neural network: *data collected in a biased fashion will train a neural network to incorporate these biases into its own algorithm and behavior.*

Impact of AI and ML in Surgery

Although AI and ML are still in their infancy within surgery (and within the field of medicine as a whole), these technologies are already being deployed in a variety of ways. Here, we examine various examples of current applications of AI, as well as potential uses which lie along the immediate horizon.

One of the logical first steps for incorporating AI into surgical practice would be to leverage its capabilities to simply *augment* the diagnostic skill and acumen which clinicians already possess. Indeed, a growing variety of examples highlight the role of AI as a kind of "helper." Colonoscopy, for instance, provides a clear opportunity for this role. While expert endoscopists can accurately make a visual distinction between hyperplastic polyps and neoplastic polyps (adenomas) during colonoscopy, research suggests that general endoscopists, without fellowship-level training, may not be as effective at making this determination [14]. As a result, diagnostic AI algorithms (known as computer-aided diagnosis, or CAD) are being developed to help endoscopists better distinguish between adenomas and hyperplastic polyps. In a multicenter study in Japan, Mori and colleagues were able to demonstrate that their CAD system was capable of distinguishing rectosigmoid adenomas from hyperplastic polyps with an accuracy of 94% and a negative predictive value of 96%, all in real time during the actual procedure [15]. While their study did have limitations – their software was only useful in the sigmoid colon and was less effective at detecting sessile, serrated polyps – it nonetheless provides an intriguing glimpse into how AI may be blended into diagnostic procedures such as upper and lower endoscopy [16].

Another potential avenue for AI to augment a surgeon's clinical skillset is through the use of automated algorithms to review radiographic imaging for detecting abnormal findings. In 2017, a group of Stanford University radiologists asked whether AI could be trained to reliably identify pneumonia on chest X-rays [17]. Beginning with a data set of over 100,000 chest X-rays, they utilized a 121-layer DNN for the task. Not only were the researchers able to demonstrate comparable accuracy in diagnosing pneumonia between their algorithm and human radiologists, they were able to show similar findings with over a dozen other pulmonary pathologies including atelectasis, effusion, nodule, pneumothorax, emphysema, fibrosis, pleural thickening, and more [17]. While few surgeons would ever relinquish reviewing their own films, it is conceivable that this type of technology could be used as an early detection system to alert a surgeon of a radiographic abnormality in a film that has not yet been viewed and interpreted by a human.

Perhaps even more fascinating than these applications – in which AI serves as a very basic helper to the surgeon – is the ability of neural networks to extract far more complex and nuanced meaning from data. Consider a rudimentary pixel. With the naked eye, clinicians can appreciate the relative brightness of pixels on a radiographic image. And by leveraging a nearly ubiquitous feature in today's PACS (picture archiving and communication system) software, clinicians can calculate Hounsfield units, allowing them to determine and quantify the radiodensity – using this approach to infer tissue (or fluid) type. DNNs, however, have the potential to unlock an entire universe of information within each pixel; such as texture, dye enhancement, signal intensity, and more [12].

At Harvard University, for instance, a group of clinicians used ML to extract new information from data (both pathology data and radiographic data) in order to make predictions not otherwise possible for a human clinician [18]. Leveraging a database of 1006 biopsy-proven, high-risk lesions (defined as lesions which included ADH, atypical lobular hyperplasia, biphasic neoplasms, flat epithelial atypia, lobular carcinoma in situ, nonspecific atypia, papillomas, and radial scars), the researchers trained an ML model to make inferences between radiographic features and the eventual definitive pathologic diagnosis. They then tested the algorithm they had developed, demonstrating the ability to successfully predict the risk of upgrading a high-risk lesion to cancer following its definitive excision. Such information could, in the future, be used to avoid surgical excision for certain patients.

As this ML application with breast lesions demonstrates, some of AI's greatest potential for surgery and medicine lies in its ability to find nuances within data and to make connections with that information in ways that human researchers might not otherwise be able to conceive. In a separate study at Harvard University, for instance, researchers leveraged a deep learning neural network to predict KRAS mutation status of colorectal liver metastases, based simply on the MRI characteristics of the lesions. Their predictions reportedly had a greater than 95% accuracy rate [19].

The more sophisticated deep neural networks become, the more ability they will have to make surprising connections and inferences from data that, to humans, might otherwise seem uninformative. In the future, AI algorithms encoded into a hospital's electronic medical record (EMR) could be used to scan a patient's real-time vital signs, connecting seemingly unrelated, mundane fluctuations in vital signs to predict an adverse event – for example, pulmonary embolism or myocardial infarction – before (or just as) the event transpires. DL algorithms may be the norm in tumor boards of the future, melding with the voices of seasoned experts in the room to predict a patient's unique response to chemotherapy or likelihood of cure from resection. It is no exaggeration to say that the possibilities are truly limitless.

Finally, while the concept of a robot surgeon that entirely replaces human surgeons in the operating room does not appear tangible, it is worth mentioning that indeed there are early prototypes of robots able to autonomously carry out specific tasks previously limited to humans. Most notable among these is the so-called STAR system, or Smart Tissue Autonomous Robot, developed by a team at Children's National Health System in Washington, DC [20]. In an in vivo porcine model, these researchers were able to demonstrate that STAR could perform a complete, end-to-end, "machine-sewn" bowel anastomosis – comparable in quality to anastomoses performed by human surgeons as controls.

Risks and Pitfalls of Artificial Intelligence

As AI and ML become increasingly integrated into surgery and medicine, it is critical for physicians to remain wary of the practical and ethical risks raised by these technologies. To date, many of the applications that leverage AI and ML in serve as tools that augment the very skills surgeons themselves already possess. An algorithm trained to recognize pneumonia can be a useful adjunct to the busy clinician, but this ultimately performs a task that the surgeon must confirm. However, as AI becomes increasingly advanced, particularly in its ability to make predictions or form connections between vast amounts of data, clinicians may increasingly find themselves in the dilemma of acting on clinical information provided by an algorithm without being able to confirm its veracity.

What happens, then, when the algorithm makes an error? Is the physician liable for this mistake, or is it the company that produced the software? Should a software algorithm be required to pass through the same FDA clearance and approval process as other therapeutics? Should patients be required to give their consent for any element of AI involved in their care? These are difficult questions that must be carefully considered now, while the field is in its infancy.

An even more insidious risk posed by the use of artificial intelligence in medicine is the potential for bias to be incorporated into neural networks. DNNs that have been trained to carry out a particular skill, such as making radiographic diagnoses or creating predictions from clinical data, must first learn these skills by being fed large volumes of data upon which to train. Unfortunately, however, bias inadvertently incorporated into this training data will ultimately be propagated through the algorithm itself. In the nonmedical world, this issue of bias within AI was famously illustrated in Google's public struggles with its own algorithms. In one study, for instance, researchers from Carnegie Mellon demonstrated that men were shown Google ads for higher-paying job opportunities than their female counterparts [21]. The US criminal justice system has also faced major concerns of bias influencing its own AI algorithms: in 2016, ProPublica published an article exploring a tool, known as COMPAS, that is used to help a judge predict the likelihood that a defendant will commit a new crime in the future. The article demonstrated how the software was biased against African Americans [22].

This same potential for bias has a very real risk in medicine. Suppose a neural network is trained to recognize breast lesions, using data from studies that predominantly included patients of white, European ancestry. If this algorithm is later generalized to a different population, *its ability to properly diagnose those same lesions in patients of other ethnicities may be compromised.* Furthermore, even less straightforward situations of bias can reverberate down the line in an algorithm's ability to be used. At what point is a set of training data generalizable to an *overall* population? How can an AI algorithm – especially one licensed from an outside vendor – be properly vetted? Careful oversight will be crucial to safe and effective use of DNNs as they become more widespread.

Will AI Replace Doctors?

Though occasionally raised by the lay press, the question of AI replacing surgeons – or, altogether displacing physicians – is *not* likely, at least for the foreseeable future.

Today, even the most sophisticated examples of DNNs are all examples of what is called "narrow AI," or AI that is focused on one specific task. Contrast this, for instance, with the type of intelligence possessed by humans, also known as *general intelligence.* The simple acts of having a conversation, or putting on a pair of shoes, or walking down a flight of steps without looking at one's feet, are all incredibly complex operations that in themselves require thousands of individual skills, all woven together. Being able to synthesize these skills – through what would be called *artificial general intelligence* – would require exponential breakthroughs not only in the field of AI as a whole, but in the very physics of modern-day computing.

From a much more pragmatic view, however, AI will revolutionize much of the world of medicine – surgery included. Despite the challenges posed by avoiding bias within neural networks and the legal risks of liability incurred by using these new technologies, it is likely that AI will touch nearly every aspect of a surgeon's clinical life – from AI screening tools built into EMR's that surface the most relevant information when it is needed most to virtual, AI scribes that let clinicians speak to a patient without typing, to sophisticated algorithms that predict likelihood of tumor recurrence, to first-assist robots capable of independently helping a solo surgeon carry out an operation in a rural setting. All of these technologies already exist in some form. Entering them into common clinical use is soon to be expected. To paraphrase a sentiment held by many of today's thought leaders in digital health and medicine: *Will AI replace doctors? No. But doctors who use AI will replace doctors who don't.*

References

1. Poole D, Mackworth A, Goebel R. Computational intelligence: a logical approach. New York: Oxford University Press; 1998.. ISBN 978-0-19-510270-3.
2. Solomonoff RJ. The time scale of artificial intelligence; reflections on social effects. Hum Syst Manag. 1985;5:149–15.
3. A proposal for the Dartmouth Summer Research Project on Artificial Intelligence. [cited 1 Oct 2019]. Available from: http://www-formal.stanford.edu/jmc/history/dartmouth/dartmouth.html.
4. Russell SJ, Norvig P. Artificial intelligence: a modern approach. 2nd ed. Upper Saddle River: Prentice Hall; 2003, ISBN 0-13-790395-2.
5. Crevier D. AI: the tumultuous search for artificial intelligence. New York: BasicBooks; 1993, ISBN 0-465-02997-3.
6. Clark J. Why 2015 was a breakthrough year in artificial intelligence. Bloomberg News. 8 Dec 2015.
7. Ransbotham S, Kiron D, Gerbert P, Reeves M. Reshaping business with artificial intelligence. MIT Sloan Manag Rev. 6 Sept 2017. Retrieved 2 May 2018.
8. Bishop CM. Pattern recognition and machine learning. New York: Springer; 2006, ISBN 978-0-387-31073-2.
9. Ashwani C, Manu S. Searching and optimization techniques in artificial intelligence: a comparative study & complexity analysis. International Journal of Advanced Research in Computer Engineering & Technology (IJARCET). 2014;3(3)
10. Zagorecki A, Orzechowski P, Hołownia K. A system for automated general medical diagnosis using Bayesian networks. Stud Health Technol Inform. 2013;192:461–5.
11. Suchánek P, Marecki F, Bucki R. Self-learning Bayesian networks in diagnosis. Procedia Computer Science. 2014;35:1426–35.
12. Topol EJ. Deep medicine: how artificial intelligence can make healthcare human again. New York: Basic Books; 2019.
13. McCulloch W, Pitts W. A logical calculus of ideas immanent in nervous activity. Bull Math Biophys. 1943;5(4):115–33. https://doi.org/10.1007/BF02478259.
14. Stegeman I, van Doorn S, Mallant-Hent R, van der Vlugt M, Mundt M, Fockens P, et al. The accuracy of polyp assessment during colonoscopy in FIT-screening is not acceptable on a routine basis. EIO. 2014;2(03):E127–32.
15. Mori Y, Kudo SE, Misawa M, et al. Real-Time Use of Artificial Intelligence in Identification of Diminutive Polyps During Colonoscopy: A Prospective Study. Ann Intern Med. 2018;169(6):357–66.
16. Holme Ø, Aabakken L. Making colonoscopy smarter with standardized computer-aided diagnosis [Internet]. Ann Intern Med. American College of Physicians; 2018 [cited 18 Oct 2019]. Available from: https://annals.org/aim/article-abstract/2697090/making-colonoscopy-smarter-standardized-computer-aided-diagnosis.
17. Rajpurkar P, Irvin J, Zhu K, Yang B, Mehta H, Duan T, et al. CheXNet: radiologist-level pneumonia detection on chest X-rays with deep learning. arXiv:171105225 [cs, stat] [Internet].14 Nov 2017 [cited 16 Oct 2019]; Available from: http://arxiv.org/abs/1711.05225.
18. Bahl M, Barzilay R, Yedidia AB, Locascio NJ, Yu L, Lehman CD. High-risk breast lesions: a machine learning model to predict pathologic upgrade and reduce unnecessary surgical excision. Radiology. 2018;286(3):810–8.
19. Machine learning can help predict KRAS mutation status [Internet]. AuntMinnie.com. [cited 1 Oct2019]. Available from: https://www.auntminnie.com/index.aspx?sec=rca&sub=rsna_2017&pag=dis&ItemID=119308.
20. Shademan A, Decker RS, Opfermann JD, Leonard S, Krieger A, Kim PCW. Supervised autonomous robotic soft tissue surgery. Sci Transl Med. 2016;8(337):337ra64.
21. University CM. Questioning the fairness of targeting ads online – news – Carnegie Mellon University [Internet]. [cited 17 Oct 2019]. Available from: http://www.cmu.edu/news/stories/archives/2015/july/online-ads-research.html.
22. Julia Angwin JL. Machine Bias [Internet]. ProPublica. 2016 [cited 17 Oct 2019]. Available from: https://www.propublica.org/article/machine-bias-risk-assessments-in-criminal-sentencing.

24 AI and Endoscopy: Future Perspectives

Daljeet Chahal, Neal Shahidi, and Michael F. Byrne

Abbreviations

ADR	Adenoma detection rate
AFI	Autofluorescence imaging
AI	Artificial intelligence
AQCS	Automated quality control system
ASGE	American Society for Gastrointestinal Endoscopy
AUROC	Area under receiver operating characteristic curve
BBPS	Boston bowel preparation score
BE	Barrett's esophagus
BLI	Blue light imaging
CE	Capsule endoscopy
CEA	Carcinoembryonic antigen
CLE	Confocal laser endomicroscopy
CNN	Convolutional neural network
CROE	Central reading of endoscopy
DL	Deep learning
EAC	Esophageal adenocarcinoma
EFTR	Endoscopic full-thickness resection
EMR	Endoscopic mucosal resection
ESCC	Esophageal squamous cell carcinoma
ESD	Endoscopic mucosal dissection
EUS	Endoscopic ultrasound
FDA	Food and Drug Administration
FICE	Flexible spectral imaging color enhancement
HP	*Helicobacter pylori*
HRME	High-resolution microendoscopy
IEE	Image-enhanced endoscopy
IPCL	Intrapapillary capillary loop
IPMN	Intraductal papillary mucinous neoplasms
LCI	Linked color images
LIFS	Laser-induced fluorescence spectroscopy
ML	Machine learning
NBI	Narrowband imaging
NICE	Narrow-Band Imaging International Colorectal Endoscopic
NPV	Negative predictive value
PIVI	Preservation and incorporation of valuable endoscopic innovations
PPV	Positive predictive value
SAE	Society of Automotive Engineers
UC	Ulcerative colitis
VLE	Volumetric laser endomicroscopy
WL	White light

D. Chahal · N. Shahidi
Department of Gastroenterology, University of British Columbia, Vancouver, BC, Canada

M. F. Byrne (✉)
Department of Gastroenterology, Vancouver General Hospital, University of British Columbia, Vancouver, BC, Canada
e-mail: michael.byrne@vch.ca

S. Atallah (ed.), *Digital Surgery*, https://doi.org/10.1007/978-3-030-49100-0_24

Introduction

Artificial intelligence (AI) refers to a set of machine and computational functions that attempts to mimic human cognitive function [1]. AI is not a new field, with inquiries into its possibilities beginning as far back as the 1950s [2]. With the exponential increase in computer processing power, AI has grown to where computers can perform a variety of tasks without explicit instruction, termed machine learning (ML) [3].

Early ML models were dependent on user-selected *features* that define an object of interest. This inherently restricted their ability to adapt and thus limited their real-world application. The introduction of deep learning (DL) and convolutional neural networks (CNNs) revived the field of AI [4], leading to the recent proliferation of AI-related research and development. AI models are now able to "learn," resulting in significant improvements in algorithm performance. This has facilitated AI's permeation into aspects of everyday life [5].

Endoscopy is a field reliant on imaging. There is a growing interest in AI's ability to increase the sensitivity and specificity of various endoscopic-enhanced imaging modalities. Recent AI platforms, based on DL, CNNs, and similar techniques, have demonstrated comparable performance characteristics to expert endoscopists. In this chapter, we will review the current and future applications of AI within the gastrointestinal tract. Moreover, we will discuss relevant ethical and regulatory considerations.

It should be noted that many AI algorithms in endoscopy have been developed in accordance with currently available endoscopic imaging modalities. Image-enhanced endoscopy (IEE) modalities include, but are not limited to, standard white light (WL) endoscopy, dye-based chromoendoscopy, virtual chromoendoscopy (e.g., narrowband imaging [NBI], flexible spectral imaging color enhancement [FICE], blue light imaging [BLI], I-scan), endocytoscopy, confocal laser endomicroscopy (CLE), laser-induced fluorescence spectroscopy (LIFS), and autofluorescence imaging (AFI). Detailed explanations of these modalities are beyond the scope of this chapter.

Colorectal Neoplasia

The ability of colonoscopy to mitigate the incidence and mortality of colorectal cancer is dependent on the endoscopist's ability to detect colorectal lesions [6, 7]. Unfortunately, the frequency of missed adenomas, advanced adenomas, and serrated lesions can be as high as 26%, 9%, and 27%, respectively [8].

With the introduction of high-definition endoscopy and IEE, the endoscopist now has the ability to predict lesion histopathology during optical evaluation. The American Society for Gastrointestinal Endoscopy (ASGE) Preservation and Incorporation of Valuable Endoscopic Innovations (PIVI) recommendations provide performance thresholds for the use of the "resect and discard" and the "diagnose and leave" strategies, whereby diminutive adenomas can be resected without histopathology review and diminutive distal hyperplastic polyps can be left in situ, respectively. However, these performance thresholds are not reliably achieved [9, 10] except by endoscopists with expertise in optical evaluation [11].

AI platforms have demonstrated the ability to improve lesion detection rates and optical evaluation performance, therefore carrying the potential to improve both patient outcomes and resource utilization [12, 13].

Adenoma Detection

Early AI validation studies for adenoma detection using non-DL technologies were experimental in nature, but have reached accuracies of greater than 90% [14–16].

A CNN for automated polyp detection, by Misawa and colleagues, achieved a sensitivity of 90% and specificity of 63% (based on evaluation of 135 videos) [17]. An alternative CNN, by Urban and colleagues, was developed on a dataset of 8641 images. The area under the receiver operating characteristic (AUROC) curve for polyp recognition was 0.991 with an accuracy of 96%; this outperformed expert endoscopists [18] (Fig. 24.1). Wang and colleagues developed a CNN from 27,113 images and 192 recordings

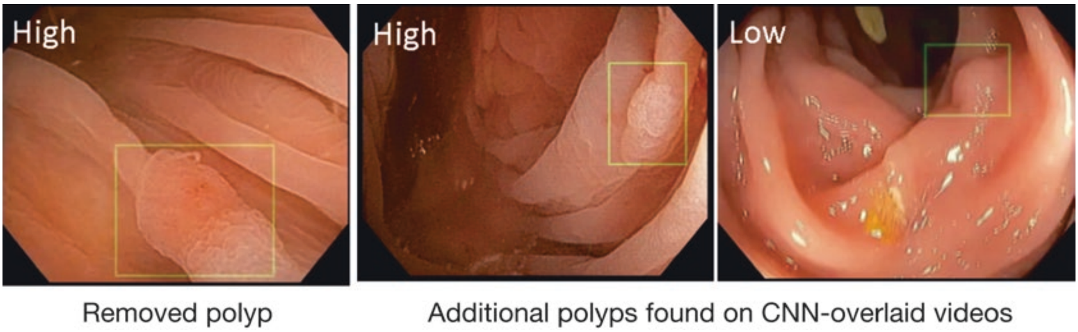

Fig. 24.1 Frame shot of CNN overlaid on colonoscopy videos. A polyp is detected with greater than 95% confidence when a green box is present. The location and size of the box are in accordance with the suspected polyp. The text in the upper left of the endoscopic image represents expert confidence of a true polyp. (Reprinted with permission from Urban et al. [18])

with validation using 612 images [19]. Sensitivity and specificity were both greater than 90%, with evaluation at 25 frames per second. Lastly, a CNN designed to segment visualized polyps from background mucosa, developed from 912 images, achieved accuracy of greater than 90% [20]. One can easily imagine how automated detection could improve endoscopist adenoma detection rate (ADR), decreasing the rate of interval cancers and resulting in improvement in overall patient outcomes.

Optical Evaluation: Narrowband Imaging

NBI is the most extensively studied modality with regards to AI polyp characterization. Early, non-DL-based methods extracted a variety of features from images and were eventually able to achieve pseudo-real-time endoscopic characterization of adenomas [21–24]. DL AI techniques have only been recently applied. A DL model, by Byrne and colleagues, using 125 unaltered endoscopic videos was able to identify adenomas with a sensitivity and specificity of 98% and 83%, respectively [25] (Fig. 24.2). The negative predictive value (NPV) was 97% and the positive predictive value (PPV) was 90%. Another DL model, by Chen and colleagues, using 284 diminutive polyps was successful in identifying hyperplastic or neoplastic polyps with a sensitivity of 96%, specificity 78%, NPV 91%, and PPV 90% [26]. Both of these studies achieved PIVI-2 per-

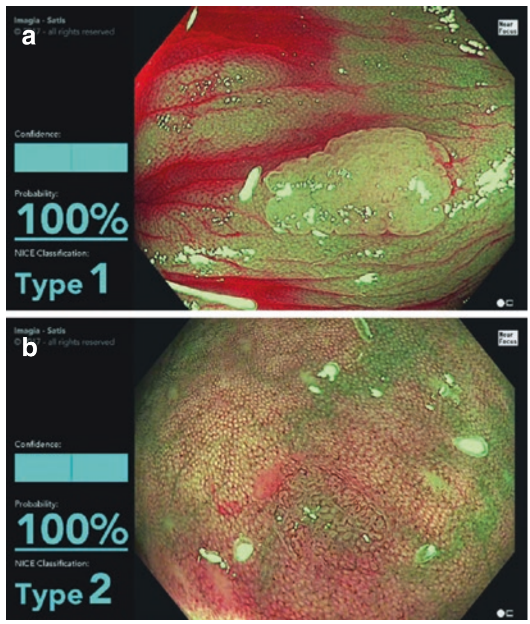

Fig. 24.2 (**a**) Evaluation of a hyperplastic polyp (NICE Type 1). The model displays the lesion type and probability. (**b**) A conventional adenoma (NICE Type 2). Again, the type of lesion and probability are displayed. NICE, Narrow-Band Imaging International Colorectal Endoscopic. Reprinted with permission from Byrne MF et al. [25]. Open access article distributed in accordance with the Creative Commons Attribution Non-Commercial (CC BY-NC 4.0)

formance thresholds for the "diagnose and leave" strategy. Such models demonstrate how real-time characterization of polyps will allow endoscopists to decide not only which polyps warrant resection, but also on an optimal resection technique.

Optical Evaluation: Chromoendoscopy, Endocytoscopy, and Confocal Laser Endomicroscopy

Chromoendoscopy non-DL AI models have been shown to improve endoscopic diagnostic capabilities [27, 28]. Nuclear areas and microvessels have also been analyzed to identify neoplastic changes and detect invasive cancer [17, 29, 30]. A prospective study using endocytoscopy and non-DL AI methodology (EndoBRAIN, Cybernet System Co., Tokyo, Japan) involving 466 diminutive polyps recently demonstrated an NPV of 94% for characterizing rectosigmoid adenomas in real time [31] (Fig. 24.3). CLE and non-DL AI methods have been combined to diagnose adenomatous colorectal polyps and colorectal adenocarcinomas with accuracies of 90% and 85%, respectively [32, 33]. DL AI techniques have yet to be applied to these modalities.

Optical Evaluation: Laser-Induced Fluorescence Spectroscopy (LIFS) and Autofluorescence Imaging (AFI)

LIFS and non-DL AI have been successfully used to differentiate adenomatous polyps [34]. Prospective studies have demonstrated conflicting NPVs of 96% and 74%, respectively [34, 35]. For

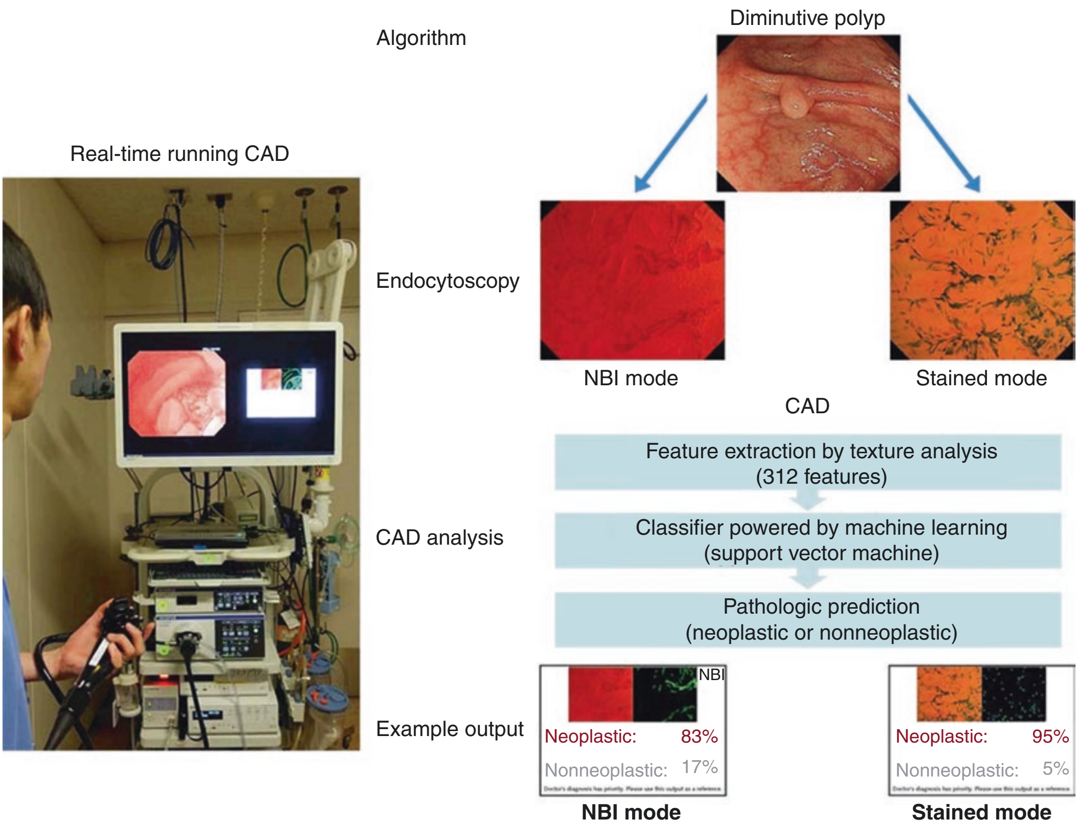

Fig. 24.3 Fully automated computer-assisted diagnosis is triggered by pushing the endoscope capture button. This algorithm analyzes texture, classifies the image, and then predicts pathology. Outputs are predicted as neoplastic or nonneoplastic, and a probability of diagnosis is provided. (Reprinted with permission from Mori et al. [31])

AFI, the ratio of green to red fluorescence after stimulation can be used to identify images with a high likelihood of neoplasia. A prospective study of 102 colorectal lesions using non-DL AI and AFI demonstrated that a green/red cutoff ratio of 1.01 could discriminate neoplastic from nonneoplastic lesions with sensitivity of 94% and specificity of 89% [36]. Again, DL methods have yet to be applied to either LIFS or AFI.

Future Possibilities in Colonoscopy

Ongoing application of AI for use in colonoscopy is only limited by our imagination. Automated adenoma detection and characterization will eventually be integrated in a seamless workflow. However, we can envision beyond this immediate possibility. What if we could predict how fast any particular adenoma could grow into invasive carcinoma? What if we could model the behavior of possible malignancy and which local structures it may invade – and thus inform radiological investigations? Could we characterize adenomas that have been incompletely resected? Could optical image data be combined with clinical metadata to predict personalized surveillance intervals? These are interesting questions which deserve further exploration.

Esophageal Neoplasia

Identification of Barrett's Esophagus and Esophageal Adenocarcinoma

Barrett's esophagus (BE) is currently sampled via random biopsies resulting in relatively low per-lesion sensitivity of 64% for dysplasia detection [37]. The ASGE has endorsed IEE modalities to carry out targeted rather than random biopsies, but NPV thresholds remain out of reach for nonexperts [38]. Non-DL algorithms based on texture and color for conventional endoscopic images as well as volumetric laser endomicroscopy (VLE) have been used to characterize neoplastic lesions with sensitivities and specificities exceeding 90% [39, 40]. DL methods for BE and esophageal adenocarcinoma (EAC) are in early stages of development. A CNN, by Fonolla and colleagues, evaluated images from only 45 patients; an AUROC of 0.96 was achieved [41]. Another CNN, by Ebigo and colleagues, trained on 148 WL and NBI images of 33 EACs as well as 41 images of nonneoplastic BE, was able to diagnose EAC with a sensitivity and specificity of 97% and 88% for WL images and 94% and 80% for NBI images, respectively [42]. Thirteen endoscopists achieved sensitivity and specificity of 86% and 80%, respectively.

Identification of Esophageal Squamous Cell Carcinoma

Identification of esophageal squamous cell carcinoma (ESCC) is currently limited by operator expertise, creating an opportunity for AI [43, 44]. A non-DL technique using contact high-resolution microendoscopy (HRME) was able to identify malignant tissue effectively [45, 46]. A DL CNN, by Horie and colleagues, developed with 8428 images of esophageal cancer from 384 patients, has demonstrated promising results [47] (Fig. 24.4). Testing on 1118 test images from 47 patients with cancer and 50 patients without cancer revealed a sensitivity of 98%. All lesions (n = 7) that were ≤10 mm in size were detected. Superficial cancer could be differentiated from advanced cancer with an accuracy of 98%. A CNN, by Everson and colleagues, based on intrapapillary capillary loop (IPCL) classification, was able to differentiate abnormal patterns with an accuracy, sensitivity, and specificity of 94%, 89%, and 98%, respectively [48]. A CNN, by Kumagai and colleagues, developed for an endocytoscopic system trained on 1141 malignant and 3574 nonmalignant images was able to diagnose ESCC with an accuracy of 91% [49].

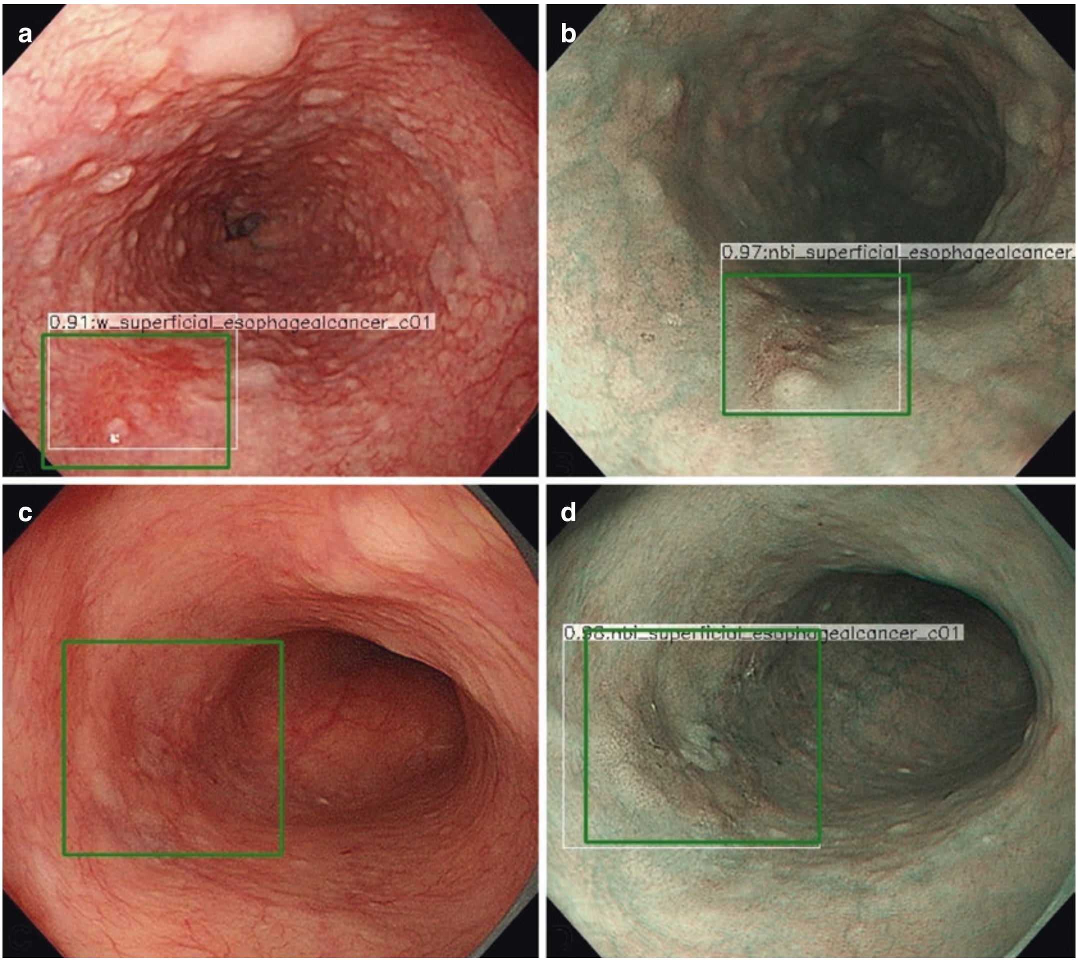

Fig. 24.4 CNN-based diagnosis of esophageal cancer using WL and NBI. In images (**a**) and (**b**), the CNN recognized cancer (white square) and was matched with the endoscopists' diagnosis (green square). In image (**c**), the CNN was unable to diagnose cancer when in WL but was able to diagnose when switched to NBI in image (**d**) (white square). (Reprinted with permission from Horie et al. [47])

Gastric Neoplasia

Identification of Gastric Cancer

The endoscopic presentation of early gastric cancer can be extremely subtle, making identification difficult, especially amongst western endoscopists. Non-DL models applied to magnifying FICE and blue laser imaging (BLI) images have been able to detect early gastric cancer with accuracy, sensitivity, and specificity all exceeding 80% [50, 51]. A CNN, by Hirasawa and colleagues, trained on 13,584 conventional endoscopic images was able to analyze 2296 test images in 47 seconds and correctly diagnosed 71 of 77 gastric cancers with a sensitivity of 92% [52]. A CNN, by Ishioka and colleagues, utilizing videos of 68 cases of early gastric cancer, was able to detect 64 of 68 cancers with a median time of 1 second [53]. Another CNN, by Wu and colleagues, trained using 3170 still gastric cancer images and 5981 benign lesions diagnosed malignancy with an accuracy of 92%, outperforming 21 endoscopists [54]. A CNN platform, by Wu and colleagues, developed to improve gastric cancer screening automatically detected blind spots and generated photo-documentation in a clinical trial of 324 patients and resulted in a 15% reduction of missed sites [55]. This platform achieved this reduction by ensuring increased inspection times and completeness of photo-documentation. Millions of patients undergo upper endoscopy every year, but the quality of endoscopy varies significantly. High-quality endoscopy is known to improve health outcomes, and as such, platforms such as this which result in better quality of procedure will have a large positive impact on patients.

Gastrointestinal Neoplasia

Depth of Invasion Assessment

Minimally invasive endoscopic resection techniques have revolutionized the management of gastrointestinal neoplasia. This includes endoscopic mucosal resection (EMR) and organ-sparing curative resection techniques such as endoscopic submucosal dissection (ESD) and endoscopic full-thickness resection (EFTR). *To select the appropriate technique, the endoscopist must predict lesion depth of invasion, as this is a core component to organ-specific definitions of a curative endoscopic resection* [56]. Optical evaluation is the primary method for predicting lesion depth of invasion, specifically for early cancers, due to the limitations of relying on lesion biopsy and radiologic evaluation. However, optical evaluation has demonstrated modest performance characteristic for clinically relevant depth of invasion stratification, even amongst experts. Therefore, AI platforms have been developed for the esophagus, stomach, and colorectum.

In relation to esophageal cancer, a CNN developed by Horie and colleagues using 8428 WL and NBI images was able to differentiate early (T1) from advanced (T2-T4) ESCC and EAC with accuracy of 98% [47]. Accuracy was higher for ESCC (99%) than EAC (90%). Another CNN, by Nakagawa and colleagues, trained on 8660 nonmagnified and 5679 magnified WL, NBI, and chromoendoscopy images differentiated M-SM1 (mucosal-submucosal) disease from SM2-3 disease in the esophagus with 91% accuracy and outperformed 16 endoscopists [57]. A CNN, by Zhao and colleagues, for differentiating esophageal invasion depth based on IPCL classification had an accuracy of 89%, outperforming junior- to mid-level endoscopists [58].

Analysis of depth of invasion of gastric cancer has also been explored [59]. A CNN developed on endoscopic images from 344 gastric cancer patients demonstrated diagnostic accuracies of 77%, 49%, 51%, and 55% for T1, T2, T3, and T4 stages, respectively. Further advancements by Zhu and colleagues resulted in an algorithm that was able to identify SM2 or deeper (>500-μm invasion into the submucosa) lesions with sensitivity of 76% and specificity of 96%, significantly better than the observed accuracy of 63% achieved by 17 endoscopists [60] (Fig. 24.5).

As for the colon, one platform has been developed to differentiate between adenomatous lesions and invasive cancer [30]. A total of 5843 endocytoscopic images from 375 colorectal lesions were used to train the model, with 200 of these same images used for validation. The model had an impressive accuracy of 94%.

The future of *depth of invasion* assessment and determination is quite exciting. Not only are there implications for therapeutic procedures, but also for the basic biology of these lesions. Much of the biologic characterization of lesions has been conducted in fully developed malignancies, specifically because such samples have been accessible after surgical resection. With appropriate depth characterization combined with EMR and ESD, early lesions will become available for study. *Combining clinical, molecular, and radiologic data with features extracted from optical endoscopy may allow us to create AI models which exquisitely characterize these lesions and predict their behavior*. In turn, such data will allow us to make even more informed decisions about which lesions warrant endoscopic resection.

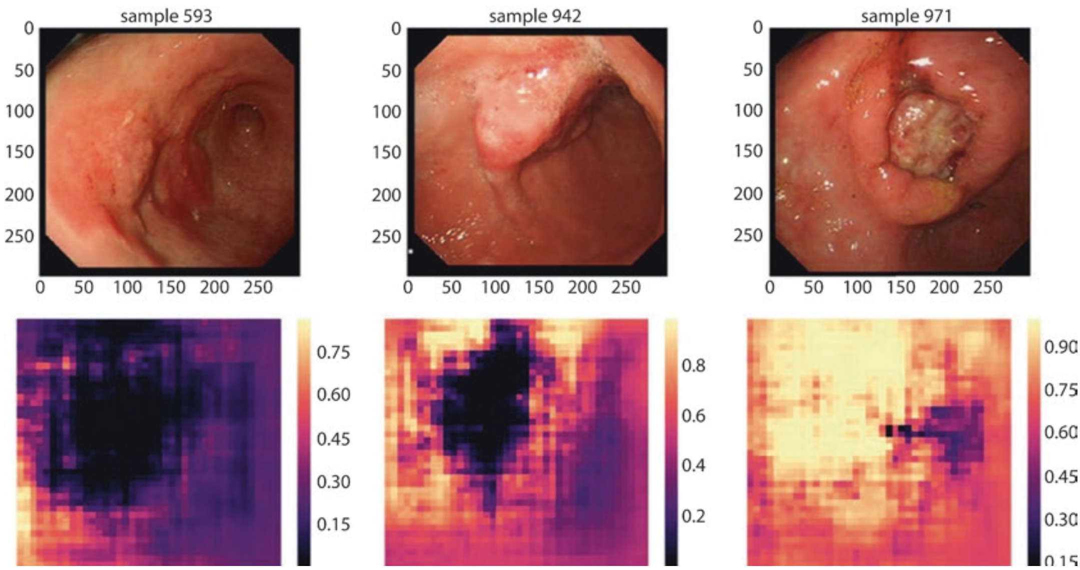

Fig. 24.5 Endoscopic images and heatmaps generated during gastric depth of invasion assessment. The heatmap represents an attempt to identify which part of the endoscopic image was most crucial to identifying lesions as SM2 or deeper. (Reprinted with permission from Zhu et al. [60])

Capsule Endoscopy

Capsule endoscopy (CE) is an operator-independent endoscopic modality intended to evaluate diseases of the gastrointestinal tract, although it is currently mostly used for evaluating the small intestine [61]. To date, colon capsule endoscopy has proved challenging for the reader. Reading capsule endoscopies in general, even for small bowel, can be a monotonous and time-intensive task, given the examination length. Diagnoses can be missed, as pathology can be isolated to a single CE frame, manifesting in interreader variability [62].

Organ Classification

Calculating small bowel transit, which is used to estimate a finding's location, is based on identifying the first part of the duodenum and cecum. This can be time consuming, and for the cecum, it can be difficult due to debris obscuring visualization. A CNN to differentiate between stomach, small intestine, and colon, by Zou and colleagues, trained on 15,000 images, demonstrated accuracy of 96% [63].

Lesion Detection

DL approaches for small bowel bleeding include a CNN by Xiao and colleagues, which evaluated 10,000 images (2850 were positive for bleeding). This demonstrated an accuracy of 99% [64]. Another AI model, by Li Panpeng and colleagues, showed an accuracy of 99% when evaluating 1300 bleeding images and 40,000 normal images [65]. A recent CNN model, by Leenhardt and colleagues, using 20,000 normal frames and 2946 frames with vascular lesions, was able to identify angioectasias with an accuracy of 96% [66]. Sensitivity was 100%, specificity 96%, PPV 96%, and NPV 100%. The reading time for an entire CE video was 39 minutes. This study demonstrates that highly accurate diagnostic AI models have been developed, in capsule endoscopy.

Erosions and ulcerations remain the most commonly seen abnormalities during CE. A recently developed CNN, by Aoki and colleagues, based on a single-shot multi-box detector, evaluated 10,440 test images in 233 seconds [67]. Sensitivity, specificity, and accuracy were 88%, 91%, and 91%, respectively.

For the colon, AI-facilitated polyp detection by CE is less developed in comparison to optical colonoscopy. However, there is evolving work in this space. For example, a DL stacked sparse auto-encoder-based approach by Yan and colleagues, which used 4000 images from 35 patients, detected polyps with an accuracy of 98% [68]. Image features were also incorporated into analysis, with each image being labeled as turbid, bubble, or clear.

An interesting application of AI is the detection of hookworms [69]. A DL edge extraction methodology using 440,000 images from 11 patients was able to detect hookworms with accuracy and sensitivity of 89% and 85%.

Detecting Multiple Lesions

Multiple pathologies can be detected during CE. Development of an "all-in-one" algorithm requires software to detect all lesions concurrently. A three-phase approach for detecting multiple lesions at once such as angioectasia, ulceration, and mass lesions, points to such a possibility [70]. This model consisted of a weakly supervised CNN for abnormality classification, deep saliency detection to detect salient points, and iterative cluster unification to localize GI anomalies. The model demonstrated good performance when a large dataset of 10,000 images was used. This approach demonstrates the potential for combining different aspects of the previously mentioned networks into a cohesive network with the potential to detect all gastrointestinal anomalies with a single AI platform.

Other Potential Applications

CE is one of the fastest-evolving fields in endoscopy, and its uses will likely expand beyond detection. The advent of AI-based methods to rapidly sort through the numerous frames obtained during CE and determine which ones are relevant may allow use of CE beyond just the small bowel. Indeed, if an AI algorithm could generate a 3D reconstruction by piecing high-quality images together, CE of the colon could also become widespread. CE is also commonly used to identify bleeding lesions which may be amenable to therapeutic modalities through small bowel balloon enteroscopy. If an AI algorithm could identify the suspect lesion during CE and match it to images obtained during enteroscopy, the endoscopist could be confident they were treating the appropriate lesion. This would lead to improved therapeutic rates and reduction in unnecessary procedures.

Inflammatory Bowel Disease

Endoscopic Severity, Mucosal Healing, and Histologic Healing

Endoscopic disease severity assessment in ulcerative colitis (UC) is a key component of effective patient management. Classification systems have been developed, but interobserver variability is dependent on endoscopist experience [71]. DL models have attempted to automate this process. A CNN, by Ozawa and colleagues, was constructed using GoogLeNet architecture [72]. A total of 26,304 images tagged with the appropriate Mayo score from 841 UC patients was used to train the model to differentiate normal mucosa (Mayo score 0) from a mucosal healing state (Mayo score 0 to 1). Validation was performed on 3981 images from 114 patients and demonstrated an AUROC of 0.86 for identifying normal mucosa and 0.98 for identifying a mucosal healing state. A CNN, by Stidham and colleagues, was trained using 16,514 images from 3082 UC patients to classify patients into a remission group (Mayo score 0 or 1) or a moderate to severe disease group (Mayo score 2 or 3) [73]. A set of 30 full-motion colonoscopy videos, unseen by the model during the training phase, were partitioned into frame-by-frame still images that were used for final validation. The AUROC for distinguishing the two groups from each other was 0.97, with sensitivity of 83% and specificity of 96% (Fig. 24.6). Model performance was similar to experienced reviewers when grading UC severity. The fact that the model could achieve these outcome metrics from

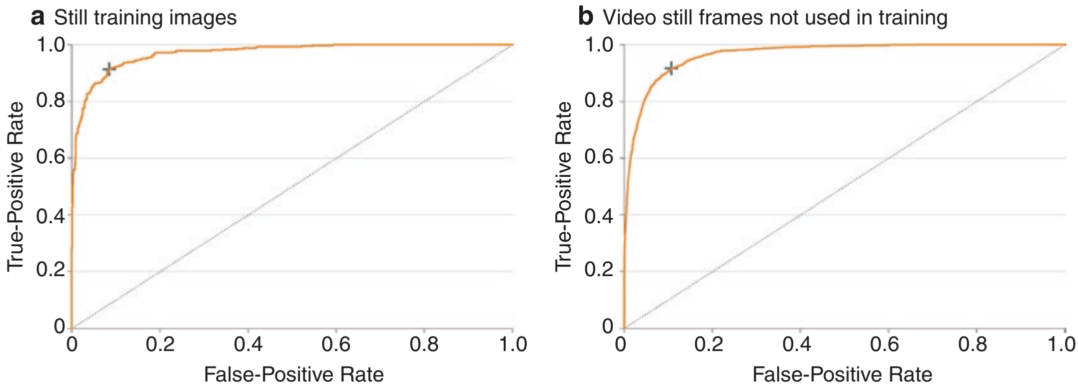

Fig. 24.6 Ability of a CNN to discriminate between endoscopic remission (Mayo 0 or 1) and moderate or severe disease (Mayo 2 or 3). The CNN had an AUROC of 0.97 using both the reference colonoscopy images (**a**) and on a separate set of images from colonoscopy videos not used for model building (**b**). (Reprinted with permission from Stidham et al. [73]. JAMA Network Open)

still images obtained from 30 external videos points towards its real-world applicability. The next step in development would be to apply such technology in real-time endoscopy.

Patient outcomes are also predicated upon histologic disease activity. In UC, persistent histologic inflammation despite mucosal healing on endoscopy increases the risk of disease exacerbation and dysplasia. A non-DL system, by Maeda and colleagues, using magnification endocytoscopy and still images has been able to predict histologic inflammation with an accuracy of 91% [74] (Fig. 24.7). Sensitivity and specificity were also at acceptable with values of 74% and 91%, respectively.

Central Reading of Endoscopy in Inflammatory Bowel Disease Trials

As technology for automated classification and assessment of mucosal healing evolves, it is likely to find use beyond routine clinical practice. A prime example is central reading of endoscopy (CROE) in IBD trials [75]. Currently, a central group of expert endoscopists assesses endoscopic disease activity in pharmaceutical clinical trials. Such an approach theoretically minimizes bias and variation when compared to letting individual centers assess disease activity. Results determine which patients qualify for trials as well as the efficacy of experimental interventions. Controversy exists about the ideal manner in which to implement CROE, with variations in blinding, number of readers, and how to reach diagnostic consensus. Although this has not been evaluated in the literature, it is not difficult to envision how a DL algorithm could overcome these limitations. At the very least, this approach could help standardize the process and improve efficiency.

Reclassification of Disease Activity

IBD management is dependent on the assessment of disease activity both clinically and endoscopically. At present, endoscopic classification is mainly limited to 3 disease severities (Mayo Score) based on endoscopic assessment by the human eye. Interestingly, we do not take into account the total surface area of bowel affected. For example: Is a bowel with 50% of its area affected by Mayo 3 activity the same as a bowel with only 10% affected? Most likely not. In reality, endoscopic disease activity may be much

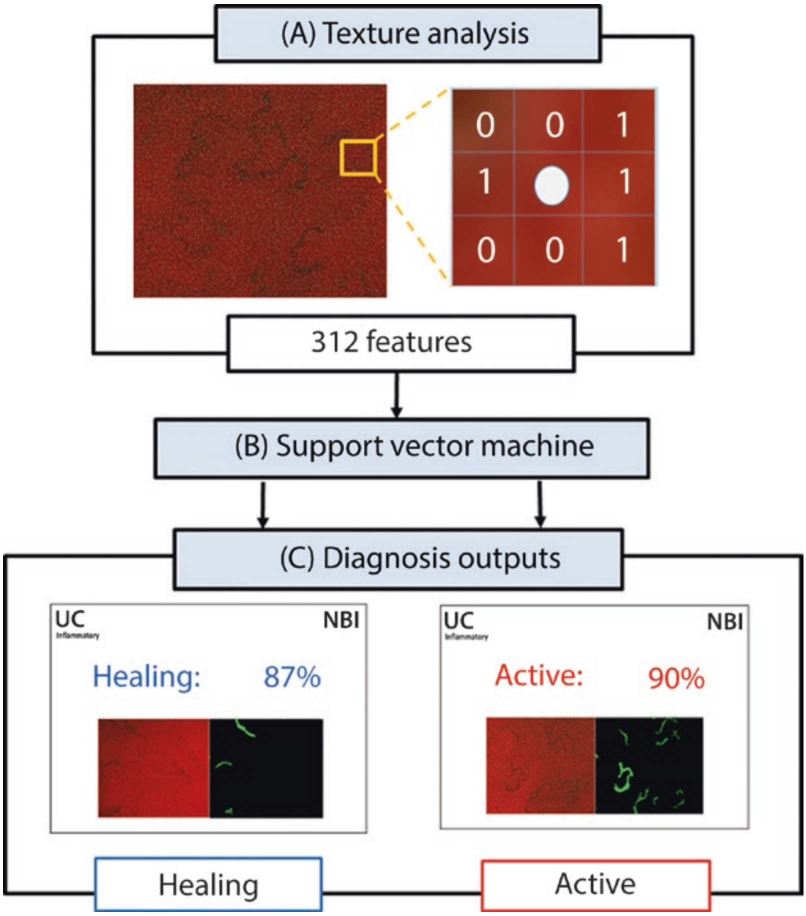

Fig. 24.7 Algorithm used during endocytoscopy to predict histologic activity. The algorithm first performed texture analysis (**a**) and then classified images using a support vector machine (**b**). The output (**c**) resulted in a diagnosis of "healing" or "active" with an associated diagnostic probability. (Reprinted with permission from Maeda et al. [74])

more complex than we currently realize. DL algorithms should be able to determine the amount of bowel surface affected and analyze thousands of subtle image features. This then raises the question of whether AI assessments will be able to provide scales of disease severity that have more clinical relevance than our current methods. We believe the increased sensitivity of such assessments will lay the groundwork for improved analysis of IBD disease activity, with significant implications for future pharmacologic regimens. Perhaps in the future, AI-based methods of assessment will help us stratify disease in a manner that refines therapeutic regimens to a degree of precision not yet imaginable. In fact, in many aspects of disease, AI will provide the gateway towards personalized and precision medicine.

Other Applications of Artificial Intelligence

Identifying *Helicobacter pylori* Infection

Helicobacter pylori (HP) infection can precipitate intestinal metaplasia and is a known risk factor for gastric cancer. The sensitivity and specificity of white light endoscopy is, at best, 62% and 89% for detecting HP, therefore creating opportunity for AI to improve detection [76]. CNNs have been able to detect HP infection with sensitivities and specificities exceeding 85% [77, 78]. Advances have thus far led to development of a CNN by Shichijo and colleagues trained on 32,208 images with sensitivity and specificity of

89% and 87%, respectively [79]. Diagnostic time was 194 seconds. Test images were also evaluated by 23 endoscopists who demonstrated sensitivity, specificity, and diagnostic time of 79%, 83%, and 230 minutes. A recent prospective study compared how a DL algorithm performed when it was used for WL, BLI, or linked color images (LCI) [80]. Patients were enrolled prospectively and still images using each modality were taken during endoscopy. Still images were then subsequently analyzed by the algorithm. The AUROC was 0.66 for WLI, 0.96 for BLI, and 0.95 for LCI.

Gastrointestinal Bleeding Triage

AI-based methods have been developed to triage gastrointestinal (GI) bleeds [81]. A recent gradient-boosting ML model using retrospective clinical data was able to identify patients who met a composite endpoint of hospital-based intervention (transfusion or hemostatic intervention) or death within 30 days, with an AUROC of 0.90, outperforming clinical scores (Glasgow-Blatchford, Rockall, and AIMS65) [82]. Data used in this model included patient characteristics, clinical variables, and biochemistry, and sensitivity at identifying low-risk patients was 100%. A recent systematic review examining AI to triage GI bleeds found that none of the included studies used endoscopic image analysis as part of the assessment [83]. Risk of rebleeding has also been evaluated using AI models, but again, based on clinical data rather than endoscopic images [84]. Risk of rebleeding due to lesions such as ulcers is generally assessed endoscopically by the Forest Classification [85]. Given the increasing use of AI, is it not unreasonable to imagine that bleed severity and risk of rebleed could be assessed via AI at time of endoscopy? Perhaps risk of rebleed risk could also be determined after endoscopic therapy. Furthermore, this type of analysis could extend to all etiologies of GI bleeding, rather than the sole classification currently used for ulcers.

Geo-Localization

A critical aspect of endoscopy is reassessment after intervention. Scar evaluation is an essential component for the management of gastrointestinal neoplasia, given the frequency of recurrence [86, 87]. Moreover, scar biopsy is commonly performed due to the potential for “invisible” recurrence [88]. However, even amongst experts, scar evaluation can sometimes be difficult. The previously mentioned examples of landmark recognition during endoscopy open up the possibility of geo-localization [89]. An algorithm could identify signature features and landmark the area. On repeat endoscopy, the algorithm would alert the endoscopist when the area of interest has been reached. This would allow for accurate reassessment after intervention. Combining this technique with those already discussed would allow seamless reassessment of scar evaluation and other disease processes of interest.

Endoscopic Ultrasound

Endoscopic ultrasound (EUS) is a rapidly evolving area of endoscopy with applications such as choledocholithiasis [90] and pancreatic neoplasia [91]. Its evolution as a diagnostic and therapeutic modality makes it a prime area for the assimilation of AI. DL algorithms have predicted whether intraductal papillary mucinous neoplasms (IPMNs) detected via EUS were malignant or benign [92]. Accuracy of malignant prediction using AI was 94%, compared to a human diagnostic accuracy of 56%. DL algorithms have also been used to predict the malignant potential of pancreatic cysts based on fluid obtained via EUS sampling [93]. Accuracy of prediction by the AI model was 93%, outperforming both CEA (61%) and cytology (48%).

EUS has also been used for elastography, the measure of hardness and straining of a tissue. A CNN for EUS elastography was able to differentiate malignant from benign masses with accuracy of 90% [94]. A prospective, blinded, multicenter study of 258 patients based on this technology was able predict focal pancreatic lesions with an AUROC of 0.94 [95]. Sensitivity, specificity, PPV, and NPV were 88%, 83%, 96%, and 57%, respectively. It should be noted that analyses in this study were not real time. Video recordings were captured during endoscopy and then analyzed by the algorithm afterwards.

Quality Indicators and Automated Reporting

Quality of colonoscopy is determined by tracking of metrics such as cecal intubation rate, withdrawal time, and adenoma detection rate (ADR) [96]. Automated recording of insertion time, withdrawal time, and cecal intubation rate has been demonstrated with similar agreement when compared to expert endoscopists [97]. Further additions to automated reporting have included real-time ADR, recommended surveillance interval, tools used, and interventions performed [98]. Complete generation of endoscopy reports using CNN algorithms continues to be worked on with promising results [99]. Automated generation of such reports promises to save time, improve efficiency, and minimize variation of reporting between endoscopists. To date, quality metrics are tracked postprocedurally but cannot be used to improve intraprocedural performance [100]. However, the recently described EndoMetric Automated-RT computer system gives feedback on mucosal inspection during endoscopy by identifying blurry frames, quantifying debris in a frame, and measuring the endoscopist's effort in inspecting the mucosa [101]. Prospective evaluation of the system demonstrated that its use led to increased effective mucosal visualization, increased removal of debris, and a longer withdrawal time [102].

Effective assessment of bowel preparations is also important. In this regard, a recent CNN model was developed using the Boston Bowel Preparation Score (BBPS) to distinguish whether image frames were of adequate (BBPS of 0 or 1) or inadequate (BBPS of 2 or 3) quality [103]. The accuracy of the model was 97% in this binary fashion, but it had difficulty with multinomial classification (classifying into 4 separate BBPS labels). Regardless, future application of such a system in real time could have implications for global preparation scoring and could be used in clinical studies. Lastly, a comprehensive, real-time, automated quality control system (AQCS), based on a deep CNN, has been developed to track withdrawal time, supervise withdrawal stability, evaluate bowel preparation, and detect polyps [104]. A prospective randomized trial of this AQCS significantly increased ADR and withdrawal time, again pointing to the benefits of technology aimed at quality assurance during colonoscopy.

Ethical, Regulatory, and Data Issues

The era of "big data" promises to influence healthcare in numerous ways [105]. AI in endoscopy is undoubtedly part of this movement, requiring large amounts of endoscopic images and videos as data. However, implementing advanced technology that continuously evolves based on increasing quantity of available data presents several challenges not yet encountered in the healthcare arena. Consideration must be given to emerging issues such as approval, regulation, data storage, and ethics.

Regulatory Approval and Surveillance

Regulatory agencies will need to adapt their policies as AI technologies become increasingly complex [106, 107]. DL algorithms, by definition, will continue to learn from new data as it becomes available. Technologies may take on new abilities and diagnostic parameters after original approval. This plasticity has caused debate as to how these technologies should be monitored after approval. Although postmarket surveillance is commonplace to record adverse events, surveillance for performance parameters of technology is not. AI technologies are not without error, and algorithms can learn incorrect patterns [108]. Because of the "black box" nature of how AI algorithms function, AI-literate staff will need to be trained to carry out surveillance [109]. An additional component of AI development will be the dataset itself. *As the function and quality of any AI algorithm is entirely dependent on the quality of data it learns from, regular auditing of data will be necessary*. Data quality should be monitored during the iterative learning cycles of AI development, but also after approval given ongoing changes to the system. Large quantities of data will make this a difficult task requiring collaborative effort between healthcare systems, commercial parties, and governmental organizations.

In keeping with these requirements, the Food and Drug Administration (FDA) recently released a package of new guidance documents detailing how it plans to regulate software designed to aid clinical decision making [110]. Low-risk software, for example, mobile applications used to help manage nonserious conditions with the aid of a physician, will not be regulated. Rather, oversight will focus on software used in serious or critical situations, as well as machine-learning-based algorithms. Because the intended user (endoscopist) may not fully understand the underlying mechanisms by which an algorithm comes to a decision, DL models in endoscopy may be regulated as medical devices.

Infrastructure and Maintenance

Greater availability of data also necessitates the creation of suitable infrastructure both for data storage and workflow integration [111, 112]. Will data be stored in-house due to privacy concerns? Or will the vast amount of data not make this a feasible option and necessitate cloud-based storage? Also, will AI algorithms be installed locally, or will they be cloud-based applications? It may be fair to say that the development of AI algorithms has outpaced the hardware capacity needed to implement such algorithms and associated data capture in real time on a larger scale. The advent of new technologies, such as 5G [113] and edge computing [114], may allow for locally accessible supercomputer AI options while maintaining connection to a larger cloud-based databank. Still, many questions remain unanswered. Will competing commercial organizations offer stand-alone AI algorithm workflows? Or will organizations develop algorithms that will be "plug and play," seamlessly integrating into current workflows? Lastly, individual organizational policies may play a role into how this aspect of the field evolves. Individual healthcare institutions may have little incentive to front the financial burden of developing advanced infrastructure. They may also be concerned about data privacy when evaluating centralized cloud-based solutions. Ultimately, there will need to be a collaborative effort between healthcare and commercial organizations to develop a suitable infrastructure and to decide on the policies required for effective workflow integration.

Data Privacy and Consent

If AI technologies begin to routinely diagnose lesions, the images will have to be stored for a yet undetermined period of time in order to ensure quality. Such images may have to be recovered periodically for reexamination in some instances – such as suspected misdiagnoses or medical-legal challenges. In all likelihood, stored data will also be of interest for commercial efforts. This need for archival data access may be at odds with patient's wishes to keep her/his data private [115]. In a world where organizations have been heavily scrutinized for using consumer data without consent, the medical community must be wary of the inherent inclination to proceed in this manner [116]. Even today, physicians routinely record endoscopic procedures without explicitly obtaining consent for storage. If data storage grows exponentially, potential for privacy breaches will probably increase substantially.

Without appropriate regulatory oversight, breaches could result in serious consequences – such as insurance discrimination, policy cancellation, or worse.

If we are to store data for AI algorithm training, we may need to begin incorporating regular consent for its storage and use into daily practice. Perhaps, as physicians, we could learn from our scientific colleagues in the sphere of genomics, who have been successful with biobanks [117]. Of course, data privacy concerns in healthcare will extend far beyond endoscopy. Healthcare organizations may need disclaimers for data storage, similar to how users for social media sites sign disclaimers for data use when first creating an account. However, this situation is in a state of rapid flux at the time of this writing.

Data Ownership and Processing

Who will *own* the data? Patients? Healthcare organizations? Commercial partners [118]? Even now, patients usually have access to recorded endoscopic pictures but do not own the data. Healthcare organizations may wish to own the data in order to ensure security, while commercial partners may wish to own data in order to improve their algorithms. If data is to be anonymized before use for AI development, will commercial organizations be required to purchase anonymized data sets? And if so, who will anonymize the data? One might conceptualize that un-anonymized data could actually be used to effectively generate patient-specific clinical insights or track patient progression over a long period of time. This, in itself, may create even more complicating issues with regards to ownership. All of this data will certainly be of value, and there will likely be financial implications surrounding data anonymization, data transfer, and data processing. In the future, we expect that new organizations may be formed, in which each address unique aspects of this data chain. For example, it is not unreasonable to expect to see start-up companies which provide secure data encryption or anonymization of data prior to its use in algorithm development.

Autonomous Technologies

AI algorithms are disruptive technologies, both for gastrointestinal endoscopy and the healthcare system at large. Successful adoption of such technologies will be reliant on appropriate education and AI literacy of those involved [119]. Most AI-based technologies have emerged as clinical support tools, serving as adjuncts to help clinicians improve diagnostic performance and patient outcomes [120]. There has long been concern that autonomous AI technologies may replace certain healthcare staff altogether, but at this point in time, this does not seem to be the case. Currently developed and emerging technologies display what the Society of Automotive Engineers (SAE) terms level 2 autonomy (on a scale of 5): a technology that aids performance but requires an ever-present human operator [121, 122]. Level 3 would be a technology that fully completes a task (e.g., a capsule endoscopy read-out) and where the human operator could review and confirm results afterwards. Level 5 describes full autonomy without need for human intervention, a scenario that not likely to transpire in the near term, given current technological understanding. However, if healthcare technologies were ever to advance to such an extent, it would be our responsibility as clinicians to determine their limits and ensure regulation.

Conclusion

AI technologies will revolutionize healthcare. The field of endoscopy has already begun to change, and improvements will no doubt continue at a rapid pace. The examples highlighted in this chapter point to how these technologies will democratize advanced endoscopic skills to healthcare practitioners at large. Patients will benefit in terms of earlier and more accurate diagnoses, as well as improved therapy. It will be up to us as a profession to ensure that any rapid developments occur ethically, with patient safety always at the forefront of mind. Regardless, we should be very excited about this "brand-new world" of AI in endoscopy. We have already passed the first inflection point.

Conflicts of Interest Daljeet Chahal and Neal Shahidi: No conflicts of interest to disclose.

Michael F. Byrne: CEO and shareholder, Satisfai Health; founder of AI4GI joint venture (Satisfai Health and Imagia). Co-development agreement between Olympus America and AI4GI in artificial intelligence and colorectal polyps.

References

1. Engelbrecht AP. Computational intelligence: an introduction. Hoboken: Wiley; 2007. 630 p.
2. Turing AM. The essential turing. Oxford/New York: Oxford University Press; 2004. 622 p.
3. Mitchell T, Buchanan B, DeJong G, Dietterich T, Rosenbloom P, Waibel A. Machine learning. Ann Rev Comput Sci. 1990;4(1):417–33.
4. LeCun Y, Bengio Y, Hinton G. Deep learning. Nature. 2015;521(7553):436–44.
5. Neumann H, Bisschops R. Artificial intelligence and the future of endoscopy. Dig Endosc. 2019;31(4):389–90.
6. Winawer SJ, Zauber AG, Ho MN, O'brien MJ, Gottlieb LS, Sternberg SS, et al. Prevention of colorectal cancer by colonoscopic polypectomy. N Engl J Med. 1993;329(27):1977–81.
7. Zauber AG, Winawer SJ, O'Brien MJ, Lansdorp-Vogelaar I, van Ballegooijen M, Hankey BF, et al. Colonoscopic polypectomy and long-term prevention of colorectal-cancer deaths. N Engl J Med. 2012;366(8):687–96.
8. Zhao S, Wang S, Pan P, Xia T, Chang X, Yang X, et al. Magnitude, risk factors, and factors associated with adenoma miss rate of tandem colonoscopy: a systematic review and meta-analysis. Gastroenterology. 2019;156(6):1661–74.e11.
9. East JE, Rees CJ. Making optical biopsy a clinical reality in colonoscopy. Lancet Gastroenterol Hepatol. 2018;3(1):10–2.
10. Parikh ND, Chaptini L, Njei B, Laine L. Diagnosis of sessile serrated adenomas/polyps with image-enhanced endoscopy: a systematic review and meta-analysis. Endoscopy. 2016;48(08):731–9.
11. Dayyeh BKA, Thosani N, Konda V, Wallace MB, Rex DK, Chauhan SS, et al. ASGE Technology Committee systematic review and meta-analysis assessing the ASGE PIVI thresholds for adopting real-time endoscopic assessment of the histology of diminutive colorectal polyps. Gastrointest Endosc. 2015;81(3):502.e1–e16.
12. Corley DA, Jensen CD, Marks AR, Zhao WK, Lee JK, Doubeni CA, et al. Adenoma detection rate and risk of colorectal cancer and death. N Engl J Med. 2014;370(14):1298–306.
13. Kessler W, Imperiale T, Klein R, Wielage R, Rex D. A quantitative assessment of the risks and cost savings of forgoing histologic examination of diminutive polyps. Endoscopy. 2011;43(08):683–91.
14. Karkanis SA, Iakovidis DK, Maroulis DE, Karras DA, Tzivras M. Computer-aided tumor detection in endoscopic video using color wavelet features. IEEE Trans Inf Technol Biomed. 2003;7(3):141–52.
15. Bernal J, Tajkbaksh N, Sánchez FJ, Matuszewski BJ, Chen H, Yu L, et al. Comparative validation of polyp detection methods in video colonoscopy: results from the MICCAI 2015 endoscopic vision challenge. IEEE Trans Med Imaging. 2017;36(6):1231–49.
16. Fernández-Esparrach G, Bernal J, López-Cerón M, Córdova H, Sánchez-Montes C, de Miguel CR, et al. Exploring the clinical potential of an automatic colonic polyp detection method based on the creation of energy maps. Endoscopy. 2016;48(09):837–42.
17. Misawa M, Kudo S-E, Mori Y, Nakamura H, Kataoka S, Maeda Y, et al. Characterization of colorectal lesions using a computer-aided diagnostic system for narrow-band imaging endocytoscopy. Gastroenterology. 2016;150(7):1531–2.e3.
18. Urban G, Tripathi P, Alkayali T, Mittal M, Jalali F, Karnes W, et al. Deep learning localizes and identifies polyps in real time with 96% accuracy in screening colonoscopy. Gastroenterology. 2018;155(4):1069–78.e8.
19. Wang P, Xiao X, Brown JRG, Berzin TM, Tu M, Xiong F, et al. Development and validation of a deep-learning algorithm for the detection of polyps during colonoscopy. Nature Biomed Eng. 2018;2(10):741.
20. Wang L, Xie C, Hu Y. IDDF2018-ABS-0260 deep learning for polyp segmentation: BMJ Publishing Group; 2018.
21. Tischendorf J, Gross S, Winograd R, Hecker H, Auer R, Behrens A, et al. Computer-aided classification of colorectal polyps based on vascular patterns: a pilot study. Endoscopy. 2010;42(03):203–7.
22. Gross S, Buchner A, Crook J, Cangemi J, Picco MF, Wolfsen HC, et al. A comparison of high definition-image enhanced colonoscopy and standard white-light colonoscopy for colorectal polyp detection. Endoscopy. 2011;43(12):1045–51.
23. Takemura Y, Yoshida S, Tanaka S, Kawase R, Onji K, Oka S, et al. Computer-aided system for predicting the histology of colorectal tumors by using narrow-band imaging magnifying colonoscopy (with video). Gastrointest Endosc. 2012;75(1):179–85.
24. Kominami Y, Yoshida S, Tanaka S, Sanomura Y, Hirakawa T, Raytchev B, et al. Computer-aided diagnosis of colorectal polyp histology by using a real-time image recognition system and narrow-

band imaging magnifying colonoscopy. Gastrointest Endosc. 2016;83(3):643–9.
25. Byrne MF, Chapados N, Soudan F, Oertel C, Pérez ML, Kelly R, et al. Real-time differentiation of adenomatous and hyperplastic diminutive colorectal polyps during analysis of unaltered videos of standard colonoscopy using a deep learning model. Gut. 2019;68(1):94–100.
26. Chen P-J, Lin M-C, Lai M-J, Lin J-C, Lu HH-S, Tseng VS. Accurate classification of diminutive colorectal polyps using computer-aided analysis. Gastroenterology. 2018;154(3):568–75.
27. Takemura Y, Yoshida S, Tanaka S, Onji K, Oka S, Tamaki T, et al. Quantitative analysis and development of a computer-aided system for identification of regular pit patterns of colorectal lesions. Gastrointest Endosc. 2010;72(5):1047–51.
28. Häfner M, Kwitt R, Uhl A, Wrba F, Gangl A, Vécsei A. Computer-assisted pit-pattern classification in different wavelet domains for supporting dignity assessment of colonic polyps. Pattern Recogn. 2009;42(6):1180–91.
29. Mori Y, Kudo S-E, Wakamura K, Misawa M, Ogawa Y, Kutsukawa M, et al. Novel computer-aided diagnostic system for colorectal lesions by using endocytoscopy (with videos). Gastrointest Endosc. 2015;81(3):621–9.
30. Takeda K, Kudo S-E, Mori Y, Misawa M, Kudo T, Wakamura K, et al. Accuracy of diagnosing invasive colorectal cancer using computer-aided endocytoscopy. Endoscopy. 2017;49(08):798–802.
31. Mori Y, Kudo S-E, Misawa M, Saito Y, Ikematsu H, Hotta K, et al. Real-time use of artificial intelligence in identification of diminutive polyps during colonoscopy: a prospective study. Ann Intern Med. 2018;169(6):357.
32. André B, Vercauteren T, Buchner AM, Krishna M, Ayache N, Wallace MB. Software for automated classification of probe-based confocal laser endomicroscopy videos of colorectal polyps. World J Gastroenterol. 2012;18(39):5560.
33. Ştefănescu D, Streba C, Cârţână ET, Săftoiu A, Gruionu G, Gruionu LG. Computer aided diagnosis for confocal laser endomicroscopy in advanced colorectal adenocarcinoma. PLoS One. 2016;11(5):e0154863.
34. Rath T, Tontini GE, Vieth M, Nägel A, Neurath MF, Neumann H. In vivo real-time assessment of colorectal polyp histology using an optical biopsy forceps system based on laser-induced fluorescence spectroscopy. Endoscopy. 2016;48(6):557–62.
35. Kuiper T, Alderlieste YA, Tytgat KM, Vlug MS, Nabuurs JA, Bastiaansen BA, et al. Automatic optical diagnosis of small colorectal lesions by laser-induced autofluorescence. Endoscopy. 2015;47(01):56–62.
36. Aihara H, Saito S, Inomata H, Ide D, Tamai N, Ohya TR, et al. Computer-aided diagnosis of neoplastic colorectal lesions using 'real-time' numerical color analysis during autofluorescence endoscopy. Eur J Gastroenterol Hepatol. 2013;25(4):488.
37. Sharma P, Hawes RH, Bansal A, Gupta N, Curvers W, Rastogi A, et al. Standard endoscopy with random biopsies versus narrow band imaging targeted biopsies in Barrett's oesophagus: a prospective, international, randomised controlled trial. Gut. 2013;62(1):15–21.
38. Sharma P, Savides TJ, Canto MI, Corley DA, Falk GW, Goldblum JR, et al. The American Society for Gastrointestinal Endoscopy PIVI (preservation and incorporation of valuable endoscopic innovations) on imaging in Barrett's esophagus. Gastrointest Endosc. 2012;76(2):252–4.
39. van der Sommen F, Klomp SR, Swager A-F, Zinger S, Curvers W, Schoon E, et al., editors. Evaluation and comparison of computer vision methods for early Barrett's cancer detection using volumetric laser endomicroscopy. NCCV'16, the Netherlands Conference on Computer Vision, December 12–13, 2016, Lunteren, The Netherlands; 2016.
40. Swager A-F, van der Sommen F, Klomp SR, Zinger S, Meijer SL, Schoon EJ, et al. Computer-aided detection of early Barrett's neoplasia using volumetric laser endomicroscopy. Gastrointest Endosc. 2017;86(5):839–46.
41. Fonollà R, Scheeve T, Struyvenberg MR, Curvers WL, de Groof AJ, van der Sommen F, et al. Ensemble of deep convolutional neural networks for classification of early Barrett's neoplasia using volumetric laser endomicroscopy. Appl Sci. 2019;9(11):2183.
42. Ebigbo A, Mendel R, Probst A, Manzeneder J, de Souza Jr LA, Papa JP, et al. Computer-aided diagnosis using deep learning in the evaluation of early oesophageal adenocarcinoma. Gut. 2019;68(7):1143–5.
43. Shimizu Y, Omori T, Yokoyama A, Yoshida T, Hirota J, Ono Y, et al. Endoscopic diagnosis of early squamous neoplasia of the esophagus with iodine staining: high-grade intra-epithelial neoplasia turns pink within a few minutes. J Gastroenterol Hepatol. 2008;23(4):546–50.
44. Muto M, Minashi K, Yano T, Saito Y, Oda I, Nonaka S, et al. Early detection of superficial squamous cell carcinoma in the head and neck region and esophagus by narrow band imaging: a multicenter randomized controlled trial. J Clin Oncol. 2010;28(9):1566.
45. Kodashima S, Fujishiro M, Takubo K, Kammori M, Nomura S, Kakushima N, et al. Ex vivo pilot study using computed analysis of endo-cytoscopic images to differentiate normal and malignant squamous cell epithelia in the oesophagus. Dig Liver Dis. 2007;39(8):762–6.
46. Shin D, Protano M-A, Polydorides AD, Dawsey SM, Pierce MC, Kim MK, et al. Quantitative analysis of high-resolution microendoscopic images for diagnosis of esophageal squamous cell carcinoma. Clin Gastroenterol Hepatol. 2015;13(2):272–9.e2.
47. Horie Y, Yoshio T, Aoyama K, Yoshimizu S, Horiuchi Y, Ishiyama A, et al. Diagnostic outcomes of esophageal cancer by artificial intelligence using

convolutional neural networks. Gastrointest Endosc. 2019;89(1):25–32.
48. Everson M, Herrera L, Li W, Luengo IM, Ahmad O, Banks M, et al. Artificial intelligence for the real-time classification of intrapapillary capillary loop patterns in the endoscopic diagnosis of early oesophageal squamous cell carcinoma: a proof-of-concept study. United European Gastroenterol J. 2019;7(2):297–306.
49. Kumagai Y, Takubo K, Kawada K, Aoyama K, Endo Y, Ozawa T, et al. Diagnosis using deep-learning artificial intelligence based on the endocytoscopic observation of the esophagus. Esophagus. 2019;16(2):180–7.
50. Miyaki R, Yoshida S, Tanaka S, Kominami Y, Sanomura Y, Matsuo T, et al. Quantitative identification of mucosal gastric cancer under magnifying endoscopy with flexible spectral imaging color enhancement. J Gastroenterol Hepatol. 2013;28(5):841–7.
51. Miyaki R, Yoshida S, Tanaka S, Kominami Y, Sanomura Y, Matsuo T, et al. A computer system to be used with laser-based endoscopy for quantitative diagnosis of early gastric cancer. J Clin Gastroenterol. 2015;49(2):108–15.
52. Hirasawa T, Aoyama K, Tanimoto T, Ishihara S, Shichijo S, Ozawa T, et al. Application of artificial intelligence using a convolutional neural network for detecting gastric cancer in endoscopic images. Gastric Cancer. 2018;21(4):653–60.
53. Ishioka M, Hirasawa T, Tada T. Detecting gastric cancer from video images using convolutional neural networks. Dig Endosc. 2019;31(2):e34–e5.
54. Wu L, Zhou W, Wan X, Zhang J, Shen L, Hu S, et al. A deep neural network improves endoscopic detection of early gastric cancer without blind spots. Endoscopy. 2019;51(6):522–31.
55. Wu L, Zhang J, Zhou W, An P, Shen L, Liu J, et al. Randomised controlled trial of WISENSE, a real-time quality improving system for monitoring blind spots during esophagogastroduodenoscopy. Gut. 2019:gutjnl-2018-317366.
56. Bourke MJ, Neuhaus H, Bergman JJ. Endoscopic submucosal dissection: indications and application in Western endoscopy practice. Gastroenterology. 2018;154(7):1887–900.e5.
57. Nakagawa K, Ishihara R, Aoyama K, Ohmori M, Nakahira H, Matsuura N, et al. Classification for invasion depth of esophageal squamous cell carcinoma using a deep neural network compared with experienced endoscopists. Gastrointest Endosc. 2019;90(3):407–14.
58. Zhao Y-Y, Xue D-X, Wang Y-L, Zhang R, Sun B, Cai Y-P, et al. Computer-assisted diagnosis of early esophageal squamous cell carcinoma using narrow-band imaging magnifying endoscopy. Endoscopy. 2019;51(04):333–41.
59. Kubota K, Kuroda J, Yoshida M, Ohta K, Kitajima M. Medical image analysis: computer-aided diagnosis of gastric cancer invasion on endoscopic images. Surg Endosc. 2012;26(5):1485–9.
60. Zhu Y, Wang Q-C, Xu M-D, Zhang Z, Cheng J, Zhong Y-S, et al. Application of convolutional neural network in the diagnosis of the invasion depth of gastric cancer based on conventional endoscopy. Gastrointest Endosc. 2019;89(4):806–15.e1.
61. Iddan G, Meron G, Glukhovsky A, Swain P. Wireless capsule endoscopy. Nature. 2000;405(6785):417.
62. Byrne MF, Donnellan F. Artificial intelligence and capsule endoscopy: is the truly "smart" capsule nearly here? Gastrointest Endosc. 2019;89(1):195–7.
63. Zou Y, Li L, Wang Y, Yu J, Li Y, Deng W, editors. Classifying digestive organs in wireless capsule endoscopy images based on deep convolutional neural network. In: 2015 IEEE international conference on digital signal processing (DSP): IEEE; 2015.
64. Jia X, Meng MQ-H, editors. A deep convolutional neural network for bleeding detection in wireless capsule endoscopy images. In: 2016 38th annual international conference of the IEEE Engineering in Medicine and Biology Society (EMBC): IEEE; 2016.
65. Li P, Li Z, Gao F, Wan L, Yu J, editors. Convolutional neural networks for intestinal hemorrhage detection in wireless capsule endoscopy images. In: 2017 IEEE international conference on multimedia and expo (ICME): IEEE; 2017.
66. Leenhardt R, Vasseur P, Li C, Saurin JC, Rahmi G, Cholet F, et al. A neural network algorithm for detection of GI angiectasia during small-bowel capsule endoscopy. Gastrointest Endosc. 2019;89(1):189–94.
67. Aoki T, Yamada A, Aoyama K, Saito H, Tsuboi A, Nakada A, et al. Automatic detection of erosions and ulcerations in wireless capsule endoscopy images based on a deep convolutional neural network. Gastrointest Endosc. 2019;89(2):357–63.e2.
68. Yuan Y, Meng MQH. Deep learning for polyp recognition in wireless capsule endoscopy images. Med Phys. 2017;44(4):1379–89.
69. He J-Y, Wu X, Jiang Y-G, Peng Q, Jain R. Hookworm detection in wireless capsule endoscopy images with deep learning. IEEE Trans Image Process. 2018;27(5):2379–92.
70. Iakovidis DK, Georgakopoulos SV, Vasilakakis M, Koulaouzidis A, Plagianakos VP. Detecting and locating gastrointestinal anomalies using deep learning and iterative cluster unification. IEEE Trans Med Imaging. 2018;37(10):2196–210.
71. De Lange T, Larsen S, Aabakken L. Inter-observer agreement in the assessment of endoscopic findings in ulcerative colitis. BMC Gastroenterol. 2004;4(1):9.
72. Ozawa T, Ishihara S, Fujishiro M, Saito H, Kumagai Y, Shichijo S, et al. Novel computer-assisted diagnosis system for endoscopic disease activity in patients with ulcerative colitis. Gastrointest Endosc. 2019;89(2):416–21.e1.
73. Stidham RW, Liu W, Bishu S, Rice MD, Higgins PDR, Zhu J, et al. Performance of a deep learning

model vs human reviewers in grading endoscopic disease severity of patients with ulcerative colitis. JAMA Netw Open. 2019;2(5):e193963.
74. Maeda Y, Kudo S-E, Mori Y, Misawa M, Ogata N, Sasanuma S, et al. Fully automated diagnostic system with artificial intelligence using endocytoscopy to identify the presence of histologic inflammation associated with ulcerative colitis (with video). Gastrointest Endosc. 2019;89(2):408–15.
75. Gottlieb K, Travis S, Feagan B, Hussain F, Sandborn WJ, Rutgeerts P. Central reading of endoscopy endpoints in inflammatory bowel disease trials. Inflamm Bowel Dis. 2015;21(10):2475–82.
76. Watanabe K, Nagata N, Shimbo T, Nakashima R, Furuhata E, Sakurai T, et al. Accuracy of endoscopic diagnosis of Helicobacter pylori infection according to level of endoscopic experience and the effect of training. BMC Gastroenterol. 2013;13(1):128.
77. Huang C-R, Sheu B-S, Chung P-C, Yang H-B. Computerized diagnosis of Helicobacter pylori infection and associated gastric inflammation from endoscopic images by refined feature selection using a neural network. Endoscopy. 2004;36(7):601–8.
78. Itoh T, Kawahira H, Nakashima H, Yata N. Deep learning analyzes Helicobacter pylori infection by upper gastrointestinal endoscopy images. Endosc Int Open. 2018;6(2):E139–E44.
79. Shichijo S, Nomura S, Aoyama K, Nishikawa Y, Miura M, Shinagawa T, et al. Application of convolutional neural networks in the diagnosis of Helicobacter pylori infection based on endoscopic images. EBioMedicine. 2017;25:106–11.
80. Nakashima H, Kawahira H, Kawachi H, Sakaki N. Artificial intelligence diagnosis of Helicobacter pylori infection using blue laser imaging-bright and linked color imaging: a single-center prospective study. Ann Gastroenterol. 2018;31(4):462.
81. Sengupta N, Leiman DA. Improving acute GI bleeding management through artificial intelligence: unnatural selection? Dig Dis Sci. 2019;64(8):2061–4.
82. Shung DL, Au B, Taylor RA, Tay JK, Laursen SB, Stanley AJ, et al. Validation of a machine learning model that outperforms clinical risk scoring systems for upper gastrointestinal bleeding. Gastroenterology. 2019;158(1):160–7.
83. Shung D, Simonov M, Gentry M, Au B, Laine L. Machine learning to predict outcomes in patients with acute gastrointestinal bleeding: a systematic review. Dig Dis Sci. 2019;64(8):2078–87.
84. Wong GL-H, Ma AJ, Deng H, Ching JY-L, Wong VW-S, Tse Y-K, et al. Machine learning model to predict recurrent ulcer bleeding in patients with history of idiopathic gastroduodenal ulcer bleeding. Aliment Pharmacol Ther. 2019;49(7):912–8.
85. Rahman SI-U, Saeian K. Nonvariceal upper gastrointestinal bleeding. Crit Care Clin. 2016;32(2):223–39.
86. Moss A, Williams SJ, Hourigan LF, Brown G, Tam W, Singh R, et al. Long-term adenoma recurrence following wide-field endoscopic mucosal resection (WF-EMR) for advanced colonic mucosal neoplasia is infrequent: results and risk factors in 1000 cases from the Australian Colonic EMR (ACE) study. Gut. 2015;64(1):57–65.
87. Tate DJ, Desomer L, Klein A, Brown G, Hourigan LF, Lee EY, et al. Adenoma recurrence after piecemeal colonic EMR is predictable: the Sydney EMR recurrence tool. Gastrointest Endosc. 2017;85(3):647–56.e6.
88. Desomer L, Tutticci N, Tate DJ, Williams SJ, McLeod D, Bourke MJ. A standardized imaging protocol is accurate in detecting recurrence after EMR. Gastrointest Endosc. 2017;85(3):518–26.
89. Wu Y, Tang F, Li H. Image-based camera localization: an overview. Vis Comput Ind Biomed Art. 2018;1(1):1–13.
90. Khan MA, Akbar A, Baron TH, Khan S, Kocak M, Alastal Y, et al. Endoscopic ultrasound-guided biliary drainage: a systematic review and meta-analysis. Dig Dis Sci. 2016;61(3):684–703.
91. Rodrigo L. Advances in pancreatic cancer: BoD – Books on Demand; 2018. 226 p.
92. Kuwahara T, Hara K, Mizuno N, Okuno N, Matsumoto S, Obata M, et al. Usefulness of deep learning analysis for the diagnosis of malignancy in intraductal papillary mucinous neoplasms of the pancreas. Clin Transl Gastroenterol. 2019;10(5):1.
93. Kurita Y, Kuwahara T, Hara K, Mizuno N, Okuno N, Matsumoto S, et al. Diagnostic ability of artificial intelligence using deep learning analysis of cyst fluid in differentiating malignant from benign pancreatic cystic lesions. Sci Rep. 2019;9(1):1–9.
94. Săftoiu A, Vilmann P, Gorunescu F, Gheonea DI, Gorunescu M, Ciurea T, et al. Neural network analysis of dynamic sequences of EUS elastography used for the differential diagnosis of chronic pancreatitis and pancreatic cancer. Gastrointest Endosc. 2008;68(6):1086–94.
95. Săftoiu A, Vilmann P, Gorunescu F, Janssen J, Hocke M, Larsen M, et al. Efficacy of an artificial neural network–based approach to endoscopic ultrasound elastography in diagnosis of focal pancreatic masses. Clin Gastroenterol Hepatol. 2012;10(1):84–90.e1.
96. Rex DK, Schoenfeld PS, Cohen J, Pike IM, Adler DG, Fennerty MB, et al. Quality indicators for colonoscopy. Am J Gastroenterol. 2015;110(1):72–90.
97. Rombaoa C, Kalra A, Dao T, Requa J, Ninh A, Samarasena JB, et al. Tu1932 automated insertion time, cecal intubation, and withdrawal time during live colonoscopy using convolutional neural networks – a video validation study. Gastrointest Endosc. 2019;89(6):AB619.
98. Karnes W, Requa J, Dao T, Massoud R, Samarasena J, Ninh A. Automated documentation of multiple colonoscopy quality measures in real-time with convolutional neural networks: 2761. Am J Gastroenterol. 2018;113:S1532.
99. Hicks S, Smedsrud PH, Riegler MA, Lange TD, Petlund A, Eskeland SL, et al. 383 Deep learning for automatic generation of endoscopy reports. Gastrointest Endosc. 2019;89(6):AB77.

100. Byrne MF, Shahidi N, Rex DK. Will computer-aided detection and diagnosis revolutionize colonoscopy? Gastroenterology. 2017;153(6):1460–4.e1.
101. Stanek SR, Tavanapong W, Wong J, Oh J, Nawarathna RD, Muthukudage J, et al. SAPPHIRE: a toolkit for building efficient stream programs for medical video analysis. Comput Methods Prog Biomed. 2013;112(3):407–21.
102. Srinivasan N, Szewczynski M, Enders F, Tavanapong W, Oh J, Wong J, et al. Real-time feedback improves the quality of colonoscopy by trainees: a controlled clinical trial: ACG/AstraZeneca Fellow Award. Am J Gastroenterol. 2012;107:S596.
103. Karnes WE, Ninh A, Dao T, Requa J, Samarasena JB. Sa1940 unambiguous real-time scoring of bowel preparation using artificial intelligence. Gastrointest Endosc. 2018;87(6):AB258.
104. Su J-R, Li Z, Shao X-J, Ji C-R, Ji R, Zhou R-C, et al. Impact of real-time automatic quality control system on colorectal polyp and adenoma detection: a prospective randomized controlled study (with video). Gastrointest Endosc. 2020;91(2):415–424.e4.
105. Murdoch TB, Detsky AS. The inevitable application of big data to health care. JAMA. 2013;309(13):1351–2.
106. He J, Baxter SL, Xu J, Xu J, Zhou X, Zhang K. The practical implementation of artificial intelligence technologies in medicine. Nat Med. 2019;25(1):30.
107. Allen B. The role of the FDA in ensuring the safety and efficacy of artificial intelligence software and devices. J Am Coll Radiol. 2019;16(2):208–10.
108. Caruana R, Lou Y, Gehrke J, Koch P, Sturm M, Elhadad N, editors. Intelligible models for healthcare: predicting pneumonia risk and hospital 30-day readmission. In: Proceedings of the 21th ACM SIGKDD international conference on knowledge discovery and data mining: ACM; 2015.
109. Rimmer A. Technology will improve doctors' relationships with patients, says Topol review: British Medical Journal Publishing Group; 2019.
110. Administration FaD. Clinical decision software: guidance for industry and food and drug administration staff. 2019.
111. Lo'ai AT, Mehmood R, Benkhlifa E, Song H. Mobile cloud computing model and big data analysis for healthcare applications. IEEE Access. 2016;4:6171–80.
112. Wang Y, Kung L, Byrd TA. Big data analytics: understanding its capabilities and potential benefits for healthcare organizations. Technol Forecast Soc Chang. 2018;126:3–13.
113. Latif S, Qadir J, Farooq S, Imran M. How 5G wireless (and concomitant technologies) will revolutionize healthcare? Future Internet. 2017;9(4):93.
114. Shi W, Cao J, Zhang Q, Li Y, Xu L. Edge computing: vision and challenges. IEEE Internet Things J. 2016;3(5):637–46.
115. Abouelmehdi K, Beni-Hessane A, Khaloufi H. Big healthcare data: preserving security and privacy. J Big Data. 2018;5(1):1.
116. Mostert M, Bredenoord AL, Biesaart MC, van Delden JJ. Big data in medical research and EU data protection law: challenges to the consent or anonymise approach. Eur J Hum Genet. 2016;24(7):956.
117. Beskow LM, Dombeck CB, Thompson CP, Watson-Ormond JK, Weinfurt KP. Informed consent for biobanking: consensus-based guidelines for adequate comprehension. Genet Med. 2015;17(3):226.
118. Kostkova P, Brewer H, de Lusignan S, Fottrell E, Goldacre B, Hart G, et al. Who owns the data? Open data for healthcare. Front Public Health. 2016;4:7.
119. Wartman SA, Combs CD. Medical education must move from the information age to the age of artificial intelligence. Acad Med. 2018;93(8):1107–9.
120. Shah P, Kendall F, Khozin S, Goosen R, Hu J, Laramie J, et al. Artificial intelligence and machine learning in clinical development: a translational perspective. NPJ Digit Med. 2019;2(1):69.
121. Topol EJ. High-performance medicine: the convergence of human and artificial intelligence. Nat Med. 2019;25(1):44.
122. Jaremko JL, Azar M, Bromwich R, Lum A, LHA C, Gibert M, et al. Canadian Association of Radiologists white paper on ethical and legal issues related to artificial intelligence in radiology. Can Assoc Radiol J. 2019;70(2):107–18.

Explainable AI for the Operating Theater

25

Frank Rudzicz and Shalmali Joshi

Machine learning (ML) can now be deployed at multiple stages of a surgical workflow. However, prediction models deployed in the workflow have limited utility unless they also provide actionable insights. This chapter reviews tools in explainable AI (XAI) research that can help bridge this gap. Explanations for an ML tool depend on several factors, including where the model is deployed in the surgical workflow, the specific decision support it is intended to provide, and the appropriate representation that is most beneficial in the specific setting. We therefore provide an overview of state-of-the-art XAI methods categorized by the type of explanation provided. Each explanation type is contextualized within potential operative scenarios, including potential shortcomings of each method. Further, an explanation may not be intended for just clinical end use but serve other purposes like retrospective or prospective AI model debugging before deployment. Finally, we provide requirements of a good explanation to serve as a guideline of how these methods should be vetted for deployment.

Introduction

As machine learning is increasingly deployed at multiple stages of a patient's trajectory through a surgical clinical workflow, these tools need to be augmented to allow clinicians, surgeons, educators, and administrators to interpret the outputs of such models. These interpretations allow stakeholders to calibrate trust in the model and enhance the *actionability* of the ML tool. The interpretations here concern specific decision outputs of a model rather than explaining overall model behavior in terms of an arbitrary summary statistic. Explaining overall model behavior is more closely related to the *simulatability* [1] of the model, whereby a human can process precisely how a model may be processing the input to provide the outcome. We do not concern ourselves with such models in this chapter and instead focus on models that may assist reliable *justification* to aid actionable interventions. For example, simply predicting a high risk of an intraoperative hemorrhage (or similar adverse event) a few minutes in advance can be insufficient. Rather, the ML model should provide information regarding

F. Rudzicz (✉)
International Centre for Surgical Safety, Toronto, ON, Canada

Li Ka Shing Knowledge Institute, St. Michael's Hospital, Toronto, ON, Canada

Department of Computer Science, University of Toronto, Toronto, ON, Canada

Surgical Safety Technologies Inc., Toronto, ON, Canada

Vector Institute for Artificial Intelligence, Toronto, ON, Canada
e-mail: frank@spoclab.com

S. Joshi
Vector Institute for Artificial Intelligence, Toronto, ON, Canada

S. Atallah (ed.), *Digital Surgery*, https://doi.org/10.1007/978-3-030-49100-0_25

the precise anomaly in the procedure that may lead to a change in its estimated risk of blood loss, allowing surgeons in the operating theater (OT) to take appropriate preventive measures. Recent arguments suggest how *explainability* can enhance decision support for preemptive management of surgical adverse events [2, 3]. Indeed, explanations can help to retrospectively improve workflow management and improve interaction between the ML tool and the clinicians who use it, which is necessitated by an increased use of ML in surgical settings [4]. Some of the most promising venues where explainability can help end users include reliable preoperative clinical decision support and augmenting ML-based intraoperative adverse event prediction.

Explanations augment conventional statistical metrics in several ways. For instance, explanations are often intended to be more personalized, characterizing patient-specific measures. Explanations related to characterizing uncertainty can be provided for individuals, as opposed to over the population sample characterized by confidence intervals. Additionally, conventional evaluation measures may serve as good indicators of whether a model is deemed safe to be deployed. On the other hand, explanations can serve multiple purposes when an ML model is deployed, potentially in real time. That is, an explanation may augment decision support, help clinicians calibrate their trust in the model for the case at hand, or even curate similar case studies from millions of other records for reference.

Considering these motivations, we organize the chapter as follows. We describe state-of-the-art XAI tools developed in literature and contextualize their utility for preoperative, inoperative, and postoperative hospital procedures. We consider different modalities of data and potential prediction tasks commonly considered in AI surgical literature. We suggest characteristics of a good explanation and describe limitations of each method. The chapter is organized around a case study of a patient who requires surgery, as determined by a preoperative AI-based decision support tool. An intraoperative surgical tool predicts the possibility of an adverse event, such as a hemorrhage. Note that we only focus on the subarea of explanation so far as its applicability to surgical end users is concerned. This requires that such methods be reliable, intuitive to users, and thoroughly evaluated.

Preliminaries

Consider a machine learning (ML) model that predicts the risk of an intraoperative hemorrhage for a patient as in Fig. 25.1. Let $x \in X$ represent a vector of patient features (i.e., independent input variables) in domain X monitored in real time (including, but not limited to, cardiogram output, blood pressure, temperature, arterial blood oxygen levels, intracranial hemoglobin levels, and blood pressure). Let $y \in Y$ represent the model's prediction label (i.e., dependent output variable). For instance, Y may be specified as "low risk, high risk" for our particular task. Let $p(y \mid x)$ be the probabilistic risk of hemorrhage, estimated by the ML model. This probability may be passed through a threshold to determine the nominal label y. In essence, even a complex deep neural network is a function that maps input features to the outcome label y, usually by minimizing the empirical estimate of the risk within some fixed function class $f \in F$. Example cost functions l include approximations of the zero-one loss or l_2 loss for regression [5]. Note that this framework can easily be modified for predictions over time, but for simplicity, we do not elaborate on that here. When such a model is deployed, an estimate of risk is not necessarily sufficient to provide utility, especially in time-constrained settings like surgery. For example, surgeons may benefit more from knowing why the risk of hemorrhage has increased in the past 2 minutes of operation and what they could do to manage the situation. In the preoperative surgery setting, X may include a biopsy report, knee X-rays, or MRI scans to decide whether, for example, an osteoarthritis patient requires knee replacement surgery (i.e., the label here indicates whether the patient needs surgery) [6, 7]. In this example, a localized region of the image, on which the model primarily based its prediction, is useful to know. In the following, we describe some of the more general state-of-the-art methods that may be useful in surgical settings to provide such functionality.

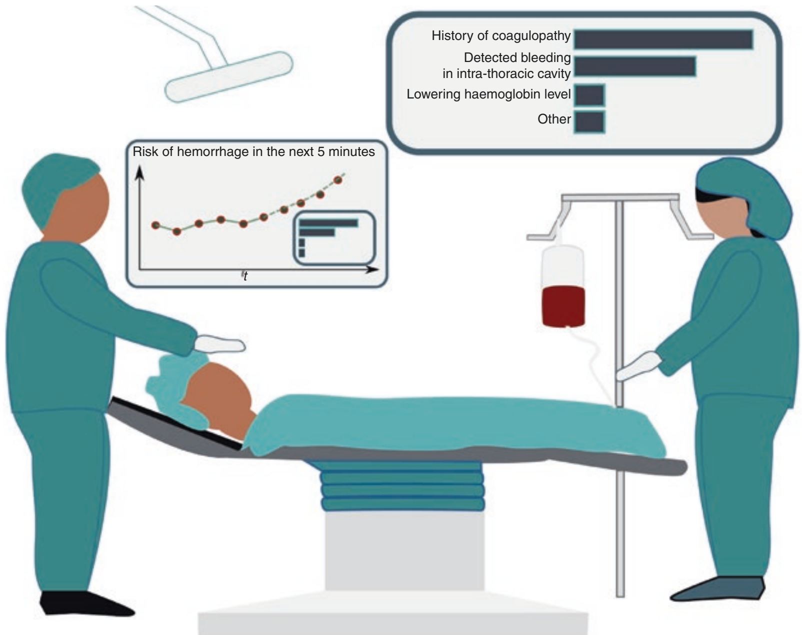

Fig. 25.1 XAI-augmented surgical workflow for intraoperative hemorrhage prediction

Overview of Methods

Explanations can serve multiple functionalities – inasmuch as augmenting model predictions are concerned. Therefore, an appropriate representation of an explanation is better determined with respect to the classification task, specifically. Here, we categorize different kinds of explanations into a few major groups, each providing different functionality. Within each category, we describe methods that may be useful for different data domains, such as images, time series, or sequential data.

Feature Importance

Feature importance refers to identifying the subset of attributes that *drive* a model's prediction, generally most associated with a change in the estimate of $p(y|x)$. For example, for a model that monitors the intraoperative risk of hemorrhage [7], whenever the risk changes to critically high, highlighting potentially relevant features can allow early intervention or even prevention. Such feature importance methods should highlight features relevant to the specific patient and their outcome. Note that determining feature importance does *not* imply causal relationships between those features and predictions; rather, the association $p(y|x)$ is affected by potential perturbations on, or removal of, the features. Figure 25.2 shows an abstract illustration of feature-based explanations for different data domains.

Feature Importance for Cross-Sectional Data

These methods are usable in intraoperative as well as postoperative retrospective data. INVASE [8], LIME [9], and Shapley values [10] are some of the known methods for deriving feature importance for an individual sample. LIME and Shapley values primarily approximate a classifier locally around the sample whose relevant features we wish to highlight, in order to derive feature importance. These methods have recently been used to augment models that predict the risk of intraoperative hypoxemia due to anesthesia [11]. The INVASE method, on the other hand, learns to select the subset of relevant features by approximating the conditional distribution $p(y|x)$ with that obtained from a selected feature subset for each sample. Recently, a deep learning neural architecture called an *attention mechanism* [12]

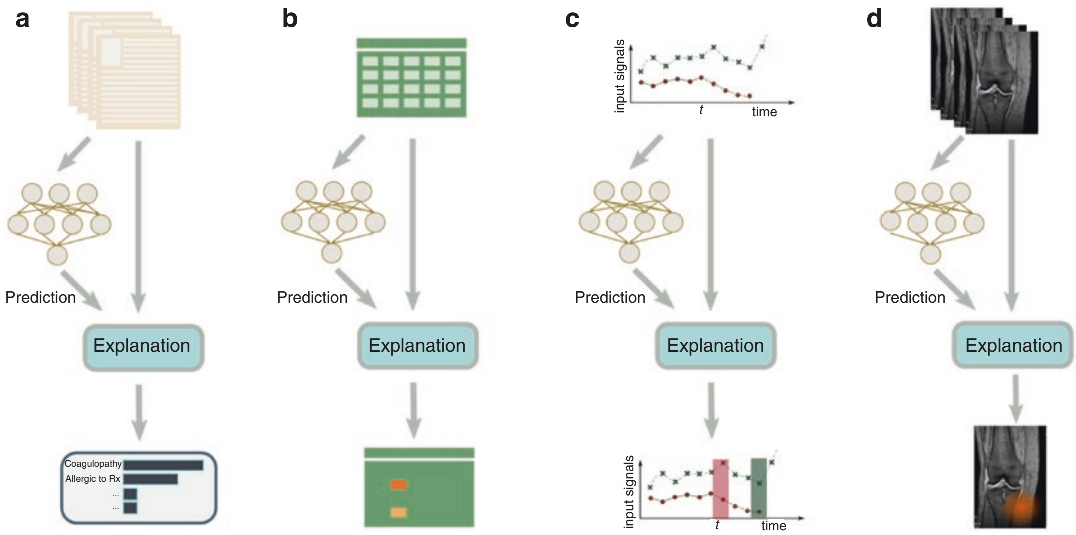

Fig. 25.2 Feature importance for different data domains

has been demonstrated to show such explainability by highlighting relevant features, although there are caveats.

For example, Jain and Wallace and Pruthi et al. [13, 14] established that the correlation between weights learned by attention models and gradient-based feature importance is low, and perturbations in attention weights lead to modest changes in model output. This architecture is known to be especially suitable and competitive for complex structured and unstructured data such as sequences [15], images [16], and time series data [17, 18]. This is an attractive property, as the ML model to which it is applied would not need to be augmented with any other auxiliary mechanisms to generate explanations. However, each method has a different mechanism of obtaining the most relevant feature for prediction and thereby differs in the clinical relevance of such explanations. As such, we recommend deploying such methods with caution. When the highlighted features do not reflect clinical relevance, interventions based on explanations can be ineffective and potentially actively harmful. As suggested in Fig. 25.2, feature importance methods can highlight which aspects of the intraoperative procedure may be driving the model prediction to increased risk of hemorrhage.

If the model has been trained only on patient data collected during intraoperative monitoring, any feature importance method will only highlight features within the subset of features being monitored. Some of these features may change over time, thereby requiring the identification of the precise times at which a change in a feature resulted in potential changes to risk. However, if the ML model has been augmented with other data sources, like patient history, the methods may highlight a potential rare disorder, like hemophilia that increases the patient propensity for hemorrhage. On the other hand, this information is relevant, but not critical to highlight throughout the procedure, as it is a *static*, albeit relevant, feature. Any good explanation algorithm should highlight static relevant features preoperatively or at the beginning of the surgical procedure, preempting surgeons to take the right precautions, but avoid highlighting it throughout the procedure as it may be distracting without being actionable.

Feature Importance for Medical Imaging

For medical imaging data, like radiographs or MRI, a carefully *segmented* group of pixels can help identify the region of the image driving the model prediction [19, 20]. Augmenting surgical instruments with such technology has the potential to improve data collection [21] by focusing on relevant views in laparoscopic surgeries or even improve diagnoses [22]. Some of the most well-known methods that highlight localized regions of importance rely on a fundamental method called *saliency maps*. Saliency methods attribute importance by evaluating how regional perturbations affect the model outcome [23–26]. As with other XAI methods, saliency maps should also be utilized or deployed with caution. Recently, Adebayo et al. [27] outlined requirements of good saliency methods, applicable to natural images, and more recent work has attempted to meet these necessary conditions [28]. This is still an area of active exploration, and its extensive applicability to medical imaging is a burgeoning area of research. For instance, saliency methods have been augmented for potential preoperative screening in tumor detection [29] and efficient retrieval for radiographs [30]. Wen et al. [31] demonstrated that, with modality-specific fine-tuning, conventional saliency methods in literature can provide reasonable heatmaps of clinically relevant regions for chest computed tomography (CT), chest X-ray images, and whole-body positron emission tomography (PET). However, these methods do not compare the more recent AI-based techniques generating saliency maps. Since such methods have not been extensively evaluated for surgical data and as surgical data explanations require domain expertise for evaluating correctness of the explanations, we demonstrate the kinds of explanations generated by such methods for a sample natural image in Fig. 25.3; Fig. 25.3a is the original sample. The AI model is meant to classify two subtypes of elephants (Africa, Indian) in the image to the class "African elephant"; here, the ears are the primary distinguishing factor between these subtypes. The

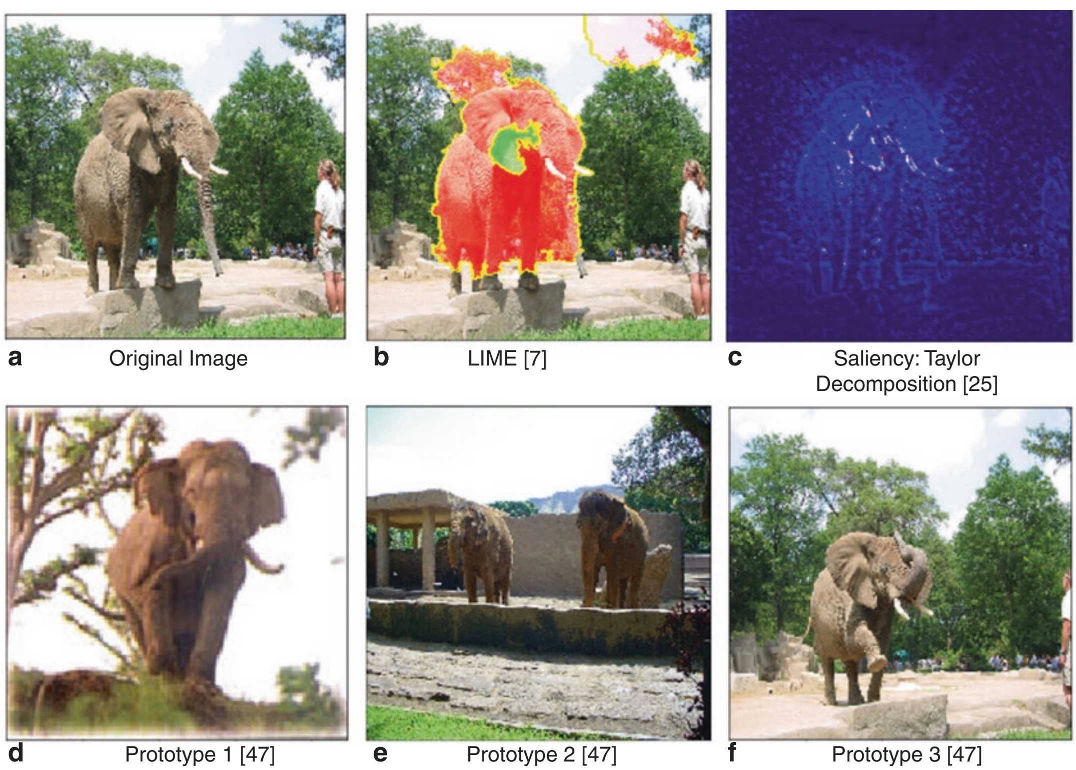

Fig. 25.3 Image domain explanations. Top row (**a**–**c**): Feature-importance-based explanations. Bottom row (**d**–**f**): Explanations using examples

non-saliency-based explanation, LIME [9], (Fig. 25.3b) highlights super pixels that are most relevant for the classifier in determining its prediction. Figure 25.3c is a saliency based on Taylor decomposition and highlights edges around the ears and tusks. Figure 25.3d–f is addressed later; see *Examples for Model Debugging.*[1]

Closely related to saliency, but serving a complementary purpose, is image segmentation in which images are partitioned into regions of importance (e.g., background, foreground, and specific objects in the foreground). This is a fundamental problem in robot-assisted surgery to track instruments using videos [32–34]. Recently, novel deep neural architectures have been developed that segment and track each individual object, called Mask R-CNN [35]. The Control & Mechatronics Lab at National University of Singapore demonstrated its utility for segmenting surgical robotic instruments.[2] Evaluating such methods is far easier compared to saliency methods due to ease of obtaining the ground truth annotation.

Feature Importance for Longitudinal Data

For time series data, as in real-time detection of adverse events, methods that highlight which features drive the model prediction are significantly rarer. Attention-based neural networks designed exclusively for time series data [17, 18] have some utility for prediction tasks in the ICU, such as mortality and length of stay, and an extension of Shapley values [10] has identified adverse risk of hypoxemia during anesthesia in surgery.

Explanations Using Examples

Explanations need not just highlight features that drive a model prediction. In fact, they can also potentially highlight which patients in the surgical cohort are responsible for model prediction or most similar to the current patient under consideration. This can be effective for preoperative clinical decision support and has been demonstrated by a few empirical studies. For instance, effective retrieval of visually similar images of tissue biopsies can be useful in augmenting the clinical workflow [36]. The result is that both clinical decision-making and AI models themselves can be improved. Additionally, explanations can come in the form of understanding which patients a classifier is most likely to classify well and those for whom it does not.

Patient Similarity

Context-based image retrieval [37–39] identifies similar patients from massive cohort histories to support clinical decision-making. This is useful for clinicians, as “similar” patients can understandably receive similar surgical interventions, by highlighting rare but similar cases and potentially highlighting consistencies that may be overlooked. Recently, deep learning methods such as convolutional neural networks have been used for this purpose [36]. When provided as an explanation, such a method can highlight patients that the AI model would classify *similarly*. In the medical field, where precedent often matters, a model that does this reliably can potentially provide precedent and justification for a specific surgical decision when based on an AI tool. However, capturing the most clinically applicable notion of similarity is challenging for machine learning methods but can be successful when results are refined by clinical experts [36]. Therefore, such methods can be used to understand whether a model is predicting reliably. Other than preoperative decision-making support, explanations that provide examples can serve debugging purposes for ML models deployed in surgery. We review some of these below.

Examples for Model Debugging

An adversarial example is a sample that is similar to another in the training set (most likely visually indecipherable or without any discernible clinical difference) but predicted to have a different outcome by the AI model. An adversarial attack is the process of creating such examples. The sim-

[1] For more details, see https://github.com/ArnoldYSYeung/interpretable_ml_showcase.

[2] https://github.com/SUYEgit/Surgery-Robot-Detection-Segmentation

plest attack is to add additive noise δ to the original example x until the model predictions change on the synthetic example $x + \delta$ [40]. This, and more sophisticated attacks, can help explain whether model predictions are truly relying on clinically relevant features or are merely sensitive to surface detail. Recently, such examples have demonstrated shortcomings of AI diagnostic models trained on chest X-ray, fundoscopic, and dermoscopic images [41–44] and nonsurgical medical data like electronic health records [45]. However, such examples are known to be unrealistic. Counterfactual examples have been identified as providing similar functionality but with images from the training cohort itself, albeit classified differently [46]. These methods are not yet extensively applied for surgical decision support debugging.

Yet another way of debugging an AI model is to evaluate which examples a model may be relying on most for a particular surgical case. For example, suppose a model suggests an increased risk of intraoperative bleeding, but the adverse event actually did not occur. For retrospective analysis, it is useful to identify which examples the model relied on most during training, to update its risk estimate. Such examples can be used to detect unexpected biases in the training data or procedure or to highlight spurious correlations the model has learned (like predicting a high risk for all patients older than 70, without discerning individual characteristics). This can be done using a method called *influence functions* [47]. Influence functions rank all training samples based on how much a test sample's prediction would change if the model was retrained without some training sample. Therefore, if a training sample was very *influential* for a particular prediction, removing it would significantly change the prediction. Note that this is different from a counterfactual as it does not necessarily find the closest sample to the test sample with a different label. This also does not guarantee finding the most similar patient to the patient being evaluated. It is only likely that the most influential *sample* may be closely related, in terms of its semantics, to the test sample.

When data is massive, as in information retrieval, it helps to identify similar samples by looking at a much smaller subset of samples. Such samples can serve different purposes. However, unlike traditional context-based information retrieval, these prototypes can actually be associated with the target black box model and provide samples that the model would classify similarly. It helps to get a sense of the classifier behavior by looking at what are known as prototypes [48]. In particular, if a black box is consistently working well for chest X-rays from one hospital, prototypes can highlight those samples. It is important to highlight not only examples that are consistently classified reliably but also those that fail to be classified. These can help identify specific subgroups or classes where the model is consistently underperforming. Figure 25.3d–f shows an example of prototypes.

In summary, using training examples as explanations can potentially provide debugging insights into the model. However, care should be taken that the employed measures of similarity reflect clinical similarity. Additionally, examples may also provide debugging insights in retrospective evaluation, highlighting potential improvements in training.

Model Uncertainty

As suggested before, model outcomes themselves cannot provide sufficient precedent for clinical action. However, if augmented with certain justifications, they may help reflect model behavior and calibrate model trust. For instance, characterizing uncertainty in outcome, input, and model parameters can characterize such uncertainty. A few issues separate traditional means of characterizing uncertainty, compared to providing uncertainty as explanations. Traditional methods have primarily focused on population estimates of uncertainty as opposed to individual sample-specific measures. Uncertainty estimation can be performed with various techniques and is generally tied to the model design. For instance, attention-based neural network models can be augmented with specific uncertainty estimates for postoperative classification tasks [49] and regression techniques commonly used for analyzing surgical workflows or estimating potential lengths of surgery [50, 51]. With advances in imaging, neural networks have been augmented with uncertainty estimates for intraoperative multispectral imaging [52], image segmentation [53], and intraoperative view imaging. More fundamentally, modern and complex neural networks are especially known to be poorly calibrated [54]. That is, probabilistic estimates of risk may be over- or underestimated by neural networks. These issues can be resolved to some extent by post hoc recalibration techniques [54] or by modeling neural networks to incorporate probabilistic estimates, in frameworks called Bayesian neural networks [55]. While this may mitigate some issues, care should be taken before relying on uncertainty estimates produced by neural networks as a means to an explanation.

Uncertainty estimation is also related to the transferability of models. That is, a high uncertainty from a well-calibrated model suggests that the samples similar to the current sample may have been rare in training or demonstrate associations that the model has not learned to predict reliably. This is especially necessary to handle in surgical settings. For instance, consider a computer vision model trained and deployed for adverse event prediction in operating room 1 at a hospital. Suppose a machine learning model performs reasonably well at predicting the risk of any adverse outcome with reasonable certainty. The same model may provide consistently high uncertainties in operating room 2, however, on a different floor in the same hospital. There could be several reasons for this which should be considered. First, the machine learning model may not generalize well if it has learned not just clinically relevant associations between the events in room 1 but also is overfit to the types of surgeries commonly done in room 1. Such confounding can be hard to detect in ML models, but knowing them *a priori*, they can be actively removed from model training using domain adaptation techniques [56, 57]. Thus, uncertainty estimation can shed light on how AI models can be improved for practical deployment. Further technical discussion of domain adaptation and transfer learning is beyond the scope of this chapter.

Transparent Design

XAI is, rightfully, a contentious topic within modern AI contexts [58]. This is because of several assumptions and myths around this area and lack of established benchmarks and evaluation measures. Wang and Rudin suggested that there exists a simple model class, like a rule-based method [59], that inherently satisfies needs of interpretability and should be preferred over any complex model (usually characterized by the number of model parameters learned during training), like a deep neural network. While this may be applicable if the performance of such models is comparable, in a vast variety of data domains like medical imaging and processing of natural language notes for information retrieval, deep neural networks have outperformed traditional methods consistently and by wide margins. In such scenarios, depending on the application and where the model fits within the clinical workflow, an appropriate choice of statistically sound and reliable method of explanation should be deployed. In any scenario, such an explanation should satisfy certain properties. In the following section, we outline some of these properties to serve as a guideline, but this is by no means comprehensive.

Evaluating the Quality of Explanations

How do we know that an explanation is appropriate, reliable, and reasonable within the clinical workflow? To summarize this section, we largely follow the outcomes that Tonekaboni et al. [60] determined as useful evaluation measures for the critical care unit and emergency departments. A study focusing on the OT is currently lacking, but we believe the broader concepts to transfer to the surgical setting as well:

1. *Domain-appropriate representation*: First, an explanation should be fit for the appropriate task at hand and relevant within the surgical workflow where the AI tool and therefore the explanation may be deployed. This may consist of one or more explanation methods suggested above. It should also be as personalized as the task appropriates. For example, in a real-time prediction task, when providing feature importance over time, an aggregate importance up to the current time point is not as actionable as highlighting the exact instance one or more features cause the risk estimates of a patient to deteriorate.
2. *Consistency*: Consistency implies that, for the same outcome y for a given test sample x, the XAI tool should provide the same set of explanations, irrespective of the choice of representation. Further, any perturbation or changes in explanations should imply or correspond to specific changes in model outcome. Therefore, any supposed explanation should be rigorously tested to possess such a statistically quantifiable property.
3. *Potential actionability*: Any explanation in the clinical setting is meant to augment decision-making. There is a massive body of work that is potentially helpful to understand the underlying model, but such explanations do not necessarily help an end user, like a surgeon or anesthesiologist, in a time-constrained surgical setting. It is therefore important to identify if the explanation is usable, can reliably provide precedent for clinical action (for an appropriate target user), and fits well within the surgical workflow [61]. For a resource on additional guidelines, refer to Lipton [1].

Closing Comments

In this chapter, we provided an overview of potential XAI tools that could be promising for the surgical workflow. We identified some of the fundamental themes around which XAI tools are developed and their utility for different aspects of the surgical workflow. We finally provide desirable properties of what explanations should provide to reliably and consistently augment AI-based tools and generally aid decision support in most settings.

References

1. Lipton ZC. The mythos of model interpretability. Commun ACM. 2018;61:36–43. Available from: https://doi.org/10.1145/3233231.
2. Gordon L, Grantcharov T, Rudzicz F. Explainable artificial intelligence for safe intraoperative decision support. JAMA Surg. 2019; Available from: https://doi.org/10.1001/jamasurg.2019.2821.
3. Chen D, Afzal N, Sohn S, Habermann EB, Naessens JM, Larson DW, et al. Postoperative bleeding risk prediction for patients undergoing colorectal surgery. Surgery. 2018;164:1209–16. Available from: https://doi.org/10.1016/j.surg.2018.05.043.
4. Shorten G. Artificial intelligence and training physicians to perform technical procedures. JAMA Netw Open. 2019;2(8):e198375.
5. Duda RO, Hart PE, Stork DG. Pattern classification. New York: Wiley; 2001. p. xx–654, ISBN: 0-471-05669-3. J Classif. 2007;24: 305–7. Available from: https://doi.org/10.1007/s00357-007-0015-9.
6. Yu D, Jordan KP, Snell KIE, Riley RD, Bedson J, Edwards JJ, et al. Development and validation of prediction models to estimate risk of primary total hip and knee replacements using data from the UK: two prospective open cohorts using the UK Clinical Practice Research Datalink. Ann Rheum Dis. 2019;78:91–9. Available from: https://doi.org/10.1136/annrheumdis-2018-213894.
7. Irita K. Risk and crisis management in intraoperative hemorrhage: human factors in hemorrhagic critical events. Korean J Anesthesiol. 2011 Mar;60(3):151–60.
8. Yoon J, Jordon J, van der Schaar M. INVASE: instance-wise variable selection using neural networks. In: International conference on learning representations; 2019. Available from: https://openreview.net/forum?id=BJg_roAcK7.
9. Ribeiro MT, Singh S, Guestrin C. Why should I trust you? Proceedings of the 22nd ACM SIGKDD international conference on knowledge discovery and data mining – KDD'16. 2016. Available from: https://doi.org/10.1145/2939672.2939778.
10. Lundberg SM, Lee S-I. A unified approach to interpreting model predictions. In: Advances in neural information processing systems. San Mateo: Morgan Kaufmann Publishers; 2017. p. 4765–74.
11. Lundberg SM, Nair B, Vavilala MS, Horibe M, Eisses MJ, Adams T, et al. Explainable machine-learning

predictions for the prevention of hypoxaemia during surgery. Nat Biomed Eng. 2018;2(10):749–60.
12. Xu K, Ba J, Kiros R, Cho K, Courville A, Salakhudinov R, et al. Show, attend and tell: neural image caption generation with visual attention. In: International conference on machine learning. 2015. p. 2048–57.
13. Jain S, Wallace BC. Attention is not explanation. In: Proceedings of the 2019 conference of the North American Chapter of the Association for Computational Linguistics: Human Language Technologies, volume 1 (long and short papers). 2019. p. 3543–56.
14. Pruthi D, Gupta M, Dhingra B, Neubig G, Lipton ZC. Learning to deceive with attention-based explanations. arXiv [cs.CL]. 2019. Available from: http://arxiv.org/abs/1909.07913.
15. Vaswani A, Shazeer N, Parmar N, Uszkoreit J, Jones L, Gomez AN, et al. Attention is all you need. In: Guyon I, Luxburg UV, Bengio S, Wallach H, Fergus R, Vishwanathan S, et al., editors. Advances in neural information processing systems 30: Curran Associates, Inc.; 2017. p. 5998–6008.
16. Fukui H, Hirakawa T, Yamashita T, Fujiyoshi H. Attention branch network: Learning of attention mechanism for visual explanation. In: Proceedings of the IEEE conference on Computer Vision and Pattern Recognition. 2019. p. 10705–14.
17. Choi E, Bahadori MT, Sun J, Kulas J, Schuetz A, Stewart W. RETAIN: an interpretable predictive model for healthcare using reverse time attention mechanism. In: Lee DD, Sugiyama M, Luxburg UV, Guyon I, Garnett R, editors. Advances in neural information processing systems 29: Curran Associates, Inc.; 2016. p. 3504–12.
18. Xu Y, Biswal S, Deshpande SR, Maher KO, Sun J. RAIM: recurrent attentive and intensive model of multimodal patient monitoring data. In: Proceedings of the 24th ACM SIGKDD International Conference on Knowledge Discovery & Data Mining. New York, NY, USA: ACM; 2018. p. 2565–73. (KDD'18).
19. Nam JG, Park S, Hwang EJ, Lee JH, Jin K-N, Lim KY, et al. Development and validation of deep learning–based automatic detection algorithm for malignant pulmonary nodules on chest radiographs. Radiology. 2019;290(1):218–28.
20. Lu MT, Ivanov A, Mayrhofer T, Hosny A, Aerts HJWL, Hoffmann U. Deep learning to assess long-term mortality from chest radiographs. JAMA Netw Open. 2019;2(7):e197416.
21. Kassahun Y, Yu B, Tibebu AT, Stoyanov D, Giannarou S, Metzen JH, et al. Surgical robotics beyond enhanced dexterity instrumentation: a survey of machine learning techniques and their role in intelligent and autonomous surgical actions. Int J Comput Assist Radiol Surg. 2016;11(4):553–68.
22. Chen P-HC, Gadepalli K, MacDonald R, Liu Y, Kadowaki S, Nagpal K, et al. An augmented reality microscope with real-time artificial intelligence integration for cancer diagnosis. Nat Med. 2019;25:1453–7. Available from: https://doi.org/10.1038/s41591-019-0539-7.
23. Baehrens D, Schroeter T, Harmeling S, Kawanabe M, Hansen K, MÃžller K-R. How to explain individual classification decisions. J Mach Learn Res. 2010;11(Jun):1803–31.
24. Bach S, Binder A, Montavon G, Klauschen F, Müller K-R, Samek W. On pixel-wise explanations for non-linear classifier decisions by layer-wise relevance propagation. PLoS One. 2015;10(7):e0130140.
25. Selvaraju RR, Cogswell M, Das A, Vedantam R, Parikh D, Batra D. Grad-cam: Visual explanations from deep networks via gradient-based localization. In: Proceedings of the IEEE international conference on computer vision. 2017. p. 618–26.
26. Montavon G, Lapuschkin S, Binder A, Samek W, Müller K-R. Explaining nonlinear classification decisions with deep Taylor decomposition. Pattern Recogn. 2017;65:211–22.
27. Adebayo J, Gilmer J, Muelly M, Goodfellow I, Hardt M, Kim B. Sanity checks for saliency maps. In: Bengio S, Wallach H, Larochelle H, Grauman K, Cesa-Bianchi N, Garnett R, editors. Advances in neural information processing systems 31: Curran Associates, Inc.; 2018. p. 9505–15.
28. Gupta A, Arora S. A simple saliency method that passes the sanity checks. arXiv [cs.LG]. 2019. Available from: http://arxiv.org/abs/1905.12152.
29. Mitra S, Banerjee S, Hayashi Y. Volumetric brain tumour detection from MRI using visual saliency. PLoS One. 2017;12(11):e0187209.
30. Ahmad J, Sajjad M, Mehmood I, Baik SW. SiNC: saliency-injected neural codes for representation and efficient retrieval of medical radiographs. PLoS One. 2017;12(8):e0181707.
31. Wen G, Rodriguez-Niño B, Pecen FY, Vining DJ, Garg N, Markey MK. Comparative study of computational visual attention models on two-dimensional medical images. J Med Imaging (Bellingham). 2017;4(2):025503.
32. Attia M, Hossny M, Nahavandi S, Asadi H. Surgical tool segmentation using a hybrid deep CNN-RNN auto encoder-decoder. 2017 IEEE International Conference on Systems, Man, and Cybernetics (SMC). 2017. Available from: https://doi.org/10.1109/smc.2017.8123151.
33. Shvets AA, Rakhlin A, Kalinin AA, Iglovikov VI. Automatic instrument segmentation in robot-assisted surgery using deep learning. 2018 17th IEEE International Conference on Machine Learning and Applications (ICMLA). 2018. Available from: https://doi.org/10.1109/icmla.2018.00100.
34. Islam M, Atputharuban DA, Ramesh R, Ren H. Real-time instrument segmentation in robotic surgery using auxiliary supervised deep adversarial learning. Vol. 4, IEEE Robotics and Automation Letters. 2019. p. 2188–95. Available from: https://doi.org/10.1109/lra.2019.2900854.
35. He K, Gkioxari G, Dollar P, Girshick R. Mask R-CNN. 2017 IEEE International Conference on

Computer Vision (ICCV). 2017. Available from: https://doi.org/10.1109/iccv.2017.322.
36. Cai CJ, Reif E, Hegde N, Hipp J, Kim B. Human-centered tools for coping with imperfect algorithms during medical decision-making. CHI Conf Proc. 2019.; Available from: https://dl.acm.org/doi/abs/10.1145/3290605.3300234.
37. Mosquera-Lopez C, Agaian S, Velez-Hoyos A, Thompson I. Computer-aided prostate cancer diagnosis from digitized histopathology: a review on texture-based systems. IEEE Rev Biomed Eng. 2015;8:98–113. Available from: https://doi.org/10.1109/rbme.2014.2340401.
38. Sklan JES, Plassard AJ, Fabbri D, Landman BA. Toward content-based image retrieval with deep convolutional neural networks. Medical imaging 2015: biomedical applications in molecular, structural, and functional imaging. 2015. Available from: https://doi.org/10.1117/12.2081551.
39. Akgül CB, Rubin DL, Napel S, Beaulieu CF, Greenspan H, Acar B. Content-based image retrieval in radiology: current status and future directions. J Digit Imaging. 2011;24(2):208–22.
40. Goodfellow IJ, Shlens J, Szegedy C. Explaining and harnessing adversarial examples. arXiv [stat.ML]. 2014. Available from: http://arxiv.org/abs/1412.6572.
41. Stoyanov D, Taylor Z, Kia SM, Oguz I, Reyes M, Martel A, et al. Understanding and interpreting machine learning in medical image computing applications: first international workshops, MLCN 2018, DLF 2018, and iMIMIC 2018, Held in Conjunction with MICCAI 2018, Granada, Spain, September 16–20, 2018, Proceedings. Springer; 2018. 149 p.
42. Finlayson SG, Chung HW, Kohane IS, Beam AL. Adversarial attacks against medical deep learning systems. arXiv [cs.CR]. 2018. Available from: http://arxiv.org/abs/1804.05296.
43. Asgari Taghanaki S, Das A, Hamarneh G. Vulnerability analysis of chest X-ray image classification against adversarial attacks. In: Understanding and interpreting machine learning in medical image computing applications: Springer International Publishing; 2018. p. 87–94.
44. Kotia J, Kotwal A, Bharti R. Risk susceptibility of brain tumor classification to adversarial attacks. Adv Intell Syst Comput. 2020:181–7. Available from: https://doi.org/10.1007/978-3-030-31964-9_17.
45. An S, Xiao C, Stewart WF, Sun J. Longitudinal adversarial attack on electronic health records data. The World Wide Web Conference on – WWW'19. 2019. Available from: https://doi.org/10.1145/3308558.3313528.
46. Wachter S, Mittelstadt B, Russell C. Counterfactual explanations without opening the black box: automated decisions and the GDPR. SSRN Electron J. Available from: https://doi.org/10.2139/ssrn.3063289.
47. Koh PW, Liang P. Understanding black-box predictions via influence functions. In: Proceedings of the 34th international conference on machine learning – volume 70. Sydney, NSW, Australia: JMLR.org; 2017. p. 1885–94. (ICML'17).
48. Kim B, Khanna R, Koyejo OO. Examples are not enough, learn to criticize! Criticism for interpretability. In: Lee DD, Sugiyama M, Luxburg UV, Guyon I, Garnett R, editors. Advances in neural information processing systems 29: Curran Associates, Inc.; 2016. p. 2280–8.
49. Heo J, Lee HB, Kim S, Lee J, Kim KJ, Yang E, et al. Uncertainty-aware attention for reliable interpretation and prediction. In: Bengio S, Wallach H, Larochelle H, Grauman K, Cesa-Bianchi N, Garnett R, editors. Advances in neural information processing systems 31: Curran Associates, Inc.; 2018. p. 909–18.
50. Bodenstedt S, Rivoir D, Jenke A, Wagner M, Breucha M, Müller-Stich B, et al. Active learning using deep Bayesian networks for surgical workflow analysis. Int J Comput Assist Radiol Surg. 2019;14(6):1079–87.
51. Ng N, Gabriel RA, McAuley J, Elkan C, Lipton ZC. Predicting surgery duration with neural heteroscedastic regression. arXiv [stat.ML]. 2017. Available from: http://arxiv.org/abs/1702.05386.
52. Adler TJ, Ardizzone L, Ayala L, Gröhl J, Vemuri A, Wirkert SJ, et al. Uncertainty handling in intra-operative multispectral imaging with invertible neural networks. 2019 [cited 2020 Mar 5]. Available from: https://openreview.net/pdf?id=Byx9RUONcE.
53. Wang G, Li W, Aertsen M, Deprest J, Ourselin S, Vercauteren T. Aleatoric uncertainty estimation with test-time augmentation for medical image segmentation with convolutional neural networks. Neurocomputing. 2019;338:34–45. Available from: https://doi.org/10.1016/j.neucom.2019.01.103.
54. Guo C, Pleiss G, Sun Y, Weinberger KQ. On calibration of modern neural networks. In: Proceedings of the 34th international conference on machine learning – volume 70. JMLR.org; 2017. p. 1321–30. (ICML'17).
55. Gal Y. Uncertainty in deep learning. University of Cambridge 2016;1:3.
56. Schulam P, Saria S. Can you trust this prediction? Auditing pointwise reliability after learning. In: Chaudhuri K, Sugiyama M, editors. Proceedings of Machine Learning Research. PMLR; 2019. p. 1022–31. (Proceedings of Machine Learning Research; vol. 89).
57. Subbaswamy A, Saria S. Counterfactual normalization: proactively addressing dataset shift using causal mechanisms. auai.org. Available from:. http://auai.org/uai2018/proceedings/papers/334.pdf.
58. Rudin C. Stop explaining black box machine learning models for high stakes decisions and use interpretable models instead. Nat Mach Intell. 2019;1:206–15. Available from: https://doi.org/10.1038/s42256-019-0048-x.
59. Wang F, Rudin C. Falling rule lists. In: Artificial intelligence and statistics. 2015. p. 1013–22.
60. Tonekaboni S, Joshi S, McCradden MD, Goldenberg A. What clinicians want: contextualizing explainable

machine learning for clinical end use. In: Doshi-Velez F, Fackler J, Jung K, Kale D, Ranganath R, Wallace B, et al., editors. Proceedings of the 4th Machine Learning for Healthcare Conference. Ann Arbor, Michigan: PMLR; 2019. p. 359–80. (Proceedings of Machine Learning Research; vol. 106).

61. Tomsett R, Braines D, Harborne D, Preece A, Chakraborty S. Interpretable to whom? A role-based model for analyzing interpretable machine learning systems. arXiv [cs.AI]. 2018. Available from: http://arxiv.org/abs/1806.07552.

26 A Digital Doorway to Global Surgery

Nadine Hachach-Haram

Guaranteeing Access to Safe Surgical Care: A Global Challenge

The concept of healthcare as a universal and inalienable human right dates back to the 1940s. It was, in fact, one of the founding principles of the World Health Organization (WHO), which in its original constitution declared its intention to promote 'the highest attainable standard of health as a fundamental right of every human being' [1].

Until very recently, however, surgery was conspicuous by its absence in definitions of specifically what *kind of care* people should be able to receive. It was due to the work of the Lancet Commission on Global Surgery, with its vision for 'universal access to safe, affordable surgical and anaesthesia care when needed', that *surgery* moved to centre stage, gaining a newfound interest in the global healthcare community [2]. In light of the commission's work, the World Health Assembly amended its position in 2015, unanimously passing a resolution to recognize surgery within the concept of universal health care (UHC) [3].

The Lancet Commission's work was based on two key premises: first, that global access to surgery is grossly unequal and, second, surgery's role in driving better outcomes in healthcare has been drastically underappreciated. The implication is that, unless the structural inequalities in access and quality of surgical services are addressed, the UHC project would be fundamentally undermined. Moreover, populations will not receive the safe, quality surgical care they are entitled to receiving, without appropriate *access* to surgery.

The sobering conclusions from the Lancet Commission's findings are now common currency – *five billion people, almost three-quarters of the global population, 'are excluded from what is often life-saving or disability-averting treatment' offered by surgery* [2]. The key reasons for this exclusion range from non-affordable care for services, to a dearth of local provisions with under-resourced and low-quality surgical care. Eyler et al. summarized the issue succinctly – *one-third of the world's burden of disease can be treated with surgery, and yet 70% of the global population lacks access to surgical care* [4, 5].

The Lancet Commission also posed the argument that access to surgical services should be enshrined *within* the broader spectrum of universal rights to healthcare. It also sets ambitious global targets for progress towards universal provisions and what this should encompass by 2030. The commission outlined six key metrics for evaluating achievement (Table 26.1) [6, 7].

The implications of these targets are considerable. There are 143 million additional surgical procedures required each year to balance the deficit. This would require a doubling of the global surgical workforce, a potential cost of $420

N. Hachach-Haram (✉)
Plastic Surgery and Clinical Innovation, Guy's & St. Thomas' NHS Foundation Trust, London, UK

S. Atallah (ed.), *Digital Surgery*, https://doi.org/10.1007/978-3-030-49100-0_26

Table 26.1 Core indicators for monitoring universal access to safe, affordable surgical and anaesthesia care when needed [6, 7]

Access to timely essential surgery	Two-hour access to the three Bellwether procedures (caesarean delivery, emergency laparotomy, and management of an open fracture) in 80% of countries.
Specialist surgical workforce density	All countries with at least 20 surgical, anaesthesia, and obstetric physicians per 100,000 population.
Surgical volume	5000 procedures per 100,000 population in all countries.
Perioperative mortality rate (POMR)	Tracked and reported by 100% of countries.
Protection against impoverishing expenditure	No individual or family should be at risk from impoverishment from out-of-pocket payments for surgical care.
Protection against catastrophic expenditure	No individual or family should be put at risk of financial ruin from out-of-pocket payments for surgical care.

billion, which is separate from the estimated $371 billion required to achieve the UN's health-related Sustainable Development Goals by 2030 [6, 8].

The Lancet Commission clearly emphasized that lower- to middle-income countries (LMICs) will face the brunt of the challenges in achieving these targets and openly framed the entire project of achieving universal surgical care in terms of redressing the imbalance between developed and undeveloped nations, between rich and poor. There are fundamental disparities which face the healthcare community if surgery is to be included as part of the UHC vision. This is underscored by the fact that three-quarters of the >300 million surgical procedures performed globally are undertaken in the *richest 33%* of nations. Meanwhile, 6% of surgeries are conducted in the *poorest 33%* [6].

Unless addressed, there is a detrimental impact of inadequate surgical services in underserved nations. The most salient of these detriments are (a) preventable death, (b) preventable disability, and (c) financial burden imposed by unaffordable surgical care. The latter will equate to a $12.3 trillion loss among LMICs [6].

Even developed nations are not guaranteed a smooth path to delivering universal access to safe, high-quality surgical care. The Lancet Commission might have formulated its 2030 vision with the aim of challenging the global community to bring surgical services across LMICs up to a workable level of baseline targets, but for those nations that already satisfy these specific criteria, renewed focus is required to ensure that all surgical provisions satisfy the parameters set forth by the UHC:

- *Equity in access* – access to healthcare services should be universal, not dependent on ability to pay.
- *Guaranteed quality of service* – care should guarantee improvement in the health of those receiving them.
- *Avoidance of financial risk* – the cost of using services should not put persons at risk of financial harm [9].

Even in nations with well-funded healthcare systems, meeting these criteria becomes problematic in the context of surgical provision. In the United States, for example – which, as a percentage of GDP, spends more on healthcare provisions than any other country – the insurance-based, pay-at-the-point-of-delivery system has been linked to widespread inequality in access to healthcare in general. Dickman et al. highlighted that 27 million uninsured US citizens are effectively excluded from healthcare services, while a disproportionate amount of financial harm, extending to indebtedness and, in some cases, bankruptcy, is inflicted upon low-income patients who access healthcare services [10].

Dr. Adil Haidler (Harvard Medical School) has conducted extensive research into racial disparities in surgical access and patient outcomes in the United States, establishing links to socioeconomic status, insurance status, and even the quality of care received by patients across differing demographics [11, 12]. By any objective standard, the US healthcare system faces substantial barriers to achieving a universal standard of surgical care.

The United Kingdom, with a free-at-point-of-delivery National Health Service (NHS), provides a contrasting service model to the United States – one that some perceive as an example of equitable, universal healthcare. However, the NHS also has shortcomings, including patient-access restrictions, variance in the quality of surgical care delivered, and, at times, patients placed at financial risk when surgical (and other) services are required.

Well-publicized complaints regarding so-called postal-code lotteries for surgical access across different regions within the UK are supported by academic studies into procedures including aesthetic surgery, cataract correction, gynecomastia reduction, and more [13–15]. Such studies have uncovered wide regional variations in operating criterion, with limitations in funding a frequently cited key factor. There has been ongoing criticism of the individual funding request approach which links provision of specialist treatments directly to cost-efficiencies [16, 17]. In extreme cases, patients are forced into difficult decisions about trying to fund their own treatments privately, raising the spectre of financial hardship often associated with access to surgery in less developed regions.

Limited resource is a key factor that affects access to surgery, even in advanced healthcare systems. For fiscal years 2017–2018, just under half (44%) of UK NHS trusts were in deficit, despite a £1.8 billion cash injection in 2015, aimed at curtailing the overspending gap [18].

A related concern is the shortage of available expertise. The Lancet Commission emphasized that much of the work required to meet the target of doubling the number of qualified surgical practitioners by 2030 would have to transpire in the *developed world.* According to the Association of American Medical Colleges (AAMC), the United States will need a minimum of 20,000 new surgeons by 2030 to meet the growing demand [19]. In the UK, one in four hospitals remains unable to offer minimally invasive procedures due to a shortage of interventionist radiologists [20].

The strain on surgical resources is, unfortunately, predicted to increase as a result of ageing populations. In the United States, it is forecast that there will be 30 million more individuals aged 65 and over by 2030 [21]. In the UK, the number of people aged 80 and over is expected to double in the same period to reach six million [22]. This shift in demographics will result in specific changes to the healthcare environment. For example, an increase in the prevalence of non-communicable disease is predicted, with greater complexity associated with the treatment of chronic conditions and comorbidity [23]. Surgery is a key part of the treatment pathway for many non-communicable diseases, yet increased age is also associated with greater risk of post-operative complications and longer hospital stays [24]. *Ageing populations will therefore raise demands in terms of surgical volumes, quality of care, and hospital capacity.*

Another important factor influencing ‘postal-code lottery’ variations in access to high-quality surgical care and upholding consistency of standards is due to a lack of consensus regarding the definition of ‘best practice’. Writing in The Lancet, Birkmeyer et al. argued that differences in illness burdens, diagnostic practices, and patient attitudes only have a modest impact on regional variations in the number of surgical procedures being performed, while ‘differences in physician beliefs about the indications for surgery’ demonstrated a much stronger correlation [25].

Appleby et al. cite the work of John Wennberg to suggest ‘that when there is strong evidence and a professional consensus that an intervention is effective, there tends to be little or no variation in clinical practice… admission rates for these conditions can be predicted’ [26]. When there is little evidence and only weak consensus about the efficacy of surgery, on the other hand, decision-making is dependent on the opinions of individual practitioners, leading to high levels of variation in admission rates and surgical outcomes. Even for standardized procedures (e.g., tonsillectomy, appendectomy), without robust professional consensus on the indicators for surgery, a patient’s likelihood of accessing treatment can vary considerably depending on where they happen to live (i.e., a postal-code lottery).

The Role of Technology in Achieving Universal Surgical Care

We can summarize that both the Lancet Commission's 2030 targets and the WHO's definition of UHC will require a durable change to the global healthcare framework, a change necessary to assure access to safe and effective surgical services. Key challenges include the following: (a) a shortage in numbers of trained surgeons, (b) an uneven distribution of expertise, (c) funding and resource deficits, and (d) a lack of consensus in best practice. Collectively, these factors can result in disparities in surgical quality of care.

The challenge of making surgery a universal patient right mandates a new paradigm. Such a paradigm should increase resource availability, redistribute surgeon expertise, reduce costs, and, as a result, improve outcomes for patients. It requires an overhaul in capacity, efficiency, collaboration, and capability that industries and service providers are seeking from a digital transformation.

The UK's Royal College of Surgeons (RCS) launched its own commission on the *Future of Surgery* to look specifically at the potential impact of technology on surgical services over the next 20 years. The final report defines four key categories of technology which its authors argue will transform surgical provision:

- Robotics and minimally invasive techniques
- Imaging technologies, including the use of virtual and augmented reality
- Intelligence technology utilizing big data, artificial intelligence, and genomics
- 'Specialist interventions', under which the commission includes innovations like stem-cell therapies and 3D bioprinting [27]

Overall, the RCS envisions a future where automation, data-driven intelligence, sophisticated imaging, and patient-specific interventions, such as tissue and organ generation for implants, drive better outcomes for the majority of surgical procedures. However, it is not entirely clear that the application of digital technology in this manner will naturally lead to resolution of surgeon shortages, rising healthcare and surgical care costs, and limits to global access. In fact, the RCS foresees that highly specialized interventions will probably remain centralized, with skills and resources concentrated in a small number of locations, requiring patients to travel to receive high-quality surgical care. However, the RCS also concluded that technology, like robotics, 'could enable more types of routine surgery to be delivered locally *if resources are available*' [emphasis added].

It is important to recognize that advanced hardware-based solutions – such as master-slave robotics for minimally invasive surgery – may represent a cost which, for many healthcare environments, is prohibitive. While automation does present one solution to the shortage of surgical expertise, it would take a considerable reduction in costs for such technology to become universally accessible. The report also accepts that, in order for such solutions to be delivered effectively, surgical teams must be made up of 'multilinguists' who combine knowledge and skills in medicine, genetics, surgery, radiotherapy, and bioengineering. This imposes an additional burden on the need to develop and distribute expertise effectively. Birkmeyer et al. suggests that new technologies and innovations in techniques can themselves contribute to variation in care because adoption tends to progress in a piecemeal fashion and often without adequate discussion about efficacy and best practice [25].

The key to driving equal distribution of (and access to) surgical care is how to radically scale such services to meet demand while reducing costs. Increasing surgical capacity to the levels set forth by the Lancet Commission and other sources will be contingent upon integration of services [4, 6]. Fortunately, there is a family of affordable technologies readily available worldwide which lend themselves to solving this problem. They are the combination of digital communication solutions and cloud-based software applications that are collectively referred to as *telemedicine*.

The concept of telemedicine specifically refers to the use of ICT and telecommunication technologies to overcome geographical barriers to service delivery – such as for the medical/surgeon expert who might be geographically divided from the patient who requires treatment [28]. Bashshur's definition of telemedicine talks about the use of technology 'as a substitute for face-to-face contact between provider and client', with specific benefits listed including improving access, addressing variations in quality standards, and controlling cost inflation [29].

Interest in telemedicine and proliferation of its solutions has accelerated in tandem with the rapid advances in digital communications over the past two decades. Faster Internet speeds, mobile technology, smartphones, livestream video, cloud data networks, and more have opened the door to significant new possibilities in how patients can be effectively connected to healthcare services over distance, as well as to how medical professionals can connect to, and collaborate with, one another. Typical patient-focused applications for telemedicine include self-diagnosis and health management routes which empower people to make better informed decisions about their own care through online information pathways, remote monitoring through wearable health-tech devices, and remote consultations via video, online messaging, or even social media networks. For healthcare professionals, tele-medical applications extend from the now commonplace use of online reference materials in making day-to-day decisions about care, to using digital collaboration platforms to connect colleagues across different clinical settings, to the use of digital resources in education and training [30].

To date, much of the academic interest in how these principles can be applied specifically to surgery – a field often referred to as *telesurgery* – have narrowed around the use of robotics to enable surgery to be managed remotely [31]. While robotic telesurgery may contribute to tackling the geographical barriers which prevent high-quality surgical access, and while robotics may solve, to some degree, the problem of surgeon shortage, focusing on this technology alone will not adequately address the core challenges of access, shortages of expertise, and variations in standards and cost, which collectively pose impediment to universal patient access to top-level surgical care. Thus, robotic surgery alone does not address the critical issue of needing to train more surgeons so as to increase the global pool of available surgical expertise [32, 33].

This is why, in order to unlock the digital doorway to global access to quality surgical care, the definition of telesurgery should be redefined to include other technologies, namely, digital technology that centres upon communication, collaboration, and information exchange. It is these technologies which are crucial in meeting the challenges outlined by the Lancet Commission and by the definitions of UHC.

A Cloud-Based Communications Platform (Proximie)

Proximie (London, UK) is a cloud-based audio-visual (AV) communications platform which supplements livestream video with augmented reality (AR). It takes the form of an app that can be downloaded on any suitable internet-ready device with a camera and a screen – such as a laptop, tablet, or smartphone. It can be used equally for real-time communication, collaboration, and video recording – with AR providing a rich digital overlay in either case. The Proximie app, therefore, comprises six core component technologies. They are as follows: (1) real-time remote communication (RTRC), (2) AV, (3) AR, (4) cloud computing, (5) ML, and (6) AI. These core components are familiar across a range of telemedicine solutions. Each can be seen to make a distinct contribution to solving the challenge of universal surgical provision. ML and AI can also further enhance the telemedicine experience by providing real-time guidance to surgeons. For instance, Fig. 26.1 demonstrates the capabilities of ML and AI as applied to polyp recognition.

Proximie was developed to help improve access to surgery. Its founding objective was to give surgical practitioners (residing in different locales) a platform that provides an interactive experience, reliable enough to allow them to collaborate on live procedures in real time, overcoming the common problem of not having a

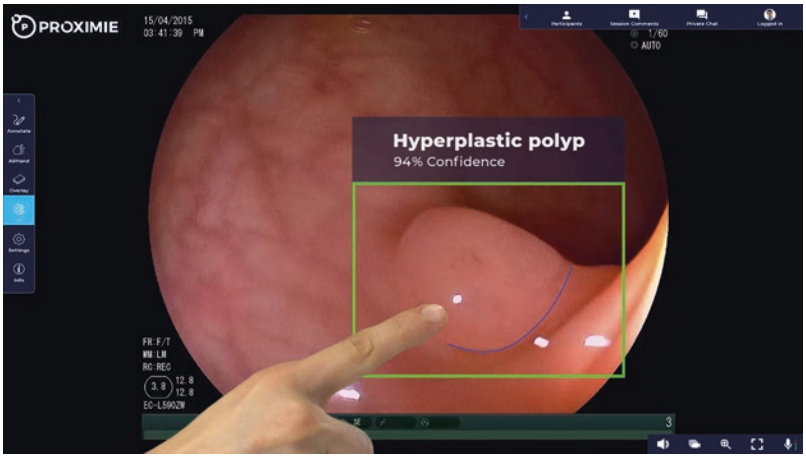

Fig. 26.1 Real-time polyp recognition and classification using integrated AI technology

Fig. 26.2 Integrating Proximie into the operating theatre setting

particular specialist available. Rather than waiting for a specialist to become available, or forcing a patient to travel for care, expertise can be 'beamed in' from varying geographical locations. In this manner, surgeons are able to effectively consult, directly guide, mentor, and demonstrate operations in such a way that they can be safely performed in local (underserved) healthcare environments (please refer to Fig. 26.2).

AR plays an important role in replicating the 'live' experience, substituting a colleague's actual physical presence in the operating room with sophisticated telepresence. This can be accomplished with tools such as digital markup of a live video image, gesture-activated demonstration, and the ability to post digital content directly to the feed. Via their cameras and screens, remote colleagues are able to interact on a more meaningful level than just watching a plain video feed and simple voice telecommunication.

RTRC technologies help to overcome geographical barriers to surgery by eliminating the inefficiency associated with waiting times and travel. This applies to all stages of the patient journey. Audiovisual communications allow for the possibility of consultants carrying out patient assessments remotely, drastically reducing the time it takes to make decisions about surgical pathways when an appropriately qualified specialist is not available at a particular hospital [34].

Many of the elements of high-quality surgical care are related to planning, preparation, and sharing of expertise. Hence, the use of technology to enable effective collaboration (wherever practitioners happen to practice) *will shorten delivery cycles and increasingly ensure complex procedures can be delivered in more locations. Better communication* thus answers the Lancet Commission's call for surgical services to be more tightly integrated across all levels of care –

from community referral networks to specialist surgical teams [6].

There is an important role for RTRC technologies in enabling 'tele-live' procedures, by connecting practitioners to remote experts as they operate: the virtual equivalent of the consultant 'looking over the shoulder' in the operating room. But this, alone, will not resolve all challenges of providing universal surgical care. Geographical barriers to access are, in part, caused by shortages and uneven distribution of surgical expertise. The only sustainable remedy to this dilemma is to increase the *global surgical skills base*, by training more surgeons, and by expanding the range of procedures they are able to perform. Communications technologies, and AV platforms in particular, have a well-established role in surgical training and skillset development, providing a means of sharing knowledge more broadly.

In general terms, the use of video technology in surgical education is widely associated across academic studies with improved resident knowledge and greater participant satisfaction [35]. Recorded video is widely used in peer-to-peer coaching across all levels of expertise [36]. Studies into the use of video review of procedures in training and development indicates better learning outcomes, with coaches and mentors able to make more teaching points per unit of time, compared to conventional feedback and guidance given during a procedure. Video reviews result in improved technical, cognitive, and decision-making skills [37, 38].

Recorded video thus provides an invaluable resource which is helping to strengthen surgical skills globally. But by combining video with RTRC technologies and also making livestreaming a core part of training and education, a radical overhaul of *how* surgical skills, standards, and how best practice are disseminated can be achieved. Ultimately, this will overcome barriers (imposed by geography) to facilitate a truly global *flow of expertise.*

As an example of real-world application, Proximie has been used in training programs at major academic centres (e.g. University College London and Yale University) to allow trainee surgeons to observe procedures carried out by specialists based in distant hospitals. Through the lens of AR enhancement, an immersive, interactive learning experience helps bridge the divide between theory and practical application. Tantamount to 'tele-observation', dozens of students can watch and learn at once – rather than the otherwise 1–2 who might be present in the operating room. Knowledge therefore spreads further and faster.

Proximie applications have been used in transnational mentoring projects to help connect globally recognized experts with local surgical teams. In Peru and Vietnam, for example, the Proximie app was used to connect local surgical teams with academic centres in the United States and UK. The remote development program at the EsSalud Hospital in Trujillo, Peru, led to the team achieving a significant increase in the number of cleft lip and cleft palate corrections it was able to perform, as a direct result of long-distance professional dialogues around best practice and via remote coaching.

Similarly, the International Society for Hip Arthroscopy (ISHA) has adopted Proximie as a means of connecting members across four continents, with the aim of establishing best practice principles and enabling effective collaboration. The organization uses both livestream and recorded video to conduct live and 'as live' training and development conferences, creating a platform for global specialists to demonstrate and discuss surgical techniques and procedural nuances in the OR. This directly aided ISHA in promoting global standards in patient care, reducing variations from region to region (by connecting practitioners in real time), and extending the professional community beyond the boundaries of a particular hospital or department.

Finally, in the context of making access to surgery a universal right that people in all parts of the world can benefit from in practice, it is important to emphasize that the digital technologies highlighted herein come with an additional cost burden (albeit minimal) and indeed may even help to improve cost-efficiency overall. The assumption is often that technological solutions are expensive, require large amounts of complex equipment, and may require years of implementation before value is achieved. But in this paradigm of telesurgery, that may no longer be a valid assessment.

Solutions which are built on readily available, affordable technologies that have become part of the fabric of everyday life – the Internet, laptops, smartphones, digital cameras – may not impose a significant new cost. Cloud-based software is not only highly cost-effective, it is also easily accessible to anyone with an Internet connection and *enormously scalable – exactly what is required when we are aiming to extend surgical services to tens of millions of people worldwide and improve access and quality for those who already have it.* Moreover, because these existing technologies are already familiar to surgeons and healthcare providers, they are *immediately ready* for rapid adoption.

Conclusion

Achieving global standards in surgical care, allowing for safe, universal access is a daunting challenge. What is clear from the scale of the task to 2030 and beyond is that old models of surgical provision must be updated and replaced by approaches that suit a truly global vision. The solution will require the use of digital technology integration across disciplines, across departments, between hospitals, regions, and nations. The paradigms described herein, increased availability of surgical expertise, standardized practice, and improved resource efficiency will all allow surgery to become more widely accessible.

In order to achieve the aims of better integration, improved collaboration, expanded knowledge sharing, and open surgeon dialogue, digital communication technology is essential. Ultimately, digital-based communication and apps represent the key which unlocks the global doorway to surgical care. It is integral to resolving the problem of surgical access. By providing remote access, timely support, open knowledge exchange, and a networked infrastructure, technology can increase the availability of surgery and quality of care without the need for an unsustainable increase in human or capital resources.

At the time of writing, telemedicine is actively being employed to respond to one of the greatest challenges ever faced by modern healthcare systems: the COVID-19 global pandemic. As the relentless spread of the virus threatens humanity as a whole, the need for clinicians and surgeons to connect remotely has never been more vital. Telemedicine is enabling healthcare providers to access expert advice and best practice solutions in real time while also containing viral spread by reducing the number of individuals required to be physically present in a clinical space. In March 2020, during the midst of the pandemic, Proximie was employed by a cardiothoracic surgeon in Beirut to connect with a medical device expert in order to perform a life-saving novel mitral clip surgery, a procedure that would have otherwise been impossible in light of the current travel restrictions. It is during these critical times, when healthcare communities must stand shoulder to shoulder, that we can recognize the true value of augmented technology solutions and appreciate their role in providing access to surgical care for all patients, regardless of location.

References

1. World Health Organization. Human rights and health. 2017 [Internet]. https://www.who.int/news-room/fact-sheets/detail/human-rights-and-health.
2. Meara JG, Greenberg SLM. Global surgery as an equal partner in health: no longer the neglected stepchild. Lancet. 2015;3:S1–2. Available from https://www.thelancet.com/journals/langlo/article/PIIS2214-109X(15)70019-7/fulltext.
3. McQueen K, Watters DA, Tangi V. World J Surg. 2017;41:5. https://doi.org/10.1007/s00268-016-3651-6.
4. Patterson R, Corley J. Do we have a right to surgery? The case for access to all. 2018. Available from https://www.globalhealthnow.org/2018-09/do-we-have-right-surgery-case-access-all.
5. Eyler L, Mohamed S, Feldhaus I, Dicker R, Juillard C. Essential surgery as a component of the right to health: a call to action. Hum Rights Q. 2018;40(3):641–62. Available from https://muse.jhu.edu/article/699507.
6. Meara JG, Leather AJM, Hagander L, et al. Global surgery 2030: evidence and solutions for achieving health, welfare, and economic development. Lancet. 2015;386:569–624. http://www.globalsurgery.info/wp-content/uploads/2015/01/Overview_GS2030.pdf.

7. Watters DA, Guest GD, Tangi V, Shrime MG, Meara JG. Global surgery system strengthening: it is all about the right metrics. Anesth Analg. 2018;126(4):1329–39. https://www.ncbi.nlm.nih.gov/pubmed/29547428.
8. World Health Organization. WHO estimates cost of reaching global health targets by 2030. 2017 [Internet]. Available from: http://www.who.int/mediacentre/news/releases/2017/cost-health-targets/en/.
9. World Health Organisation. What is health financing for universal coverage? 2019 [Internet]. https://www.who.int/health_financing/universal_coverage_definition/en/.
10. Dickman S, Himmelstein D, Woolhandler S. Inequality and the health-care system in the USA. Lancet. 2017;389:1431–41. Available at http://www.rootcausecoalition.org/wp-content/uploads/2017/04/Inequality-and-the-health-care-system-in-the-USA.pdf.
11. Haider AH, Scott VK, Rehman KA, et al. Racial disparities in surgical care and outcomes in the United States: a comprehensive review of patient, provider, and systemic factors. J Am Coll Surg. 2013;216(3):482–92.e12. Available at https://www.ncbi.nlm.nih.gov/pmc/articles/PMC5995336/.
12. Haider AH, Weygandt PL, Bentley JM, et al. Disparities in trauma care and outcomes in the United States: a systematic review and meta-analysis. J Trauma Acute Care Surg. 2013;74(5):1195–205. Available at https://www.ncbi.nlm.nih.gov/pmc/articles/PMC3641534/.
13. Henderson J. The plastic surgery postcode lottery in England. Int J Surg. 2009;7(6):550–8. Available at https://www.ncbi.nlm.nih.gov/pubmed/19800037.
14. Burdon M. End the postcode lottery for cataract surgery. BMJ. 2019;365:l2293. Available at https://www.bmj.com/content/365/bmj.l2293.full.
15. Stevens R, Stevens S, Rusby J. The "postcode lottery" for the surgical correction of gynaecomastia in NHS England. Int J Surg. 2015;22:22–7. Available at https://www.sciencedirect.com/science/article/pii/S1743919115010602.
16. Blennerhassett M. Individual funding request process is bad for everyone. BMJ. 2018;362:k3833. Available at https://www.bmj.com/content/362/bmj.k3833.
17. Beerstecher H. I accuse NHS England of a lack of transparency. BMJ. 2018;362:k3028. Available at https://www.bmj.com/content/362/bmj.k3028/rr.
18. The King's Fund. Trusts in deficit. 2018 [Internet]. https://www.kingsfund.org.uk/projects/nhs-in-a-nutshell/trusts-deficit.
19. Mann S. Research shows shortage of more than 100,000 doctors by 2030. 2017 [Internet] https://www.aamc.org/news-insights/research-shows-shortage-more-100000-doctors-2030.
20. Lack of specialist surgeons 'putting patients at risk'. 2017 [Internet]. https://www.theguardian.com/politics/2017/dec/31/lack-of-specialist-surgeons-putting-patients-at-risk.
21. Etzioni DA, Ko CY. Providing surgical care to an aging population: implications for the surgical workforce. In: Rosenthal R, Zenilman M, Katlic M, editors. Principles and practice of geriatric surgery. New York: Springer; 2011. https://doi.org/10.1007/978-1-4419-6999-6_12.
22. Thompson C. Meeting the challenges of an ageing population. 2015 [Internet]. https://www.england.nhs.uk/blog/catherine-thompson/.
23. Government Office for Science. Future of an ageing population. 2016. https://assets.publishing.service.gov.uk/government/uploads/system/uploads/attachment_data/file/816458/future-of-an-ageing-population.pdf.
24. McVeigh TP, Al-Azawi D, O'Donoghue GT, Kerin MJ. Assessing the impact of an ageing population on complication rates and in-patient length of stay. Int J Surg. 2013;11(9):872–5. Available from https://www.ncbi.nlm.nih.gov/pubmed/23917211.
25. Birkmeyer JD, Reames BN, McCulloch P, Carr AJ, Campbell WB, Wennberg JE. Understanding of regional variation in the use of surgery. Lancet. 2013;382(9898):1121–9. Available from https://www.ncbi.nlm.nih.gov/pmc/articles/PMC4211114/.
26. Appleby J, Raleigh V, Frosini F, Bevan G, Gao H, Lyscom T, Variations in health care: the good, the bad and the inexplicable. 2011 The King's Fund. https://www.kingsfund.org.uk/sites/default/files/Variations-in-health-care-good-bad-inexplicable-report-The-Kings-Fund-April-2011.pdf.
27. Pitruzella B, Leahy P. The future of surgery. Royal College of Surgeons. 2018. https://www.rcseng.ac.uk/standards-and-research/future-of-surgery/.
28. World Health Organisation. Telemedicine: opportunities and developments in member states. 2010. Available from https://www.who.int/goe/publications/goe_telemedicine_2010.pdf.
29. Bashshur R. On the definition and evaluation of telemedicine. *Telemedicine Journal* 1:1. https://doi.org/10.1089/tmj.1.1995.1.19.
30. Hjelm N. Benefits and drawbacks of telemedicine. J Telemed Telecare. 2005;11:60–70. Available at https://www.researchgate.net/profile/Nils_Hjelm/publication/7908107_Benefits_and_drawbacks_of_telemedicine/links/568825f308aebccc4e155b68/Benefits-and-drawbacks-of-telemedicine.pdf.
31. Choi P, Oskouian R, Tubbs RS. Telesurgery: past, present, and future. Cureus. 2018;10(5):e2716. https://doi.org/10.7759/cureus.2716.
32. Wilensky G. Robotic surgery: an example of when newer is not always better but clearly more expensive. Milbank Q. 2016;94(1):43–6. https://doi.org/10.1111/1468-0009.12178.
33. Shah N, Laungani R, Kaufman M. Financial considerations in robotic surgery. SAGES Atlas Robot Surg. 2018:45–51. https://doi.org/10.1007/978-3-319-91045-1_5.
34. Greenhalgh T, Vijayaraghavan S, Wherton J, et al. Virtual online consultations: advantages and limitations (VOCAL) study. BMJ Open. 2016;6:e009388.

https://doi.org/10.1136/bmjopen-2015-009388.. Available from https://www.health.org.uk/sites/default/files/Virtual%20online%20consultations%20BMJ%20article.pdf.

35. Green J, Suresh V, Bittar P, et al. The utilization of video technology in surgical education: a systematic review. J Surg Res. 2019;235:171–80. https://doi.org/10.1016/j.jss.2018.09.015.
36. Hu Y, Peyre SE, Arriaga A, et al. Postgame analysis: using video-based coaching for continuous professional development. J Am Coll Surg. 2012;214(1):115–24. Available at https://www.ncbi.nlm.nih.gov/pubmed/22192924.
37. Hu Y, Mazer L, Yule S, et al. Complementing operating room teaching with video-based coaching. JAMA Surg. 2017;152(4):318–25. Available at https://www.ncbi.nlm.nih.gov/pubmed/27973648.
38. Greenberg C, Ghousseini H, Pavuluri Quamme S, et al. A statewide surgical coaching program provides opportunity for continuous professional development. Ann Surg. 2018;267(5):868–73. Available at https://www.ncbi.nlm.nih.gov/pubmed/28650360.

Telementoring for Minimally Invasive Surgery

27

Justin W. Collins, Runzhuo Ma, Yanick Beaulieu, and Andrew J. Hung

Introduction

Telemedicine is the ability for a clinician to provide clinical healthcare or advice from a remote location using telecommunication technologies. To date, telementoring has been implemented in many areas of healthcare management including teleradiology and remote management of intensive care units or international patients [1–4]. In surgical training, minimally invasive surgery using video has greatly improved opportunities for sharing surgical technique and education and for providing feedback on performance.

The implementation of innovative technologies has given rise to *surgical telementoring* – the application of telemedicine in the field of surgical instruction. Telementoring has existed in various forms for more than 20 years and has been shown to positively impact patient outcomes [5]. As an example, in a study by Pahlsson et al., telementoring delivered from a high-volume surgeon at a tertiary hospital to a low-volume surgeon at a rural hospital increased their cannulation rate in endoscopic retrograde cholangiopancreatography from 85% (one of the lowest in the country) to 99%, equaling the highest success rate in the national statistics [6]. This higher success rate was also maintained after the telementoring support was removed.

While robotic surgery continues to evolve quickly, it has high initial start-up costs, including the investment in a surgeons' learning curve for learning both established and new techniques. Maximum service value is only realized once the team is experienced, working safely and efficiently with patient outcomes optimized. There are various elements to an optimized service, and there are recognized different skill sets between different tertiary centers of excellence [7]. Successful training delivered remotely, with an expert surgeon having the ability to observe real-time video of surgical operations and to provide guidance to trainee surgeons outside of the main operating room, has the potential to shorten learning curves [8]. Expert mentors can then disseminate their knowledge from a distance, without the need or costs for the mentor or mentee to travel. While the opportunities are large, the safe integration of any new technology requires understanding of both the rewards and risks.

Verbal guidance, telestration, and tele-assist are forms of surgical telementoring that differ in

J. W. Collins (✉)
Department of Urology, University College London Hospitals NHS, London, UK
e-mail: Justin.collins@ucl.ac.uk

R. Ma · A. J. Hung
Catherine & Joseph Aresty Department of Urology, University of Southern California Institute of Urology, Center for Robotic Simulation & Education, Keck School of Medicine, University of Southern California, Los Angeles, CA, USA

Y. Beaulieu
Cardiology and Critical Care, Hôpital Sacré-Coeur de Montréal and Montreal Heart Institute, Montreal, QC, Canada

S. Atallah (ed.), *Digital Surgery*, https://doi.org/10.1007/978-3-030-49100-0_27

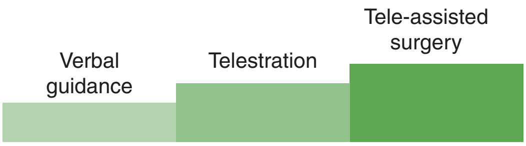

Fig. 27.1 Stepwise upgrade of telementoring

the degree of intervention an expert surgeon is able to provide and the equipment required. The different forms of surgical telementoring allow proctor surgeons to offer verbal guidance, provide visual aid (telestration), or even take control over the robotic instruments (tele-assisted surgery) (Fig. 27.1). This chapter serves to provide insight on the applications, development, and challenges for the integration of telemedicine in minimally invasive surgery.

Background

The conceptual idea of robotic surgery began more than 50 years ago [9]. However, the first usable systems were not developed until the late 1980s with Robodoc (Integrated Surgical Systems, Sacramento, CA); this orthopedic image-guided system was developed by Hap Paul and William Bargar, for use in prosthetic hip replacement [10]. Around the same time, a similar project developing a urologic robot for prostate surgery was being developed by Brian Davies and John Wickham [11]. These were procedure-specific, computer-assisted, and image-guided systems that proved both the concept and potential value of robotic surgery systems (computer-assisted surgery). The first multipurpose teleoperated robotic systems were initially developed by SRI International and the Defense Advanced Research Projects Agency (DARPA), resulting in the surgeon console-controlled multifunctional robotic surgery systems we are now familiar with [12]. The drive to develop these remotely controlled systems by DARPA was driven by the identified need to provide additional expertise and technical skills to help decrease morbidity and mortality in battlefield casualties. The principle of providing surgical expertise from a remote geographical location remains pertinent to various operating room scenarios including learning curves – as well as emergency and "unfamiliar" situations, where the alternative is to convert to an open or laparoscopic procedure.

While the early goals of surgical robotics were focused on long-distance telesurgery, there are few examples of this being attempted due to the limitations of cost, available infrastructure, and legal and safety issues [13]. On September 7, 2001, Professor Jacques Marescaux and his team from the Institute for Research into Cancer of the Digestive System (IRCAD) successfully completed the first transatlantic operation. The Lindbergh Operation was a complete telesurgical minimally invasive cholecystectomy operation carried out on a patient in Strasbourg, France, with the surgeon located in New York, using high-speed ISDN fiber-optic services and the ZEUS robotic platform [14].

This transatlantic robotic cholecystectomy was completed with data traveling around distance of approximately 8700 miles with average round time delay (RTD) of only 155 ms achieved due to the lack of interruptions from bridges, routers, and gateways (hops) that a dedicated transatlantic connection benefits from. The project was supported by the French telecommunication company ACTEL with costs estimated to be greater than €1 million without proven benefit to patient outcomes [15]. However, the implications of utilizing this technology are immense. Speaking at the time, in 2001, Professor Marescaux commented: "*The demonstration of the feasibility of a trans-Atlantic procedure, dubbed 'Operation Lindbergh,' is a richly symbolic milestone. It lays the foundations for the globalization of surgical procedures, making it possible to imagine that a surgeon could perform an operation on a patient anywhere in the world.*"

In 2001, the FDA approved Socrates, the telementoring system developed by Computer Motion that could integrate an operating room for telementoring services. Also, in 2001, the world's first national telesurgery initiative was launched in Canada with the goal of disseminating expertise from large tertiary hospitals to remote and rural medical centers [16–18].

The Centre for Minimal Access Surgery group led by Dr. Mehran Anvari, located at McMaster University and St. Joseph's Hospital in Ontario, Canada, trained surgeons through telementoring, as well as completing numerous successful tele-assisted surgeries utilizing a dedicated virtual private network (VPN) [17, 18]. Procedures completed included Nissen fundoplication, hemicolectomies, sigmoid colon resections, and other procedures [19, 20]. The potential and effectiveness of telementoring as an educational tool were demonstrated, with an average RTD of 150 to 200 ms. At the time (circa 2005), Dr. Anvari commented that while surgery may be possible with up to a 200 ms lag, the effects of visual cue and proprioception mismatch at greater levels of lag result in extreme difficulty for the operator, and even nausea [21].

On the January 8, 2019, a surgeon in China, in the southeastern province of Fujian, performed the world's first remote operation using 5G technology. The tele-assisted robotic surgery was reported in the *South China Morning Post* with the surgeon utilizing the 5G network to remotely control the robot from a location 30 miles away [22]. During the procedure, the surgeon removed the liver of a laboratory test animal over the 5G connection with a latency (lag time) of just 0.1 seconds. This experimental procedure proved that 5G can meet the requirements of telementoring and even tele-assisted surgery and that it offers exciting new opportunities to the application and accessibility of telemedicine services.

Infrastructure

Telecommunication can currently be achieved via cables, radio waves, or Wi-Fi. All three modalities, depending on their underlying infrastructure, have wide variability in quality assurance regarding access, bandwidth, and latency or round time delay (RTD). Robotic networks, delivering telementoring services, can have a dedicated infrastructure, a so-called virtual private network (VPN), with predefined quality assurance. The infrastructure can comprise optic cables, 4 or 5G, Wi-Fi, cloud computing, or more likely a combination. In a hospital setting, a VPN is called a local access network (LAN), and with a wider geographical access, connecting multiple sites, it is termed a wide access network (WAN). Both LANs and WANs can be quality assured with regard to bandwidth and latency, and they can also have associated dedicated services, such as data storage services that can be delivered through a framework of cloud computing.

Optimized cable infrastructure is currently provided with fiber-optic cables and is the most reliable infrastructure but has high setup and running costs [14]. The 4G or 5G radio wave communication both have bandwidth sufficient to provide telementoring and tele-assisted surgery services [22]. The 5G (5th Generation) is the latest generation of cellular mobile communications. Improved performance targets of 5G include high data rate, reduced latency, cost reduction, higher system capacity, and the potential for multiple device connectivity.

Cloud computing enables computer system resources, such as storage and computing power, that are available on demand without direct active management by the user. Cloud computing is generally used to describe data centers available to many users over the Internet. Clouds may be limited to a single organization (enterprise clouds) or be available to many organizations (public cloud) or a combination of both (hybrid cloud). Large clouds currently predominate, with services distributed over multiple locations from central servers.

Wi-Fi is a wireless network technology that delivers local wireless networks. Different versions of Wi-Fi exist, with different ranges, radio bands, and speeds. Wi-Fi most commonly uses the 2.4 GHz UHF and 5 GHz SHF ISM radio bands. These wavelengths work best for line-of-sight connectivity, being absorbed or reflected by materials, which further restricts range. At close range, some versions of Wi-Fi, running on suitable hardware, can achieve speeds of over 1 Gb/s. The most common Wi-Fi is a local area network (LAN) that uses high-frequency radio signals to transmit and receive data over distances of a few hundred feet, using ethernet protocol. Wi-Fi has been shown to be capable of providing telementoring services within a hospital LAN [23].

The identified needs for setting up a telementoring infrastructure with a secure, reliable network of sufficient bandwidth, with ability to prioritize data transfer (without latency), have, to date, kept service costs high and limited accessibility to telementoring across greater distances. The more expensive a procedure, the harder it is to deliver value, so this has previously been a limiting step in the progression of telementoring and tele-assisted surgery [8]. In an optimized robotic network, telementoring services would include tele-assist surgery. However, this service requires minimal latency [21].

The launch of 5G networks offers exciting opportunities for telementoring compared to the previous data transmission standards available; it has been successfully utilized to telementor two laparoscopic surgeries in 2019 [24]. However, the increased bandwidth and speed of 5G transmission also highlights concerns regarding the security of health data transfer.

Telementoring can currently be delivered with different network infrastructures with theoretically different goals ranging from intervention in emergency scenarios to elective (planned) guidance of live surgery to dissemination of expertise via livestreamed surgery with real-time interaction delivered via social media [25] (Table 27.1).

Besides network, latency can also arise from *codec,* which is a software for encoding/decoding a digital data stream or signal [26]. For a given bandwidth, a trade-off exists between video quality (resolution and frame rate) and encoding/decoding of the video. Increase of either resolution or frame rate aggravates network burden – because of the requirement for deeper compression and decompression, which lengthens transmission latency. In order to shorten the latency, one study proposed AI software using shallow convolutional neural networks to automatically code the surgical incision region in *high* quality whereas the background region in *low* quality [27].

Verbal Guidance

The simplest form of surgical telementoring is verbal guidance. With these cases, a surgical mentor is typically presented with a one-way transmitted real-time video of the surgical operation and is able to provide verbal feedback or instruction to those present in the operating room [5, 28–36] (Table 27.2). Operating rooms equipped with standard laparoscopic, endoscopic, or interventional radiologic (IR) systems require no major upgrade of the current systems. The operating rooms can be supplemented with

Table 27.1 Potential levels of telementoring

Level	Network	Quality assured	Latency	Telestration	Tele-assist surgery	Access	Potential for skill transfer	Cost
1	VPN	Yes	<100 ms (dependent on distance covered and hops)	Yes	Yes	Low	High	High
2	5G	5G coverage-related variability	<100 ms (dependent on 5G coverage)	Potentially	Yes	High	High	Low
3	Open point-to-point	Internet-variable reliability	Minimal delays	Variable functionality	No	High	Variable	Variable (hardware)
4	Cloud based	Cloud-variable reliability	10- to 30-second delays	Potentially	No	High	Variable	Low

Table 27.2 Studies of telementoring with verbal guidance

Research	Specialty	Procedure	Distance	Equipment in local operation room	Equipment for remote proctor site	Connection	Outcome
2008 Gambadauro et al. [28]	Gynecology	Abdominal, vaginal, and laparoscopic surgery	Not mentioned	Standard laparoscopic/endoscopic/robotic system or interventional radiologic system, external camera system, a multidirectional microphone, and computer installed with video and audio transmission software	Video monitor with speakers, a multidirectional microphone, or a real-time multimedia conferencing platform	Not mentioned	Not mentioned
2005 Sebajang et al. [29]	General surgery	Laparoscopic bowel resections, Nissen fundoplications, splenectomies, reversal of a Hartmann procedure, and ventral hernia repair	400 km			ISDN lines with bandwidths from 385 kbps to 1.2 Mbps	No intraoperative complications. Two major postoperative complications occurred.
2013 Treter et al. [30]	Endocrinology	Posterior retroperitoneoscopic adrenalectomy	2400 km			Not mentioned	Procedures were performed uneventful.
2016 Clifford et al. [31]	Urology	Robotic prostatectomy and nephrectomy	77 km			3200 Mbps or 800 Mbps	All procedures were completed without complication or adverse events.
2005 Challacombe et al. [5]	Urology	Hand-assisted laparoscopic living donor nephrectomy	Transatlantic			Four ISDN lines 128 kbps × 4	All procedures were completed without complication or adverse events.
2005 Di Valentino et al. [32]	Vascular surgery	Endovascular aortic aneurysm repair	250 km			Four ISDN lines with a total transmission rate of 384 kbps	Surgery operated by the local team with telementoring support had comparable results to experienced interventionist.
2007 Agarwal et al. [33]	Urology	Laparoscopic radical nephrectomy/partial cystectomy	5 miles			Not mentioned	Procedures were performed uneventful.
2009 Rothenberg et al. [34]	Pediatrics	Laparoscopic pediatric surgery	1500 miles			Not mentioned	Procedures were performed uneventful.
2013 Anderson et al. [36]	Urology	Diagnostic flexible cystoscopy	Two adjacent rooms			Not mentioned	Telementoring was highly acceptable to patients undergoing endoscopic procedures.
2015 Safir et al. [35]	Urology	Endoscopic training	<5 m			Not mentioned	Telementoring enhanced resident education and endoscopic training.

commercially available equipment – such as an external camera, a multidirectional microphone, and a computer installed with telecommunication software. On the other hand, the mentor's remote office only requires a video monitor with speakers and a microphone. With this framework, a video feed of the laparoscopic and external views and two-way audio signals can be transferred between the two locations. For IR procedures, signal transfer of fluoroscopic images and intravenous ultrasound replaces the laparoscopic feed.

There are many verbal telementoring software and hardware systems that are commercially available to medical institutions [28–31]. Personal computers can download telecommunication software such as UltraVNC™ and NetMeeting™ in order to achieve video and audio signal transmission [4]. Telementoring hardware systems for verbal guidance include Comstation (Zydacron, UK), incorporating Z360 telementoring CODEC (coder/decoder) (Zydacron, UK) [5] and integrated endourology suites (IES) [35, 36]. A commercially available videoconferencing system (Eykona; Aethra S.p.A., Ancona, Italy) was used to transmit the data over 4 ISDN lines with a total transmission rate of 384 kbps [32]. With the Remote Presence-7 (RP-7 InTouch Health, Santa Barbara, California, USA), a proctor can control a remote presence robotic system using a laptop control station. From a remote locale, the proctor is able to communicate via real-time, two-way audio-video communication using a robot fitted with two advanced digital cameras, an audio microphone, and amplification circuitry. The proctor also has control over the robot's moveable head, allowing them to pan, zoom, and tilt their video feed accordingly [34].

Verbal guidance telementoring can easily be implemented into an operating room at relatively low cost due to widely available systems, mature technology, and its ability to function at a low bandwidth. The most evident drawback is that verbal guidance offers one of the lowest levels of interaction between proctor and trainee surgeons in the field of surgical telementoring.

Guidance with Telestration

Telestration improves upon verbal guidance by offering additional instruction to trainee surgeons through the use of visual aids. Telestration allows the remote proctor to add illustrations and/or annotations that overlay the view of the operating field on monitors in the operating room (i.e., to draw or sketch on a video screen image). These visual instructions allow mentors to indicate target areas in real time thereby enhancing the teaching experience. For robotic cases, telestration can be two-dimensional (2D) or three-dimensional (3D) based on the visual effect of the illustration and/or annotation.

2D Telestration

The current mainstream application of telestration in surgical telementoring is 2D telestration [23, 37–45] (Table 27.3). Beyond equipment necessary for verbal guidance telementoring, the mentor's office only requires an additional telestration interface to draw on (termed a *telestrator*). By drawing on this interface, the mentor produces illustrations that simply overlay the operating surgeon's field on view on monitors present in the operating room.

Stryker Doctor's Office System (Stryker Canada, Hamilton) supports verbal guidance and telestration. The remote office is equipped with a touch-sensitive annotator screen that displays the operative field of view. The mentor is able to use a stylus to draw directly on the screen, producing a superimposed image on accessory monitors in the operating room [37–42]. For robotic cases, Connect™ (Intuitive Surgical, Sunnyvale, CA) is a software solution that supports telestration and is integrated into the da Vinci Surgical System. The mentor can offer verbal guidance and telestration by using a mouse or trackpad to draw annotations. With this program, the illustrations overlay the operating surgeon's field of view directly within the robotic surgeon console,

Table 27.3 Studies of surgical telestration

Research	Specialty	Procedure	Distance	Equipment in local operation room	Equipment for remote proctor site	Connection	Outcome
2015 Shin et al. [23]	Urology	Robotic-assisted radical prostatectomy and robotic partial nephrectomy	0.35 km	Standard laparoscopic system or robotic surgical system, external camera system, a multidirectional microphone, and a computer equipped with telecommunication or telestration software	2D or 3D video monitor with speakers, a multidirectional microphone, a telestrator video sketch pad, a touch-screen computer, or a touch-sensitive annotator screen	Not mentioned	Comparable between in-room and remote mentored cases. Wired connections had lower latency and better data transfer than wireless connection.
2009 Schlachta et al. [37]	Colorectal Surgery	Laparoscopic colon surgery	60 km			768 kbps	No intraoperative complications. Telementored cases took longer operating time. Post-operation complications were equivalent to compare group.
2016 Bruns et al. [38]	Pediatrics	Laparoscopic appendectomy and thoracoscopic total thymectomy	6320 km			700 kbps	Procedures completed successfullywith "high satisfaction" from telementors and telementees
2016 Snyderman et al. [39]	Laryngology	Endoscopic endonasal procedures	7260 km			Not mentioned	Nine of 10 cases obtained adequate audio and video communications telestration instructions.
2015 Forgione et al. [40]	Gastroenterology	Laparoscopic colorectal surgery	2868 km			256 kbps	Two procedures were successfully performed.
2014 Ponsky et al. [41]	General surgery	Video-assisted thoracic surgery lower lobectomy, gastric stimulator placements, and laparoscopic inguinal hernia repairs	2140 km			700 kbps	All procedures completed successfully without loss of transmission or complications
2005 Bruschi et al. [42]	Endocrinology	Laparoscopic adrenalectomy	430 km			Four ISDN lines, 128 kbps × 4	All the procedures were successfully performed.
2014 Hinata, at el [43]	Urology	Robotic-assisted radical prostatectomy	230 km			1 Gbps	Similar results and postoperative outcomes between telementoring surgeries and in-room mentoring surgeries
2016 Fuertes-Guiro et al. [44]	Bariatric surgery	Laparoscopic bariatric surgery	Not mentioned			1.2 Mbps	Patients undergoing laparoscopic bariatric surgery by community surgeons receiving telementoring had shorter surgical time, less conversion rate, and shorter hospital stay.
2017 Meijer, at el [45]	Urology	Laparoscopic partial nephrectomy in a porcine model	1970 km			12 Mbps download speed and 5 Mbps upload speed	The procedures were successfully performed.

therefore eliminating the need for the operating surgeon to view a separate video input [23]. Other telestration setups are possible using verbal guidance telementoring systems with the addition of a telestration sketch pad or touch-screen personal computer [43–45].

3D Telestration

For robotic cases on the da Vinci Surgical System, the surgeon console provides operating surgeons with a 3D view and depth perception of their operating field. Ali et al. developed a video algorithm that transforms a proctor's 2D telestration into a 3D telestration viewed on the console's display [46]. The software algorithm processes the original 2D illustration and calculates a corresponding image in the parallax view (i.e., for the contralateral eye). In this process, the 2D annotation becomes a true 3D telestration image that more accurately pinpoints areas of interest for the operating surgeon.

Jarc et al. advanced telestration techniques by introducing three types of 3D tools to enhance learning: 3D pointers (3Dpointers), 3D cartoon hands (3Dhands), and 3D instruments (3Dinstruments) [47]. These 3D tools are semi-transparent virtual images that can be superimposed and shifted on the operating surgeon's endoscopic view. In remote offices, mentors control these virtual tools using Razer™ Hydra motion controllers (Sixense Entertainment, Inc., Los Gatos, CA, USA), a third-party gaming controller. In addition to the basic illustration capabilities of telestration, the 3D tools provide an opportunity to present the operating surgeon with visual cues on how to physically manipulate the robot console and control robotic instruments. 3Dpointers is the most basic tool, allowing mentors to point and draw in 3D. 3Dhands is a visualization of cartoon hands that allow proctors to demonstrate hand positioning and grasping, as perceived by the opening and closing of the index finger and thumb. 3Dinstruments depicts a da Vinci Endowrist Large Needle Driver instrument that also conveys positioning and grasping through the opening and closing of the instrument jaws. In a subsequent study, Jarc et al. validated the effectiveness of the 3D proctoring tools for interactions between mentors and trainees during live porcine surgical tasks [48].

Telestration improves upon verbal guidance by providing more precise instruction through the use of visual aids. However, it not only requires additional hardware (i.e., telestration screen interface) but also mandates a higher level of bandwidth to accommodate for the greater data signal being transferred. Without upgrading the bandwidth level, delays in signal transfer can compromise communication and affect this teaching approach. While there is no current literature on signal delays during telestration, telesurgery provides us with insight on the effect of temporal delays.

Guidance with Tele-assist

The development of robot-assisted surgical cases has provided fertile ground for the field of surgical telementoring in the form of tele-assist. For these robotic cases, an operating surgeon has the ability to control a robotic arm not only from across the operating room but also from remote locations. Using tele-assist, a surgical mentor can control the robotic scope and instruments without being present in the operating room [17, 49–56] (Table 27.4). This form of telementoring is the highest level of interaction between mentor and trainee, allowing the mentors to extend their hand into the operating room and participate in the surgery – perhaps by physically readjusting the endoscope to enhance the visual field or by applying traction for better exposure. Contrary to previous methods of surgical telementoring, this method requires the operating room to be upgraded with a surgical robot equipped with a camera and minimally invasive surgical instruments. The robotic arms could then be controlled by the trainee surgeon on the surgeon console or a mentor in a remote office.

In 1994, the FDA approved the Automated Endoscopic System for Optimal Positioning (AESOP®, Computer Motion, Inc.), a robotic arm that has since been extensively utilized dur-

Table 27.4 Studies of tele-assisted surgery

Research	Specialty	Procedure	Distance	Equipment in local operation room	Equipment for remote proctor site	Connection	Outcomes
2005 Mendez et al. [49]	Neurosurgery	Craniotomies for brain tumors, arteriovenous malformation, carotid endarterectomy, and lumbar laminectomy	400 km	Standard laparoscopic system and robotic surgical system, external camera system, a multidirectional microphone, and a computer equipped with telecommunication software	Control station consists of a laptop computer, a headset with earphones and a microphone, and a joystick control.	Four ISDN lines, 128 kbps × 4	No surgical complications. All procedures were performed uneventfully.
2004 Rafiq et al. [50]	Endocrinology	Thyroid dissection	Not mentioned			384 kbps	Procedures were completed successfully. Patients had uneventful recovery.
2003 Netto et al. [51]	Urology	Laparoscopic varicocelectomy and percutaneous renal access	Not mentioned			Four ISDN lines, 128 kbps × 4	Procedures were completed successfully. Patients had uneventful recovery.
2000 Bauer et al. [52]	Urology	Laparoscopic varicocelectomy, adrenalectomy, and nephrectomy	4500 to 11, 000 miles			Not mentioned	Procedures were completed without intraoperative complications. Outcomes were similar to the expected non-mentored procedures.
2001 Bauer et al. [56]	Urology	Robotic percutaneous renal access	7158 km			Not mentioned	Obtaining percutaneous access within 20 min, with two attempts to obtain entry into the collecting system
2000 Micali et al. [53]	Urology	Laparoscopic spermatic vein ligations, retroperitoneal renal biopsies, laparoscopic nephrectomies, pyeloplasty, and percutaneous renal access	8000 km			Four ISDN lines, 128 kbps × 4	All procedures were accomplished with an uneventful postoperative course.
2003 Bove et al. [54]	Urology	Laparoscopic spermatic vein ligations, retroperitoneal renal biopsies, simple nephrectomies, pyeloplasty, and percutaneous renal access	9230 km			Four ISDN lines, 128 kbps × 4	Ten cases were telementored successfully. Failed to establish a connection to the remote site in five cases. Two procedures were converted to open surgery because of intraoperative complications.
2006 Sebajang et al. [55]	Colorectal surgery	The role of telementoring and telerobotic assistance in the provision of laparoscopic colorectal surgery in rural areas	400 km			384 kbps for telementoring, 1–15 Mbps for the tele-assist	Two minor intraoperative complications
2005 Anvari et al. [17]	Colorectal surgery	Laparoscopic fundoplications, sigmoid resections, right hemicolectomies, anterior resection, and inguinal hernia repairs	400 km			15 Mbps	No major intraoperative complications. Hospital stays were equivalent to the tertiary institution.

ing robotic-assisted cardiac, abdominal, and urological surgeries. This robotic arm is physically attached to the side of the surgical table and has an adapter system capable of carrying the endoscope camera. AESOP® could be controlled by voice control of the operating surgeon or remote control from a mentor using tele-assist systems [51–54]. The Socrates system (Computer Motion, Inc.) was the first robotic tele-collaboration device approved by the FDA. The Socrates system made it possible for expert surgeons to control AESOP® from remote locations through complex data transmissions. It not only supported two-way video and audio communication in real time between the mentor's location and the primary site but also provided telestration capabilities. The mentor could use the provided electronic stylus (telestrator) to annotate the operating surgeon's field of view for further instruction [49, 50]. As tele-assist systems developed, additional equipment, such as the PAKY® (Percutaneous Access to the Kidney, Urobotics Laboratory JHMI, Baltimore, MD), could be controlled from remote locations. PAKY® is a percutaneous nephrostomy robot that is mounted on a custom-designed rigid side rail and subsequently secured to the operating room table. Needle insertion is driven by a battery-powered variable-speed DC motor, which can be controlled with a joystick from either the operating room or a remote office [51, 53, 54].

In October 2001, ZEUS (Computer Motion, Inc.) was approved by the FDA. ZEUS is a three-armed robot mounted to the side of the operating table. One of the robotic arms was AESOP® and therefore carried the endoscopic camera. The other two arms assisted in the manipulation of blunt dissectors, retractors, graspers, and stabilizers during laparoscopic surgeries and could be controlled by an operating surgeon via an independent console [53]. ZEUS is utilized at the Centre for Minimal Access Surgery (CMAS) at McMaster University in Canada, who in present history has the most substantial and comprehensive experience with remote tele-assisted surgery [17, 55]. CMAS has established remote colorectal and general surgical services between their location in Hamilton, Ontario, Canada, and North Bay General Hospital (North Bay, Ontario, Canada), a location 400 km away. The systems are linked via a redundant Internet protocol virtual private network (VPN) at a bandwidth of up to 15 MB per second. Through several studies, they have reported a potential transmission latency of 140 milliseconds, a time frame easily adaptable for operating surgeons.

Guidance with Augmented Reality

New, innovative telemedicine software solutions have emerged (Reacts ®, Proximie ®) that integrate the use of augmented reality to superimpose video feeds, images, virtual pointers, and other multimedia assets to live video feeds from the surgical laparoscopic systems (Figs. 27.2 and 27.3). These software solutions use inexpensive hardware such as webcams, laptops, and off-the-shelf video converters as well as standard Internet connectivity. They allow for a remote proctor to provide a type of remote surgical assistance that is highly interactive as the proctor can superimpose images, 3D objects, videos, or his/her own hands virtually over the livestream of the surgical system video feed.

Being able to provide AR as a more interactive type of remote education and assistance brings a new dimension to telementoring for minimally invasive surgery and represents a simple, efficient, and innovative way to improve remote proctoring [57].

Applications

Resident Training and Surgical Continuing Education

Telementoring provides more possibilities of surgical education. By using 2D/3D telestration, tele-assist, or even tele-augmented reality, mentors can demonstrate surgery procedures in a more straightforward method, instead of just verbal guidance. This may improve the efficiency of teaching, saving valuable time of both mentors and trainees. Likewise, telementoring may facili-

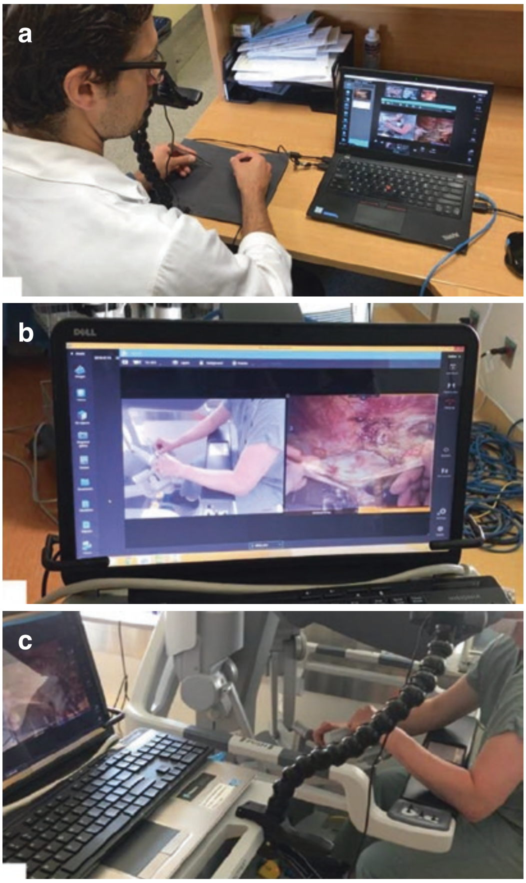

Fig. 27.2 Virtual guidance using augmented reality during live surgery. (**a**) A remote proctor can view the live video feeds (surgical endoscopic camera as well as two webcams) of a surgeon performing a procedure on a robotic surgical system. The proctor can provide direct remote virtual guidance using the Reacts ® platform by superimposing his own hands over the surgical video feed. The surgeon sees the remote proctor's hands appear in "augmented reality" over his live video feeds on a laptop (**b**) located right beside him in the operating room (**c**)

tate continuing education of surgeons and spread state-of-the-art skills. Nowadays, surgical technique is constantly involving. Surgeons not only need to be trained during their residency but also are required to learn throughout their career. Telementoring may help the surgeon community provide more current services to their patients.

Several studies have proved telementoring as an effective training tool. One study showed that residents in a telementoring group performed significantly better compared to a non-mentoring group ($p < 0.001$) [58]. The safety of telementoring has also been established. In a systematic review, the author summed up a total of 11 studies. Nine out of them concluded that telementoring did not prolong surgery time compared to on-site mentoring, none of them reported increased morbidity, and only 3% of the total number of cases reported technical issues [59]. Of note, a study conducted by Byrne included 34 telementoring cases of laparoscopic cholecystectomies. Results showed no intervention was necessary in 68% of cases, verbal advice was given in 26% of cases, and in two cases, the mentor had to come to the OR from their remote location and scrub into the case. The authors concluded that telementoring may be used as bridge between on-site supervision and totally unsupervised performance [60].

Emergency or Extreme Scenarios

Imagine if you are a young medic in a battlefield, a soldier needs a lower limb fasciotomy, but you have never done it by yourself before. What if you have a portable telementoring system that can connect you to an expert at a trauma center and effectively walk you through the operation in real time? Or imagine if you are a urologist who caused a severe rectal injury by accident when doing robotic-assisted radical prostatectomy. No colorectal surgeon in the OR is available, and you probably need to wait for >1 hour for one to arrive. What if you have a telementoring system which can connect you to an expert who can guide you through the repair, determine if diversion of the fecal stream is indicated, or even tele-assist with the robotic repair of the defect?

Under these hypothetical scenarios, the advantages of telementoring were highlighted. It saves significant time and facilitates experts applying their surgery knowledge without physical presence. Actually, one of the original purposes of developing telementoring was for usage in austere environments. In 1999, Cubano and colleagues successfully connected USS Abraham

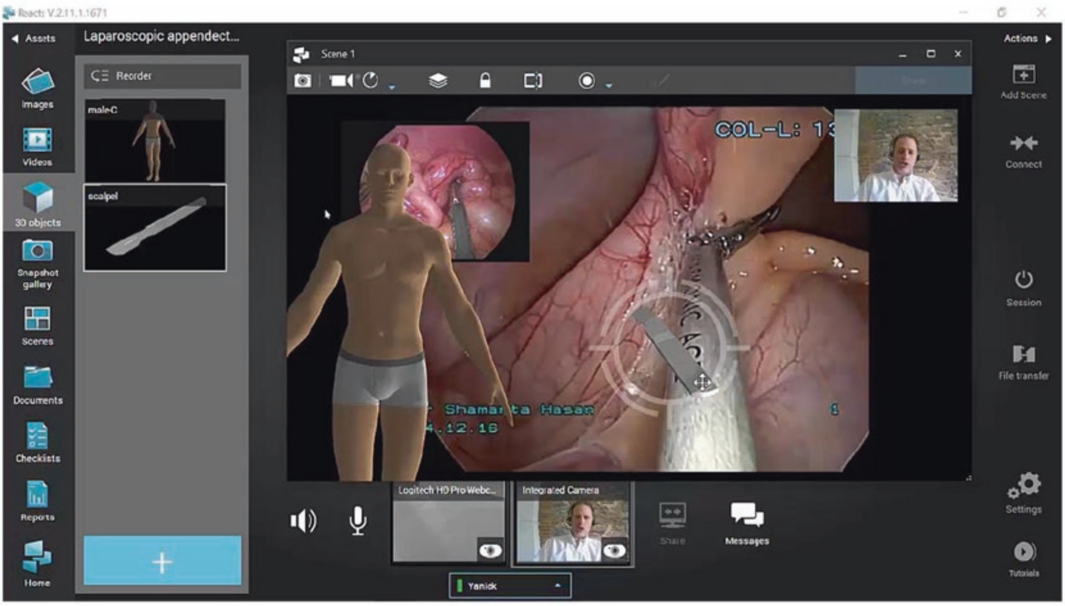

Fig. 27.3 "Augmented" remote proctoring using virtual overlays. Screenshot of a live Reacts session during a laparoscopic appendectomy procedure, demonstrating the use of image and 3D object overlays as well as the use of a virtual scalpel superimposed on the live laparoscopic video bringing highly interactive support and assistance to the remote surgeon

Lincoln aircraft with land-based surgical mentor and finished five laparoscopic hernia repairs under telementoring guidance [61]. Subsequently, Rogers et al. demonstrated that telementoring between trauma center and community hospital resulted in 7% lifesaving consultations and 83% approval rating for improved patient care. Interestingly, only 25% agreed telephone alone would have resulted in a similar effect [62].

Surgery Assistance/Education to Rural Areas

To date, the first telementoring program was for the purpose of continuing medical education in remote areas [63]. Traditional surgical education requires the mentor to be physically present during instruction with mentees. Without sufficient expert surgeons in rural areas, an important limitation exists for the *traditional* surgical education in such less populated regions. In this respect, telementoring has its natural advantages for rural surgery, especially combining with minimal invasive surgeries.

Outside surgery field, a telementoring program called "Extension for Community Healthcare Outcomes (ECHO)" has helped thousands of primary care practitioners in underserved areas acquire the knowledge they need to treat patients with complex health problems – including hepatitis C, HIV, chronic pain, opioid addiction, mental illness, diabetes, and cancer [64]. Similarly, in the field of surgery, *Project 6* was proposed by the Society of American Gastrointestinal and Endoscopic Surgeons (SAGES) in 2015 and aimed to promote the development of surgical telementoring [65]. But one of the limitations now is that surgical telementoring has a higher requirement for bandwidth than other telehealth mentoring – and rural areas usually lack such bandwidth. Hopefully, with the development of new Internet technology like 5G, this barrier will be overcome in the near future [24].

Challenges to Adopting Surgical Telementoring

Even though the development of advanced telecommunication and bioengineering technology has greatly facilitated surgical telementoring, there are many hurdles preventing the full adoption of these techniques in the clinical field.

Safety Considerations

One of the aims of surgical telementoring is to deliver professional instructions from academic centers to community hospitals so as to aid surgical training, improve outcomes, and ensure surgical safety worldwide [6, 44]. However, the technology of surgical telementoring has its inherited safety concerns. In Bove et al.'s study, 5 out of 17 planned telementoring procedures experienced connection failure to the proctoring site [54]. In two surgeries, the robotic arm AESOP™ failed to operate properly due to limited surgical space and severe tissue adhesions.

Signal delay caused by insufficient bandwidth can also compromise the safety during surgical telementoring and potentially place the patient at risk for harm [55]. Latency was noticeable during surgical telementoring at 135 to 140 milliseconds, but this did not compromise the fluidity of the procedure [17, 55]. When the latency increased to 200 milliseconds, the impact on robotic instrument movement during tele-assisted surgery was mild, and the surgeons were still able to adapt and operate safely and effectively [66]. However, the impact becomes more prominent when there is a 300 to 700 millisecond delay and eventually unable to operate if the delay is 800 to 1,000 milliseconds.

Cyberattack also poses a danger to surgical telementoring. Bonaci et al. reported multiple possibilities of cyberattacks during tele-assisted surgery, such as network- and communications-based attacks [67]. In their study, they found that the Raven™ II, a commercially available, open-source robot design, was vulnerable to cyberattacks that could manipulate the intent of the surgeon's actions, delay specific actions, or completely block actions. Preventive strategies to ensure the safety of surgical telementoring include data encryption before transmitting between the proctoring site and the operative room, as well as a telecommunication monitoring system that could assess the network and identify when multiple streams of data are being transmitted to the operating room [67].

Legal Considerations

Legal considerations linked to surgical telementoring have also prevented its widespread adoption in the clinical field. Currently, there is no clear legislation and credentialing on licensure applicability to surgical telementoring. However, in the context of telemedicine, the Federation of State Medical Boards has adopted the Interstate Medical Licensure Compact, which can facilitate and expedite licensure for telephysicians. Some have suggested a mobile patient-telephysician relationship wherein the physician is geographically tied to his or her current practicing state and the patient is seemingly "transported" to the physician location for the duration of that healthcare interaction. However, such an approach has not yet been approved, and the standard model remains multistate licensure and treatment of the physician-patient relationship by location of the patient [68–70].

Financial and Economic Considerations

Previous studies have failed to consider relative costs across the different approaches within surgical telementoring. For an increasingly cost-constrained healthcare environment, it is important to consider the financial implications of developing medical approaches on institutional and individual levels.

From an institutional standpoint, the primary expenditures for onboarding surgical telementoring systems include the cost of required equipment and network connection fees. However, these costs may be potentially offset by the reduction of expenses associated with the time and travel costs of an expert surgeon required for on-site mentoring.

As seen in the case of Virginia, state-level legislation may have incorporated the use of telemedicine into Medicaid budgeting; however, this allowance does not include coverage for the cost of providing telemedicine services or technical fees. The varying fees between verbal guidance, telementoring, and tele-assist services are to be managed by individual existing healthcare infrastructures [71].

Lastly, the financial relationship between the payer and the surgical telementoring team has yet to be clarified. It has not been determined whether the mentor is to be billed as a second healthcare-providing physician or whether the allocated payments are distributed between the telementor and tele-assistant. Surgical telementoring services are still in their early development phase and will be dependent on a changing healthcare landscape. The change in this market could have a lasting effect (either positive or negative) on the healthcare economy – as well as the overall cost of delivering surgical training and patient care.

Discussion

For the vision of telementoring and tele-assisted surgery to be realized, it will require more than secure, high-speed network connections – it will need trust and understanding of the standardized surgical approaches and patient management protocols agreed between the parties involved. As well as the demonstration of surgical techniques, the ability of the mentor to convey ideas and inspire learning is crucial to optimizing the learning experience. A good mentor is an expert in his/her discipline, is someone who likes to teach, is patient, has availability to train, and can mitigate the stress and challenges imposed upon mentee surgeons [72]. Telementoring adds to the complexity of this mentor/mentee relationship while giving new opportunities related to accessibility to expertise in both elective and unplanned operating room scenarios, when support and guidance may be most needed.

Using the telementoring resources currently available will help disseminate surgical expertise. Proctorship and preceptorship requirements will vary for different surgeons and organizations – and different patients will be in need of varying levels of expertise. The expert mentors, who are likely to be in greatest demand, will be those who are pushing the boundaries of robotic surgery in complex case selection or as a result of their new techniques or novel approaches. If the future infrastructure for worldwide robotic networks are realized, they could literally be in demand 24 hour/day [73]. In today's age of the telecommunication, data and ideas are spread more readily and can be adopted more quickly. What we choose to share reflects who we are, but what we search for reflects who we aspire to be. However, rapid dissemination of novel approaches to surgery also presents its own risks and further highlights the need for guidance regarding the use of telementoring, which should be limited to evidence-based practice, and trainers should be appropriately trained and certified [72].

Simulators have been successfully used in healthcare and are a standard tool in the aviation industry to measure both proficiency and technical skill learning [74]. Although robotic surgical simulation has not yet reached a stage where advanced procedural training replicates all aspects of robotic surgical procedures and team training, it has already shown potential to accelerate trainees along their learning curve and improve outcomes [74]. A simulator's greatest future value may be aligned with the data and feedback that robotic networks will provide, replicating the roles of airport control centers and flight simulators [75].

With better understanding of surgical learning curves and the ability to score and differentiate between performance levels, data collected via networks may also have a future regulatory role for surgeons [8]. International collaborative telementoring networks also have the potential to help achieve balance between the continual cycle of optimization and standardization of robotic surgical techniques. Standardized live surgery broadcast from home institutions could support and promote both telementoring and the benefits of standardized surgical techniques [76]. Standardization is critical to developing cohesive networks with defined agreement between mentors and mentees. Standardization also aids identification of the "hazard" steps in complex multistep procedures, enabling strategies to avoid the associated complications [77].

Sharing of expertise requires shared goals. In highly competitive healthcare systems, where hospitals compete in attracting patients, there is inherent resistance to sharing. If suitable quantitative datapoints are identified and the beneficial effects of sharing are confirmed, new thinking in robotic surgery is likely. With the increasing requirement to publish results and the natural competition that comes from market forces, there are drivers in place to promote collaboration that will result in improved surgical outcomes for patients [8]. Change is driven on varying scales from local discussion to national and international opinion and debate. While telementoring technologies will undoubtedly enhance communication between surgeons, it is the development of networks across greater distances, connecting the centers with the largest differences in surgeon skill set, which may deliver the greatest global health benefit. If these benefits to surgical outcomes and improved patient safety using telementoring are realized, then legal, ethical, and reimbursement issues will likely be resolved.

Conclusions

With telementoring, trainers hold the potential to drive standardization in training via centralization designed in principle to disseminate knowledge from a distance, without the need for mentor or mentee to travel. Collaborative telementoring via robotic networks has the potential not only to enable but also to drive advancement in multiple areas of robotic surgery through crowdsourcing and sharing of knowledge. Future studies should acknowledge the challenges of ethical and legal concerns and the need to prioritize patient safety. The development of this novel approach to training will need careful evaluation and validation with predefined service goals.

References

1. Guljas R, Ahmed A, Chang K, et al. Impact of telemedicine in managing type 1 diabetes among school-age children and adolescents: an integrative review. J Pediatr Nurs. 2014;29(3):198–204.
2. Eadie L, Seifalian A, Davidson B. Telemedicine in surgery. Br J Surg. 2003;90(6):647–58.
3. Weinstein R, Lopez A, Joseph B, et al. Telemedicine, telehealth, and mobile health applications that work: opportunities and barriers. Am J Med. 2014;127(3):183–7.
4. Mars M. Telemedicine and advances in urban and rural healthcare delivery in Africa. Prog Cardiovasc Dis. 2013;56(3):326–35.
5. Challacombe B, Kandaswamy R, Dasgupta P, Mamode N. Telementoring facilitates independent hand-assisted laparoscopic living donor nephrectomy. Transplant Proc. 2005;37:613–6.
6. Pahlsson HI, Groth K, Permert J, et al. Telemedicine: an important aid to perform high-quality endoscopic retrograde cholangiopancreatography in low-volume centers. Endoscopy. 2013;45:357–61.
7. Collins JW, Sooriakumaran P, Wiklund NP. Launching and evolving a robotic cystectomy service by developing your 'FORTE'. BJU Int. 2014;113(4):520–2.
8. Collins J, Akre O, Challacombe B, Karim O, Wiklund P. Robotic networks: delivering empowerment through integration. BJU Int. 2015;116(2):167–8.
9. Corliss WR, Johnson EG. Teleoperators and human augmentation. An AEC-NASA technology survey. Washington, DC: Office of Technology Utilization, National Aeronautics and Space Administration; 1967.
10. Paul HA, Bargar WL, Mittlestadt B, et al. Development of a surgical robot for cementless total hip arthroplasty. Clin Orthop Relat Res. 1992;285:57–66.
11. Davies BL, Ng W, Hibberd RD. Prostatic resection: an example of safe robotic surgery. Robotica. 1993;11:561–6.
12. Satava RM. Robotic surgery: from past to future: a personal journey. Surg Clin North Am. 2003;83:1491–500.
13. George EI, Brand TC, LaPorta A, Marescaux J, Satava RM. Origins of robotic surgery: from skepticism to standard of care. JSLS. 2018;22(4):e2018.00039.
14. Marescaux J, Leroy J, Gagner M, et al. Transatlantic robot-assisted telesurgery. Nature. 2001;413(6854):379–80.
15. Marescaux J, Leroy J, Rubino F, Vix M, Simone M, Mutter D. Transcontinental robot assisted remote telesurgery: feasibility and potential applications. Ann Surg. 2002;235:487–92.
16. Anvari M. Remote telepresence surgery: the Canadian experience. Surg Endosc. 2007;21:537–41.
17. Anvari M, McKinley C, Stein H. Establishment of the world's first telerobotic remote surgical service: for

provision of advanced laparoscopic surgery in a rural community. Ann Surg. 2005;241:460–4.
18. Anvari M. Reaching the rural world through robotic surgical programs. Eur Surg. 2005;37:284–92.
19. Anvari M. Telesurgery: remote knowledge translation in clinical surgery. World J Surg. 2007;31:1545–50.
20. Anvari M. Robot-assisted remote telepresence surgery. Semin Laparosc Surg. 2004;11:123–8.
21. Anvari M, Broderick T, Stein H, et al. The impact of latency on surgical precision and task completion during robotic-assisted remote telepresence surgery. Comput Aided Surg. 2005;10:93–9.
22. https://www.scmp.com/video/china/2181656/china-completes-worlds-first-5g-remote-surgery-test-animal.
23. Shin D, Dalag L, Azhar R, et al. A novel interface for the telementoring of robotic surgery. BJU Int. 2015;116(2):302–8.
24. Lacy AM, Bravo R, Otero-Piñeiro AM, Pena R, De Lacy FB, Menchaca R, et al. 5G-assisted telementored surgery. Br J Surg. 2019;106:1576–9. https://doi.org/10.1002/bjs.11364.
25. Collins JW, Verhagen H, Mottrie A, Wiklund PN. Application and integration of live streaming from leading robotic centres can enhance surgical education. Eur Urol. 2015;68(5):747–9.
26. Bogen EM, Schlachta CM, Ponsky T. White paper: technology for surgical telementoring-SAGES Project 6 Technology Working Group. Surg Endosc. 2019;33:684–90. https://doi.org/10.1007/s00464-018-06631-8.
27. Hassan A, Ghafoor M, Tariq SA, Zia T, Ahmad W. High efficiency video coding (HEVC)-based surgical telementoring system using shallow convolutional neural network. J Digit Imaging. 2019;32:1027–43. https://doi.org/10.1007/s10278-019-00206-2.
28. Gambadauro P, Magos A. NEST (network enhanced surgical training): a PC-based system for telementoring in gynecological surgery. Eur J Obstet Gynecol Reprod Biol. 2008;139(2):222–5.
29. Sebajang H, Trudeau P, Dougall A, et al. Telementoring: an important enabling tool for the community surgeon. Surg Innov. 2005;12(4):327–31.
30. Treter S, Perrier N, Sosa JA, et al. Telementoring: a multi-institutional experience with the introduction of a novel surgical approach for adrenalectomy. Ann Surg Oncol. 2013;20(8):2754–8.
31. Clifford TG, Dajani D, Khooshabeh P, Hwang E, Desai MM, Gill IS, et al. MP23-18 inter-hospital telementoring for robotic surgery. J Urol. 2016;195(4S): e268-e269. https://www.auajournals.org/doi/pdf/10.1016/j.juro.2016.02.740.
32. Di Valentino M, Alerci M, Bogen M, et al. Telementoring during endovascular treatment of abdominal aortic aneurysms: a prospective study. J Endovasc Ther. 2005;12(2):200–5.
33. Agarwal R, Levinson A, Allaf M, et al. The RoboConsultant: telementoring and remote presence in the operating room during minimally invasive urologic surgeries using a novel mobile robotic interface. Urology. 2007;70(5):970–4.
34. Rothenberg S, Yoder S, Kay S, et al. Initial experience with surgical telementoring in pediatric laparoscopic surgery using remote presence technology. J Laparoendosc Adv Surg Tech A. 2009;19(Suppl 1):S219–22.
35. Safir IJ, Shrewsberry AB, Issa IM, Ogan K, Ritenour CWM, Sullivan J, et al. Impact of remote monitoring and supervision on resident training using new ACGME milestone criteria. Can J Urol. 2015;22:7959–64.
36. Anderson SM, Kapp BB, Angell JM, Abd TT, Thompson NJ, Ritenour CWM, et al. Remote monitoring and supervision of urology residents utilizing integrated endourology suites – a prospective study of patients' opinions. J Endourol. 2013;27:96–100. https://doi.org/10.1089/end.2012.0406.
37. Schlachta C, Sorsdahl A, Lefebvre K, et al. A model for longitudinal mentoring and telementoring of laparoscopic colon surgery. Surg Endosc. 2009;23(7):1634–8.
38. Bruns NE, Irtan S, Rothenberg SS, et al. Trans-atlantic telementoring with pediatric surgeons: technical considerations and lessons learned. J Laparoendosc Adv Surg Tech A. 2016;26:75.
39. Snyderman CH, Gardner PA, Lanisnik B, et al. Surgical telementoring: a new model for surgical training. Laryngoscope. 2016;126:1334.
40. Forgione A, Kislov V, Guraya SY, et al. Safe introduction of laparoscopic colorectal surgery even in remote areas of the world: the value of a comprehensive telementoring training program. J Laparoendosc Adv Surg Tech A. 2015;25:37.
41. Ponsky TA, Bobanga ID, Schwachter M, et al. Transcontinental telementoring with pediatric surgeons: proof of concept and technical considerations. J Laparoendosc Adv Surg Tech A. 2014;24:892.
42. Bruschi M, Micali S, Porpiglia F, et al. Laparoscopic telementored adrenalectomy: the Italian experience. Surg Endosc. 2005;19(6):836–40.
43. Hinata N, Miyake H, Kurahashi T, et al. Novel telementoring system for robot-assisted radical prostatectomy: impact on the learning curve. Urology. 2014;83(5):1088–92.
44. Fuertes-Guiró F, Vitali-Erion E, Rodriguez-Franco A. A program of telementoring in laparoscopic bariatric surgery. Minim Invasive Ther Allied Technol. 2016;25:8.
45. Meijer HAW, Sánchez Margallo JA, Sánchez Margallo FM, et al. Wearable technology in an international telementoring setting during surgery: a feasibility study. BMJ Innov. 2017;3:189–95.
46. Ali M, Loggins J, Fuller W, et al. 3-D telestration: a teaching tool for robotic surgery. J Laparoendosc Adv Surg Tech A. 2008;18(1):107–12.

47. Jarc A, Shah S, Adebar T, et al. Beyond 2D telestration: an evaluation of novel proctoring tools for robot-assisted minimally invasive surgery. J Robot Surg. 2016;10(2):103–9.
48. Jarc A, Stanley A, Clifford T, et al. Proctors exploit three-dimensional ghost tools during clinical-like training scenarios: a preliminary study. World J Urol. 2017;35(6):957–65.
49. Mendez I, Hill R, Clarke D, et al. Robotic long-distance telementoring in neurosurgery. Neurosurgery. 2005;56(3):434–40.
50. Rafiq A, Moore JA, Zhao X, et al. Digital video capture and synchronous consultation in open surgery. Ann Surg. 2004;239(4):567–73.
51. Rodrigues Netto N, Mitre A, Lima S, et al. Telementoring between Brazil and the United States: initial experience. J Endourol. 2003;17(4):217–20.
52. Bauer J, Lee B, Bishoff J, et al. International surgical telementoring using a robotic arm: our experience. Telemed J. 2000;6(1):25–31.
53. Micali S, Virgili G, Vannozzi E, et al. Feasibility of telementoring between Baltimore (USA) and Rome (Italy): the first five cases. J Endourol. 2000;14(6):493–6.
54. Bove P, Stoianovici D, Micali S, et al. Is telesurgery a new reality? Our experience with laparoscopic and percutaneous procedures. J Endourol. 2003;17(3):137–42.
55. Sebajang H, Trudeau P, Dougall A, et al. The role of telementoring and telerobotic assistance in the provision of laparoscopic colorectal surgery in rural areas. Surg Endosc. 2006;20(9):1389–93.
56. Bauer J, Lee BR, Stoianovici D, Bishoff JT, Micali S, Micali F, et al. Remote percutaneous renal access using a new automated telesurgical robotic system. Telemed J E Health. 2001;7:341–6. https://doi.org/10.1089/15305620152814746.
57. Andersen DS, Cabrera ME, Rojas-Muñoz EJ, et al. Augmented reality future step visualization for robust surgical telementoring. Simul Healthc. 2019;14(1):59–66. https://doi.org/10.1097/SIH.0000000000000334.
58. Panait L, Rafiq A, Tomulescu V, Boanca C, Popescu I, Carbonell A, et al. Telementoring versus on-site mentoring in virtual reality-based surgical training. Surg Endosc. 2006;20:113–8. https://doi.org/10.1007/s00464-005-0113-x.
59. Bilgic E, Turkdogan S, Watanabe Y, Madani A, Landry T, Lavigne D, et al. Effectiveness of telementoring in surgery compared with on-site mentoring: a systematic review. Surg Innov. 2017;24:379–85. https://doi.org/10.1177/1553350617708725.
60. Byrne JP, Mughal MM. Telementoring as an adjunct to training and competence-based assessment in laparoscopic cholecystectomy. Surg Endosc. 2000;14:1159–61. https://doi.org/10.1007/s004640000264.
61. Cubano M, Poulose BK, Talamini MA, Stewart R, Antosek LE, Lentz R, et al. Long distance telementoring. A novel tool for laparoscopy aboard the USS Abraham Lincoln. Surg Endosc. 1999;13:673–8. https://doi.org/10.1007/s004649901071.
62. Rogers FB, Ricci M, Caputo M, Shackford S, Sartorelli K, Callas P, et al. The use of telemedicine for real-time video consultation between trauma center and community hospital in a rural setting improves early trauma care: preliminary results. J Trauma. 2001;51:1037–41. https://doi.org/10.1097/00005373-200112000-00002.
63. St Julien J, Perrier ND. Video telementoring to accelerate learning of new surgical techniques. JAMA Surg. 2016;151:671–2. https://doi.org/10.1001/jamasurg.2016.0054.
64. McBain RK, Sousa JL, Rose AJ, Baxi SM, Faherty LJ, Taplin C, et al. Impact of project ECHO models of medical tele-education: a systematic review. J Gen Intern Med. 2019;34:2842–57. https://doi.org/10.1007/s11606-019-05291-1.
65. Schlachta CM, Nguyen NT, Ponsky T, Dunkin B. Project 6 Summit: SAGES telementoring initiative. Surg Endosc, vol. 30, Springer US; 2016, pp. 3665–72. https://doi.org/10.1007/s00464-016-4988-5.
66. Xu S, Perez M, Yang K, et al. Determination of the latency effects on surgical performance and the acceptable latency levels in telesurgery using the dV-Trainer_ simulator. Surg Endosc. 2014; 28:2569.
67. Bonaci T, Herron J, Yusuf T et al. To make a robot secure: an experimental analysis of cyber security threats against teleoperated surgical robots. 12 May 2015; arXiv: 1504:04339v2 [cs.RO].
68. Silva E III. The interstate medical licensure compact. J Am Coll Radiol. 2015;12:511.
69. Federation of State Medical Boards. Interstate medical licensure compact prepares launch of new pathway for multi-state physician licensing. 17 Oct 2016. Available at http://www.fsmb.org/Media/Default/PDF/Publications/IMLCC_Oct2016_meeting.pdf. Accessed 12 June 2014.
70. Kempen P. The interstate telemedicine compact and the agenda of the Federation of State Medical Boards. J Am Phys Surg. 2015;20:57.
71. Virginia's Legislative Information System. 2010 Session: SB 675 Health insurance; mandated coverage for telemedicine services. Available at https://lis.virginia.gov/cgi-bin/legp604.exe?101+sum+SB675.
72. Collins JW, Levy J, Stefanidis D et al. Utilising the Delphi process to develop a proficiency-based progression train-the-trainer course for robotic surgery training. Eur Urol. 2019. pii: S0302-2838(19)30001-6. https://doi.org/10.1016/j.eururo.2018.12.044. [Epub ahead of print] Review.
73. Collins J, Dasgupta P, Kirby R, Gill I. Globalization of surgical expertise without losing the human touch: utilising the network, old and new. BJU Int. 2012;109(8):1129–31.

74. Brunckhorst O, Volpe A, van der Poel H, Mottrie A, Ahmed K. Training, simulation, the learning curve, and how to reduce complications in urology. Eur Urol Focus. 2016;2(1):10–8.
75. Saied N. Virtual reality and medicine--from the cockpit to the operating room: are we there yet? Mo Med. 2005;102(5):450–5.
76. Collins JW, Akre O, Wiklund PN. Re: Walter Artibani, Vincenzo Ficarra, Ben J. Challacombe et al. EAU policy on live surgery events. Eur Urol 2014; 66: 87–97. Eur Urol. 2014;66:e121–2.
77. Collins JW, Tyritzis S, Nyberg T, et al. Robot-assisted radical cystectomy – description of an evolved approach to radical cystectomy. Eur Urol. 2013;64:654–63.

Digital Medical School: New Paradigms for Tomorrow's Surgical Education

28

Joanna Ashby, Isaac Ndayishimiye, Arsen Muhumuza, and Sylvine Niyoyita

Introduction

Medical schools around the world are set to enter a new era of transformation as digital technologies are gradually incorporated into education for the next generation of surgeons [1]. Broadly, digital technologies could help to address access to healthcare challenges by addressing workforce shortages, by improving the availability of clinical expertise and thereby improving safety and quality of care, and by supporting local priorities and thereby preparing for demographic changes [2]. But while there has been a rapid wave of emerging early stage applications of digital technologies into medical and surgical education, as well as across innovative health systems around the world [3], little attention has been placed on how today's traditional and outdated "one-size-fits-all" approach to medical education will appropriately prepare medical students for a future of digital surgery [4].

After a century of rapid progress in medical education that was initiated in the Western medical system by the 1910 Flexner Report [5], today students are all trained the same way without really considering a need for alternative career paths of work following graduation. In 2010, the global independent Lancet Commission on the Education of Health Professionals for the Twenty-First Century was launched, and the key message was as follows: "All health professionals in all countries should be educated to mobilize knowledge and to engage in critical reasoning and ethical conduct so that they are competent to participate in patient and population-centered health systems as members of locally responsive and globally connected teams" [1]. Also proposed in the commission was a novel "systems" approach to reform, whereby medical education must overlap with the health system it attempts to serve. The commission provided medical education systems around the world with principles required to better address the health needs of their local populations, but better more, a need for increased recognition into the local and global demands for integrated education and digital leadership [6].

Reflecting upon generations globally, the world currently has the largest youth generation in its history with more than half of the global population aged 30 or younger [7]. Yet workforce shortages are a challenge for systems worldwide: in the UK, it is believed that 8000 more general practitioners are needed for primary care delivery; in the USA, achieving universal health coverage is still not reality; and globally, health and surgical burdens are at their greatest, with local

J. Ashby (✉)
Program in Global Surgery and Social Change, Harvard Medical School, Boston, MA, USA

I. Ndayishimiye · S. Niyoyita
Medicine and Surgery, University of Rwanda, Kigali, Rwanda

A. Muhumuza
Medicine and Surgery, University Teaching Hospital of Kigali, Kigali, Rwanda

S. Atallah (ed.), *Digital Surgery*, https://doi.org/10.1007/978-3-030-49100-0_28

systems of care at their most vulnerable. Medical students do not only want to be involved in accelerating the future augmented by digital technologies but are in fact necessary partners in preparing, shaping, and implementing effective processes and initiatives for digital transformation in their own medical schools [8]. The exclusion of young people at all levels of medical education leadership and the lack of opportunities for integration delay progress and negatively impact the quality of patient care in the long run. Achieving a future surgical workforce empowered with the skills required for future healthcare delivery will require innovative and evidence-based approaches to learning that would be tailored to the needs of patients and populations [9], and this will not be possible without the meaningful engagement of today's medical students.

In this review, we explore ways in which digital technologies will augment surgical education, prepare future surgical trainees to join the workforce, and provide an essential global perspective in the context of digital transformation for global surgery. We discuss how medical students can prepare for the future and how governments, academic intuitions, and organizations can empower students all around the world to develop the essential skills required to enable the rediscovery of healthcare democracy and access to surgical care that is safe, affordable, and timely for all populations through leveraging digital technologies.

Education in the Digital Medical School

It is expected that future medical students will be part of the digital transformation process that takes place throughout their working careers in their respective health systems; therefore, it makes sense that they are prepared for what lies ahead in their practice. As new technologies and platforms are increasingly introduced into surgical education, new core skill competencies must, too, be integrated into curricula, allowing innovation ecosystems to flourish which in turn will strengthen health system innovation. In this section, we highlight several state-of-the-art technologies that are either already adopted or will soon be realized in medical schools around the world over the coming years. Following this, the new specialized skills that will require training to effectively support these technologies within the framework of an innovation ecosystem will be discussed.

Digital Technologies Impacting Medical and Surgical Education

New digital approaches are swiftly entering the medical and surgical education playing field, and among those are massive open online courses, "flipped classrooms," digital badges, virtual anatomy, and medical holograms [10–12].

- *Massive open online courses* (MOOCs) are open-access courses that are available online and have been available for at least two decades. However, the concept of an MOOC was popularized by a group of researchers when a course on "Connectivism and Connected Knowledge" in 2008 attracted over 23,000 worldwide participants. MOOCs aim to promote active, retrieval-based learning, real-time collaboration, customized feedback based on analysis of vast amounts of data generated by students' performance, and peer learning while also creating an experience that mimics one-on-one tutoring. Overall, MOOCs ensure access to many students who otherwise might not be able to enter such courses, and they help to build a virtual, multidisciplinary, and collaborative environment.
- *Flipped classrooms* refer to an alternative educational setup whereby students receive and master new knowledge outside the classroom, and the teachers then use the classroom time to reinforce learning and address students' questions. They are part of a series of powerful, online-based disruptive changes in the educational landscape. A similar example of this model is Khan Academy which started in 2006 and has delivered over 180 million lessons to date. The site offers practice tests for skill building in the form of a series of short

Web-accessible (e.g., YouTube) videos that are created by an individual with only basic laptop and Internet connection.

- *Digital badges* are another disruptive tool in the education world which also has real-world implications outside medical education. Digital badges are a way to provide concrete evidence of skills, achievements, and qualities in a more granular manner than traditional grades and degrees. They reflect mastery of real-life skills and are valued by employers looking for evidence of expertise not often reflected by solely a college degree. As a parallel medical application of this technology, a badge could indicate information regarding a patient's procedure and details regarding whether it was performed as an example.
- *Virtual anatomy* is a powerful tool that involves the digitization of the traditional cadaver dissection sessions at medical school, allowing for easy manipulation and presentation of any disease or condition in physiology, anatomy, dissection, or/and pathology.
- *Medical holograms* allow for complete visualization of the human body in a third dimension, displaying a 360° view of a virtual human body. However, unlike the dissection tables, hologram technology can showcase specific organs in relation to other parts of the body. It is also possible to perform small-scale procedures on the virtual body, such as inserting an intravenous line, in order to assist with student understanding of a practical skill or clinical exam in a lot more depth than would be possible with a textbook.

The Evolution of Core Competencies

We believe the future digital medical student will require the following five core skill competencies (Fig. 28.1):

1. *Multidisciplinary collaborator*: Specialized leadership skills required to resolve solutions between teams of different training backgrounds. For example, coordinating discussions between surgeons, data scientists, and software engineers.
2. *Data-driven decision-maker*: Proficient in digital health technologies; able to adopt, implement, and evaluate new technologies as they enter the system.
3. *Digital leader*: Fluency in use of all frequently used digital health platforms and digital technologies, allowing for more comprehensive patient care that is more personalized, preventative, and predictive care.
4. *Super-communicator*: Sophisticated professionalism and specialized communication skills adapted for digital health and AI-driven technologies.
5. *Community leader*: Awareness and advocacy for the sociopolitical, economical, and environmental factors that impact individual and population health.

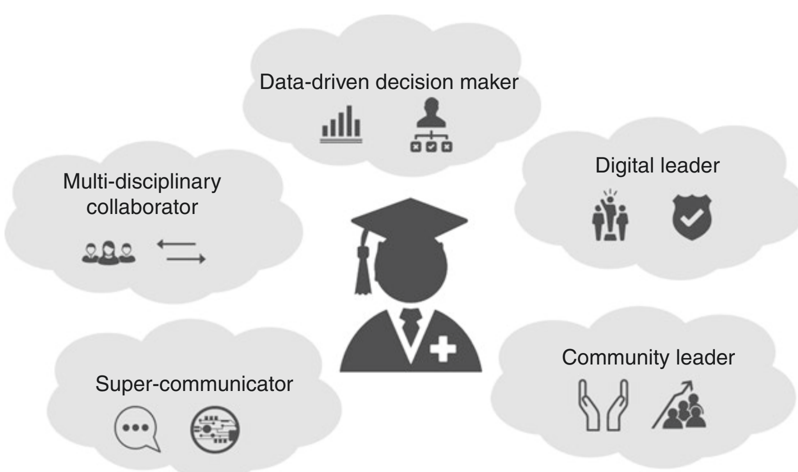

Fig. 28.1 Core competencies of the future digital medical student. (Illustration created by the authors, adapted from [1, 3, 10])

In more detail, the specialized role of a multidisciplinary collaborator would require several languages of communication, where conversation between the primary two languages would switch between “clinical” and “coding” languages. A data-driven decision-maker would have a comprehensive education in data analysis skills to improve digital systems, as well as critical judgement evaluation skills to assess factors such as risks, benefits, and regulations. A leader in digital health technologies would have a comprehensive understanding of imaging and digital health platforms and systems and a competency in health, digital, and eHealth literacy. They would have specialized training on the development, deployment, evaluation, and interpretation of AI-driven technologies, as well as training for new robots in health and surgery, telemedicine, wearables, and sensors. Alongside specialized communication and professionals’ skills, a super-communicator would also require training in the appropriate use and delivery of the online doctor-patient consultation and training in the performance of accurate surgical procedures using augmented and virtual reality platforms. A community leader would have an understanding of the underlying political and economic factors that impact local and global health inequity. This might involve having an appreciation for some of the high-level policy frameworks in health, including the World Health Organization and World Bank. They would also have an awareness for national health priorities and know how to integrate these policies into the regional and district levels of care. Table 28.1 reviews the core technologies impacting the digital medical school both from the perspective of surgical education for the medical student and from the perspective of the future surgical trainee toward the end of medical school.

Training the Future Digital Surgeon

For medical students and emerging surgical trainees beyond 2020, there will be a sea of opportunity for learning that will be augmented by digital technologies. Alongside skill-building opportunities, the very nature of surgical care and role of the surgeon will also evolve with increasing adoption of digital technologies; therefore, the competition of preparedness training will also be essential before completing medical school. Herein, the impact of digital surgical technologies when preparing for surgical training while still at medical school is highlighted.

Digital Technologies Impacting Surgical Education

A selection of key digital technologies that are impacting surgical training and education today include surgical robots, next-generation minimally invasive surgery, and artificial intelligence [11]. Surgical robots and minimally invasive approaches via advanced laparoscopy are changing surgery globally by reducing morbidity and mortality of operations that were once performed with traditional open methods. As a result, surgery is becoming more dependent on technology, and accordingly, the surgeon’s skill set is expanding to accommodate for these new techniques. In accordance with this transition, the technical and nontechnical skills of surgeons must be adaptive. Surgeons will have to learn new technical skill approaches as new robotic platforms and minimally invasive techniques are incorporated into the surgeons’ workflow, as well as more specialized nontechnical digital communication skills for online and virtual provision of care.

Changes to Training and the Surgeon’s Role

As we are entering a new digital era in healthcare, it is important to appreciate the opportunities that digital technologies hold for surgical care – an indivisible and indispensable part of healthcare. While there are real efforts to scale, develop, integrate, and distribute digitized services in surgical training today, there are still many gaps that need to be addressed – for example, in the context of workforce where only 12% of the world’s specialist surgeons reside in Africa and Southeast Asia,

Table 28.1 The impact of digital technology on medical school training and surgical training roles

Technology	Digital domain	Use case and description	Medical education: New learning requirements	Surgical training: New skill preparedness
Digital medicine	Telemedicine.	Virtual fracture clinics: telephone consultation and self-management service provided online.	Upskilling in specialist areas, including imaging, digital technologies, and fracture management.	Care provided virtually with faster access for patients. New roles for advanced digital practitioners.
	Smartphone applications.	Computerized cognitive behavioral therapy (CBT).	Data analysis skills to improve regulation of digital therapeutics. Critical judgment evaluation skills (risks, benefits, regulation).	Scalable solutions to care provision using fully automated, advanced, algorithm-driven app. New roles for data interpreters, digital prescribers, and phone consultants.
	Web applications.	Online clinical consultations with electronic prescribing, notification, and health surveillance.	Understanding of new specialized components including health literacy, digital literacy, and eHealth literacy. Training in use and delivery of online doctor-patient consultations.	Training for new roles in monitoring and management of patients using telephone consultations via an online interface.
	Sensors and wearables for remote diagnostics and monitoring.	Ultrasensitive bio-nanotechnologies: rapid diagnosis of disease at point-of-care, faster access to care, and improved antimicrobial stewardship.	Training and understanding of sensors, wearables, and algorithms for safe patient monitoring.	Training on patient data sharing, privacy, and security in the context of real-time monitoring of vitals, diagnosis, and remote management.
	Virtual and augmented reality.	Immersive technologies combining computer-generated visual, auditory, and sensory data with physical world.	Teaching in virtual and augmented reality technology. Introduction to surgical training for procedures using AR/VR platforms.	Surgical training delivered using online AR/VR technology using smart data-driven educational platforms.
Artificial intelligence and robotics	Automatic image interpretation.	Enhanced diagnostics via automated image interpretation using digitized medical data.	Specialized education on AI-driven radiological interpretation, monitoring, and evaluation. Communication training for patient-generated consultations (e.g., diagnosis of skin lesion via app using smartphone camera).	Training in the analysis and evaluation of AI-driven image diagnostic platforms.

(continued)

Table 28.1 (continued)

Technology	Digital domain	Use case and description	Medical education: New learning requirements	Surgical training: New skill preparedness
	Speech recognition and natural language processing (NLP).	Voice assistants that interpret human speech and response via smart speakers.	Specialized communication skills for verbal and nonverbal aspects of clinical consultation. Training in natural language processing and speech recognition.	Smart consultation training with specialized patient-physician interaction involving the computer and smart speaker. Training on nuances of primary care provision in the context of text and voice inputs.
	Interventional and rehabilitative robotics.	Healthcare robots that address specific procedural technical challenges and rehabilitative robots (prosthesis, exoskeletons, brain-computer interfaces, etc.)	Teaching on underlying technology of new robots in healthcare and surgery. New multidisciplinary aspect involving orthotists, physiotherapists, and occupational therapists for holistic rehabilitative care.	Robotic training on new platforms for surgeons and theater staff. Nontechnical skills to ensure smooth integration and performance of robots within the rehabilitative multidisciplinary team.
	Predictive analytics using artificial intelligence.	Predicting future outcomes using data mining, statistics, and machine learning-based modelling.	Training on the AI applications in healthcare and predictive analytics, including interpretation, evaluation, development, and deployment.	Specialized roles involving algorithm-driven patient triage and risk prediction in the context of personalized medicine.
Genomics	Reading and writing the genome.	Revolutionary specific gene-editing system allowing for specific corrections in an individual's DNA.	Education on the potential of genome reading, writing, and editing and understanding of applications.	Training in comprehensive genomic care in the context of gene-editing systems.

Adapted by the authors from [1–3, 11]

where 33% of the world population resides [12]. Despite the significant health inequities and uneven distribution of healthcare workers around the world, digital technologies are expected to provide solutions to such challenges.

Accordingly, new roles will arise within the specialist surgical workforce as new technologies are developed and gradually adopted. Some examples of these new roles include advanced digital practitioners, data interpreters, digital prescribers, and virtual surgeons for online consultations [3]. In addition to evolving roles within the workforce, new skill sets will also arise to better cope with the increased complexity in tasks. Some of these new tasks include training on data sharing, privacy, and security in the context of surgical sensors and wearables for monitoring, diagnosis, and remote management, with an increased focus on nontechnical skills [2]. Looking forward, it will be important that medical students who have surgical ambitions are aware of the technologies that will impact their day-to-day work as well as the new specialized training they will have to complete in order to provide high-standard care that is digitally augmented.

Preparing the Future Global Surgeon in the Digital Era

Global Burden of Surgical Disease

There are many challenges ahead in global surgery that are amenable to digital health technologies as well as a vast potential for advancement of health and social justice. In 2015, the Lancet Commission on Global Surgery estimated that 5 billion people lack access to safe, affordable, and timely surgical and anesthesia care [12, 13]. An estimated 16.9 million lives – 32.9% of all deaths worldwide – are lost as a result of surgically preventable conditions every year. Without surgical care, universal health coverage and other global health goals, at both the local and national levels, will be impossible to achieve [13]. Furthermore, every year 81 million patients are forced into poverty as a result of the cost of surgery, if they are able to access surgical care at all [14]. It is estimated that one-third of the global disease burden is surgical in nature [15]. The report states how there are common conditions such as appendicitis that require surgical care and are easily treatable but frequently result in high morbidity and mortality due to lack of access to care. Remarkably, the risk of maternal death following cesarean section reaches up to 50 times higher when performed in low- and middle-income countries (LMICs) compared to high-income countries (HICs) [16]. If the future surgical workforces around the world were empowered with the skills required to transform health systems, would it then be possible to begin to tackle some of these international global health priorities?

Digital Technologies, Innovation, and Global Opportunities

Three broad challenges within global surgery that are amenable to digital health have been selected in the context of their importance to the future medical student experience [17–20]. These primarily relate to workforce shortages, the urgent need for clinical expertise expansion, and future projections for population changes. As the future workforce, it is critical to be able to address these shortages with effective and efficient approaches to service delivery that is honed through the years of preparation in medical school.

- *Workforce shortage*: While human resources are the backbone of healthcare systems, major shortages exist within surgical systems worldwide which, in turn, are further compounded by misdistribution of existing workforce both within and between countries. This results in gross inequity. Global access to healthcare is particularly pronounced in rural settings where there is little access to care. However, tomorrow's digital health infrastructure transcends the geographic divide and has shown potential in improving healthcare delivery and access through rapid and virtual diagnosis, treatment, and remote care. In addition, automation offers huge benefits in improving workflow efficiency and reducing burdens on the existing workforce.
- *Clinical expertise expansion*: While there is a definite need to prepare the current and future workforce in digitally enabled technologies, there might be other shorter-term solutions that could be achieved with the aid of technology. In settings where clinical expertise is limited, digital and AI systems are able to assist with quality and provision of care that is accurate and safe. This assistance could be in the form of diagnostic or management support, clinical decision systems that integrate electronic health records with the most recent up-to-date medical evidence, or through automated, AI-enhanced triage systems.
- *Population changes*: The healthcare demands of future populations are constantly shifting. Noncommunicable diseases are estimated to account for 80% of global disease burden by 2020, which indicates an increased importance in a specific group of conditions – for example, the management of diabetes mellitus and hypertension. Digital technologies could help to address these profound projected burdens by optimizing efficiency and cost-effectiveness of current care. However, the

demands for ever-increasing specialized communication skills will also increase as healthcare workers and specialists work in closer collaboration with machines.

Recommendations

Key recommendations outlined in this section have been put forward by a number of thought leaders, academic institutions, and governments as they begin to prepare for how digital technologies will impact education and training for both medical students and surgical trainees [2, 3, 13, 17, 19]. For this review, they have been summarized in the following three broad categories: (1) partnerships and capacity, (2) ecosystems and evidence, and (3) investment and engagement.

1. *Partnerships and capacity*. Establish and support partnerships that advance education, research, and advocacy for digital transformation in healthcare. Nurture connections between institution and disciplines to encourage multidisciplinary collaboration.
2. *Ecosystems and evidence*. Support early research and innovation opportunities for medical students and surgical trainees to accelerate a future of evidence-based, data-driven surgical system strengthening.
3. *Investment and engagement*. Provide funding to strengthen student leadership initiatives that encourage skill development of digital technologies in the context of advancing health and economic growth.

Partnerships that advance education, research, and advocacy for digital transformation in healthcare will support capacity-building initiatives and encourage multidisciplinary collaboration. As medical students will play a vital role in revitalizing medical education as well as prepare students for a future practice with digital surgery, it is important that they participate in the leadership discussions that surround forging these connections between institutions and disciplines, building on shared collective experience in national and international student organizations for social good.

Government, industry and academic initiatives that strengthen healthcare ecosystems sustainably will provide an infrastructure for future digital transformation. These initiatives will build on evidence that will be generated from real-world clinical research and population-level trials. Early exposure to these specialized research practices and principles for medical students and surgical trainees alike will encourage knowledge sharing and early adoption of technologies, which in turn will encourage deployment and evaluation that is safe, accurate, and reliable.

Finally, ecosystems and partnerships will require investment in order to ensure sustainability and growth. Investment in such student- and trainee-based initiatives will not just advance local capacity and support research but will also recognize that the future of surgical workforce represents a magnitude of human potential with massive unrealized benefits for socioeconomic growth, population health, and individual health advancement. Medical students offer a unique opportunity to create the most urgent digital surgery solutions as a result of their native fluency in digital technologies and influence on social media platforms. Recognizing the need to appropriately prepare the generation for the digital future of surgery will reflect on the lived realities of these students around the world, it will impact their experiences, and it will empower them to create the solutions needed to address some of the world's most pressing challenges. Achieving the wider health goals will not be possible without the leadership and engagement of the emerging generation in training, particularly in the field of surgery. While we applaud progress that has already been made to advance digital health leadership in medical and surgical education, more must be done to position the future of the workforce as equal stakeholders in the realization of digital transformation in local, national, and global health priorities.

Conclusions

The potential for digital technologies to transform the future medical and surgical education cannot be understated. This chapter acts as a basis for further discussion and action. We emphasize the importance of involving students and learners from different disciplines in the digital transformation process as we strongly believe in the benefits of varied perspectives on the technological improvement of health on both an individual and societal level. In order to address potential future workforce shortages and other challenges ahead, medical schools around the world will need to seek reform in order to empower fellow medical students to deliver the care that their local populations need, utilizing a digital framework. Without such adjustments, achieving universal health coverage – both nationally and globally – will not be attainable. Such a shift in curricula and mindset will be necessary to lead new forms of digitally driven medical education for the future surgical workforce, which in turn will shape the direction of healthcare and surgery for a shared digital future that will benefit all mankind.

References

1. Horton R. A new epoch for health professionals' education. Lancet Lond Engl. 2010;376(9756):1875–7.
2. Topol EJ. High-performance medicine: the convergence of human and artificial intelligence. Nat Med. 2019;25(1):44.
3. Topol E. The Topol review – NHS Health Education England [Internet]. 2019 [cited 2019 Jul 16]. Available from: https://topol.hee.nhs.uk/.
4. Barras C. Training the physician of the future. Nat Med. 2019;25(4):532–4.
5. Stigler FL, Duvivier RJ, Weggemans M, Salzer HJ. Health professionals for the 21st century: a students' view. Lancet. 2010;376(9756):1877–8.
6. Green M, Wayne DB, Neilson EG. Medical education 2020—charting a path forward. JAMA. 2019;322(10):934–5.
7. Bulc B, Al-Wahdani B, Bustreo F, Choonara S, Demaio A, Jácome DI, et al. Urgency for transformation: youth engagement in global health. Lancet Glob Health. 2019;7(7):e839–40.
8. Simpson T. Medical education in the digital age: personal reflection on a simulation fellowship. Scott Med J. 2015;60(4):182–4.
9. Lilic N. Murmurs of politics and economics. N Engl J Med. 2018;379:1202–3.
10. Wartman SA, Combs CD. Reimagining medical education in the age of AI. AMA J Ethics. 2019;21(2):E146–52.
11. Pitruzella B, Leahy P. Future of surgery. RCS. 2018 [online]. Available on https://futureofsurgery.rcseng.ac.uk/.
12. Meara JG, Leather AJM, Hagander L, Alkire BC, Alonso N, Ameh EA, et al. Global Surgery 2030: evidence and solutions for achieving health, welfare, and economic development. Lancet. 2015;386(9993):569–624.
13. World Health Assembly. Resolution 68.15 strengthening emergency and essential surgical care and anaesthesia as a component of universal health coverage. Geneva: WHO; 2015.
14. Shrime MG, Dare AJ, Alkire BC, O'Neill K, Meara JG. Catastrophic expenditure to pay for surgery worldwide: a modelling study. Lancet Glob Health. 2015;3(Suppl 2):S38–44.
15. Shrime MG, Bickler SW, Alkire BC, Mock C. Global burden of surgical disease: an estimation from the provider perspective. Lancet Glob Health. 2015;3(Suppl 2):S8–9.
16. Bishop D, Dyer RA, Maswime S, Rodseth RN, van Dyk D, Kluyts H-L, et al. Maternal and neonatal outcomes after caesarean delivery in the African Surgical Outcomes Study: a 7-day prospective observational cohort study. Lancet Glob Health. 2019;7(4):e513–22.
17. Tangcharoensathien V, Mills A, Palu T. Accelerating health equity: the key role of universal health coverage in the sustainable development goals. BMC Med. 2015;13(1):101.
18. Lin Y, Scott JW, Yi S, Taylor KK, Ntakiyiruta G, Ntirenganya F, et al. Improving surgical safety and nontechnical skills in variable-resource contexts: a novel educational curriculum. J Surg Educ. 2018;75(4):1014–21.
19. The World Bank. World Development Indicators; 2018. http://databank.worldbank.org/data/reports.aspx?source=world-development-indicators. Accessed 1 Apr 2018.
20. The program in global surgery and social change. National surgical, obstetric, and anaesthesia planning (NSOAP) workshop, Harvard Medical School; 2018. https://www.pgssc.org/dubai-nsoap-workshop. Accessed 1 Nov 2019.

3D Simulation and Modeling for Surgeon Education and Patient Engagement

29

Anna Przedlacka, Przemyslaw Korzeniowski, Paris Tekkis, Fernando Bello, and Christos Kontovounisios

Surgical Education

Surgical training has evolved enormously in the last decades. Traditionally, it involved an apprentice-like model outlined by Halstead in the beginning of twentieth century [1]. It was based on a high-volume, hands-on training with a gradually decaying level of supervision, until the trainee was judged by the mentor competent enough to operate on their own. With time, the structure and the content of the educational material have become more defined, and detailed curricula have been developed. Regardless of the educational model, the aim of surgical training has always been focused on producing a highly skilled operator capable of performing independently at the safest possible level.

A. Przedlacka
Department of Surgery and Cancer, Imperial College London – Chelsea and Westminster Hospital, London, UK

P. Korzeniowski
Department of Surgery and Cancer, Imperial College London, London, UK

P. Tekkis · C. Kontovounisios (✉)
Department of Surgery and Cancer, Imperial College London – Chelsea and Westminster and the Royal Marsden Campus, London, UK
e-mail: c.kontovounisios@imperial.ac.uk

F. Bello
Centre for Engagement and Simulation Science, Imperial College London, London, UK

Due to the reduction in working hours and a substantial increase in knowledge and patient safety requirements, the traditional model of surgical education is no longer sustainable. The development of digital technologies has allowed an introduction of new methods of learning surgery, with an aim to utilize the reduced time more efficiently and effectively. A significant proportion of the surgical training have now moved outside of the traditional setting of the operating theatre into the skill and simulation labs. The question regarding the simulation training has shifted from *"Is it effective?"* to *"How can it be best embedded, supported and funded?"* [2].

Gaining core surgical skills on animals or cadavers is expensive and raises ethical concerns, thus restricting their use in everyday training [3]. Using inexpensive, low-fidelity task physical trainers can provide effective training of the key elements of the procedure, but this paradigm lacks (in most instances) the real-life effect of surgery. Moreover, animals and cadavers, as well as foam, silicon or plastic parts used in task trainers, lack the physiological behaviour and different biomechanical properties, compared to living human tissue. Hence, these methods do not provide sufficient realism. Finally, they require feedback from a tutor.

The rapid increase in computer power and emergence of haptic technology [4] resulted in an alternative approach – a computer-based simulation system enabling training on a virtual patient [5]. Such systems, often referred to as

S. Atallah (ed.), *Digital Surgery*, https://doi.org/10.1007/978-3-030-49100-0_29

virtual reality (VR) simulators, typically consist of a 2D or 3D display, a computer running the simulation software and a physical human-computer interface device mimicking the surgical instruments.

The device tracks the manipulation of the instruments and often can recreate the sense of touch by providing force feedback to the user (a haptic device). The software is responsible for taking input from the input device, simulating the interactions between the instruments and the virtual anatomy, rendering the 3D image of the surgical site and, if supported, calculating the forces sent to the user via the haptic device. Additionally, the software can record, analyze and store user performance.

The advances in 3D technologies have added new advantages to the already established application of simulation technology. They have led to the development of environments and scenarios which are more complex and thus able to more closely resemble real operations. 3D modeling has a central, paramount role in this evolution – it produces models that can be used independently as a sophisticated depiction of the anatomy or form the basis for the 3D simulation tools. 3D printing, or additive printing technology, has broadened the surgical horizons even further. The physical 3D models are manufactured through layering of printing materials based on digital 3D models.

Hybrid simulation, which combines the advantages of a physical 3D printed model (haptic feedback, deformability) with advantages of a VR simulator (building complex interfaces and environments), is an especially exciting joint application of both technologies [6]. The inclusion of haptic feedback seems to be an important factor in the training on VR, and the lack of haptic feedback might prove the application of VR less successful than a standard black box simulator [7].

Since the 1990s, virtual reality (VR) simulators have been expected to become as important for surgery as flight simulators are for aviation [8]. In 2001, Satava stated that "*The greatest power of virtual reality is the ability to try and fail without consequence to animal or patient. It is only through failure – and learning the cause of failure – that the true pathway to success lies*" [9].

High-fidelity virtual reality simulators have several advantages over the traditional methods of surgical training. They offer a safe, controllable and configurable training environment free from ethical issues in which clinicians can repetitively practice their skills.

VR simulators improve patient safety – not only because patients are not at risk during actual training but also because surgeons trained on VR simulators show higher competencies [10, 11].

VR simulators improve the educational experience by providing a wide selection of training scenarios diversified in terms of virtual patient's anatomy and pathologies. This overcomes the problem of waiting for a suitable real-life case and allows for controlled clinical exposure, where trainees start with basic cases moving gradually to more complex ones when they feel confident to do so.

Training on VR simulators does not require the presence of a supervising expert. By analyzing user performance in real-time, simulators can give immediate feedback during the procedure, which is crucial for efficient training [12]. The formative and summative assessment at the end of each training session helps to track user's learning progress that may be used in the future for credentialing and certification [13].

VR simulators have low maintenance costs and, except for calibration, practically require no preparation before or during the training session. Students and delegate surgeons can train on their own, whenever the equipment is available. They are reusable allowing for repetitive training of the same procedure countless times without incurring additional costs.

Experts can also benefit from simulation by practicing rare/complex cases, to maintain and improve their skills or even to "warm up" before performing real surgery [14]. VR simulators can be used to explore new ways of performing a procedure or to become familiar with new surgical techniques or new surgical devices [15].

Some VR simulators can assist during preoperative planning or intraoperative navigation

[16]. By reading patient-specific data obtained from medical imaging (CT or MRI), VR simulators can help to plan a surgery in order to avoid potential complications and to assure a safe outcome.

High development costs and corresponding final high price are usually mentioned as key disadvantages of VR simulators. However, when considering the wider economic benefits of better-trained surgeons, error reduction, faster completion times and savings on instructor time, VR simulators can, in fact, be cost-effective [10, 17, 18].

Lastly, there is an increasing body of evidence, which supports the transferability of surgical skills acquired through the virtual training [19]. The novel technologies have been utilized to address all aspects of modern surgical training – from learning anatomy, through development of clinical judgement and surgical planning, to acquisition of operative skills.

Anatomy

Meticulous knowledge of anatomy underpins any successful surgical training. Traditionally, anatomy has been taught through a combination of prosection, didactic lectures and self-directed textbook study. The role of cadavers has significantly decreased over the last decade, partly due to their reduced availability and the ethical issues surrounding their use [20, 21].

Various anatomical models have always been used to depict the complexities of human anatomy. The introduction of different adjuncts facilitates the creation of a mental image of a complex structure; such adjuncts also improve the efficiency of the process of memorizing and the reliability of recall. The development and advances in 3D modeling and printing, as well as simulation, have allowed for creation of new generation of high-fidelity models, which can be based on patient-specific anatomy, allowing for rehearsal of patient-tailored surgery. They can be freely moved, rotated and dissected and allow for assessment of the organ from different points of view.

Virtual models can be accessed remotely on PCs or mobile phones. Complete Anatomy by 3D4Medical and 3D Atlas by Anatomy Learning are examples of free smartphone apps that present virtual three-dimensional models. Visual Human Projects by National Library of Medicine, a free database of 3D anatomy, provides virtual models based on volumetric reconstruction of transverse CT, MRI and cryosectional photographs of the entire male and female body [22, 23].

Virtual reality platforms like Anatomage, Biodigital, Netter3DAnatomy, Visible Body, Primal Pictures and Electronic Anatomy Atlas are other examples of modern anatomy resources. 3D models can be dissected, and students can easily transfer between the microscopic and macroscopic views. This technology is also multi-user-friendly, thus facilitating a group study approach [20].

The 3D models are especially useful for complex anatomy, such as the liver, brain, vascular, pelvic or craniofacial anatomy. Organ-specific resources, such as VIRTUAL LIVER, often depict the 3D virtual models along the relevant 2D radiological studies (CT, MRI, cholangiogram) and textual information [24].

Pelvic colorectal anatomy with its complex intricacies presents significant challenges to both students and colorectal trainees. The virtual display of a 3D pelvis and its compartments [25], as well as depiction of a rectal tumour [26], or benign pathologies, such as fistula-in-ano [27], allows the learner to manipulate the image, to inspect it in detail from different perspectives and, with different transparencies of each layer, to form a comprehensive mental image of this complex anatomical region (Fig. 29.1).

Anatomical concepts can be equally difficult to comprehend, yet their full appreciation and recognition is crucial for the safety of surgical procedures. An inguinal hernia, and the distinction between the direct and indirect sacs, is one such example, where students and junior trainees commonly struggle to form the mental image. The use of 3D virtual reconstruction appears to significantly improve the understanding and is highly valued as an addition to traditional

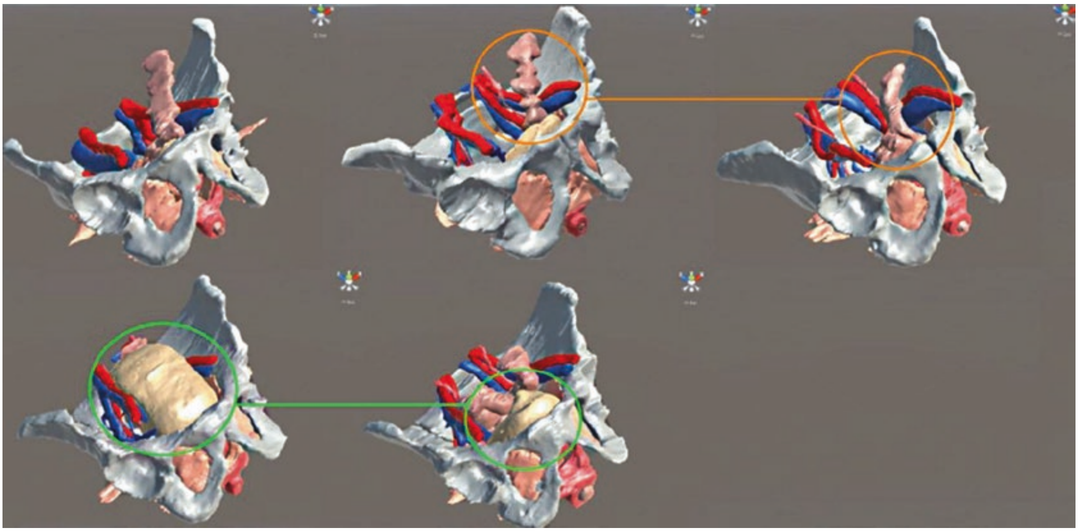

Fig. 29.1 3D models of five healthy male volunteers illustrating anatomical variation (orange) and organ distension (green)

methods. Students find preoperative review of 3D anatomy very useful for comprehension of complex intraoperative anatomy such as encountered during laparoscopic transabdominal preperitoneal repair (TAPP) [28]. Along with the virtual models, 3D printed physical models are used. These add a benefit of haptic feedback which further enhances recognition and learning [29].

Surgical Planning

Accurate operative planning is integral to the process of becoming an independent, mature surgeon. This often relies on the ability to mentally reconstruct complex two-dimensional radiological scans into three-dimensional images and then being able to interpret such reconstructions during live surgery. While there is broad evidence that 3D technology aids in surgical planning in general, it is still not widely included in surgical curricula; students report that they are not taught surgical planning enough in their training [30].

Trainees value 3D visualization highly as a useful adjunct for surgical planning. Lyn et al. found that surgical trainees assess the resectability and staging of pancreatic tumours more accurately using 3D visualization when compared with 2D staging images. It appears that 3D modeling facilitates the anatomy-image-surgery translation [31].

The same improvement in the accuracy of surgical planning and decrease in time required for that was found when virtual 3D models were used in liver surgery. Trainees saw a difference between using the 2D radiological images and 3D virtual models and reported increased confidence when forming surgical strategy with the use of 3D technology [32].

A question exists as to whether 3D *virtual* or 3D *physical* models are more efficacious. For some purposes, virtual 3D models displayed on screens offer enough information to enhance learning. However, in more complex cases, 3D printed models might be superior since they can provide the benefit of haptic feedback.

No conclusive answer exists at present; however, Zheng et al. compared the accuracy of surgical operative planning amongst students using either 3D computer or 3D printed models of patient-specific pancreatic anatomy in patients with three different types of pancreatic cancer which would require different surgical approaches. Students using the 3D printed models were able to formulate a higher-quality and more accurate operative plans [33]. This might be due to the incorporation of haptic feedback to the assessment. The authors believe that a physical model also has a more significant impact on the development of hand-eye coordination skill.

3D printed models can significantly improve inaccuracies in surgical operative planning and reduce time required for decision-making. Craniofacial surgery involves complex decision-making based on difficult anatomy that trainees are not closely familiar with. 3D printed models of craniofacial anatomy have been validated to improve these skills based on four anomalies included in the curriculum [34].

Surgical Operative Skills

One of the first medical VR simulators was developed in 1987 at Stanford University to practice Achilles tendon repair [35]. The simulator could also be used for preoperative planning. It allowed students and trainees to "walk the leg" and visualize the effect of the procedure on gait. A few years later, Lanier and Satava [8] developed a first simulator for simplified intra-abdominal surgery.

The first commercially successful VR surgical simulator was the Minimally Invasive Surgery Trainer-VR or MIST-VR [36], by Mentice AB, Sweden (www.mentice.com). It was based on abstract graphics and consisted of fundamental laparoscopic tasks emphasizing motor skills acquisition. Seymour et al. [10] demonstrated its validity and estimated a 29% reduction in operating time and an 85% decrease in number of errors during gallbladder dissection in a laparoscopic cholecystectomy procedure.

Currently, there are simulators for many subspecialties, such as laparoscopic surgery (e.g., LAP Mentor, Fig. 29.2, www.simbionix.com), endovascular surgery (e.g., Vist-Lab, www.mentice.com), endoscopy (e.g., EndoSim), etc. [37].

Patient safety is one of the main concerns in surgical training. It is especially important in the field of neurosurgery. The Immersive Touch technology has been used to develop a realistic VR platform which allows surgical trainees to perform placement of a ventriculostomy catheter. It employs 3D modeling based on a patient's CT

Fig. 29.2 Simbionix LAP Mentor laparoscopic training simulator from 3D Systems. (Courtesy of Healthcare 3D Systems, Israel)

images, combined with VR, dynamic 3D stereoscopic vision and haptic feedback. It realistically simulates the changing resistance during the passage through the brain parenchyma while the 3D visual perspective changes with the user's head movement [38].

Mental preparation is an important step in improving practice in high-performance disciplines such as extreme sports or combat aviation. Its role is being also explored in surgical education; however, unequivocal conclusions have yet to be drawn. Yiasemidou et al. argue that mental preparation in surgical trainees can be enhanced by the use of interactive models of task-relevant anatomy. This study showed that students who used interactive 3D visual models while preparing for laparoscopic cholecystectomy completed the procedure in shorter time with a smaller number of movements. It showed a promising role of 3D visualization during mental preparation for minimally invasive surgery [39].

This novel technology can be utilized to increase the objectivity of assessment of surgical skill. When the assessment is conducted on a patient, frequently, trainees are not able to perform the entire procedure and therefore only parts of it are assessed. Often, it is delivered in a descriptive way, assigning levels of competency according to a predetermined scale. Simulation, however, allows for an assessment, where the outcomes can be measured objectively. The 3D model can be easily scrutinized following the completion of the procedure which enhances the delivery of feedback as well.

Choi et al. introduced a 3D printed model of prostate, which serves both as a training and an assessment tool for surgeons. A 3D physical model has been moulded to depict with high-fidelity two distinctive zones of the prostate – it is crucial to distinguish reliably between these to perform safe transurethral resection of the prostate gland. Through applying different materials to construct these, a real-life scenario is created where a surgeon relies on haptic feedback during this minimally invasive procedure. Different sonographic contrast is applied to each zone which then allows for an objective assessment of the safety and completion of the resection [40].

Transfer of skills remains an important area specific to the development of surgeons in residency and fellowship training, which justifies the funding applied towards the use of the new technologies in surgical and medical education. It is not fully understood whether the transfer of skills is more efficient based on the similarity of the learning context [41] or the similarity of the learning process required for completion of the task [42]. Both components should be addressed in the design of simulation technologies.

VR has been employed by some groups to test educational theories. Yang et al. assessed the skill and knowledge transfer between two common types of general laparoscopic operations in surgical novices – appendectomy and cholecystectomy. It showed that previous exposure to laparoscopic appendectomy does not necessarily translate into reduction of operative time or overall safety of the procedure in laparoscopic cholecystectomy. However, it positively affected the ergonomy of surgeon movements. This study leads to the conclusion that procedure-specific learning curricula are necessary to develop skills relevant to each procedure [43]. More research in this area is required.

Adjunctively, video games – which are keenly dependent on the honing of hand-eye coordination – are being explored as tools for surgical training as well. There is some evidence that that the acquisition and practice of video gaming skills translate into surgical skills. In fact, laparoscopic surgeons who played video games regularly made fewer surgical errors [44] and were observed to be faster [45, 46] than those who did not play, suggesting a correlation with achieving adeptness at the technical aspects of operating. Similar correlations were found for endoscopic or gastroscopic skills [47, 48]. Perhaps not surprisingly, students, including those who do not play video games, support their application of video gaming as an adjunct to surgical training and, specifically, towards the acquisition of technique-based advanced surgical skill pertaining to minimally invasive surgery.

Patient Engagement

The patient's role, both in individual care and in shaping healthcare systems in general, has evolved enormously in recent years. Increasingly more focus is being placed on patient safety, measurable outcomes and overall satisfaction. Simultaneously, patients have gained an important voice in shaping clinical research and healthcare systems. A fruitful communication is paramount in achieving these goals. It leads to better adherence to treatment plans and reduced anxiety, and it achieves greater satisfaction with an overall improved patient experience.

3D modeling, simulation and VR have all been explored and show promising potential for patient engagement. The novel technologies have been explored to achieve various aims – to improve healthcare literacy, to engage the public and promote healthy habits and to design healthcare systems and research programs, further supporting the implementation of evidence-based medicine.

Improving Patient Knowledge and Health Literacy

Virtual or physical three-dimensional models of organs affected by the disease can improve patient's understanding of pathology and facilitate a more informed consent process and a more satisfactory formation of treatment plans. These models can depict generic anatomy or patient-specific pathology in a manner that laypersons, including patients, can more easily comprehend. Increasingly, more reports and clinical examples are emerging for the modeling of common pathologies, as well as complex and rare conditions [49].

Bernhard et al. assessed the impact on a patient's understanding of pathology and treatment using a 3D printed life-size, patient-specific model of renal tumours during the consent process for partial nephrectomy. They found an improved knowledge of basic kidney anatomy and physiology, as well as tumour characteristics and proposed surgical procedure, when the 3D printed models (based on patient-specific CT scans) were used [50].

Zhuang et al. explored the effectiveness of 3D virtual reconstructions and printed models of individualized patient anatomy (specifically, lumbar pathology) in increasing patient understanding of their condition and surgical plan. The group found that patients' knowledge and satisfaction were significantly improved when 3D *printed* models were used, compared to 3D *virtual* reconstructions or traditional approach using the CT and MRI images only [51].

Similarly, Kim et al. assessed the usefulness of 3D printed patient-specific models of cerebral aneurysms as an educational tool for those undergoing surgery for cerebral artery aneurysm clipping. Again, they observed an improved understanding and satisfaction of the explanation compared to the use of traditional two-dimensional CTA images [52].

Mobile applications can be used to facilitate 3D visualization of surgery leading to better patient understanding. Pulijala et al. showed that patients who used a mobile application with 3D animations (related to orthognathic surgery) retain more knowledge of the proposed procedures and their complications than a cohort of patients who receive verbal explanation only [53].

Virtual reality platforms and immersive image viewing experience have also been successfully applied to improve patient education related to specific medical conditions. Pandrangi et al. introduced standardized 3D models of abdominal aortic aneurysm (AAA) viewed in VR through Google Cardboard VR headset in patients with this condition. Despite mostly having no previous experience with use of VR, this technology was positively received by the majority of patients who felt that it significantly improved their understanding of the condition and overall engagement in their care. The overwhelming majority of patients felt comfortable using this technology and would like to see it used more frequently in their care [54].

The application of VR technology can reduce anxiety related to surgical procedures as well. Yang et al. found that patients who were familiarized with a 3D model of their own knee anatomy watched through a VR headset experienced a reduced level of anxiety prior to knee arthroscopy, when compared to the patients who received standard information regarding their preoperative MRI [55].

3D models and 3D simulation play a significant role in aesthetic surgery, where addressing and managing patient expectations might be especially paramount. The novel technology has been used as a tool for visualization of desired outcomes in breast augmentation surgery or rhinoplasty. Interestingly, despite the lack of concrete evidence that this technology improves measurable outcomes, patients had a favourable view for application of VR for select types of cosmetic surgery, such as breast augmentation [56].

The transfer of knowledge between the doctor and the patient is equally important following the surgical procedure, as it is during the planning phase. It is estimated that patients recall as little as 50% of information provided by the healthcare providers. Equally importantly, research has demonstrated that in 66% of consultations, doctors can unwillingly omit at least some of the crucial information related to patient surgical care delivery [57]. VR has been successfully tested in overcoming these barriers by constructing virtual environments, where patient-doctor interactions take place. HealthVoyager is a platform designed for children with gastrointestinal pathologies, which utilizes customizable VR software compatible with smartphones or tablets (Fig. 29.3). Through creation of an avatar, it allows a patient and their parents to familiarize themselves with the child's individual anatomy, as well as relevant clinical and procedural data. The personalized information is presented in a visual, rather than text-based way and applies an active (rather than passive) learning method. Patients can also return to and review the discussions at later time to be able to apply the clinical instructions more accurately [58]. This is important as at the time of physician-patient encounter, a high level of stress can prevent the patient and their family from absorbing details of relevance.

Novel Technologies to Treat Pain

Pain is a leading complaint in majority of surgical presentations, and most patients experience acute or chronic pain during the course of their illness. Management of pain is therefore a crucial part of surgical care. VR and video gaming have proven to be successful in management of both acute and chronic pain. Their mechanism of action is based on providing distraction during the occurrence of an unpleasant stimulus and has been validated with the use of functional MRI. Immersive VR technologies have a better analgesic effect than non-immersive technology [59].

Virtual reality distraction (VRD) has been shown to be effective in management of experimentally induced thermal pain. Patterson et al. tested the virtual reality hypnosis (VRH) by creating virtual environment where patients experienced gliding through frozen landscapes and throwing snowballs. While there might be a synergistic effect when combined with post-hypnotic suggestion, VRD has been shown to be effective, and this is independent of "hypnotizability" of the subject [60].

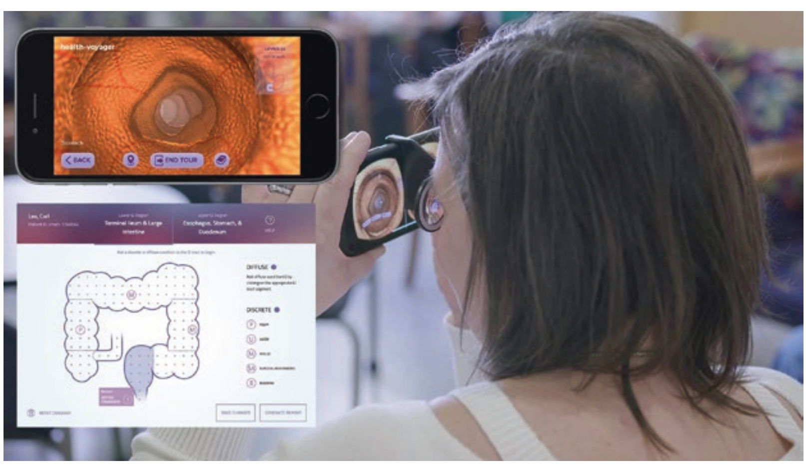

Fig. 29.3 HealthVoyager software application, with an inlay of the patient VR experience (top left) and a sample report from the physician's notes (bottom left). (From Palanica et al. [58]. Copyright © 2019, Springer Nature, Creative Commons CC BY license)

Hoffman et al. explored the use of VR in pain management in children with severe burns >10% of body surface cared for in the intensive care unit. A significant reduction in the level of most severe pain was observed when VR immersive reality (involving playing the SnowWorld, a 3D snowy canyon) was used during the wound care, when compared to patients who did not utilize VR [61].

VR technology shows promising potential as an alternative or additional treatment of chronic pain as well. Sato et al. applied virtual reality mirror visual feedback in patients with complex regional pain syndrome. A virtual environment was developed using Autodesk 3DS Max (San Rafael, USA), where the exercises are target-oriented motor-controlled tasks via various movements like reaching out, grasping, transferring and placing. In this study, 50% reduction in pain was observed in 4 out of 5 patients; furthermore, 2 out of 5 patients were able to discontinue pain clinic visits altogether [62].

Enhancing Patients' Attitudes and Promoting Healthy Lifestyle

Engaging the general public, as well as specific subgroups of patients, is important in promoting lifestyle changes. Serious video gaming has been proven to be successful in management of weight in young adults and in rehabilitation in patients with stroke or following traumatic brain injury [63–65]. It has also been used for mood management in patients with metastatic cancer.

Shaping the Future of the Healthcare Systems

There has been an important shift in the recent years from a "paternalistic" approach to healthcare, where the healthcare providers are the main decision-makers, to a model of partnership – where both patient and the care provider meet as equals with different levels of expertise. Patient and public involvement is paramount for shaping the healthcare systems and for designing clinical research.

Novel 3D technologies have been explored as a potential means to facilitate this engagement. One of the forms of obtaining patient views and arriving at solutions is a focused group discussion. Virtual worlds such as Second Life can facilitate this process through creating virtual 3D environments where meetings between patients, care providers and researchers (represented by their avatars) can take place. It can be especially attractive for patients with mobility or other restrictions, which often pose significant impedance to partaking in face-to-face interactions and dialogue. In essence, novel 3D technologies are opening new avenues for peer-led support and engagement [66].

References

1. Halsted W. The training of the surgeon. 1904.
2. Kneebone RL. Simulation reframed. Adv Simul (Lond). 2016;1:27.
3. Rosen KR. The history of medical simulation. J Crit Care. 2008;23(2):157–66.
4. Salisbury K, Conti F, Barbagli F. Haptic rendering: introductory concepts. IEEE Comput Graph. 2004;24(2):24–32.
5. Gallagher AG, Ritter EM, Champion H, Higgins G, Fried MP, Moses G, et al. Virtual reality simulation for the operating room: proficiency-based training as a paradigm shift in surgical skills training. Ann Surg. 2005;241(2):364–72.
6. Condino S, Carbone M, Ferrari V, Faggioni L, Peri A, Ferrari M, et al. How to build patient-specific synthetic abdominal anatomies. An innovative approach from physical toward hybrid surgical simulators. Int J Med Robot. 2011;7(2):202–13.
7. Jensen K, Ringsted C, Hansen HJ, Petersen RH, Konge L. Simulation-based training for thoracoscopic lobectomy: a randomized controlled trial: virtual-reality versus black-box simulation. Surg Endosc. 2014;28(6):1821–9.
8. Satava RM. Virtual reality surgical simulator. The first steps. Surg Endosc. 1993;7(3):203–5.
9. Satava RM. Accomplishments and challenges of surgical simulation. Surg Endosc. 2001;15(3):232–41.
10. Seymour NE, Gallagher AG, Roman SA, O'Brien MK, Bansal VK, Andersen DK, et al. Virtual reality training improves operating room performance: results of a randomized, double-blinded study. Ann Surg. 2002;236(4):458–63; discussion 63–4.
11. Youngblood PL, Srivastava S, Curet M, Heinrichs WL, Dev P, Wren SM. Comparison of training on

two laparoscopic simulators and assessment of skills transfer to surgical performance. J Am Coll Surg. 2005;200(4):546–51.
12. Zendejas B, Brydges R, Hamstra SJ, Cook DA. State of the evidence on simulation-based training for laparoscopic surgery: a systematic review. Ann Surg. 2013;257(4):586–93.
13. de Visser H, Watson MO, Salvado O, Passenger JD. Progress in virtual reality simulators for surgical training and certification. Med J Aust. 2011;194(4):S38–40.
14. Kahol K, Satava RM, Ferrara J, Smith ML. Effect of short-term pretrial practice on surgical proficiency in simulated environments: a randomized trial of the "preoperative warm-up" effect. J Am Coll Surg. 2009;208(2):255–68.
15. Punak S, Kurenov S. A simulation framework for wound closure by suture for the endo stitch suturing instrument. Stud Health Technol Inform. 2011;163:461–5.
16. Kockro RA, Serra L, Tseng-Tsai Y, Chan C, Yih-Yian S, Gim-Guan C, et al. Planning and simulation of neurosurgery in a virtual reality environment. Neurosurgery. 2000;46(1):118–35; discussion 35–7.
17. Bridges M, Diamond DL. The financial impact of teaching surgical residents in the operating room. Am J Surg. 1999;177(1):28–32.
18. Aggarwal R, Ward J, Balasundaram I, Sains P, Athanasiou T, Darzi A. Proving the effectiveness of virtual reality simulation for training in laparoscopic surgery. Ann Surg. 2007;246(5):771–9.
19. Gallagher AG, Seymour NE, Jordan-Black JA, Bunting BP, McGlade K, Satava RM. Prospective, randomized assessment of transfer of training (ToT) and transfer effectiveness ratio (TER) of virtual reality simulation training for laparoscopic skill acquisition. Ann Surg. 2013;257(6):1025–31.
20. Bisht B, Hope A, Paul MK. From papyrus leaves to bioprinting and virtual reality: history and innovation in anatomy. Anat Cell Biol. 2019;52(3):226–35.
21. Davis CR, Bates AS, Ellis H, Roberts AM. Human anatomy: let the students tell us how to teach. Anat Sci Educ. 2014;7(4):262–72.
22. Spitzer VM, Whitlock DG. The Visible Human Dataset: the anatomical platform for human simulation. Anat Rec. 1998;253(2):49–57.
23. Dai JX, Chung MS, Qu RM, Yuan L, Liu SW, Shin DS. The Visible Human Projects in Korea and China with improved images and diverse applications. Surg Radiol Anat. 2012;34(6):527–34.
24. Crossingham JL, Jenkinson J, Woolridge N, Gallinger S, Tait GA, Moulton CA. Interpreting three-dimensional structures from two-dimensional images: a web-based interactive 3D teaching model of surgical liver anatomy. HPB (Oxford). 2009;11(6):523–8.
25. Kontovounisios C, Tekkis P, Bello F. 3D imaging and printing in pelvic colorectal cancer: 'The New Kid on the Block'. Tech Coloproctol. 2019;23(2):171–3.
26. Sahnan K, Pellino G, Adegbola SO, Tozer PJ, Chandrasinghe P, Miskovic D, et al. Development of a model of three-dimensional imaging for the preoperative planning of TaTME. Tech Coloproctol. 2018;22(1):59–63.
27. Sahnan K, Adegbola SO, Tozer PJ, Gupta A, Baldwin-Cleland R, Yassin N, et al. Improving the understanding of perianal Crohn fistula through 3D modeling. Ann Surg. 2018;267(6):e105–e7.
28. Wada Y, Nishi M, Yoshikawa K, Higashijima J, Miyatani T, Tokunaga T, et al. Usefulness of virtual three-dimensional image analysis in inguinal hernia as an educational tool. Surg Endosc. 2019;34(5):1923–8.
29. Marconi S, Pugliese L, Botti M, Peri A, Cavazzi E, Latteri S, et al. Value of 3D printing for the comprehension of surgical anatomy. Surg Endosc. 2017;31(10):4102–10.
30. Snyder RA, Tarpley MJ, Tarpley JL, Davidson M, Brophy C, Dattilo JB. Teaching in the operating room: results of a national survey. J Surg Educ. 2012;69(5):643–9.
31. Lin C, Gao J, Zheng H, Zhao J, Yang H, Lin G, et al. Three-dimensional visualization technology used in pancreatic surgery: a valuable tool for surgical trainees. J Gastrointest Surg. 2019;24(4):866–73.
32. Yeo CT, MacDonald A, Ungi T, Lasso A, Jalink D, Zevin B, et al. Utility of 3D reconstruction of 2D liver computed tomography/magnetic resonance images as a surgical planning tool for residents in liver resection surgery. J Surg Educ. 2018;75(3):792–7.
33. Zheng YX, Yu DF, Zhao JG, Wu YL, Zheng B. 3D Printout models vs. 3D-rendered images: which is better for preoperative planning? J Surg Educ. 2016;73(3):518–23.
34. Lobb DC, Cottler P, Dart D, Black JS. The use of patient-specific three-dimensional printed surgical models enhances plastic surgery resident education in craniofacial surgery. J Craniofac Surg. 2019;30(2):339–41.
35. Delp SL, Loan JP, Hoy MG, Zajac FE, Topp EL, Rosen JM. An interactive graphics-based model of the lower extremity to study orthopaedic surgical procedures. IEEE Trans Biomed Eng. 1990;37(8):757–67.
36. Wilson MS, Middlebrook A, Sutton C, Stone R, McCloy RF. MIST VR: a virtual reality trainer for laparoscopic surgery assesses performance. Ann R Coll Surg Engl. 1997;79(6):403–4.
37. Dunkin B, Adrales GL, Apelgren K, Mellinger JD. Surgical simulation: a current review. Surg Endosc Other Interv Tech. 2007;21(3):357–66.
38. Lemole GM Jr, Banerjee PP, Luciano C, Neckrysh S, Charbel FT. Virtual reality in neurosurgical education: part-task ventriculostomy simulation with dynamic visual and haptic feedback. Neurosurgery. 2007;61(1):142–8; discussion 8–9.
39. Yiasemidou M, Glassman D, Mushtaq F, Athanasiou C, Williams MM, Jayne D, et al. Mental practice with interactive 3D visual aids enhances surgical performance. Surg Endosc. 2017;31(10):4111–7.
40. Choi E, Adams F, Palagi S, Gengenbacher A, Schlager D, Muller PF, et al. A high-fidelity phantom for the simulation and quantitative evaluation of transure-

thral resection of the prostate. Ann Biomed Eng. 2019;48(1):437–46.
41. Thorndike EL. Educational Psychology. Science. 1923;57(1476):430.
42. Lee T. Transfer-appropriate processing: a framework for conceptualizing practice effects in motor learning. Adv Psychol. 1988;50:201–15.
43. Yang C, Kalinitschenko U, Helmert JR, Weitz J, Reissfelder C, Mees ST. Transferability of laparoscopic skills using the virtual reality simulator. Surg Endosc. 2018;32(10):4132–7.
44. Grantcharov TP, Bardram L, Funch-Jensen P, Rosenberg J. Impact of hand dominance, gender, and experience with computer games on performance in virtual reality laparoscopy. Surg Endosc. 2003;17(7):1082–5.
45. Rosser JC Jr, Lynch PJ, Cuddihy L, Gentile DA, Klonsky J, Merrell R. The impact of video games on training surgeons in the 21st century. Arch Surg. 2007;142(2):181–6; discussion 6.
46. Schlickum MK, Hedman L, Enochsson L, Kjellin A, Fellander-Tsai L. Systematic video game training in surgical novices improves performance in virtual reality endoscopic surgical simulators: a prospective randomized study. World J Surg. 2009;33(11):2360–7.
47. Stefanidis D, Acker C, Heniford BT. Proficiency-based laparoscopic simulator training leads to improved operating room skill that is resistant to decay. Surg Innov. 2008;15(1):69–73.
48. Westman B, Ritter EM, Kjellin A, Torkvist L, Wredmark T, Fellander-Tsai L, et al. Visuospatial abilities correlate with performance of senior endoscopy specialist in simulated colonoscopy. J Gastrointest Surg. 2006;10(4):593–9.
49. Aroney N, Markham R, Putrino A, Crowhurst J, Wall D, Scalia G, et al. Three-dimensional printed cardiac fistulae: a case series. Eur Heart J Case Rep. 2019;3(2)
50. Bernhard JC, Isotani S, Matsugasumi T, Duddalwar V, Hung AJ, Suer E, et al. Personalized 3D printed model of kidney and tumor anatomy: a useful tool for patient education. World J Urol. 2016;34(3):337–45.
51. Zhuang YD, Zhou MC, Liu SC, Wu JF, Wang R, Chen CM. Effectiveness of personalized 3D printed models for patient education in degenerative lumbar disease. Patient Educ Couns. 2019;102(10):1875–81.
52. Kim PS, Choi CH, Han IH, Lee JH, Choi HJ, Lee JI. Obtaining informed consent using patient specific 3D printing cerebral aneurysm model. J Korean Neurosurg Soc. 2019;62(4):398–404.
53. Pulijala Y, Ma M, Ju X, Benington P, Ayoub A. Efficacy of three-dimensional visualization in mobile apps for patient education regarding orthognathic surgery. Int J Oral Maxillofac Surg. 2016;45(9):1081–5.
54. Pandrangi VC, Gaston B, Appelbaum NP, Albuquerque FC Jr, Levy MM, Larson RA. The application of virtual reality in patient education. Ann Vasc Surg. 2019;59:184–9.
55. Yang JH, Ryu JJ, Nam E, Lee HS, Lee JK. Effects of preoperative virtual reality magnetic resonance imaging on preoperative anxiety in patients undergoing arthroscopic knee surgery: a randomized controlled study. Arthroscopy. 2019;35(8):2394–9.
56. Overschmidt B, Qureshi AA, Parikh RP, Yan Y, Tenenbaum MM, Myckatyn TM. A prospective evaluation of three-dimensional image simulation: patient-reported outcomes and mammometrics in primary breast augmentation. Plast Reconstr Surg. 2018;142(2):133e–44e.
57. Tarn DM, Heritage J, Paterniti DA, Hays RD, Kravitz RL, Wenger NS. Physician communication when prescribing new medications. Arch Intern Med. 2006;166(17):1855–62.
58. Palanica A, Docktor MJ, Lee A, Fossat Y. Using mobile virtual reality to enhance medical comprehension and satisfaction in patients and their families. Perspect Med Educ. 2019;8(2):123–7. https://doi.org/10.1007/s40037-019-0504-7.
59. Gold JI, Kim SH, Kant AJ, Joseph MH, Rizzo AS. Effectiveness of virtual reality for pediatric pain distraction during i.v. placement. Cyberpsychol Behav. 2006;9(2):207–12.
60. Patterson DR, Hoffman HG, Palacios AG, Jensen MJ. Analgesic effects of posthypnotic suggestions and virtual reality distraction on thermal pain. J Abnorm Psychol. 2006;115(4):834–41.
61. Hoffman HG, Rodriguez RA, Gonzalez M, Bernardy M, Pena R, Beck W, et al. Immersive virtual reality as an adjunctive non-opioid analgesic for predominantly Latin American children with large severe burn wounds during burn wound cleaning in the intensive care unit: a pilot study. Front Hum Neurosci. 2019;13:262.
62. Sato K, Fukumori S, Matsusaki T, Maruo T, Ishikawa S, Nishie H, et al. Nonimmersive virtual reality mirror visual feedback therapy and its application for the treatment of complex regional pain syndrome: an open-label pilot study. Pain Med. 2010;11(4):622–9.
63. Sietsema JM, Nelson DL, Mulder RM, Mervau-Scheidel D, White BE. The use of a game to promote arm reach in persons with traumatic brain injury. Am J Occup Ther. 1993;47(1):19–24.
64. Caglio M, Latini-Corazzini L, D'Agata F, Cauda F, Sacco K, Monteverdi S, et al. Video game play changes spatial and verbal memory: rehabilitation of a single case with traumatic brain injury. Cogn Process. 2009;10(Suppl 2):S195–7.
65. Caglio M, Latini-Corazzini L, D'Agata F, Cauda F, Sacco K, Monteverdi S, et al. Virtual navigation for memory rehabilitation in a traumatic brain injured patient. Neurocase. 2012;18(2):123–31.
66. Taylor MJ, Kaur M, Sharma U, Taylor D, Reed JE, Darzi A. Using virtual worlds for patient and public engagement. Int J Technol Knowl Soc. 2013;9(2):31–48.

30 Next-Generation Surgical Robots

Shinil K. Shah, Melissa M. Felinski, Todd D. Wilson, Kulvinder S. Bajwa, and Erik B. Wilson

Introduction

The technology surrounding robotic surgery is discussed most often in relation to commercially available platforms. However, the use of robotic technology in medicine has occurred for over 30 years. In 1985, the programmable universal machine for assembly (PUMA) robot was first used for biopsies of brain tumors [1, 2]. The birth of the most widely used current robotic platform in general surgery arose out of research funded by the US Department of Defense and NASA, with initial intentions for remote surgery in space or on the battlefield [3]. Although remote surgery was performed in 2001 using the ZEUS system (Computer Motion, Inc., Goleta, CA), telesurgery has to date not been the major application of robotic technology in surgery [4].

Growth of Robotic Surgery

While the growth of robotic surgery was by some measures slow in the initial years, an inflection point appears to be developing – where surgeons, rather than questioning why operate *with* a robot, are instead asking why *not* operate with a robot. Although there is current debate in many intellectual circles about the value of robotics and its appropriate application, the worldwide growth of robotic surgery continues. In 2018, there were over 750,000 robotic surgical procedures performed in the United States and nearly 250,000 additional procedures performed internationally [5]. There appears to be no evidence of annual volume dropping going forward. Most experts project a continued increase in uptake unless major economic pressures on health care alter this trend. However, proponents argue that even if health-care dollars were contracting, the robotic market is so well established that it could adapt and survive.

The future of robotic surgery cannot be easily predicted. Certain assumptions can however safely be made by evaluating the past and asking questions of those forward thinkers who are working on developing new robotic platforms. There are over 70 different companies developing platforms for nearly every surgical subspecialty [6]. Some of the companies that are actively designing and discussing surgical robotics in addition to Intuitive Surgical, Inc. (Sunnyvale, CA) include Activ Surgical, Inc. (Boston, MA), Auris Health, Inc. (Redwood City, CA), CMR Surgical Ltd. (Cambridge, United Kingdom), ColubrisMX, Inc. (Houston, TX), Human Xtensions (Netanya, Israel), TransEnterix, Inc. (Morrisville, NC), Verb Surgical, Inc. (Santa

S. K. Shah (✉) · M. M. Felinski · T. D. Wilson
K. S. Bajwa · E. B. Wilson
Department of Surgery, UT Health McGovern Medical School, Houston, TX, USA
e-mail: shinil.k.shah@uth.tmc.edu

S. Atallah (ed.), *Digital Surgery*, https://doi.org/10.1007/978-3-030-49100-0_30

Clara, CA), Medtronic (Minneapolis, MN), Medrobotics (Raynham, MA), Titan Medical, Inc. (Toronto, Ontario, Canada), and Virtual Incision Corporation (Lincoln, NE).

Future of Robotics

When discussing the future of robotics, there are several important concepts to discuss. These themes include the design of the surgical console or interface, the number of access ports used (which are dependent upon the specific robotic system), the modularity or integration of the robotic surgical arms, the size of the robotic ports, use of simulation in training, reality augmentation (both visually and haptic), and the use of computer autonomy in the surgical tasks performed. Other issues include the cost of the systems in the future, the future of data analytics, and how the value proposition of these systems evolve over time.

Surgeon Side Cart/Interface

Surgeon robotic consoles will have varying approaches. Some will be immersive, such as the family of Intuitive Surgical, Inc. platforms, but most new platforms are focusing on an open visual console to allow for more room presence of the surgeon visual field and for the added surgeon flexibility. This includes robotic systems being designed by TransEnterix, Inc., CMR Surgical Ltd., Medtronic [7], Titan Medical, Inc., Medrobotics, and ColubrisMx. The debate exists as to whether it is more advantageous to be immersed inside the patient (via the surgeon console/interface) with no peripheral distractions or whether an open console allows for better surgeon perspective of what is happening at the bedside. There may also be some ergonomic advantages. In addition to an open versus closed visual console, there is also debate about the design of surgeon controls. These designs range from hand controls that mimic the movements of the fingers, as in open surgery, to hand controls that resemble the handles of traditional laparoscopic instruments or new control systems that may resemble video gaming controllers, remote control interfaces, or entirely new designs [8]. There is also debate about the integration of haptic feedback at the surgeon side cart [8, 9]. At present, only one system currently available incorporates haptic feedback (TransEnterix, Inc.) [10]. There is little clinical data that demonstrates an advantage/disadvantage of haptic feedback in robotic surgical systems [10].

Port Design

Surgical robots are being designed for a variety of applications, including multiple-port design, single-port design, or endoluminal flexible design. Most multiport systems are set up around three to four ports (including the camera) being robotically controlled, but research into the development of up to six robotically controlled arms delivered via multi-access ports has also been proposed. As more ports (with corresponding robotic arms) are positioned into a body cavity, more flexibility and control become possible by a single surgeon – but that must be balanced with interference and collision between the arms. Computer-based management of external and internal interferences will likely evolve as multiport robotic systems expand.

Single-port robotic systems are designed to eliminate external interferences and allow for only one incision and scar, which could be cosmetically superior in concept, if not yet in practice. Single-port systems make sense in confined work areas where an extraction of a specimen is needed through the one larger port in the case. Single-port systems potentially allow for greater movement around a cavity without external interferences but have less width and breadth of movement of each individual instrument compared to multiport systems currently. Single-port systems have been/are being designed by Intuitive Surgical, Inc., Medrobotics, Titan Medical, Inc., Auris Health, Inc., Virtual Incision Corporation, and ColubrisMx (Fig. 30.1).

Additionally, single-port robotic systems can be placed transorally and endoluminally and

Fig. 30.1 (**a**) An emerging robotic single-port system by ColubrisMx with open console and single boom robotic beside cart is shown. (**b**) Close-up detail illustrating the single-port design of the new robotic system that is pending FDA approval. (Photographs courtesy ColubrisMx, with permission)

function as endoluminal platforms, but the ultimate promise of endoluminal systems are flexible, single-port systems that can move larger distances inside a hollow lumen. These ultimately could allow for complex natural orifice transluminal endoscopic surgery (NOTES), a concept developed nearly 15 years ago, but not practical because the mechanical tools and technology of the time were much too crude to allow for safe, efficient, and widespread adoption. It is also important to note the development of single-port/single-access robotic systems for catheters (cardiac and vascular applications; Sensei X robotic catheter system (Hansen Medical, Inc. (now Auris Health, Inc.), Redwood City, CA) and colonoscopy/flexible endoscopy (Invendoscopy E200 system (Invendo Medical GmbH, Germany), NeoGuide Endoscopy System (NeoGuide Endoscopy System, Inc., Los Gatos, CA), ViaCath System (BIOTRONIK, Berlin, Germany)) as well as other robotic systems being designed for NOTES procedures [11]. The promise of robotics is to allow for intraluminal and transluminal surgery to be performed, but this concept is still currently in its early infancy. Endoluminal surgery is growing with a variety of mechanical platforms being designed to work through a natural orifice. Digital platforms equip these mechanical instruments with the capacity to improve a surgeon's operative precision inside organs and near critical anatomic targets.

Patient Side Robotic Design: Integrated Versus Modular

The design of how the surgical robotic arms are managed in the system is also varied, is debated by experts, and is currently in evolution. The Intuitive Surgical, Inc. platform is an integrated boom design with all the arms linked together to a patient bedside cart. Other non-single incision systems are now focusing on each arm being maintained on its own cart to allow variability of arms used based upon the specific case (TransEnterix, Inc., Medtronic, and CMR Surgical, Ltd.). A modular arm system could also potentially be configured to quickly access and control large body cavity spaces with more separate (i.e., modular) arms than the more conventional single boom-mounted approach. However, this modular approach does require more software for the robotic device to recognize each of the other arms (especially in relation to one another) because they are no longer physically linked.

Some companies are taking the modular design to the hand itself by developing laparoscopic handheld instruments which have robotically driven movements (Human Xtensions). This approach eliminates a separate remote (from the patient's bedside) surgeon-based console/ interface because the surgeon remains at the bedside; an additional benefit is that such a system reduces cost dramatically. However, some experts believe the lower cost may not offset the advantages gained from more complex emerging robotic systems.

Table-mounted arm systems are also being developed, and this allows the bed and the robotic arms to be a singular unit. Table systems are even more physically integrated than boom-mounted systems which could reduce clutter in the operative field and operating theater. These systems include systems being designed by Verb Surgical, Inc. and Virtual Incision Corporation. As robotic systems increase in complexity, it is likely that we will see particular robots designed for very specific applications.

Robotic Instrument Size (Diameter)

Robotic instrument size and corresponding port diameter are variable. Multiport systems often use 12 mm, 8 mm, and 5 mm instruments depending upon the complexity of the instrument and its function. Some 3 mm diameter. instruments have been developed as well though none are currently available with articulating wrists. The drive to single-port robotics and endoluminal platforms will likely result in smaller effector arms because, intuitively, smaller single-access systems require smaller instruments to fit inside the single-access systems.

Cost

Cost is often a point of contention when discussing robotic surgery. Over the years, experts have varied in their prediction about how cost will change as more competitive systems emerge. The majority of experts believe the costs of the robotic systems will fall over the next decade. Many have said the capital costs will be absorbed into the procedure costs of each case. Different models of cost sharing between the hospitals and companies are being proposed and used [12].

Autonomy

Autonomy of robotic systems is a complex topic. The spectrum of autonomy ranges from surgical robots functioning as pure master slave interfaces (with little to no machine-based decision assist) to the extreme opposite, with the hope and promise of completely autonomous artificial intelligence-driven surgical robots capable of completing an entire surgical task, start to finish, with minimal human supervision and input. Fully autonomous systems will likely take decades to mature. There is ongoing research in this area, including by companies such as Activ Surgical, Inc. Autonomous surgical tasks, in specific settings, have been proven to be feasible. Recently, this has been reported in a study highlighting the ability of the Smart Tissue Autonomous Robot (STAR), in which an in vivo intestinal anastomosis was created [13]. Robotic surgical systems offer wide opportunities for data integration and analytics, perhaps more so than laparoscopy. As the field moves toward an integrated digital surgery, variability in procedures will be reduced, and artificial intelligence for surgical field guidance (i.e., no-fly zones during surgery to protect vital structures) is expected to emerge [9, 14]. Using predictive technology may be a substitution to haptic feedback; in addition to the concept of no-fly zones, there is research centered upon visual or auditory cues to help surgeons gauge force (visual force feedback) [10].

Redefining Telesurgery

Although the initial ideal of remote surgery using robotic systems was not widely adopted with the introduction of robotic surgical systems, advances in communication technology may usher in a new era of remote applications. This may include remote proctoring, expert assistance, and real-time intraoperative consultation [12].

Conclusions

Next-generation robotic platforms with new technology are emerging at unprecedented rates. Such surgical innovation has opened an immense array of possibilities for the future of robotic surgery. These advancements will not only continue to increase the applicability of surgical robots but will also allow translate points of access from the requirement for multiple incisions, to smaller incisions, to single incisions with a single-port platform, and even to no incisions with endoluminal designs. Finally, with the development of artificial intelligence and virtual reality technology, autonomous surgery and remote proctoring are on the horizon.

References

1. Kwoh YS, Hou J, Jonckheere EA, Hayati S. A robot with improved absolute positioning accuracy for CT guided stereotactic brain surgery. IEEE Trans Biomed Eng. 1988;35(2):153–60.
2. Schleer P, Drobinsky S, de la Fuente M, Radermacher K. Toward versatile cooperative surgical robotics: a review and future challenges. Int J Comput Assist Radiol Surg. 2019;14(10):1673–86.
3. Leal Ghezzi T, Campos CO. 30 Years of robotic surgery. World J Surg. 2016;40(10):2550–7.
4. Hockstein NG, Gourin CG, Faust RA, Terris DJ. A history of robots: from science fiction to surgical robotics. J Robot Surg. 2007;1(2):113–8.
5. Intuitive Surgical I. Annual report 2018. 2018. Available from: http://www.annualreports.com/HostedData/AnnualReports/PDF/NASDAQ_ISRG_2018.pdf.
6. Smith R. Robotic surgery: the future is already here. 2019. Available from: https://www.linkedin.com/pulse/robotic-surgery-future-already-here-roger-smith.
7. Medtronic. Robotic-assisted surgery (RAS) analyst. Updated 2019. Updated 24 Sept 2019. Available from: http://investorrelations.medtronic.com/static-files/75f6cb56-5c12-440f-8e1a-1cc7bc6182e1.
8. Namdarian B, Dasgupta P. What robot for tomorrow and what improvement can we expect? Curr Opin Urol. 2018;28(2):143–52.
9. Gosrisirikul C, Don Chang K, Raheem AA, Rha KH. New era of robotic surgical systems. Asian J Endosc Surg. 2018;11(4):291–9.
10. Brodie A, Vasdev N. The future of robotic surgery. Ann R Coll Surg Engl. 2018;100(Suppl 7):4–13.
11. Peters BS, Armijo PR, Krause C, Choudhury SA, Oleynikov D. Review of emerging surgical robotic technology. Surg Endosc. 2018;32(4):1636–55.
12. Aruni G, Amit G, Dasgupta P. New surgical robots on the horizon and the potential role of artificial intelligence. Investig Clin Urol. 2018;59(4):221–2.
13. Leonard S, Wu KL, Kim Y, Krieger A, Kim PC. Smart tissue anastomosis robot (STAR): a vision-guided robotics system for laparoscopic suturing. IEEE Trans Biomed Eng. 2014;61(4):1305–17.
14. Marecik S, Kochar K, Park JJ. Current status and future of robotic colorectal surgery. Dis Colon Rectum. 2019;62(9):1025–7.

31 Artificial Intelligence and Computer Vision

Sam Atallah

Introduction

Vision. It is one of the most important aspects of human cognition. The evolution of visual systems in living organisms is so important that it is believed to have led to a relative sudden diversity in the types of species on Earth some 540 million years ago [1]. Nearly one-half of the human brain, and the brain of most primates, is dedicated to visual processing, enabling the ability to see and interact with the environment. As humans, vision-based perception of our surroundings and our ability to interpret our surroundings occur effortlessly.

Although vision is instinctive for us, it is a very complex challenge for machines. While computer vision and human vision are fundamentally different, there are important aspects of cerebral processing of visual stimuli that are the basis for modern computer vision. Therefore, we must first understand the process of animal vision. One key study was performed in the late 1950s by Hubel and Wiesel et al. [2], where electrophysiology was used to study visual perception in cats. In this animal model, they studied which visual stimuli would cause neurons to be activated in the primary visual cortex. Importantly, the experimentation showed that simple images of *oriented edges* provided this neuronal activation, and it appeared that visual perception "begins" with *an interpretation of these object borders and oriented edges* [2].

In 1963, Larry Roberts published a thesis that would represent one of the original insights into computer vision, essentially using the idea of defining geometric shapes by defining the shape edges [3]. In the 1970s, David Marr built upon the foundation of Hubel and Wiesel, intuitively suggesting that an image can be broken down in to a "primal sketch" – meaning an image could be deconstructed into its key boundaries, edges, and borders first in order to render an actual 3D representation of the visual field [4].

In the 1970s, however, computer speed, computer power, and graphic image rendering capabilities were extremely poor compared to today's standard, making the creation of computer vision impractical and much more theoretical. Approaches utilizing *pictorial structures* [5] and *generalized cylinders* [6] were two approaches to deconstructing imagery into simpler parts or geometric features. For example, the image of a truck can be deconstructed into circles to represent wheels and rectangles to represent the carriage. Thus, complex objects and images are *simplified into geometric primitive parts,* and the distance between those parts and the relation to one another is what allows a machine to classify an image.

S. Atallah (✉)
University of Central Florida, College of Medicine, Orlando, FL, USA
e-mail: atallah@post.harvard.edu

S. Atallah (ed.), *Digital Surgery*, https://doi.org/10.1007/978-3-030-49100-0_31

Such approaches that decompose images into their primitive parts continued into the 1980s [7].

With limited computer power, and in the era predating the Internet, digital cameras, and image acquisition and storage, computer vision was quite limited and was not suitable for real-world utilization. Notwithstanding, research into computer vision continued, and in the late 1990s, the idea of deconstructing a scene or image into "parts that go together" was explored [8]. Here, a computer would group parts of an image that go together in the same way a human would place similar pieces of a large jigsaw puzzle together, even if the image of the puzzle is unknown. In this analogy, a person may group like pieces together knowing only that they look similar, but not knowing what the actual picture will end up being. Instead of jigsaw puzzle pieces, however, computers use pixels, placing likewise pixels *together* in an image, in a process termed *image segmentation* [8].

Today, we know that even complex and unique digital images – such as the human face – can be recognized by fascial recognition software, and this is quite commonplace in many airport security facilities, smartphones (e.g., iPhone X and later), and a variety of social media platforms (e.g., Facebook). But before there could be *individual* fascial recognition, there had to be the development of computers to simply recognize the human face. In 2001, real-time face detection technology was introduced [9], and by the mid-2000s, the first digital cameras to include human face recognition (often appearing as a neon green square outlining human face(s) seen on the camera's view finder) were made available.

Around the time (general) face detection was developed, the concept of using *image features* as the definable characteristic of an image was advocated in use with computer vision. What this meant was that *any object can be decomposed into smaller features*. For example, a face is made up of features – including eyes, a nose, lips, ears, jaw, and so on. The idea of decomposing an image into its root features is that it makes it much easier for machines to recognize objects when they appear in different vantage points and positions relative to the camera angle. This allows machines to "see" and track the smaller aspects of an object and thus recognize that object when the viewpoint (for example) is changed [10]. Further advancements came in 2006 with the development of spatial pyramid matching [11], which essentially allows computers to determine what scene any given picture represents by its given feature. For example, if a feature of a scene is identified as the sun, then this would clue the machine to look for the surrounding as probably being the sky. In a similar fashion, the *histogram of gradients* (HoG) [12] and the *deformable part model* [13] were used to help machines recognize the human form.

As computer power increased in the mid-2000s and as the volume and quality of digital images on the Internet increased, large-scale image analysis became achievable, and the ability for computer scientists to assess various algorithms in real-world environments became more practical. Thus, projects such as the *PASCAL visual object challenge* with 20 image classes and 10,000 images per category were used to train machines to recognize various objects, with accuracy gradually improving to approximately 40% by 2010 [14–17]. This was followed by a more ambitious project called *Imagenet* [18]. The objective was to categorize most (22,000) objects using 14 million images.

Initial accuracy for image classification with Imagenet revealed 28% of images were incorrectly classified, but this improved dramatically in 2012, when the classification error rate dropped to 16.4%. This was a major milestone for computer vision. This was the year convolutional neural networks (ConvNets) were first applied to Imagenet demonstrating significant accuracy. By 2015, the use of ConvNets for image classification had become the standard for computer vision; it was further modified, and the accuracy improved to an error rate of just 3.57%, which is less than the recorded error rate of humans (5.1%) for the same dataset. The seminal work by Krizhevsky et al. in 2012 [19] applying ConvNets to image recognition was based on ideas proposed by Lecun et al. in 1998 [20], and the methodologies mirror one another quite closely.

By 2020, most of the data exchanged and bandwidth along the Internet have become image and video based, and the volume of image-based data has been increasing at a dramatic rate. As an example, in the 10 seconds it takes for you to read this sentence, an additional 50 hours of video will have been uploaded to YouTube. It is content like this that can be fed into machines to provide training sets important for machine learning and computer vision.

Machine Learning

Machine learning represents an important branch of artificial intelligence and can be used for *classification* (such as image classification) and *prediction* (especially with an ability to make predictions based on multidimensional data). Machine learning can be either (a) ***statistical learning,*** which consists of *natural language processing* and *speech recognition,* or (b) ***deep learning.*** *Convolutional neural networks* (ConvNets) used in modern computer vision utilize deep learning, which, as we shall see, consists of several layers or stacks. *The deeper the stack, the more sophisticated the ConvNet.* Machine learning can also be of differing categories: (1) *supervised learning,* (2) *unsupervised learning,* and (3) *reinforcement learning* (Fig. 31.1). In *supervised learning,* a machine is trained on a dataset that contains the answer or solution. For example, in surgery, imagine we would train the computer recognize various anatomic targets by teaching the computer (i.e., pointing to the target and telling it this is the liver, for example). With *unsupervised learning,* the computer must figure out the solution or determine the image classification on its own. With *reinforcement learning,* the computer is given a goal (such as winning a game), programmed to follow specific rules, and then allowed to operate and improve over iterations, by trial and error. In other words, the computer learns from its mistakes.

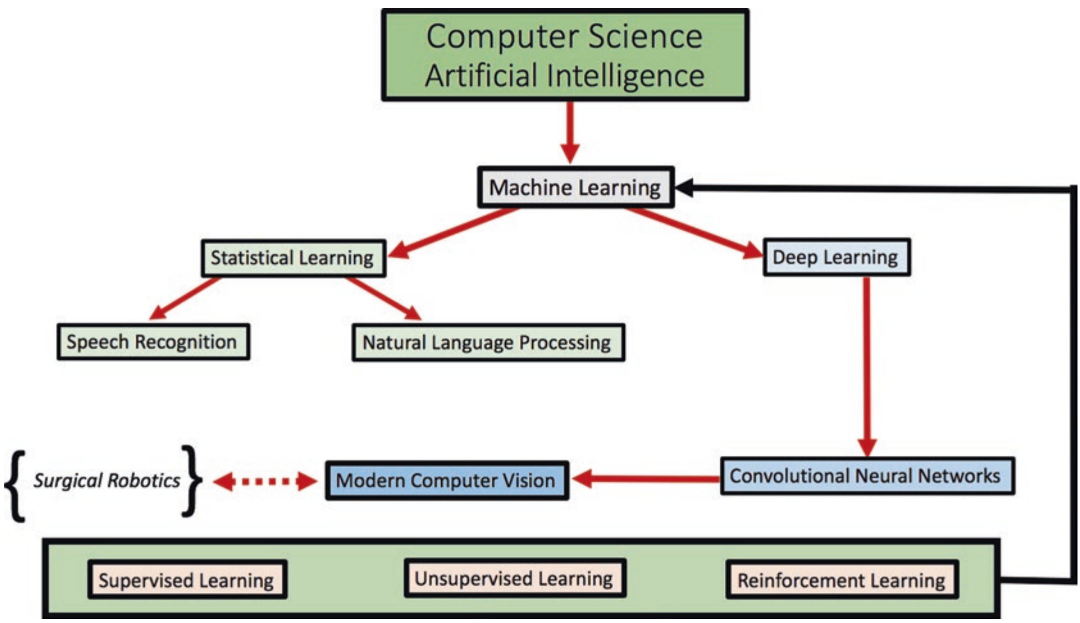

Fig. 31.1 A schematic representation of artificial intelligence is shown highlighting how machine learning can be divided into two categories, deep learning and statistical learning. Convolutional neural networks involve deep learning and represent an important pathway toward the advancement of computer vision over the next decade. Machine learning can also be classified based on the method utilized. There are three main categories of machine learning – supervised, unsupervised, and reinforcement learning

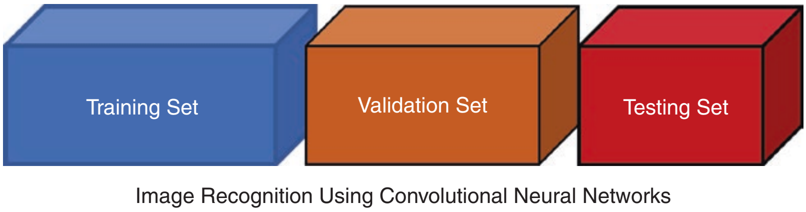

Fig. 31.2 The pathway of machine learning for computer vision is illustrated in this diagram. It is important that test images are used to assess the convolutional neural network in the example of computer vision. The validation image set allows the image classification accuracy to be established before implementation in a real-world setting

Assessment of image classification requires a *training* image set, a *validation* image set, and finally a *testing* image set (Fig. 31.2). ConvNets and the idea of image recognition are forms of unsupervised machine learning in which a computer uses known information – such as image ***features*** – to determine the ***label*** (i.e., the name) of any given object. In the surgical application, this would be an anatomical structure. The objective is to harness the capability of machine learning, possibly via a cloud interface, to help identify critical structures and operative landmarks during surgery. Ultimately, such technology could be incorporated into next-generation robotic systems.

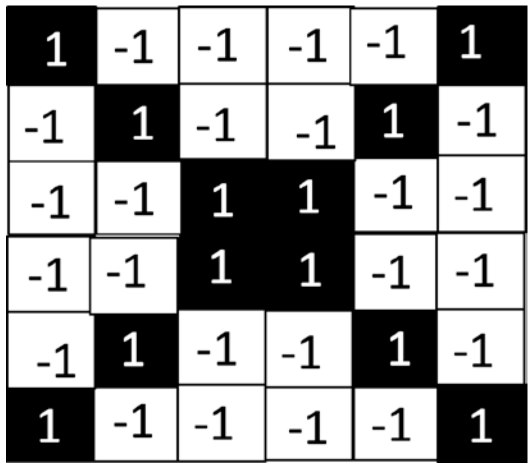

Fig. 31.3 The example image is a 6 × 6 pixel array of the capital letter X. In this simple example, pixels are either all black (+1) or all white (−1). This will be used throughout the chapter to illustrate principles of machine learning and convolutional neural networks

Understanding Convolutional Neural Networks

ConvNets are not as difficult to understand as you might think. Let's use a very simple example to illustrate how a ConvNet works to recognize an image: the capital letter "X." This can be broken down into a 2D array of pixels. Let us suppose the X is represented by an array of 6 × 6 pixels (Fig. 31.3). The pixel array then can be decomposed such that each pixel is represented quantitatively and given a value, which, because we have chosen a simple example, can be represented as one of two values, +1 for any pixel that appears black and −1 for any pixel that is white in the array. Now, the objective here is to have a computer determine what it is that it is looking at (the letter X) regardless of variances that can occur, such as with different handwriting. In other words, we need a computer to not just be able to recognize a "textbook" version of the letter X; we need it to recognize variant forms. In surgery, for example, we would want computer vision to recognize critical structures such as the common bile duct, or ureter, despite variances from the examples provided to machines during the training phase. Remember, computers are very literal. This means that if we were to train them to recognize the letter X, or any image, and then show the machine that exact image, they will recognize it, but if it is only slightly changed, without deep learning algorithms, they will not.

ConvNets are used to help computers recognize structures and objects despite variations by breaking down images into smaller features. In our example of the letter X, the pixels can be broken down into four diagonal lines, two of them up slanted and two of them down slanted, with a central point of intersection. So, in this example, let us define each diagonal line as the specific feature for

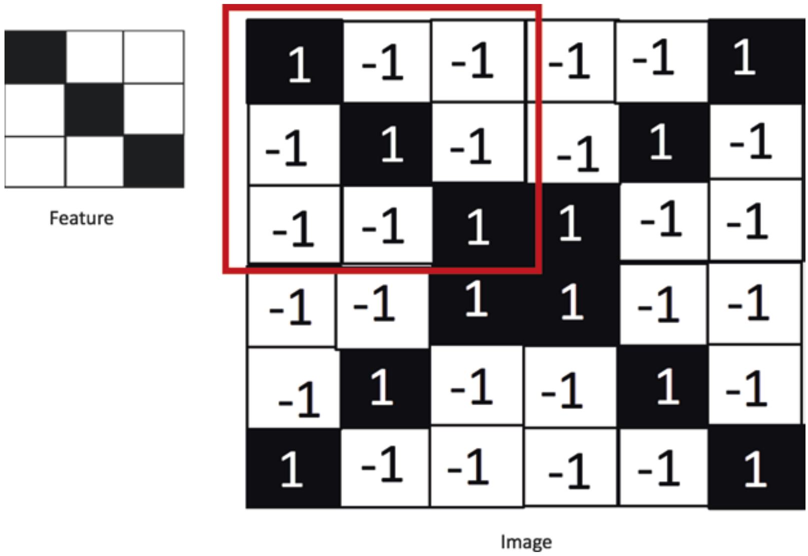

Fig. 31.4 All images can be decomposed into their smaller parts, called features. Here, we have identified one of two features that make up the letter X, namely, the downward slanted diagonal line shown and highlighted with the red square. This same feature appears in two places in the 6 × 6 pixel array

this image (Fig. 31.4), and since two of the diagonal lines are the same, the X is composed of only two features. We could have defined the cross point of the X as a feature, but for simplicity's sake, we have limited the "X" to just two features (an up slant (/) and a down slant (\) line).

The first step in a ConvNet occurs when known features are compared to the image at hand. In our example, a 3 × 3 feature (data known from a given training set) is compared against the image of the "X" to see if it fits and how well it fits into the image – a process called *filtering*. Think of it as being a way a computer can tell how well a given feature matches a given image (where the feature is known, but the image being analyzed is not known to the computer). *The act of trying to fit and assessing the closeness of match in every possible part of the image defines a* ***convolution,*** often denoted with the symbol ⊗. Figure 31.5 demonstrates the act of convolution as would be performed by a computer. Although the computer calculates values for each of the 3 × 3 pixel arrays to mathematically determine the similarity or difference between a known feature and the image of the "X," it is analogous to how humans would look at a puzzle and ask to themselves, "Does the puzzle piece fit here … or there?" while trying every possible position in a jigsaw puzzle.

A computer does not see like you and I do, so it has to turn pixels into numbers representing pixel color shade and brightness. It multiplies together the pixels and then divides by the total pixels in a given frame. Here, our feature is a 3 × 3 pixel array, and the objective is to compare the pixels. Let's consider a pattern in which a test image *nearly* matches the feature – differing by only a single pixel (Fig. 31.6).

Mathematically, this can be represented as:

$$\begin{array}{ccc} +1 & -1 & -1 \\ -1 & +1 & -1 \\ -1 & -1 & +1 \end{array} \qquad \begin{array}{ccc} +1 & +1 & -1 \\ -1 & +1 & -1 \\ -1 & -1 & +1 \end{array}$$

Now multiplying corresponding pixels from the known feature versus the image, we can compute the similarity:

$$\frac{(1\times 1)+(-1\times 1)+(-1\times -1)+(-1\times -1)+(1\times 1)+(-1\times -1)+(-1\times -1)+(-1\times -1)+(1\times 1)}{9}$$

$$\frac{1+-1+1+1+1+1+1+1+1}{9}$$

$$\frac{8}{9}=.89$$

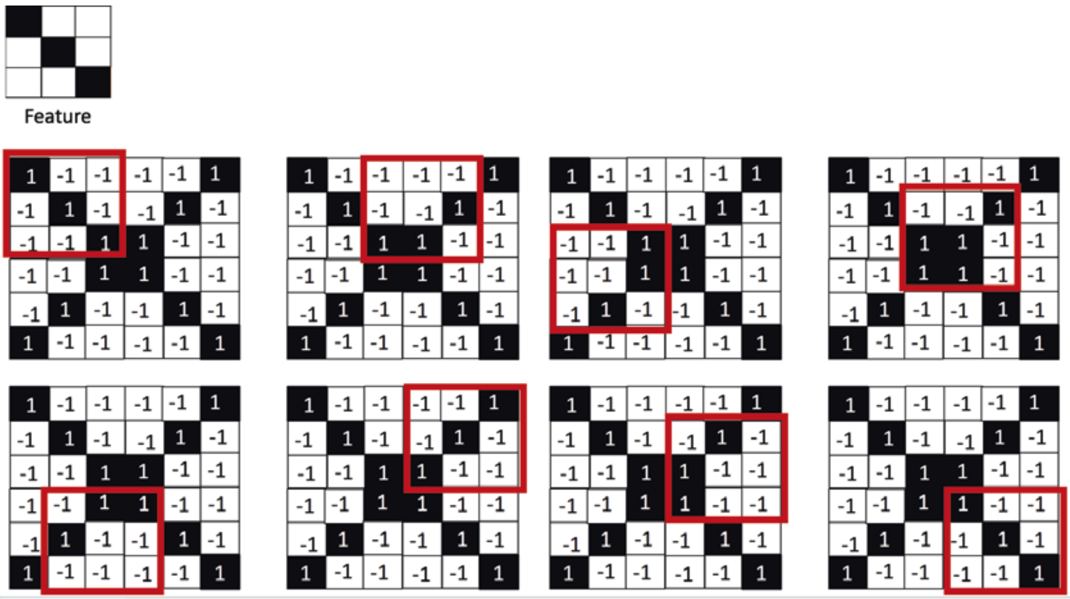

Fig. 31.5 The main principle of a convolutional neural network is shown. Here, the computer systematically tries to place the feature in every possible position in the image (red squares) looking for the best match (the process of filtering). This is just as a human might try to place the piece of a jigsaw puzzle in every possible place until a best fit is found. The act of trying every possible position in an image in order to find the best fit for a given feature is called *convolution* and is often represented by the symbol ⊗. Thus, convolution is just a way for the computer to find the best match for known features

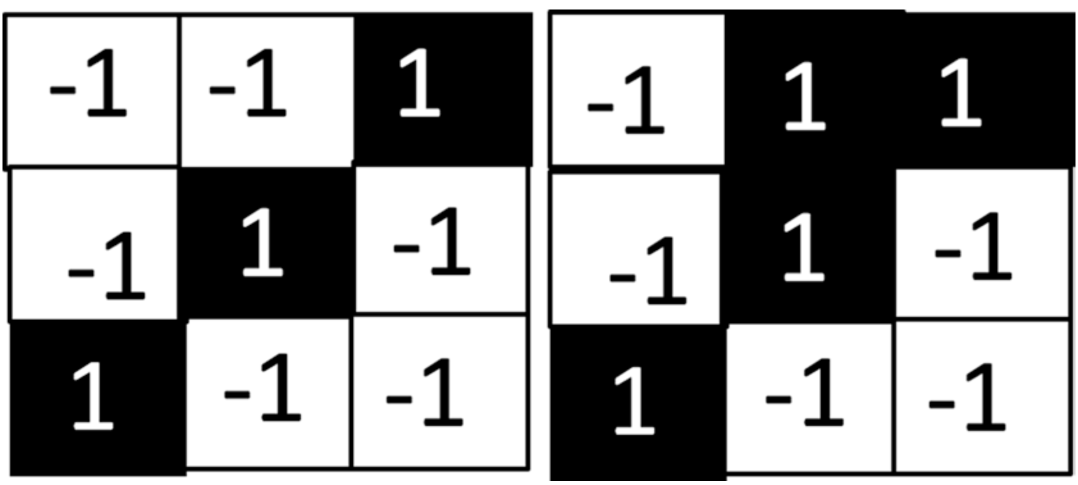

Fig. 31.6 ConvNets are not trying to teach computers to recognize exact matches but rather to recognize images that are *inexact* so that if they are close and similar enough, they will be classified in the same category. Here, a known feature (left) is shown next to a test image (right). The 3 × 3 pixel arrays differ by a single black pixel instead of a white pixel. Mathematical models can predict this variance and ultimately determine whether the training and test image are similar enough to be categorized as the same

In a sense, the two figures can be thought of as being 89% similar, as they differ by only one pixel. More generally, for any feature array (x_a, y_a), the similarity with the image array (x_b, y_b):

$$\begin{matrix} a_1 & a_2 & a_3 \\ a_4 & a_5 & a_6 \\ a_7 & a_8 & a_9 \end{matrix} \qquad \begin{matrix} b_1 & b_2 & b_3 \\ b_4 & b_5 & b_6 \\ b_7 & b_8 & b_9 \end{matrix}$$

Sigma notation can be used to express the product of any two pixel matrices as follows:

$$\sum_{x=1}^{n}\sum_{y=1}^{n}\left(a_{x,y} \times b_{x,y}\right)$$

Now the sum of the products can be divided by the number of pixels in the array, n_p, as follows:

$$\frac{\sum_{x=1}^{n}\sum_{y=1}^{n}\left(a_{x,y} \times b_{x,y}\right)}{n_p}$$

This is a general equation for determining the degree of similarity (likelihood of feature match) between a training set feature and a test image.

Returning to our example of the image "X," we can perform convolutions with the *down slant* feature (\) and the *upward slant* feature (/). Using all known features and *convolving* them to every possible position in the image; looking for a best match creates convolution *layers*. That is, every feature outputs a "map" denoting its best match in the image. Each of these represents an additional level of information, helping the computer to mathematically "see" the overall image. So, just like physical layers, the layers can be *stacked,* and we can determine or set the number of layers, and their relative arrangement since they are modular. One important concept in ConvNets is that they work very well in a stackable arrangement, like stacking Lego pieces or even like making a sandwich, where you can decide to stack cheese on top of meat or stack tomatoes between two slices of cheese, with a slice of toast stacked in the middle, etc. *Being able to arrange the ConvNet stacks in any order we want is an important aspect of this design.*

So now, we have taken our dataset, performed one or more convolutions ⊗, and placed them into a stack. The next step is called *pooling (expressed as the symbol* ⊳), and this is very important in the process of image recognition. Pooling ⊳will do two things. First, it will dramatically reduce the overall image to a more manageable size. Second, and perhaps more importantly, *it will allow for more variability in interpreting the image.*

Pooling ⊳ entails walking across the filtered images using preset window sizes and strides, assigning a maximum value for the pixels in any given window. So let us suppose the window size is four pixels, and the highest value in the group of four pixels here is 0.95. Then that group of four pixels will be reduced to *one* pooled pixel, with a maximum value of 0.95. It does not matter where the 0.9 pixel was in the four-pixel array during pooling, *and thus this builds in a certain flexibility that is accepting of variation and thus "humanizes" computer vision and makes it less literal.* This is extremely important in allowing for the recognition of imperfections; variations due to, for example, camera angles; and other real-world obstacles to image and pattern recognition.

The next step, or layer, in the ConvNet is called *normalization,* and this is the process of normalizing filtered pixels values using rectified linear units (ReLUs, $\mathcal{R}$); the methodology of ReLUs is beyond the scope of this introductory chapter. Then, filtered and refiltered output of the ConvNet passes through a final, so-called voting phase in what is known as the *fully connected layer* (Fig. 31.7). Here, the computer must make a final decision and determine what is the image based on the analysis of the ConvNet. It lists the pixels in a linear array or vector (i.e., feature values), and then each pixel value counts toward the overall vote on labeling the object. This is because object classifiers have to select from an established set of image categories, so the end output is actually a numerical vote ranking each of the categories. The computer thus produces a weighted score of the image being the letter "X" and, for example, a weighted score that is the letter "T" and the letter "O." The votes are weighted

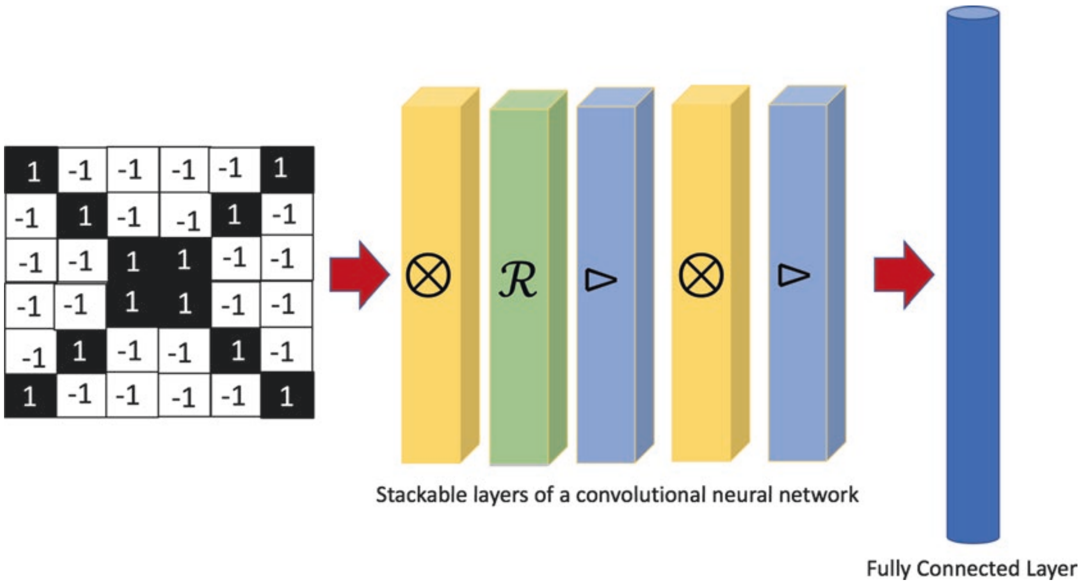

Fig. 31.7 A model of a ConvNet architecture is illustrated showing how an initial image (our familiar example of the capital letter “X”) is analyzed by first convolution ⊗, then normalization with ReLUs, $\mathcal{R}$, then pooling ▷, followed by an additional convolution layer ⊗ and an additional layer of pooling ▷before entering one of the final steps, the fully connected “voting” layer(s). An important aspect of ConvNets is the ability to arrange, or ‘stack’, these layers in multiple ways, as though arranging Lego blocks

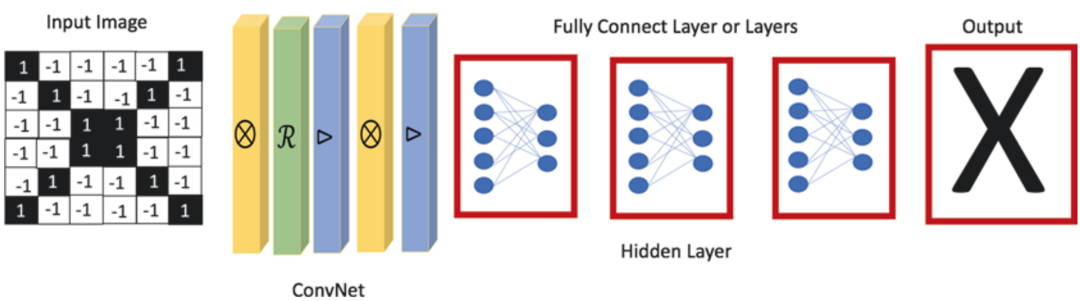

Fig. 31.8 Here, the entire ConvNet is illustrated from test image input to final computer labeling output. Note that the fully connected layers can also be stacked. This means that there are middle (hidden) layers whose output feeds the input of the next. Only the final output, in this case the label of the letter X, is provided. This is a very simplified view as usually, in computer vision, the computer assigns a score to the final label; a high score is indicative of a higher certainty that the image is correctly classified

such that those that positively predict the image carry more weight than those which do not.

Again, it is important to understand that the fully connected layer can itself be stacked, Lego-style. This means the computer can “vote,” and the output of the vote can be used for the input of the next vote. Such intermediate votes are not counted. In fact, they are not part of the final answer in the image recognition. Therefore, they are often termed *hidden layers* (Fig. 31.8).

Hyperparameters

Hyperparameters allow computer engineers to control various settings within the neural network. It is *not* something learned by the computer but rather parameters that are set with *full user control.* Examples include setting feature specifics, such as the number and pixel size of features. For example, a feature could be *the human eye* – or the user can include multiple features within this – such as the eyelid, the iris, eyebrow, and sclera. The pooling ⊳window size and stride can also be set by the user, and parameters within a fully connected network can also be modified. So then, hyperparameters are like having manual control over the system, allowing a computer scientist to architect and experiment with different settings by toggling though various parameters in the ConvNet.

Loss Functions

In computer vision, it is important to represent the error rate. More expressly, we need to know the times we asked the computer to label an object, and the computer got it wrong. This is essentially called a loss score or *loss function* L_i. The loss function L_i, where in the example (x_i, y_i),where x_i is the image (pixel array), y_i is the integer label (i.e., the item or object we want our computer to be able to predict), often expressed as:

$$\{(x_i, y_i)\} \lim_{i=1} N$$

With image score, $s = f(x_i, W)$, where W is the *weight* or parameter assigned to the image (parametric approach, summarizing all of the information derived from the training data), then:

$$L_i = \sum_{j \neq y_i} \max\left(0, s_j - s_{y_i} + 1\right)$$

What is this equation telling us? This means that when the computer correctly classifies an object and the nearest score(s) is at a safety margin of +1 or more, then the loss incurred (error rate) is zero: the computer got it right. But when the computer incorrectly classifies an object, or it correctly classifies the object, but the score of another object is <1 from the score given to the correct object, then it is either too close or altogether incorrect, and a loss is incurred – the more incorrect the compute value, the higher the loss function, and the worse the computer is at recognizing objects.

To understand this, let us suppose three training examples on three different classes of objects. We will use clinical images as shown in Fig. 31.9. Here, the computer must be able to identify a *hook cautery,* the *pancreas,* and the *ileocecal*

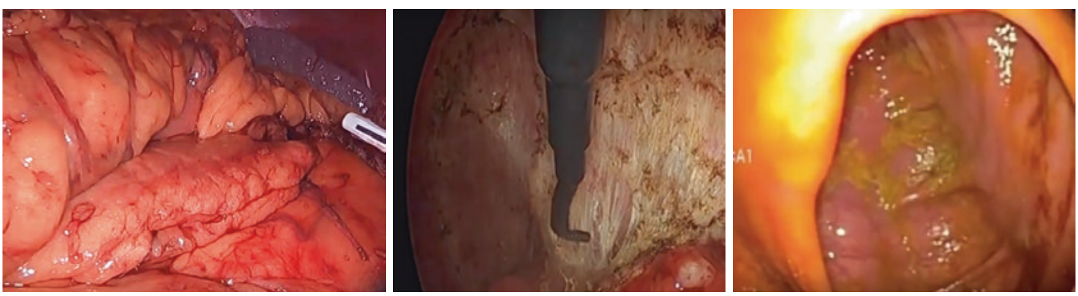

Image Classifiled As (highest score)	Score - image of pancreas shown	Score - image of hook cautery shown	Image of ileocecal Valve shown
Pancreas	5.6	4.0	**5.3**
Hook Cautery	-2.3	**10.8**	-4.6
Ileocecal Valve	**8.1**	2.3	2.3
Loss Function	***3.5***	***0***	***4.0***

Fig. 31.9 The test images are shown from real-world surgical case videos. The computer is challenged to classify each of the items. Usually, the output is represented as a numerical score: the higher the score, the more likely the image is correctly classified. In this hypothetical example, only the hook cautery was correctly classified. Incorrect classifications represent a loss function (error rate) and must be assessed. Here, the loss values for each of the image categories are computed (refer to text)

valve from real-world scenes. Hypothetical output scores are displayed in the image, and the highest score represents the computer's final decision on the image classification. You can see in this example that the hook cautery was correctly identified, but the ileocecal valve and pancreas were incorrectly identified. Let us use the above formula to calculate the loss for each of these. For the *pancreas image*, the ileocecal valve had the higher score of 8.1; the pancreas score was greater than the score for the hook cautery with more than a +1 margin, so the loss between those two objects is 0, but the loss between the pancreas (5.6) and ileocecal valve (8.1) is the absolute difference between the two, plus one: or $|(5.6 - 8.1)| + 1 = 3.5$. Similarly, the loss function L_i for the *ileocecal valve image* is 4.0. The computer correctly classified the hook cautery, and both other objects in the training set (pancreas and ileocecal valve) had scores of > +1 from the hook cautery score, so the loss L_i for this training sample is zero.

We can determine the *total* loss function for the training set provided. It is the summation of the losses divided by the N number of image categories:

$$\frac{(3.5+0+4.0)}{3} = 2.5$$

More generally, this can be expressed as follows:

$$L = \frac{1}{N}\sum_{i=1}^{N} L_i$$

Finally, data loss should include a *regularization term* which prevents the model from becoming overly complex; it is based on the axiom that a simpler approach is usually a better approach than one that is serpiginous. The full expression can be written as:

$$L(W) = \frac{1}{N}\sum_{i=1}^{N} L_i\left(f\left(x_i, W\right), y_i\right) + \lambda R(W)$$

For the score function for a dataset (x, y), $s = f(x; W) \rightarrow Wx$ (which is effectively a linear classifier). Here, the term $\lambda R(W)$ has been added and denotes a regularization factor for the model. For our purposes, the value of the constant is not important and is far beyond the scope of this chapter.

Nevertheless, the error signal (difference between *actual* answer and the *right* answer) is used in *backpropagation,* whereby the network automatically adjusts and learns from its error, thus adjusting aspects in the network such as voting weights. Gradient descent is the process of making small changes in ConvNet parameters so as to minimize error and maximize correct image identification.

References

1. Parker A. In the blink of an eye: how vision sparked the big bang of evolution. Cambridge, MA: Perseus Publishing; 2003.
2. Hubel DH, Wiesel TN. Receptive fields of single neurones in the cat's striate cortex. J Physiol. 1959;148(3):574–91.
3. Roberts LG. Machine perception of three-dimensional solids. (Doctoral dissertation, Massachusetts Institute of Technology) 1963.
4. Marr D, Poggio T. A computational theory of human stereo vision. Proc R Soc Lond B Biol Sci. 1979;204(1156):301–28.
5. Fischler MA, Elschlager RA. The representation and matching of pictorial structures. IEEE Trans Comput. 1973;100(1):67–92.
6. Brooks RA, Creiner R, Binford TO. The ACRONYM model-based vision system. In: Proceedings of the 6th international joint conference on artificial intelligence – volume 1, 20 Aug 1979 (pp. 105–113).
7. Lowe DG. Three-dimensional object recognition from single two-dimensional images. Artif Intell. 1987;31(3):355–95.
8. Shi J, Malik J. Normalized cuts and image segmentation. IEEE Trans Pattern Anal Mach Intell. 2000;22(8):888–905.
9. Viola P, Jones M. Rapid object detection using a boosted cascade of simple features. In: Proceedings of the 2001 IEEE computer society conference on computer vision and pattern recognition. CVPR 2001, 8 Dec 2001 (Vol. 1, p. I). IEEE.
10. Lowe DG. Object recognition from local scale-invariant features. In: Proceedings of the seventh IEEE international conference on computer vision, 20 Sep 1999 (Vol. 2, pp. 1150–57). IEEE.
11. Lazebnik S, Schmid C, Ponce J. Beyond bags of features: Spatial pyramid matching for recognizing natural scene categories. In: 2006 IEEE Computer Society Conference on Computer Vision and Pattern

Recognition (CVPR'06), 17 June 2006 (Vol. 2, pp. 2169–78).
12. Dalal N, Triggs B. Histograms of oriented gradients for human detection. In: 2005 IEEE computer society conference on computer vision and pattern recognition (CVPR'05), 25 Jun 2005 (Vol. 1, pp. 886–93). IEEE.
13. Felzenszwalb P, McAllester D, Ramanan D. A discriminatively trained, multiscale, deformable part model. In: 2008 IEEE Conference on Computer Vision and Pattern Recognition, 23 Jun 2008 (pp. 1–8). IEEE.
14. Everingham M, Van Gool L, Williams CK, Winn J, Zisserman A. The pascal visual object classes (voc) challenge. Int J Comput Vis. 2010;88(2):303–38.
15. Everingham M, Van Gool L, Williams CK, Winn J, Zisserman A. The PASCAL visual object classes challenge 2007 (VOC2007) results.
16. Everingham M, Zisserman A, Williams CK, Van Gool L, Allan M, Bishop CM, Chapelle O, Dalal N, Deselaers T, Dorkó G, Duffner S. The 2005 pascal visual object classes challenge. In: Machine Learning Challenges Workshop, 11 Apr 2005 (pp. 117–76). Springer, Berlin, Heidelberg.
17. Everingham M, Eslami SA, Van Gool L, Williams CK, Winn J, Zisserman A. The pascal visual object classes challenge: a retrospective. Int J Comput Vis. 2015;111(1):98–136.
18. Russakovsky O, Deng J, Su H, Krause J, Satheesh S, Ma S, Huang Z, Karpathy A, Khosla A, Bernstein M, Berg AC. Imagenet large scale visual recognition challenge. Int J Comput Vis. 2015;115(3):211–52.
19. Krizhevsky A, Sutskever I, Hinton GE. Imagenet classification with deep convolutional neural networks. In: Advances in neural information processing systems, 2012. (pp. 1097–105).
20. LeCun Y, Bottou L, Bengio Y, Haffner P. Gradient-based learning applied to document recognition. Proc IEEE. 1998;86(11):2278–324.

32 The Future of Surgery

Rebecca A. Fisher, Suewan Kim,
and Prokar Dasgupta

Introduction

It is impossible to predict exactly what the future holds for a field as dynamic as surgery. With hindsight, it seems it has often been the most unexpected advances that have changed the face of surgery, such as the discovery of the role of *Helicobacter pylori* in gastric cancer. In this chapter, we will outline some themes we feel may impact the future of surgery in the next 50 years. To minimize our own embarrassment when rereading this in the future, we have chosen a group of themes that we think are likely to be sources of significant advances in surgery but are currently limited by advancement of technology, most of which are currently in early stages of use. As the Topol Review in the United Kingdom summarized in 2019, the changes we discuss will require significant investment in people as well as technology, including a focus on development of technology [1].

We will begin with advances in biomedical sciences that will change our ability to treat patients at a cellular level using genomics and regenerative medicine. We will then discuss technology used to teach surgeons and patients such as virtual reality, augmented reality and three-dimensional (3D) printing technologies. Finally, we discuss challenges we expect to see in an evolving world of digital surgery, such as issues with data protection and medical ethics.

R. A. Fisher (✉) · S. Kim · P. Dasgupta
MRC Centre for Transplantation, King's College London, London, UK
e-mail: Rebecca.r.fisher@kcl.ac.uk

Genomics

An increasingly prominent theme in the future is likely to be the use of genomics in routine practice. The widest use of genetic testing at present is in rare diseases and cancers, for example, BRCA genes in breast and ovarian cancer and patients with multiple endocrine neoplasia.

In the United Kingdom, the 100,000 Genome Project has been ongoing since 2012. Access to National Health Service data means the whole genomes that are sequenced can be coupled with patients' medical records. In December 2018, 100,000 whole genomes had been sequenced [2]. The aim of the project is to improve our understanding of the genome at an individual and a population level and presents a challenge for the future as to how we harness this so-called big data to identify genetic sequences that are diagnostically or prognostically useful [3]. Large projects such as this are also contributing to an improvement in technology that is making genetic testing cheaper and faster, and therefore accessible to more patients.

As this access becomes wider, we may see genomics becoming a more routine part of multidisciplinary team decisions, allowing tailored genetic approaches to patients with known

S. Atallah (ed.), *Digital Surgery*, https://doi.org/10.1007/978-3-030-49100-0_32

conditions (i.e., personalized medicine). We may also see an increase in preventative surgery for patients at risk of familial cancers, such as the current approach to offer prophylactic mastectomies to patients with germ line BRCA mutations.

Another aspect of genetic testing we may see more in the future is testing for cancer through 'liquid biopsies' via peripheral blood sampling, where blood tests capture cell-free tumour DNA or RNA that is released into the bloodstream [4, 5]. This could reduce the need for invasive biopsies and their associated morbidity – as well as the costly healthcare burden for patients, physicians, and hospital systems.

Regenerative Medicine

Another area that focuses on advances at a cellular level is regenerative medicine. This field focuses on healing, replacing, or regenerating tissues that have impaired function due to age, congenital defects, diseases, and trauma [6]. It involves technologies such as tissue engineering and entails the use of therapeutic stem cells and gene therapy.

One method to regenerate tissue is to stimulate tissues to heal themselves with implantation of a synthetic substance such as bioactive glass. Examples include Bioglass, a material with osteogenic properties [7]. Bonalive® is an example of bioactive glass that is currently being used for trauma, osteomyelitis, spine surgery, and mastoid surgery. This serves to stimulate bone formation whilst preventing bacterial growth [8, 9].

When the body cannot heal itself, there are now increasing options to grow tissues in vitro and implant them to restore function. There are a multitude of therapies currently available clinically, with the main products aiming for cartilage or skin repair [10]. Cartilage has thus far been the leading tissue in this technology because cartilage does not have its own vascular infrastructure, which has always been a challenge to create in vitro. An example is Carticel®, which is composed of autologous cultured chondrocytes. These are harvested products from a patient's own femoral cartilage which is then cultured in vitro before being replaced into the site of the defect. Carticel® has been clinically available for some time and was the first cell therapy to be approved by the United States Food and Drug Administration (FDA) in 1997. It is used for symptomatic cartilage defects of the femoral condyle following acute or repetitive trauma [11]. However, although pre-existing therapies focus on repair and regeneration, they cannot fully resolve injuries or diseases [12].

The holy grail of regenerative medicine is the in vitro production of genetically matched functioning human organs for transplantation. As Western populations are ageing, the demand for organ transplantation is greater than ever before, which poses a serious healthcare challenge – particularly for organs such as the heart, whereby transplants can only be donated from previously healthy deceased donors. From April 2018 to March 2019 in the United Kingdom, there were 290 patients awaiting heart transplantation whereas only 181 hearts were available, exemplifying the substantial organ shortage [13]. For transplant recipients, the allogeneic tissue presents lifelong risks of rejection and side effects of immunosuppression (i.e., graft-versus-host disease).

Three of the methods currently in development to solve this problem include (a) fabrication of human organs in live porcine animal bodies, (b) transplantation of 'organ buds' into the patient's body that then develop viable vascularization, and (c) regeneration of organs by filling cytoskeleton scaffolds with cells [14].

Three-Dimensional Printing

Three-dimensional (3D) printing enables conversion of digital 3D models into physical objects. These objects are produced from a computer-aided design (CAD) which builds models layer by layer. There have been many applications of this technology over the past decades in a variety of fields, including orthopaedic surgery, neurosurgery, and cardiac surgery. The technology

Fig. 32.1 A selection of 3D printed prosthetic hands in different sizes made by charity e-NABLE (Photo by Jen Owen. 3D printed hands created by the e-NABLE Community. enablingthefuture.org)

allows customized prosthetics, preoperative surgical planning, and medical education [15]. Moreover, there is an emerging trend towards four-dimensional (4D) printing, where the time component is taken into account. For example, 4D models can portray the changing positions of bones with movement, allowing visualization of spatiotemporal relationship between structures [16].

One aspect of 3D printing increasingly in clinical use is customized prosthetics, to replace tissues absent due to congenital malformations, cancer, or trauma. They provide a cost-effective modality to create a unique prosthesis – particularly when needs change rapidly in patients such as growing children with prosthetic limbs (Fig. 32.1). In the future, there may be more prosthetics that expand according to growth of an individual [17]. It also presents hope for global healthcare as the inexpensive nature of these prostheses means charities such as e-NABLE are able to provide them in war zones and areas of natural disasters [18]. There has been development of 3D printed prosthesis of facial organs of sense, such as the nose, eyes, and ears. In patients involved in traumatic accidents or facial cancer, where significant proportion of the face is lost, functional and aesthetic restoration is provided. Various materials with range of different colours and mechanical properties could be used to 3D print, which is important as colour of prosthesis needs to precisely match patient skin colour so as to minimize the discrepancy, thus improving the cosmetic result [19, 20].

Solely based on 2D imaging, it may be difficult to appreciate the complexity of an individual's anatomy. With the use of 3D printing technology, surgeons can plan complex or demanding surgeries preoperatively with more accuracy [21]. This correlates with improved clinical outcomes – such as decreased operation time, decreased blood loss, and achieving negative resection margins [22]. This technology is already commonly used in maxillofacial and orthopaedic surgery, but more specialties are beginning to use it, particularly for planning procedures in areas with complex anatomy, such as patient-specific cerebral aneurysm models to practise applying clips preoperatively [23]. Models can also be sterilized to be used intraoperatively. In the future, there will potentially be a method for these models to be made more routinely – which will also allow surgeons to use them in clinic for patient education as well as for their own learning.

Virtual Reality Education

One advance in digital technology that is likely to affect the future of surgery is the availability of virtual reality technology – a platform which involves real-time interaction within a 3D computer-generated environment. This can be used for education of patients, medical students, and doctors.

In recent years, pressures have mounted on surgical training. Time is increasingly limited for training due to increasing clinical workload and reduced working hours in some countries due to legislation such as the European Working Time Directive and, in the United States, the 80-hr/week, restriction for general surgery residents imposed by the Accreditation Council of Graduate Medical Education. The surgical mantra of 'See one, Do one, Teach one' is no longer deemed appropriate, due to intensifying emphasis on patient safety and litigation in everyday practice. This means that the risks associated with a trainee's learning curve are no longer acceptable in clinical practice. As a reaction, we have seen an increase in simulation-based skills training in surgery: current trainees are very familiar with digital manikins for resuscitation simulation and box simulators for laparoscopic skills training. We expect in the future that this training will involve virtual reality simulation; as surgical training involves recognition of structures and surgical planes, it lends itself well to high-fidelity virtual reality content. Until now, virtual reality training has been limited by the expense of simulators that have high enough fidelity to be useful for clinical training. However, in the future, it is hoped this will become an affordable option for more centres [24].

Some centres, such as the virtual reality neuroanatomy lab at Stanford University, have described use of virtual reality in a clinic setting for patient education [25]. We believe that this could become more widespread as a way to explain complex pathology to patients. It is already being used increasingly at medical schools to help students visualize 3D anatomy, which is expected to become a standard part of teaching as this technology becomes more affordable.

Augmented Reality

Augmented reality is different from virtual reality as it connects the real, physical environment with the digital world. It does this by superimposing virtual computer-generated imagery on top of real images. A popular example of this technology is the game Pokémon Go, the mobile game that went viral in 2016. Advanced forms of augmented reality are also known as *mixed reality*, which usually means there is a larger element of interaction between the overlaid images and objects in the real world.

In a surgical setting, most applications of augmented reality technology involve adding information to the clinician's visual field. This can include patient-related information such as scan images or images derived from sensors intraoperatively. An example of the latter is AccuVein (AccuVein Inc., NY, USA), a device that projects live images of veins onto the skin surface to help clinicians locate them for venepuncture and cannulation (Fig. 32.2). In surgery, many technologies being developed overlay preoperative imaging onto live video, for example to estimate the location of an anatomical structure during minimally invasive surgery. At present, this is limited by the capability of current computers, as it requires the ability to anchor the virtual images to real-life structures, with accurate rendering and minimal lag. It is anticipated that future technology will allow accurate live application of patient scan data, meaning surgeons will be able to see locations of tumours and key structures intraoperatively in routine practice [27].

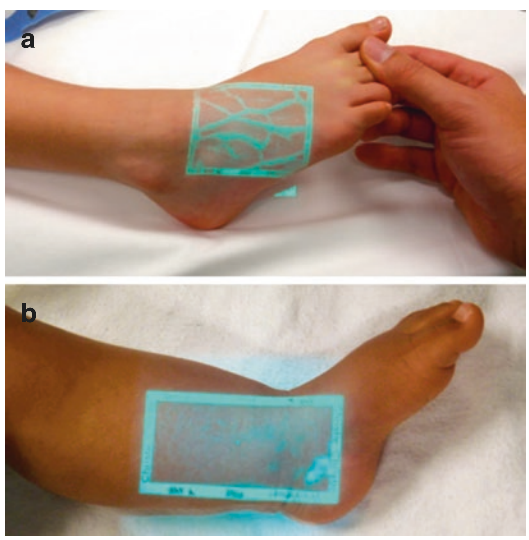

Fig. 32.2 Use of AccuVein in clinical practice. (From Pirotte [26]. Reprinted with permission)

Telementoring

One aspect of surgery that is likely to develop dramatically in the future is the routine use of telementoring. Telementoring in surgery usually involves geographically separated surgeons communicating via an internet connection to learn from one another. Although there are a vast number of applications for telemedicine, such as in an outpatient setting, there are important challenges for intraoperative telementoring [28]. Many technologies used thus far for telementoring have either struggled due to variable internet connection stability or required a dedicated internet connection as was often set up for pioneering cases in telesurgery [29]. There has been significant excitement around the potential of 5G internet in this field [30], with other companies striving to offer reliable telementoring on slower native wireless connections (for example the telementoring company Proximie (Proximie Ltd., London, UK)) [31, 32]. 5G tactile internet will enable recognition of haptic movements, allowing accurate, real-time information of a surgeon's precise movements to be known and recorded. In addition, 5G tactile networks will aid surgeons to get tactile feedback [30]. The potential of telementoring is that greater ability to communicate with other surgeons can help us move towards the standardization of surgical techniques worldwide. This global interconnection also presents an opportunity to reduce the amount of travel needed to learn new or complex procedures [33]. The many uses of telementoring are summarized by Proximie's telementoring model dubbed the "3 Ps" – Prepare, Perform, and Perfect (Fig. 32.3).

Artificial Intelligence

Artificial intelligence (AI) algorithm enables machines to execute tasks that previously required human intelligence by recognition, processing and prediction. AI in healthcare is expanding as we are learning to use big data to make predictions via pattern recognition, allowing progress in machine learning and deep learning. This is being applied to healthcare by enhancing the detection of abnormalities [34].

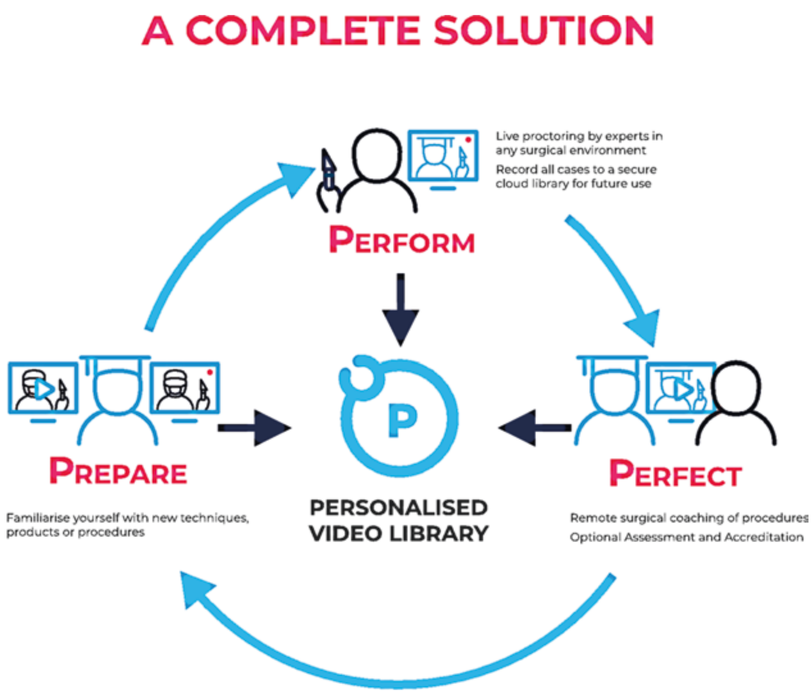

Fig. 32.3 The Proximie 3 Ps used to outline uses of telementoring in clinical practice: Prepare, Perform, and Perfect. (Image with permission from Proximie Ltd)

Fig. 32.4 Da Vinci Xi. It has four arms that are beneficial for multi-quadrant procedures [40]. (©2020 Intuitive Surgical, Inc. Used with permission)

In specialties such as pathology and radiology, AI algorithms can be used to improve the ability to identify malignant lymph nodes, including the identification of those at highest risk.

The CAMELYON16 (Cancer Metastases in Lymph Nodes Challenge) took place in November 2016, where over 200 slides were analyzed by both pathologists and AI algorithms with time limits. The algorithms were proved to be similar to (if not better than) 11 pathologists who took part, although it should be noted that pathologists were as good or better when they had no time limit [35]. It is believed that use of AI to increase accuracy in diagnosis and prognostication could improve patient outcomes in the future [36, 37].

Robotics

Robotic devices have many advantages, such as performing tasks that are hazardous to humans, carrying out repetitive tasks without getting tired, and helping complex surgery to be more precise [38]. Robots are currently widely used in many specialties. Compared to laparoscopy or open surgery, robotic surgery provides many advantages, including 3D visualization, image magnification, tremor cancellation, and motion scaling. Some studies also suggest other benefits of robotic surgery compared to open surgery – including decreased blood loss, diminished post-operative pain, shorter hospital stays and fewer complications [39].

The current generation of the da Vinci series (Fig. 32.4) is the main commercially available robot in surgery – although new robotic systems from Auris Health, Medtronic, Inc., CMR Surgical, and Verb Surgical, Inc. are poised to have (or have already) entered clinical use, and the landscape of robotics in surgery is expected to change dramatically during the ‘20s. Notwithstanding, the da Vinci family of robots remain the most utilized surgical system worldwide. It is designed to have thinner arms and is ergonomically enhanced, and it allows 3D HD camera to be used at each of the four arms, which is useful for multi-quadrant procedures. There are other competitor robots appearing in the market, such as Revo-I. Revo-I has features including open console and four-arm system, and it was approved by the Korean government for commercial use in 2017, followed by successful clinical trial in 2018 [34, 41].

Despite the benefits of robotic master-slave systems, human errors can still be made and there is room for improvement. Continuous developments are taking place to enhance robotic function. The next generation of robots may offer features like haptic gloves for more accurate tactile feedback or cellular image guidance [34]. Future robotic system will likely include more automation and AI-based computer-driven technology.

Challenges for the Future of Surgery

Data Security

One aspect of the future of surgery that is still unknown is how healthcare systems will embrace digital technology whilst maintaining the confidentiality and security of patient data. At present, healthcare systems often lag significantly behind technology used in other large organizations because of data security concerns. For example, there is a current drive in the United Kingdom to stop using fax machines and pager systems – technologies that have not been used in the corporate world for decades [42]. In order for many of the technologies discussed in this book to move from the research realm to mainstream healthcare, significant work needs to be done to address the ethical and technical issues related to the generation of this data. On one hand, data needs to be more secure, especially since healthcare is one of the most common industries for cybercrime [43], but on the other hand, making this big data accessible to the appropriate stakeholders could lead to important developments and discovery in medical research [44].

Financial and Ethical Implications

Another issue with many of the technologies discussed here is their cost. Introduction of technologies that can be used for individual patients creates a further stretch in resources for health systems, particularly in countries such as the United Kingdom that have to address the social justice of using expensive technologies for limited patients. With more expensive options for surgical training available (such as virtual reality), it could also mean that trainees in less wealthy institutions are further disadvantaged, and only patients in these institutions are involved in early training cases.

Sustainability is also a concern for all medical fields in the future and an area where surgery currently lags behind other professions. We have grown accustomed to surgery not being eco-friendly, with sterility meaning a large amount of surgical equipment is plastic and single use, generating a large amount of waste [45]. New technological developments also require hospitals to invest in devices that may be outdated or unusable in 5 years, which could be financially unsustainable in the long term. There is also mounting social pressure to reduce unnecessary travel so as to curtail the global carbon footprint. Thus, we expect, in the near future, that international surgical training and collaboration may become more reliant on telemedicine solutions. This may also impact outpatient follow-up of patients [46].

Conclusion

The developments in digital surgery described in this book have set the foundations for a bright future in surgery. It is likely that these advances in technology can increase our ability to prevent and treat disease at a cellular level and allow surgery to be tailored to individuals. AI, VR, AR, and advancements in robotics will provide the foundation and framework for digital surgery during its period of growth throughout the '20s. Surgeons will be able to improve the landscape of global surgery, allowing more of the world's population to have access to standardized and advanced surgical care.

References

1. Topol E. The Topol review: preparing the healthcare workforce to deliver the digital future. HEE, Leeds [Google Scholar]. 2019.
2. The UK has sequenced 100,000 whole genomes in the NHS. 2018. Available from: https://www.genomicsengland.co.uk/the-uk-has-sequenced-100000-whole-genomes-in-the-nhs/.
3. Pitruzzella B. The future of surgery report. England: The Royal College of Surgeons; 2018.
4. Schwarzenbach HH, Hoon DSB, Pantel K. Cell-free nucleic acids as biomarkers in cancer patients. Nat Rev Cancer. 2011;11(6):426.
5. Diaz LA, Bardelli A. Liquid biopsies: genotyping circulating tumor DNA. J Clin Oncol. 2014;32(6):579.
6. Rouchi AH, Mahdavi-Mazdeh M. Regenerative medicine in organ and tissue transplantation: shortly and practically achievable? Int J Organ Transplant Med. 2015;6(3):93.
7. Jones JR, Brauer DS, Hupa L, Greenspan DC. Bioglass and bioactive glasses and their impact on healthcare. Int J Appl Glas Sci. 2016;7(4):423–34.
8. Bonalive official website. Available from: https://www.bonalive.com.

9. Adams M, Reddy E, McNaboe T. Mastoid cavity obliteration using bonalive bioactive glass. J Laryngol Otol. 2016;130(S3):S15–S6.
10. Huang H, Xu H, Zhang J. Current tissue engineering approaches for cartilage regeneration: IntechOpen; 2019.
11. Hentze H, Graichen R, Colman A. Cell therapy and the safety of embryonic stem cell-derived grafts. Trends Biotechnol. 2007;25(1):24–32.
12. Mao AS, Mooney DJ. Regenerative medicine: current therapies and future directions. Proc Natl Acad Sci. 2015;112(47):14452–9.
13. Transplant statistics 2019 NHS Blood and Transplant Website. 2019. Available from: https://nhsbtdbe.blob.core.windows.net/umbraco-assets-corp/15720/annual_stats.pdf.
14. Kobayashi E. Challenges for production of human transplantable organ grafts. Cell Med. 2017;9(1–2):9–14.
15. Tack P, Victor J, Gemmel P, Annemans L. 3D-printing techniques in a medical setting: a systematic literature review. Biomed Eng Online. 2016;15(1):115
16. Gao B, Yang Q, Zhao X, Jin G, Ma Y, Xu F. 4D bioprinting for biomedical applications. Trends Biotechnol. 2016;34(9):746–56.
17. Dodziuk H. Applications of 3D printing in healthcare. Polish J Cardio-Thoracic Surg. 2016;3:283–93.
18. E-NABLE. Enabling the future E-NABLE website. 2019. Available from: https://enablingthefuture.org.
19. Mohammed M, Tatineni J, Cadd B, Peart P, Gibson I, editors. Applications of 3D topography scanning and multi-material additive manufacturing for facial prosthesis development and production. Proceedings of the 27th Annual International Solid Freeform Fabrication Symposium; 2016.
20. Nuseir A, Hatamleh MM, Alnazzawi A, Al-Rabab'ah M, Kamel B, Jaradat E. Direct 3D printing of flexible nasal prosthesis: optimized digital workflow from scan to fit. J Prosthodont. 2019;28(1):10–4.
21. Malik HH, Darwood ARJ, Shaunak S, Kulatilake P, El-Hilly AA, Mulki O, et al. Three-dimensional printing in surgery: a review of current surgical applications. J Surg Res. 2015;199(2):512–22.
22. Witowski JS, Pedziwiatr M, Major P, Budzynski A. Cost-effective, personalized, 3D-printed liver model for preoperative planning before laparoscopic liver hemihepatectomy for colorectal cancer metastases. Int J Comput Assist Radiol Surg. 2017;12(12):2047–54.
23. Baskaran V, Strkalj G, Strkalj M, Di Ieva A. Current applications and future perspectives of the use of 3D printing in anatomical training and neurosurgery. Front Neuroanat. 2016;10:69.
24. Satava RM. The future of surgical simulation. In: Stefanidis D, Korndorffer Jr JR, Sweet R, editors. Comprehensive healthcare simulation: surgery and surgical subspecialties. Cham: Springer International Publishing; 2019. p. 379–87.
25. Lanese N. New neuroanatomy lab bridges virtual reality, operating room Stanford Medicine News Center. 2018. Available from: https://med.stanford.edu/news/all-news/2018/03/new-neuroanatomy-lab-bridges-virtual-reality-operating-room.html.
26. Pirotte T. Vascular access in the perioperative period. In: Astuto M, Ingelmo P, editors. Perioperative medicine in pediatric anesthesia. Anesthesia, intensive care and pain in neonates and children. Cham: Springer; 2016. p. 285–340.
27. Vávra P, Roman J, Zonča P, Ihnát P, Němec M, Kumar J, et al. Recent development of augmented reality in surgery: a review. J Healthc Eng. 2017;2017:1–9.
28. Khor WS, Baker B, Amin K, Chan A, Patel K, Wong J. Augmented and virtual reality in surgery-the digital surgical environment: applications, limitations and legal pitfalls. Ann Transl Med. 2016;4(23):454.
29. Micali S, Virgili G, Vannozzi E, Grassi N, Jarrett T, Bauer J, et al. Feasibility of telementoring between Baltimore (USA) and Rome (Italy): the first five cases. J Endourol. 2000;14(6):493–6.
30. Miao Y, Jiang Y, Peng L, Hossain MS, Muhammad G. Telesurgery robot based on 5G tactile Internet. Mobile Netw Appl. 2018;23(6):1645–54.
31. Greenfield MJ, Luck J, Billingsley ML, Heyes R, Smith OJ, Mosahebi A, et al. Demonstration of the effectiveness of augmented reality telesurgery in complex hand reconstruction in Gaza. Plast Reconstr Surg Glob Open. 2018;6(3):e1708.
32. Kim SSY, Dohler M, Dasgupta P. The Internet of skills: use of fifth-generation telecommunications, haptics and artificial intelligence in robotic surgery. BJU Int. 2018;
33. Schlachta CM, Nguyen NT, Ponsky T, Dunkin B. Project 6 Summit: SAGES telementoring initiative. Surg Endosc. 2016;30(9):3665–72.
34. Rassweiler JJ, Autorino R, Klein J, Mottrie A, Goezen AS, Stolzenburg JU, et al. Future of robotic surgery in urology. BJU Int. 2017;120(6):822–41.
35. Golden JA. Deep learning algorithms for detection of lymph node metastases from breast cancer. JAMA. 2017;318(22):2184.
36. Panesar S, Cagle Y, Chander D, Morey J, Fernandez-Miranda J, Kliot M. Artificial intelligence and the future of surgical robotics. Ann Surg. 2019;270(2):223–6.
37. Hashimoto DA, Rosman G, Rus D, Meireles OR. Artificial intelligence in surgery: promises and perils. Ann Surg. 2018;268(1):70–6.
38. Diana M, Marescaux J. Robotic surgery. Br J Surg. 2015;102(2):e15–28.
39. Ludwig WW, Badaan S, Stoianovici D. Robotic systems in urological surgery: current state and future directions. In: Hemal AK, Menon M, editors. Robotics in genitourinary surgery. Cham: Springer International Publishing; 2018. p. 901–8.
40. Da Vinci Surgery website. 19/12/2019. Available from: https://www.davincisurgery.com/da-vinci-systems/about-da-vinci-systems##.
41. Chang KD, Abdel Raheem A, Choi YD, Chung BH, Rha KH. Retzius-sparing robot-assisted radical prostatectomy using the Revo-i robotic surgical system:

surgical technique and results of the first human trial. BJU Int. 2018;122(3):441–8.
42. Thomas K. Wanted: a WhatsApp alternative for clinicians. BMJ. 2018;360:k622.
43. Fuentes MR. Cybercrime and other threats faced by the healthcare industry.
44. Salas-Vega S, Haimann A, Mossialos E. Big data and health care: challenges and opportunities for coordinated policy development in the EU. Health Syst Reform. 2015;1(4):285–300.
45. Wyssusek KH, Keys MT, van Zundert AAJ. Operating room greening initiatives – the old, the new, and the way forward: A narrative review. Waste Manag Res. 2018;37(1):3–19.
46. Dullet NW, Geraghty EM, Kaufman T, Kissee JL, King J, Dharmar M, et al. Impact of a university-based outpatient telemedicine program on time savings, travel costs, and environmental pollutants. Value Health. 2017;20(4):542–6.

Index

S. Atallah (ed.), *Digital Surgery*, https://doi.org/10.1007/978-3-030-49100-0

M

N

O

P

U

V

W